UNIVERSITY OF CAPE TOWN
IYUNIVESITHI YASEKAPA • UNIVERSITEIT VAN KAAPSTAD

THE EFFECT OF VISCOELASTIC DEFORMATION IN PIPE CRACKS ON LEAKAGE RESPONSE TO VARIATIONS IN PRESSURE

A dissertation submitted in partial fulfilment of

MASTER OF SCIENCE IN CIVIL ENGINEERING

By

Ssozi Eva Nantongo

(sszeva001)

Supervisor: Prof J.E. Van Zyl

Co supervisor: Prof B.D. Reddy

Declaration

1. I know that plagiarism is wrong. Plagiarism is to use another's work and to pretend that it is one's own.
2. I have used the Harvard Convention for citation and referencing. Each significant contribution to and quotation in this report form the work or works of other people has been attributed and has been cited and referenced.
3. This report is my own work
4. I have not allowed and will not allow anyone to copy my work with the intension of passing it as his or her own work.

Signature _____ Date: ____29th August 2014___

Acknowledgements

I would like to thank and acknowledge the following people for their various roles during this project:

Prof J.E Van Zyl of the department of Civil Engineering at the University of Cape Town for his assistance and guidance during this project.

Prof B.D Reddy of CERECAM at the University of Cape Town for his insight and guidance throughout the course of this project.

Mr. Hellmut Bowles of FEAS Cape Town, for his guidance and help with the python scripting and results extraction.

Bukenya Patrick of the COMSIRU at the University of Cape Town for reading through this dissertation and commenting on writing and presentation.

The CERECAM and Water Distribution Systems research groups for their support and lastly but not least,

My family and friends who were an excellent support system during the duration of this project.

Abstract

Water is an important and increasingly scarce resource in the world today. Unfortunately, a lot of water is lost through leakage since most distribution systems are deteriorating. Therefore research in leakage management is necessary in order to improve the utilization of water resources. Leakage may be reduced by managing the water pressure in water distribution systems. One of the important factors affecting the pressure-leakage relationship is pipe material behaviour (Van Zyl & Clayton 2007; Greyvenstein & Van Zyl 2007). The pressure – leakage relationship has been described by several relationships such as the Torricelli equation, the Fixed and Variable Area Discharge (FAVAD) concept and the conventional equation.

Pipe material behaviour affects leakage parameters in the pressure-leakage relationship such as the leak area and the leak exponent (Cassa et al. 2010). For this project, the pressure-leakage relationships in High Density Polyethylene (HDPE) and Polyvinylchloride (PVC) pipes are investigated. HDPE and PVC are polymeric materials and therefore exhibit a viscoelastic response to applied stress and applied strain. Viscoelastic responses include creep, relaxation, hysteresis and time dependency. When these pipes experience stresses due to water pressures, failure and fracture may occur as leaks. The viscoelastic properties of these materials therefore affect how the leaks respond to pressure change.

The effect of viscoelastic deformations in leaks was investigated using Finite Element Analysis (FEA) software, Abaqus. Round holes and longitudinal cracks were represented as individual leaks in HDPE and PVC pipes in Abaqus. Pressure was applied to each pipe model for different time periods, and the deformed leak areas were obtained. Further analysis was carried out to determine the effects of pressure on leak parameters such as the gradient of the leak area-pressure relationship, leak exponent and the leakage number.

The analysis shows that viscoelastic deformations have an effect on the pressure-leakage relationship. A linear relationship exists between the leak area and pressure for all time periods investigated and therefore gradients could be obtained. Deformed leak areas, gradients and leak exponents all increased with time and therefore confirmed that the time dependency of viscoelastic materials affected the pressure-leakage relationship. The leakage exponents for both materials were found to vary between 0.5 and 1.5 for both HDPE and PVC. HDPE also exhibited higher leak exponents, gradients and larger deformed leak areas than PVC for the same leaks. It was also found that leakage in viscoelastic materials may be analysed using the leakage number, developed for elastically deforming materials by Van Zyl & Cassa (2013).

Table of Contents

List of Figures

List of Tables

List of symbols and abbreviations

A	-Area
C	-Leakage coefficient
C_d	-Discharge coefficient
D	-Inner diameter
D^*	-Standard Dimension Ratio
E	-Young's Modulus/elastic modulus
F	-Force
$G(t)$	-Shear modulus
$J(t)$	-Creep modulus
K	-Stress concentration
L_N	-Leakage number
M	-Bulk Modulus
$N1$	-Leak exponent/leakage exponent
Q	-Discharge
R^2	-Coefficient of determination
S	-Stress in plate
V	-Velocity
ΔE	-Elastic change in area
ΔT	-Total change in area
c_w	-Decompression wave speed
e	-Extension
g	-Gravitational constant
g_1^p	-Dimensionless shear modulus
h	-Pressure head

l	-Length
m	-Gradient
p	-Pressure
$t*$	-Thickness
t	-Time
u	-Displacement
ε	-Strain
η	-Viscosity
ν	-Poisson's ratio
θ	-Angle
ρ	-Density
σ	-Stress
τ	-Relaxation time

FEA	-Finite Element Analysis
FEM	-Finite Element Method
HDPE	-High Density Polyethylene
PVC	-Polyvinylchloride
RCP	-Rapid Crack Propagation
SANS	-South African National Standards
SCG	-Slow Crack Growth
SDR	-Standard Dimension Ratio

1 Introduction

1.1 Background

Water is an essential resource in any country's economy due to its various purposes for agriculture, industrial, household, recreational and environmental activities. Population increase in the world has led to substantial increase in water demand from distribution systems. Water resources are also becoming scarce therefore water losses are costly to both distribution companies and consumers; hence efficient management of water resources is important. However, water demand needs are not met sufficiently since water loss through leakage is a persistent problem in water distribution systems in the world.

One of the ways in which water losses occur is through pipe leaks (Van Zyl & Clayton 2007; Puust et al. 2010). Pipe leakages become more common as water distribution systems age and deteriorate, therefore increasing water losses. Water losses that occur through leakage present a challenge to effective management of water resources.

Several researchers around the world have conducted studies concerning leakage, which involved investigating and understanding the behaviour of leak holes and cracks in distribution systems. This has in turn provided guidelines for effective water resource management, reducing the amount of water lost through leakage and thus increasing the amount of water available for consumption.

1.2 Present state

In order to control water losses through leakages, an understanding of leakage and how it varies with pressure is essential. The pressure – leakage relationship is an important factor for leakage in distribution systems. Knowledge of this relationship therefore aids in improving water management (Lambert 2001). The behaviour of leak openings in pipes makes leakage a complex issue to characterise. The application of pressure management to control leakage depends on the accurate definition of the pressure – leakage relationship.

Currently, the pressure – leakage relationship is described either by the Torricelli equation or power law equation (Van Zyl & Cassa 2014). The Torricelli equation is a hydraulic equation also known as the orifice equation which states that the area of the leak openings is constant even as water pressure applied in the pipe increases. However, the variations of leak opening characteristics such as area have been shown to have an effect on the pressure – leakage relationship. This effect can be quantified by studying the behaviour of area of the leak openings, and the leak exponent of the leak.

Several investigations have been carried out to date concerning the response of leak openings to pressure changes. Cassa et al. (2010) numerically investigated the response of leak openings to pressure in elastically deforming materials. Greyvenstein & Van Zyl (2007) and Ferrante (2012) also carried out practical investigations in various materials. The most important factor affecting leak opening behaviour is the pipe material behaviour (Clayton & Van Zyl 2007; Greyvenstein & Van Zyl 2007). The water pressure in pipes is transmitted as stresses in the pipe material, which causes the leakage openings to deform accordingly. Clayton & Van Zyl (2007) observed that pipe deformation affects both the area of the leak opening and the leak exponent, and presented a model that incorporated material response to pressure in order to predict the pressure – leakage relationship. The model included a material property, Young's Modulus (E), which is important since mechanical responses to pressure vary from material to material.

Ferrante (2012) observed that pipe material behaviour has an effect on leakage behaviour by investigating the response of a longitudinal crack in different materials such as steel and polyethylene. The cracks were allowed to deform according to the pipe material properties, and it was found that different materials gave rise to unique pressure – leakage relationships. This was confirmed by Ferrante (2012), Massari et al. (2012) and Meniconi et al (2013) who found that the viscoelastic behaviour of a polyethylene pipe gave rise to a hysteric pressure-leakage relationship, which could not be explained by the Torricelli equation.

Therefore, different materials and types of leak openings respond differently to the application of pressure, and have different effects on the pressure-leakage relationship. Cassa, Van Zyl, & Laubscher (2010) investigated the effects of pressure on different leak openings and materials, and observed a linear relationship between leak area and pressure for each material. The leak area and leak exponent were found to vary with pressure. This is in contrast to the orifice equation, which assumes that leak area and exponent are constant with pressure changes. The study by Cassa et al. (2010) did not take into account deformations other than elastic deformation and leak exponents greater than 1.5. Leak exponents have been observed to be as high as 2.79 (Farley & Trow 2003). It is against this background that the effects of viscoelastic deformations of leak openings in High Density Polyethylene (HDPE) and Polyvinylchloride (PVC) pipes are investigated in this project.

1.3 Scope

Previous work by Cassa et al. (2010) only concentrated on the elastic deformation behaviour of leak openings in pipes and the variation with pressure. Since pipe material behaviour affects leak opening behaviour, the study of viscoelastic deformation is essential.

The purpose of the current investigation was to determine the effects of viscoelastic deformation on the pressure – leakage relationship by observing leak area deformation using the Finite Element Method (FEM). The pipes investigated were modelled as viscoelastic materials and therefore instantaneous and time dependent deformations was investigated.

Two pipe materials were investigated, and these included PVC (polyvinylchloride) and HDPE (High Density Polyethylene) pipes. The leakage openings studied were round holes and longitudinal cracks, of which different initial sizes were considered. More details are provided in methodology chapter 5. The investigation was based on a PVC pipe of pressure class 6.

The results obtained from the Finite Element Analysis program, (Abaqus), were compared to results obtained by earlier researchers such as the linear Fixed and Variable Area Discharges (FAVAD) model by Cassa et al. (2010) and practical investigations by Buckley (2007) and Ferrante (2012).

1.4 Problem statement, aims and objectives of the project

1.4.1 Problem statement

Accurate estimation of water losses in distribution systems involves studying the behaviour of distribution system leak openings and their effect on the pressure – leakage relationship. In particular, this project seeks to investigate how viscoelastic deformation of pipes affects the relationship between pressure and leakage.

Elastic deformation is the reversible change in shape or size of the leak opening when a load or stress is applied, whereas for viscoelastic deformation, the stress and strain of a body are time dependent (Banks et al. 2011). Cassa et al. (2010) found that for elastic deformation, the relationship between pressure and the leak area is linear.

The linear relationship between area of the leak openings and pressure was then further developed by use of the Fixed and Variable Areas approach (Van Zyl & Cassa, 2011) and linked to the leak exponent. The leak exponent for elastic deformation was theoretically found to have a maximum value of 1.5 (Cassa et al., 2010). Therefore elastic deformation could not explain leakage exponent values higher than 1.5. In some cases, the leak exponent was observed to be below 0.5.

Plastic pipes are commonly used and therefore the viscoelastic deformation behaviour of leaks may have an effect of the leak area and leak exponent. Hence, this project seeks to investigate the effect of viscoelastic deformation on the pressure - leakage relationship.

1.4.2 Objectives

The main goal of this research was to investigate and understand the impact of viscoelastic deformation of existing leak openings due to variations in pressure. This goal was achieved by:

i. Carrying out a literature review to gain an understanding of the following:
   - Background research work by various researchers. This includes an understanding of how pressure and leakage are linked through the various pressure-leakage relationships, and the individual parameters that describe this relationship. The main parameter to be discussed in detail is the leak area, and how its variation with pressure affects the pressure-leakage relationship.
   - To understand how stresses due to water pressure affect the response of leaks in the pipes.
   - To understand the structural and chemical properties of the two pipe materials, HDPE and PVC.
   - To understand the mechanical properties of the pipe materials, in particular viscoelasticity and their fracture behaviour when subjected to loads as well as the material structure and properties.
   - To provide better understanding of the Finite Element Analysis (FEA) software, Abaqus, which is to be used for the project, including modelling time dependent and cyclic deformation.

ii. Modelling leak openings (round holes and longitudinal cracks) in viscoelastic pipe materials with the help of Abaqus, which is a finite element modelling software.
iii. Investigating the effect of pressure on the deformation behaviour and area of existing leak openings.
iv. Investigating the pressure – leakage relationship for the leak openings, by linking the area variation of the leak openings to the leak exponent and comparing the results with the observations of other researchers.
v. Deducing the impact of viscoelastic deformation on the pressure - leakage relationship of pipe leaks. This includes both the impact of non-cyclic and cyclic pressure simulations on the leakage exponent and comparing results with previous numerical investigations for elastically deforming materials.

1.5 Organisation of dissertation

This dissertation is divided into 6 main chapters as follows:

Chapter one is an introduction of the project, and includes the background and present state of the research topic. The problem statement, aims and objectives are included and explained. The objective of the project is to investigate the impact of viscoelastic deformations on pipe leaks and the pressure-leakage relationship.

Chapter two and three are the literature reviews. Chapter two covers leak hydraulics while chapter three covers material behaviour of the pipe materials investigated. The literature review was carried out by reading various journal articles, conference papers, text books and web pages. The literature review explains the pressure-leakage relationship and the stress and strain behaviour of the pipe materials.

Chapter four is the methodology chapter. An explanation of the finite element method and software used in this project is included in this chapter. The method implemented is described and material parameters are listed.

Chapter five is the results and analysis chapter. Two pipe leaks are explained (one round hole and one longitudinal crack) and the analysis process is described. The results of all the leaks are also summarised and compared.

Chapter six contains the conclusions and recommendations drawn from this project. This is followed by the bibliography and appendix.

2 Effect of pressure on leak openings behaviour in pipes

Pressure from water flow in distribution systems is taken up as longitudinal and circumferential stresses in pipe walls. Longitudinal stresses arise from the internal pressure acting in the axial direction of the pipe while circumferential stresses arise from water pressure acting on the internal pipe walls. These stresses are given by the following expressions adapted from Griffel (1966) which are a result of water pressure acting perpendicularly onto the pipe walls. The stresses are illustrated in the equations 2.1 and 2.2 as well as figure 2-1 below:

Circumferential stresses:

$$\sigma_{circ} = \frac{pD}{2t^*} \tag{2.1}$$

Longitudinal stresses

$$\sigma_{long} = \frac{pD}{4t^*} \tag{2.2}$$

Where σ is the stress in the pipe material, p is the water pressure, t^* is the pipe thickness and D is inner diameter of the pipe.

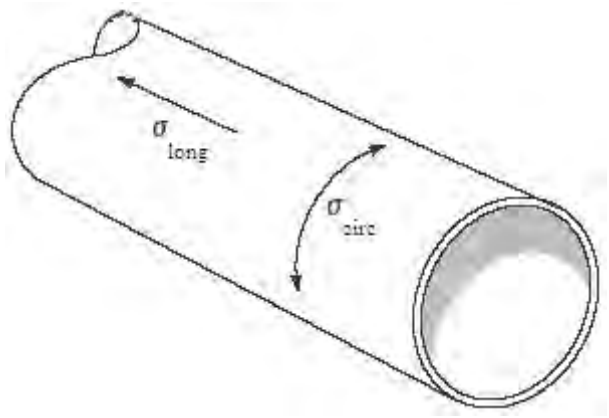

Figure 2-1: Longitudinal and circumferential stresses (Source: open.jorum.ac.uk)

These induced stresses cause the area of existing leak openings to increase or decrease depending on the magnitude of the stresses, pipe material behaviour and shape (round hole, circumferential or longitudinal crack) of the leak opening.

Changes in pressure and therefore pipe stresses affect both area of the leak opening and the leakage exponent, N1. For example, a study reported by Clayton & Van Zyl (2007) found that in uPVC pipes, the leakage exponent could be less than 0.5 indicating that the opening has contracted with increase in pressure. In the study, the experimental setup did not allow longitudinal stresses to develop in pipe. Circumferential stresses instead caused the cracks under observation to elongate, and therefore contract.

Pipe material behaviour has been studied to gain a deeper understanding of its effect on the pressure – leakage relationship when pipes experience stresses from applied pressure. Cassa et al. (2010) focused on four aspects for leakage research. These aspects were:

i. Stress distribution in pipes
ii. Effect of the size of the leak opening on leak behaviour
iii. Relationship between pressure and leak area
iv. Implications of the above three aspects on the leakage exponent.

The above aspects are each discussed in the sections that follow.

2.1 Stress distribution in pipes

As stated before, stresses and the resulting stress distributions in the pipe wall are due to water pressure in the pipe. A leak opening will affect the stress distribution in pipe walls. With the help of a thin plate with a round hole, Timoshenko & Goodier (1951) showed that the effect of a hole in a material is localised, and stresses become more uniform as the distance from the edge of the hole increases. In their theoretical study, the plate was subjected to uniform tension at its edges as illustrated below in figure 2-2.

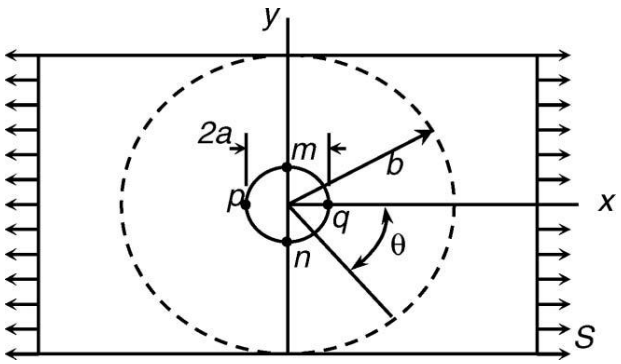

Figure 2-2: Plate subjected to uniform stresses at the ends (Source: Cassa et al, 2010)

Timoshenko and Goodier (1951) also showed that stress at the hole edge is given by equation (2.3) below.

$$\sigma_\theta = S - 2S\cos 2\theta \tag{2.3}$$

Where θ is the angle shown in figure 2-2 above and S is the stress applied to the plate.

It can be seen from equation (2.3) and figure 2-2 that points p and q experience compressive stresses. This explains the deformation of round holes to elliptical shapes as observed in previous research by Cassa et al. (2010).

From equation (2.3), it is also seen that the maximum and minimum stresses (σ_{max} and σ_{min} respectively) around the hole edges would occur at the hole edges as illustrated by the stress distributions in the figure 2-3 below.

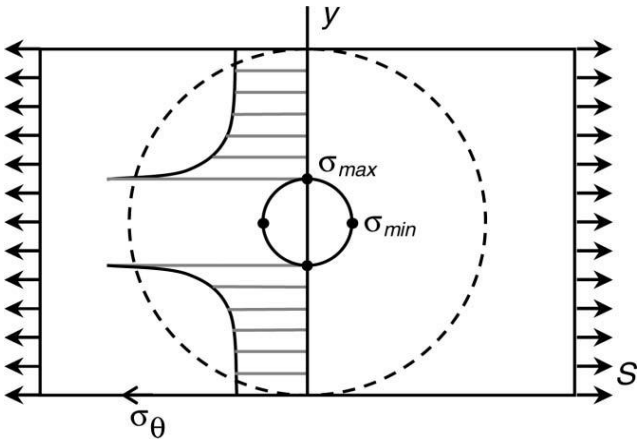

Figure 2-3: Location of maximum and minimum stresses in a plate with a round hole (Source: Timoshenko, 1951)

Maximum stress occurring around a leak opening is usually significantly higher than stresses in the rest of the pipe wall. This stress effect of a hole on the pipe material behaviour can be expressed by the use of a stress concentration factor, K. This factor is the ratio of maximum stress to nominal stress in the material. This is shown by the following equation:

$$K = \frac{\sigma_{\max}}{\sigma_{nom}} \tag{2.4}$$

Where σ_{max} is the maximum stress in the material and σ_{min} is the nominal stress in the pipe material. Stress concentrations occur at pipe defects and abrupt changes in pipe geometry or direction.

At the edge of a leak opening, only circumferential stresses exist, but longitudinal stresses still exist in the rest of the pipe material. The biaxial stress state is defined as the state in which both the longitudinal and circumferential stresses exist in the pipe, while the uniaxial stress state is the state in which only circumferential stresses exist in the pipe. The resultant stress distribution in pipes usually lies somewhere in between the extremes of the biaxial and uniaxial stress states. It is the resultant stress distribution that is responsible for leak opening behaviour.

Observing stress distribution assists in explaining leak opening behaviour. For example, in a pipe with a round opening under uniaxial loading, the highest stresses are likely to occur at the opposite edges of the opening, along the length of the pipe (Cassa et al. 2010). This explains why a round hole deforms to an elliptical shape along the pipe length. This is illustrated in the figure 2-4 below.

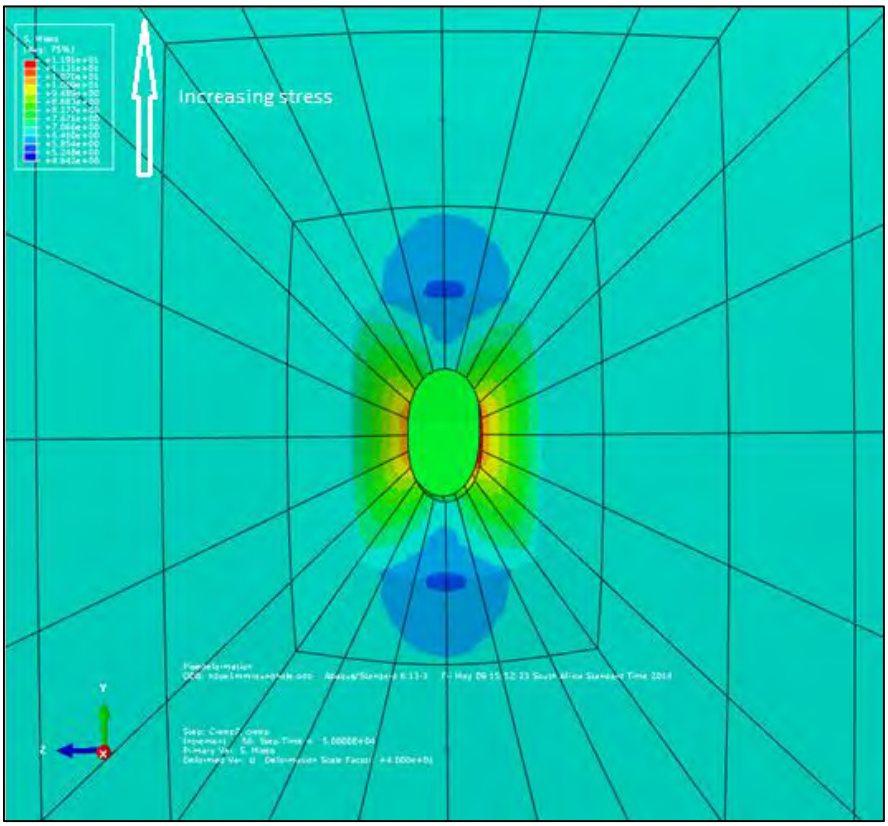

Figure 2-4: Stress distributions for a 1mm round hole deformed to an ellipitical shape, deformation scale factor = 40 (Source: Abaqus)

Stresses can sometimes be sufficiently high to cause permanent deformation such as plastic deformation.

In the case of a crack transverse to loading direction, the highest stresses would be located at the crack tips. As pressure is increased, the stress at the tips approaches the elastic limit of the material. For an ideally sharp crack tip, linear elasticity would predict infinite stress at the tips (Cassa et al, 2010). In practice, this condition does not exist and instead the material undergoes plastic deformation and load redistribution resulting in crack propagation. The stress intensity of a leak opening is a function of its orientation relative to the applied stress and length or size of the opening. As the area of leak openings is altered by stress, the relationship between pressure and leakage is duly affected. Circular holes, longitudinal cracks and circumferential cracks all result in different stress distributions in pipes.

Circular openings are deformed into an elliptical shape as stress in the pipe wall increases. Cassa et al (2010) showed that for a round hole in a pressurised PVC pipe, the highest stresses occurred at the furthest edges along the length of the pipe for all pressures and loading states. The lowest stresses were observed at the furthest edge in a transverse direction. This can be seen in figure 2-4 above. Scaling up the deformations showed that the hole is slightly pulled into the pipe and it resembles an ellipse. Stress concentrations for round holes were also found to increase linearly with increasing diameter of the opening. This linear behaviour was also observed in other materials such as steel and cast iron pipes.

The maximum stresses at an opening can be higher than nominal pipe stresses; therefore allowable stress to cause plastic deformation can easily be exceeded when a leak is present. As stress increases, the hole area increases to a point when the yield strength of the material is exceeded (Cassa 2005; Cassa et al. 2010). For both longitudinal and circumferential cracks, the highest stresses occur at the ends of the crack. In particular, for circumferential cracks, maximum deformation occurs at and around the crack. The crack opens up as a result of pressure in the pipe.

Therefore, it can be concluded that pipe stress distributions are significantly affected by leak openings. Certain regions of leak openings experience higher stresses, such as the crack tips and edges along pipe lengths. At high stresses, pipe materials may either undergo plastic deformation or bursts may occur when the fracture toughness of the material is exceeded.

2.2 Pressure – leakage relationship

The pressure – leakage relationship can be modelled in two ways. They include the power law concept and the Fixed and Variable Area Discharges (FAVAD) concept.

An important aspect in the pressure – leakage relationship that is evident in the FAVAD concept is the relationship between leak area and pressure head in the pipe. This relationship has been studied to various extents, for example Cassa et al. (2010), who investigated the relationship under elastic deformation and found that it is a linear relationship. Allowing for plastic deformation, Ferrante (2012) found that this linear relationship adequately described the pressure – leakage relationship until plastic deformation occurred.

In this section, the power law and FAVAD concepts are discussed fully and then two parameters of the pressure-leakage relationship, that is, leakage area and leakage exponent are also explained.

2.2.1 FAVAD approach

The FAVAD concept was first proposed by (May 1994) and developed from the orifice equation by Van Zyl & Cassa (2011). Unlike the original orifice equation whose leakage exponent is fixed at 0.5, the FAVAD equation allowed for variation of the leakage exponent. The FAVAD equation was developed assuming only elastic behaviour. The development of the FAVAD equation from the orifice equation by Van Zyl & Cassa (2011) is explained in the paragraphs below.

The original orifice equation models the leak opening as an orifice with defined properties such as the discharge coefficient. In essence, leak openings are hydraulically similar to orifices. The principle of conservation of energy is applied to obtain a relationship between pressure head and velocity of water through an opening. This principle is given by the equation 2.5 below also known as the Torricelli equation:

$$V = C_v\sqrt{2gh} \tag{2.5}$$

Where V is the velocity of the water in the pipe, C_v is the velocity coefficient, g is the gravitational constant, and h is the total head. In water distribution systems, the total head can be assumed to be the water pressure. The velocity coefficient is ratio of the actual velocity to the velocity that would occur if there were no frictional losses in the orifice (Finnemore & Frazini 2009). The velocity is then multiplied by the cross sectional area A, and the coefficient of contraction C_c to obtain the actual leakage rate, Q. The coefficient of contraction is the ratio of the area of the water jet out of the orifice to the area of the orifice (Finnemore & Frazini 2009). The result is the orifice equation below:

$$Q = C_c A C_v \sqrt{2gh} \quad (2.5b)$$

Equation 2.5b can be simplified as:

$$Q = C_d A \sqrt{2gh} \quad (2.6)$$

In equation 2.6 above, $C_d = C_c C_v$ and is known as the discharge coefficient. The properties of the orifice therefore include the discharge coefficient and the cross-sectional area of the orifice. The discharge coefficient therefore accounts for frictional losses at the orifice and also contraction of the water jet downstream from the orifice (Van Zyl & Cassa 2014). The discharge coefficient, C_d is defined as the ratio of actual discharge rate to ideal discharge rate. (Finnemore & Frazini 2009). The ideal discharge rate occurs when there are no frictional losses and contraction of the water jet at the orifice.

The discharge coefficient varies due to flow conditions (Lambert 2001; Finnemore & Frazini 2009). Flow conditions depend on the Reynolds number, which is a way of establishing if the flow is laminar, transitional or turbulent. Reynolds number is defined as the ratio of inertia forces to viscous forces in fluid flow (Finnemore & Frazini 2009). For Reynolds numbers of 200000 and higher, the discharge coefficient is constant (Finnemore & Frazini 2009). The high Reynolds number indicates turbulent flow, which is a good approximation for water flow through leaks. Furthermore, the square root relationship between the discharge rate of the orifice and pressure head is only valid for turbulent flow, which occurs at Reynolds numbers greater than 4000-5000 (Van Zyl & Cassa 2014). Therefore the assumption of a constant discharge coefficient is reasonable.

The orifice equation (as presented in equation 2.6), can lead to inaccurate results as since it does not consider the effect of change in area due to pipe material deformation when pressure is applied. For example, materials with a high Young's modulus may have less expansion and therefore lower leakage exponents, compared to the value of 0.5 of the orifice equation (Greyvenstein 2007). Also negative pressures are not taken into account (Todini 2003) in the orifice equation. Therefore various efforts have been made to improve the orifice equation. Van Zyl & Cassa (2011) illustrated a transformation from the original orifice equation to a FAVAD equation form described below.

Using the finite element method, Cassa (2005) established that the area of leak openings in elastically deforming pipes varied linearly with pressure. Different materials and different loading conditions led to different linear equations, under the assumption of elastic deformation.

This alternative FAVAD approach describes a linear relationship between the area of leak openings and the pressure. This linear relationship is of the form:

$$A = \left(A_0 + mh\right) \tag{2.7}$$

Where A_0 is the original area of the leak opening, A is the area of the leak opening after pressure head h has been applied and m is the gradient of the linear pressure-leakage relationship.

This expression was then substituted into the original orifice (equation 2.6) and the result was as shown below:

$$Q = C_d \sqrt{2g}\left(A_0 h^{0.5} + mh^{1.5}\right) \tag{2.8}$$

Where Q is the discharge, C_d is the discharge coefficient, A_0 is the original area of discharge, g is the gravitational constant, h is the pressure head and m is the slope of the linear relationship of area against pressure head.

The relationship between leak opening area and pressure head has been shown to be affected by pipe material deformation behaviour by different researchers as explained in the previous chapters. Attempts have been made to quantify and verify the relationship between leak area and pressure, for different materials and different leak openings. Change in leak area due to pressure is a result of the stress distributions in the pipe and resultant pipe deformations. Different materials experience different types of deformations, such as plastic, elastic and viscoelastic deformations. Viscoelastic deformations are the relevant deformations for this project and are discussed in greater detail in the literature review (chapter 3).

The original Torricelli equation, (equation 2.6), assumes that the area of the leak opening is constant even as pressure increases or decreases. This assumption has been shown to be incorrect by researchers such as Ferrante (2012) and Van Zyl & Cassa (2011) who observed that the area of leak openings varies according to the pressure applied.

The relationship between leak area and pressure has been verified to be a linear relationship for elastically deforming materials. This relationship is described earlier by equation (2.7) and was developed by Cassa et al. (2010) for four different materials which included cast iron, asbestos cement, PVC and steel pipes and three leak types (round holes, circumferential cracks and longitudinal cracks). A similar relationship was also proposed earlier by May (1994). Cassa et al.

(2010) found that the maximum value of leakage exponent given by this linear relationship was 1.5 and recommended the investigation of plastic deformation to offer an explanation for leak exponents higher than 1.5.

A practical investigation by Ferrante (2012) also showed that the relationship developed by Cassa et al. (2010) was only valid up to a certain point for an elastoplastic material. Experiments were carried out in which plastic deformation was allowed to occur. For these experiments, leaks of the same dimensions were machined into 4 pipe materials, namely non-deformable steel, elastoplastic steel, elastic steel; and HDPE. The pipes were subjected to certain flow rates that were varied in order to vary pressure. The effective areas of the leaks were thereafter calculated from the Torricelli equation. The dimensionless effective area was plotted against the pressure head as shown in figure 2-5 for each material test. The data for the elastoplastic pipe (test 2 in figure 2-5) was fitted to the linear relationship developed by Cassa et al. (2010) (equation 2.7) by calculating the predicted dimensionless area for each pressure. The linear relationship is abbreviated as CAS in figure 2-5.

Ferrante (2012) found that at a pressure of 20m, the data deviated away from the prediction of the CAS model. In addition, on closer inspection and measurement of the leak it was clear that plastic deformation of the leak had occurred and the crack had propagated through the pipe. The occurrence of plastic deformation was verified both by observation and measurement of the leak cracks tested before and after the application of pressure. The relationship between area of the crack and pressure head beyond 20m (after plastic deformation occurred) was not discussed in his paper.

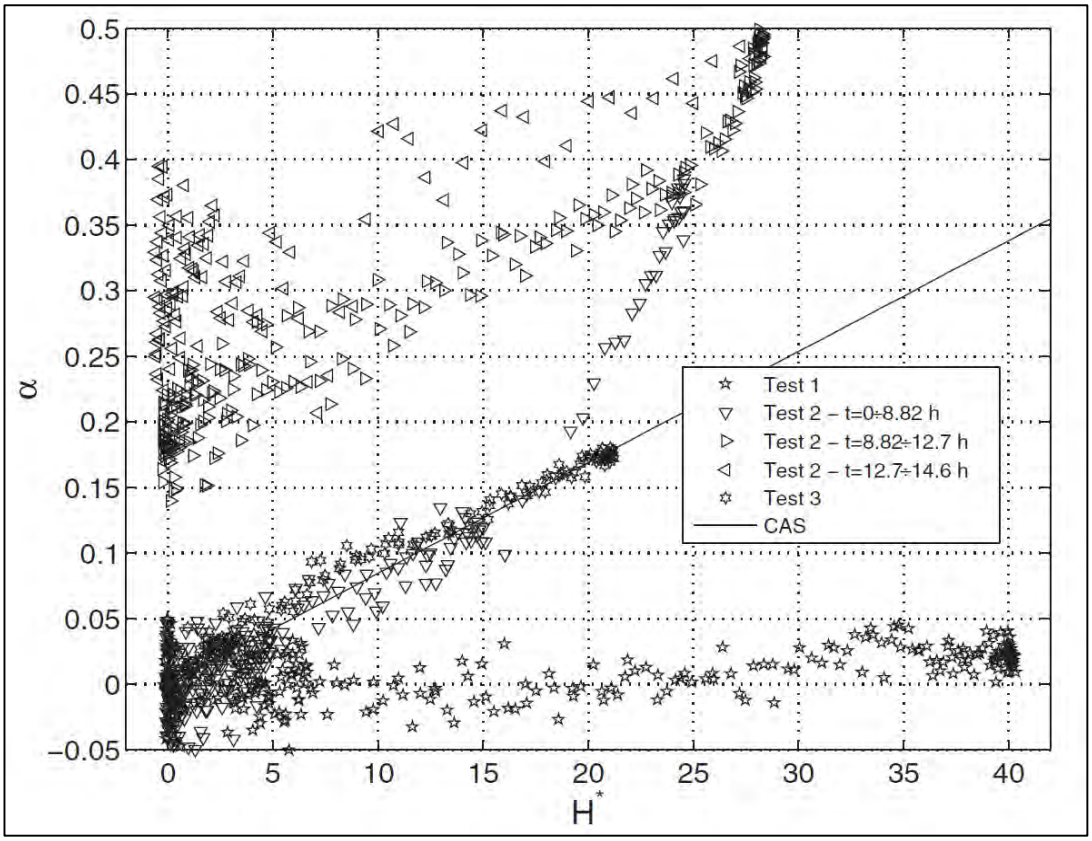

Figure 2-5: Difference between experimental data and Cassa et al. (2010) model when dimensionless leak area is plotted against pressure (Source: Ferrante, 2012))

Further analysis by Ferrante (2012) showed that the leak area – pressure relationship for plastics such as PVC and HDPE was different from that of metallic materials such as steel and cast iron. A hysteric relationship between effective area and pressure head was observed by Ferrante et al. (2011) for a longitudinal leak in a polyethylene pipe. A hysteric relationship is characterised by different loading and unloading cycles. The figure 2-6 below shows the hysteric loop formed as a result of the viscoelastic deformation behaviour of the polyethylene pipe material.

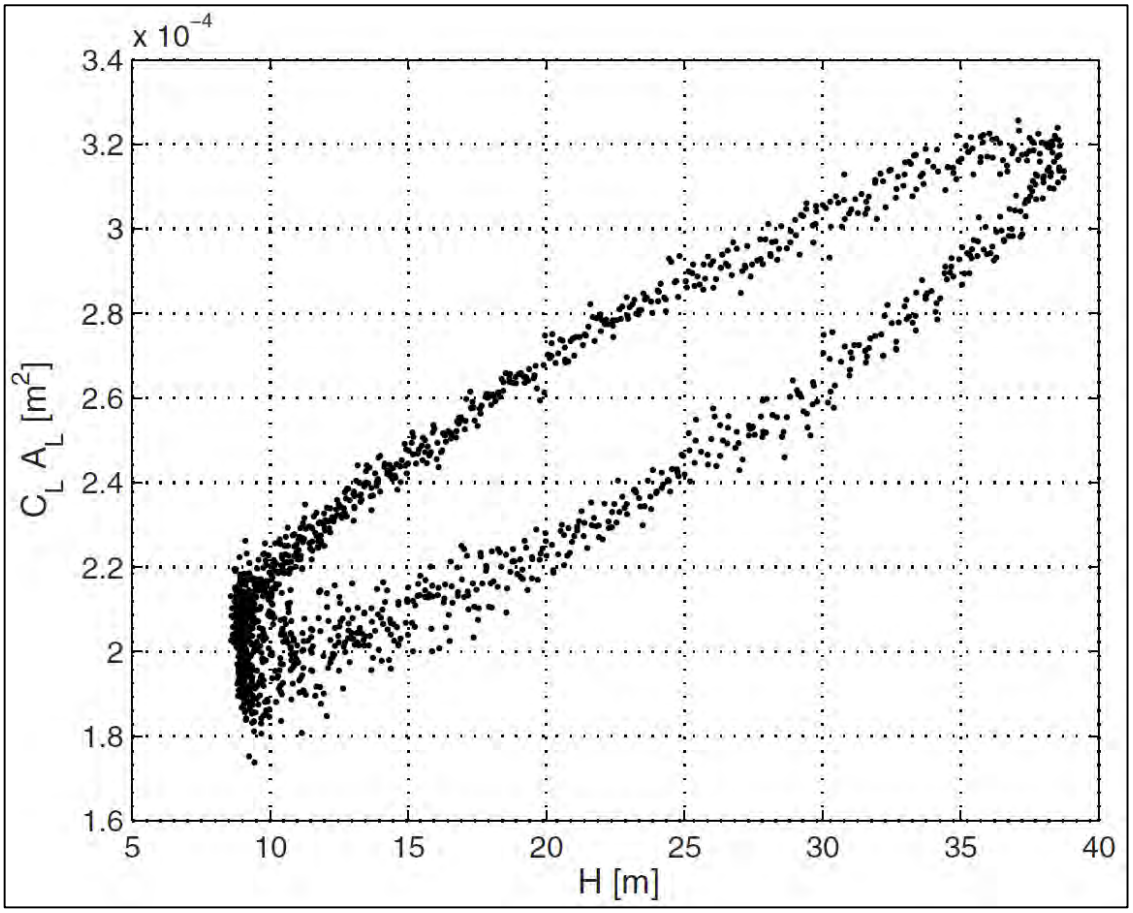

Figure 2-6: Effective area against pressure head for a polyethylene pipe (Source: Ferrante et al, (2011))

From figure 2-6, it is seen that the assumption of a constant area made by the Torricelli equation and the linear model developed by Cassa et al. (2010) will not adequately describe the leak area – pressure relationship for a polyethylene pipe. Since PVC also exhibits viscoelastic deformation behaviour, a similar loop would be observed. These results were further verified by measuring the radial strains around the leak opening. A hysteric loop was also obtained for the relationship between the radial strains and pressure, which confirmed that the hysteric loops in the leak area – pressure graph were indeed due to the pipe material behaviour.

Clearly, as seen as from figures 2-5 and 2-6, the effect of material behaviour on the leak area – pressure relationship cannot be ignored for the purpose of accurate description of the pressure – leakage relationship of deformable pipe materials.

2.2.2 Power law approach

Alternatively, the power law approach for modelling leakage behaviour was developed by leakage practitioners after the orifice equation was discovered to be inadequate for leakage characterisation.

$$Q = Ch^{N1} \tag{2.9}$$

This approach is a more general form of the Torricelli equation, commonly used by leakage practitioners. A leak opening is modelled with a fixed leakage coefficient (C) and varying leakage exponent (N1). However the leakage coefficient is not necessarily constant and can vary with flow conditions such as Reynolds' number.

Water Losses Task Force (Thornton & Lambert, 2005) developed a simple law from equation (2.9) above as a physical and practical way of presenting the pressure - leakage relationship. Their power law states that leakage, Q, varies with pressure head h, raised to an exponent N1. The relationship is normally used in ratio form. It is derived as follows for pressure and leakage at two times, 0 and 1:

$$Q_0 = Ch_0^{N1} \tag{2.10}$$

$$Q_1 = Ch_1^{N1} \tag{2.11}$$

Where Q_0 and Q_1 are leakage rates and h_0 and h_1 are pressure heads at the respective times. For example, if pressure changes from h_0 to h_1, leakage will change from Q_0 to Q_1 and the extent to which leakage changes depends on the leakage exponent, N1. In leakage practice, C is often assumed constant leading to the following equation:

$$\frac{Q_1}{Q_0} = \left(\frac{h_1}{h_0}\right)^{N1} \tag{2.12}$$

The relationship between the ratio of leakages, $\frac{Q_1}{Q_0}$ and the ratio of pressures, $\frac{h_1}{h_0}$ for different leak exponents is illustrated in figure 2-7 below.

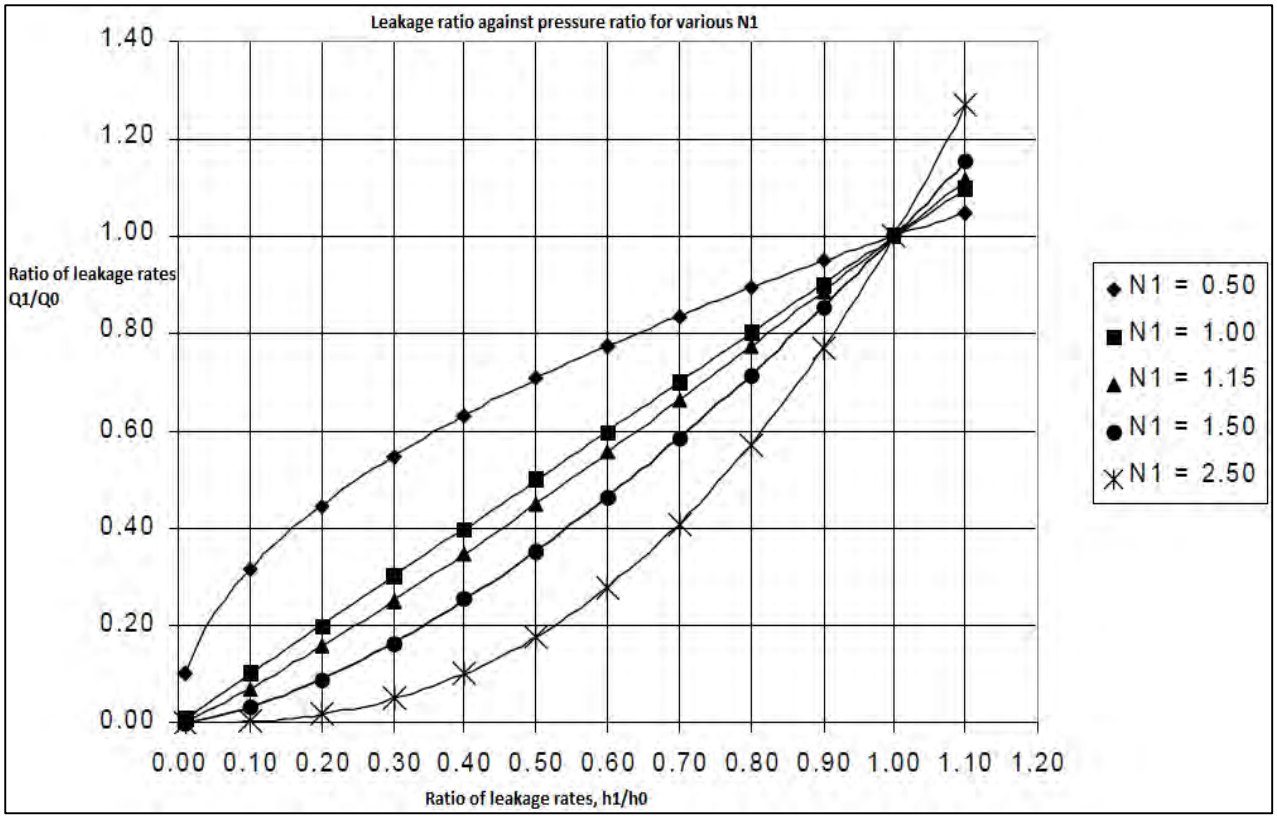

Figure 2-7: Relationship between ratio of leakage and ratio of pressure (Source: Lambert & Thornton, (2005))

N1 for the power law (equation 2.9) typically lies between 0.5 and 1.5, but may reach values as high as 2.5. The value of N1 obtained from this equation could also vary depending on whether a leak opens in one dimension or two dimensions (Lambert 2001). The leakage exponent (N1) depends on the pipe material behaviour under loading and nature of the opening or fracture and this has been proved from international test data. Material deformations can therefore be expected to have an impact on N1 and the area of the opening, and therefore the pressure – leakage relationship.

The Torricelli equation assumes a fixed N1 value of 0.5. As stated before, the fixed value does not take into account other exponent values that have been found by leakage researchers. Work done by Greyvenstein (2007) shows that the leakage exponent varies between 0.5 and 2.79. Therefore the FAVAD concept (equation 2.7) was also developed by Cassa et al. (2010) as a better way of approximating leakage in distribution systems. Cassa et al. (2010) investigated elastic deformation in various leaks and found that the leakage exponent for elastically deformable materials varied between 0.5 and 1.5.

The FAVAD equation developed by Cassa et al. (2010) was substituted into the Torricelli equation and from equation (2.8), it is seen that the leakage exponent varies from 0.5 to 1.5, if one assumes that the pipe material only undergoes elastic deformation. However, Farley & Trow (2003) state that the leakage exponent usually varies between 0.5 and 2.79, and values below 0.5 could also be obtained. It was suggested that research allowing for plastic deformation in leak openings could explain this variation. The large range of exponent values reported by Farley & Trow (2003) indicates that leakage can be quite sensitive to pressure. Hence, accurate models are essential in estimating and predicting leakage losses.

2.2.3 Relationship between FAVAD and power equations

The area of a leak opening also varies with pressure. This is illustrated by the FAVAD concept, equation (2.7) which shows that the leak area and pressure are related via a linear relationship if the pipe material is only allowed to deform elastically. The power equation was developed by leakage practitioners as alternative to the orifice equation.

Van Zyl & Cassa (2014) investigated the power equation and found that it had three limitations. Firstly, the power trend line equation did not adequately describe the pressure-leakage relationship for pressures higher or lower than the investigated pressure range. Secondly, the fit quality of the power trend line reduced significantly when more low pressure points were included. Lastly, the discharge coefficient and leak exponent were calculated for small changes in pressure and were found to vary for the same leak opening. Data collected by Van Zyl & Cassa (2011) showed that the leakage exponent could vary substantially over a range of experimented pressures for the same opening. For example, in figure 2-8 below, it is observed that there was a 150% increase in the leakage exponents for the experimented pressures in a 60mm longitudinal crack. These values of N1 were calculated using the leakage coefficients obtained from equation (2.9) during the experiments.

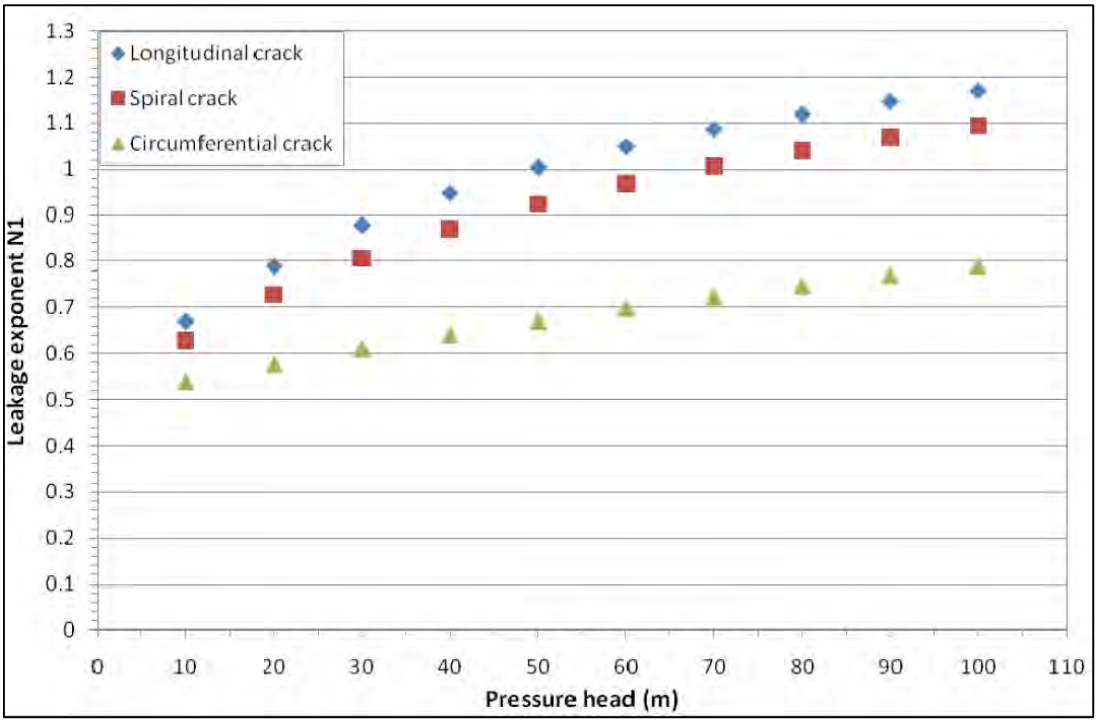

Figure 2-8: Leakage exponent against pressure head for 60mm crack in PVC (Source: Van Zyl & Cassa, (2014))

To further understand the relationship between area of the leak opening and leakage exponent for elastic deformation, the FAVAD and power law equations were equated after establishing the linear relationship between pressure and area from finite element modelling (Van Zyl & Cassa, 2011). This was done by equating the two equations (2.8) and (2.9), and dividing both sides by the orifice equation, equation 2.6. A leakage number, L_N, was established. L_N is given by:

$$L_N = \frac{mh}{A_0} \tag{2.13}$$

Where m is the gradient of the linear relationship between area and pressure, h is the pressure head and A_0 is the original area of the leak.

Van Zyl & Cassa (2011) then illustrated how this leakage number L_N could be used to convert between m and N1. After further manipulation, an expression that enabled direct conversion from L_N to N1 was developed. This expression is stated below:

$$N1 = \frac{In(L_N + 1) - In(C^1)}{In(h)} + \frac{1}{2} \tag{2.14}$$

Where,

$$C^1 = \frac{C}{C_d A_0 \sqrt{2g}} \tag{2.15}$$

Further investigation showed that plotting N1 against L_N always plotted on the same line as shown in the figure 2-9 below, irrespective of the values of A_0, m and h. In figure 2-9, it is observed that for leakage numbers less than 1, leak exponents were less 1. For leakage numbers greater than 1, leak exponents were also greater than 1. Leak exponents were approximately 0.5 for leakage numbers less than 0.01. Leak exponents were also approximately 1.5 for leakage numbers greater than 100. A formula for calculating leak exponents from leakage numbers was therefore derived as:

$$N1 = \frac{1.5L_N + 0.5}{L_N + 1} \tag{2.16}$$

Equation (2.16) was derived from the FAVAD concept, and was therefore applicable to elastic deformation. The leakage number was therefore a more consistent measure of leak behaviour and this was proven by plotting values of the leakage exponent against values obtained for the corresponding leakage numbers. With the leakage number known, leak exponents for any crack at any given pressure could be obtained. In figure 2-9 below, A0 is the area of the un-deformed leak.

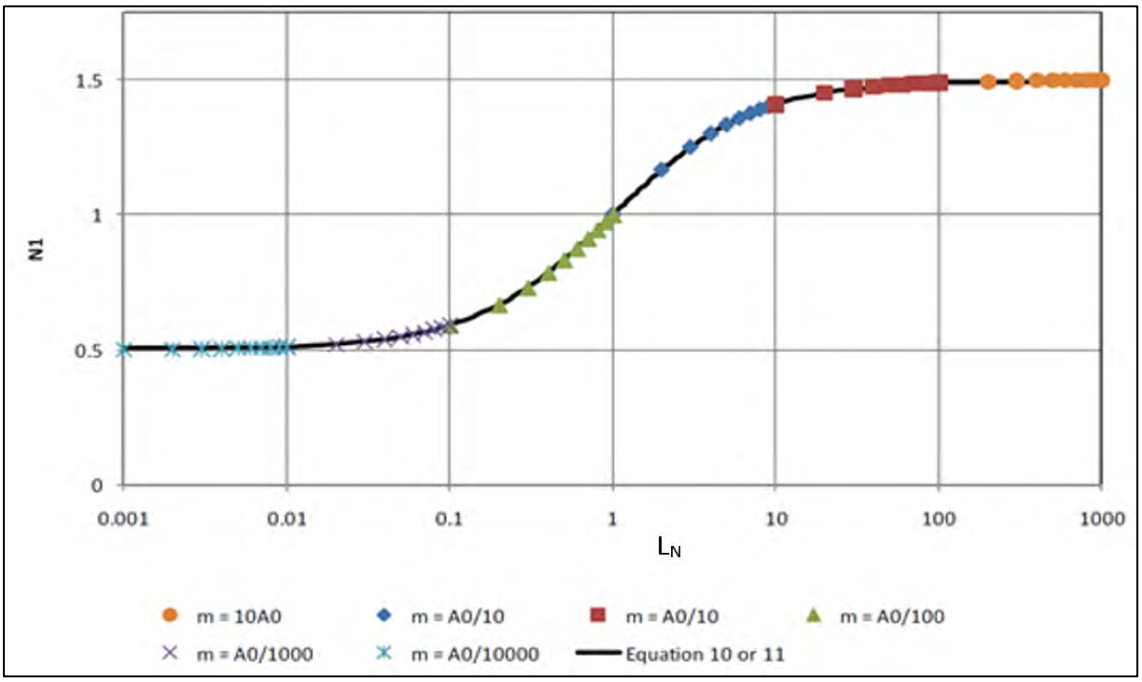

Figure 2-9: Relationship between leakage exponent N1 and leakage number N_L (Source: Van Zyl & Cassa, (2011))

Chapter two has presented a discussion on leakage behaviour. Leak behaviour is influenced by the stress distributions occurring in pipes. The leak behaviour is explained by studying the pressure-leakage relationship. The pressure-leakage relationship has been studied by various researchers and two approaches were discussed in this chapter, the FAVAD approach and the power law. The two concepts differ from the original Torricelli equation since they allow for leak area deformation. Two parameters within the pressure-leakage relationship were discussed and they include the leak area and the leak exponent. The leak area and leak exponent have been found to vary with pressure in the various pipe materials studied. The variations of the leak area are mainly due to the pipe material behaviour and resulting stress distributions. In the next chapter, the structure and mechanical properties of the pipe materials for this study are discussed in order to understand the resulting leak deformations.

3 Properties of PVC and HDPE pipe materials

Polyvinyl Chloride (PVC) and High Density Polyethylene (HDPE) are both polymeric materials, but with different properties. The reason for this lies in their chemical structure. This section is a review of the chemical structures of PVC and HDPE. Also, their advantages and disadvantages as pipe materials are discussed and a summary of the production process is also included. This will provide greater insight in accounting for the difference in material, yield and fracture behaviour for latter sections of the literature review.

3.1 Structural properties of PVC and HDPE

PVC and HDPE pipes are plastic pipes which are manufactured from polymer materials. A polymer is defined as a large molecule made up of one or more repeating units which are linked together by covalent bonds (Moore & Kline 1984) to form long chains. Plastics are defined as polymers which contain additives that include stabilisers or plasticizers (Farshad 2006). Polymers are substances synthesized from monomers, which can be defined as molecular compounds used to produce a polymer. Monomers contain mainly carbon and hydrogen atoms, but other atoms such as chlorine may be present. The monomer for PVC is known as Vinyl chloride while that for HDPE is ethylene.

Polymers are formed from a process known as polymerization in which a polymer is formed from its monomer (Moore & Kline 1984). PVC and HDPE polymers are also both termed as thermoplastic polymers. Painter & Coleman (2009) define thermoplastic polymers as a group of polymers that can be reheated and remoulded repeatedly without degradation. Thermoplastic polymers do not contain cross links within their structure and therefore flow when heat is applied to them. Cross links are additional covalent bonds in a material induced chemically to strengthen a material (Moore & Kline 1984). PVC and HDPE differ in structure as explained below in sections 3.1.1 and 3.1.2.

3.1.1 Polyvinylchloride (PVC)

PVC polymer is formed from its monomer vinyl chloride, by suspension polymerisation. In suspension polymerisation processes, the monomer is added to water and stirred continuously to maintain a suspension (Moore & Kline 1984). This continuous stirring is necessary to prevent coalescence of the monomer droplets. Vinyl chloride is a gas at room temperatures (Billmeyer 1984) and is normally stored as a liquid under pressure. Vinyl chloride is obtained from ethylene dichloride, which is a product of ethylene and chlorine. However vinyl chloride is carcinogenic, highly flammable and explosive and should therefore be handled with great care and minimum exposure.

PVC is an amorphous polymer, which means that it has an irregular structure and a low degree of crystallinity. Crystallinity is the degree to which molecules of a substance are arranged in an ordered pattern (Moore & Kline 1984). PVC structure contains polar chlorine atoms spread throughout the carbon–hydrogen molecular structure which gives rise to unique properties. The structure is further complicated by branching within its chains and association due to the polar chlorine atoms in the covalent bonds. The structures of Vinyl chloride and PVC are illustrated in the figures 3-1 and 3-2 below.

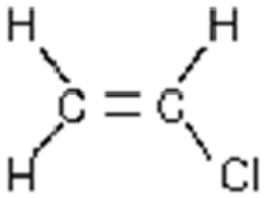

Figure 3-1: Vinyl chloride monomer (Source: www.lenntech.com)

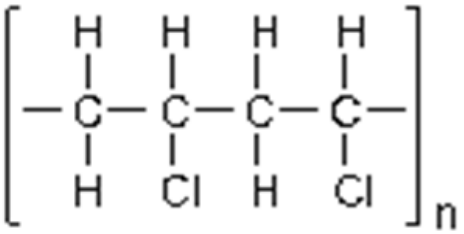

Figure 3-2: Polyvinyl chloride (Source: www.lenntech.com)

For the figures 3-1 and 3-2, C are the carbon atoms, H are the hydrogen atoms, Cl are the chlorine atoms and n is a whole number indicating the number of similar chains that make up the polymer. PVC in its original form after the polymerisation process is rigid therefore plasticizers are added to soften it for manufacturing processes such as extrusion and other functions.

PVC material has been observed to be thermally unstable (Farshad 2006; Billmeyer 1984). The thermal instability of PVC is usually initiated by exposure to ultra violet (UV) radiation at unsaturated sites in the polymer. Unsaturated sites occur as a result of the loss of chlorine and hydrogen atoms. These atoms react to form hydrochloric acid (HCl) and set off a chain reaction through the material. More chlorine is regenerated and this leads to the formation of structural abnormalities at the unsaturated sites (Billmeyer 1984). This process gradually leads to degeneration of the PVC material

and ketonic structures may form. Thermal instability is usually improved by the addition of stabilisers to PVC during manufacture such as metallic salts, oxides and epoxy plasticizers. These stabilizers are added during the industrial manufacturing process. PVC pipe has various advantages and disadvantages some of which are discussed below.

3.1.1.1 Advantages of PVC pipe

i. PVC requires a less amount of petrochemicals during the manufacturing process compared to metallic pipe materials (Myles 1998). More energy and thus petrochemicals are required to mould cast iron and steel pipes compared to the entire manufacturing process of PVC pipes. Therefore the manufacture of PVC pipe results in less pressure on the diminishing petrochemical resources.

ii. PVC pipe is lighter than metallic pipes of the same diameter due its lower density (about 0.94-0.96kg/m^3 compared to 7850kg/m^3 for steel and 6800kg/m^3 – 7800kg/m^3 for cast iron). The lighter weight makes PVC easier to install and therefore lower costs are incurred during construction.

iii. PVC material is not corroded easily by aggressive soils and other particles that may be present in water compared to steel and cast iron pipe. This means that it maintains a smooth bore and therefore good flow characteristics where abrasion is a factor resulting in less pumping costs for the duration of design life. According to Myles (1998) a 30% reduction in head loss due to friction in the pipe bore is possible compared to head loss occurring in metallic and asbestos cement pipes.

iv. PVC pipes are more flexible than metallic pipes and therefore affected by settlement to a lesser extent.

v. PVC pipes provide the highest stiffness per unit cost of all engineering plastics (Myles 1998), thus providing an economic and durable solution in many cases.

vi. PVC pipes exhibit low flammability due to the chlorine content. The chlorine makes the pipe self-extinguishing once the flame is removed and therefore reduces damage that may be incurred during fires.

vii. PVC pipe bell and spigot jointing is cheaper than other metallic pipe and HDPE jointing as it does not require welding. Welding equipment is expensive, hence the economical savings when working with PVC pipe.

3.1.1.2 Disadvantages of PVC pipe

i. PVC material is brittle at low temperatures below the brittle-ductile transition. The brittle-ductile transition is that point when the fracture behaviour of a material changes from brittle

behaviour to ductile behaviour (Andrews 1968). In ductile fracture, significant plastic deformation is observed at the fracture surfaces while in brittle fracture, there is almost (or none) no plastic deformation observed. This makes PVC pipe susceptible to certain failures such as brittle cracking where cracks can rapidly move through the entire pipe length.

ii. PVC pipes are cannot be welded as they are susceptible to failure by rapidly propagating brittle cracks which can move through welded joints from one pipe to another. Alternative jointing methods are employed such as the bell and spigot joint.

iii. PVC pipes are manufactured in shorter lengths of 6m or 12m and maximum diameter of 500mm due to the high probability of brittle failure. Shorter pipe lengths result in easier replacement but result in more joints for a single pipeline compared to HDPE pipe that can be longer than 24m.

iv. PVC pipe also exhibits a lower abrasion resistance compared to HDPE pipe and therefore wears out faster and might not be suitable for abrasive contents.

v. PVC also has lower tensile strength compared to HDPE pipe material and is therefore less ductile.

vi. The PVC monomer known as vinyl chloride is carcinogenic and therefore extra care must be taken to reduce exposure levels during the manufacturing process. It therefore poses a health risk to industrial workers and the extra precautions that must be taken may increase the cost of the manufacturing process.

3.1.2 High Density Polyethylene (HDPE)

HDPE is an olefin polymer formed from a monomer known as ethylene. Olefin polymers are those polymers that contain only carbon and hydrogen in their structures. Ethylene is obtained from ethane gas which is in turn derived from natural gas. HDPE has a linear structure as it does not contain so many branches and has a high degree of crystallinity of over 90% (Billmeyer 1984). This means that in the main chain of the polymer, there is less than one side chain per 200 carbon atoms. The structure of the ethylene monomer and the HDPE polymer are illustrated below in figures 3-3 and 3-4.

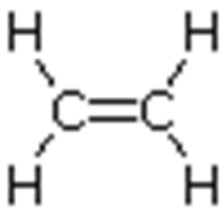

Figure 3-3: Ethylene monomer (Source: www2.chemistry.msu.edu)

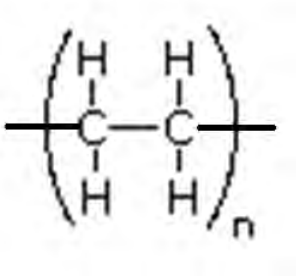

Figure 3-4: Polyethylene (Source: www2.chemistry.msu.edu)

HDPE has a high degree of crystallinity compared to Low Density Polyethylene (LDPE). The higher degree of crystallinity results in HDPE exhibiting a higher tensile modulus, melting point and hardness than LDPE. Crystallinity affects the material properties of polymers because it influences the strength of the bonds within the material. Brittleness, chemical resistance, permeability to gases and therefore resistance to environmental stress cracking are also improved due to the high crystallinity. In HDPE manufacturing, cross linking or the entanglement of molecules is chemically induced to improve stability, environmental stress cracking resistance and tensile strength. For pipe manufacture, chemical cross linking is achieved by the addition of stable peroxides. HDPE is a semi crystalline polymer. Semi crystalline means that the polymer has both crystalline and amorphous regions. The advantages and disadvantages of HDPE as a pipe material are discussed below.

3.1.2.1 Advantages of HDPE pipe

i. HDPE pipes can be welded which results in the formation of smooth joints.
ii. HDPE pipes also have a higher tensile strength than PVC pipes especially at the joints since welding is normally employed as opposed to PVC pipes that are joined using the bell and spigot joints.
iii. HDPE pipes are manufactured and supplied in long lengths of typically 24m and larger diameters of 1m since they are less likely to fail by rapid crack propagation compared to PVC pipes. This is because HDPE is ductile compared to PVC which is brittle especially at low temperatures.
iv. HDPE pipes exhibit higher abrasion resistance compared to PVC pipes and can be expected to have a longer service life if abrasion is a factor in the required application.
v. HDPE and its monomer are non-toxic and hence extra costs and risks during the manufacturing process are reduced.
vi. HDPE pipes are also lighter than metallic pipes making installation and transportation easier.
vii. HDPE pipes have a smooth surface and therefore low friction losses and lower pumping costs are incurred.

viii. HDPE material is corrosion resistant therefore flow is improved since the formation of abrasive structures is reduced. The pipe bore remains smooth and no protection is necessary.

ix. HDPE pipes are also more flexible and ductile than PVC pipes and are therefore frequently relined during maintenance procedures. They are also less affected by settlement as a result.

3.1.2.2 Disadvantages of HDPE pipe

i. HDPE pipe joints are expensive as high costs are incurred due to the welding equipment required. The joints are also prone to failure if welding is not done well.

ii. HDPE pipe material is flammable and unlike PVC pipe is not self-extinguishing. This might mean higher replacement costs in case of fire incidences.

The advantages and disadvantages listed above illustrate the benefits and risks associated with the use of PVC and HDPE as pipe materials. Before either material is chosen for a particular application, these characteristics, the working conditions and the various standards for water distribution systems should be taken into account. HDPE pipe was implemented as a pipe material later than PVC and further development can be expected as more research is conducted.

The properties of PVC and HDPE that make them desirable as pipe materials are due to their chemical and molecular structures that have been discussed above. HDPE pipe in particular exhibits good stress cracking resistance and PVC is durable due to its high stiffness and self-extinguishing properties when exposed to fire (Myles 1998). Both pipe materials are durable and resistant to corrosion which is a common occurrence in steel and cast iron pipes. This has contributed to the rapid increase in the use of plastic pipes for water distribution systems, sometimes replacing metallic pipes.

Plastic pipes are manufactured from the raw material polymer which is processed into a final product. The next section is a summary of the production and manufacturing process of PVC and HDPE pipe from the raw material polymer to the final pipe product. The main process starts with polymerisation of the monomer to extrusion of the final product.

3.1.3 Manufacture process of PVC and HDPE pipes

The manufacturing process of both PVC and HDPE pipes starts with the formation of the polymer from the monomer during polymerisation. Most PVC polymer in industry is formed through suspension polymerisation while HDPE polymer is typically formed by solution polymerisation (Moore & Kline 1984). Details of the polymerisation process are beyond the scope of this study. Plastic pipes are through polymerisation by a thermoplastic extrusion process (Billmeyer 1984;

Moore & Kline 1984). Extrusion is the process by which a polymer material is propelled by a screw through an extruder. The extruder has high temperature and pressure regions so that the polymer material can be melted, compacted and shaped into the final product. The extrusion process is summarised in the figure 3-5 below.

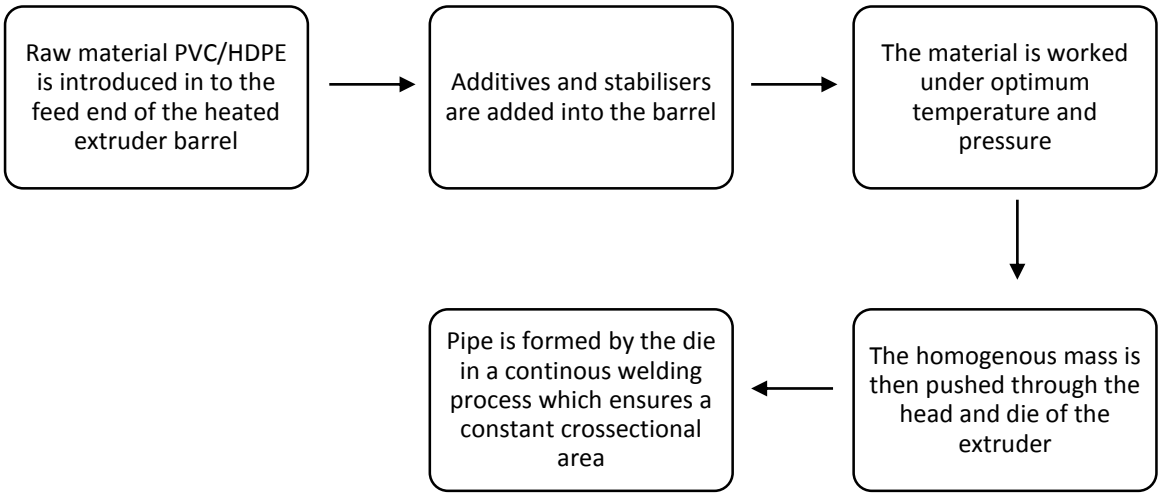

Figure 3-5: Process of pipe extrusion from polymer raw material

Extrusion is carried out with the help of an extruder. The extruder consists of a number of sections, each with different functions which include feeding the polymer into the extruder barrel, compaction and melting of the polymer material, and mixing and working of the molten plastic before it is forced through the head and die. Plenty of the heat required to melt the polymer is provided by friction within the extruder contents.

Section 3.1 is a summary of the physical properties and chemical structure of PVC and HDPE materials. It is these structural properties that give HDPE and PVC pipe their characteristics. The advantages and disadvantages of each materials were also discussed. The next section is a review of the mechanical properties of HDPE and PVC and the models that are developed for the mathematical presentation of these mechanical properties.

3.2 Mechanical properties of pipe materials HDPE and PVC: Viscoelasticity

The properties of the pipe material influence the pipe deformation behaviour when it is subjected to a load. This section describes the mechanical properties of the pipe materials that influence the deformation behaviour of the pipes and pipe leaks. Like all other materials, mechanical properties of polymers are characterized by their response to applied stress and strain under tension. The response is monitored with standardized tests from which the stress-strain modulus and strength of the polymer are determined under various conditions.

To understand pipe deformations, a complete study of the mechanical response of the materials when a load is applied is important. Unlike metallic materials whose mechanical properties are independent of their surroundings, polymers' responses to loads are complicated since the properties are dependent on prevailing conditions. These conditions include but are not limited to: rate of load application, temperature and rate of strain (Ward 1971). Low temperatures combined with a high strain rate gives a high modulus and the polymer behaves like a brittle material. High temperatures and low strain rates give large strains and temporary deformations, and polymers behave like rubber with a low modulus. Higher temperatures may result in permanent deformation and viscous behaviour (Ward 1971; Farshad 2006). At intermediate temperatures, polymers are neither fully brittle nor ductile and are termed as viscoelastic, a combination of the two responses. In this chapter viscoelastic behaviour is discussed as a mechanical response of polymers below their yield stress. Polymers therefore exhibit elastic, viscous, and brittle behaviour under different conditions, which are usually due to variations in temperature and time scale of loading. The effects of temperature and other factors are fully discussed in section 3.2.4 after defining viscoelastic behaviour.

The response of a polymer to stress and strain is also dependent upon its internal structure, flexibility, molecular weight, presence of cross links, crystallinity and loading history. (Moore & Kline, 1984, Painter & Coleman, 2009). For example, low flexibility and high strength of intermolecular bonds within a material will tend to increase the stress-strain modulus. The reverse is also true. The presence of defects and the resulting stress concentrations in a material will also impact the overall strength of polymers.

PVC and HDPE are amorphous and semi crystalline materials respectively. Whereas amorphous polymers are fully expected to experience viscoelasticity, semi crystalline polymers only experience viscoelasticity in the amorphous regions of their structure. (Andrews 1968). Semi crystalline

polymers may not obey viscoelasticity completely, but their yield behaviour has been observed to be similar to that of the amorphous polymers.

Viscoelasticity is the property of materials that exhibit both viscous and elastic behaviour (Banks et al. 2011). In order to understand the phenomenon of viscoelasticity, one must first understand viscous and elastic behaviour. Viscous materials are materials in which the stress in the material is a function of the strain rate while elastic materials are those in which the stress in a material is a function of the strain (Moore & Kline 1984). For purely elastic materials, deformations are independent of load history and strain rate (Ward 1971). In reality, all materials exhibit both viscous and elastic behaviour to a certain extent and no material is perfectly elastic or viscous.

A material is classified as either viscous or elastic, depending on how much the strain and strain rate contribute to the stress. For materials considered to be elastic, the strain rate response to time is small enough to be ignored, while for materials considered to be viscous, the strain response to time is small enough to be ignored. Elasticity and viscosity are defined as follows:

Elasticity

Elasticity is described by Hooke's law given by

$$\sigma_E = E\varepsilon\,. \tag{3.1}$$

Where σ_E is the stress due to strain in the material, E is Young's modulus and ε is the strain in the material.

Viscosity

Viscosity is described by a Newtonian relationship given by

$$\sigma_V = \eta\left(\frac{\partial V}{\partial y}\right) = \eta\left(\frac{\partial \varepsilon}{\partial t}\right). \tag{3.2a}$$

Note that:

$$\frac{\partial V}{\partial y} = \frac{\partial}{\partial y}\left(\frac{\partial u}{\partial t}\right) = \frac{\partial}{\partial t}\left(\frac{\partial u}{\partial y}\right) = \frac{\partial \varepsilon}{\partial t} \tag{3.2b}$$

where σ_v is the stress due to strain rate in the material, η is the viscosity, $\frac{\partial V}{\partial y}$ is the velocity gradient $\frac{\partial \varepsilon}{\partial t}$ is the strain rate and u is the displacement in the direction y. In the viscous materials, it can be seen from the above relationship that as the strain rate increases, the stress in the material is also increased. The reverse is also true.

Unlike metals and water that can be classified as elastic and viscous materials respectively, it is not the case for polymers. Polymers are classified as viscoelastic materials since both strain and strain rate effects occur concurrently.

Viscoelastic behaviour is further characterised by three main features namely:

i. Creep
ii. Stress relaxation
iii. Hysteresis

Creep and stress relaxation behaviour are applicable as long term responses while hysteresis is only applicable for short term cyclic loading. The three features are explained below.

3.2.1 Creep

Creep is defined as the increase of strain with time in a material (Andrews 1968). During creep, a constant stress is applied to a polymeric material and the increase in strain over a time period is measured. Time dependent strain is observed and the creep modulus is calculated from the following equation:

$$J(t) = \frac{\sigma}{\varepsilon(t)} \tag{3.3}$$

Where J(t) is the time dependent creep modulus, σ is the constant nominal stress and ε(t) is the time dependent strain. This time dependent strain is the strain measured at certain time intervals. The time scale can vary from seconds to years.

The stress-time and strain-time relationships of a viscoelastic material experiencing creep are shown below in the figure 3-6. A load is applied to the material or body at time t_0 and left until time t. When the load is applied, an instantaneous elastic strain is observed followed by a creep strain which increases over time. When the load is removed at time t, a part of the strain that is, the elastic

strain, is recovered immediately. Partial recovery then proceeds at a slower rate, until a permanent deformation known as the residual strain is left (Moore & Kline 1984).

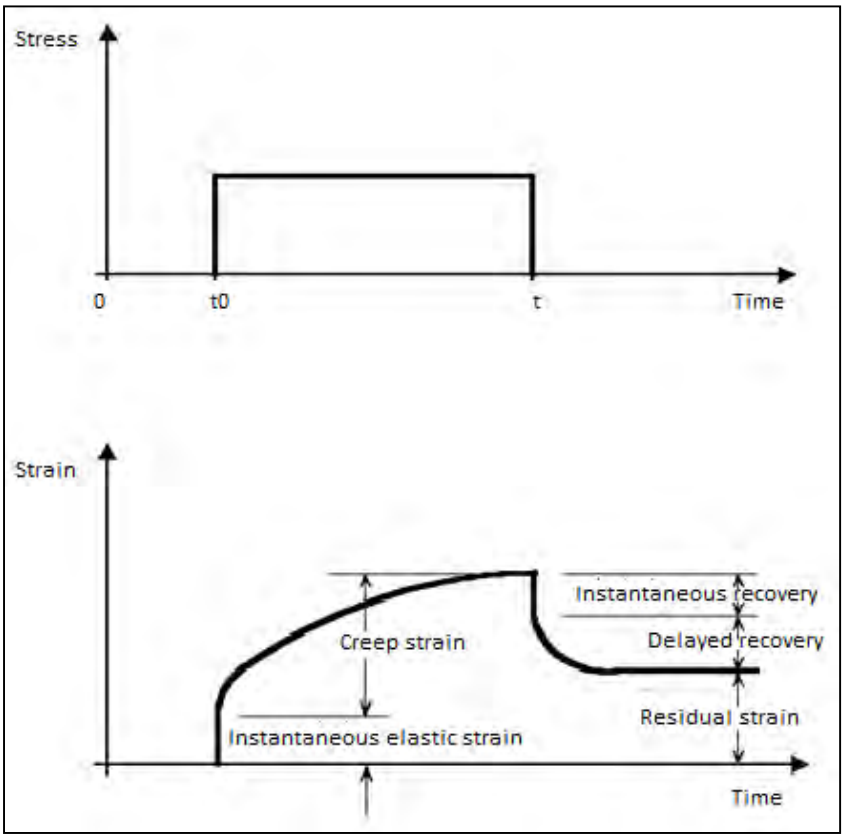

Figure 3-6: Graph showing creep response in a viscoelastic material over time

(Source: www.fgg.uni-lj.si/kmk/esdep/master/wg10/l0520.htm)

In comparison, strain in elastic materials is independent of time and no additional elongation occurs after the initial elastic response of the material to the load. In viscous materials, there is no elastic response, and only time dependent response is observed.

For the case of linear viscoelasticity, the total strain is regarded as the sum of the immediate elastic deformation, the deformation occurring over a period of time and the viscous deformation (Ward 1971). Creep is therefore a function of the entire loading history in polymer materials.

When a load is applied to a viscoelastic material for a sufficient time, creep rupture might occur. For design purposes, creep rupture is used to calculate and compare allowable stress levels for different materials after appropriate design life and safety factors have been determined accordingly.

3.2.2 Stress relaxation

Stress relaxation refers to the decrease of stress in a material with time (Andrews 1968). Stress relaxation can be illustrated by rapidly stretching a material to a given elongation and the stress that is required to maintain that elongation for a certain period is measured. A time dependent stress is observed and a time dependent relaxation modulus is therefore calculated as follows:

$$G(t) = \frac{\sigma(t)}{\varepsilon} \tag{3.4}$$

Where G(t) is the time dependent relaxation modulus, ε is the applied strain and σ(t) is the time dependent residual stress. However, creep modulus is not the inverse of the relaxation modulus. That is,

$$J(t) \neq \frac{1}{G(t)} \tag{3.5}$$

The stress-time and strain-time relationships of a material experiencing stress relaxation are illustrated below in the figure 3-7. A strain is applied to the material or body at time t0 (0 seconds) by rapid stretching. Over time, the stress required to maintain this strain or elongation is observed to decrease. This is called stress relaxation. The stress in the body continues to decrease until a time when it is constant. The stress that is required to maintain the elongation is called the residual stress.

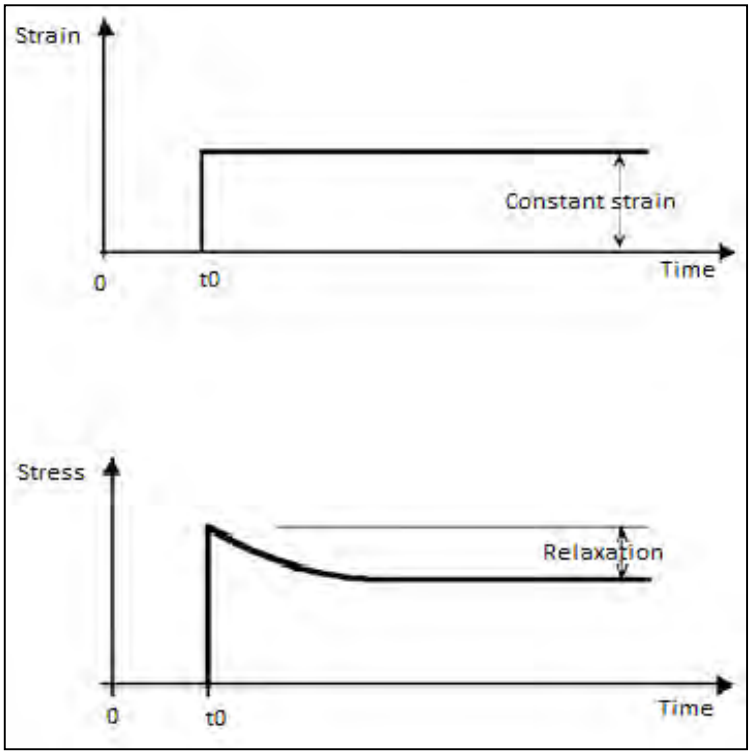

Figure 3-7: Graph showing stress relaxation in a viscoelastic material over time

(Source: www.fgg.uni-lj.si/kmk/esdep/master/wg10/l0520.htm)

In viscous flow, the residual stress may decay to zero after a sufficient time, and for "no viscous flow" situations, the stress decays to a finite value and the relaxation modulus at infinite time can be calculated (Ward 1971). However viscoelastic flow lies between the two extremes of no stress decay and complete stress decay, such that the relaxation modulus is observed to reduce from an initial value at very short time intervals to a final constant relaxation modulus at long time periods.

A common term in the manufacture and design of polymeric parts is the relaxation time (λ). It is defined as the time taken for stress in a material to reduce to $\frac{1}{e}$ of its original value (Moore & Kline 1984), where e is the natural number.

3.2.3 Hysteresis

Hysteresis is also a characteristic of polymeric materials and is defined as the phenomenon whereby the stress-strain relationship of a material follows different paths when it is subjected to cyclic loading (Fung 1993). Hysteresis has been observed in polymeric materials (Andrews 1968; Ferrante et al. 2011) and occurs at both large and small strains. At high strains, fracture may occur in the material due to high stress concentrations or the entire part undergoes yielding and failure. Stress concentrations are due to high stresses and strains close to the crack site.

Hysteresis is also characterised by the amount of energy released in the stress-strain cycles generated during cyclic loading in a material. When a load is applied and gradually increased, material close to the crack undergo full stress and strain cycles as the crack propagates through the material (Andrews 1968). When the load is finally removed from the polymer material, a residual strain may be observed that is only recovered after sometime. For this reason, hysteresis effects may be confused with plastic deformation.

During hysteresis, the unloading curve of a polymer differs from the loading curve. An example was included in figure 3-8. The area enclosed by the loop is a measure of the energy dissipated (Tanaka & van Eijden 2003). The smaller the area enclosed, the less energy is dissipated and therefore the material is more elastic. In purely elastic materials, there is no energy dissipation. The reverse is also true. This behaviour highlights the load history dependent properties of polymers and the effects on fracture behaviour. This may be an important consideration for leak response when controlling leakage by varying pressures applied to the pipe.

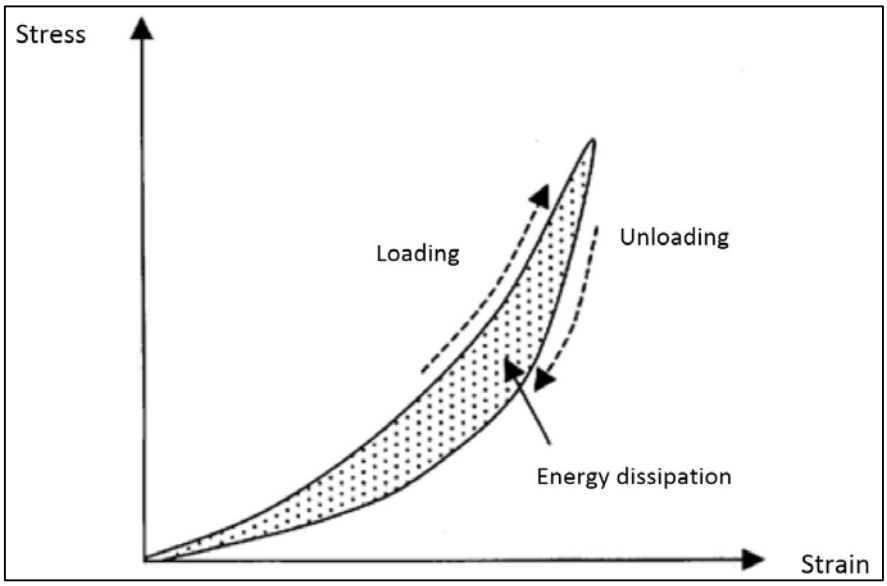

Figure 3-8: Hysteresis in a viscoelastic material (Source: Tanaka & van Eijden (2003))

Creep, stress relaxation and hysteresis are features of viscoelasticity and its time dependent properties. PVC and HDPE experience viscoelastic deformations at room temperature since both materials contain amorphous regions in their microstructure. (PVC is an amorphous polymer while HDPE is a semi crystalline polymer). To understand deformations in the polymeric material, deformations in both the crystalline and amorphous regions should be considered. Deformations in the crystalline regions can be approximated by linear elasticity.

The next section is a discussion of the factors that affect creep stress relaxation and hysteresis in materials. The material properties of polymeric materials depend on their surroundings and loading history. It is also essential to understand why these viscoelastic deformations occur so that their negative effects in pipes can be minimised. Leak occurrences due to material defects may also be minimised if the factors affecting viscoelastic behaviour are known and understood.

3.2.4 Factors affecting creep, stress relaxation and hysteresis in materials

Creep and stress relaxation responses are influenced by the time dependent motion of molecules which occurs within the material when a stress is applied. For very short loading times, the only distortion that occurs is the bond distance between molecules and not in the bulk polymer. This results in low strains and high creep and relaxation moduli (Moore & Kline 1984), as illustrated by equations (3.3) and (3.4). As the loading time is increased, large scale distortion of molecular bonding becomes possible and molecular segments within the polymer begin to slip. Stress relaxation is observed in the bulk polymer, and therefore the values of both moduli reduce.

Deformation of polymeric materials occurs when the molecular segments slip past each other. There are different factors that influence the amount of slippage experienced in these materials and they include crystallinity, crosslinking, molecular weight and temperature. Understanding how these factors influence polymer response to applied stress is essential.

Crystallinity

Crystallinity relates to the arrangement of crystals in a material. A material that is said to be crystalline is made up of well-arranged crystals. Crystalline materials are generally tougher than non-crystalline materials, unless other factors come into play. The role played by crystallinity during stress relaxation and creep is a complex one due to the possibility of recrystallization and slip plane movement within the material. Overall it is agreed that the presence of crystals in a polymer tends to reduce creep, and the lowest creep occurs in the orientation direction of the crystal lattice.

Crosslinking

Crosslinking in polymers reduces creep by reducing the amount of slippage that occurs between molecules. When a stress is applied to a cross-linked material, the cross-linked molecules uncoil and slip past each other. However, when crosslinks are fully stretched, no more slipping can occur unless the covalent bonds that form the crosslinks are broken. The higher the number of crosslinks present, the lower the amount creep observed.

Molecular weight

Higher molecular weight polymers result in greater entanglement of polymer molecules compared to lower molecular weight polymers. Creep is therefore less in higher molecular weight polymers as greater entanglement restricts the amount of slippage that can occur in a certain time.

Temperature

An increase in temperature results in the weakening of intermolecular bonds in polymers and therefore increases the amount of creep that occurs. This effect of temperature can be applied to predict creep and stress relaxation responses for long periods of time that may be impractical to replicate in the testing laboratory. This is referred to as time-temperature super positioning. In time-temperature super positioning, a change in temperature is equivalent to changing the time scale in creep and stress relaxation situations (Ward 1971). For example, to calculate the creep modulus of a material for a given stress at 5 years and 23°C, a test may be ran for a shorter period of time at elevated temperatures.

The response of polymers to stresses at different temperatures depends on their internal structure, for example amorphous polymers exhibit high creep rates at temperatures near their glass transition temperature since intermolecular bonds are considerably weakened at this temperature. The glass transition temperature is that temperature above which solid polymers soften and behave like rubber due to loosening of molecular bonds when temperature is increased (Andrews 1968; Moore & Kline 1984). Crystalline polymers will exhibit very high creep rates close to their melting points, at which bonds are considerably weakened. An increase in the crystallinity of polymer materials also increases the temperature range of the polymer by increasing the constraints within the polymer (Andrews 1968). These constraints are stronger molecular bonds and result in higher melting points.

Creep, stress relaxation and hysteresis are characteristic responses of viscoelastic materials and occur in day to day life applications. It is therefore important to consider them in design processes involving the use of viscoelastic materials. Accepted standards and norms must be applied for their

use in different environments as they are affected by temperature. Plastic water pipes may experience viscoelastic deformations when pressure is applied. The pipe and leak hole deformations in turn affect the amount of water lost through the leaks. A number of mathematical models have been developed to illustrate and explain viscoelastic deformations. These models are discussed in the next section, section 3.2.5.

3.2.5 Viscoelasticity models

Various models have been developed to illustrate and explain viscoelastic responses analytically. These models provide an insight into the different aspects of viscoelasticity, as well as establishing a mathematical basis for this mechanical behaviour. Viscoelasticity can be modelled as linear or non-linear. In linear viscoelasticity, the stress in a material is linearly proportional to the strain history of the material (Banks et al. 2011). The shape of the material response curve is not linear as seen on the figures 3-6, 3-7 and 3-8 above. Linear viscoelasticity is a good approximation for small strains and linear materials. For this project, HDPE and PVC are modelled as linear viscoelastic materials. The four models therefore discussed in this section are only applicable to linear viscoelasticity. These models include:

i. The Boltzmann superposition theory
ii. Maxwell model
iii. Voigt model
iv. Standard linear solid model.

Non-linear viscoelasticity is observed when large strain deformation occurs (Banks et al. 2011). It is more complex and will not be covered in this study. For large strains both strain rate and rotation of material elements must be included, thus complicating the calculation of the stress rate (Fung 1993). However, non-linear viscoelasticity can be accounted for by extension of the superposition principle of the Voigt model (Ward 1971).

3.2.5.1 Boltzmann superposition theory

The Boltzmann superposition theory is a mathematical theory that states that strain is a linear function of stress (Billmeyer 1984). Therefore the total effect of applying several stresses is the same as the sum of the effects of applying each one separately. The Maxwell, Voigt and standard linear models are all formulations of the Boltzmann superposition theory and therefore are models of linear viscoelasticity.

The Boltzmann superposition principle applies to both static stresses and time dependent stresses which are common in polymers. Examples of static stresses and time dependent stresses include creep and stress relaxation situations respectively. Applying the principle to viscoelastic polymers makes it possible to determine or predict their response to a range of loads.

Under the Boltzmann principle, the total creep in a material is illustrated as a function of the material's entire loading history. Each load increment results in an independent and additive contribution to the total deformation of the material. This independent contribution thus allows the response to be termed as linear.

From this principle, the total creep is therefore the sum of the products of the stress increment and the creep modulus (creep compliance) function at each step in time(Ward 1971). Creep in linear viscoelasticity can be expressed as a function of position x and time t below (Fung 1993):

$$\varepsilon_{ij}\left(\underline{x},t\right)=\int_{-\infty}^{t} J_{ijkl}\left(\underline{x},t-\tau\right)\frac{\partial\sigma_{kl}}{\partial\tau}\left(\underline{x},\tau\right)d\tau \tag{3.6}$$

Where ε, σ and J are the creep, stress and creep compliance respectively, all expressed as functions of position x and time t.

Equation (3.6) may be simplified as:

$$\varepsilon\left(t\right)=\Delta\sigma_1 J\left(t-t_1\right)+\Delta\sigma_2 J\left(t-t_2\right)+\Delta\sigma_3 J\left(t-t_3\right)+\ldots\ldots \tag{3.7}$$

Where t is the total time, $\Delta\sigma_1$, $\Delta\sigma_2$, $\Delta\sigma_3$ are the stress increments added at times t_1, t_2, and t_3 respectively and J is the creep compliance function. The creep compliance is a function of the total time of the experiment t, and time of application of stress increment for each step, t_1, t_2, t_3 and so on.

Since the Boltzmann superposition principle is linear, equation (3.7) shows that the additional creep in a material resulting from adding a stress say σ_0 is equal to the creep that would occur if σ_0 is applied to the material with no loading history at the same instant in time.

Also, due to the linearity of this principle, the recovery response that occurs if the same stress that caused a certain creep is removed is equal in magnitude to the creep.

Similarly, the equation for stress relaxation in linear viscoelasticity as defined by the same principle is:

$$\sigma_{ij}(\underline{x},t)=\int_{-\infty}^{t} G_{ijkl}(\underline{x},t-\tau)\frac{\partial \varepsilon_{kl}}{\partial \tau}(\underline{x},\tau)d\tau \qquad (3.8)$$

Where ε, σ and G are the creep, stress and stress relaxation modulus respectively, all expressed as functions of position x and time t.

Equation (3.8) may be simplifies as:

$$\sigma(t)=\Delta\varepsilon_1 G(t-t_1)+\Delta\varepsilon_2 G(t-t_2)+\Delta\varepsilon_3 G(t-t_3)+..... \qquad (3.9)$$

Where t is the total time, $\Delta\varepsilon_1$, $\Delta\varepsilon_2$, $\Delta\varepsilon_3$ are the strain increments added at times t_1, t_2, and t_3 respectively, and G is the stress relaxation modulus. The stress relaxation modulus is a function of total time t, and time of application of stress increment for each step, t_1, t_2, t_3 and so on. The additional stress in a material resulting from adding a strain is equal to the strain that would occur if that strain was applied to a material with no prior loading history.

As a result of the Boltzmann superposition theory, a mathematical relationship between the creep and stress relaxation of a material for n increments can be stated as:

$$\int_0^t G(t_n)J(t-t_n)dt_n = t \qquad (3.10)$$

3.2.5.2 Maxwell model

The Maxwell model for viscoelasticity consists of one elastic spring and one dash pot connected in series as shown in figure 3-9 below. When a load is applied to the set-up, an immediate deflection is induced in the elastic spring followed by creep of the dashpot.

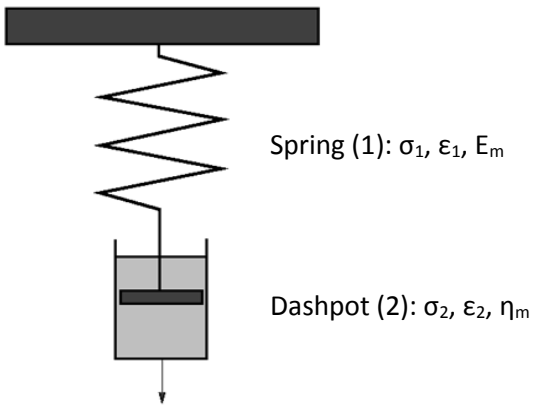

Figure 3-9: Maxwell model for viscoelasticity

(Source: www.see.ed.ac.uk/~johnc/teaching/fluidmechanics4/2003-04/visco/)

The spring is elastic and obeys Hooke's law (equation 3.1), while the dash pot is viscous and obeys Newton's law (equation 3.2).

The mathematical analysis for this arrangement is as below:

For the spring (1), Hooke's law states that:

$$\sigma_1 = E_m \varepsilon_1 \tag{3.11}$$

For the dashpot (2), Newton's law states that:

$$\sigma_2 = \eta_m \frac{d\varepsilon_2}{dt} \tag{3.12}$$

The stress in the spring and dash pot is identical since they are connected in series. Therefore $\sigma_1 = \sigma_2 = \sigma$.

From equation (3.11) above,

$$\frac{d\sigma_1}{dt} = E_m \frac{d\varepsilon_1}{dt} \tag{3.13}$$

By linear viscoelasticity, the total strain is the sum of the individual strains. From equations (3.12) and (3.13), the total strain can be obtained as:

$$\frac{d\varepsilon}{dt} = \frac{d\varepsilon_1}{dt} + \frac{d\varepsilon_2}{dt} = \frac{1}{E_m}\frac{d\sigma_1}{dt} + \frac{\sigma_2}{\eta_m} \tag{3.14}$$

Therefore the final expression that relates the total strain to the stress in the model is given as:

$$\frac{d\varepsilon}{dt} = \frac{1}{E_m}\frac{d\sigma}{dt} + \frac{\sigma}{\eta_m} \tag{3.15}$$

It is important to note that the Maxwell model is of great importance for only stress relaxation situations (Ward 1971) since it states that for constant stress conditions, the material response is defined completely by Newtonian's law for viscosity, which is not true for viscoelastic materials.

That is, in conditions of constant stress, $\frac{d\sigma}{dt} = 0$ and the equation (3.15) becomes $\frac{d\varepsilon}{dt} = \frac{\sigma}{\eta_m}$ which is the same as the law of viscosity which is given by equation (3.2).

3.2.5.3 Voigt model

The Voigt model consists of an elastic spring obeying Hooke's law and a dash pot obeying Newton's law for viscosity which are connected in parallel. This is shown in figure 3-10 below.

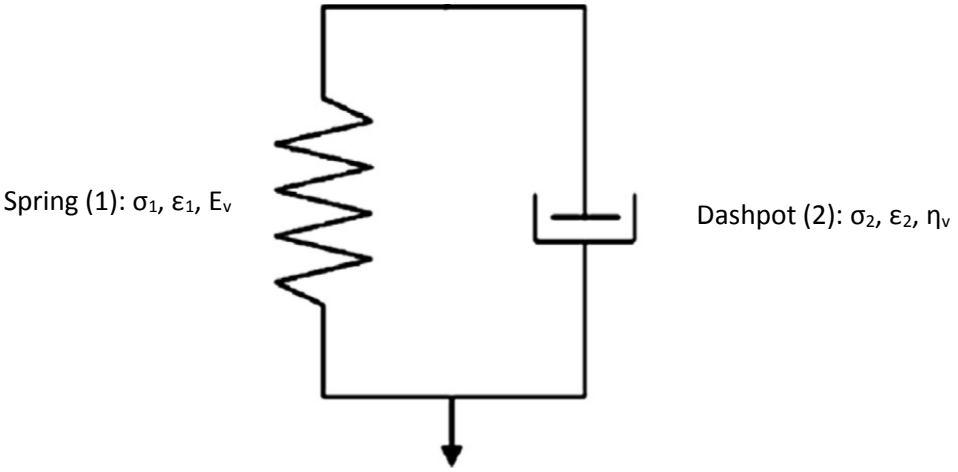

Figure 3-10: Voigt model for viscoelasticity (Source: Saffar & Abdullah (2013))

A sudden load application to the set-up illustrated in figure 3-10 does not cause an immediate deflection due to the dash pot. The deflection increases gradually with time, and the elastic spring takes an increasing share of the load (Fung 1993). The displacement of the dash pot relaxes exponentially.

In the Voigt model, the rate at which the deformation or strain increases is governed by the dash pot until the load applied is equal to the restoring force in the spring.

The mathematical analysis is as follows:

For the spring (1), Hooke's law states that:

$$\sigma_1 = E_v \varepsilon_1 \tag{3.16}$$

For the dashpot (2), Newton's law states that:

$$\sigma_2 = \eta_v \frac{d\varepsilon_2}{dt} \tag{3.17}$$

In this case, the strain in the spring and dash pot is identical since they are connected in parallel. Therefore, $\varepsilon_1 = \varepsilon_2 = \varepsilon$.

By linear viscoelasticity the total stress σ is the sum of the individual stresses of the spring and the dash pot, therefore adding equations (3.16) and (3.17):

$$\sigma = \sigma_1 + \sigma_2 = E_v \varepsilon_1 + \eta_v \frac{d\varepsilon_2}{dt} \tag{3.18}$$

Therefore,

$$\sigma = E_v \varepsilon + \eta_v \frac{d\varepsilon}{dt} \tag{3.19}$$

The Voigt model is a good approximation for creep situations but not stress relaxation. This is because for stress relaxation where the strain rate is constant ($\frac{d\varepsilon}{dt} = 0$), the equation (3.19) becomes, $\sigma = E_v \varepsilon$ which is Hooke's law for elasticity (equation 3.1) and therefore does not adequately describe viscoelastic behaviour.

3.2.5.4 Standard linear solid model

The Maxwell and Voigt models have been found to be inadequate for the first approximations of viscoelasticity, that is constant stress (creep) and constant strain (stress relaxation) respectively. In real life viscoelasticity, both creep and stress relaxations occur at all times. The standard linear model was developed to offer an alternative to the Voigt and Maxwell models.

The standard linear model is attributed to Zener (1948) and provides an approximation which predicts an exponential response for viscoelastic behaviour. In its simplest form the standard linear solid model consists of a single spring connected in parallel to another spring and dash pot (figure 3-11).

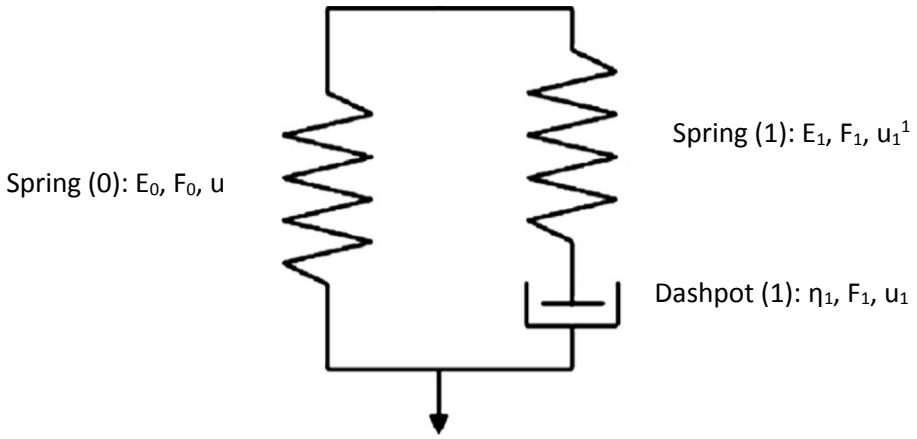

Figure 3-11: Standard linear model for viscoelasticity (Source: Saffar & Abdullah (2013))

The mathematical analysis is adapted from Fung (1993):

From the figure above, the following expressions may be formulated:

$$u = u_1 + u_1^1 \tag{3.20}$$

$$F = F_0 + F_1 \tag{3.21}$$

$$F_0 = E_0 u \tag{3.22}$$

$$F_1 = \eta_1 \frac{du_1}{dt} = E_1 u_1^1 \tag{3.23}$$

Where u is the displacement of the respective spring or dashpot, and F is the force.

From the above expressions,

$$F = F_0 + F_1 = E_0 u + E_1 u_1^1 = (E_0 + E_1)u - E_1 u_1 \tag{3.24}$$

The term $\frac{\eta_1}{E_1}\left(\frac{dF}{dt}\right)$ is added to both sides of expression 3.24 and the following is the result:

$$F + \frac{\eta_1}{E_1}\left(\frac{dF}{dt}\right) = E_0 u + \eta_1\left(1 + \frac{E_0}{E_1}\right)\frac{du}{dt} \tag{3.25}$$

Equation (3.25) is then simplified to what is known as the Standard linear solid model:

$$F + \tau_\varepsilon \frac{dF}{dt} = E_R\left(u + \tau_\sigma \frac{du}{dt}\right) \tag{3.26}$$

Where

$$\tau_\varepsilon = \frac{\eta_1}{E_1},\ \tau_\sigma = \frac{\eta_1}{E_0}\left(1 + \frac{E_0}{E_1}\right) \text{ and } E_R = E_0. \tag{3.27}$$

τ_ε is defined as the relaxation time of the load during constant strain and τ_σ is defined as the relaxation time of strain during a constant load (Fung 1993). The relaxation time is defined as the time taken to achieve a steady stress state during a relaxation test (Tanaka & van Eijden 2003). When a load is applied to the set up in figure 3-10 for an infinite time, the dash pot completely

relaxes and the relationship between stress and strain is defined by the spring 0. Hence its constant E_0 is the relaxation modulus E_R of the model.

An expression for creep may be obtained from equation (3.26) by solving for the deflection u(t) when the force F(t) is a unit step function, 1(t). This creep expression derived from the standard linear solid model is:

$$c(t) = \frac{1}{E_R}\left[1 - \left(1 - \frac{\tau_\varepsilon}{\tau_\sigma}\right)e^{-t/\tau_\sigma}\right]1(t) \tag{3.28}$$

Where c(t) = u(t) when F(t) = 1(t). Similarly, an expression for stress relaxation may be obtained from the standard linear solid model by solving for F(t) when the deflection u(t) is a unit step function. Only the creep expression is stated here since the material constants for this project were derived from creep data.

The material parameters in equation (3.28) may be obtained by the use of a Prony series and experimental data. This is because viscoelastic properties in Abaqus are defined by a Prony series. A short review of the Prony series is included in the next section. Thereafter its application to the linear viscoelastic model in Abaqus is derived.

3.2.6 Prony series in linear viscoelasticity

The Prony method was developed by De Prony in 1975. The method is used for solving a non-linear system of equations that arises from an exponential approximation function (Hildebrand 1974). The background to the series is purely mathematical and is not covered in this dissertation. The short review described here is adapted from lecture notes from the University of California by Prof Govindjee (2011) included in the bibliography. The Prony series method has been used extensively in determination of viscoelastic parameters.

A Prony series for viscoelasticity is of the form:

$$f(t) = \sum_{j=1}^{n} A_j e^{\lambda_j t} \tag{3.29}$$

To solve for the material constants of the series which are A and λ_j, experimental relaxation data is collected for a selection of time periods, t. The challenge in determining an appropriate series is that the appropriate number of terms (n) in equation (3.29) above is unknown. Therefore, n has to be chosen beforehand and relies on the intuition and understanding of the material. The function

$f(t)$ is also non-linear. De Prony (1975) proposed a method to express $f(t)$ as a set of linear equations:

If we know $f(0), f(\Delta t), f(2\Delta t)$.....

And set $\alpha_j = e^{\lambda_j \Delta t}$, we can solve for α_j and then A_j. Then it is seen that,

$$f(k\Delta t) = \sum A_j \alpha_j^k \qquad (k = 0, 1, 2.....) \tag{3.30}$$

We also set α_j to be a root of the polynomial below:

$$P(\alpha) = \prod_{j=1}^{n} (\alpha - \alpha_j) = \alpha^n + c_{n-1}\alpha^{n-1} + ... + c_0 \tag{3.31}$$

Where c_{n-1}.....c_0 are constants.

Using the equations for $f(k\Delta t)$ and $P(\alpha)$, a system of linear equations can be obtained and solved for c_j .Consequently, α_j and A_j can be solved for.

The Prony series parameters are then converted to an Abaqus specific format which is available in the Abaqus documentation. In Abaqus, the viscoelastic series may be expressed as an exponential approximation of the relaxation modulus similar to equation (3.29):

$$G(t) = G_\infty + \sum_{i=1}^{N} G_i e^{-t/\tau_i} \tag{3.32}$$

Where $G(t)$ is the time dependent relaxation modulus, G_∞ is the long term shear modulus, τ is the relaxation time, t is the time and *i* refers to the ith term in the series.

To obtain the Prony series parameters for Abaqus, we set t = 0 seconds and therefore obtain the following expression for G_0. From equation (3.32),

$$G_0 = G(0) = G_\infty + \sum_{i=1}^{N} G_i \tag{3.33}$$

The expression for G_∞ is obtained from equation (3.33) above and then we substitute for G_∞ in the equation (3.32).

An expression for $G(t)$ is thus obtained as follows:

$$G(t) = G_0 - \sum_{i=1}^{N} G_i (1 - e^{-t/\tau_i}) \tag{3.34}$$

In Abaqus, equation (3.34) is expressed as:

$$G(t) = G_0 \left[1 - \sum_{i=1}^{N} g_i^p \left(1 - e^{-t/\tau_i}\right)\right] \tag{3.35}$$

Where:

$$g_i^p = \frac{G_i}{G_0} \tag{3.36}$$

For a single term series (N=1) equation (3.35) above yields:

$$G(t) = G_0 - G_0 g_1^p + G_0 g_1^p e^{-t/\tau_\sigma} \tag{3.37}$$

Where $\tau_i = \tau_1 = \tau_\sigma$.

Equation (3.37) above is then compared to the standard linear solid model in terms of the shear modulus for creep in viscoelasticity which is given by:

$$G(t) = G_R - G_R\left(1 - \frac{\tau_\sigma}{\tau_\varepsilon}\right)e^{-t/\tau_\varepsilon} \tag{3.38}$$

Note that $G_R = G_\infty$.

From the comparison we see that:

$$G_0\left(1 - g_1^p\right) = G_R \tag{3.39}$$

And

$$G_0 g_1^p = G_R\left(\frac{\tau_\sigma}{\tau_\varepsilon} - 1\right) \tag{3.40}$$

Eliminating g_1^p from the equations (3.39) and (3.40) gives:

$$G_0 = G_R \frac{\tau_\sigma}{\tau_\varepsilon} \tag{3.41}$$

Also from equations (3.39) and (3.40) it is seen that:

$$g_1^p = \left(1 - \frac{G_R}{G_0}\right) = \left(1 - \frac{\tau_\varepsilon}{\tau_\sigma}\right) \tag{3.42}$$

The required parameters for direct specification of a single term Prony series in Abaqus are g_1^p and τ_ε. g_1^p is the dimensionless form of the shear relaxation modulus and τ_ε is the relaxation time.

3.3 A review of yield behaviour, failure and fracture in plastic pipes

This section focuses on the material behaviour of polymeric materials experiencing stress above their yield point as defined in section 3.3.2 below. The yield point is defined as the point where plastic deformations starts to occur. The section begins with a description of the stress-strain behaviour and then explains failure and fracture in pipes. Important aspects of the failure and fracture behaviour in polymeric materials are also discussed.

When a load is applied to an amorphous polymeric material the response is initially viscoelastic (Andrews 1968).When the yield point of the material is exceeded, the material is said to have failed. If the load is further increased beyond yield point the material might eventually fracture. The failure and fracture behaviour of pipes is determined by the mechanical properties and yield behaviour of the pipe materials, in this case Polyvinylchloride (PVC) and High Density Polyethylene (HDPE).

In plastic materials, failure occurs when molecular bonds are weakened. In the process, molecular chains are separated and fracture surfaces between existing small cracks are widened as a result of the applied loads. For the thermoplastic materials such as PVC and HDPE, when a tensile force is applied, the molecular chains are stretched and aligned to the direction of the force applied. Deformation occurs when the molecular chains begin to slip past each other. Eventually cracking and permanent deformation are observed when the chains are stretched beyond their limit. When a part or material is said to have failed, it means that it is unfit for its intended function.

Fracture is one of the many modes of failure and is defined as the creation of new surfaces in a body or material (Andrews 1968). To understand fracture behaviour, it is important to understand the stress – strain relationship of the material and its yield behaviour, which are studied with the help of tension tests. The yield point and fracture point assist in quantifying plastic deformation of polymers, since the deformation which occurs beyond these points in a material is usually considered irrecoverable (Ward 1971). Shear, flexure, torsion and compression tests are also carried out for other applications. For this section, stress – strain behaviour and yield behaviour observed from tension tests at unspecified load rates and temperatures will be discussed.

The results of tension tests for polymeric materials obtained from short term tensile tests should be used carefully. This is because of the time and temperature dependence of polymer properties (Krishnaswamy, 2005; Moore & Kline, 1984). Plastic pipes are tested for design life and maximum stresses by carrying out creep rupture tests at different temperatures. These tests apply the principle of time-temperature super positioning since pipes are expected to function for long periods of time which may not be practical. During the tests, loads on the pipes are exerted in form of steady

hydrostatic pressures for certain time periods and failure is allowed to occur which is observed as a pipe burst or crack formation. Actual design life and allowable stress in these tests depends on the intended function and the environmental conditions.

Other modes of failure apart from fracture may include creep deformation and plastic flow. Creep deformation and plastic flow may ultimately contribute to the fracture process in the material.

Stress-strain behaviour may be categorised into two modes, namely fatigue and impact strength. The next section discusses fatigue and impact strength in polymeric materials.

3.3.1 Stress-strain behaviour

The stress – strain behaviour of polymers influences failure and fracture and can be classified into three modes namely, static fatigue, cyclic fatigue and impact strength. In the following paragraphs, the three modes are defined and their occurrence explained.

3.3.1.1 Static fatigue

Static fatigue or creep rupture is that deformation which occurs when a stationary non oscillating load is applied to a material over time (Farshard, 2006). The resistance of a material to static fatigue can be estimated by the use of static fatigue curves.

Static fatigue or creep rupture curves for plastic pipes are obtained from long term internal pressure tests carried out at elevated temperatures. This is the process of time – temperature super positioning. In creep rupture testing if the failure mode is ductile, the time to failure depends on the applied pressure (Krishnaswamy 2005). For brittle failure to occur there must be other factors such as stress cracking due to environmental conditions. During the fatigue process a transition from ductile to brittle behaviour may be observed. The transition is composed of three main regions and these include: ductile behaviour for a certain time period followed by transitional behaviour, after which brittle behaviour is observed for longer time periods.

3.3.1.2 Cyclic fatigue

Cyclic fatigue in polymers is defined as the loss of strength and other mechanical properties due to oscillating or varying stress (Farshad 2006; Moore & Kline 1984). In plastic pipes, sometimes an unstable pressure load is said to cause cyclic fatigue and is therefore referred to as a dynamic load (Krishnaswamy 2005).

Fatigue in polymers is characterized by cyclic fatigue life and endurance limit. Cyclic fatigue life is the number of load cycles that a material can withstand without failing (Farshad 2006) while endurance

limit is the stress below which the material can withstand an unlimited number of load cycles (Moore & Kline 1984). The endurance limit of polymers is often just 20% - 40% of the static ultimate tensile strength. Therefore, polymers experiencing fatigue fail at stresses lower than their ultimate tensile strength. The endurance limit is therefore an important design aspect in polymeric materials. Ultimate tensile strength is the maximum stress that can be withstood by a material under a static load. The resistance to cyclic fatigue is associated with fatigue life.

It is therefore important to consider both static and cyclic fatigue such that design life is correctly estimated.

3.3.1.3 Impact strength

Impact strength is the strength required to break a material with the application of a high loading rate (Moore & Kline 1984; Ward 1971). The impact strength of polymeric material is normally determined using a 120D impact tester. The impact tester consists of a pendulum with a large striking edge which is allowed to hit the test specimen. The energy required to break the specimen is the impact strength and it is calculated from the path travelled by the pendulum after breaking the specimen. Impact strength of a polymeric material depends on temperature and the presence of other agents in the polymer such as plasticizers, fillers and reinforcing agents.

Fatigue and impact strength are different modes of the stress-strain behaviour that eventually lead to yielding and failure of polymeric materials. The next section of this chapter, explains yield behaviour, and the processes that commonly occur in the pipe materials when a material yields.

3.3.2 Yielding in plastic pipes

Yielding behaviour in plastic pipes is illustrated using the stress-strain curve of polymeric materials. The stress-strain curve is normally obtained from tension tests conducted at a constant strain rate. Strain rates are normally specified and range from 1% to 100% per minute (Billmeyer 1984). This is due to the fact that polymer properties are sensitive to strain rates. As the strain rate increases, the tensile strength and modulus of the polymeric material increases. The total elongation before fracture however decreases. A general stress-strain curve of a polymer at a constant and unspecified strain rate and temperature is illustrated below in figure 3-12.

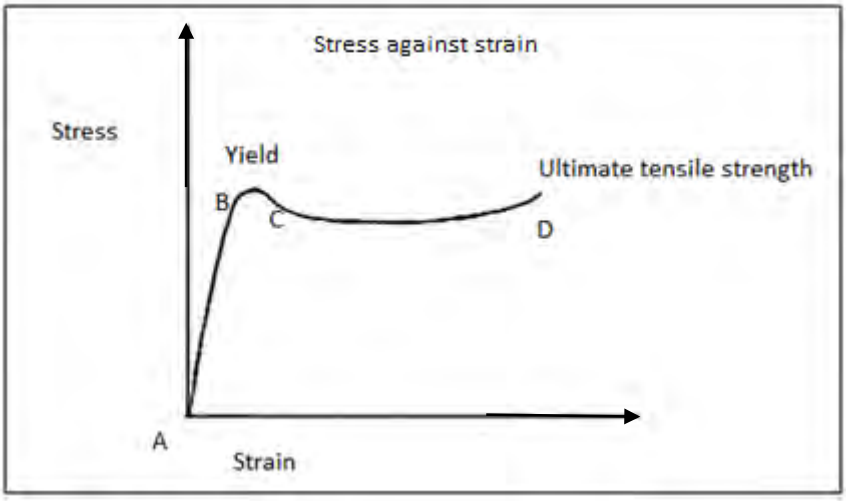

Figure 3-12: Typical stress-strain curve of a polymeric material (Source: Pascu & Vasile (2005))

A load is applied onto a polymeric material and a graph of stress against strain is obtained as shown in figure 3-12. As the load on the polymeric material is increased from A to B, the strain also increases and uniform deformation takes place until point B. Point B, which is the yield point, is the point at which necking starts. The stress at point B is the yield stress, and usually defines the start of plastic deformation and practical limit of the material in the case of ductile failure.

Necking is characterised by the observed cross section getting smaller and the engineering stress calculated with the original cross-sectional area therefore reduces as seen from point B to C. The true stress calculated from the actual cross-sectional area would continue to rise in this region. From point C, necking continues in the specimen, and the specimen elongates further, until a point D at which the specimen finally breaks or fractures (Ward 1971). Strains at fracture can be as high as several times the strain at the yield point and this is common in semi-crystalline polymers such as HDPE (Andrews 1968). This means a great amount of plastic deformation is possible before fracture depending on the ductility of the material. The stress at point D is known as the ultimate tensile strength of the polymer. The ultimate tensile strength is normally the practical limit of a polymer exhibiting brittle failure.

Necking can also occur in a particular part of a material that is experiencing higher stress concentrations compared to the rest of the material (Ward 1971). This is known as localised necking. If these stress concentrations are higher than the yield stress of the material, localised yielding and necking occurs at these parts of the material. Crack tips in pipes are examples of high stress concentration areas that may experience yielding and necking before the rest of the pipe. Variation

of mechanical properties in different parts of a material that may lead to non-uniform temperature and stress distributions which in turn may cause localised necking. Necking may begin at an initial point in the material until it is stabilised and then other surrounding parts are also brought to their yield stresses. In this way the neck propagates through the material. The extent of necking before failure is dependent on the ductility of the material and may not be observed in brittle materials.

The stress-strain curves of polymers are dependent on temperature and strain rate as their properties vary with temperature and strain rate. The test temperatures and strain rates stated in industry are chosen to satisfy conditions for yield behaviour for the specific intended functions. The variation of these stress-strain curves with temperature and strain rate is shown below in figure 3-13:

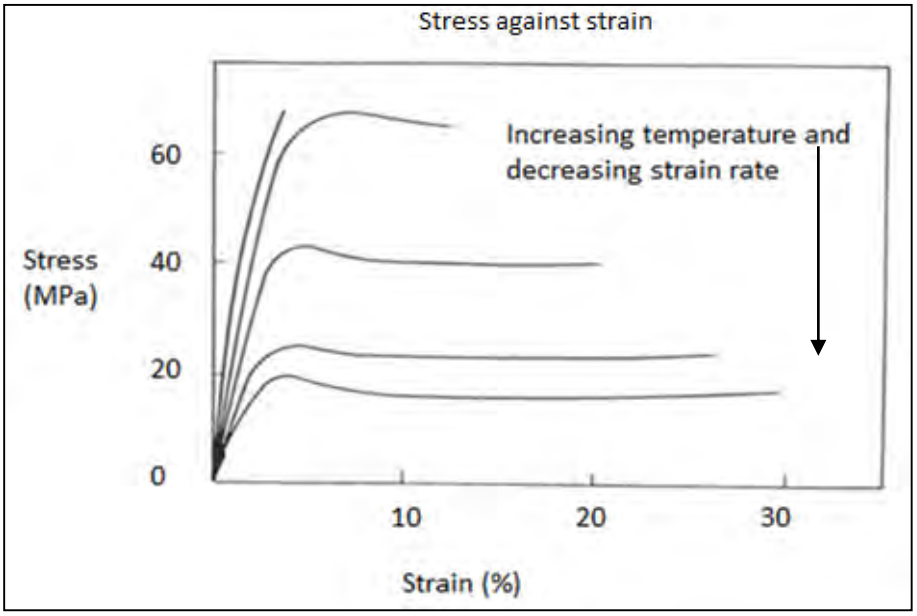

Figure 3-13: Effect of temperature and strain rate on stress -strain curves of a polymer

(Source: http://gertrude-old.case.edu/276/materials/04.htm)

Material properties of polymers are therefore not easily quantified as fixed numbers but have a range of variation since they change with temperature, strain rate, loading history, material composition and the environmental conditions. Manufacturers therefore often state values such as temperature and strain rate for the required polymer materials.

When the tensile strength of a polymer is exceeded, the polymer ruptures and the material is said to have failed. Yield stress however defines the failure point of most polymers since the usefulness of

polymeric materials ceases when yielding occurs (Ward 1971); unless the polymer fails by brittle failure in which case the ultimate tensile stress defines the failure point.

Failures due to yielding in plastic pipes occur due to various causes. Some of the causes of failure are discussed in the next section.

3.3.3 Causes of failure in plastic pipes

Plastic pipe systems are affected by various factors that contribute to failure thus rendering them vulnerable to leakage. Failures in plastic pipes occur when pipes can no longer perform the intended function. Failures may be caused by inadequate material type for specified function, poor design, inadequate manufacturing processes and inadequate storage facilities. Aging also contributes to failure in pipes, since the properties of plastic pipes are time and loading history dependent (Ferrante et al. 2011) and also deteriorate with time and loading cycles (Farshad 2006). The response of plastic pipes to long term loads should be investigated since plastic pipes may withstand sustained internal water pressure. Creep rupture tests and time-temperature super positioning are applied in industry to determine the long term behaviour of plastic pipes for practical purposes.

The following causes of failure are adapted from Farshard (2006).

Inadequate material for intended function

Inadequate material type for the intended function may lead to failures in plastic pipes. Pipe materials are usually selected using various criteria and standards. Materials chosen should be durable, safe and should require easy maintenance. Plastic pipes in particular are light weight and easy to manufacture compared to metallic pipes and can easily be connected. However, some aspects such as sensitivity to ultraviolet (UV) radiation, environmental stress sensitivity and temperature should be taken into consideration as these can lead to failure. For example, PVC material weakens with exposure to UV light.

Inadequate design

Pipes and pipe systems that are not designed properly according to purpose are prone to failure. Pipes should be designed with the help of standards, computational methods and guidelines that have been proved and tested over time. This is important so that the designed pipe will be able to withstand loads and other factors during the design life. Pipe systems should also be tested to make sure that all loading scenarios have been considered. Inadequate design can lead to failure in a system.

Improper manufacturing processes

Impurities introduced during the manufacturing process can contribute to failure in pipes before or during the pipe design life. Some impurities absorb UV light which weakens plastics such as PVC. This can be prevented by addition of stabilizers such as carbon black.

Residual stresses in the pipe and the system connections as a result of manufacturing procedures can lead to or increase the possibility of failure. Residual stresses occur as a result of temperature gradients within the pipe core incurred during cooling in the manufacturing process. Different cooling rates between the inner and outer surfaces of the pipe cause the temperature gradient and residual stresses within the pipe core. Residual stresses accelerate the failure process in pipes since the pipes may eventually experience stresses higher than their tensile strengths. The effects of residual stresses may be reduced by annealing the pipe at specified high temperatures which relaxes the residual stresses and therefore reduces the total stresses imposed in the pipe.

Storage, transport and installation problems

Poor storage facilities and transportation also contribute to the occurrence of pipe failures by causing deformation and damage. Some materials such as PVC react to UV radiation and should thus be protected from sunlight during storage and transportation. UV radiation excites the atoms in the plastic material. In the presence of oxygen, this excitation leads to the formation of oxygen hydro peroxides resulting in a brittle material and therefore brittle failure.

Improper transport and installation can also lead to breakage. During installation, pipes should be properly handled and connected with suitable bedding in the pipe trench.

Poor service conditions

The conditions to which a pipe is exposed during service life can also contribute to pipe failure. Such conditions include extension of service life beyond the intended design life, incorrect maintenance and repair procedures and the use of inadequate connections and valves. Unpredictable conditions such as loads above the design maximum may contribute to failure. Also, chemical and biological attacks resulting from the environment that were not foreseen before installation may lead to pipe failure.

Third party damages

Third party damages are damages to the pipe that are a result of activities carried out close to existing pipe lines, for example, excavation and road construction equipment. This equipment can

strike and damage pipes causing rupture of pipes and leakage. Constant construction and drilling next to pipes also contributes to the gradual weakening of pipes. However, during failure investigation, all possible causes should be ruled out to avoid blaming innocent parties for pipe damages.

Ageing and deterioration

Plastic pipes are manufactured from polymeric materials whose properties are time and loading history dependent. Therefore plastic pipes age and deteriorate with time thus weakening and accelerating failure. Mechanical wear and exposure to high temperatures also contribute to the weakening and aging process of plastic pipe systems.

Insitu failures

Insitu failures can be defined as those failures which occur as a result of the conditions the pipe is subjected to while in the trench during service. These failures occur as a result of hydrostatic internal pressures, water hammers, surrounding soil pressure, incorrect jointing and point loads due to large rocks and wooden pieces left in the trench during construction. Hydrostatic pressures weaken the plastic pipe through the process of static fatigue since the pipe may experience a sustained pressure for a long period. A water hammer is a momentary increase in water pressure which arises due to sudden changes in the water flow direction or velocity. Sometimes, this sudden increase in pressure can be high enough to cause failure in the pipe by rupturing or bursting.

Negative pressures may also cause the collapse and subsequent failure of a pipe. Negative pressures arise when excessive amounts of water are drawn from specific points of the distribution network, leading to a fall in pressures at other points in the network. For example, in firefighting, a lot of water is drawn from specific places in the network which may induce over drawing and negative pressures at other points. Distribution systems should therefore be designed to support fire flow demands.

Thrust due to internal pressures may also cause pipe failure. Thrusts are unbalanced forces that arise from changes in flow direction and pressure. The effects of thrust are minimised by the use of concrete thrust blocks in the pipe trench to hold the pipe in place.

Large rocks and wood pieces may increase the load at specific points along the pipe, leading to failure. Pipe bedding should also be laid properly so that pressures from surrounding soil and other ground loads do not cause failure.

Joint connections are also a common cause of pipeline failure if not installed properly. Incorrect joints can increase stress concentrations and therefore increase the possibility of leak occurrence.

There are various failures that may occur in plastic pipes due to the causes discussed above. These pipe failures may be categorised accordingly. The types of pipe failures may be grouped according to their causes and these types are discussed in the next section.

3.3.4 Types of failures in plastic pipes

The types of failures are characterised according to the processes that lead to them. According to Farshard (2006) failures in pipes may occur as a result of a combination of two or more causes.

Mechanical failures

Mechanical failures occur due to applied forces exceeding the stress-strain limits of a material. This normally results in breaking, cracking and bursting of pipes or anything that is a result of loading above the material limit. These failures occur in both the short and long term. Longitudinal cracks are a common type of failure that results from mechanical causes. Point loads have been documented as a common cause of longitudinal cracks in PVC pipe (Myles 1998). These longitudinal cracks mainly occur in large diameter pipes.

Thermal failures

Thermal failures in pipes occur when the material is exposed to extremely high or low temperatures beyond which the material deforms and cannot be used for the intended purpose. The properties of plastic pipes vary with temperature since polymer properties are temperature dependent (Billmeyer 1984). Plastics are generally brittle at low temperatures and at high temperatures can soften, warp, twist, melt or even burn. Cracks may also occur as a result of extreme thermal changes.

Chemical failures

Water and some chemical agents also affect the properties of plastic pipes, leading to deterioration of mechanical, physical and surface properties (Farshad 2006). Stress and high temperatures may worsen the impacts of chemical failure in plastic pipes since the polymer properties depend on temperature and loading history.

Environmental failures

Aggressive environments also contribute to failure in pipes. The aggressive aspects of the environment include UV radiation, humidity, micro-organisms, ozone, extremely low or high

temperatures, solvents, oils and others (Farshad 2006). These may affect the pipe material properties by breaking down the polymer structure and are manifested by change in colour and cracking. Slow crack growth (SCG) which is the development of small brittle cracks in a material is one common phenomenon that may result from aggressive environments.

Brittle and ductile failures

At room temperature and low loading rates, plastic materials are generally ductile and their fracture behaviour is ductile. However at low temperatures and high loading rates, plastics are brittle and undergo brittle fracture. This temperature dependence of polymer behaviour is a result of a phenomenon known as the brittle-ductile transition. The brittle-ductile transition in fracture behaviour is not only induced by changes in temperature but also loading/strain rate (Andrews 1968). High loading rates may induce brittle failure while low loading rates induce ductile failure. Brittle and ductile failures manifest through various ways such as slow crack growth and rapid crack propagation in brittle failure.

The occurrence of brittle or ductile failure is also influenced by material properties such as molecular weight of polymer molecules, presence of additives, degree of crystallinity and degree of crosslinking. High molecular weight, low crystallinity and high crosslinking degree may result in brittle failure while low molecular weight, high crystallinity and low crosslinking may result in a greater degree of ductile failure. In particular, crystallinity is a very important factor in determining the ductility of a material. As a result, HDPE is more ductile than PVC due to its higher degree of crystallinity. The effect of plasticisers varies according to the type of plasticizer is added.

Brittle and ductile failures can be differentiated in various ways. In ductile failure a large amount of plastic deformation can be observed on the fracture surface, such as necking or ballooning of the pipe at the location of the leak hole. In brittle fracture little or no plastic deformation is observed and the growth of a crack is initiated as soon the yield stress is exceeded. Cracks may also be initiated at sites of high stress concentrations or defects. This is known as slow crack growth and this process is common in HDPE pipes. Also in HDPE pipes, ductile failures occur at higher stresses while brittle failures occur at lower stresses (Krishnaswamy 2005). A small degree of ductility in the form of plastic deformation maybe observed at the tip of a propagating brittle crack.

Another difference is that for brittle failure, the eventual fracture is usually perpendicular to the stress causing it while in ductile failure; the eventual fracture is oblique (at angle between 90° and 180°) to the stress system causing it, therefore indicating a shear stress component (Andrews 1968).

Figure 3-14 below illustrates an example of a ductile failure as a ballooned crack in a polyethylene pipe.

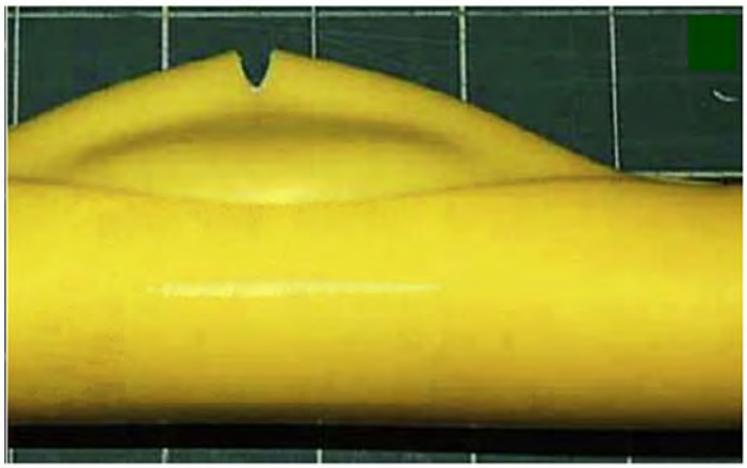

Figure 3-14: Example of ductile failure in a polyethylene pipe as seen from the side (Source: Chudnovsky et al. (2012))

Section 3.3.4 discussed failure in plastics by describing the causes and types of failures in plastic pipes. Failure can manifest in various forms such as fracturing, cracking, bursting, tearing and crazing. Most of these forms of failure occur concurrently, each contributing to the fracture process.

The next section, defines and describes the brittle–ductile transition behaviour in fracture behaviour. This transition is a common occurrence in polymer materials due to their environmental dependent characteristics.

3.3.5 Brittle-ductile transition of fracture behaviour

Brittle and ductile fracture behaviour are both observed in polymeric materials and the two are often presented as distinct processes occurring in polymers with different properties. However owing to the changing properties of polymers due to temperature and environment variations, both fracture processes have been researched in polymeric materials. These conditions result in the material responding differently in all conditions and therefore a material can experience both brittle and ductile cracking. Plastic materials display brittle or ductile crack behaviour depending on various conditions present when the fracture toughness limit is reached.

In ductile failure, the material undergoes a considerable amount of plastic deformation before it breaks. In HDPE pipes, ductile failure is a function of the applied tensile stress and the yield stress of the material (Krishnaswamy 2005). Yield stress marks the onset of ductile failure. The ductile crack

progresses slowly and may not grow unless a greater stress is applied due to strain hardening processes at the crack tip. In brittle cracking there is little or no plastic deformation observed and the crack progresses with a high speed, sometimes amounting to the speed of sound (Farshad 2006). Also, ductile cracks have larger necking regions than brittle cracks.

In brittle fracture behaviour, the polymer material fails at maximum stress which is termed as the ultimate tensile stress. Total strains at failure are low compared to ductile fracture, with typical values at 20% elongation for brittle failure (Ward 1971). The difference between brittle and ductile fracture behaviour can also be observed from fracture surfaces and from the energy released during fracture. The energy released may be determined by an impact tester.

The difference in fracture behaviour of the same material is due to the temperature and loading rate dependence of polymer material properties. Fracture behaviour for pipe materials such as PVC and HDPE at room temperature is normally ductile creep behaviour. However brittle fracture in normally ductile materials may occur if loading or straining rates are increased.

At low temperatures, the stress-strain relationship in most polymers is linear and brittle fracture is prevalent. In thermoplastic materials such as PVC and HDPE, brittle fracture occurs when temperature is below the brittle-ductile transition temperature. From figure 3-13, the brittle fracture curve is almost linear right up to the point at which failure by brittle fracture occurs. The total elongation at fracture is low.

As temperatures are increased, the polymer undergoes ductile fracture (Andrews 1968) and distinct yield points are observed. The stress in the material reduces and the necking process may be observed. If the neck stabilizes, strain hardening may ensue before the material breaks. When a ductile polymer undergoes strain hardening, the fracture stress is higher than the yield stress and therefore yield occurs first (Ward 1971). In case strain hardening does not occur, the fracture stress may however be lower than the yield stress. If temperature is increased further, the viscosity of polymeric materials increases and therefore behave like rubber which is characterised by large strain deformations compared to viscoelastic deformations. The specifics of rubber behaviour are out of the scope of this project.

The phenomenon by which a polymeric material displays a change from brittle to ductile fracture behaviour or vice versa is termed as the brittle-ductile transition. The brittle-ductile transition can be explained with the help of the Ludwik-Davidenka-Orowan hypothesis. According to this hypothesis, for any polymer, brittle fracture occurs when the yield stress at the prevailing conditions exceeds a certain critical value. The hypothesis assumes that yield behaviour together with plastic deformation

and brittle fracture of a material are both independent processes (Ward 1971; Andrews 1968). The yield stress (which marks the onset of plastic deformation) and brittle fracture stress are both functions of temperature and are measured at a constant strain rate. The fracture process which can occur at a lower stress in the given conditions is the one that eventually occurs in the material. Figure 3-15 illustrates how the brittle and yield stresses vary with temperature.

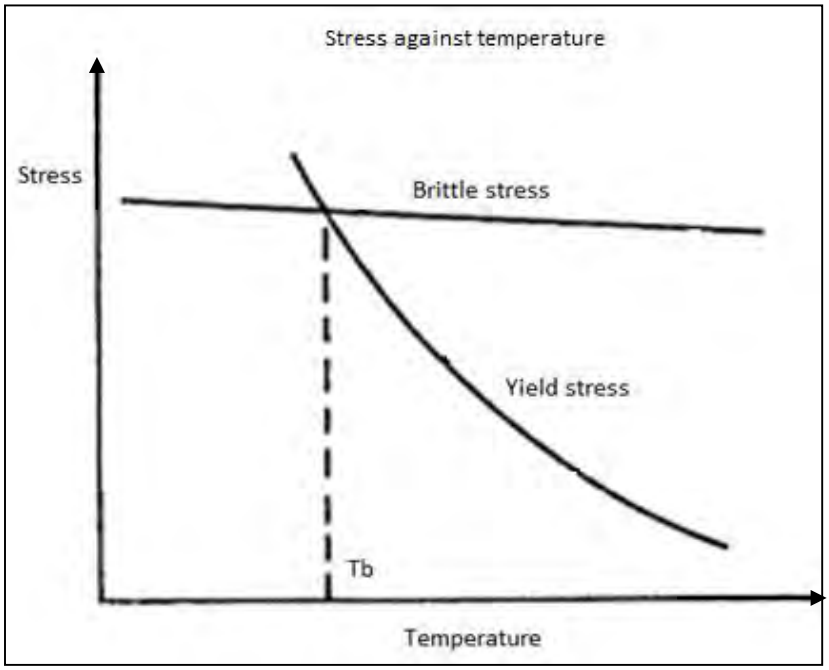

Figure 3-15: Graph illustrating the brittle-ductile transition behaviour (Source: Argon & Cohen (2003))

In figure 3-15 the intersection of the brittle fracture stress and the yield stress marks the brittle-ductile transition point (Tb). At temperatures above this point, the yield stress is lower than the brittle stress and therefore ductile fracture occurs. At temperatures below Tb, brittle stress is lower than yield stress and therefore brittle fracture is prevalent in the material. This is because the material first attains the lower stress of yield or brittle stress. The yield and brittle stress are temperature dependent, confirming that polymers exhibit viscoelastic behaviour.

From the figure 3-15 above, as temperature is increased, the yield stress decreased more rapidly than the brittle stress of the same material. The yield stress and therefore ductile fracture behaviour are more dependent on strain rate and temperature than brittle stress. Yield stress and brittle stress both increase with strain rate and decrease with temperature due to the temperature and loading rate dependence of polymeric material properties.

A brittle-ductile transition is also observed during creep rupture tests when a graph of hydrostatic hoop stress is plotted against the time to failure at constant temperature. This transition point is known as the mechanical knee (Krishnaswamy 2005) and is used to illustrated the point at which failure changes from brittle to ductile. The mechanical knee is illustrated in figure 3-16 below:

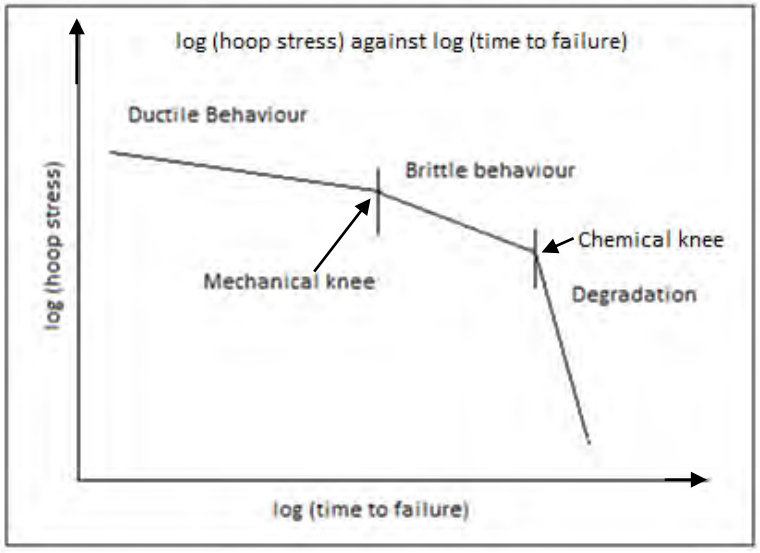

Figure 3-16: Mechanical and chemical knee in polyethylene pipe (Source: Krishnaswamy (2005))

Figure 3-16 also shows that when stresses are applied for a longer time, degradation occurs. This degradation is due to chemical failure and the time to failure in this region is independent of the applied stress. The transition from brittle behaviour to chemical degradation is known as the chemical knee (Krishnaswamy 2005). The figures 3-15 and 3-16 indicate that polymeric materials experience brittle or ductile failure behaviour depending on the prevailing conditions. Therefore it is possible for a polymeric material to exhibit both brittle and ductile failure.

An important factor which affects the transition point is the degree of crystallinity in the material observed. As the degree of crystallinity increases, the transition point of brittle-ductile behaviour becomes more defined (Andrews 1968). Since HDPE is semi-crystalline, it has a clearer transition point as compared to PVC which is an amorphous polymer, making it easier to predict the transition from brittle to ductile behaviour of fracture in HDPE. This brittle-ductile transition temperature is not related to the glass transition temperature in section 3.1.

Crystallinity also affects the strain hardening process in ductile polymers by affecting ductility of the material (Krishnaswamy 2005). This is because it affects the ability of molecular planes to slide past

each other, a process essential in strain hardening and therefore ductile behaviour. An increase in crystallinity may also increase the degree of cross linking in a material, resulting in less ductility but higher fracture strength. If strain hardening is allowed to occur a higher fracture strength may be obtained than before strain hardening.

The brittle-ductile transition is important in fracture behaviour. The transition point assists in predicting the possible occurrence of fracture and in failure analysis. Questions pertaining to the cause and nature of the crack may be answered by deciding if the fracture is brittle or ductile and the transition point offers a way of deciding this. Failures in plastic pipes may manifest as fracture. Fracture of pipes leads to the formation of leaks.

3.3.6 Fracture in plastic pipes

One of the most common failure modes occurring in plastic pipes is fracture. The resistance of a material to fracture is known as the fracture toughness of the material. Farshard (2006) defines fracture toughness as the ability of a material which already contains cracks to withstand an applied load. Fracture toughness therefore indicates the resistance of a material to the growth of imperfections such as cracks. Fracture is a failure mode that indicates that fracture toughness limit of a material has been reached. The initial presence of cracks in a material may cause the stress concentrations to increase at their location in the material, and thus cause localised failure before the entire material reaches the fracture toughness limit. Pipe fracture results in a loss of strength and function.

In pipes, there are various types of fractures classified into bursts and background leaks. Bursts are those that can be detected with or without specialised equipment while background leaks are fractures that are too small to be detected individually.

There are three ways through which fracturing may occur. These include opening mode also known as mode I, in plane shear mode or mode II and out of plane shear mode or mode III. The modes are illustrated below in figure 3-17. The arrows in the figure 3-17 indicate the direction of the acting forces.

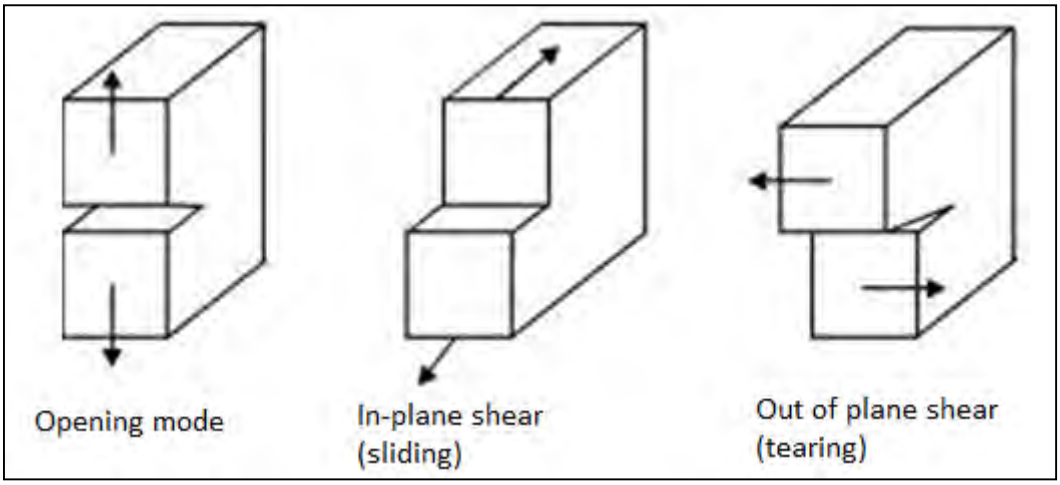

Figure 3-17: Modes of fracture

(Source: http://www.afgrow.net/applications/DTDHandbook/sections/page2_2_0.aspx)

Brittle failure is normally a result of the opening mode while ductile failure is normally due to in plane and out of plane shear.

Fractures are often a result of various sub processes. These processes lead to fracture either independently or together and include tensile fracture, crack propagation, fatigue, creep fracture, wear, crazing, and environmental stress cracking. Some of these modes or sub divisions have already been presented in the previous sections of this chapter and will be linked to fracture in the following sections. All processes of failure and fracture essentially involve the loosening and breaking of molecular bonds which leads to the growth of cracks.

3.3.6.1 Fatigue fracture

Fatigue fracture is the process through which a material fractures from steadily applied stresses lower than that required to cause fracture under direct load (Andrews 1968). During the fatigue process, small cracks or fissures and flaws are formed which may eventually propagate through the material until failure by fracture occurs. In the case of static fatigue, the stress applied to the material is constant whereas in direct loading situations, the true stress may increase due to a reduction in cross sectional area. Tensile loading is an example of a direct loading situation. In static fatigue, the stress is constant until fracture occurs.

Due to the time and temperature dependent properties of polymer materials the strength to resist fracture is also dependent on the loading history and prevailing temperatures. The longer the time

allowed for stress to act, the less the stress required to achieve fracture. For shorter time intervals, higher stresses are required to cause fracture.

3.3.6.2 Wear

Wear is also a mode of fracture since it involves the breaking off of small particles of a material (Andrews 1968). In wear, the stresses are not high enough to cause yielding, but cumulative damage occurs. This cumulative damage is observed in high speed, high temperature and high friction conditions. Pipes that carry water under pressure may undergo wearing due to the friction in the pipe which is usually interpreted as head losses in hydraulics. Wear may also be an indication of aging or end of service life (Farshad 2006). Wear is a complex process, involving mechanical and chemical processes.

3.3.6.3 Crazing

Actual fracture in pipes may be preceded by a process known as crazing. Farshard (2006) defines crazing as the formation of small cracks whose surfaces are still bonded by fibrils of 10nm. Fibrils are molecular filaments of polymer chains oriented at 90° to the craze surface (Mark 2007; Farshad 2006). Fibrils span the entire craze width and form a sponge structure. Crazes differ from cracks in that for cracks, surfaces are completely separated and do not have fibrils which are present in crazing. Crazing occurs due to microscopic yielding of a material's molecular bonds as a result of high stress concentrations. This results in the formation of micro yield zones which join and form a craze.

Corrosive environments, material defects and the presence of residual stresses can contribute to the process of crazing by increasing stress concentrations in the material. Also a combination of small stresses and an aggressive environment may lead to crazing which may eventually result in environmental stress cracking.

A craze develops into a crack in three steps namely craze initiation, craze propagation and craze-crack transition (McCarthy & Deblieck 2008). In the initiation stage, a deformation zone is formed at the tip of an existing defect or crack. This occurs when the stress at a point in the material reaches yield stress. Formation of the deformation zone also depends on the stiffness of the material. The deformation zone spreads through the material and in this way craze propagation occurs. Craze fibrils within the spreading deformation zone are stretched and strain hardened until fracture occurs. The point at which craze fibrils fracture is known as the craze-crack initiation. At this point, a crack is formed.

3.3.6.4 Tensile fracture

Tensile fracture falls under the mechanical failures in pipes. A tensile fracture is a fracture that occurs when the part or material is subjected to tensile forces until the fracture toughness of the material is exceeded. This type of fracture process can result in either brittle or ductile fracture depending on the material, environment and loading conditions. In ductile fracture, plastic deformation is observed at the fracture site and fracture surfaces are relatively rough while in brittle fracture there is little or no plastic deformation observed and the fracture surfaces are relatively smooth. Fibril length is also used to classify fractures. Brittle fracture is characterised by fibril length of 1µm or less while in ductile fracture, fibril length is greater than 1µm (Farshad 2006) after fracture.

3.3.6.5 Environmental stress cracking

Polymeric materials are susceptible to damage from chemically active environments, and sometimes the damage manifests as cracking. This process is known as environmental stress cracking and a common example is corrosion in metallic pipes. In plastic pipes, the material may slowly disintegrate due to chemical reactions, crazing due to solvents or the process of stress cracking may contribute to aging of the pipes. The energy required for fracture in this case is provided by these chemical processes and applied mechanical stress if any.

The stress required to cause fracture in environmental stress cracking is lower than that stress necessary for the case of direct loading (Andrews 1968). Lower stresses such as residual stresses from manufacturing processes in the material experienced over time are sufficient to cause cracking. The stress to cause fracture depends on the environmental conditions and the type of material. The cracks normally start at the surface of the pipe and propagate in a perpendicular direction to the resultant stress system. This crack propagation as a result of environmental stress cracking further illustrates that the process of fracturing is a combination of many sub processes.

Tests carried out on HDPE pipes have shown that the resistance to stress cracking reduces gradually when it is exposed to water and other surface active substances for increasing periods of time (Andrews 1968). However stress cracking can be counteracted by increasing the degree of crosslinking in HDPE material for pipes. Crosslinking increases the fracture toughness of the pipe, making it harder to break molecular bonds. High temperatures have also been observed to increase the process of environmental stress cracking as the molecular bonds are weakened.

3.3.6.6 Crack propagation

Crack propagation characterises the movement or growth of a crack through a part or material from an initiation point and occurs in all other modes of fracture. Propagation of the crack (or cracks) is controlled by the resultant stress system in the material. For example, in the process of tearing the length of the tear is controlled by the amount of surface energy supplied. Surface energy is the minimum amount of required energy for the formation of new surfaces (Andrews 1968). Surface energy is derived from the resultant stress system acting on the material. The extra energy is given off as heat sound or kinetic energy.

Crack propagation could also be described as fast propagation or slow propagation. Fast crack propagation is usually attributed to mechanical (tensile) fracture while slow crack propagation is attributed to creep, static or environmental stress fracture.

In practice, fracture usually occurs as a result of combination of the modes discussed above. To reduce the incidence of fracture, it is important to understand some of the underlying mechanisms of the fracture process. These mechanisms influence the initiation, growth and propagation of cracks through a material. Some of the mechanisms that have been introduced thus far in this chapter include the brittle-ductile transition of fracture behaviour and crack propagation. These mechanisms are common in almost all modes of fracture of water pipes.

Crack propagation is a common phenomenon in the failure process of plastic pipes. Pipe failures in the field are sometimes due to crack propagation. In the next section, the mechanisms of crack propagation are discussed.

3.3.7 Crack propagation

Crack propagation is the movement or growth of a crack through a material and occurs in all modes of fracture. Crack propagation is affected by the microstructure of the material, notch sensitivity and is characterised as either rapid crack propagation (RCP) or slow crack growth (SCG). These factors greatly influence the movement of a crack through a material.

3.3.7.1 Microstructure

Crack propagation is influenced by the microstructure of the material to a great extent. The microstructure determines the mechanical and fracture response of the materials when a load is applied to it. This microstructure also affects the stress distribution such that the fracture toughness is increased or decreased. In fibre reinforced plastics the fibres carry most of the load applied to the material and inhibit crack propagation hence fracture toughness is increased (Andrews 1968). In the

absence of fibres, strain hardening may occur as a result of plastic deformation and further propagation is then inhibited.

In other polymer materials, the microstructure may cause high stress concentrations at crack tips and notch tips and therefore the material fails at stress levels below the fracture toughness. The microstructure of the plastic material may also offer a path of weakness to the propagating crack and these are normally the boundaries of molecular planes (Andrews 1968). These regions may also provide points of entry for corrosive media, thus enhancing stress corrosion processes.

Another important aspect in the microstructure is the crystalline-amorphous texture found in polymeric materials. The crystalline regions in polymers consist of regular patterns of atoms with strong covalent bonds while the amorphous regions consist of less regular weakly bound molecules. The crystalline regions' response to mechanical behaviour is easily interpreted as elastic and plastic deformation. This is not the case in the amorphous regions where the response is better approximated as viscoelastic deformation (Andrews 1968). Understanding the deformation and fracture processes in each region may not necessarily assist in understanding the processes where both regions co-exist since the proportions usually vary and materials are not homogenous. A crack will propagate through the weaker regions, or along the boundaries of the crystalline-amorphous regions.

It is observed that as the degree of crystallinity increases, the strength of the polymer increases (Andrews 1968; Moore & Kline 1984). This is why HDPE which is semi-crystalline has a higher strength and fracture toughness than PVC which is amorphous. A higher degree of crystallinity increases the number of the strong covalent bonds making HDPE harder to break, compared to PVC. The molecular bonds act as crosslinks which reduce the amount of deformation allowed. The fracture toughness and resistance to deformation is therefore increased. Depending on how much of the material is crystalline or amorphous, the fracture behaviour is governed by the relative proportions.

3.3.7.2 Notch sensitivity

The study of the effects of a notch or notches in a material is important as they can potentially modify failure and fracture behaviour in a material. In a specimen with a notch, failure may occur at stresses below the ultimate tensile strength (Andrews 1968) because of the induced stress concentrations at the tip of the notch. These stress concentrations result in localised yielding and failure while the rest of the material is still experiencing a stress lower than the yield stress. The crack therefore propagates through the material starting from the tip of the notch.

The presence of a notch might give rise to notch embrittlement. Notch embrittlement is the process whereby a material fails in a brittle manner due to the presence of a notch, even if ductile failure would normally occur if the notch was absent (Andrews 1968). This is again due to the presence of stress concentrations that make the stress at the notch tip higher than in the rest of the material and therefore resulting in brittle failure. For example from figure 3-14 showing brittle-ductile transition, at temperatures above the transition temperature, the material's brittle stress is higher than the yield stress. The material would therefore be expected to experience ductile failure before brittle failure. However, due to stress concentrations at the tip of the notch, the stresses are likely to be sufficiently high for brittle stress to occur.

However, not all materials are sensitive to notches and in some materials such as HDPE, plastic deformation that occurs at the notch tip may actually inhibit crack propagation. This is because plastic deformation leads to the molecular planes slipping past each other and results in strain hardening. Some plastic materials also exhibit crack stopping mechanisms since they have additives that act as physical barriers to the growth and movement of the crack.

3.3.7.3 Rapid crack propagation

Rapid crack propagation (RCP) is a phenomenon in which failure occurs in a material by a brittle crack moving through the part in use (Farshad 2006). Rapid crack propagation is also known as high/fast speed fracture and is described as uncontrolled fracture. In this type of crack propagation, the velocity of the growing crack can be as high as 0.5V, where V is the velocity of transverse stress waves propagating in the material (Andrews 1968). Transverse waves are waves where the particle motion is perpendicular to the direction of propagation of the wave (Lai et al. 1999). The velocity of the stress wave is related to the stress level in the material. Estimation of the velocity is further complicated by the possibility of several cracks propagating at the same time in the same material. These cracks will possess different but stable velocities. Since brittle fractures also experience an amount of local plastic deformation at the crack tips the velocity may differ from the calculated estimate.

The effects of RCP in plastic pipes are observed as longitudinal cracks that occur by brittle failure. These longitudinal cracks occur as a result of point loads, pressure surges, water hammers and stress concentrations due to pipe defects. The cracks can move through an entire pipe length in a straight line or sinusoidal wave pattern depending on the velocity of the crack. Greenshields & Leevers (1996) observed that in pipes completely filled and pressurised by water, crack paths are always completely or almost straight. Sinusoidal paths occurred in air/water pressurised pipes. The cracks travel through butt fusion joints but are arrested at other joint types such as the bell and spigot joint

in PVC pipes. A single crack or several cracks branching out from one major crack may be observed. The cracks move through the pipe as a result of energy supplied by the pressurized pipe system until the pressure has dissipated or the entire pipe is shattered.

The brittle cracks in pipes due to RCP occur at pressures above a certain critical pressure. Once the pressure drops below the critical value, the crack growth slows down and is eventually arrested because the energy from the pressure is no longer enough to sustain it. The reduction in pressure is normally due to a decompression wave travelling through the water. When the decompression wave velocity exceeds the crack propagation velocity, the crack is arrested (Greenshields & Leevers 1996). Crack arrest therefore means that the pressure and energy available to drive the crack dissipate more rapidly than the crack can travel. This effect of the decompression wave is the opposite of the compression wave that can actually cause fracture if the pressure surge is above critical pressure. Decompression and compression waves occur during water hammer.

The decompression wave velocity therefore estimates the minimum crack velocity. The minimum crack velocity is the crack velocity below which RCP cannot be sustained. Crack velocity is increased by the presence of notches and when crack velocity exceeds the decompression wave velocity RCP may occur. The decompression wave may be approximated from the following equation (Greenshields & Leevers 1996):

$$c_w = \left[\left(\frac{M}{\rho} \right) \frac{1}{1 + \frac{M}{\rho E}\left(D^* - 1 + 2\nu \right)} \right]^{1/2} \tag{3.43}$$

Where c_w is the decompression wave speed, D* is the standard dimensional ratio (SDR) of the pipe, ρ is the density of water at atmospheric pressure, E is the dynamic tensile modulus of the material of the pipe, v is Poission ratio of the pipe material and M is the bulk modulus of the fluid in the pipe, in this case water. D* is calculated from:

$$D^* = \frac{D}{t^*} \tag{3.44}$$

Where D is the external pipe diameter and t* is the thickness of the pipe.

RCP is more common in PVC pipes than HDPE pipes because HDPE has a higher ductility and toughness, therefore preventing brittle fracture. This is due to the fact that at room temperature (20°C) HDPE is above its glass transition temperature while PVC is below resulting in ductile

behaviour and strain hardening in HDPE. According to Hall (1989), the glass transition temperatures for PVC and polyethylene are about 85°C and -90°C/-35°C respectively. The ductility of HDPE due to its low glass transition temperature reduces the crack velocity and may eventually force its arrest. Also, for most HDPE pipes, the critical pressure is higher than the allowable pressures of the pipe system (Greenshields & Leevers 1996). In PVC, the critical pressure has been found to be below allowable pressure and therefore RCP easily occurs. Presence of a notch in an HDPE pipe also gives rise to stress concentrations which may result in stresses higher than its ultimate strength. This may eventually cause RCP.

Cracks due to RCP can travel through butt fusion joints. Therefore in designing PVC pipes with butt fusion joints, the critical pressure is normally taken to be half of the pressure rating of the pipe. As a result thicker PVC pipes of lower diameter to thickness ratio (dimensional ratio) are used in practice. Most manufactured PVC pipes are however thin walled and therefore their allowable pressures should be reduced to avoid incidence of RCP. RCP can also be avoided by ensuring that the velocity of the decompression wave is higher than the crack velocity. For this to be achieved, required pipe dimensions are determined by dynamic fracture methods which are beyond the scope of this dissertation.

An example of the of the dynamic fracture methods is the Irwin-Corten analysis. The Irwin-Corten analysis assumes that the crack is driven by only and all the strain energy stored in the pipe wall, therefore no energy is converted to kinetic energy. However for high speeds, the effect of inertia is significant and therefore the assumption is not true (Greenshields & Leevers 1996). The crack driving force given by the Irwin-Corten analysis is given by the following equation:

$$G = \frac{\pi p_0^2}{8E} D\left(D^* - 2\right)^2 \left[1 - \frac{1}{D^*}\right] \tag{3.45}$$

Where G is the driving force or energy required to drive the crack and p_0 is the initial internal pressure of the pipe.

The driving force G in the Irwin-Corten analysis equation (3.45) is obtained from the strain energy which is calculated assuming thin walled pipes (Greig et al. 1992). However plastic pipes are thick walled with most having a standard dimensional ratio less than 20. A modified form of the Irwin-Corten analysis was proposed by Greenshields & Leevers (1996) to calculate the strain energy and therefore the driving force for thicker pipes (SDR > 5) accurately. The modified form is:

$$G = \frac{\pi p_0^2}{8E} D\left(D^* - 1\right)\left(D^* - 2\right)\left[1 + \frac{2\left(D^* - 1\right)}{D^{*2}}\left(v - 1\right)\right] \tag{3.46}$$

The modified analysis leads to minimum dimension ratios of 13 and 29 for PVC and HDPE respectively (Greenshields & Leevers 1996) for resistance against RCP. Despite this, most PVC pipe available on the market is thin walled and therefore susceptible to RCP.

Above a certain critical thickness RCP cannot be sustained (Farshad 2006) and therefore the pipe should have a thickness above the critical thickness. This is because as the pipe thickness is increased, the pressure due to a water hammer and other surges decreases faster than the crack speed Greenshields & Leevers (1996). This critical thickness (t*) can be determined from the equations (3.46) and (3.44) above after the driving force necessary to cause RCP has been established. The critical pressure and thickness also depend on various conditions such as the environment, material properties, pipe dimensions, residual stresses due to manufacturing processes, service conditions, age and type of fluid being transported. RCP has also been found to occur as a result of high impact stresses during service life. These factors all influence the behaviour of the pipe under pressure and hence the fracture response.

RCP is only possible if a crack occurs in the material during the fracture initiation stage. Formation of a crack would be termed as failure since leakage would occur and the pipe would have lost its intended function. Failure of plastic water pipes by brittle cracking is fairly common and therefore study of RCP in plastic pipes is essential to determine their reliability, and increase design life.

The resistance of a pipe to RCP depends on a combination of factors which include the material toughness, impact strength, notch sensitivity and fatigue strength. Since HDPE has a higher toughness, impact strength and fatigue strength than PVC, it is less susceptible to RCP as compared to PVC. The mechanical properties of the material assist in predicting the effects of residual stresses, age, pressure and environmental conditions the pipe is exposed to during design life. It is important to note that although RCP is more common in PVC pipes compared to HDPE pipes, it is caused by not only inferior pipe properties but other external factors such as environmental conditions, pipe dimensions and water pressure also contribute to occurrence of RCP. The figure 3-18 below shows a PVC pipe failure where the pipe failed due to RCP and would have to be replaced.

Figure 3-18: Rapid crack propagation in PVC pipe (Source: Long (2012))

3.3.7.4 Slow crack growth

Slow crack growth (SCG) is a sub process of failure in plastic pipes present in the initiation stages of environmental stress cracking and brittle failure due to high stress concentrations or defects. SCG has contributed to most of the HDPE pipe failures that occur in the field (Krishnaswamy 2005), therefore making it an essential mode of failure in testing HDPE pipes. Testing for failure by SCG is also essential due to the growing demand for extended design life beyond 50 years, such as 100 years. Since it occurs as brittle fracture, it is normally referred to as stage II failure of the rupture process illustrated in figure 3-17. SCG has been identified as the critical failure mechanism for HDPE pipes and occurs in two ways, namely fatigue cracking and environmental stress cracking (McCarthy & Deblieck 2008). The result of these processes and SCG is brittle cracks that occur internally or externally.

SCG in plastic pipes is normally preceded by crazing. The process is initiated by the continuous application of stresses below the yield stress of a material with imperfections such as notches. Crazes are formed at these sites and are tiny cracks whose surfaces are still joined by micro fibrils. The crazes grow when a deformation zone is formed at existing craze tips due to the high stress concentrations in these areas. The high stress concentrations may exceed the yield stress of the material causing strain hardening of the craze fibrils and then cracking when the fibrils break at

craze-crack transition. Brittle cracking is then initiated. The entire process is repeated at the crack tip, leading to failure due to SCG.

Environmental stress cracking is a form of SCG in plastic pipes and failure times depend on the media transported within the pipes. Although water has been known to cause SCG in HDPE (Andrews 1968), its failure times are rather high for industrial testing. Therefore reagents such as Igepal CO-630 are used to cause stress cracking and reduce time to failure. The reagents plasticize the amorphous regions of the polymeric materials and this initiates craze formation which eventually results in SCG. Stress reagents are also said to cause plastic deformation by lubricating the molecular planes which then slide past each other easily, an essential process in strain hardening (McCarthy & Deblieck 2008).

Time-temperature super-positioning methods are also applied to reduce the testing time for SCG. However, increasing temperature to reduce the testing time may lead to ductile failure instead of brittle fracture observed in SCG. Other factors that influence SCG in polymeric materials are presence of notches, molecular weight and microstructure. Resistance to SCG increases as molecular weight and crystallinity increases.

SCG has contributed to various pipe failures (Krishnaswamy 2005) and therefore tests have been developed to measure the resistance against SCG. Resistance to SCG in HDPE pipes is measured by standard tensile tests such as the Pennsylvania Notch Tensile (PENT) test. Stress cracking reagents may be added and temperatures raised to reduce testing time as explained above. However due to the uncertainty concerning the exact impact of these reagents to the material structure and the possibility of ductile fracture at high temperatures, a new accelerated method was proposed by McCarthy et al. (2008) and it is based on the Kramer-Brown model. The Kramer-Brown model links craze propagation and craze failure to the strain hardening in a material. Craze propagation and failure are initiation stages of SCG. The accelerated method makes use of strain hardening by applying tensile stress-strain behaviour to measure the SCG resistance of HDPE. The Kramer-Brown model also shows that the higher the strain hardening a material undergoes, the higher its resistance to craze initiation and therefore a higher resistance to the onset of SCG. The amount of strain hardening in a material increases with crosslinks and entanglements, and these increase the resistance to SCG.

3.3.8 Preventing fracture in water pipe systems

Failure by fracture in plastic pipes can be prevented by considering and eliminating the possible causes of fracture. Conditions which favour fracture processes and errors during construction and maintenance should be eliminated or minimised. Relevant standards should be employed for choosing pipe materials. Also, consideration should be given to mode of construction and length of design life. It is essential to remember that design life may be shortened by aggressive environmental conditions or third party damages therefore regular checks and maintenance are necessary. Proper maintenance procedures should be followed since some failures have been reported to be a result of poor maintenance and repair procedure.

The following checks are important during design, construction and maintenance process:

i. Implementation of proper planning procedures for the system in question. This includes the design phase, construction and maintenance phase. Plastic pipe standards should be utilised since plastic pipe properties differ from other pipe materials such as metals due to their temperature and load dependent characteristics.
ii. The right material and joints to join pipes should be used and this is done with the help of the standards available. For example welded joints are not suitable for PVC pipe due to susceptibility to brittle cracking by RCP, therefore bell and spigot jointing is used.
iii. There should be regular and adequate monitoring and servicing of the system to identify potential pipe failure sites such as bends, chemically eroded pipes and point loads. For example, PVC pipes are weakened by UV exposure and therefore exposed PVC pipes should be monitored.
iv. For the course of the design life, proper maintenance procedures should be followed so that pipes are not fractured by careless handling.

Chapter 3 is a summary of the properties of PVC and HDPE polymers. The section begins with a description of the chemical structure and properties of these polymers that influence the behaviour of the manufactured pipe. Both PVC and HDPE are thermoplastic polymers, with PVC containing carbon, hydrogen and chlorine while HDPE contains only carbon and hydrogen. The polymers are formed from the monomers during the respective polymerisation processes.

A description of the mechanical properties that are prevalent in polymeric materials then follows. This focuses on the behaviour of polymeric materials when loads are applied to them, before they reach the yield point and initiation of fracture. Polymeric materials undergo viscoelastic deformation

when loads are applied. Creep, stress relaxations and hysteresis were introduced as aspects of viscoelastic behaviour. The factors affecting these aspects were discussed to explain how they are dependent on time history and environmental conditions. Four models, one mathematical and the other three mechanical were introduced to explain viscoelasticity.

Finally an overview of the expected failure and fracture behaviour of a polymeric material is included. Failure and fracture occur after the yield point of the material has been exceeded. It was seen that failure and therefore fracture can result from various causes such as mechanical, thermal, chemical and environmental processes. Fracture was then discussed as a result of several sub processes which include tensile fracture, crack propagation, fatigue fracture, wear, crazing and environmental stresses. These sub processes may lead to fracture either independently or concurrently. The process of fracture is observed as the growth of crack through a material. Crack growth as a result of fracture was then explained, with reference to the effect of the microstructure of materials and presence of defects such as notches on crack behaviour. The growth of cracks through the material was classified into RCP and SCG, and it was seen that RCP is prevalent in PVC pipes while HDPE pipes fail by SCG. A discussion on how fracture can be prevented in water distribution systems to reduce the occurrence of leakage was included.

The next chapter is the methodology chapter, which explains how the objectives of the project were achieved.

4 Methodology

This chapter describes the Finite Element Method (FEM) and the commercial software Abaqus, used for this project. The chapter also describes how the objectives of this project were achieved.

4.1 The Finite Element Method

4.1.1 Background of the Finite Element Method

The Finite Element Method is a numerical analysis technique that is used for the evaluation of structures and systems and providing accurate predictions of a structure's response when it is subjected to structural and thermal loads (Huebner et al. 2001). The method is used to analyse structures with complex geometries, subjected to various loading conditions and the structure's response is predicted within acceptable limits. Various engineering problems have been solved using the Finite Element Method within a variety of finite element software that is available. The Finite Element Method is a very accurate tool for analysing failure modes, behaviour of defects, fatigue and code compliance among other uses. It also serves as a good visual aid since the material response is presented as graphics. In essence, the Finite Element Method is a numerical method for solving differential or integral equations.

The name "Finite Element Method" was first published in an applied mathematics paper in 1960. The paper which was published by Clough (Huebner et al. 2001) contained ideas that were however developed and applied before 1960. The first ideas of the Finite Element Method (FEM) were developed separately by mathematicians, physicists and engineers for their own applications.

In mathematics, the ideas of the FEM were applied to solve boundary value problems for continuum mechanics. In physics, similar ideas were developed to obtain piecewise approximations of functions so as to approximate solutions to continuous functions in continuum mechanics. In engineering, the increasing complexities encountered in aerospace engineering necessitated the development of FEM concepts. Engineers were required to work out the stiffness coefficients of shell structures reinforced with ribs and spars.

The use of piecewise continuous functions was first published by Courant (Huebner et al. 2001) in an applied mathematical paper in 1943. The paper described how triangular elements and the principle of minimum potential energy were applied to study the Saint Venant Torsion problem. This process of representing a continuum in terms of small elements is known as discretization. It was only after a decade that discretization was applied again by mathematicians investigating boundary value problems. Discretization was again demonstrated in 1959 by Greenstadt (Huebner et al. 2001) using

cells to represent the continuum investigated. Each cell had its own mathematical function, and these individual functions altogether represented the unknown function of the entire continuum. Greenstadt applied continuity requirements to bind the cell equations together after the evaluation of a variational principle for each cell.

For the engineering community, the development of FEM concepts first appeared in the 1930s (Huebner et al. 2001). Structural engineers discovered that a truss problem could be solved by viewing the truss as an assembly of small parts such as beams and rods. The responses of these beams and rods were known, hence enabling calculation of the response of the entire truss using equilibrium laws. The method was further developed to include more complicated applications such as plates. In 1960, White and Fredrichs (Huebner et al. 2001) also used triangular elements to develop equations from variational principles. These developments all supported the spread and growth of FEM in engineering analysis.

The FEM is applied in various software packages today such as Abaqus and Ansys. To solve problems, it is implemented in three phases, which include the pre-processing phase, the analysis phase and the post-processing phase. Each of these phases is explained below.

4.1.1.1 Pre-processing phase

In this phase, the structure or continuum to be investigated is first divided into elements. There are various elements types available such as beam elements, triangular and quadrilateral elements. Elements types are listed in the FEA software manuals such as the Abaqus manual which is listed in the references as Abaqus Documentation. Various element shapes and sizes may be used for one structure depending on the type of problem to be solved. Engineering judgement, sensitivity analyses and consultations with previous work are normally used to determine the number and size of elements. The analytical structure model is therefore interpreted as a region of interconnected small elements, in which the governing equations are solved. Elements are connected to each other via nodes.

For a specific problem, approximation functions are generated for each element, and the field variables to be solved for are at the nodes (Huebner et al. 2001). Approximation functions are also called interpolation functions. Field variables such as temperature and displacement may be scalars, vectors or tensors. Nodes must lie at least at corners and vertices of elements. The approximations at nodes as a result of the functions in the elements give rise to a piece wise approximation of the problem. Therefore functions should be chosen so that solutions within each element are compatible. This means that the field variables at nodes between elements (or the derivatives of the

function) should be continuous across the element boundaries. The method applied to solve for the variables is determined by the nature of the problem.

4.1.1.2 Analysis phase

In the analysis phase, the matrix equations for the individual elements are set up. This is done using any of these four methods which will not be discussed in detail in this dissertation:

i. Direct approach
ii. Variational approach
iii. The weighted residual approach
iv. The energy balance approach

The element equations are then assembled to form the overall system matrix. Boundary conditions are incorporated into the system matrix equations. Boundary conditions are added in terms of fixed nodal values at the relevant nodes.

The FEA method formulates solutions for each individual element and then assembles the elements to obtain the solution to the entire problem. Complex problems are therefore solved by obtaining solutions to a number of simplified problems. For example to solve for the forces and displacement in a structure, the finite element method finds the solutions for each element. The element solutions are then assembled to find the force and displacement in the entire structure.

Depending on the problem, linear or nonlinear equations maybe generated. These equations are solved by either the elimination method or the wavefront method (Fagan 1992).

4.1.1.3 Post-processing phase

In the post processing phase, the unknown field variables are presented in the desired format and may also be used to calculate further system responses. Results are plotted, printed or presented as required.

4.1.2 Sources of error in Finite Element Analysis

A basic understanding of the physical problem to be solved and the finite element concept is essential. This prevents errors from going unnoticed, which can lead to inaccurate results. Common sources of error associated with the FEA method include:

i. Geometric errors. These may be due to inconsistent units of parameters, highly skewed elements and incorrect connections between elements and missing elements.

ii. Material properties errors. These could also be due to inconsistent units, or the use of wrong values for material properties.

iii. Applied forces may sometimes be wrongly placed or of wrong magnitude and direction.

4.1.3 Applications of the Finite Element Method

The finite element method has a wide range of applications for different problems. Applications may be divided into three groups. These are summarised in the table 4-1 below:

Problem to be solved	Applications of FEA
Equilibrium and time independent problems	Calculation of stress, displacement, temperature, velocity and pressure distributions among others.
Eigenvalue problems in solid and fluid mechanics	Problems that require the determination of frequencies and free vibrations. Examples include interactions between dams and water bodies, fuel in flexible tanks and structural stability.
Time dependent and propagation problems	Solving for any of the above two problems when a time dimension is added.

Table 4-1: Applications of the Finite Element Analysis Method (Huebner et al. 2001)

It should be noted that the FEM is only one of the many methods that can be implemented to solve various problems. All methods have their advantages and disadvantages when compared to others. The final choice of the method used depends on feasibility studies, availability of computer facilities and software, time and resources required. For the FEA method, different software packages have been developed that are used by engineers and companies to solve problems. Examples of such packages are Abaqus and ANSYS among others. For this project, Abaqus was used since it is already available to the University of Cape Town as a research tool.

4.1.4 Abaqus software package.

Abaqus is only one of the types of software available for analysing finite element problems. Abaqus is a general purpose simulation tool, built to cover a diverse range of applications. Applications include electromagnetic problems, stress problems, heat transfer and soil mechanics among others. The software is capable of handling both simple linear problems and complex nonlinear problems. Abaqus is equipped with an extensive element library for all geometries (Cassa 2005). The software allows for both a graphical user interface and the use of the command prompt commands. Abaqus also has an inbuilt scripting tool that uses the Python programming language. This scripting tool offers great flexibility to experienced users and programmers.

In Abaqus, the user builds the model and thus defines the model database which is the input file for the Analysis phase. The input file may also be directly imported into Abaqus. Analysis is carried out using Abaqus/Standard or Abaqus/Explicit depending on the problem to be solved. An output database is created during analysis based on the requested outputs defined by the user. Results of the analysis may be viewed in visualization mode. Simulations in Abaqus may take seconds, days or months to complete, depending on the complexity of the problem and the available computational resources. This systematic process is implemented within the ten modules of Abaqus. The modules are explained below.

4.1.4.1 Part module

In the part module of Abaqus, model parts are created and stored as an ordered list of features. Features may include cuts, extrusions and datum planes. Parameters of features such as cuts and extrusions can be edited and regenerated. The characteristics of the part are also assigned, that is rigid or deformable as well as other options not described here. For this project, a deformable part was created. Sections for the leak openings were modelled as cuts. The cut and pipe sections were represented as two dimensional sketches on datum planes before extrusion depths were assigned.

Since the area of the leak hole was required, the boundary of the leak opening or cut was saved to a set named “HolePerimeterOD.” This set name would later be implemented in a python script to read deformed coordinates of the leak opening boundary from the analysis output.

4.1.4.2 Property module

In the property module, material and sectional properties are defined. Material properties and parameters must be edited so as to achieve the objectives of the investigation. For example, to analyse for viscoelastic deformations, both elastic and viscoelastic parameters are required. Detailed explanations are included in the Abaqus manual. Material properties are edited in the material editor.

Sectional properties are related to the cross sectional area and moments of inertia. For some analyses, sections chosen must be consistent with the element type to be used. For example, beam sections should be used for beam elements and truss sections for truss element types. For the project, a solid homogenous section was created, and linked to the relevant material properties which were HDPE or PVC.

4.1.4.3 Assembly module

Models are assembled in the assembly module. An assembly can be modified accordingly if a feature of a part is modified by allowing Abaqus to regenerate the assembly. An assembly is composed of a

number of instances of parts or instances of other models. The different parts are positioned and assembled in a global coordinate system. In this particular project, there was only one part for each model which was a pipe with a hole.

4.1.4.4 Step module

Analysis steps are created in the step module. Abaqus creates a default analysis step, the initial step in which boundary conditions are implemented. Analysis steps also capture changes in load and boundary condition sequences. It is therefore important to note if loads, boundary conditions or interactions are propagated through all the steps or are modified for some steps.

Output requests from the output database are defined in this module, both under field output and history output requests. Field output requests refer to the entire model while history output requests refer to a smaller part or particular set of the points on model. Requested outputs may include displacements, stresses and coordinates. The set "HolePerimeterOD" was specified in the history output requests for deformed coordinates.

4.1.4.5 Interaction module

The interaction module is used to define interactions or couplings within a model. Interactions and couplings may be defined between regions of a single model or models and their surroundings. Interactions are step dependent and therefore the active steps must be defined. In Abaqus, mechanical contact is not recognised unless it is defined in the interaction module. No interactions were required for this project.

4.1.4.6 Load module

The load module is used to define and manage loads, boundary conditions, predefined fields and load cases. Loads and boundary conditions are step dependent and therefore active steps should be defined accordingly.

4.1.4.7 Mesh module

Meshes are generated in the mesh module. Meshes may be generated on parts or assemblies. Meshes can be verified for analysis errors and warnings. Mesh attributes include seeds, meshing techniques, and element types. Seeds are markers placed along the edges of a region to specify and target the desired mesh density in the region (Abaqus Documentation). Mesh attributes are assigned by the user according to analysis and desired output. In the mesh module, the model is coloured according to the possible meshing technique. Meshes can be regenerated when parts are modified.

4.1.4.8 Optimization module

The optimization module is used to create optimisation tasks. Optimisation tasks are iterative processes and may be carried out for topology and model shapes when a set of objectives and restrictions is defined. Optimisation tasks, design responses, objective functions, constraints, geometric restrictions and stop conditions can all be investigated using the optimization module.

4.1.4.9 Job module

The job module is used to create and manage analysis jobs after the model has been defined. Progress of a job can be monitored and multiple jobs can be run simultaneously. The job module also enables the creation of analysis input files which may be submitted separately.

4.1.4.10 Sketch module

The sketch module is used to create two dimensional representations in Abaqus. Sketches are normally representations of parts in two dimensions. Within the sketch module, sections from which parts are extruded, swept or revolved to form the three dimensional representation are drawn or edited. Sketches may be modified, after which the corresponding features are regenerated.

4.1.5 Viscoelasticity in Abaqus

Viscoelastic materials are also analysed with finite element analysis techniques in Abaqus. The purpose of this section is to provide a detailed account of implementing the viscoelastic analysis for this project in Abaqus.

Since HDPE and PVC are classified as viscoelastic materials in this dissertation, viscoelastic inputs are required for the analysis process. It should be noted that Cassa et al. (2006) modelled PVC as a linear elastic material. Therefore this section will also provide insight in the difference between a linear elastic analysis and a viscoelastic analysis. The viscoelastic inputs for the models were calculated based on the method followed by Jasinoski & Reddy (2012) to study the mechanics of cranial sutures in pigs during cyclic loading.

To model viscoelasticity in Abaqus, one has to choose between the time domain viscoelastic material model and the frequency domain viscoelastic model. The time domain model is applied to deformations that differ considerably with time while the frequency domain is applied for studying harmonic oscillations. Since one of the objectives of this project was to model pipe deformations over time, the time domain viscoelastic model was implemented. It should also be noted that viscoelastic behaviour in Abaqus can only be investigated when one of linear elastic parameters,

hyperelastic parameters of rubberlike materials or hyperelastic parameters of elastomers are specified. Therefore the parameters required for this model include linear elastic inputs as well as viscoelastic inputs. Linear elastic parameters predict the rate independent response of a material and are applicable for small strains. Hyperelastic parameters are more suitable for materials that experience large strains, such as rubber.

The linear elastic inputs are Young's Modulus (E), Poisson's ratio (ν) while viscoelastic behaviour is described by a Prony series. The Prony series may be defined directly by the user or calculated by Abaqus from creep test data, relaxation test data or combined test data. For this project a single term Prony series was specified directly. The series parameters were separately calculated from stress-strain data taken from Janson (2003). The process through which the Prony series parameters were extracted was explained earlier in the literature review. Sample calculations for the Prony series parameters of a viscoelastic material are provided in the appendix A. A Prony series expresses material relaxation constants such as the time dependent shear strain and modulus in terms of Abaqus constants.

4.2 Project Model

4.2.1 Materials and Specifications

The method detailed in this section is based on similar investigations by Jasinoski & Reddy (2012) and Cassa et al. (2010). Jasinoski & Reddy (2012) investigated viscoelastic behaviour of cranial sutures (fibrous tissue that holds skull bones together) while Cassa et al. (2010) investigated the effect of pressure on holes and cracks in pipes, assuming elastic deformation.

Two types of leak openings were investigated in this study and these were longitudinal cracks and round holes. The leak openings were modelled in two materials, HDPE and PVC which were classified as viscoelastic materials in this study. To model viscoelasticity, both elastic deformation and linear viscoelastic analyses were carried out in Abaqus for comparison with elastic deformation studies by Cassa et al. (2010) and practical investigations by Ferrante (2012). Material properties required for these analyses were defined according to South African National Standards (SANS).

Material properties are summarised in the table 4-2 below. HDPE and PVC pipe allowable stress and safety factor specifications were chosen according to SANS 966-1:2004. The elastic modulus and viscoelastic parameters were calculated based on pipe creep test data obtained from Janson (2003). Sample calculations for each material are included in the appendix A.

Elastic Properties		
Property	**PVC**	**HDPE**
Elastic Modulus (MPa)	3421.143	1126.760
Poisson's ratio (V)	0.4	0.4
Allowable stress (MPa)	10.4	8.0
Safety Factor	4.80	1.25
Prony series parameters for Viscoelasticity		
g_1^p	0.208	0.564
τ_ε (s)	3382.788	4348.761

Table 4-2: Material properties

The initial round holes and longitudinal cracks tested were of different dimensions as shown in the table 4-3 below. The area of the leak holes was calculated as a projection on to the y-z plane in Abaqus, hence a 2 dimensional projected area is used. As seen in table 4-3, the calculated area and measured area by python script differed by a small degree. Since a python script would be implemented to measured deformed areas, the measured areas by the script were taken as the un-deformed area (A_0) before the application of any pressure at time t = 0 seconds.

Round holes				
Diameter(mm)	**Undeformed projected Area (mm^2) as calculated**	**Undeformed projected Area (mm^2) as measured with python script in Abaqus (A_0)**		
1	0.7854	0.7832		
12	113.097	112.98		
Longitudinal cracks				
Length (mm)	**Width (mm)**	**Crack tip radius (mm)**	**Undeformed projected Area (mm^2) as calculated**	**Undeformed projected Area (mm^2) as with python script measured in Abaqus (A_0)**
10	1	0.5	9.7854	9.77
40	1	0.5	39.7854	39.785
80	1	0.5	79.7854	79.765

Table 4-3: Dimensions of leak openings investigated

These leak openings were placed in the middle of the pipe models. The Abaqus pipe models were chosen to be 500mm in length based on previous investigations by Cassa (2005) and (Ssozi 2012). PVC pipe of pressure class 6 was modelled and corresponds to a working pressure of 600kPa

(0.6MPa). The inner diameter of a PVC pipe for this pressure class is 104mm. To calculate the thickness of the PVC pipe to be modelled the allowable stress from table 4-2, internal diameter and working pressures were applied to the following equation for the circumferential stress (discussed in the literature review chapter 2) in the pipe:

$$\sigma = \frac{PD}{2t^*} \tag{4.1}$$

Where σ is the allowable stress, P is the working pressure of 600kPa, D is the inner diameter and t* is the pipe thickness.

Since an HDPE pipe of inner diameter 104mm is not of the same pressure class, equation (4.1) above and the allowable stress given in table 4-2 were applied to obtain a thickness of HDPE pipe that would have the same working pressure of 600kPa. According to Marley Pipe Systems (Pty) Ltd, the nearest commercially available HDPE pipe for the same pressure class that meets the required allowable stress of 8MPa (table 4-2) has an inner diameter of 101mm, with a thickness of 4.2mm. The final pipe model dimensions in this project for the two materials are illustrated in the table 4-4 below.

Material	Internal diameter (mm)	Thickness (mm)	Outer diameter(mm)
PVC	104	3.00	110.00
HDPE	104	3.90	111.80

Table 4-4: Pipe model dimensions in Abaqus

For every model, three pressure levels were investigated and these were 0.2MPa, 0.4MPa and 0.6MPa. Within the viscoelastic analysis, creep deformation over seven different times was investigated. To test creep deformation, viscoelastic simulations were carried out for a duration of 100 000s, while noting deformations after 10s, 100s, 1000s, 5000s, 10 000s, 50 000s and 100 000s.

In addition, two loading states were investigated in every case, the uniaxial and biaxial stress states. This was necessary since longitudinal pipe stresses vary greatly from zero upwards (Cassa et al. 2010). For the uniaxial stress state, pressure was only applied to the internal walls of the pipe while for the biaxial stress state; pressures were applied to both the internal walls and as well as a tensile stress to the ends of the pipe. These additional tensile stresses applied are the longitudinal stresses as discussed in the literature review to simulate a biaxial loading state. The uniaxial stress state was therefore due to the presence of only circumferential stresses.

A summary of the pressure and longitudinal stresses applied to the pipes in both stress states is included below in table 4-5. The longitudinal stresses for the biaxial stress state are calculated from the equation (2.2) in the literature review.

Pressure (MPa)	Thickness (mm)	Internal Diameter (mm)	Longitudinal stress (MPa)
HDPE			
0.2	3.9	104	1.333
0.4	3.9	104	2.667
0.6	3.9	104	4.000
PVC			
0.2	3.0	104	1.733
0.4	3.0	104	3.467
0.6	3.0	104	5.200

Table 4-5: Pressure and stresses applied to pipe models in Abaqus

Cyclic simulations were also carried for the 1mm hole and 1mm by 10mm crack in both HDPE and PVC pipe. Cyclic simulations were carried out in the biaxial stress state for two loading and unloading phases. The pressure exerted on the pipe was increased from 0.2MPa to 0.4MPa and finally to 0.6MPa, before reducing the pressure to 0.4MPa and then 0.2MPa. This cycle was then repeated once more. Each pressure step duration was 100 000s.

The design procedure and model set up in Abaqus are described in detail in the next section.

4.2.2 Design procedure and model set up

The steps taken in carrying out the project are outlined here:

4.2.2.1 Pipe and leak opening geometry

Geometry of the pipe segments with one leakage opening for each pipe is generated in Abaqus. Each pipe was constructed as a solid extrusion, extruded from its inner and outer diameter cross-section. The length of the pipe extrusion was 500mm, which was the chosen length of the pipe segments.

Leak openings were then constructed in each pipe, one leak opening to each pipe model. The leak openings were located in the middle of the pipe segments. Leak openings were constructed as cut extrusions into the pipe from their sections. The leak opening sections were drawn from a datum plane above the pipe. Figure 4-1 below shows an example of a part created in Abaqus. The yellow dotted lines show the datum planes and line used for construction of the pipe.

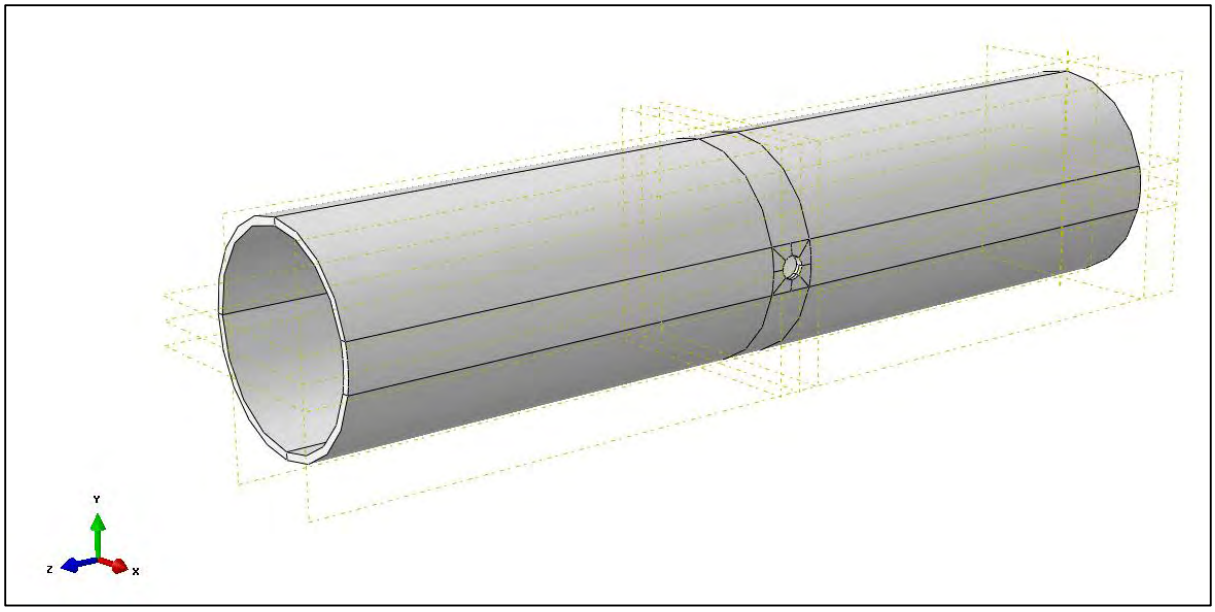

Figure 4-1: Pipe with a 12mm diameter hole in the part module (Source: Abaqus)

4.2.2.2 Section and material properties

Section properties were then assigned to the models in the property module. The models were defined as solid homogenous sections. Material properties were then edited accordingly and this involved entering the elastic and viscoelastic parameters for each model depending on the analysis. This investigation required the Young's modulus, Poisson's ratio, the dimensionless viscoelastic constant $\overline{g}_1^P$ and the relaxation time τ_ε of the material. These material constants were edited accordingly for each type of material.

4.2.2.3 Definition of analysis steps

The necessary steps were then defined in Abaqus step module for each model. Nine steps were required for each non cyclic investigation. These included the initial step, the elastic (instantaneous) deformation step and seven creep steps of different durations. The initial step is created by default in Abaqus as explained in section 4.1.4. The elastic deformation step for a viscoelastic analysis occurs at the first time step, 1s. The seven creep steps each had their own time durations starting from 10s and adding up to 100 000s for the last step. The default output requests were edited to include coordinates of the deformed leak opening and stress distribution. For the cyclic simulations, additional steps were added, changing the pressure applied at the appropriate times.

4.2.2.4 Meshing and partitioning technique

The models were then meshed appropriately. The meshing technique applied was the structured hex meshing technique. The type of element allocated to the models was the C3D20. These elements are quadratic brick elements with 20 nodes. The C320D element belongs to the family of serendipity elements. Serendipity elements are elements that have no nodes in their interior or in the middle of their faces (Abaqus Documentation). Elimination of the internal nodes reduces the size of the element functions therefore reducing computing power required. All nodes are located on the sides. Figure 4-2 illustrates a C3D20 element before deformation.

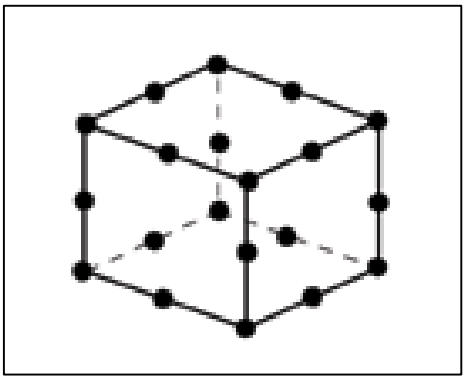

Figure 4-2: C3D20 un-deformed quadratic element with nodes (Source: Abaqus Documentation)

To use the hex meshing technique, each model had to be partitioned so that Abaqus could generate a mesh. An example of a partitioned model is shown in figure 4-1 above. After appropriate partitioning the model is coloured green in the mesh module to indicate that Abaqus can generate a mesh with the hex technique. The partitioning technique employed aimed at separating the pipe models into regions as seen from the figure 4-1. The leak opening is contained in a cell which is further partitioned to generate a mesh pattern as seen in figures 4-3 and 4-4 below.

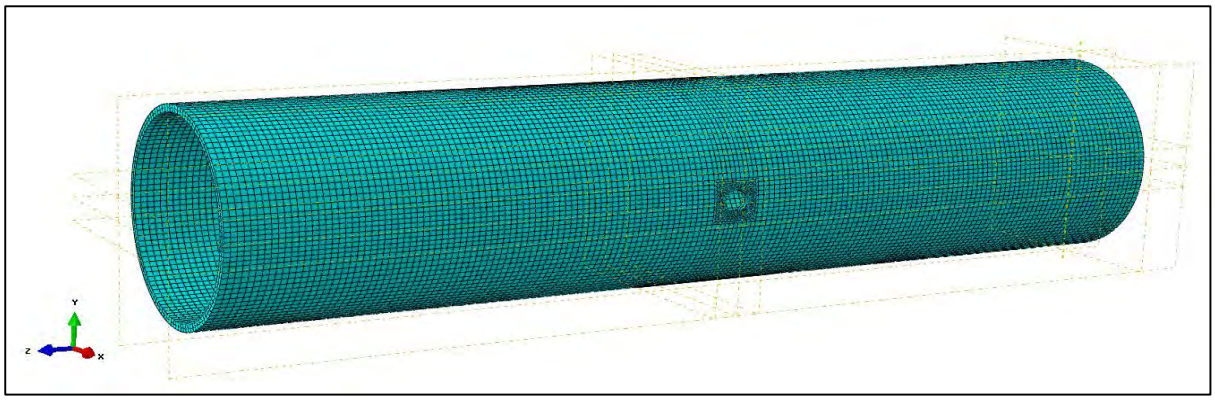

Figure 4-3: Mesh pattern on a pipe section before deformation (Source: Abaqus)

Mesh seed sizes were chosen after a sensitivity analysis which was carried out for each model since crack sizes varied. The purpose of the sensitivity analysis was to determine the global seed size for the model. The seed sizes at the leak were also allowed to vary during the sensitivity analysis. Automatic verification checks were carried out in Abaqus to ensure that there no distorted elements and analysis warnings. The final seed sizes were chosen taking into account the verification checks and sensitivity analysis.

The partitioning strategy used also ensured that seed sizes were smaller at the leak opening. This meant that the area of deformed leak openings could be measured accurately since the leak boundary has more nodes and therefore co-ordinates. The small sizes of elements at the leak opening were not used for the entire pipe in order to save computational time and memory. Due to this size difference, verification checks were necessary to make sure that there were no distorted elements near the leak opening. The figure 4-4 below illustrates the different mesh patterns of the pipe and around the leak opening.

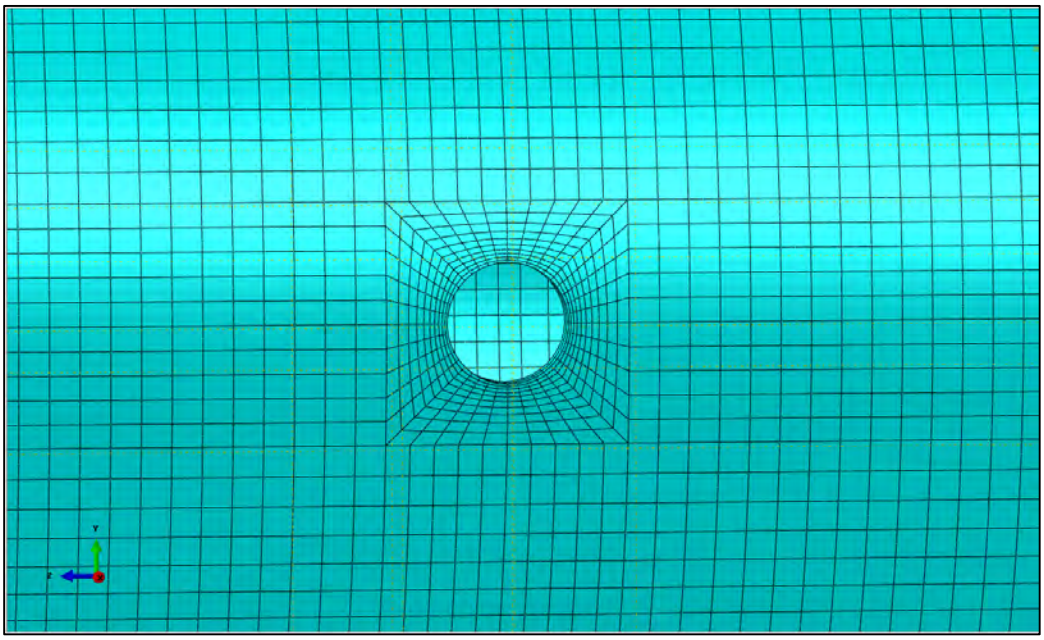

Figure 4-4: Mesh pattern around a 12mm round hole opening before deformation

(Source: Abaqus)

4.2.2.5 Load application and boundary conditions

The next step was to apply the respective loads and boundary conditions to the models. For each model, an internal pressure was applied to the pipe. To simulate the uniaxial state only the internal pressure was needed. For the biaxial stress state, an additional longitudinal stress as calculated from

equation (2.2) was also applied to the pipe ends. The value of the load was changed according to the analysis carried out, that is, 0.2MPa, 0.4MPa or 0.6MPa.

Two boundary conditions were required in this project to prevent rotation and translation of the pipe. These boundary conditions were located in such a way that their effect on the leak opening deformation would be minimised. They included:

i. Fixing an internal line on the pipe directly opposite the hole in the x and y directions.
ii. Fixing a point adjacent to the internal line on the exterior of the pipe in the x, y and z directions.

The two boundary conditions are illustrated in the figure 4-5 below with orange and blue arrows.

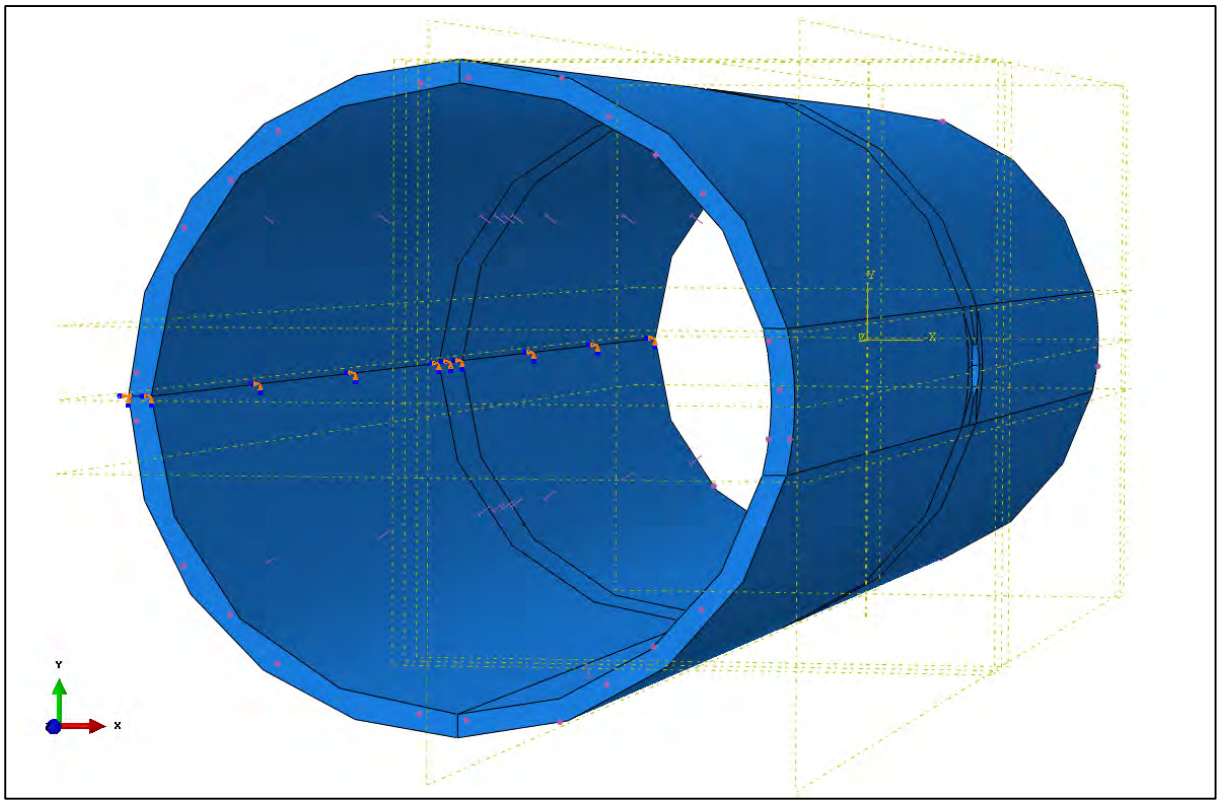

Figure 4-5: Positions of the boundary conditions (Source: Abaqus)

4.2.2.6 Job definition and submission

After loads and boundary conditions are allocated, a job is created in Abaqus so as to run the simulations.

4.2.2.7 Results analysis

The deformation results were stored in different directories for future reference. A python script was implemented at the end of each job to measure the area of the deformed leak opening. The python script which is included in the appendix extracts the boundary co-ordinates of the deformed leak opening at the end of the analysis steps and projects them onto a flat surface for area calculation. The script extracts deformed co-ordinates after the elastic and all the creep steps.

The above steps were carried out for every leak opening and the deformed areas were recorded in MS Excel for further analysis.

4.2.3 Assumptions

The following assumptions were made in this project:

i. Stresses applied on pipes are only due to the water pressure inside the pipes. Stresses that may result from external loads such as surrounding soil and traffic are ignored.
ii. The stress distribution near the leak opening is not affected by the ends of pipe and the boundary conditions.
iii. The two materials (PVC and HDPE) investigated are assumed to be linear viscoelastic materials based on the literature review. Both materials contain amorphous and crystalline regions to varying degrees and their properties vary with time and temperature. Hence the parameters for the Prony series were derived using the standard linear model which is a linear viscoelastic model.

For calculating the viscoelastic parameters, Young's modulus at 0 seconds (E_0) was assumed to be equal to Young's modulus at 3mins. This is because the data that was derived from Janson (2003) only provided 3mins as the shortest recorded time period for stress-strain data.

4.2.4 Sensitivity Analysis procedure

The purpose of the sensitivity analysis was to determine the appropriate mesh seed sizes for both the PVC and HDPE models. Since the two materials have different thicknesses, it was unlikely that the same seed size would be appropriate in each. A further sensitivity analysis in conjunction with mesh verification checks in Abaqus determined the mesh seed size for elements surrounding the hole. The sensitivity analysis was therefore carried out in two phases.

The first phase aimed at finding a suitable size for the global seeds of the whole model. For this, an arbitrary point that did not lie along the positions for the boundary conditions or the leak opening was chosen and noted as a set "out." Various mesh seed sizes were allocated to the model and

elastic deformation simulations carried out. The stress at the point "out" was noted for each seed size. The seed sizes were reduced from 12 or 10 to 3 or 2 depending on the model. The final seed size was determined at a point where the stresses started converging.

The second phase aimed at finding the suitable seed size surrounding each leak opening. The size of the elements in the leak vicinity was determined by the default size allocated by Abaqus while carrying out verification checks. This is because partitioning strategy and meshing technique applied did not allow for seed size variation for the hole without forming a poor quality mesh in the rest of the pipe. The size allocated during the global sensitivity analysis was taken as the final mesh size.

Sensitivity analysis for the 1mm by 80mm longitudinal cracks was carried out as described above however with a different meshing technique. Due to the length of the crack and meshing technique the elements at the crack tips were severely distorted and therefore a swept mesh technique was used for these cracks as shown below in figure 4-6. The mesh was verified to check for analysis warnings and errors.

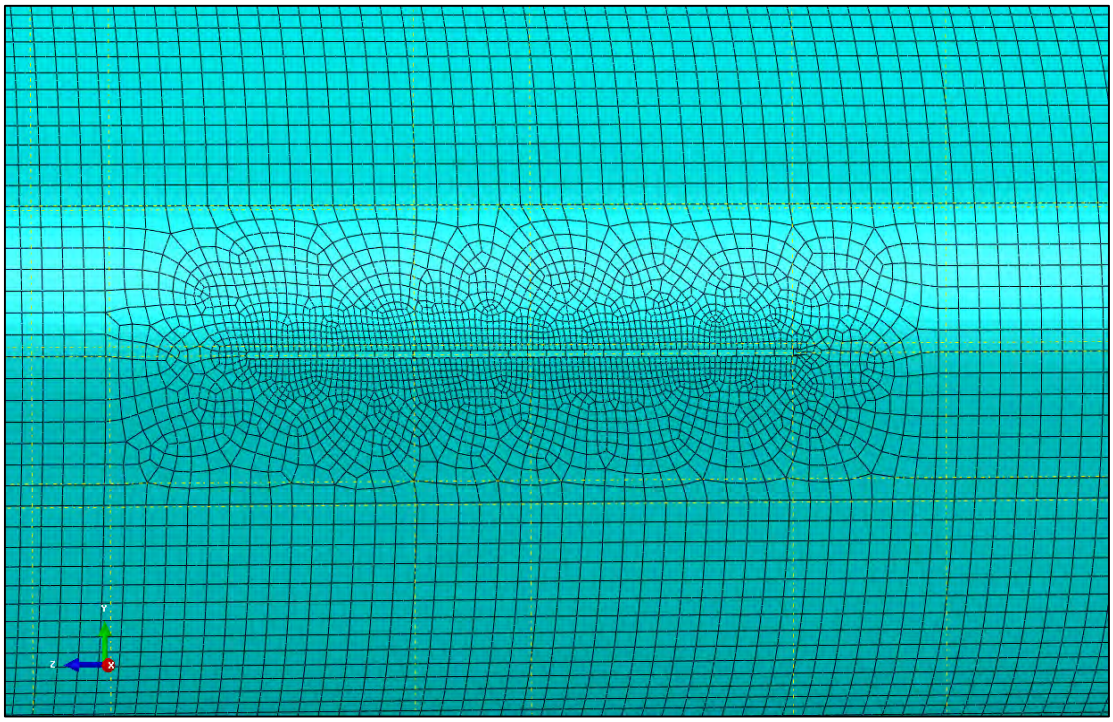

Figure 4-6: Swept mesh pattern around the 1mm by 80mm longitudinal crack (Source: Abaqus)

4.2.5 Estimation of leak hole area after deformation

One of the objectives of this project was to determine the area of leak openings after deformation due to an applied pressure. Therefore there was need to establish a method that would enable accurate calculation or measurement of the area.

The area of the leak hole could not be determined in Abaqus without a certain degree of post-processing of the results. This is due to the fact that Abaqus is designed to extract mass properties of elements and not of empty space/holes. This problem was solved by obtaining the coordinates of the leak hole boundaries and saving them to a set named “HolePerimeterOD.” The set is illustrated in the figure 4-7 below as a red circle on the inner surface of the pipe.

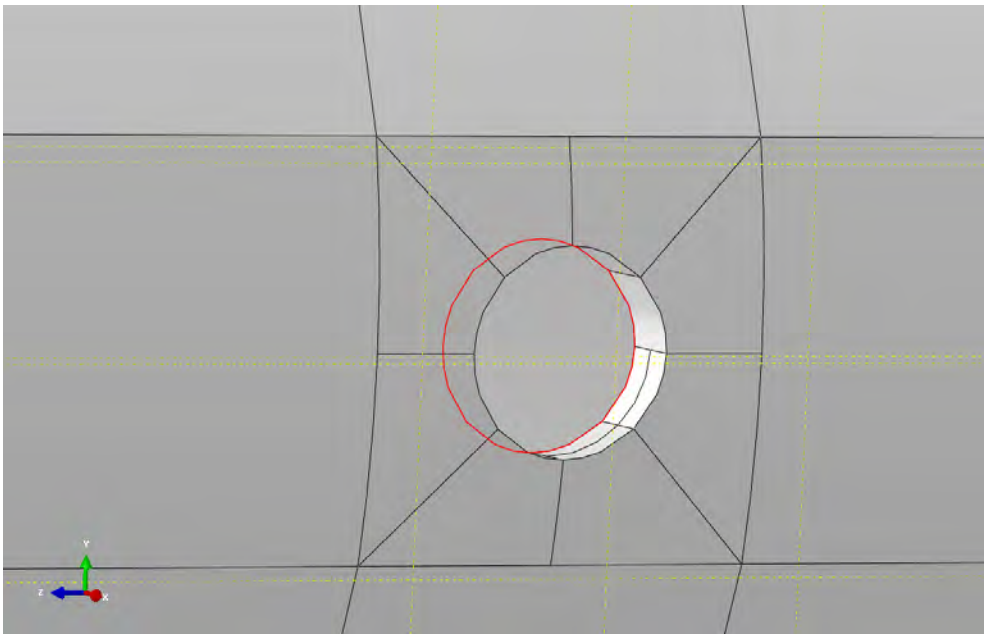

Figure 4-7: Illustration of set "HolePerimeterOD" for a 12mm hole (Source: Abaqus)

A python script was then written to project these boundary coordinates onto the y-z plane from which the projected area was calculated by Abaqus.

The python script ensured that all areas were calculated in the same way, leaving no room for errors that could occur if one was to manually export the coordinates to a drawing program such as AutoCAD. The python script was also efficient in that one was able to increase the number of elements and nodes at the hole boundary whilst reducing the time spent and possible errors in exporting the coordinates to AutoCAD format. Due to the use of a boundary set, all nodes that

surrounded the leak opening were included in the area calculation. Without the script, it was very easy to miss a few nodes and hence introduce error in the area calculation.

4.2.6 Rectangular block analysis

A simple rectangular block analysis was carried out in Abaqus to give an overview of elastic and viscoelastic deformation without the influence of complex geometry like the leak openings in pipes. The dimensions of the rectangular block were 200mm x 20mm x 25mm. The block is illustrated in the figure 4-8 below.

The block was designed to be of HDPE material, with the same property values listed in table 4-1. The block was allocated a uniform mesh seed size of 5, with the same C3D20 elements. Tensile stresses of 0.2MPa, 0.4MPa and 0.6MPa were applied in turns to the ends of the block as illustrated by the purple arrows in the figure 4-8 below. Both elastic and viscoelastic simulations were carried out as for the pipe models. Viscoelastic simulations were carried out for 1s, 10s and 100s.

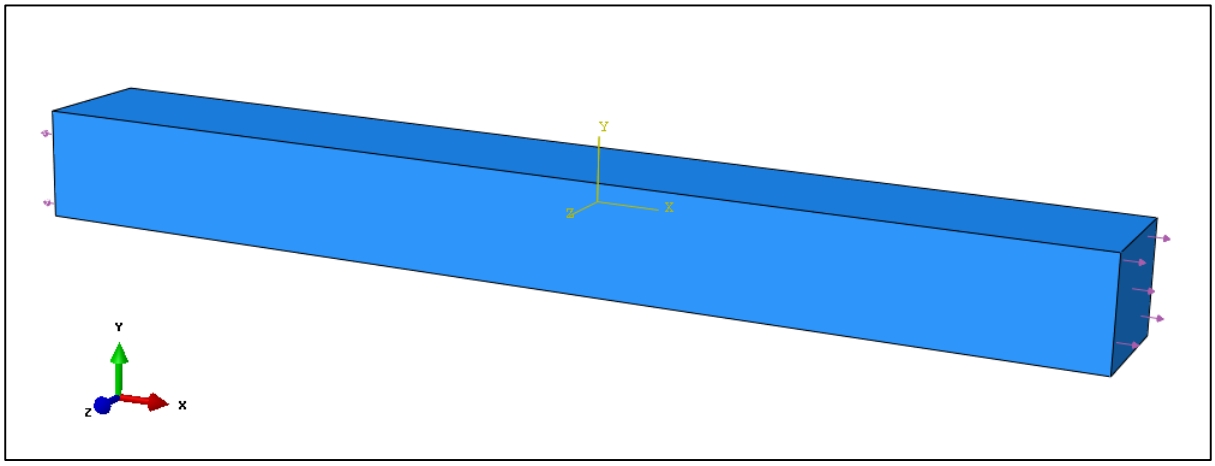

Figure 4-8: Rectangular block with tensile load at the ends (Source: Abaqus)

For each simulation, a graph of load against strain was plotted on the same graph. The strain was calculated as follows:

The length (l) of the deformed block was noted after each simulation and the extension (e) was calculated as using

$$e = l_0 - l, \tag{4.2}$$

where; l_0 is the original length and l is the deformed length. The strain of the block in the longitudinal direction is then calculated from

$$\varepsilon = \frac{e}{l_0} \tag{4.3}$$

where; ε is the strain.

A full analysis of the rectangular block results is included in Chapter 5.

In summary, chapter four is an account of the method followed to achieve the objectives of this project with the help of the Finite Element Method (FEM). The background of FEM in different fields such as mathematics, physics and engineering was described. Finite element methods have been implemented for various uses in commercially available software. The finite element software used for this investigation was Abaqus. The modules of the Abaqus software and how it is used to analyse viscoelastic behaviour were also discussed. Thereafter, the specifications of the pipe models and materials were described. The setup of the models was also included step by step. The results were collected by the use of a python script. A simple rectangular block was also analysed as HDPE material to give an idea of how the viscoelastic results would vary with time. Chapter five presents the results collected, how they were analysed and includes a discussion at the end of the chapter.

5 Results analysis and discussion

The results analysis and discussion chapter is an account of the results of the model set ups and simulations which were outlined in the methodology chapter. When a pressure was applied to each pipe model, the leak holes deformed due to the resulting stress distribution in the pipe. Stresses in the pipe differed according to the pressure load applied and time step. A discussion of all the results is also included.

After each simulation was completed, the area of the deformed leak hole was obtained with the help of a Python Script as described in chapter four. The deformed area for each pressure load, loading state and time step is noted. In the results chapter, the deformed areas are presented and analysed with the help of MS Excel. Further analysis is also carried out to show how the pressure-leakage relationship is affected by the change in area. Parameters of this relationship such as the leakage exponent and gradient variation are also investigated and discussed. Cyclic creep results are also included.

For each leak opening and simulation, the following graphs are presented and analysed:

i. Deformed area against time
ii. Deformed area against pressure
iii. Percentage change in area against pressure
iv. Leak discharge against time
v. Leak discharge against pressure
vi. Gradient (m) against time
vii. Leakage exponent (N1) against time
viii. Ratio of creep strain to elastic strain against time
ix. Pressure and area against time for cyclic loading.

For each of the graphs of deformed area against pressure and leak discharge against pressure, trend lines with best fit were assigned. The best fit is determined by the use of the R squared value as calculated by MS Excel. An R squared value of 1 describes a perfect correlation of data while an R squared value of 0 means there is no correlation. The equations for each area-pressure relationship and discharge-pressure relationship are obtained since the gradients (m) and powers (N1) are required for further analysis. For the time graphs, data labelled “elastic” means a time duration of 0s while data labelled “visco” refers to creep analysis with the indicated duration in seconds.

The results for the rectangular block are discussed first followed by the round holes and finally the longitudinal cracks.

5.1 Rectangular Block

As explained in the chapter 4, a simple rectangular block was modelled to provide an overview of the effects of lengthening time periods on the deformation of a viscoelastic material. An HDPE block (figure 4-7) with no cracks or hole was modelled, with a uniform mesh seed size of 5. A structured mesh technique was applied, and quadrilateral elements were assigned to the block. Tensile stresses of 0.2MPa, 0.4MPa and 0.6MPa were applied to the ends of the block.

An elastic deformation simulation was carried out as well as a viscoelastic simulation for creep. The final length of the block was measured after elastic deformation and creep deformation at 1s, 10s and 100s. The strain in the x direction of the block was computed from equation (4.3) and a graph of load against strain was derived as shown in figure 5-1 below. For each simulation, a linear trend line is fitted to the data as illustrated in figure 5-1, with the corresponding equation and the R squared value. The results for the rectangular block are illustrated below in figure 5-1.

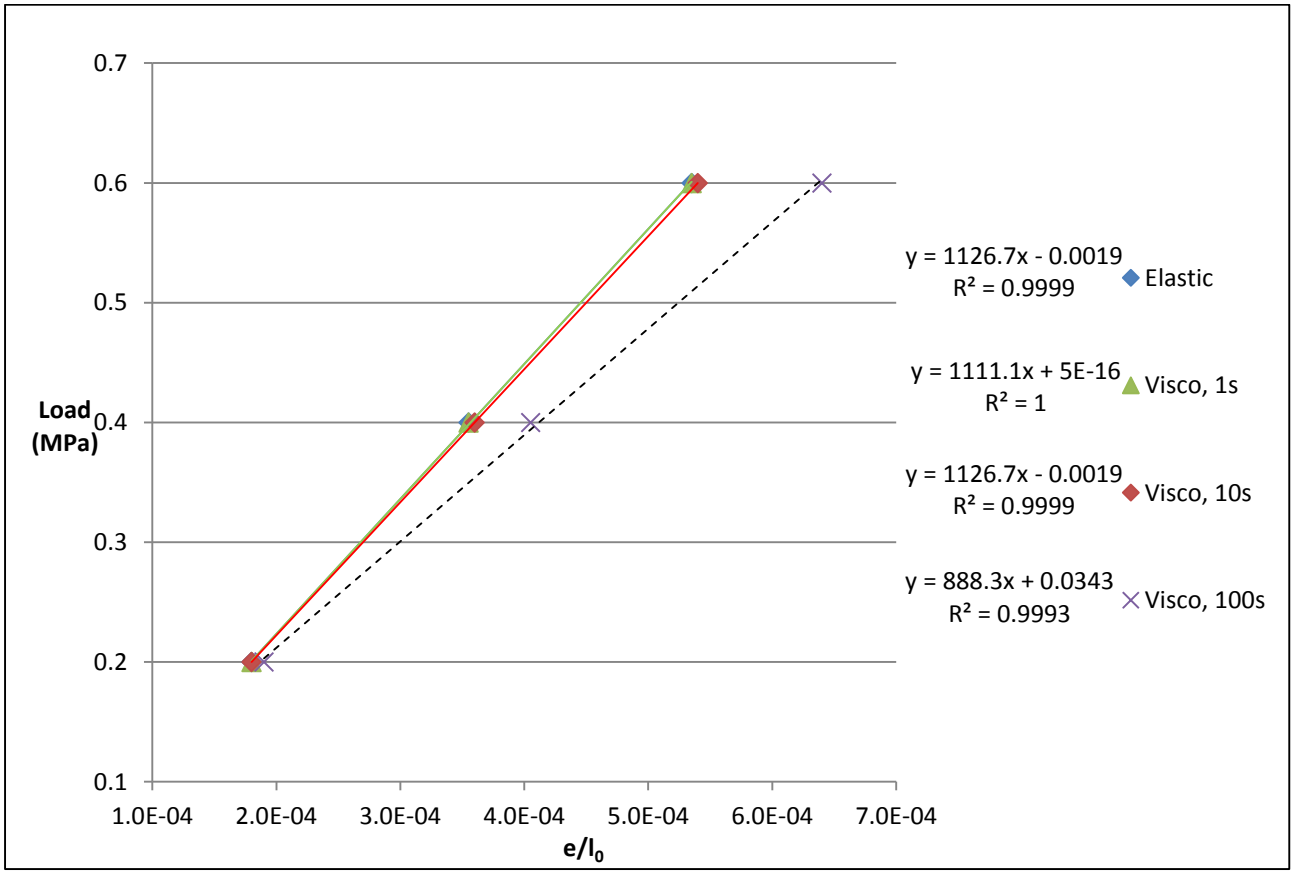

Figure 5-1: Load against strain for the rectangular beam section

In the figure 5-1, it is observed that the data for both elastic and viscoelastic simulations is adequately described by linear relationships and the R squared values are above 0.999. It is also observed that the total strain for viscoelastic deformation exceeds the elastic strain results, which is expected since the elastic modulus used is the instantaneous elastic modulus (E_0). An instantaneous modulus is measured at a time period of 0s.

Furthermore, it is observed that the elastic deformation line and the creep deformation lines of 1s and 10s are very close to each other. This is expected since the elastic analysis for this project was carried out with an instantaneous elastic modulus, that is, elastic modulus measured at 0s. Viscoelastic deformation for this project is therefore a total of the instantaneous elastic deformation and the creep deformation that occurs over a set time period. Hence, the viscoelastic analysis gave larger deformations compared to the elastic deformation analysis. Also, the total deformation for the rectangular block increased with time. These observations provided a guide to the expected viscoelastic deformation behaviour of the pipe models.

5.2 Sensitivity analysis results for pipe models

5.2.1 Global seed (element) size of pipe models

As explained in the methodology chapter, the sensitivity analysis was carried out in two phases. The first phase was to determine the global seed size, while the second phase determined the size of the elements at the crack/hole site. Since the pipe lengths were the same for all crack types and materials, only one global sensitive analysis was carried out for each of HDPE and PVC. This was done by allocating seed sizes to the entire model and noting the stress at a certain point (set out) after an elastic deformation simulation.

The seed sizes were decreased from 12mm while keeping the set out at a constant location on the pipe models. The final seed size was taken at the point where the stress at the set "out" started converging. The applied stress during the sensitivity analysis is 0.2MPa. The results of this sensitivity analysis procedure are illustrated in the graphs below, figures 5-2 and 5-3.

Figures 5-2 and 5-3, show that the stresses for different seed sizes started to converge at seed size 4mm. The final seed size was chosen as 3 which was appropriate for both HDPE and PVC pipes whose thicknesses were 3.9mm and 3mm respectively. This was true for all models with their individual leaks.

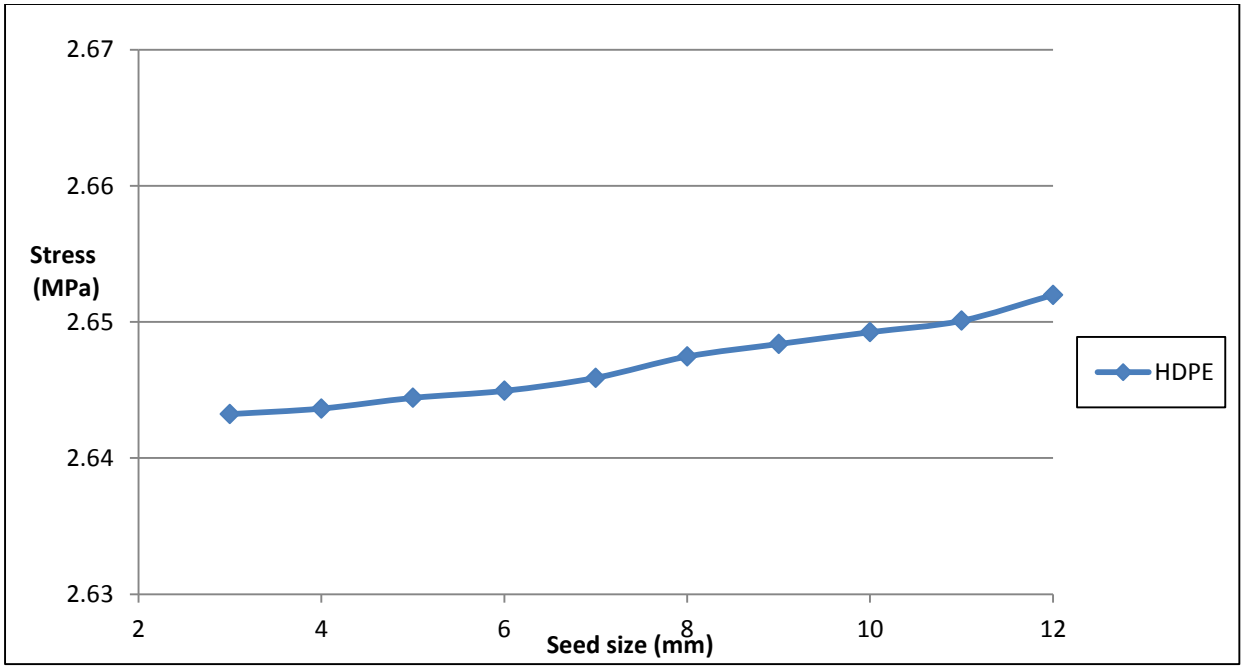

Figure 5-2: Sensitivity analysis graph of stress at set out against global seed size for HDPE

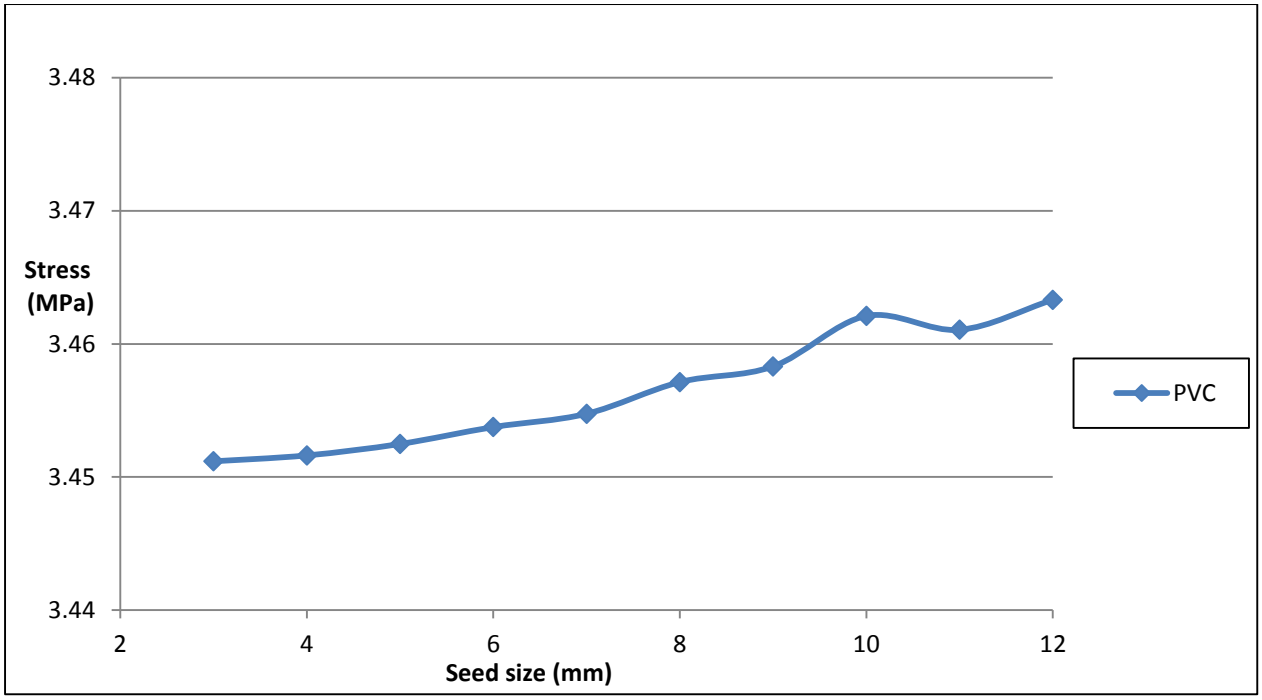

Figure 5-3: Sensitivity analysis graph of stress at set out against global seed size for PVC

5.2.2 Seed (element) size for elements at leak

The size of the elements was determined by the default size allocated by Abaqus during the global sensitivity analysis for each model. This is because partitioning strategy and meshing technique applied did not allow for seed size variation for the leaks without forming a poor quality mesh in the rest of the pipe. The seed size for the holes was therefore 0.39mm for both HDPE and PVC. Since 0.39mm is small compared to the pipe thickness and diameter of the hole, it was regarded as acceptable.

For the longitudinal cracks, the default size allocated by Abaqus was applied. The elements at the crack tip were 0.39mm and the elements along the crack length were 1mm.

5.3 Detailed simulation results for 1mm round holes

Round holes of diameter 1mm were investigated in both HDPE and PVC pipe materials under two different loading states namely uniaxial and biaxial state. This section is an account of the stress distribution and pressure analysis results obtained from the investigations.

5.3.1 Stress distribution

The leak hole deformations are a result of the stress distributions within the pipe models during the pressure simulations. The stress distributions in Abaqus are viewed with the help of a colour legend. In the figure 5-4 below, the maximum stresses in the pipe are observed at the opposite ends, of the hole's inner edges in the Z direction. Minimum stresses occurred at the opposite ends in the y direction. The blue colour indicates minimum stresses while the red colour indicates maximum stress as is indicated in the colour legend. The hole deforms into an elliptical shape as a result of the stress distributions in the pipe. The deformations were scaled to improve visibility of actual deformations.

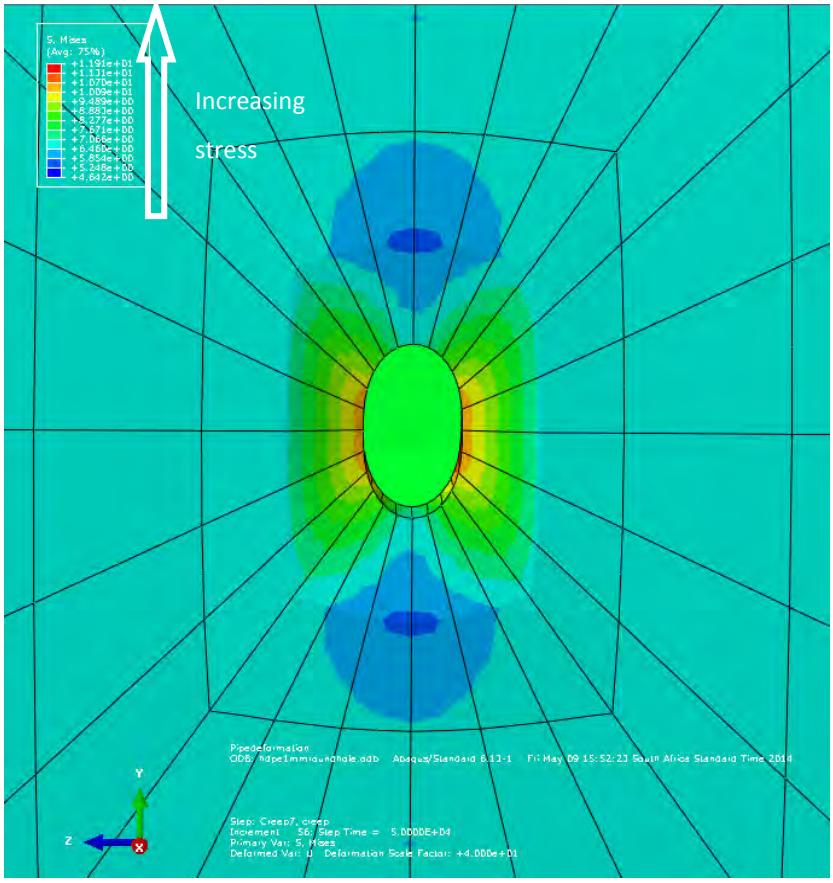

Figure 5-4: Stress distribution around a deformed 1mm round hole, HDPE, deformation scale factor = 40 (Source: Abaqus)

A similar stress distribution pattern was observed for all round holes analysed in this project, both HDPE and PVC pipe. The round holes deformed into elliptical shapes, however exact stress values differed for each pipe material, applied pressure and leak type.

5.3.2 Variation of leak area with time

As outlined in the methodology chapter, internal pressures of 0.2MPa, 0.4MPa and 0.6MPa were applied to the pipe models in turn for a total time of 100 000s. The deformed areas for both the uniaxial and biaxial load states were noted after applying each pressure for time periods of 0s, 10s, 100s, 1000s, 5000s, 10 000s, 50 000s and 100 000s.

For each pressure, an instant elastic deformation was observed, followed by creep deformation due to the viscoelastic properties of the pipe material. In the figure 5-5 below, the deformation of a 1mm hole in HDPE pipe in the biaxial state at 0.6MPa is illustrated. The un-deformed area (7.832E-7m^2) of the hole is also shown as a straight purple line. The elastic and creep deformations of the hole are also illustrated.

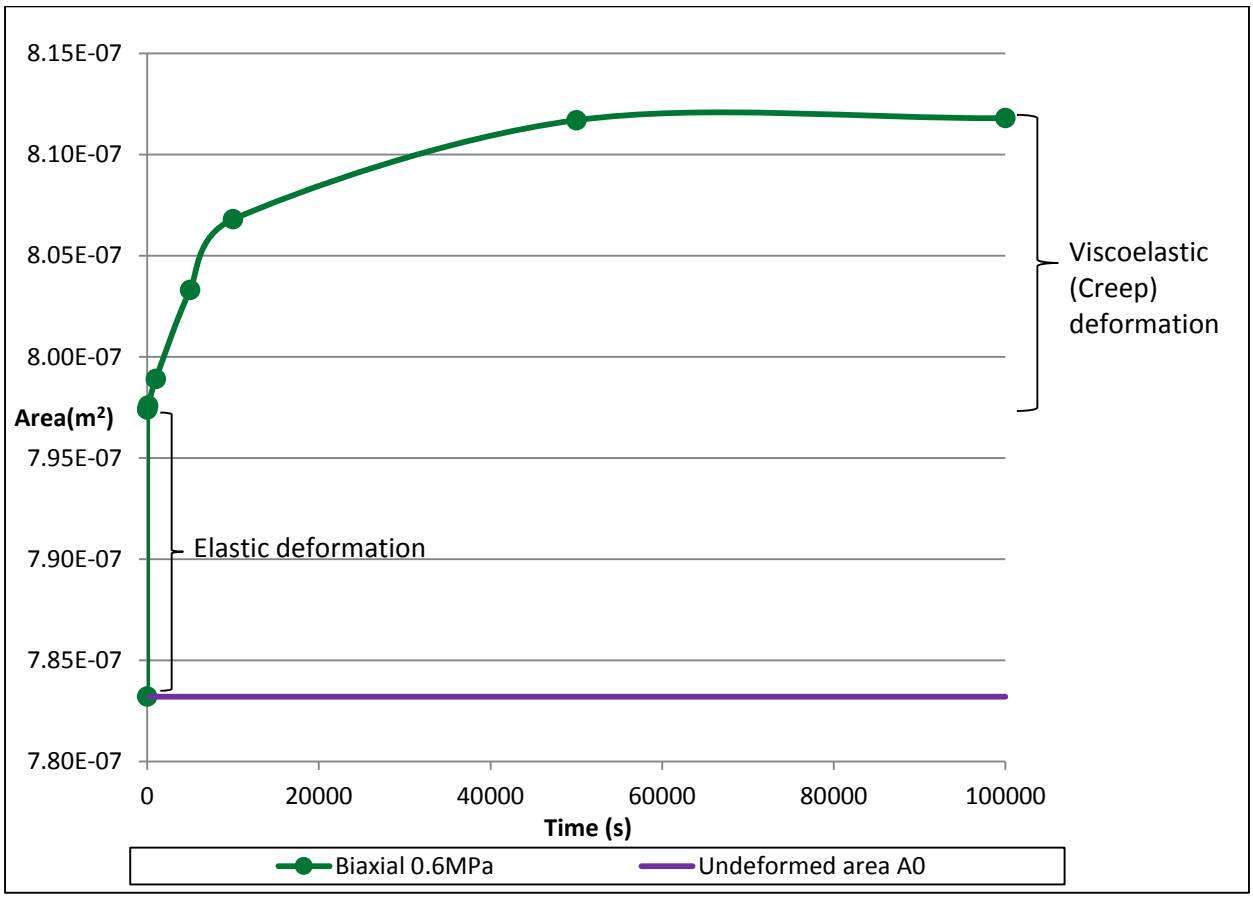

Figure 5-5: Area against time for 1mm round hole in HDPE at 0.6MPa, biaxial state

Additionally, it was observed that the deformed leak area due uniaxial loading was less than that due to biaxial loading. This was true for both elastic and creep deformations, as illustrated in figure 5-6 below. A similar pattern was observed for all round holes whose full results are included in the appendix.

In the figures 5-5 and 5-6, it was noted that the lines obtained in MS Excel did not illustrate the deformation behaviour of the leak accurately. The deformed leak areas stabilised at 50 000s and 100 000s and therefore the line should be straight in-between the two times. The line drawn by Excel is therefore not a good approximation. This should be noted for all subsequent graphs. More time steps should have been recorded, ideally at 30 000s.

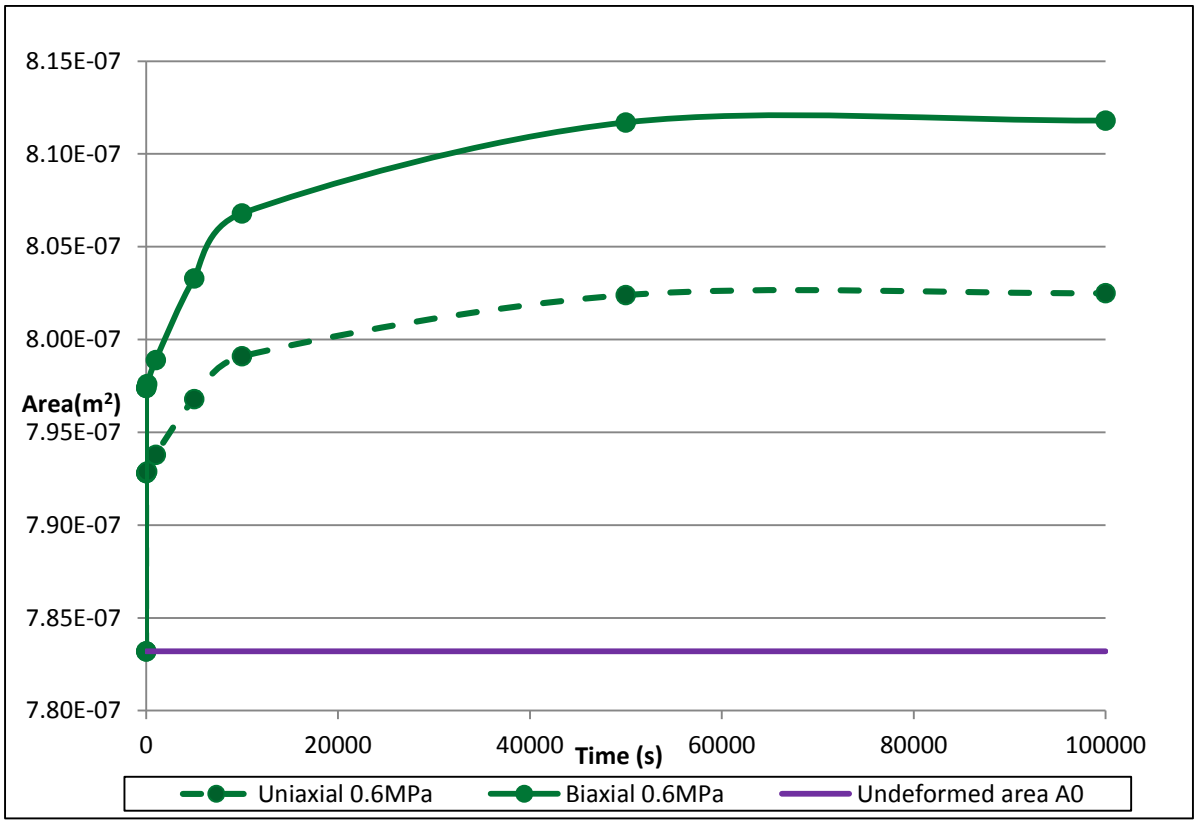

Figure 5-6: Area against time for 1mm round hole in HDPE, at 0.6MPa, uniaxial and biaxial states

The leak area deformations increased with pressure. For each pressure applied, the uniaxial state deformations were lower than that of the biaxial state deformations. This illustrated in figure 5-7 below. Each pressure was applied on to the pipes for the time periods mentioned above and the corresponding leaks areas obtained. The graph in figure 5-7 therefore illustrates how the area varied after a pressure is applied for a certain length of time. A summary of the exact areas for each time

period and load state is presented below in table 5-1. Similar figures and tables are included for all round holes in the relevant appendices.

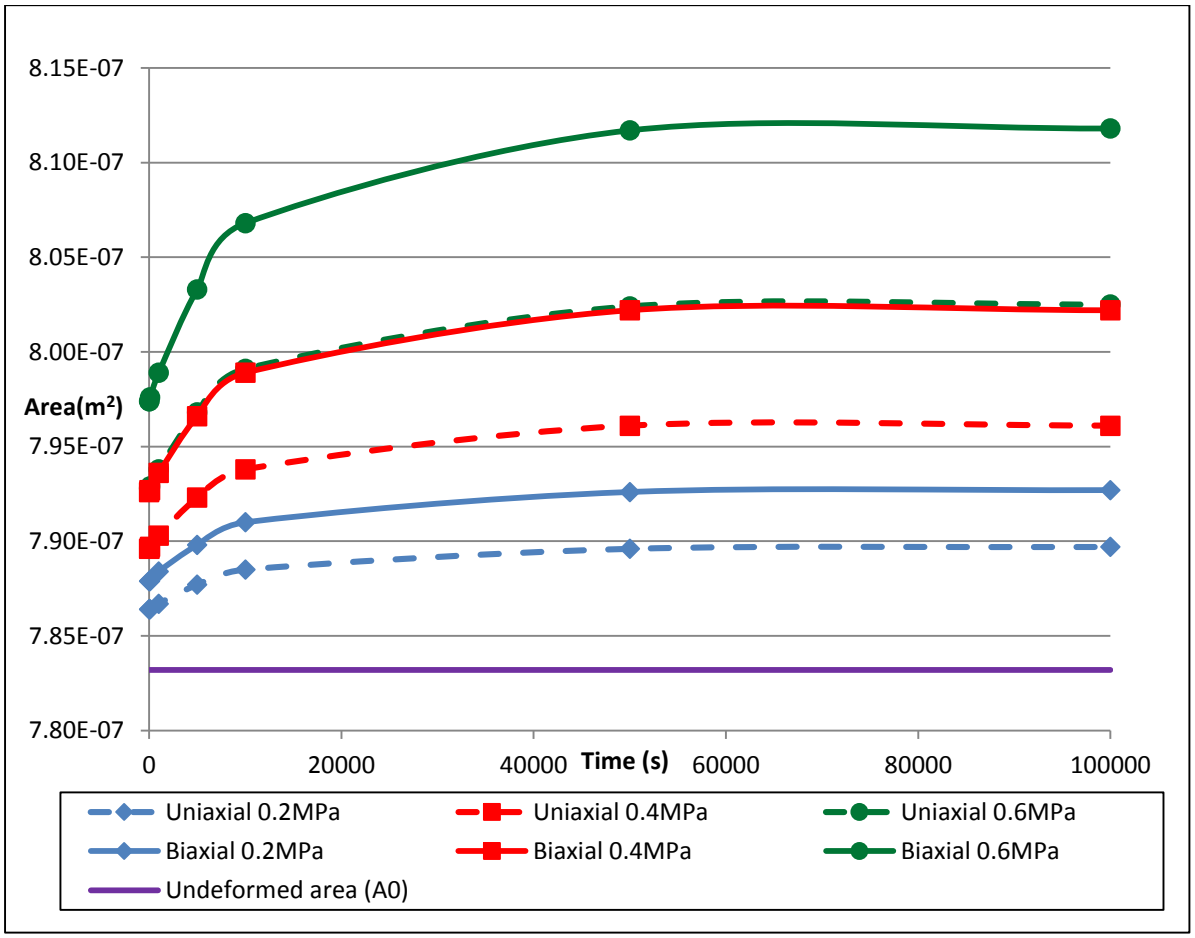

Figure 5-7: Area against time for the 1mm hole in HDPE, all pressures

HDPE	Area of deformed holes with A_0 =0.7832mm²					
Pressure (MPa)	0.2		0.4		0.6	
Time (s)	Uniaxial	Biaxial	Uniaxial	Biaxial	Uniaxial	Biaxial
0 (Elastic)	0.7864	0.7879	0.7896	0.7926	0.7928	0.7974
10	0.7864	0.7879	0.7896	0.7927	0.7928	0.7974
100	0.7864	0.7879	0.7897	0.7927	0.7929	0.7976
1000	0.7867	0.7884	0.7903	0.7936	0.7938	0.7989
5000	0.7877	0.7898	0.7923	0.7966	0.7968	0.8033
10 000	0.7885	0.7910	0.7938	0.7989	0.7991	0.8068
50 000	0.7896	0.7926	0.7961	0.8022	0.8024	0.8117
100 000	0.7897	0.7927	0.7961	0.8022	0.8025	0.8118

Table 5-1: Deformed areas for the 1mm hole in HDPE

Deformed areas for the 1mm hole in PVC pipe were observed to be less than the HDPE leak holes for the same pressure and load state conditions. The un-deformed area for the 1mm hole in PVC was also 7.832E-07m^2. The difference in area of the deformed leak holes can be attributed to the different material properties of HDPE and PVC materials. For example, the PVC pipe for this project has a higher elastic modulus and hence requires a greater load to obtain the same amount of deformation as the HDPE pipe. The uniaxial deformed areas for the 1mm hole in HDPE and PVC pipe are illustrated below in the figures 5-8 and 5-9 respectively.

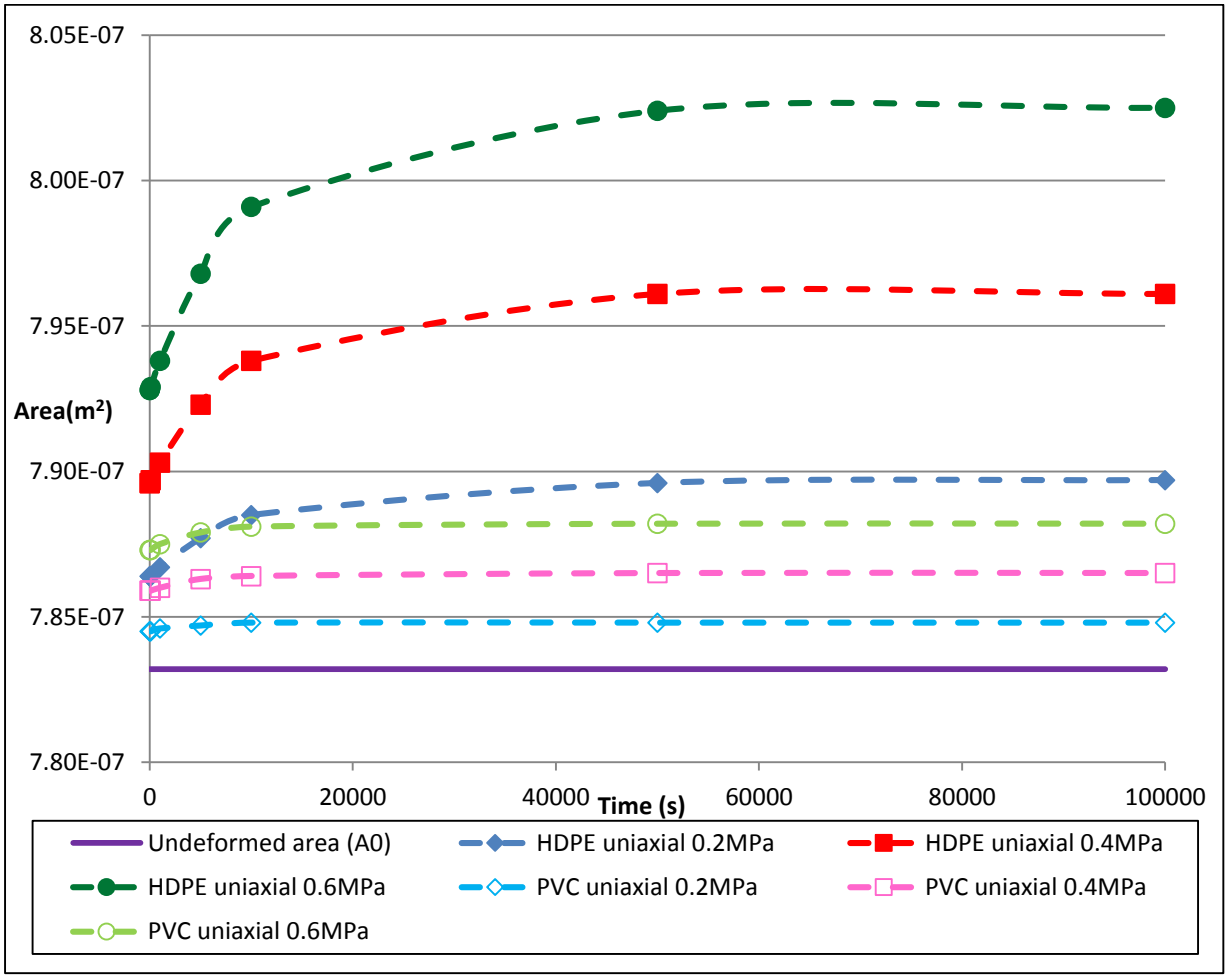

Figure 5-8: Area against time for 1mm holes in HDPE and PVC, uniaxial

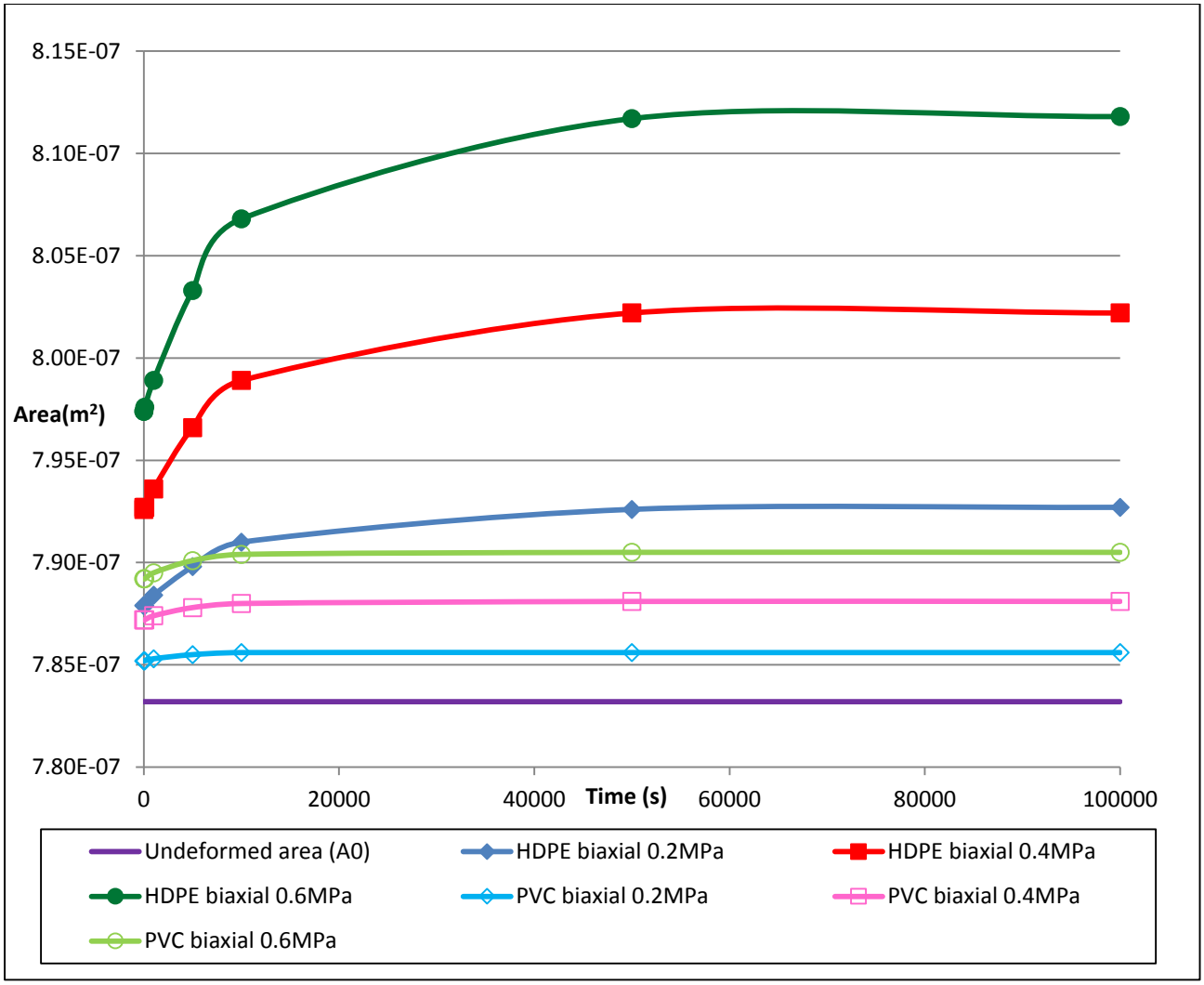

Figure 5-9: Area against time for 1mm holes in HDPE and PVC, biaxial

In figures 5-8 and 5-9, the deformed area in HDPE is seen to range from 0.785mm^2 to 0.815mm^2 while the hole in PVC ranges from 0.784mm^2 to 0.791m^2. All pipes were subjected to the same loading conditions.

Furthermore, creep deformation hole areas are observed to have stabilised by 100 000s after an initial increase occurring from 0s to about 10 000s. This deformation behaviour pattern is characteristic of linear viscoelastic materials undergoing creep as described in the literature review chapter 3. Since HDPE and PVC were modelled as viscoelastic materials, this is an expected result. Graphs illustrating deformation of all leak types are included in the appendices B to K.

5.3.3 Leak area-pressure head relationship

The deformed leak hole areas were then plotted against the corresponding pressure for each creep time period and also elastic deformation. The creep graphs are labelled “visco” with the creep time duration in seconds.

A linear relationship offered the best fit for the leak area-time data for both elastic and viscoelastic results. The high R squared values (0.999 to 1) show that the area and pressure are strongly correlated. In figure 5-10 below, the area-pressure relationships for the 1mm hole in HDPE pipe, uniaxial state are shown. The lines in the figure 5-10 show the leak areas after the different pressures have been applied for specific time periods. The straight lines show that if pressures are varied for constant time periods, the leak area varies linearly with the pressure applied. For each time period, the linear equations and the R squared values are shown as obtained in MS Excel.

Since the leak area-pressure relationships for each time period are linear, the gradient (m) for each time tested was obtained for further analysis.

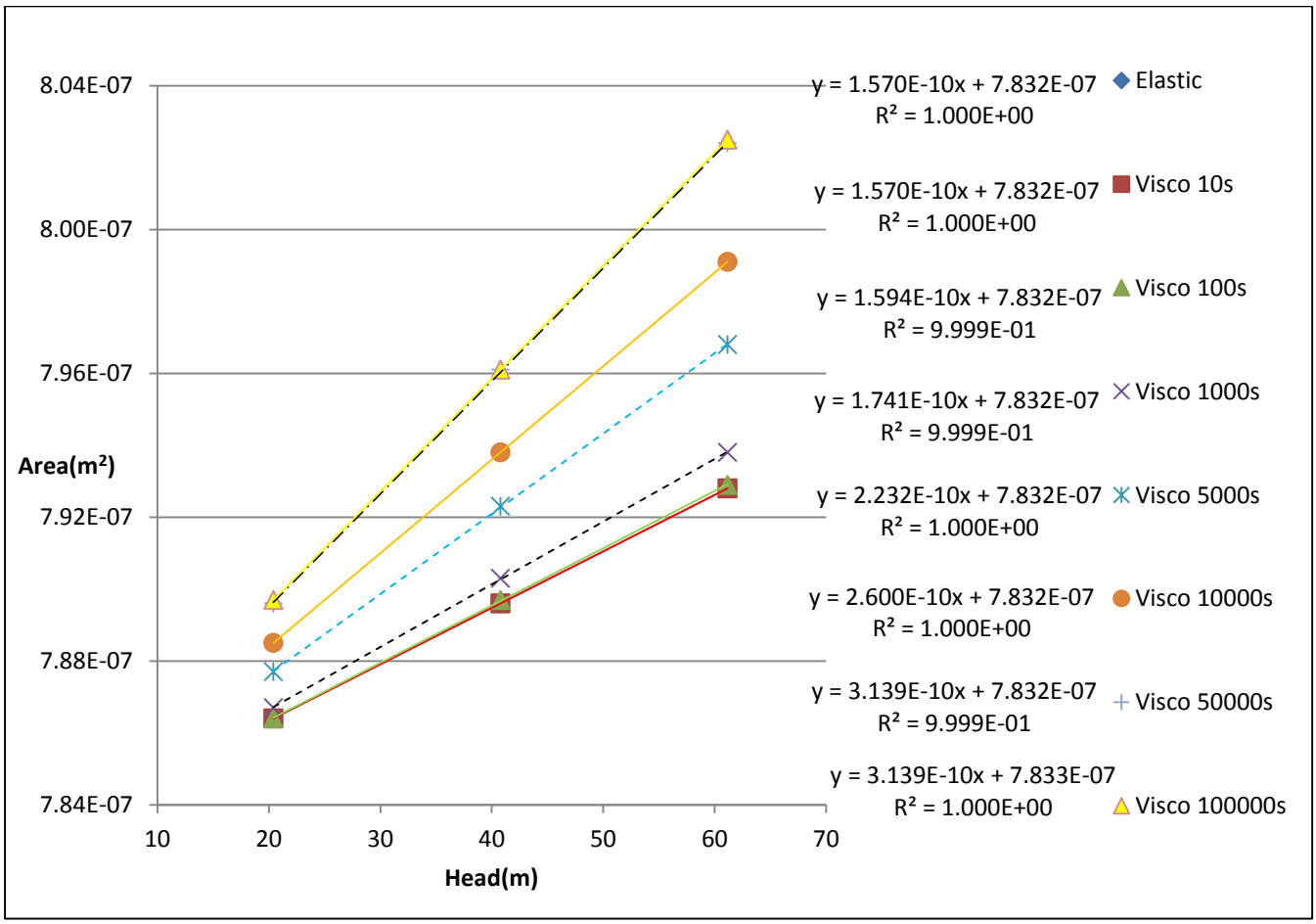

Figure 5-10: Area against pressure for 1mm hole in HDPE pipe, uniaxial state

The gradients for each time including elastic deformation (time = 0s) were obtained from the corresponding linear equation for further analysis. From figure 5-10, it is observed that the gradient increased with time. Similar graphs were plotted for all other round holes and load states and are included in the relevant appendices.

5.3.3.1 Gradient (m) of the leak are-pressure head relationship

The gradient (m) for each time period, leak type and material were plotted for further analysis. Figure 5-11 below illustrates the relationship between gradient and time for 1mm round holes in HDPE and PVC. From figure 5-11, it is observed that gradient of the 1mm diameter hole in HDPE is higher than gradient for 1mm diameter hole PVC pipe. Also, gradient for the uniaxial load state is lower than gradient for the corresponding biaxial state.

In figure 5-11, the curves representing the relationship between m and time are similar to the creep deformation curves for viscoelastic materials described in the literature review. This indicates that the gradient, a parameter of the pressure-leakage relationship is influenced by the viscoelastic behaviour of HDPE and PVC pipe materials.

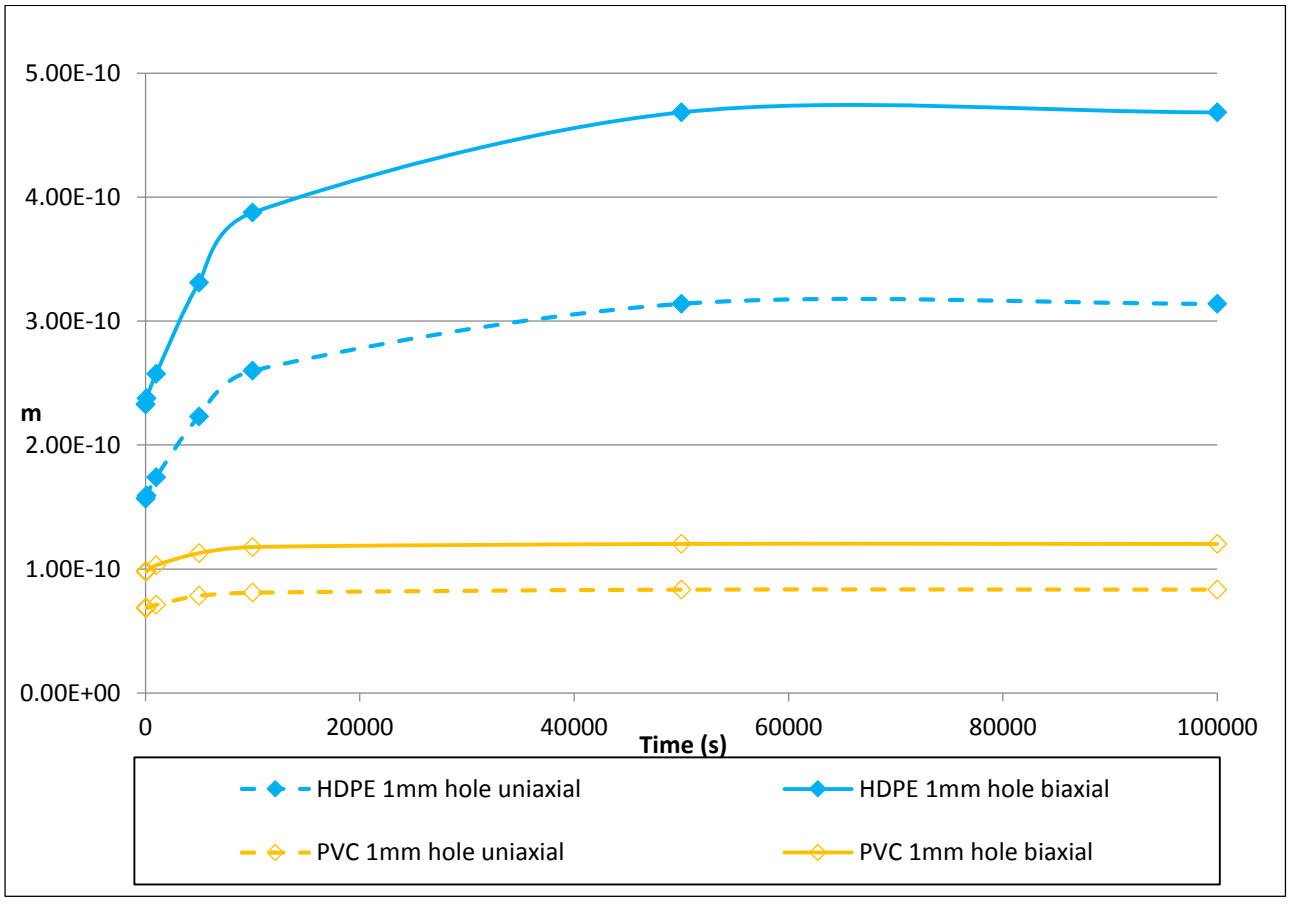

Figure 5-11: m against time for the 1mm hole in HDPE and PVC

5.3.4 Leakage exponent (N1)

To estimate the leakage exponent (N1) for the leak holes, the leakage discharge for the investigated leak types was calculated according to the Torricelli equation, equation (2.6) replacing the area with the deformed leak area. The discharge was calculated for each deformed leak area and time period.

A graph of discharge against pressure was plotted for each hole and load state as illustrated in figure 5-12 for the 1mm round hole in HDPE. The calculated data was fitted to a power relationship in MS Excel, to obtain equations similar to the power law equation applied by leakage practitioners, equation (2.9). Similar graphs are included in the relevant appendix chapters for all leak types. The lines in the figure 5-12 show the estimated leak discharges when the different pressures have been applied for specific time periods.

The estimated leakage exponents for each leak are obtained from the trend line equations generated in MS Excel using the R squared value as an indication of best fit. A power equation trend line was used so as to match the power law concept with the results. The equations for a 1mm diameter round hole in HDPE in the uniaxial load state are displayed in the figure 5-12 for elastic and viscoelastic simulations. For the 1mm diameter hole in HDPE in the uniaxial load state, the estimated leakage exponent varies from 0.5072 for elastic deformation to 0.5143 for a creep duration of 100 000s. The leakage exponent increases with time for all leak types as illustrated in the relevant graphs included in appendix.

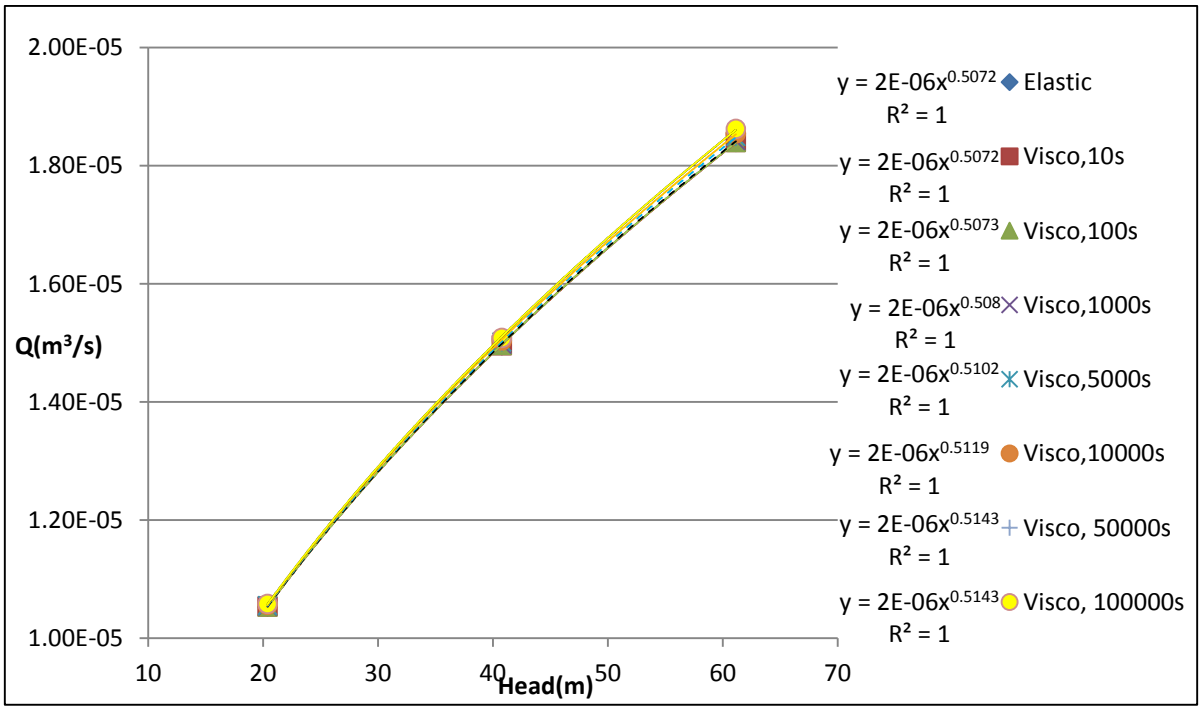

Figure 5-12: Discharge against pressure head for the 1mm hole in HDPE, uniaxial state

A graph illustrating the variation of the leakage exponent (N1) with time as obtained from the discharge-pressure graphs can be obtained for each leak type as shown in figure 5-13 below. The figure 5-13 illustrates the relationship between N1 and time for the round holes in both HDPE and PVC. From this graph, The N1 values for HDPE are higher than the corresponding values for PVC for the same leak type, pressure load and time. The leakage exponent for an un-deformed hole is 0.5 and is also included in figure 5-13. A variation in leak area therefore leads to a variation in leak exponent from its value in the Torricelli equation.

The leakage exponent for 1mm in HDPE is higher than the leakage exponent in PVC. This behaviour is similar to that observed for the gradient as seen in figure 5-11. The N1 curves in figure 5-13 are also similar to the creep curves discussed in the literature review. This suggests that the leakage exponent variation is influenced by the behaviour of the material under investigation. Since N1 is a parameter of pressure-leakage relationships in pipes, it suggests that material behaviour is an important factor of pressure-leakage relationships.

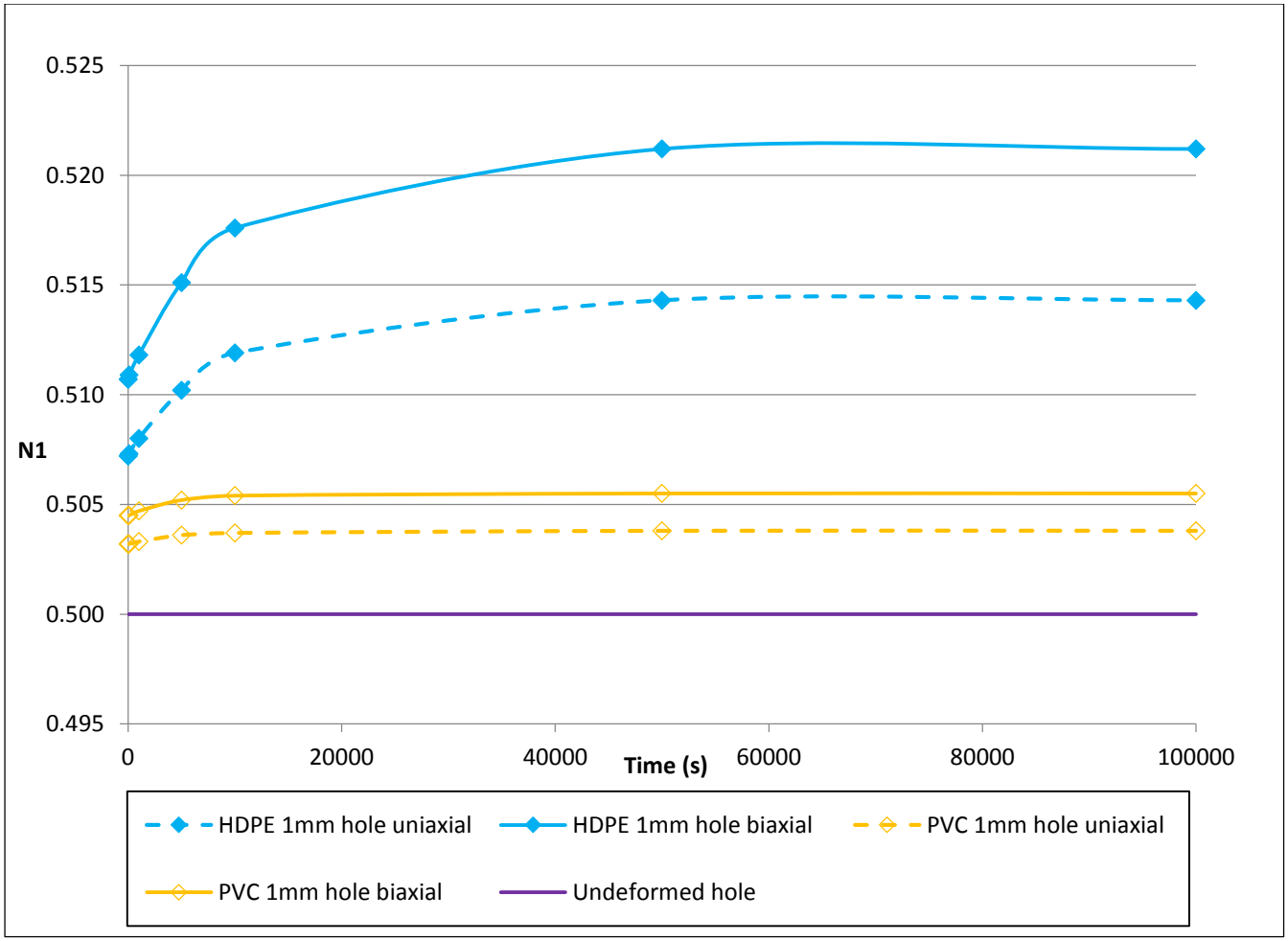

Figure 5-13: N1 against time in 1mm round holes, HDPE and PVC

A summary of the gradients (m) and leak exponents (N1) values for the 1mm hole in HDPE is shown in the table 5-2 below. The N1 and m values increase with time until stabilisation occurs at 50 000s and 100 000s. Similar tables are included in the appendix for each leak type.

HDPE	Uniaxial		Biaxial	
Time (s)	N1	m	N1	m
0 (Elastic)	0.5072	1.570E-10	0.5107	2.330E-10
10	0.5072	1.570E-10	0.5107	2.330E-10
100	0.5073	1.594E-10	0.5109	2.379E-10
1000	0.5080	1.741E-10	0.5118	2.575E-10
5000	0.5102	2.232E-10	0.5151	3.311E-10
10000	0.5119	2.600E-10	0.5176	3.875E-10
50000	0.5143	3.139E-10	0.5212	4.684E-10
100000	0.5143	3.139E-10	0.5212	4.684E-10

Table 5-2: Gradient (m) and leakage exponent (N1) values for the 1mm hole in HDPE

5.3.5 Percentage change in area against pressure

The percentage change in area was computed for each time and load state. Percentage change in area was computed using the following equation:

$$\left(\frac{A_D - A_0}{A_0} \right) \times 100 \tag{5.1}$$

Where A_D and A_0 are the deformed area and un-deformed area respectively. An example of the results obtained for this case is presented below in figure 5-14 for the 1mm round hole in HDPE pipe. A linear relationship is observed for each time and leak hole. Similar graphs for all leak holes investigated are included in the appendix. The percentage change in area for a 1mm hole in HDPE varies from 0% to about 4% as shown. The percentage changes for the uniaxial state are lower than the percentage changes for the biaxial state at corresponding times.

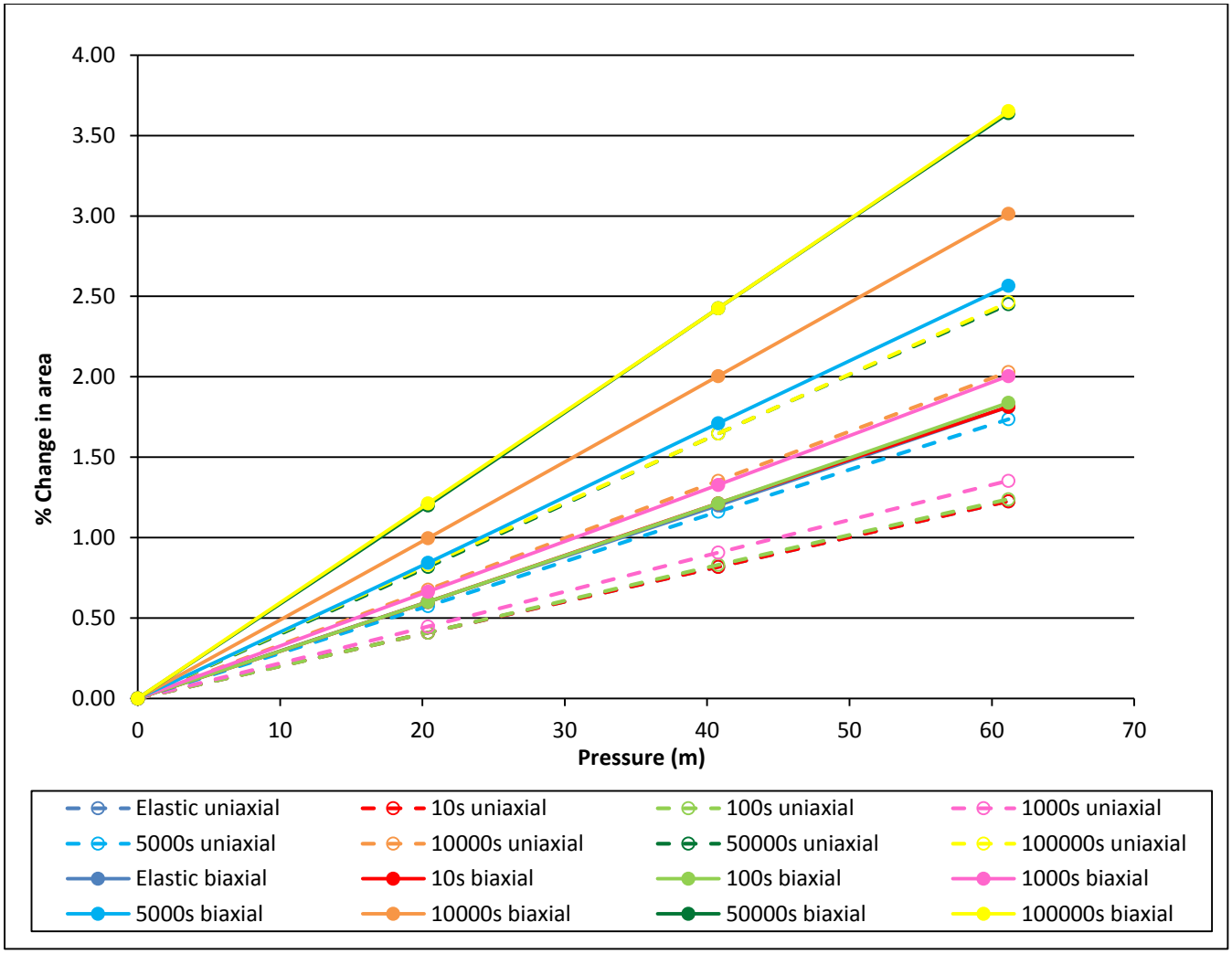

Figure 5-14: Percentage change in area against pressure for 1mm hole in HDPE

5.3.6 Ratio of total change in area to elastic change in area and gradient to elastic gradient

The total change in area and elastic change in area of each leak hole were obtained from Abaqus and the ratio of total change in area to elastic change in area obtained. This was done to investigate the relationship between elastic and viscoelastic deformation.

Elastic change in area (ΔE) is the difference between the deformed area due to elastic deformation (area at 0 seconds) and the un-deformed area. Elastic change in area was calculated as shown below in equation (5.2):

$$\Delta E = A_E - A_0 \tag{5.2}$$

Where A_E is the deformed area due to elastic deformation and A_0 is the un-deformed area.

Total change in area (ΔT) is the difference between the deformed area at any given time and the un-deformed area. Total change in area is calculated as shown below in equation (5.3):

$$\Delta T = A_D - A_0 \tag{5.3}$$

Where, A_D is the deformed area at a time t for each leak type, the ratio of ΔT to ΔE was then computed and plotted against corresponding times as shown below in figure 5-15 for a 1mm hole in HDPE.

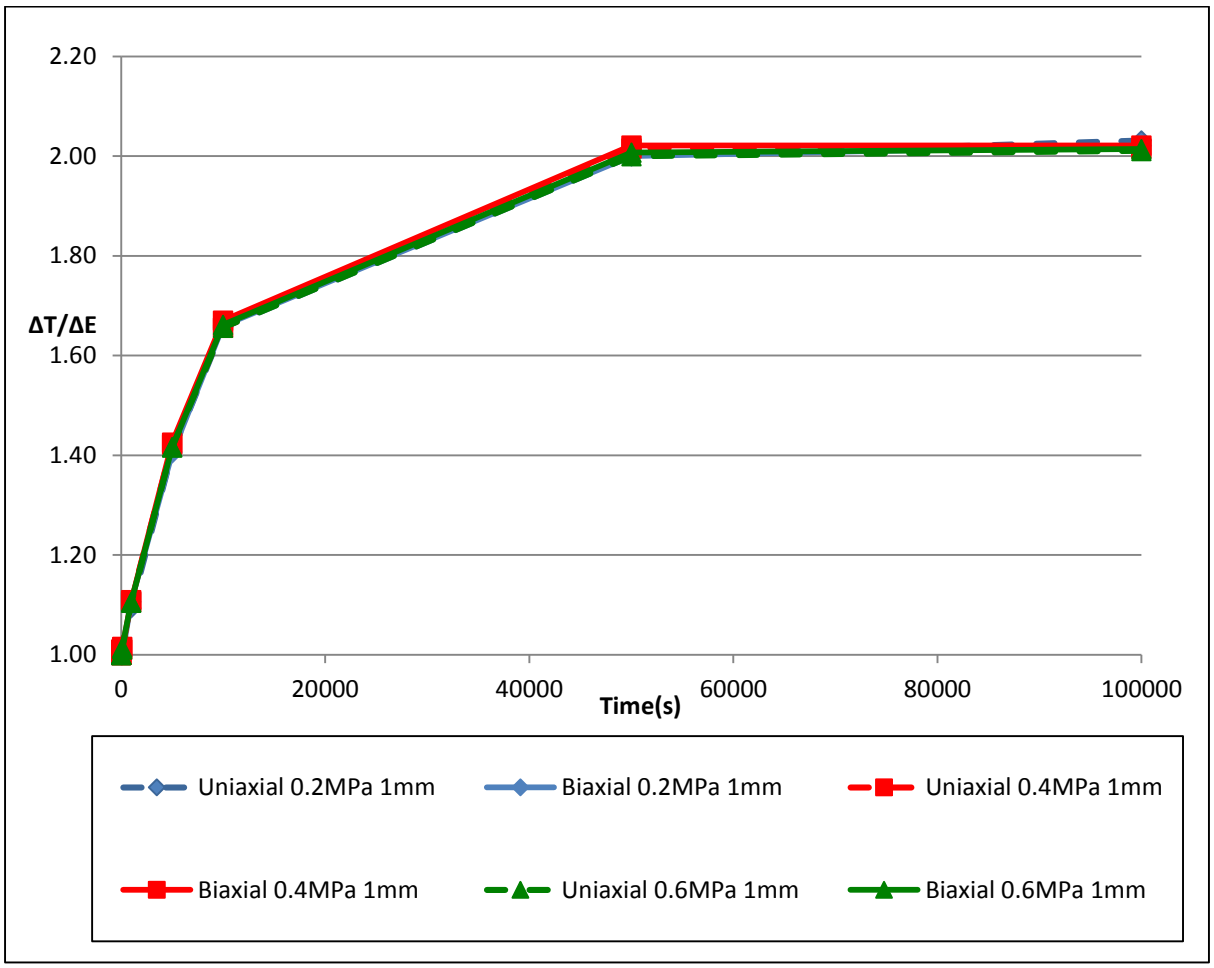

Figure 5-15: ΔT/ΔE for a 1mm round hole in HDPE

The ΔT:ΔE ratio for a 1mm hole is almost equal for all pressures, as observed in figure 5-15 above. The ΔT:ΔE ratio ranges from 0 for the elastic deformation to just above 2.0 for the longest creep period of 100 000s. This graph is also similar to the viscoelastic material creep behaviour graph in the literature review. Similar graphs are included in the appendix for all leak holes.

Similarly, the ratio of gradient to elastic gradient was calculated. The elastic gradient, m_E, is the gradient of the pressure-leakage relationship at 0 seconds, which is marked as "elastic" in figure 5-10. The ratio was calculated for each time period and the results for a 1mm hole in HDPE are presented in the figure 5-16 below.

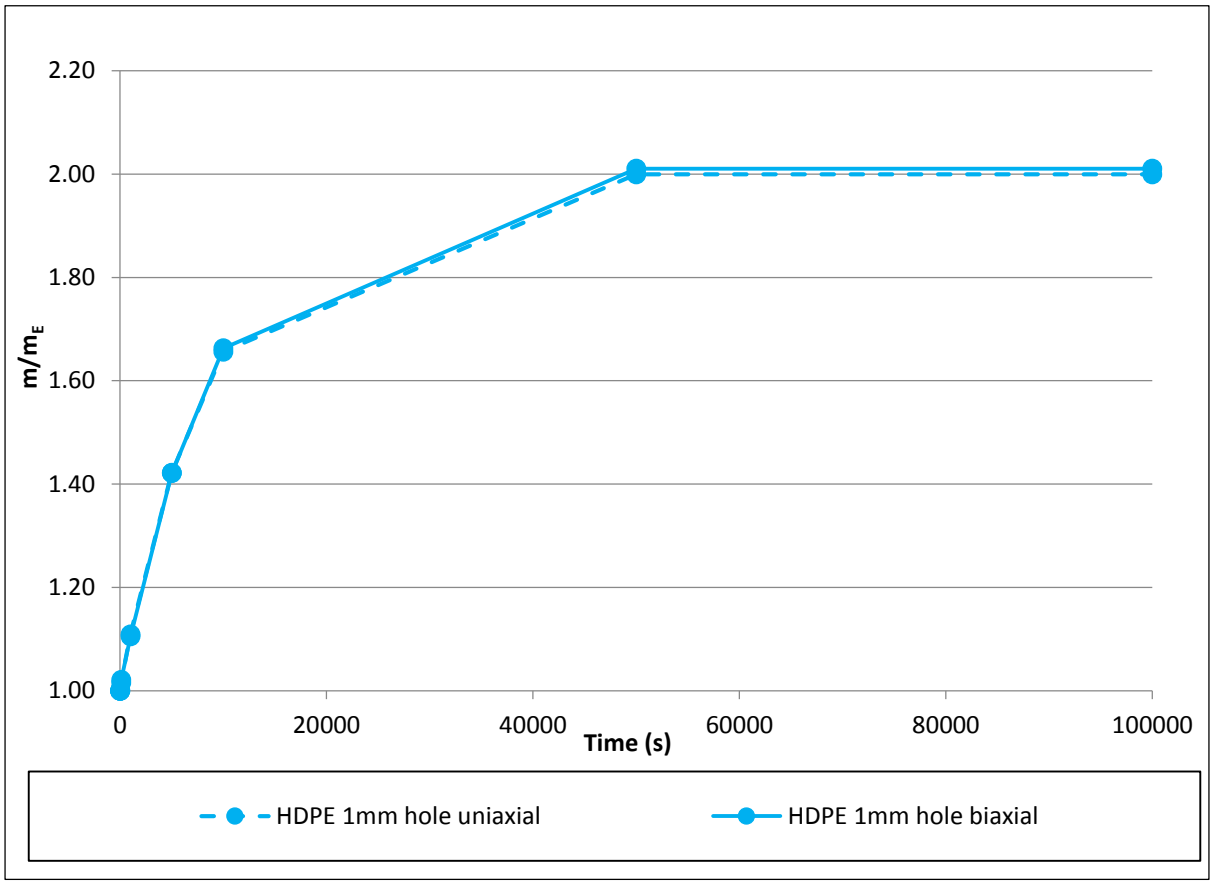

Figure 5-16: m/m_E for a 1mm hole in HDPE

Figure 5-16 can be compared to figure 5-15 since the gradient can be obtained by any two pressures at a particular time. It is seen that the $\Delta T/\Delta E$ and m/m_E ratios are similar, starting at 1.0 with the maximum at around 2.0. This indicates that the increase in gradient is similar to the increase in area over time.

5.3.7 Cyclic results for 1mm round hole in HDPE

Cyclic simulations were carried out for a selection of leak holes in the biaxial load state. The leaks investigated under cyclic loading where the 1mm round holes and 1mm by 10mm cracks in both HDPE and PVC pipe. The pipes were subjected to cyclic loading by applying pressure of 0.2MPa, 0.4MPa and 0.6MPa for a duration of 100 000s (27.8 hours) for each load. The pressure loads and corresponding deformed area for a 1mm round hole in HDPE are illustrated in the figures 5-17 and 5-18 below. In figure 5-18, both cyclic results and non-cyclic results are represented. The cyclic results are the red round dots. The non-cyclic results are the blue, pink and green diamonds and represent the pressure load applied to the pipe for 100 000s.

The cyclic results display the time dependent creep property of viscoelastic materials. This property has been observed in practical investigations of a PVC pipe by Ferrante et al. (2013). Another property that was not observed in this project was hysteresis. Hysteresis was defined in the literature review as the loading history dependent behaviour of a material. Hysteresis was not observed in this project since the loading times were greater than the relaxation time of the material and the assumption of linear viscoelasticity. The material therefore had enough time to recover. Ferrante et al. (2010) observed hysteresis in a leak in a polyethylene pipe that was tested for 12 hours, less than the 27.8 hour cycles for this project. The results obtained in the current investigation showed that there was complete recovery of the deformed areas as illustrated by the similarity of the loading curves of the cyclic simulations and the curves of the non-cyclic simulations.

Furthermore, the increase in deformation for each 0.2MPa increase or decrease was equal, for all pressures after 100 000s. This means that the total change in area from 0 to 100 000s was equal to that from 100 000s to 200 000s and so on. The reason for this is most likely due to the assumption of linear viscoelasticity.

The graphs showing the deformed area for a 1mm round hole in PVC are included in the appendix C.

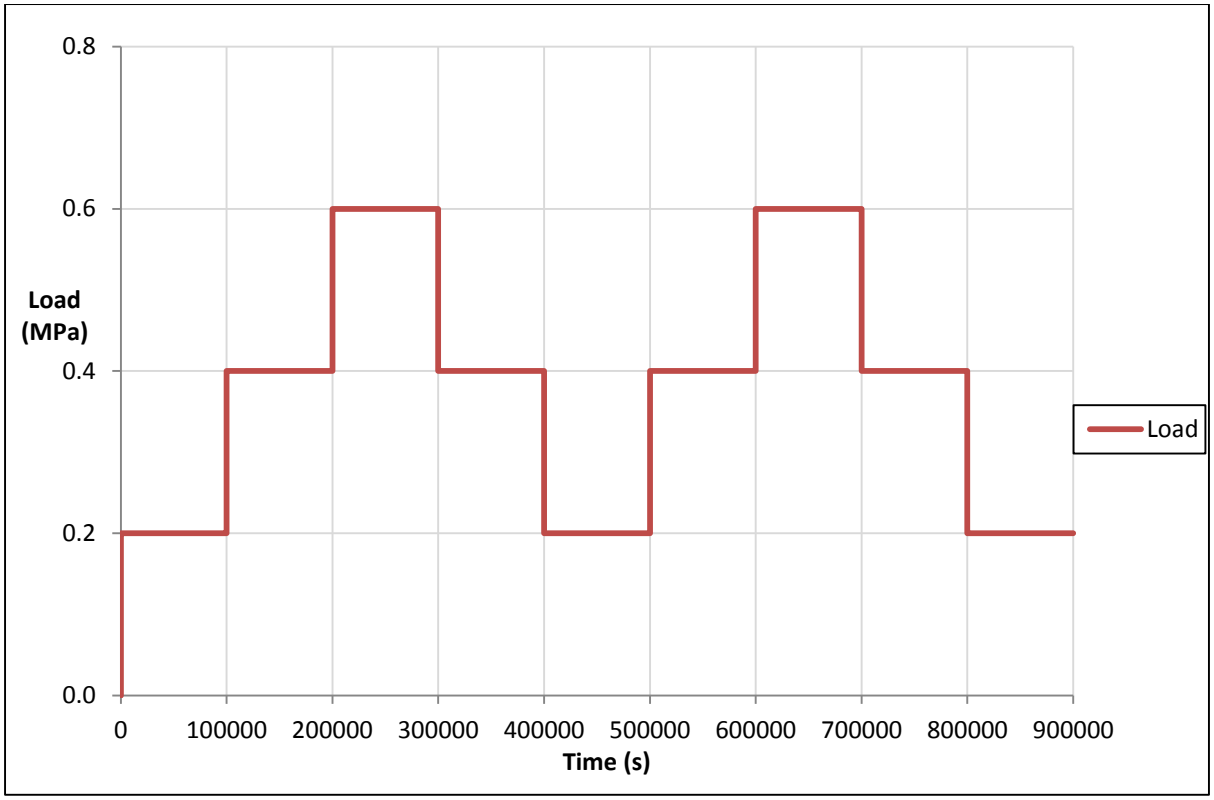

Figure 5-17: Cyclic loading for a 1mm round hole in HDPE pipe

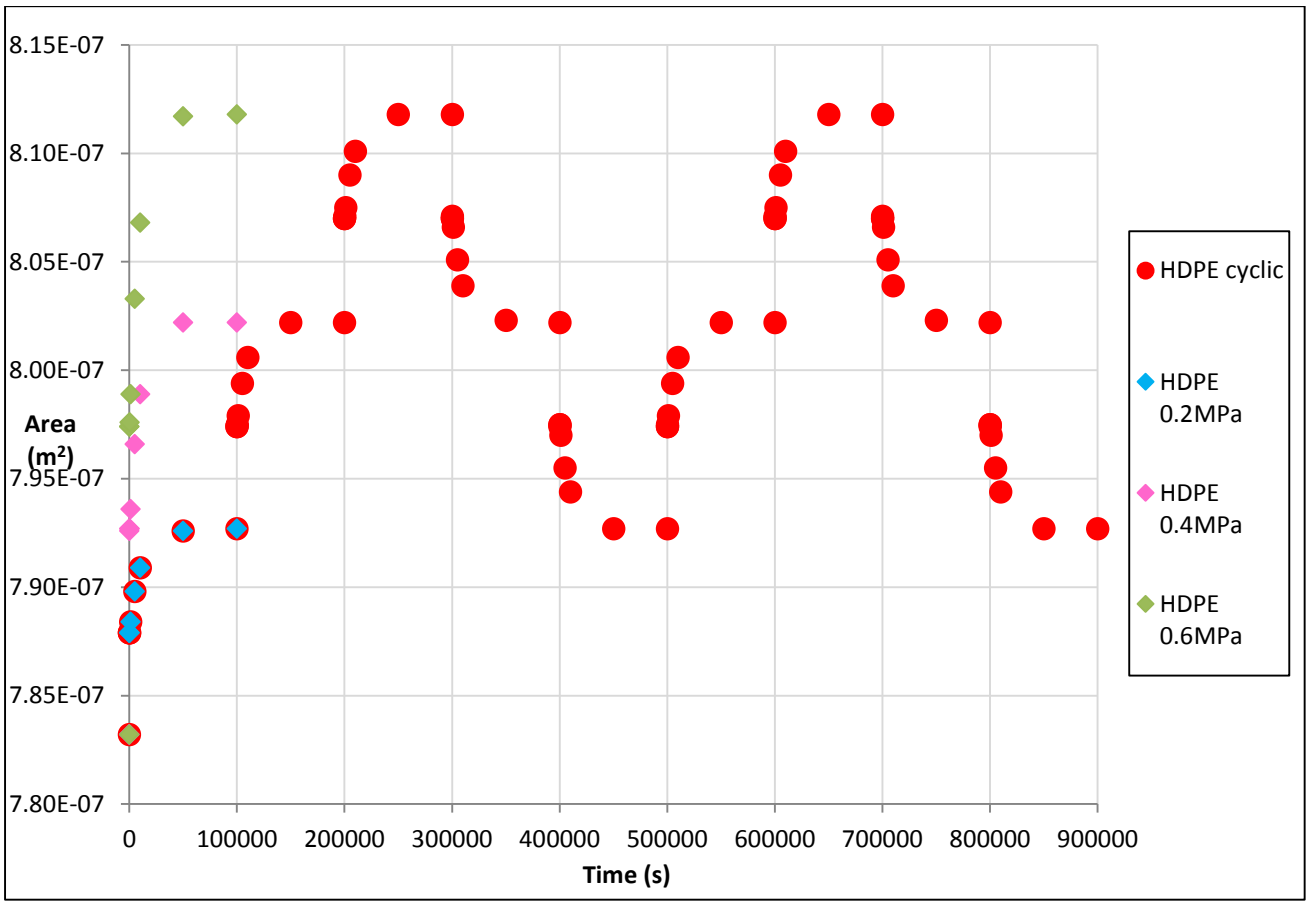

Figure 5-18: Deformed area against time for a 1mm round hole in HDPE during cyclic loading

5.4 Comparison of round holes in HDPE and PVC

The results of the round holes in HDPE and PVC are laid out in detail the appendix. For further analysis, the gradients, leakage exponents, percentage area changes $\Delta T/\Delta E$ and m/m_E ratios are compared and discussed in this section.

5.4.1 Gradient (m) of the pressure-leakage relationship in round holes

Gradients were obtained from the linear trend line for each time period over the three pressures tested. The gradients of the 1mm holes and 12mm holes in HDPE and PVC pipe obtained from the leak area-pressure relationships at the different time periods are plotted as shown below in figure 5-19. In figure 5-19, the gradients of the 12mm holes are higher than the gradients of the 1mm holes for both pipe materials. This corresponds to observations by Cassa et al. (2010) where m was observed to increase with hole diameter.

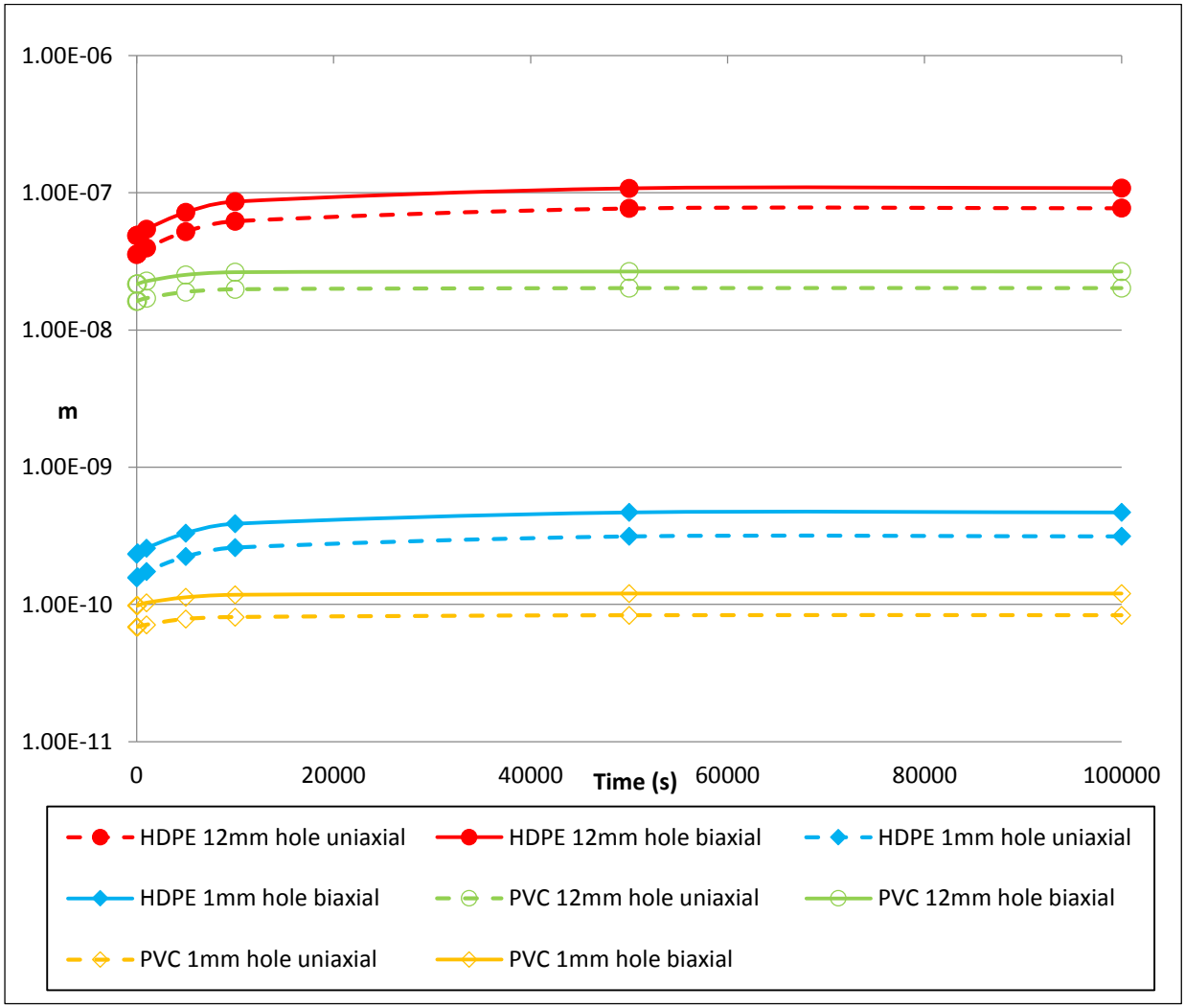

Figure 5-19: Variation of gradient (m) with time for round holes in HDPE and PVC

Additionally, the gradients in HDPE are higher than those of PVC for both hole diameters and this may be attributed to the difference in pipe material behaviour.

5.4.2 Leakage exponent (N1) in round holes

The leakage exponents for both 12mm and 1mm hole diameters and materials were also compared as shown in figure 5-20 below. For the leakage exponents it is seen that HDPE 12mm and 1mm holes have higher exponents than PVC 12mm and 1mm holes. The leakage exponents are all above 0.5. a leak exponent of 0.5 corresponds to an un-deformed hole. Leakage exponents also corresponded to specific times over the three different pressures tested.

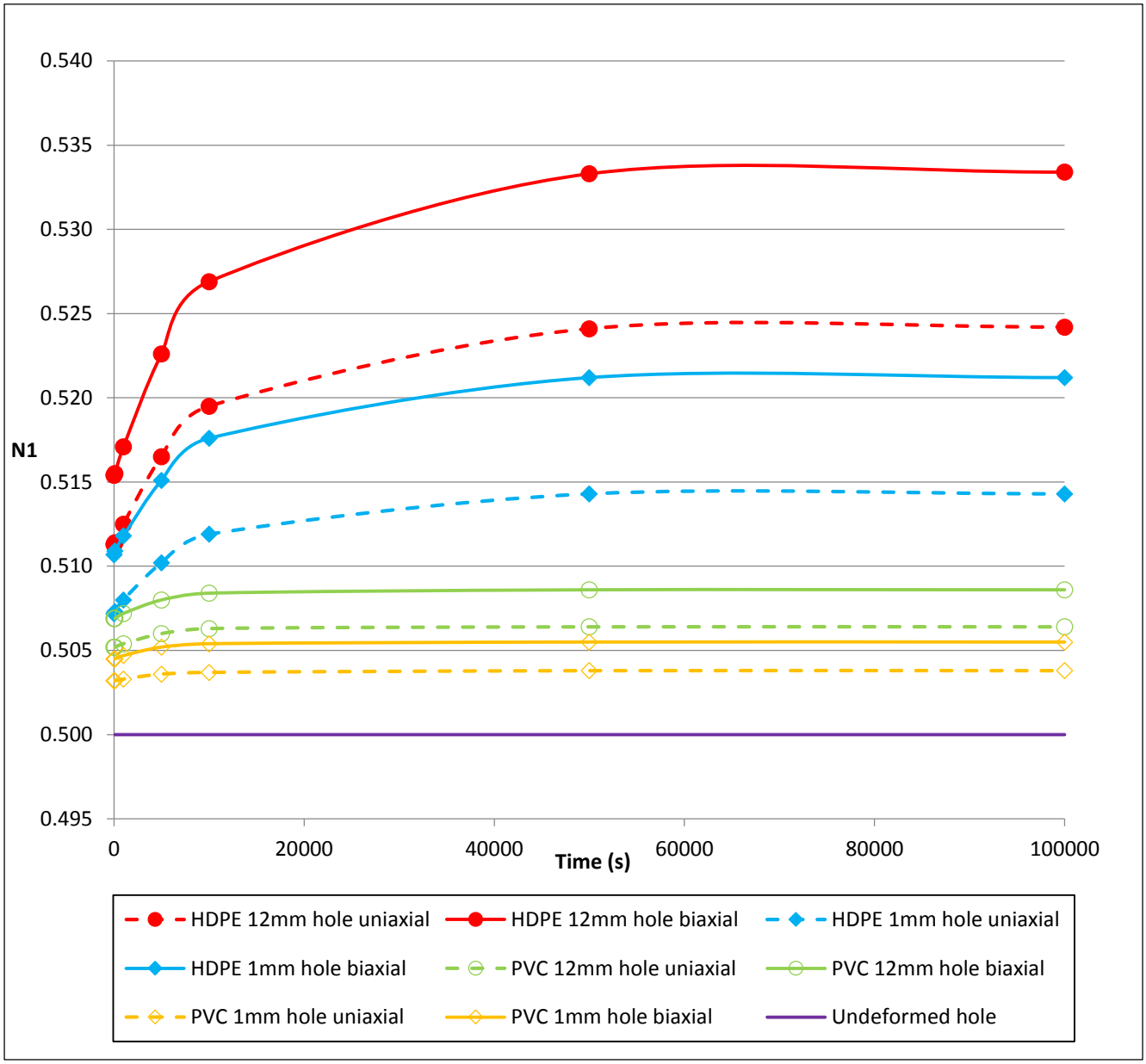

Figure 5-20: Variation of leakage exponent (N1) with time for round holes

The leakage exponents for the 12mm holes are higher than the leakage exponents for the 1mm holes in both materials. This trend was also observed by Cassa et al. (2010). The leak exponent against time graphs were similar to the creep curve of a viscoelastic material.

5.4.3 Percentage change in area for the round holes

Percentage area changes for each round were computed and compared. In the figure 5-21 below, only the round holes in HDPE, biaxial state are presented. Similar graphs for other round holes are included in the relevant appendices.

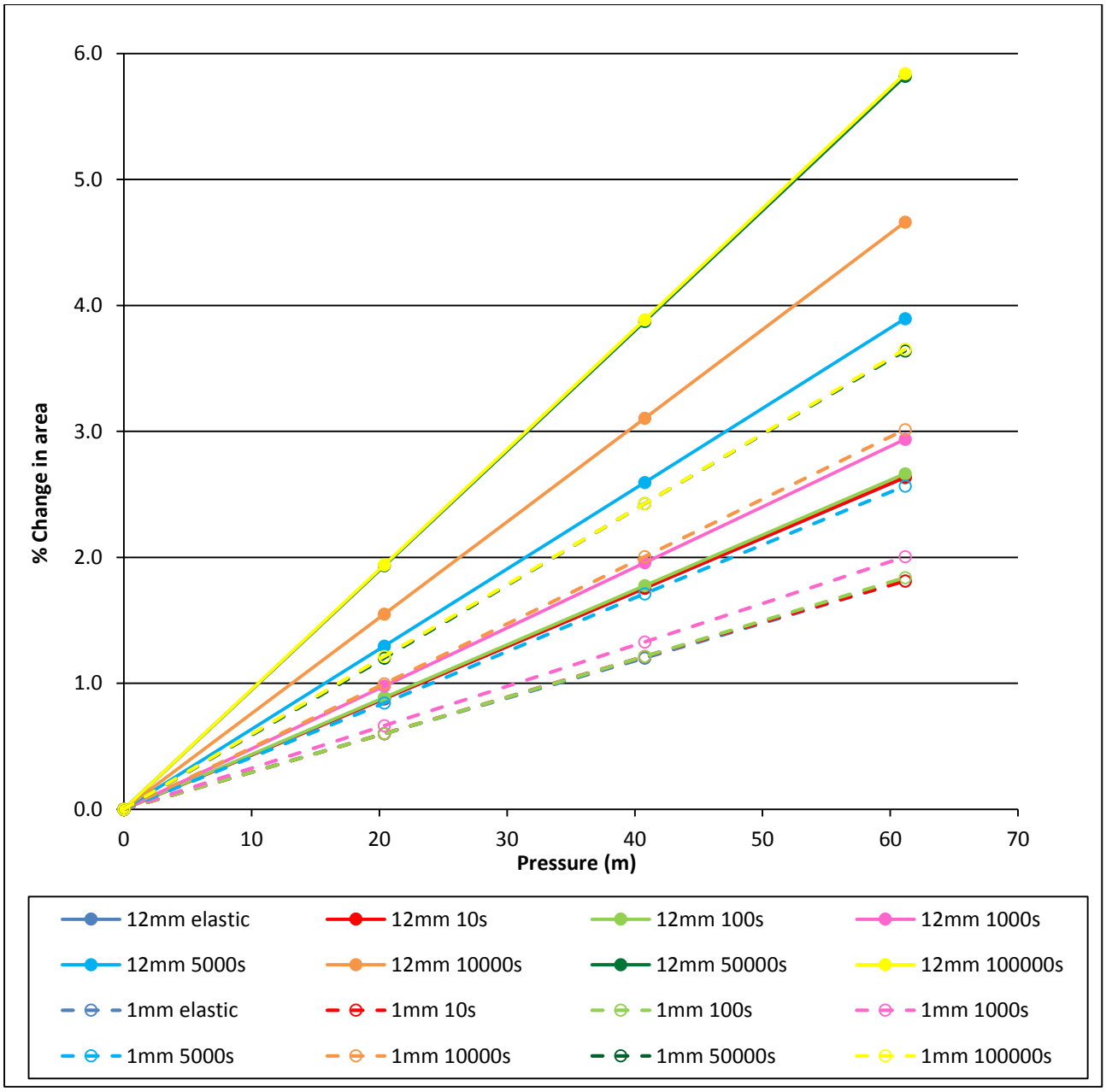

Figure 5-21: Percentage change in area against pressure for round holes in HDPE, biaxial state

From figure 5-21, it is clear 12mm holes have higher percentage increases in area compared to 1mm holes experiencing the same load conditions. This is expected since stress concentrations increase with hole diameter (Cassa 2005). Higher stress concentrations result in greater deformations hence higher percentage increases for a larger hole. The same trend is observed in PVC whose graphs are included in the appendix. This suggests that smaller diameter holes have lower expansion rates compared to larger diameter holes under the same pressure conditions, a trend that was also observed by Buckley (2007).

5.4.4 Ratio of total change in area to elastic change in area and gradient to elastic gradient

The ratios of total change in area to elastic change in area and gradient to elastic gradient for HDPE and PVC are illustrated below in the figures 5-22, 5-23, 5-24 and 5-25 below.

In figures 5-22 and 5-23 for round holes in HDPE, the $\Delta T/\Delta E$ ratios are similar to the m/m_E ratios for each time. The same observation is made for the round holes in PVC as seen in figures 5-24 and 5-25. The similarity of the $\Delta T/\Delta E$ and m/m_E graphs is significant as it indicates that the analysis by Cassa et al. (2010) for elastic pipe materials can be applied to linear viscoelastic materials. Additionally, the 12mm round holes have higher $\Delta T/\Delta E$ and m/m_E ratios compared to the 1mm holes in both HDPE and PVC pipe materials. The 12mm holes in HDPE display a maximum ratio of about 2.20 while the 1mm holes display a maximum ratio of about 2.0.

In PVC pipe, the maximum ratio for 12m holes is around 1.25 while that for the 1mm hole occurs about half way 1.20 and 1.25. There is greater variation for the 1mm hole in PVC compared to the other round holes. The scatter of the results in figure 5-24 at 10 000s may be as a result of the mesh not being fine enough at the leak.

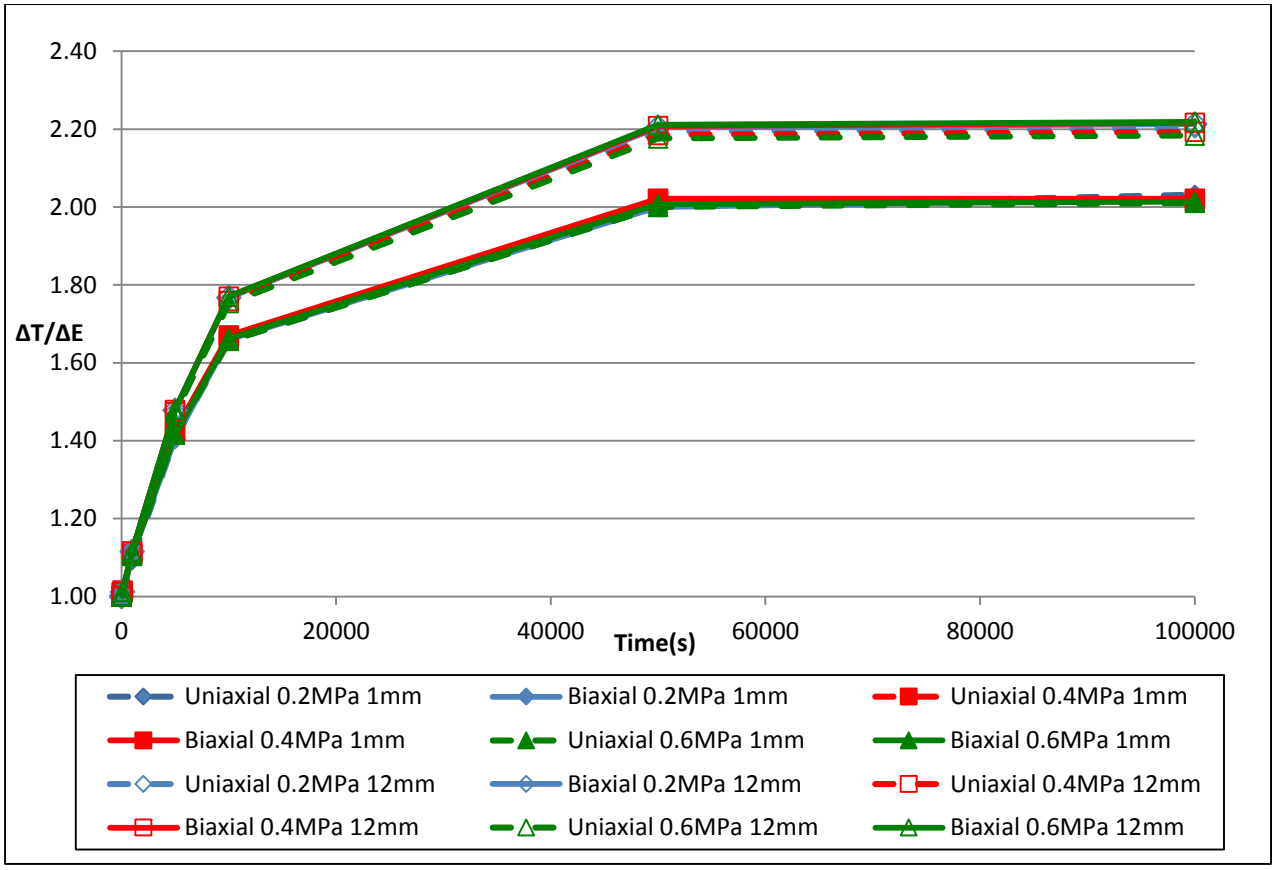

Figure 5-22: ΔT/ΔE for round holes in HDPE

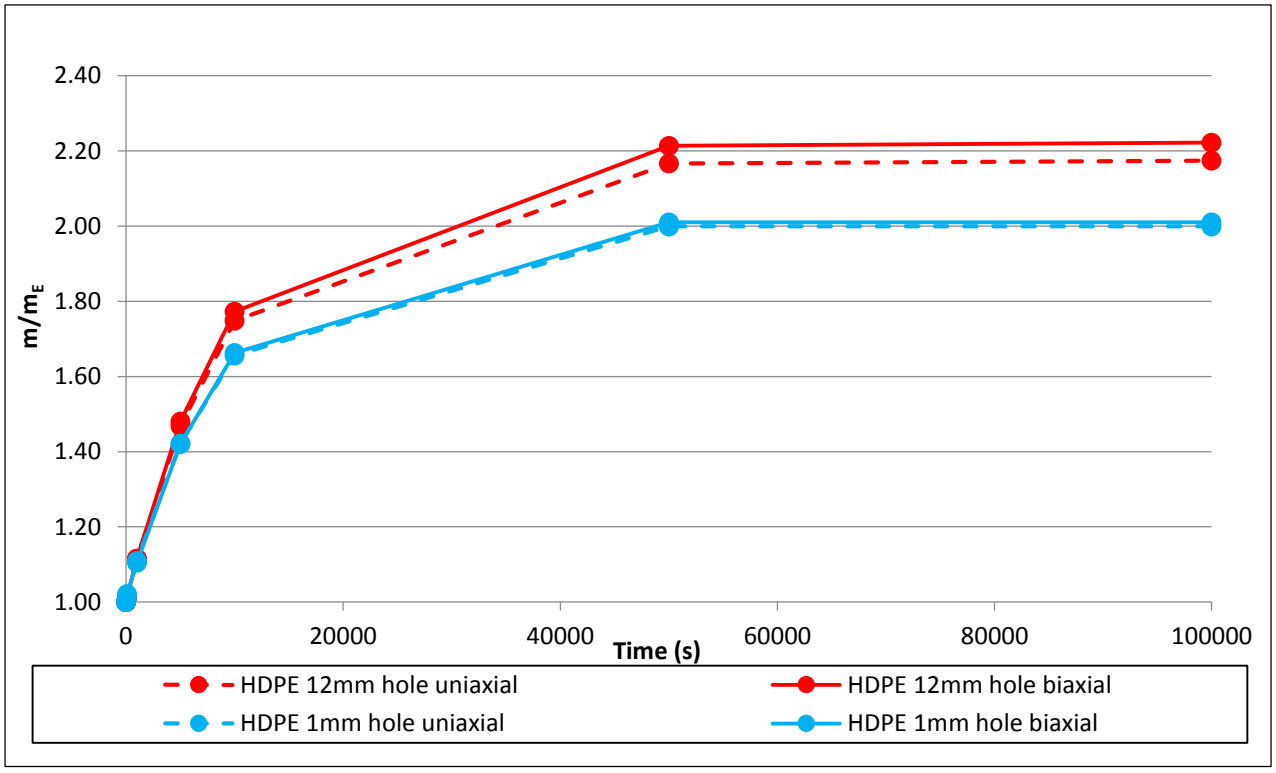

Figure 5-23: m/m_E for round holes in HDPE

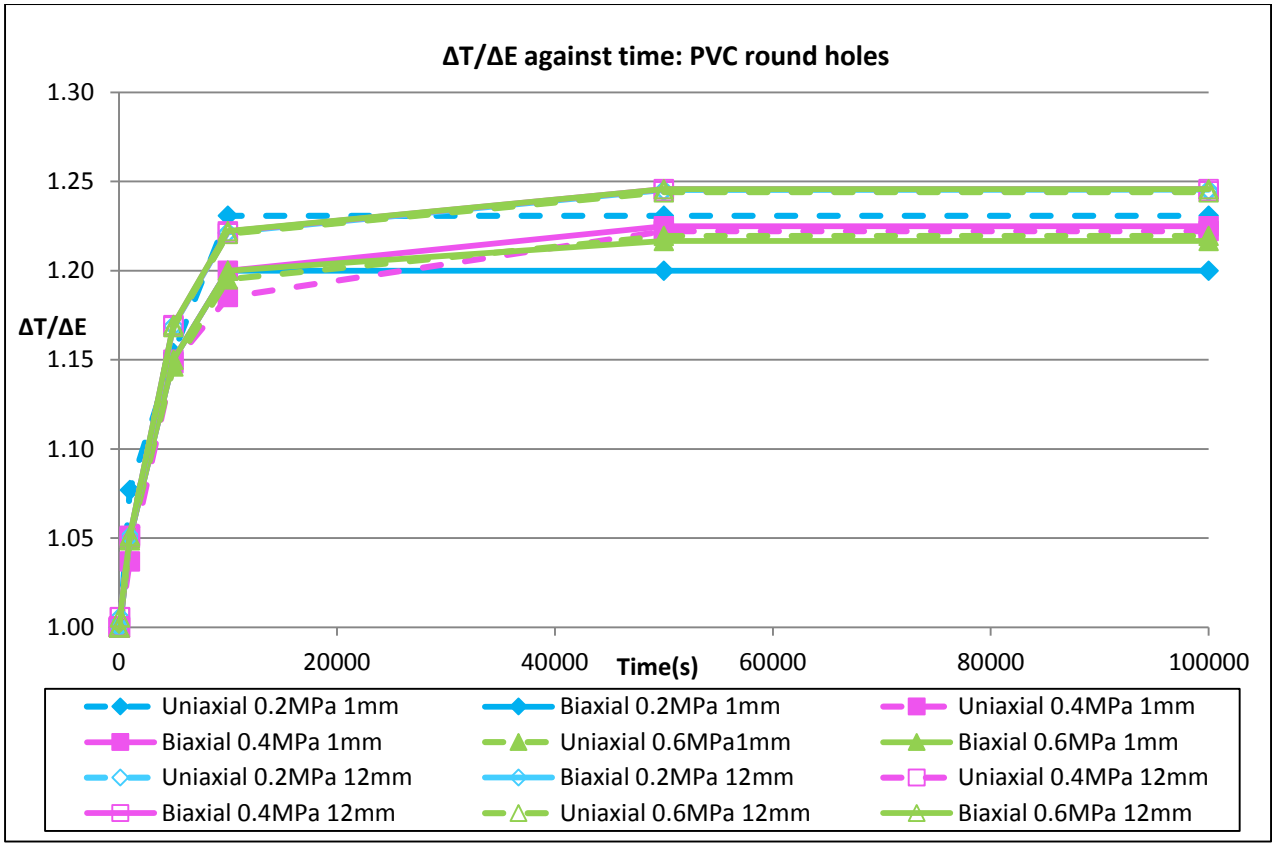

Figure 5-24: Ratio of creep strain to elastic strain for round holes in PVC

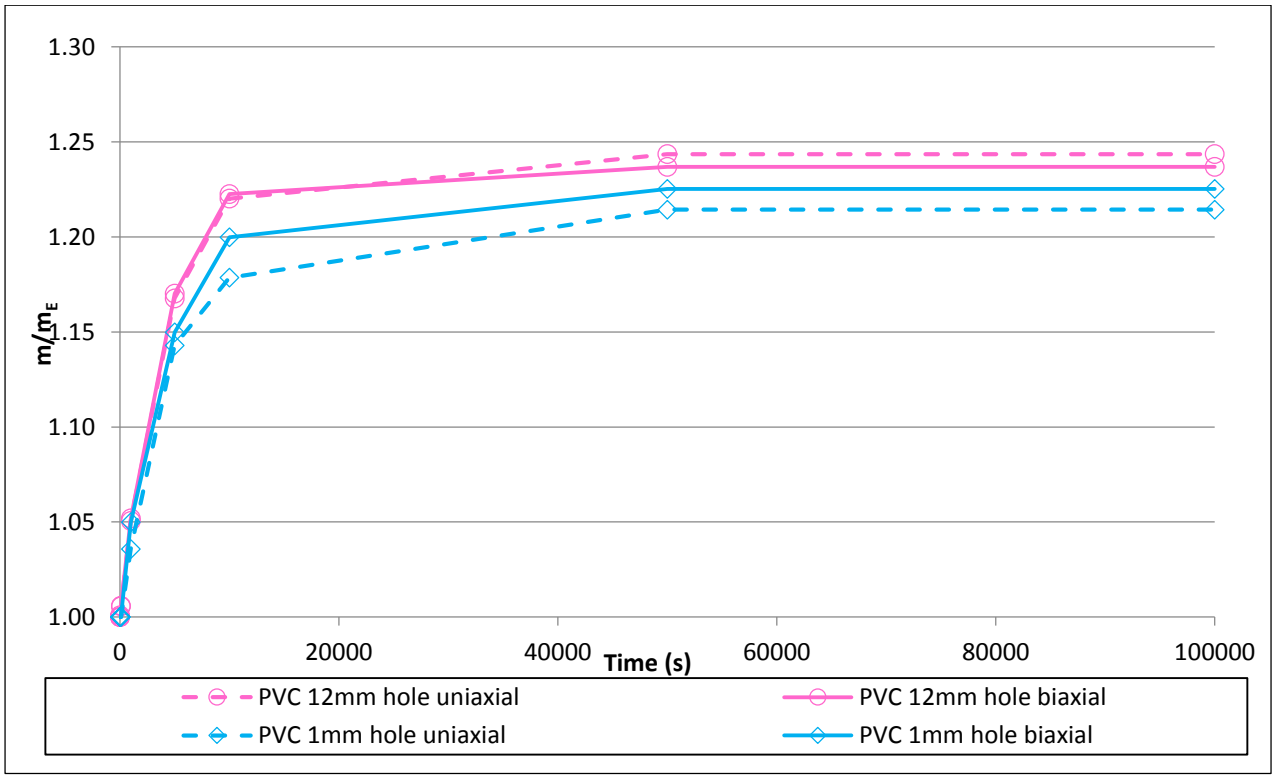

Figure 5-25: m/m_E for round holes in PVC

5.5 Detailed simulation results for 1mm by 10mm longitudinal cracks

5.5.1 Stress distribution

The stress distribution for a 1mm by 10mm longitudinal crack in HDPE is illustrated in figure 5-26 below. From figure 5-26, it is observed that maximum stresses occurred at the crack tips (in the z-direction) while minimum stresses occurred at the crack long edges in the y direction. The resultant stress distribution forces the crack to deform as illustrated. The crack was also observed to protrude from the pipe

The high stresses at the crack tips are a result of the high stress concentrations at crack tips, as discussed in the literature review. In real life situations these stress concentrations may exceed the tensile strength of the pipe material, resulting in crack propagation. The stress distribution for the rest of the longitudinal cracks was similar to that illustrated in figure 5-26. The deformations were scaled to improve visibility of actual deformations.

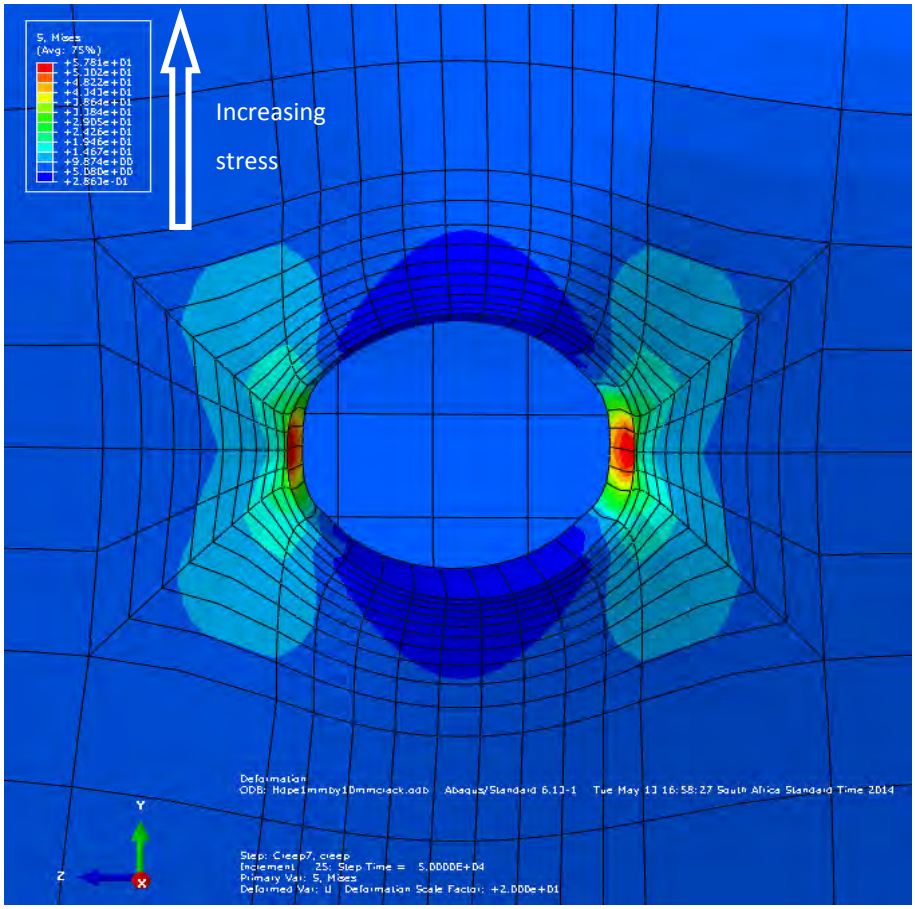

Figure 5-26: Stress distribution around a deformed 1mm by 10mm longitudinal crack, HDPE, deformation scale factor = 20

5.5.2 Variation of leak area with time

The deformed leak area for the longitudinal cracks was also plotted as illustrated in figure 5-27 below. Graphs for the other longitudinal cracks are included in the relevant appendix. For the longitudinal cracks, the deformed areas for the uniaxial and biaxial states did not vary as much as the round holes. Similar observations for the uniaxial and biaxial deformed areas were made by Cassa (2005) for longitudinal cracks in elastic materials. A summary of the deformed areas for the 1mm by 10mm crack in HDPE is included in table 5-3.

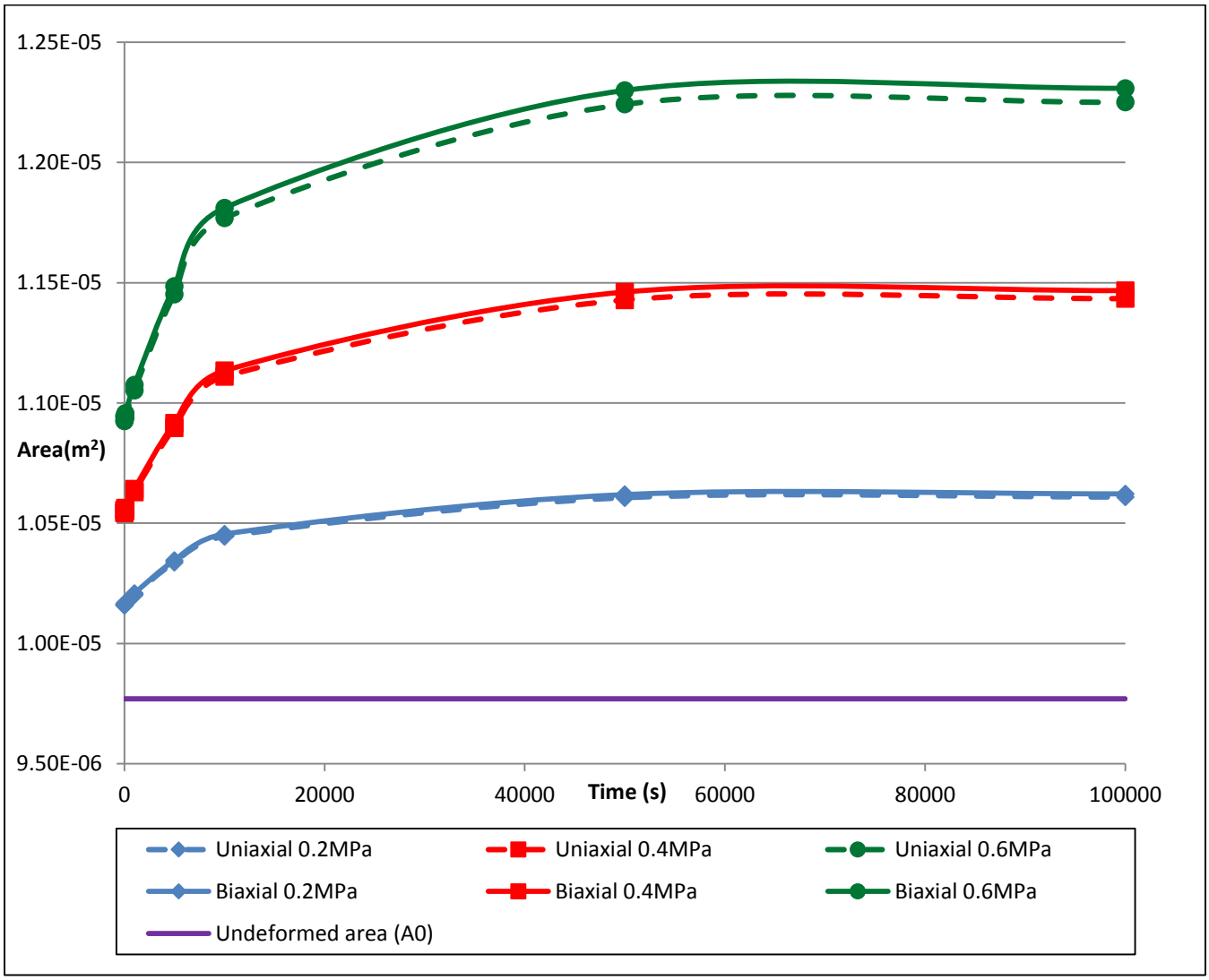

Figure 5-27: Area against time for 1mm by 10mm longitudinal crack in HDPE pipe, all pressures

HDPE	Area of deformed cracks with $A_0 = 9.77mm^2$					
Pressure (MPa)	**0.2**		**0.4**		**0.6**	
Time (s)	**Uniaxial**	**Biaxial**	**Uniaxial**	**Biaxial**	**Uniaxial**	**Biaxial**
0 (Elastic)	10.1587	10.1640	10.5425	10.5543	10.9243	10.9438
10	10.1592	10.1645	10.5434	10.5553	10.9256	10.9452
100	10.1633	10.1686	10.5515	10.5635	10.9377	10.9575
1000	10.2019	10.2080	10.6285	10.6420	11.0525	11.0750
5000	10.3370	10.3453	10.8967	10.9160	11.4519	11.4848
10000	10.4444	10.4548	11.1097	11.1341	11.7687	11.8108
50000	10.6054	10.6190	11.4284	11.4612	12.2416	12.2993
100000	10.6084	10.6220	11.4341	11.4671	12.2501	12.3082

Table 5-3: Deformed areas for the 1mm by 10mm longitudinal crack in HDPE

Figure 5-28 below shows that the deformed crack areas in PVC were less than those in HDPE and this is due to the difference in material properties as for the round holes.

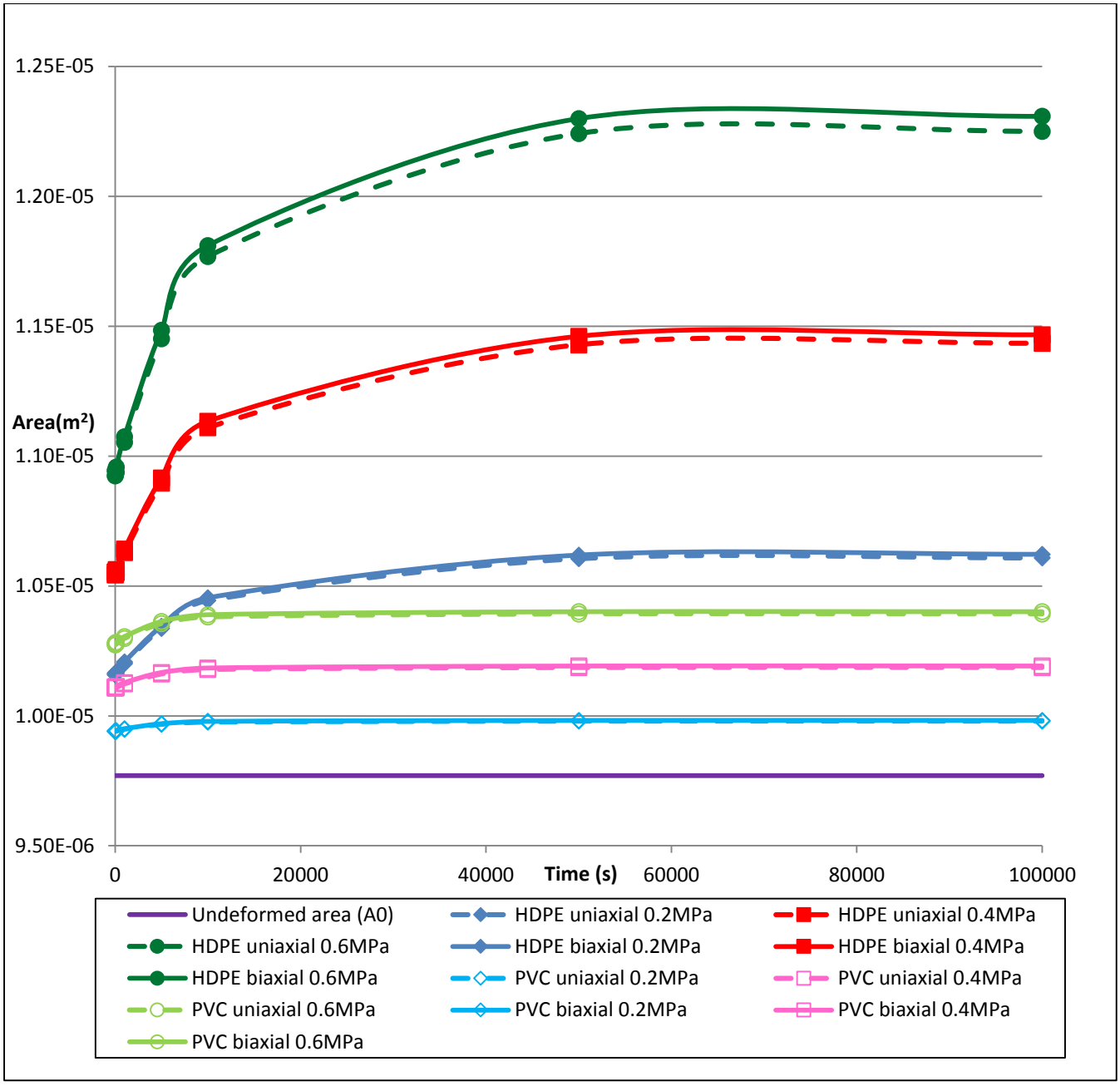

Figure 5-28: Area against time for 1mm by 10mm longitudinal crack in HDPE and PVC pipe

5.5.3 Gradient (m) of the pressure-leakage relationship

The gradients of the longitudinal cracks were obtained through the same process as for the round holes. Figure 5-29 shows the relationship between time and gradient for the 1mm by 10mm longitudinal cracks in both HDPE and PVC materials.

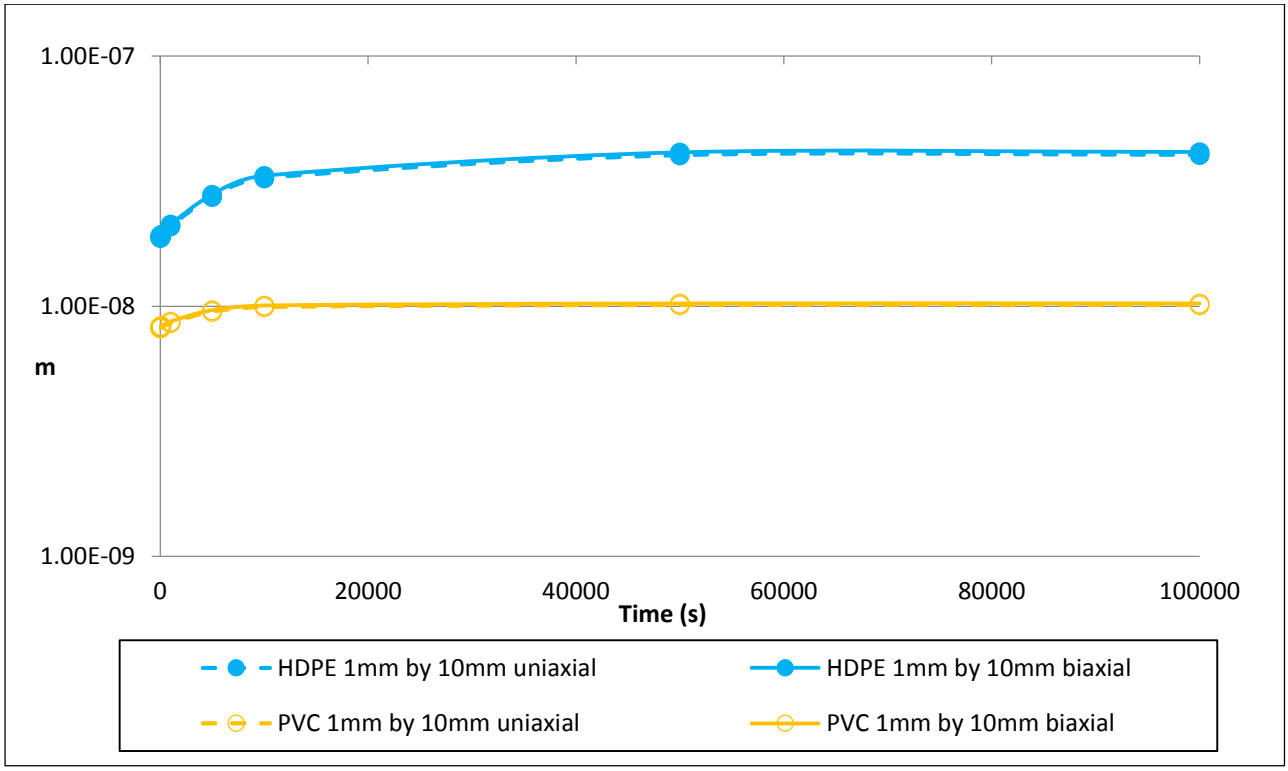

Figure 5-29: Gradient (m) against time for 1mm by 10mm longitudinal crack in HDPE and PVC

The figure above shows that the gradients for the biaxial and uniaxial states of both materials are quite similar. This is in contrast to round holes where gradients for the two loading states differed considerably. Cassa (2005) observed a similar trend for longitudinal cracks. Also, gradients for HDPE cracks are higher than the gradients for PVC cracks due to a difference in material properties.

5.5.4 Leakage exponent (N1)

The leakage exponents were also obtained in a process similar to that of the round holes. Figure 5-30 illustrates the relationship between leakage exponent and time for the 1mm by 10mm longitudinal cracks in HDPE and PVC pipes. Leakage exponents for HDPE are higher than those in PVC, and the exponents for the uniaxial and biaxial states are quite similar.

A summary of the leakage exponents and gradients in included in table 5-4 below.

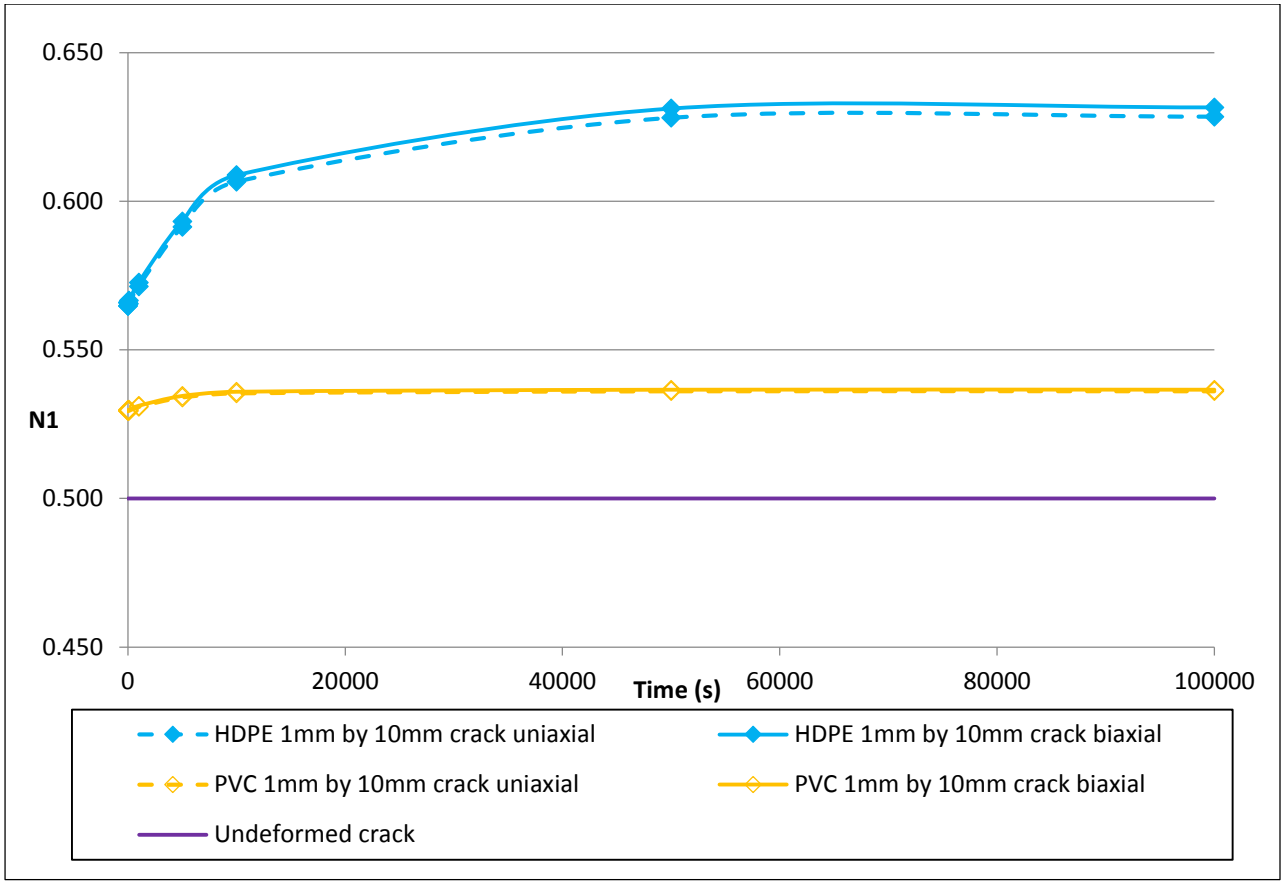

Figure 5-30: Leakage exponent (N1) against time for 1mm by 10mm longitudinal crack in HDPE and PVC

HDPE	Uniaxial		Biaxial	
Time (s)	N1	m	N1	m
0 (Elastic)	0.5648	1.878E-08	0.5659	1.912E-08
10	0.5648	1.880E-08	0.566	1.915E-08
100	0.5655	1.899E-08	0.5666	1.935E-08
1000	0.5714	2.086E-08	0.5727	2.126E-08
5000	0.5914	2.734E-08	0.5932	2.795E-08
10000	0.6066	3.248E-08	0.6088	3.326E-08
50000	0.6281	4.013E-08	0.6312	4.121E-08
100000	0.6285	4.026E-08	0.6316	4.135E-08

Table 5-4:Gradient (m) and leakage exponent (N1) values for 1mm by 10mm longitudinal crack in HDPE

5.5.5 Percentage change in area against pressure

Percentage change in area was also computed for the longitudinal cracks. Figure 5-31 illustrates the percentage change in area for the 1mm by 10mm longitudinal crack in HDPE, for each time period. The relationship between percentage area change and pressure is linear and ranges from 0% to just above 25%. The difference between the uniaxial state and biaxial state is almost negligible. Similar graphs for all longitudinal cracks are presented in the relevant appendices.

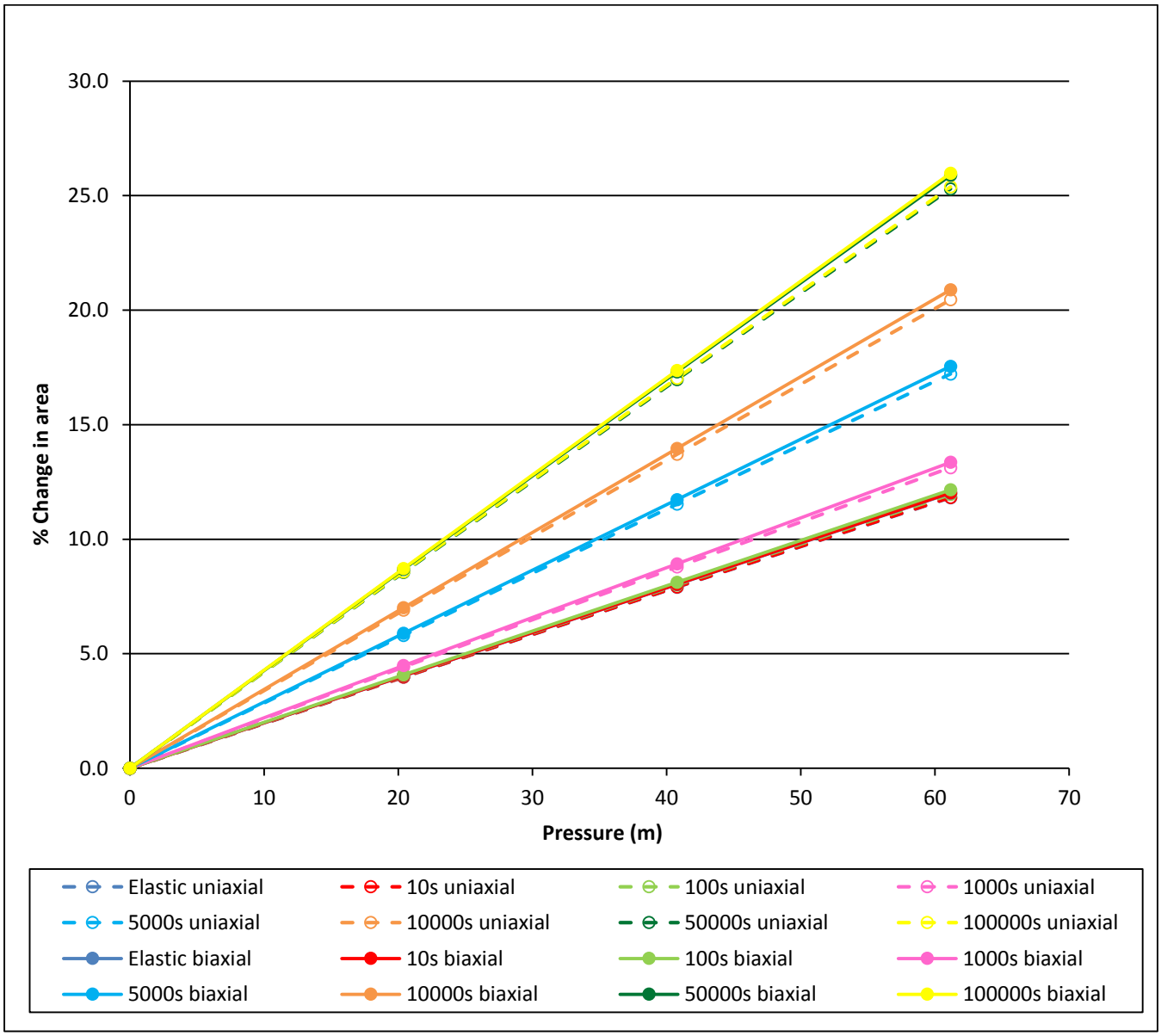

Figure 5-31: Percentage change in area against pressure for 1mm by 10mm longitudinal crack in HDPE

5.5.6 Ratio of total change in area to elastic change in area and gradient to elastic gradient

The ΔT/ΔE ratios of the 1mm by 10mm longitudinal crack in HDPE were calculated and presented in the figure 5-32 below. It is observed that the ΔT/ΔE ratios are also uniform for all pressures, ranging from 0 to just below 2.2 at 100 000s.

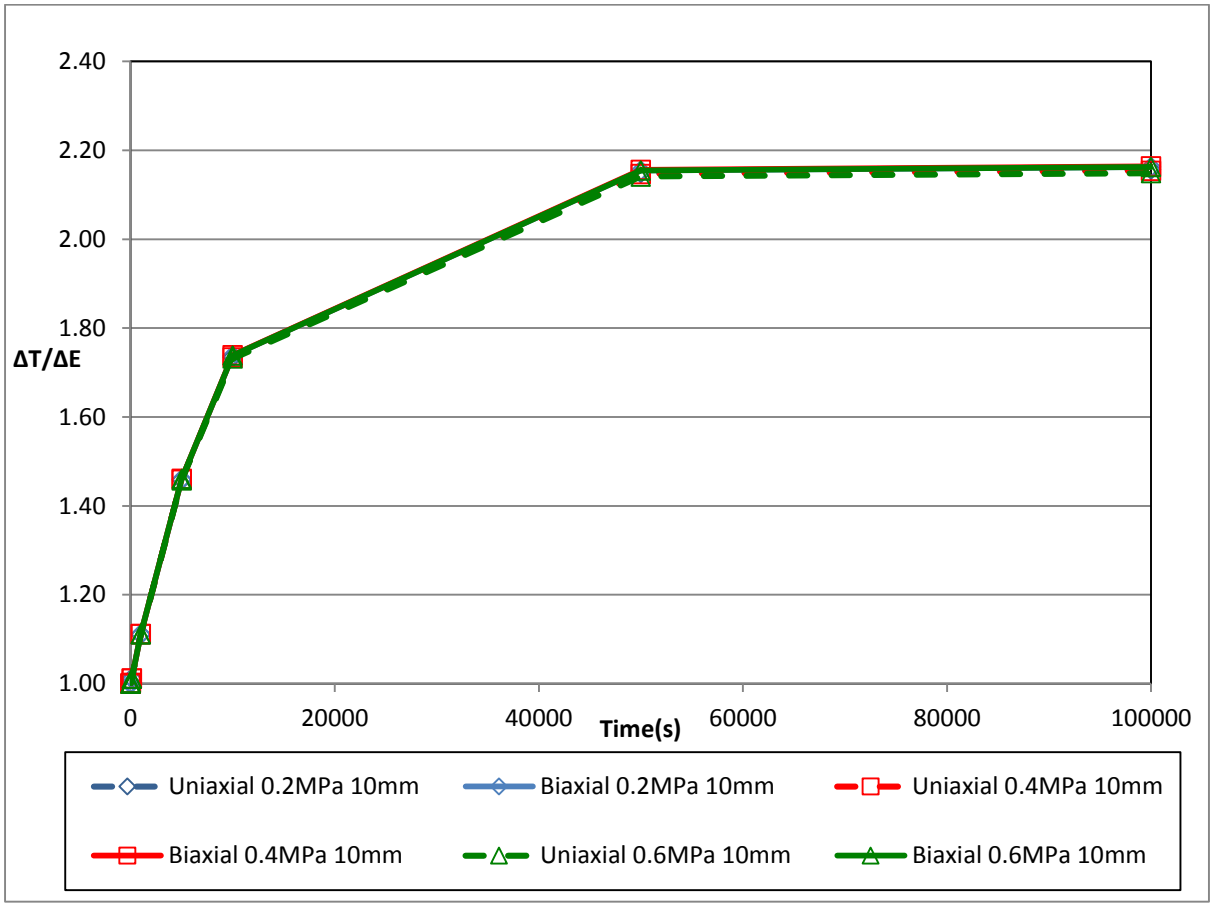

Figure 5-32: ΔT/ΔE for a 1mm by 10mm longitudinal crack in HDPE

A similar graph for m/m_E for the 1mm by 10mm longitudinal crack in HDPE is shown below in figure 5-33. The graph is similar to figure 5-32, with the m/m_E ratio attaining a maximum value just below 2.2 at 100 000s. This was similar to the behaviour observed for the round holes.

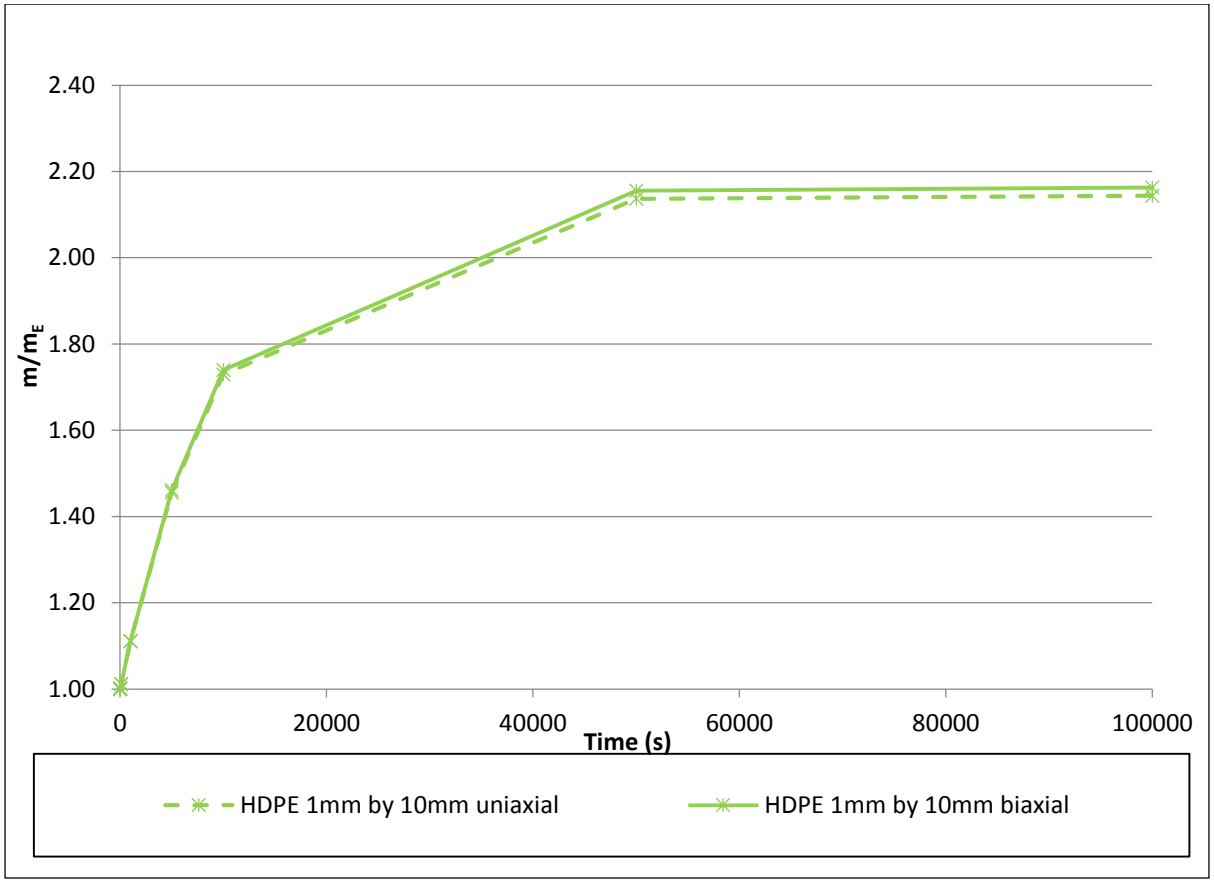

Figure 5-33: m/m_E for 1mm by 10mm longitudinal crack in HDPE

5.5.7 Cyclic results for longitudinal cracks

The pipe with a 1mm by 10mm longitudinal crack was subjected to cyclic loading by applying pressure of 0.2MPa, 0.4MPa and 0.6MPa for a duration of 100 000s (27.8 hours) for each load. The pressure loads and corresponding deformed area for a 1mm by 10mm crack in HDPE are illustrated in the figures 5-34 and 5-35 below. In figure 5-35, both cyclic results and non-cyclic results are represented. The cyclic results are the red round dots. The non-cyclic results are the blue, pink and green diamonds and represent the pressure load applied to the pipe for 100 000s.

The cyclic simulation results for a 1mm by 10mm longitudinal crack in HDPE are illustrated in figures 5-34 and 5-35 below. The 1mm by 10mm longitudinal crack shows a similar trend to the 1mm round hole, as the hole regains its shape if enough time is allowed for it to stabilise within every load cycle. The non-cyclic deformed areas from the loading phase are also shown and show that if stabilisation is allowed, there is no hysteresis observed. A similar graph for the 1mm by 10mm longitudinal crack in PVC is included in the appendix. The graphs showing the deformed area for a 1mm by 10mm longitudinal crack in PVC are included in the appendix.

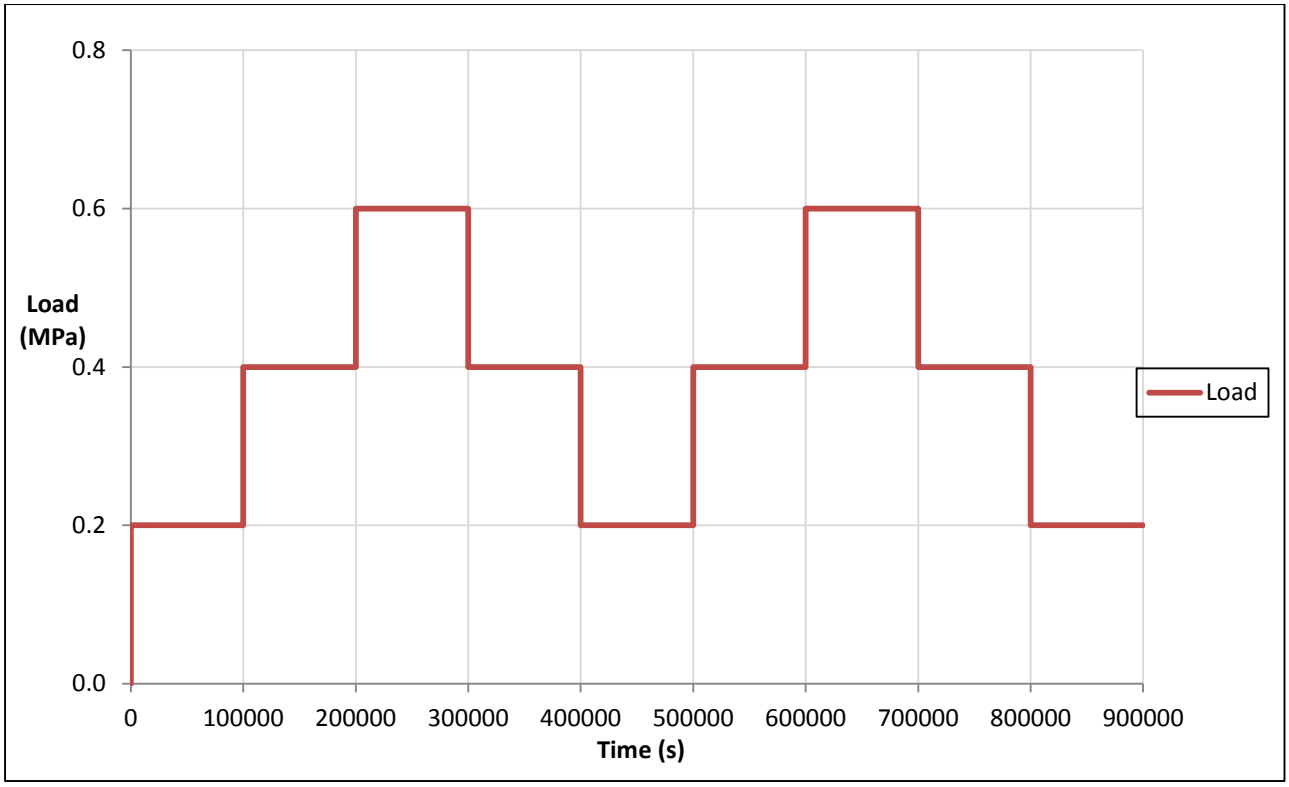

Figure 5-34: Cyclic loading for a 1mm by 10mm longitudinal crack in HDPE pipe

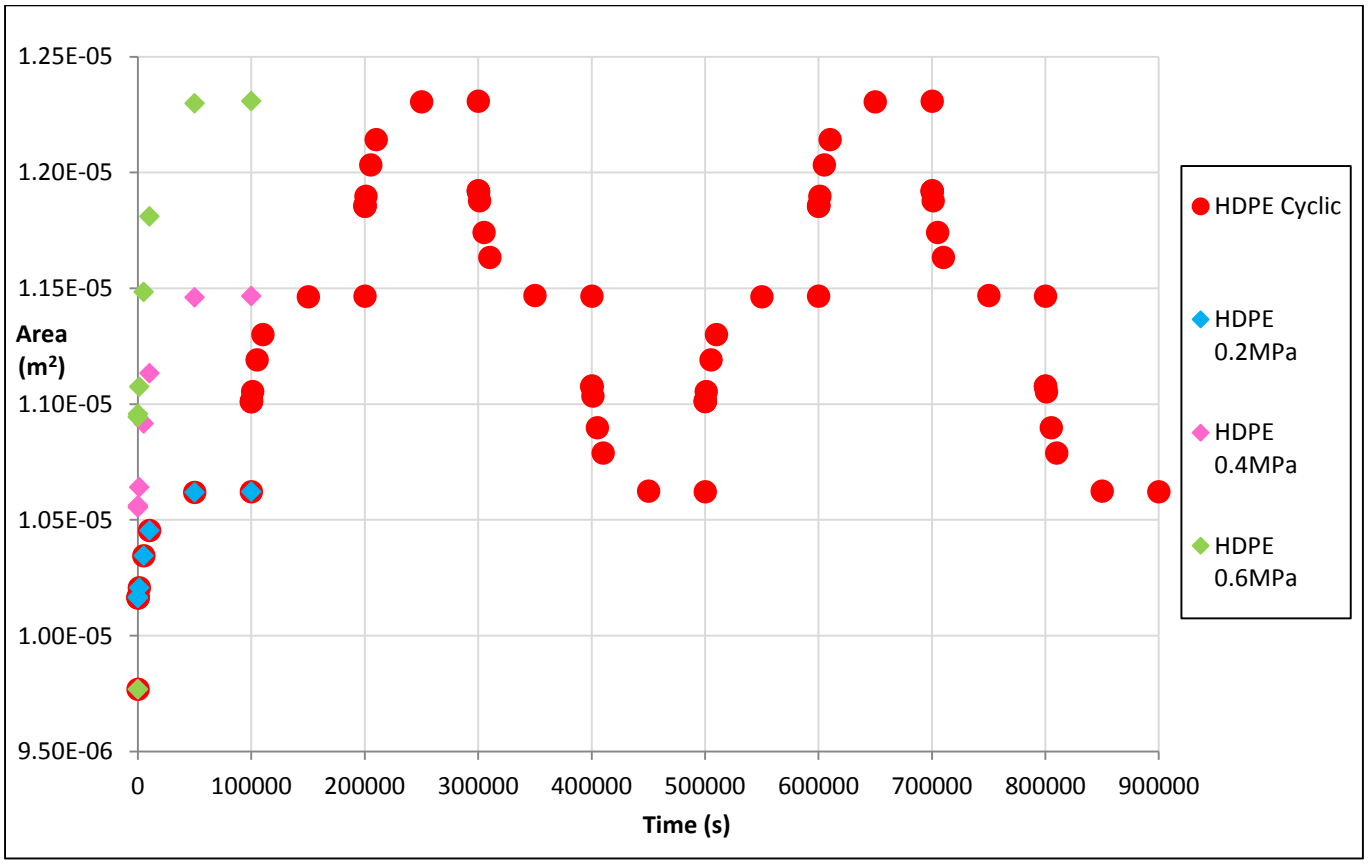

Figure 5-35: Deformed area against time for a 1mm by 10mm longitudinal crack during cyclic loading

5.6 Comparison of longitudinal cracks in HDPE and PVC

5.6.1 Gradient (m) of the pressure-leakage relationships in longitudinal cracks

The gradients of the longitudinal cracks were plotted on a graph as illustrated in figure 5-36 below.

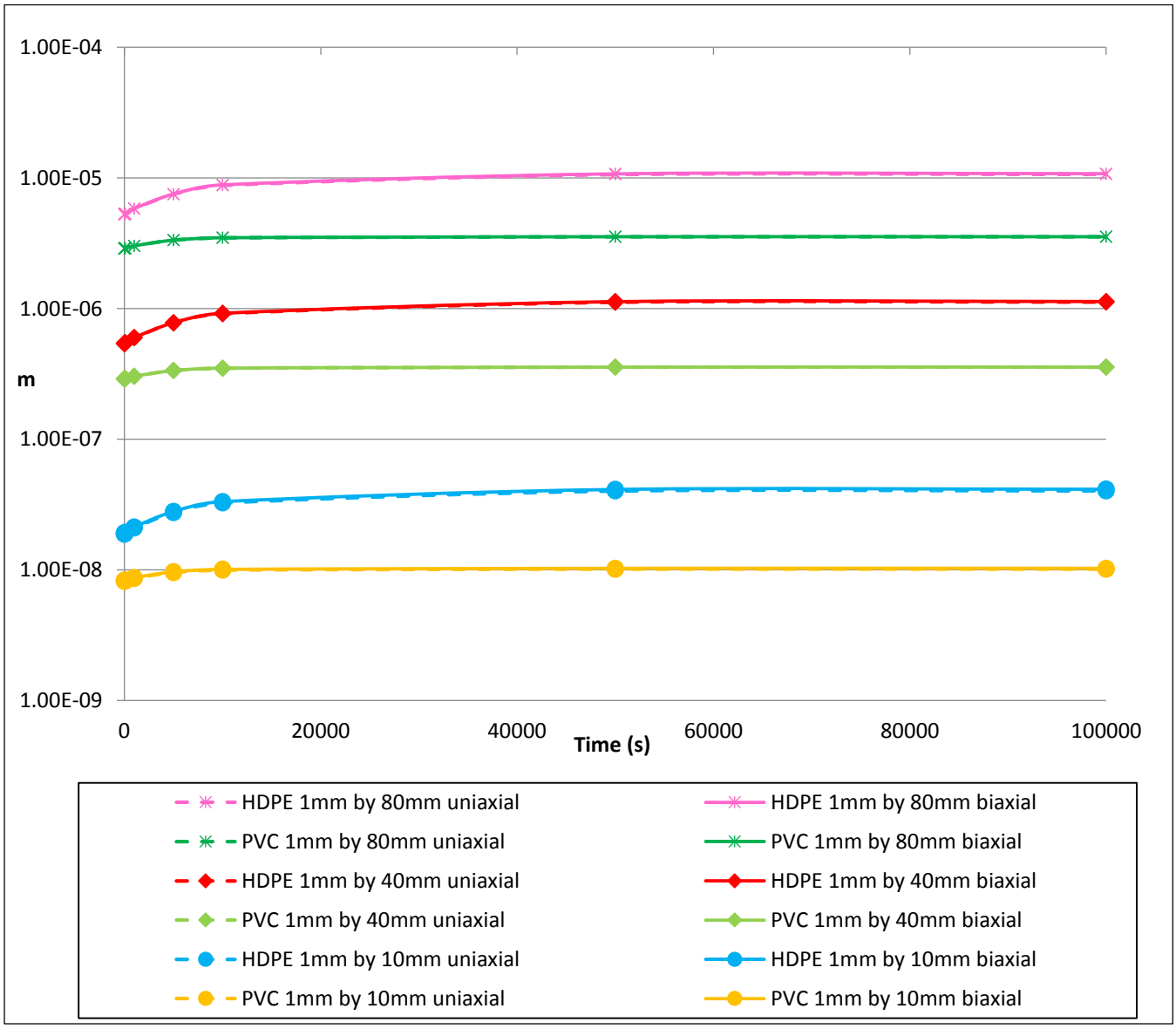

Figure 5-36: Variation of gradient (m) with time for longitudinal cracks in HDPE and PVC

Figure 5-36 illustrates that gradient (m) increases with the length of the crack, a trend also observed by Cassa et al. (2010) for elastic deformation in PVC pipes. Also, there is no notable difference between the uniaxial and biaxial load states.

5.6.2 Leakage exponent (N1) in longitudinal cracks

Leakage exponents of longitudinal cracks were also plotted against time in figure 5-37 below.

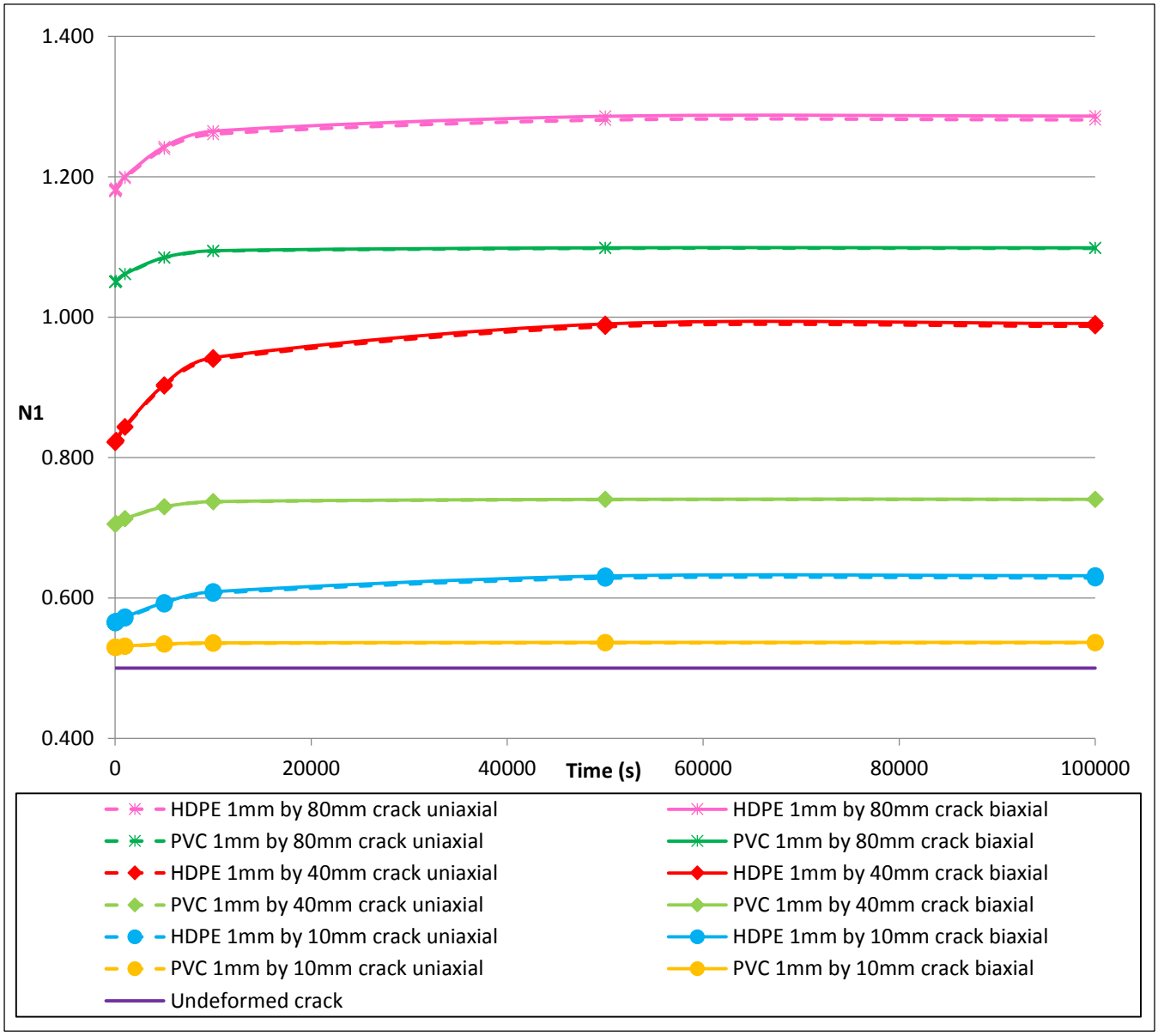

Figure 5-37: Variation of leakage exponent (N1) with time for longitudinal cracks in HDPE and PVC

In figure 5-37, N1 also increases with crack length in both HDPE and PVC pipes a trend similar to that observed by Cassa et al. (2010) for elastically deforming PVC pipes. This is in contrast to the round holes where N1 values for the 1mm hole in HDPE were higher than N1 values for the 12mm hole in PVC. This suggests that N1 in round holes is largely dependent on pipe material while N1 in longitudinal cracks is largely dependent on crack length. The N1 values of the tested cracks are all above 0.5 and almost identical for both the uniaxial and biaxial load states.

5.6.3 Percentage change in area of longitudinal cracks

The percentage changes in area for all the longitudinal cracks in HDPE (biaxial state) are compared in the figure 5-38 below. Similar graphs for all cracks are included in the relevant appendices.

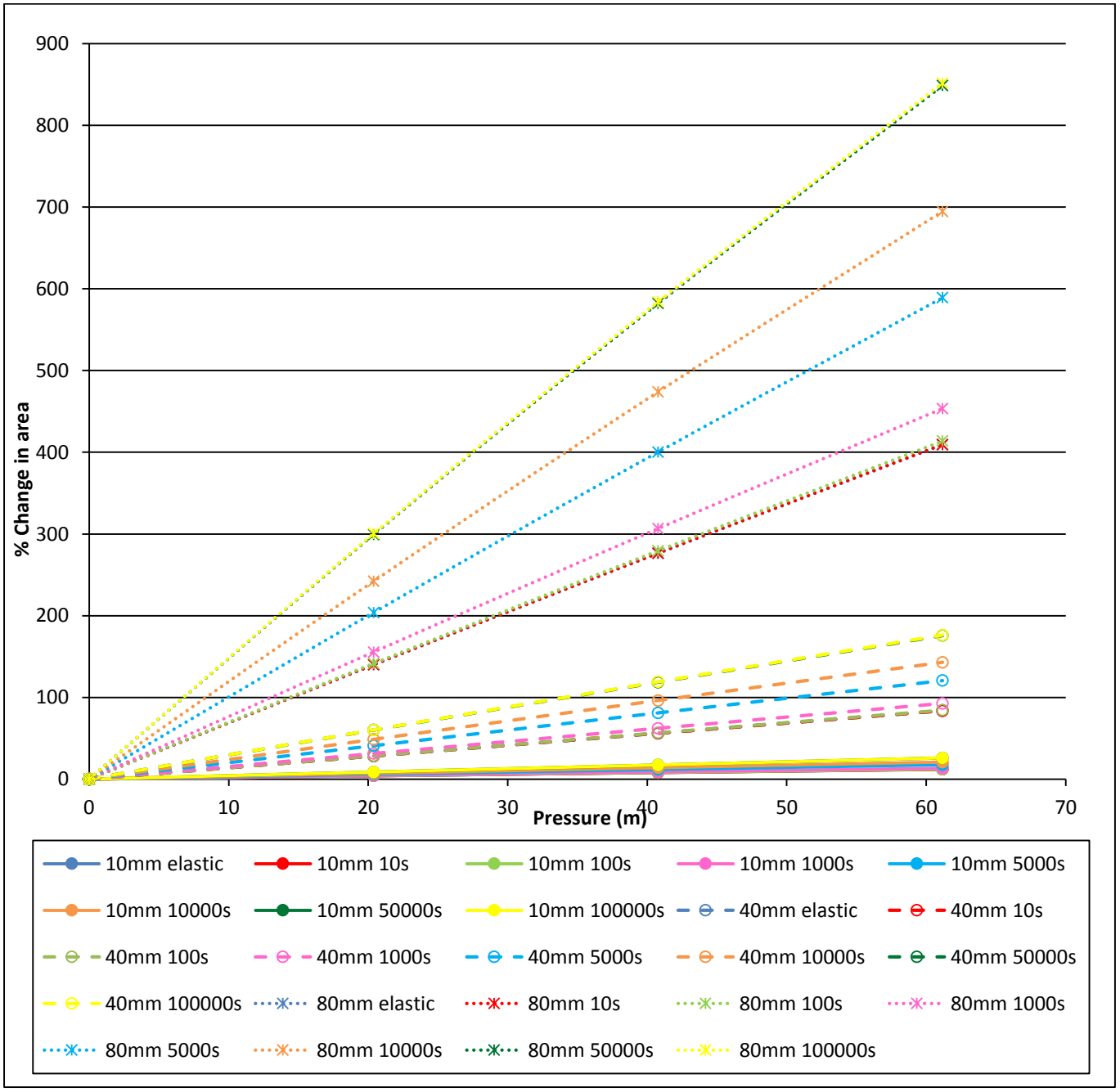

Figure 5-38: Percentage change in area against pressure for longitudinal cracks in HDPE, biaxial state

From figure 5-38, it is seen that percentage change in area of longitudinal cracks increases with crack length and time period. The 80mm longitudinal crack at 100 000s has the largest percentage

increase and the 10mm crack has the smallest increase. Range of increases for the cracks also increases with length, with the 80mm crack having a larger range 400% to about 850% and the 1mm crack having the smallest range (about 10%-25%).

5.6.4 Ratio of total change in area to elastic change in area and gradient to elastic gradient

The ratios of total change in area to elastic change in area and gradient to elastic gradient for HDPE and PVC are illustrated below in the figures 5-39, 5-40, 5-41 and 5-42 below.

In figures 5-39 and 5-40 for longitudinal cracks in HDPE, the $\Delta T/\Delta E$ ratios are similar to the m/m_E ratios for each time. The same observation is made for the round holes in PVC as seen in figures 5-41 and 5-42. The similarity of the $\Delta T/\Delta E$ and m/m_E graphs is significant as it indicates that the analysis by Cassa et al. (2010) for elastic pipe materials can be applied to linear viscoelastic materials.

The longitudinal cracks in HDPE display maximum ratios between 2.0 and 2.20 at 100 000s while the longitudinal cracks display maximum ratios between 1.20 and 1.25 at 100 000s. From the m/m_E graphs (figures 5-40 and 5-42), it is seen that the 1mm by 10mm cracks have the highest m/m_E ratio, followed by the 1mm by 40mm and lastly the 1mm by 80mm longitudinal crack. However it is not possible to determine if $\Delta T/\Delta E$ and m/m_E follow a particular trend based on crack size as the lines in the figures are so close together.

The similarity between the $\Delta T/\Delta E$ and m/m_E graphs means that the analysis for elastic materials by Cassa et al. (2010) may be adapted for linear viscoelastic materials.

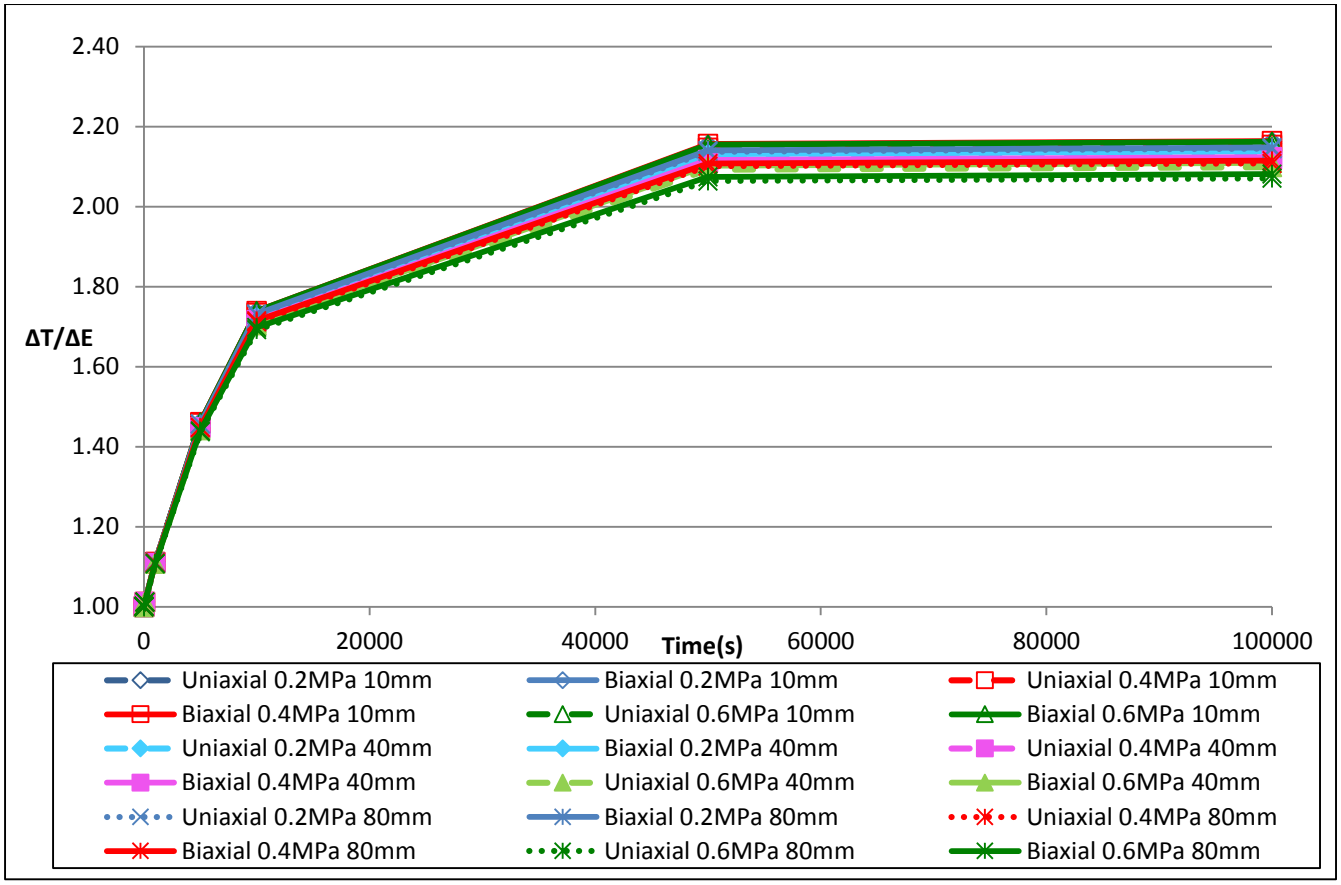

Figure 5-39: ΔT/ΔE for longitudinal cracks in HDPE

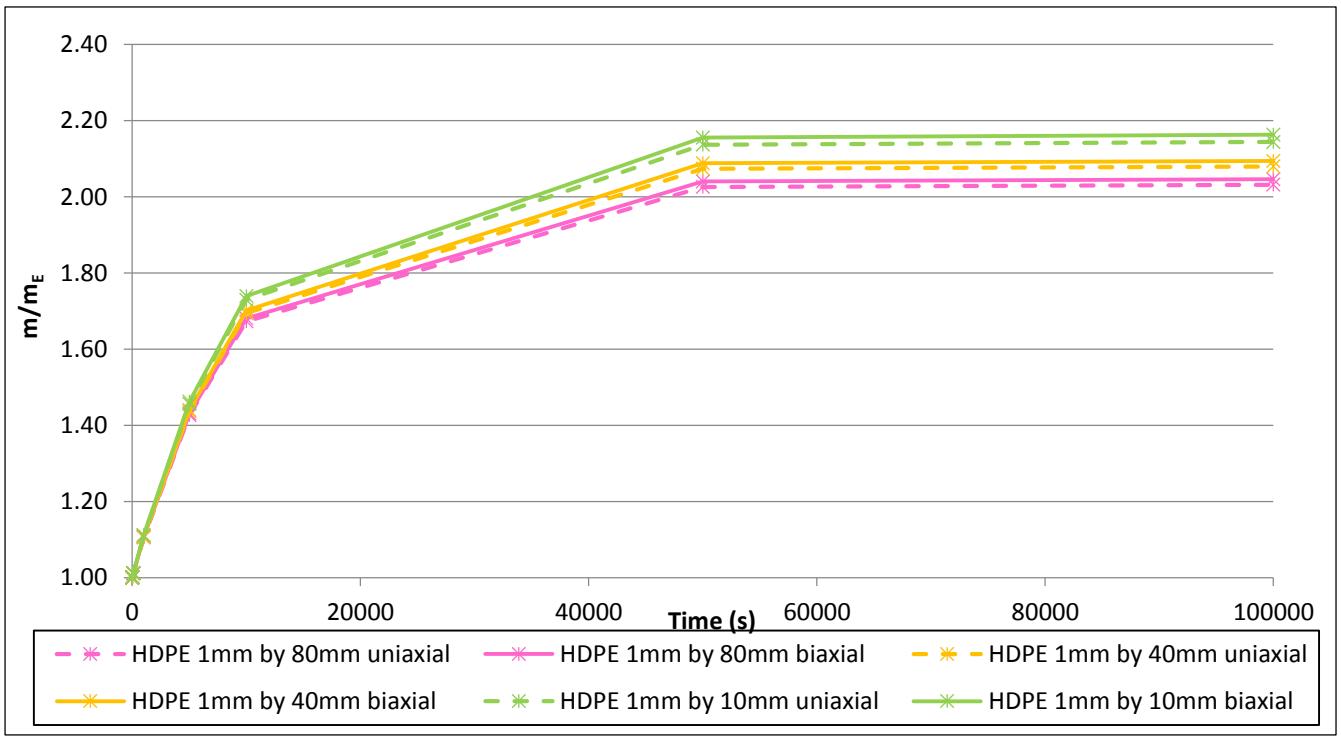

Figure 5-40: m/m_E for longitudinal cracks in HDPE

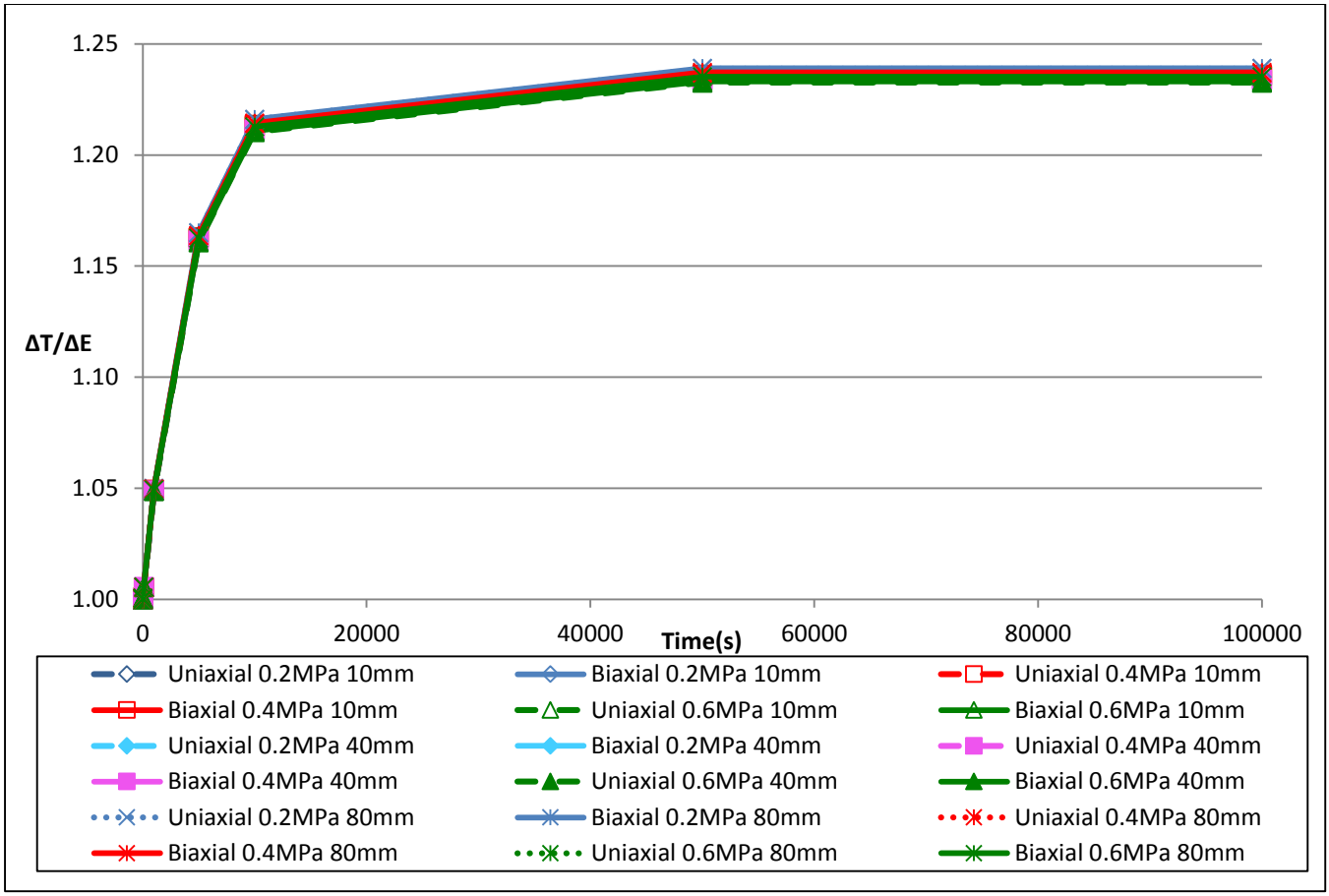

Figure 5-41: ΔT/ΔE for longitudinal cracks in PVC

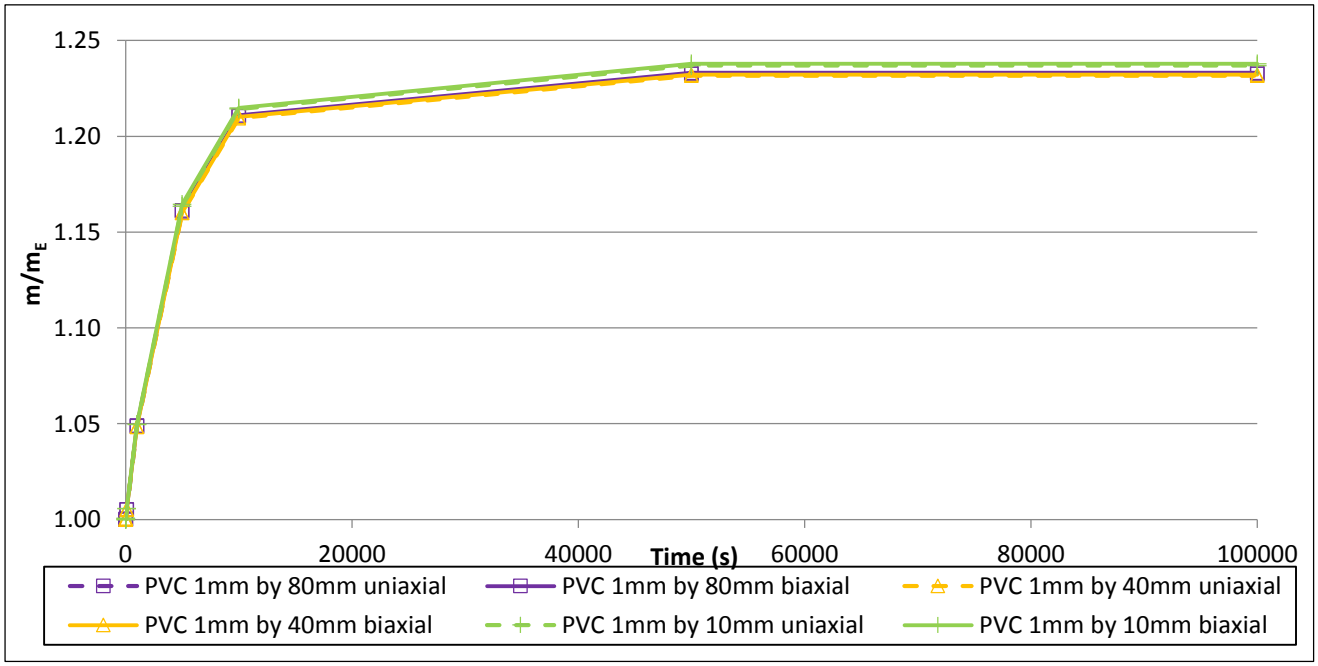

Figure 5-42: m/m_E for longitudinal cracks in PVC

5.7 Discussion

In the sections above, a summary of the results obtained in the investigation is presented. The parameters of the pressure-leakage relationship for the two leak types and materials are presented and explained. In this section it is discussed how the gradients, leakage exponents and leakage numbers as parameters of the pressure-leakage relationship are affected by creep deformations.

5.7.1 Leak area-pressure relationship and gradient (m)

The relationship between leak area and pressure for the linear viscoelastic materials investigated was found to be linear for both round holes and longitudinal cracks. This behaviour is similar to that of leaks in elastic pipe materials as investigated by Cassa et al. (2010) and for a leak in a steel pipe just before plastic deformation occurs as investigated by Ferrante (2012). However due to the creep property of viscoelastic materials, time dependent pressure loading was investigated. It was seen that as the time period increased, the leak areas also increased. For the different pressures at each time period, linear relationships between pressure and leak area were observed.

Since the leak area – pressure relationships were linear, the gradient (m) of these relationships for each time period was calculated. The gradient of the linear pressure-leakage relationship has been identified as an important parameter in similar studies such as Cassa et al. (2010) for characterisation of leaks in elastic pipe materials. The results for the current study show that the gradient for viscoelastic materials gradually increased from the elastic state and had stabilised by time period of 50 000s and 100 000s for both HDPE and PVC pipes. Since elastic deformation behaviour is not time dependent, this behaviour was not observed in elastic deformation investigations.

The linear relationship between area and pressure means that m is constant for a specific time period. When the gradients of the different leaks and materials were plotted against time, the curves resembled the creep curves of the materials, suggesting that material behaviour does play an important role in the pressure-leakage relationship. Studies by Greyvenstein (2007) and Cassa (2005) also show that material behaviour has an effect on the pressure-leakage relationship, a factor also recognized in the results of this investigation. The gradients of PVC were lower than that of HDPE for all leak types, even though both were modelled as viscoelastic materials as seen in figures 5-19 and 5-36.

5.7.2 Leakage exponent (N1)

The leakage exponent (N1) is another important parameter of the pressure leakage relationship. The leakage exponent may be determined from either the FAVAD concept or the power law as discussed in the literature review.

The FAVAD concept proposed by May (1994) and developed by Cassa (2005) may also be applied to the results discussed in this project since a linear relationship exists between leak area and pressure. The FAVAD concept (equation 2.8) gives a range of 0.5-1.5 for the leakage exponent for materials in which the relationship between leak area and pressure is linear. For easy reference the FAVAD equation is repeated below:

$$Q = C_d \sqrt{2g}\left(A_0 h^{0.5} + m h^{1.5}\right) \tag{5.3}$$

In equation (5.3), the equation maybe separated into two parts, the fixed part and the variable part. The fixed part is characterised by a fixed area (A_0) and an exponent of 0.5. The variable part is characterized by the gradient (m) and a leakage exponent of 1.5. The variable part is due to the change in the value of m for different pipe materials. For viscoelastic materials, m also changes with time. The value of m will therefore have an effect on the contribution of the variable part of the FAVAD equation to leak discharge. An increase in pressure for a pipe material with a relatively high m will result in a larger leak discharge calculated compared to a material of lower m. Since m for viscoelastic materials also increases with time, the effect of the variable component will also vary with time.

The power law equation is commonly used by leakage practitioners to characterise leakage in distribution systems. The equation was applied to the leak discharge as discussed above in section 5.3.4. Power equations were generated in MS Excel to determine the value of N1. The full results of the N1 values are included in the appendices. The value of the N1 for all leak holes was found to be above 0.5 with the highest being 0.9910 for a 1mm by 80mm crack in HDPE, biaxial state. Values of all leakage exponents are included in the appendices.

This variation in leakage exponent values shows that the original Torricelli equation with an N1 of 0.5 does not describe the pressure-leakage relationship in the pipe materials investigated adequately. The reason for this is that the Torricelli equation does not allow for deformable leak areas. Cassa et al. (2010), Buckley (2007) and Greyvenstein & Van Zyl (2007) also observed that the leakage exponent varied from 0.5. A direct comparison of leak exponents was done for the leaks investigated in this study and earlier studies as shown in the table 5-5 below. For the current study,

values for the elastic deformation phase are used since the study by Cassa (2005) assumed only elastic deformation.

Leak type in PVC pipe, Class 6	Leakage exponent values					
	Cassa (2005)		Buckley (2007)		Current study	
	Uniaxial	Biaxial	Uniaxial	Biaxial	Uniaxial	Biaxial
12mm round hole	0.5055	0.5081	0.5150	0.5091	0.5052	0.5069
1mm by 10mm longitudinal crack	0.5327	0.5327	-	-	0.5294	0.5298
1mm by 40mm longitudinal crack	0.6887	0.6873	0.9040	0.8413	0.7050	0.7051

Table 5-5: Comparison of leak exponents from power law equation in PVC pipe, class 6

From the table above, the leakage exponent values of the numerical study of Cassa (2005) are close to the results of the current investigation. Buckley (2007) obtained the leak exponent values from a practical investigation and this may explain the variation in his results compared to the numerical studies.

5.7.3 Leakage number (L_N)

The leakage number was developed by Van Zyl & Cassa (2013) as a better way of characterising leakage since it depends on the fixed leak characteristics such as un-deformed area and pressure. The leakage number is calculated using equation (2.13). The leakage numbers of the leaks investigated in this study were calculated using the average pressure of this study (0.4MPa) and the N1 subsequently calculated from equation (2.14). The calculated values of L_N and N1 were compared to the figure 2-9. The values of N1 obtained for the leaks are in agreement with those predicted by figure 2-9. A summary of the L_N values for the 1mm hole and 1mm by 80mm longitudinal crack in HDPE, biaxial state are included in the tables 5-6 and 5-7 below.

ime (s)	N1 from power law	m	L_N	Calculated N1	m/A_0
0	0.5107	2.330E-10	0.0121	0.5120	0.0003
10	0.5107	2.330E-10	0.0121	0.5120	0.0003
100	0.5109	2.379E-10	0.0124	0.5122	0.0003
1000	0.5118	2.575E-10	0.0134	0.5132	0.0003
5000	0.5151	3.311E-10	0.0172	0.5169	0.0004
10000	0.5176	3.875E-10	0.0202	0.5198	0.0005
50000	0.5212	4.684E-10	0.0244	0.5238	0.0006
100000	0.5212	4.684E-10	0.0244	0.5238	0.0006

Table 5-6: Leakage numbers and calculated leakage exponents for the 1mm hole in HDPE, biaxial, 0.4MPa

Time (s)	N1 from power law	m	L_N	Calculated N1	m/A_0
0	1.0504	2.877E-06	1.4707	1.0953	0.0361
10	1.0505	2.878E-06	1.4712	1.0953	0.0361
100	1.0517	2.892E-06	1.4783	1.0965	0.0363
1000	1.0616	3.018E-06	1.5428	1.1067	0.0378
5000	1.0851	3.341E-06	1.7079	1.1307	0.0419
10000	1.0946	3.484E-06	1.7810	1.1404	0.0437
50000	1.0988	3.548E-06	1.8137	1.1446	0.0445
100000	1.0988	3.548E-06	1.8137	1.1446	0.0445

Table 5-7: Leakage numbers and calculated leakage exponents for the 1mm by 80mm longitudinal crack in HDPE, biaxial, 0.4MPa

From the tables 5-6 and 5-7, it is seen that the leakage exponent values calculated from the leakage number are higher than those obtained from the power law. Leakage numbers and calculated leakage exponents for all leak types are included in the relevant appendices.

5.7.4 Ratio of total change in area to elastic change in area and gradient to elastic gradient

The graphs of $\Delta T/\Delta E$ and m/m_E for the leaks investigated illustrated that the FAVAD and leakage number concepts developed by Van Zyl & Cassa (2013) may be adapted for viscoelastic pipe materials. The figures in sections 5.4.4 for round holes 5.6.4 for longitudinal cracks show similar patterns for $\Delta T/\Delta E$ and m/m_E against time in both HDPE and PVC pipe materials. At 100 000s the $\Delta T/\Delta E$ and m/m_E values range from 2.0 to 2.2 in HDPE and 1.20 to 1.25 in PVC, with round holes showing greater variation than longitudinal cracks for both materials. This behaviour has the following implications for pressure-leakage management:

i. When pressure is altered in distributions systems, viscoelastic deformations would have essentially stabilised by 50 000s (13.89 hours). This was observed from the leak area against time graphs in the results chapter. If the system is allowed sufficient time to stabilise the total change in leak area experienced in HDPE can be estimated as:

$$\Delta T = 2.2 \times \Delta E \tag{5.4}$$

And that for PVC may be estimated as:

$$\Delta T = 1.25 \times \Delta E \tag{5.5}$$

ii. For time periods less than 50 000s, the graphs provided in sections 5.4.4 and 5.6.4 may be used to estimate the viscoelastic leak area deformation.

iii. Since the m/m_E against time graphs show a similar pattern to that of the $\Delta T/\Delta E$ against time graphs, equations (5.4) and (5.5) can also be applied to calculate the gradient of viscoelastic pipe materials. ΔE is replaced with m_E to find m after enough time is allowed for deformations to stabilise. m_E for round holes may be determined from numerical investigation methods while m_E for longitudinal cracks may be determined from the following equation (5.6) proposed by Van Zyl & Cassa (2013):

$$m_E = \frac{2.93157 \times D^{0.3379} \times l^{4.80} \times 10^{0.5997(\log l)^2} \times \rho \times g}{E \times (t^*)^{1.746}} \tag{5.6}$$

Where D is the inner pipe diameter, l is the length of the crack, ρ is the density of the fluid that flows through the pipe, g is the gravitational constant, E is the elastic modulus and t* is the pipe thickness.

iv. The determination of a viscoelastic gradient (m) from an elastic gradient allows the calculation of a leak exponent via the leakage number. The effect of the viscoelastic deformation on the gradient and thus the leakage number can be expressed as a function of the elastic deformation gradient. For this investigation, the effect on the gradient (m) after enough time (50 000s) is allowed for deformation to stabilise may be summarised as follows:
For HDPE:

$$m = 2.2 \times m_E \tag{5.7}$$

And for PVC:

$$m = 1.25 \times m_E \tag{5.8}$$

Thereafter, the leakage number for a viscoelastic pipe maybe calculated using equation (2.13), with the gradient determined from equations (5.7) or (5.8).

The relationship between the leakage number and leak exponent for viscoelastic materials may therefore be deduced using figure 2-9 developed from elastically deforming materials. From figure 2-9, equations (5.7), (5.8) and (2.13), it follows that if L_N is less than 0.01 or greater than 100, the

leakage exponent is not affected so much by variations in pressure or leak area. If the leakage number is in between 0.01 and 100, then the equations (5.7), (5.8), (2.13) and figure 2-9 may be used to predict the leak exponent.

5.7.5 Cyclic simulations implications

Cyclic simulation results suggest that for linear viscoelastic materials, no hysteresis is evident if enough time is allowed for stabilisation. All loading and unloading cycles were 100 000s (27.8 hours). Ferrante et al. (2011) observed hysteresis in a polyethylene pipe after a loading time of 12hours, which is less than the 27.8 hours for this project.

During the cyclic simulations, pressure was increased and then decreased by 0.2MPa for each step. It was found that the increase in deformation for each 0.2MPa increase or decrease was equal, for all pressures. The change in deformation was expressed as a percentage of the total deformation for each load step. Graphs can therefore be obtained to predict the amount of deformation to occur for any decrease or increase in pressure.

These changes in deformation are shown for the 1mm holes in both HDPE and PVC in the figures below (figure 5-43 to figure 5-46). Since the percentage change in deformation was calculated with respect to the total deformation after a pressure change, the graphs in figures 5-43 to figure 5-46 are valid for any pressure change. Similar figures for the 1mm by 10mm longitudinal crack are included in the appendices. The figures illustrate how the leak area deformation changes over a period of 100 000s (27.8 hours) when the pressure is increased or decreased. The change in deformation at each time was calculated as a percentage of the total deformation at 100 000s for every pressure step. Unlike equations (5.4) and (5.5) that only predict deformation at 100 000s, the graphs in figures 5-43 to 5-46 may be used to predict the actual deformed area between 0s and 100 000s. For example, equations (5.4) and (5.5) may be used to calculate the excess area due to deformation (ΔT) and then percentages obtained from the figures 5-43 to 5-44 are applied to calculate deformation for times between 0s and 100 000s.

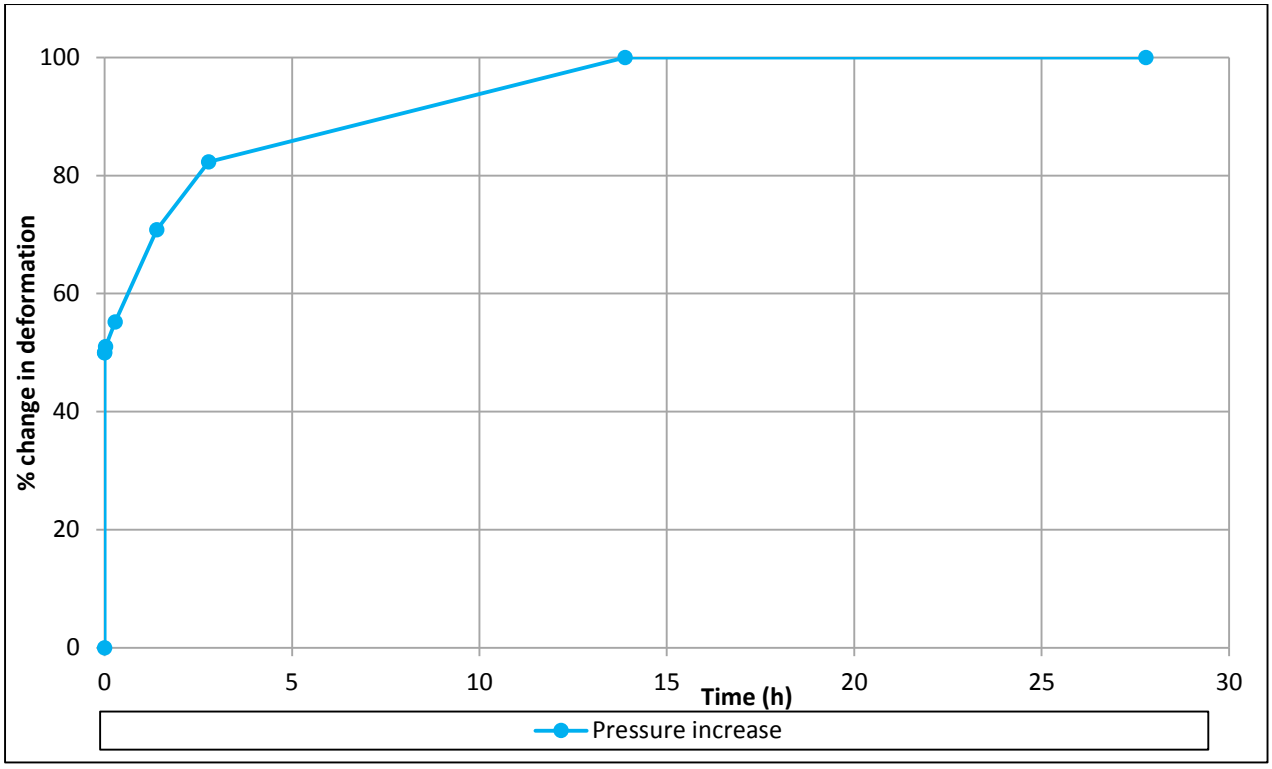

Figure 5-43: Percentage change in deformation against time for an increase in pressure, 1mm hole in HDPE, biaxial

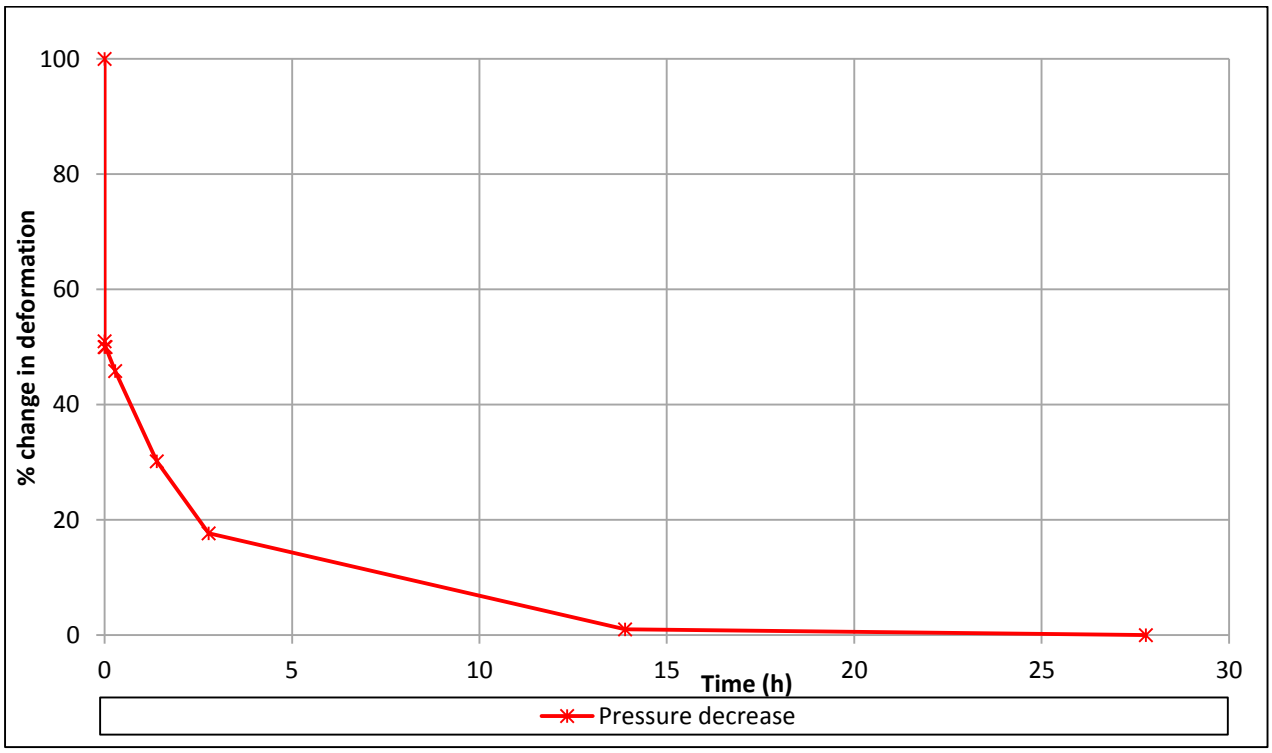

Figure 5-44: Percentage change in deformation against time for a decrease in pressure, 1mm hole in HDPE, biaxial

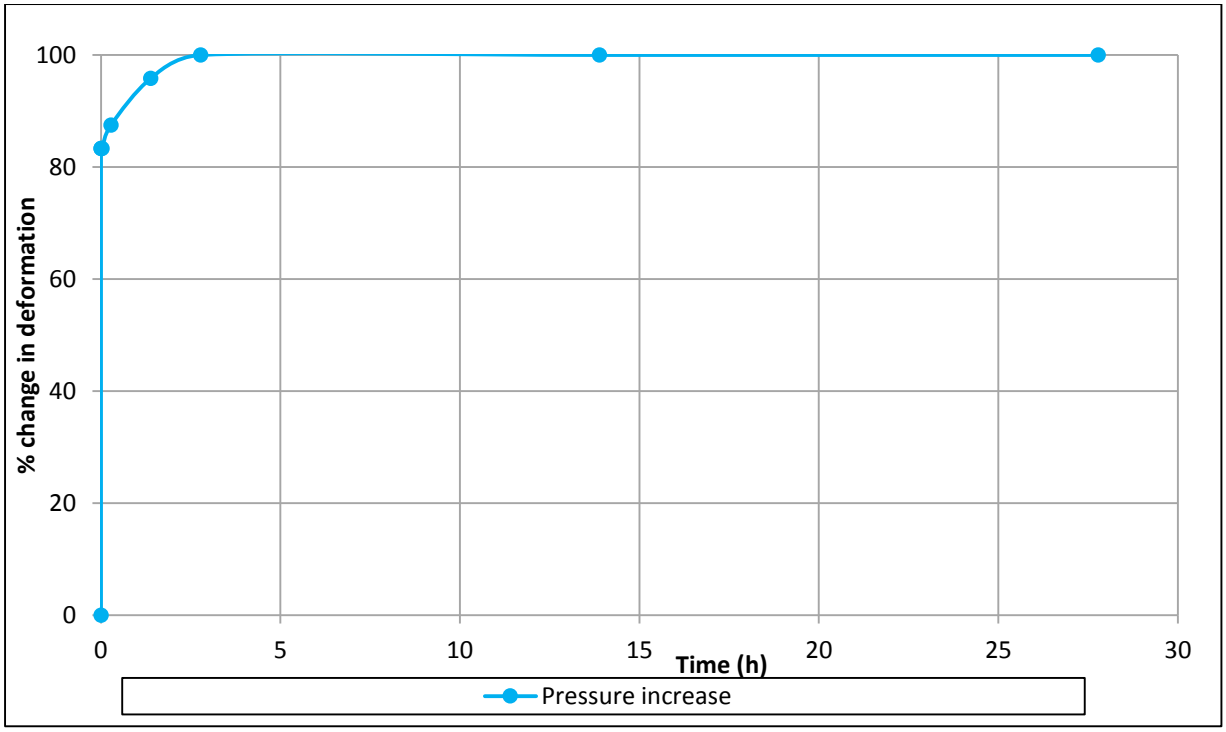

Figure 5-45: Percentage change in deformation against time for an increase in pressure, 1mm hole in PVC, biaxial

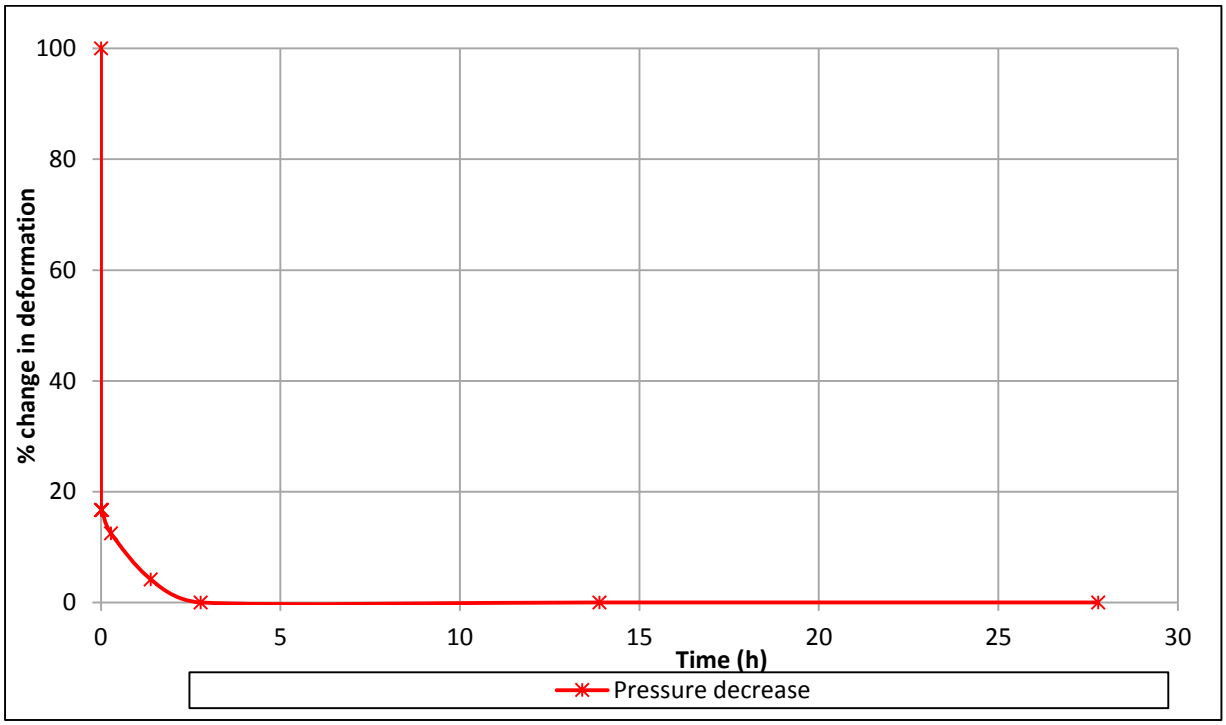

Figure 5-46: Percentage change in deformation against time for a decrease in pressure, 1mm hole in PVC, biaxial

5.7.6 Change in area due to creep and elastic deformation

The ratio of change in area due to creep at 100 000s to change in area due to elastic deformation for all the leak types was calculated and presented in the bar chart below (figure 5-43). The elastic change in area was calculated as shown earlier in equation (5.2).

Change in area due to creep (ΔC) is the defined as the difference between the total change in area and the elastic change in area as shown in equation 5.9 below. The total change in area is calculated from equation 5.3.

$$\Delta C = \Delta T - \Delta E = A_D - A_E \tag{5.9}$$

The chart in figure 5-43 shows that the highest ΔC:ΔE ratios occur in the 12mm round hole for both HDPE and PVC. This means that the 12mm round hole has the highest increase in creep deformation when compared to its elastic deformation. The 1mm round hole has the lowest increase and the longitudinal cracks lie somewhere between the 12mm and 1mm round holes.

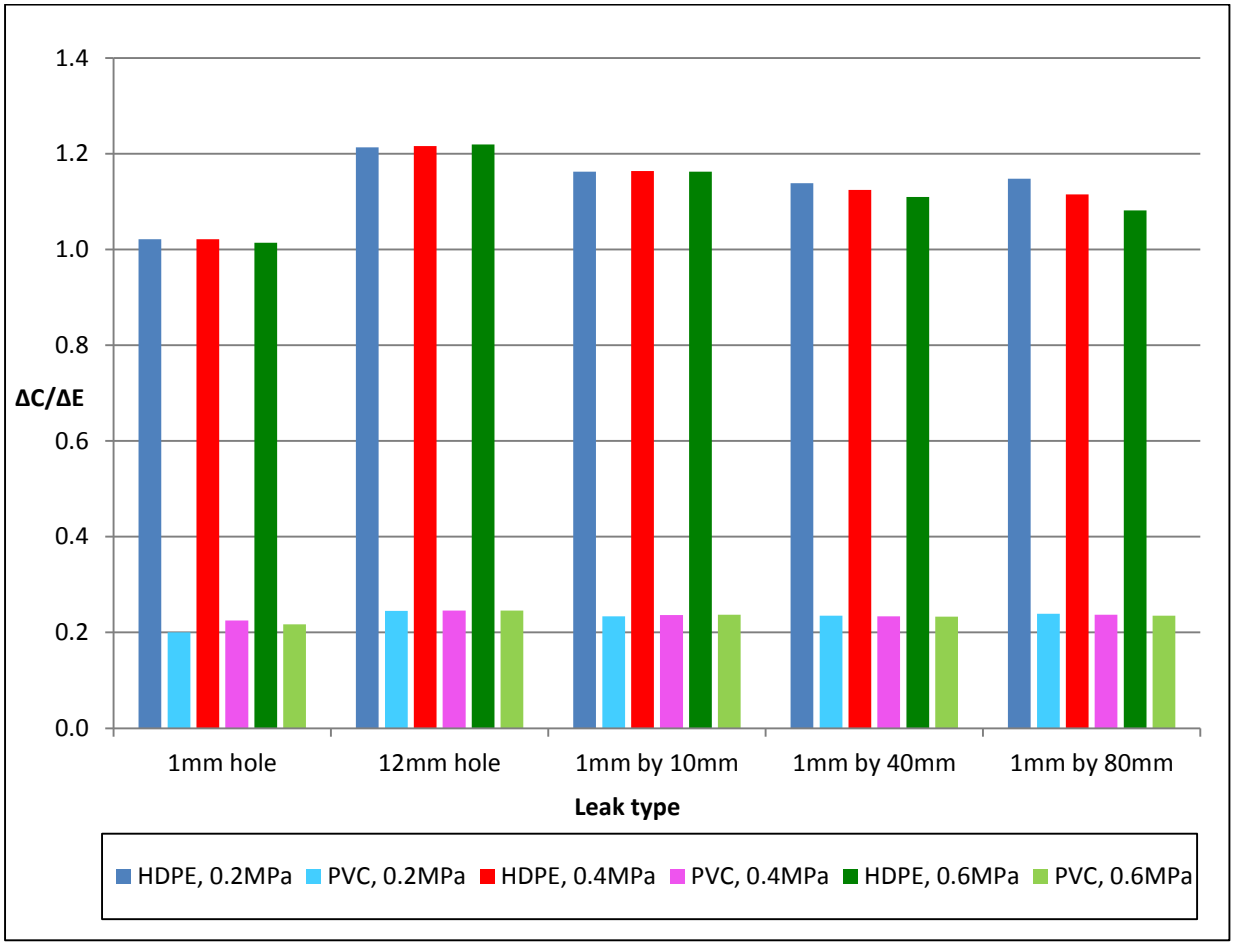

Figure 5-47: ΔC/ΔE for all leaks at 100000s, biaxial state

6 Conclusions and Recommendations

6.1 Conclusions

This project was carried out to investigate the effect of viscoelastic deformations on the parameters of the pressure – leakage relationship. The investigation was carried out with the help of finite element modelling software, Abaqus. The leak types investigated included round holes and longitudinal cracks of varying sizes. Two viscoelastic materials were investigated namely, HDPE and PVC.

The pressure-leakage relationship parameters investigated in this dissertation were the leak area, the gradient of the leak area – pressure relationship, the leak exponent and the leakage number. HDPE and PVC pipes were modelled in Abaqus with individual leaks. Pressure was applied to the pipes to simulate both the uniaxial and biaxial load states and the pipes were allowed to deform for various time periods.

Since the pipe materials were modelled as linear viscoelastic, both elastic and creep deformation was observed to occur. Results obtained from the investigation included the leak areas after pressure was applied for a certain time. In the result analysis, the deformed leak areas were then linked to the gradient, leak exponent and leakage number. The following conclusions may be drawn from the results analysis.

6.1.1 Leak area and leak exponent

The viscoelastic behaviour of the pipe materials affects the leak area deformations. From the results presented in chapter 5, it is seen that the shape of the leak area-time graphs resembles the creep deformation graph of a viscoelastic material shown in the literature review. The graphs of leak area against time showed an initial elastic deformation followed by creep for a total time period of 100 000s. This confirms previous research work by Ferrante (2012), Cassa (2005), and Greyvenstein (2007) that shows that material behaviour is an important factor in the pressure-leakage relationship in pipes. The deformed leak areas for the biaxial state were larger than the deformed areas in the uniaxial load state an observation also made by Cassa (2005).

Leak areas were also observed to increase linearly with pressure for all the time periods investigated, until stabilisation of the deformed leak areas occurred at 50 000s and 100 000s. The gradients of these linear relationships were also observed to increase with time, and the gradient-time graphs of the leaks resembled the creep graphs in the literature review. The linear relationship between the leak areas and pressure meant that the FAVAD concept first proposed by May (1994)

and applied to elastically deforming pipes by Cassa et al. (2010) could also be used for linear viscoelastic materials.

The use of the FAVAD concept led to the conclusion that the leakage exponent varied from 0.5 to 1.5 in the HDPE and PVC pipes investigated. The contribution of the exponent of 1.5 depended on the gradient of the material as discussed in the results chapter. However the FAVAD concept does not give an exact value of the leak exponent of a leak. The discharge of the leaks was therefore estimated and the power law fitted to the data in MS Excel to obtain the leak exponents for each time period. For an average pressure of 0.4MPa applied for a time period of 100 000s, the leak exponents from this method were found to vary from 0.514-0.533 for round holes in HDPE and 0.504-0.509 for round holes in PVC. Leak exponents for the longitudinal cracks varied from 0.629-1.286 for HDPE and 0.536-1.099 for PVC. N1 values increased with time, in a similar way to the creep graphs, therefore showing that material behaviour is an important aspect of the pressure-leakage relationship.

Van Zyl & Cassa (2013) however found that the leak exponent was not a good measure characterising leakage and developed the concept of the leakage number. The leakage numbers of the leaks investigated in this project were therefore calculated and new leakage exponents were calculated from the leakage number. For an average pressure of 0.4MPa applied for a period of 100 000s, the calculated leakage exponents for round holes in HDPE varied from 0.516-0.538 and for PVC leak exponents varied from 0.504-0.510. The calculated leak exponents for the longitudinal cracks varied from 0.644-1.346 in HDPE and 0.541-1.145 in PVC. From the ranges stated here one can observe that the leak exponents calculated from the leakage number are higher than those obtained from the power law graphs. Also, the leak exponents differ from 0.5 showing that the orifice equation is inadequate for leak modelling, an observation also made by Cassa et al. (2010) for elastically deforming materials.

For all time periods and pressures investigated, PVC pipes had lower deformed areas, leak exponent values and gradients for the same leak types in HDPE pipes. This is probably due to the difference in material behaviour, as PVC has a higher elastic modulus and lower relaxation time compared to HDPE. These leak parameters all increased with time and their graphs had a shape similar to the creep graph of viscoelastic materials.

6.1.2 Leakage number

The leakage number was originally developed by Van Zyl & Cassa (2013) for the characterisation of leak behaviour in elastic materials. Since the leak area – pressure relationship for viscoelastic materials was found to be linear as for elastic materials, the leakage number concept could be applied to the results of the current viscoelastic investigation. The leakage number enables the calculation of the leak exponent, once the gradient is known.

To confirm that figure 2-9 could be applied to viscoelastic materials, the leakage number was calculated for an average pressure of 0.4MPa. The ratio of gradient to original area (m/A_0) and leak exponents were also calculated. The leakage number and calculated leak exponent results corresponded with the values predicted by the graph in figure 2-9.

From the results analysis and discussion, it was observed that the ratio of the gradient to elastic gradient (m/m_E) of HDPE and PVC were 2.20 and 1.25 respectively, at a time period of 50 000s. Leak area deformation in both materials had stabilised by 50 000s. In the discussion (section 5.7), it was shown how the gradient for these viscoelastic materials could be deduced using equations (5.7) and (5.8).

The new leakage number calculated with these modified gradients therefore accounts for viscoelastic deformation. Consequently, the leak exponent for leaks in these materials may be obtained from the figure 2.9 or equation (2.13) as for elastically deforming materials. For time periods less than the time required for leak deformation to stabilise, the figures 5-23, 5-25, 5-40 and 5-42 that show the variation of m/m_E with time may be used to calculate the viscoelastic gradient.

6.1.3 Cyclic simulations implications

The results of the cyclic simulations showed that for linear viscoelasticity, there is no hysteresis observed if enough time is allowed for the leaks to stabilise. Complete recovery occurred when the pressure loads were applied or removed. The change in deformation was calculated as a percentage of the total deformation for each time period and this was observed to be equal for each pressure step as seen from the cyclic loading graphs (figures 5-18 and 5-35).

Graphs shown in figures 5-43 to 5-46 were therefore obtained to illustrate how the deformation varies over time for each material. Since the deformation at 100 000s is expressed as 100%, it follows that if the total deformation is known, the deformations at time periods less than 100 000s may be determined from the percentages in figures 5-43 to 5-46.

In conclusion, the results of this project show that the time dependent property of viscoelastic pipe materials has an impact on the leak behaviour and the pressure-leakage relationship due to the following:

i. The leak area and leak exponents of leaks in viscoelastic materials vary with pressure and time, and therefore the orifice equation is not an adequate description of the pressure-leakage relationship.
ii. The leak area against time graphs, gradient against time graphs and leak exponents against time graphs are all similar to the creep graphs of a viscoelastic material. Material behaviour is therefore an important factor in the pressure-leakage relationship.
iii. The leak area-pressure relationship was observed to be linear for both round holes and longitudinal cracks, similar to observations for elastically deforming materials. Therefore the FAVAD and leakage number concepts developed for elastic materials may be adapted for defining pressure-leakage relationships of linear viscoelastic pipe materials. This is true if the time dependency of the gradient is taken into account.
iv. Lastly, analysis of the cyclic simulations results showed that the change in deformation of leaks over time can be predicted if the elastic deformation is known.

6.2 Recommendations

For future study, the following recommendations are made:

i. The consideration of non-linear viscoelasticity to model polymeric pipe materials.
ii. Different pressure classes and pipe diameters may also be investigated. This is because pressure class and pipe thickness are related (equation 4.1). A different pressure class means a difference in thickness and Cassa (2011) also showed that gradient decreased with an increase in pipe thickness.
iii. Increase the frequency of area estimations during the investigation, for example include readings for deformation after 20 000s and 30 000s.
iv. Actual field pipe failures may also be modelled to compare numerical results to field investigations.
v. Longer pipe models with more than one leak may be investigated since actual pipes may have more than one leak.

7 References

1. *Abaqus 6.13 Documentation.* Simulia.
2. *DTD Handbook | Fundamentals of Damage Tolerance | Fracture Mechanics Fundamentals | Fracture Mechanics Fundamentals.* Available: http://www.afgrow.net/applications/DTDHandbook/sections/page2_2_0.aspx [2nd August 2013].
3. *Leakage explained.* Available: http://www.edie.net/abb/view_entry.asp?id=4268 [5th August 2014].
4. *Leakage Management and Control - A Best Practice Manual.* Geneva: World Health Organisation (WHO).
5. *Lecture 10.5.2: Design for Serviceability - II.* Available: http://www.fgg.uni-lj.si/kmk/esdep/master/wg10/l0520.htm [18 June 2013].
6. *Pipe materials.* Available: http://water.me.vccs.edu/concepts/material.html.
7. *Technical Note PP-838-TN Preventing Rapid Crack Propagation In Fused Water Pipelines.* Available: http://www.performancepipe.com/en-us/Documents/PP%20838-TN%20Preventing%20RCP%20in%20Fused%20Water%20Pipelines%2010-2010.pdf [05th August 2013].
8. *What is Water Hammer?* Available: http://www.bakercorp.com/pdfs/BKR_WhitePaper_WaterHammer.pdf [17th July 2013].
9. *Pipes and Pipelines: Principles and Practice.* 1998. K Myles and Associates.
10. *HDPE Pressure Pipe Overview.*2010. Available: http://www.marleypipesystems.co.za/images/pdfdownloads/productbrochures/hdpe_overview.pdf [12 May 2013].
11. *Polyvinyl Chloride.*2013. Available: http://www.lenntech.com/polyvinyl-chloride-pvc.htm [17th September 2013].
12. Andrews, E.H. 1968. *Fracture in polymers.* 1st ed. London: Oliver and Boyd Ltd.
13. Argon, A.S. & Cohen, R.E. 2003. Toughenability of polymers. *Polymer.* 44(19): 6013-6032. DOI:http://dx.doi.org/10.1016/S0032-3861(03)00546-9.
14. Balmer, D. *Mathematical models of viscoelastic behaviour.* Available: http://www.see.ed.ac.uk/~johnc/teaching/fluidmechanics4/2003-04/visco/ [18 June 2013].
15. Banks, H.T., Hu, S. & Kenz, Z.R. 2010. A brief review of elasticity and viscoelasticity. *Advances in Applied Mathematics and Mechanics.* 3(1): 1-51. DOI:10.4208/aamm.10-m1030.

16. Belonshenko, V.A., Beigel'zimmer, Y.E., Varyukhin, V.N. & Voznyak, Y.V. 2006. Strain hysteresis of polymers. *Doklady Physical Chemistry.* 409(1): 207-209.
17. Billmeyer, F.W. 1984. *Textbook of Polymer Science.* 3rd ed. Singapore: John Wiley & Sons, Inc.
18. Buckley, R.S. 2007. Theoretical investigation and experimentation into the expansion of round holes and cracks within pressurised pipes. Master of Science in Civil Engineering. University of Johannesburg.
19. Cassa, A.M. 2011. A numerical investigation into the behaviour of cracks in uPVC pipes under pressure. Doctor Ingenriae in Civil Engineering. University of Johannesburg.
20. Cassa, A.M. & Van Zyl, J.E. 2011. Predicting the head-area slopes and leakage exponents of cracks in pipes. *CCWI 2011: Computing and Control for the Water Industry: Urban Water Management - Challenges and Opportunities.*
21. Cassa, A.M., Van Zyl, J.E. & Laubscher, R.F. 2006. A numerical investigation into the behaviour of leak openings in uPVC pipes under pressure. *Biennial Conference and Exhibition, South Africa.* WISA.
22. Cassa, A.M., Van Zyl, J.E. & Laubscher, R.F. 2010. A numerical investigation into the effect of pressure on holes and cracks in water supply pipes. *Urban Water Journal.* 7(2): 109-120. DOI:10.1080/15730620903447613.
23. Cassa, A.M. 2005. A numerical investigation into the behaviour of leak openings in pipes under pressure. Master Ingeneriae in Civil Engineering. University of Johannesburg.
24. Cassa, A.M. & Van Zyl, J.E. 2014. Predicting the leakage exponents of elastically deforming cracks in pipes. *Procedia Engineering.* 70(2014): 302-310.
25. Chudnovsky, A., Zhou, Z., Zhang, H. & Sehanobish, K. 2012. Lifetime assessment of engineering thermoplastics. *International Journal of Engineering Science.* 59(2012): 108-139.
26. De Miranda, S., Molari, L., Scalet, G. & Ubertini, F. 2011. *The effect of pressure on leakage in longitudnally cracked pipes.* Available: http://www.lamc.ing.unibo.it/aimeta2011/dati/.../MEM-222-1.pdf.
27. Farley, M. & Trow, S. 2003. *Losses in Water Distribution Networks.* IWA Publishing.
28. Farshad, M. 2006. *Plastic Pipe Systems.*
29. Ferrante, M., Massari, C., Brunone, B. & Meniconi, S. 2013. Leak behaviour in pressurized PVC pipes. *Water Science & Technology: Water Supply.* 13(4): 987-992.
30. Ferrante, M. 2012. Experimental investigation of the effects of pipe material on the leak head-discharge relationship. *Journal of Hydraulic Engineering.* 138(August): 736-743.

31. Ferrante, M., Massari, C., Brunone, B. & Meniconi, S. 2011. Experimental evidence of hysteresis in the head-discharge relationship for a leak in a polyethylene pipe. *Journal of Hydraulic Engineering.* 137(7): 775-780.
32. Finnemore, E.J. & Frazini, J.B. 2009. *Fluid Mechanics with Engineering Applications.* 10th ed. Singapore: McGraw Hill.
33. Fung, Y.C 1993. Viscoelasticity. In *Biomechanics: Mechanical Properties of Living Tissues.* 2nd ed. Springer-Verlag, New York. 41-52.
34. Govindjee, S. *Fitting Prony's Series.* Available: http://www.ce.berkeley.edu/~sanjay/ce231mse211/prony.pdf [2014, June 5].
35. Greenshields, C.J. & Leevers, P.S. 1996. Rapid crack propagation in plastic water pipes: measurement of dynamic fracture resistance. *International Journal of Fracture.* 79(1): 85-95.
36. Greig, J., Leevers, P. & Yayla, P. 1992. Rapid crack propagation in pressurised plastic pipe—I. Full-scale and small-scale RCP testing. *Engineering Fracture Mechanics.* 42(4): 663-673.
37. Greyvenstein, B. 2007. An experimental investigation into the pressure-leakage relationship of fractured water pipes. Magister Ingenriae in Civil Engineering. University of Johannesburg.
38. Greyvenstein, B. & Van Zyl, J.E. 2007. An experimental investigation into the pressure - Leakage relationship of some failed water pipes. *Journal of Water Supply: Research and Technology - AQUA.* 56(2): 117-124.
39. Griffel, W. 1966. Discontinuity Stresses in Pressure Vessels. In *Handbook of Formulas for Stress and Strain.* F. Ungar Publishing Company. 221.
40. Haager, M., Pinter, G. & Lang, R.W. 2006. Ranking of PE-HD Pipe Grades By Fatigue Crack Growth Performance. *Plastic Pipes XIII.* 1-11.
41. Hall, C. 1989. Morphology. In *Polymer Materials: An Introduction for Technologists and Scientists.* 2nd ed. Macmillan Education Ltd. 51.
42. Hildebrand, F.B. 1974. Exponential Approximation. In *Introduction to Numerical Analysis.* J.L. Farnsworth & S.L. Langman, Eds. 2nd ed. USA: McGraw-Hill, Inc. 457-458.
43. Huebner, K., Dewhirst, D., Smith, D. & Byrom, T. 2001. *The Finite Element Method for Engineers.* 4th ed. John Wiley & Sons.
44. Janson, L. 2003. *Plastic Pipes for Water Supply and Sewage Disposal.* 4th ed.
45. Jasinoski, S.C. & Reddy, B.D. 2012. Mechanics of cranial sutures during simulated cyclic loading. *Journal of Biomechanics.* 45(11): 2050-2054.
46. Jasinoski, S.C., Reddy, B.D., Louw, K. & Chinsamy, A. 2010. Mechanics of cranial sutures using the finite element method. *Journal of Biomechanics.* 43(16): 3104-3111.

47. Krishnaswamy, R.K. 2005. Analysis of ductile and brittle failures from creep rupture testing of high-density polyethylene (HDPE) pipes. *Polymer.* 46(25): 11664-11672.
48. Lai, M.W., Rubin, D. & Krempl, E. 1999. The Elastic Solid. In *Introduction to Continuum Mechanics.* 3rd ed. Butterworth-Heinemann. 242.
49. Lakes, R. *Viscoelastic Materials.* Available: http://silver.neep.wisc.edu/~lakes/VE.html.
50. Lambert, A. 2001. What do we know about pressure-leakage relationships in distribution systems. *IWA Conference on Systems Approach to Leakage Control and Water Distribution System Management.*
51. Long, W. *How to design against long running cracks in plastic pipe for water applications.* Available: https://c.ymcdn.com/sites/www.isawwa.org/resource/resmgr/WATERCON2012-Wednesday-pdf/wedconboth730_long.pdf [17th July 2013].
52. Mark, J.E. 2007. Mechnical Properties. In *Physical properties of polymers.* J.E. Mark, Ed. Springer Science+Business Media, LLC ed.427.
53. May, J. 1994. Pressure dependent leakage. *World Water and Environmental Engineering.*
54. McCarthy, M., Deblieck, R., Mindermann, P., Kloth, R., Kurelec, L. & Martens, H. 2008. New accelerated method to determine slow crack growth behaviour of polyethylene pipe materials. *Plastic Pipes XIV.*
55. Meniconi, S., Brunone, B., Ferrante, M. & Massari, C. 2013. Numerical and experimental investigation of leaks in viscoelastic pressurized pipe flow. *Water Eng.Sci.* 6(1): 11-16.
56. Moore, G. & Kline, D. 1984. Mechanical properties of polymers Viscoelasticity. In *Properties and processing of polymers for engineers.* Englewood Cliffs, NJ: Prentice Hall. 92-114.
57. Necati C.F. *CES 6116 Finite Element Analysis (Overview).* Available: http://www.cece.ucf.edu/people/catbas/CES%206116-FEM/CES6116-WEB/CES%206116%20FEM%20Summary.pdf.
58. O'Donnell Consulting Engineers, I. 2011. *Description of the finite element method.* Available: http://www.odonnellconsulting.com/forensicfea.html.
59. Painter, P.C. & Coleman, M.M. 2009. *Essentials of Polymer Science and Engineering.* Lancaster: DEStech Publications, Inc.
60. Pascu, M. & Vasile, C. 2005. *A practical guide to polyethylene.* iSmithers Rapra Publishing.
61. Priddy, D. *Why do PVC and CPVC pipes occasionally fail?* Available: http://www.californiasprinklerfitters.org/files/WhyCPVC-OccasFail.pdf [31st July 2013].
62. Puust, R., Kapelan, Z., Savic, D.A. & Koppel, T. 2010. A review of methods for leakage management in pipe networks. *Urban Water Journal.* 7(1): 25-45.

63. Redhead, A., Frank, A. & Pinter, G. 2013. Investigation of slow crack growth initiation in polyethylene pipe grades with accelerated cyclic tests. *Engineering Fracture Mechanics.* 101(2013): 2-9. DOI:http://dx.doi.org/10.1016/j.engfracmech.2012.09.022.
64. Reusch, W. 5th May 2013. *Polymers.* Available: https://www2.chemistry.msu.edu/faculty/reusch/virttxtjml/polymers.htm [17th September 2013].
65. Saffar, S. & Abdullah, A. 2013. Longitudinal wave propagation in multi cylindrical viscoelastic matching layers of airborne ultrasonic transducer: New method to consider the matching layer's diameter (frequency< 100kHz). *Ultrasonics.* 53(6): 1174-1184.
66. Sethna, J. 1994. *What's Hysteresis?* Available: http://www.lassp.cornell.edu/sethna/hysteresis/WhatIsHysteresis.html.
67. Ssozi, E.N. 2012. Investigating the impact of plastic deformation on the pressure-leakage relationship. Bachelor of Science in Civil Engineering. University of Cape Town.
68. Tampa, R.B. *Environmental Stress Crack Resistance of Polyethylene Pipe Materials.* Available: http://www.ineos.com/Global/Olefins%20and%20Polymers%20USA/Products/Technical%20information/aga_escr.pdf [5th August 2013].
69. Tanaka, E. & van Eijden, T. 2003. Biomechanical behavior of the temporomandibular joint disc. *Critical Reviews in Oral Biology and Medicine : An Official Publication of the American Association of Oral Biologists.* 14(2): 138-150. DOI:14/2/138 [pii].
70. Thornton, J. & Lambert, A. 2005. Progress in practical prediction of pressure: leakage, pressure: burst frequency and pressure: consumption relationships. *Proceedings of IWA Special Conference'Leakage.* 12.
71. Thornton, J. 2003. Managing leakage by managing pressure: a practical approach. *Water21.* 5(5): 43-44.
72. Timoshenko S.P, Goodier.J.N. 1951. *Theory of Elasticity.* 2nd ed. McGraw-Hill.
73. Todini, E. 2003. A more realisitic approach to the extended period simulation of water distribution networks. *International Conference on Advances in Water Supply Management.* London: Balkema.
74. Uday S. Dixit 2011. *Finite element method: An introduction.* Available: http://www.iitg.ernet.in/engfac/rtiwari/resume/usdixit.pdf.
75. Van Zyl, J.E. & Clayton, C.R.I. 2007. The Effect of Pressure on Leakage in Water Distribution Systems. *Proceedings of ICE: Water Management.* 160(2): 109-114.
76. Van Zyl, J.E. & Cassa, A.M. 2014. Modeling Elastically Deforming Leaks in Water Distribution Pipes. *Journal of Hydraulic Engineering.* 140(2): 182-189.

77. Van Zyl, J.E. & Cassa, A.M. 2011. Linking the power and FAVAD equations for modelling the effect of pressure on leakage. *Proc., 11th Int. Conf. on Computing and Control of the Water Industry (CCWI 2011)—Urban Water Management Challenges and Opportunities, DA Savic, Z. Kapelan, and D. Butler, Eds., Univ. of Exeter, Exeter, UK.*
78. Wang, E., Nelson, T. & Rauch, R. 2004. Back to elements-tetrahedra vs. hexahedra. *2004 International ANSYS Conference Proceedings.*
79. Ward, I.M. 1971. *Mechanical Properties of Solid Polymers.* London: John Wiley & Sons Ltd.
80. Zener, C. 1948. *Elasticity and Anelasticity.* Chicago University Press.

Appendix

A Sample calculations and python script

1. Sample calculations

- Calculation of Young's and Shear moduli (E and G) from data in Janson (2003):

Stress data in the table A-1 below was taken from Creep test curves (20°C) in Janson (2003). The data included stress values (σ) and corresponding strains (ε) at the respect times (t) shown in table A-1 below.

Time (h)	Time (s)	t	σ (MPa)	ε	E (MPa)	G (MPa)
0	0	t_0	8	0.0071	1126.7606	402.4145
1	3600	t_1	8	0.0104	769.2308	274.7253
10	36000	t_{10}	8	0.0163	492.3077	175.8242

Table A-1: Young and shear moduli data for HDPE at certain times

Young's modulus E, was calculated from the equation A.1 below:

$$E = \frac{\sigma}{\varepsilon}$$

(A.1)

Thereafter, G, the shear modulus for each time was calculated from:

$$G = \frac{E}{2(1+\nu)} \tag{A.2}$$

- From the standard linear model given by equation 3.28 and setting

$$z = e^{t_1/\tau_\varepsilon}, \tag{A.3}$$

- We can obtain a polynomial relating the Shear moduli at the three times shown in table A-1 above (G_0, G_1 and G_{10}):

$$(G_0 - G_1)z^{10} - (G_0 - G_{10})z + (G_1 - G_{10}) = 0 \tag{A.4}$$

- Using the values in the table A-1 and the Newton Raphson method, we solve for z:

$$z = 0.437$$

And

τ_{ε} = 1.208h = 4348.761s

- Applying equation 3.38 for G0 and G1 (or G0 and G10) we solve for τ_{σ} and also $\bar{g}_1^p$ from equation 3.42:

τ_{σ} = 9965.119s

And

$\bar{g}_1^p$ = 0.564

The same procedure is applied to calculate prony series parameters for the PVC material, using PVC creep test curves from Janson (2003). A summary of the material parameters is provided below:

Elastic Properties		
Property	**PVC**	**HDPE**
Elastic Modulus (GPa)	3421.143	1126.760
Poisson's ratio (v)	0.4	0.4
Allowable stress (MPa)	10.4	8.0
Safety Factor	4.80	1.25
Prony series parameters for Viscoelasticity		
$\bar{g}_1^p$	0.208	0.564
τ_{ε} (s)	3382.788	4348.761

Table A-2: Material parameters for HDPE and PVC pipe models

2. Python script

```
# script to determine the projected are of an external opening after an analysis. The
# opening perimenter is defined by the set "HolePerimeterOD". The script
# assumes that there is only 1 instance in the ODB.
#

from abaqus import *
from abaqusConstants import *
import string
import numpy
import copy
from textRepr import prettyPrint as pp

# User to define the set name defining the perimeter of the opening
setName = 'HOLEPERIMETEROD'

def findElementWithNodeNum(nodeNum, elements):
  """return list of elements whose connectivity includes the particular node number"""
  elementList = [elm for elm in elements if nodeNum in elm.connectivity]
  return elementList

def findNodeSequenceInElement(startNodeNum, nodeSet, element):
  """define the sequence of node number along the edge in the node set"""
  nodeLabels = [node.label for node in nodeSet if node.label in element.connectivity]
  nodeNumList = [startNodeNum]
  nodeLabels.remove(startNodeNum)
  if len(nodeLabels) == 1:
    nodeNumList.append(nodeLabels[-1])
  else:
```

```
    if 'C3D10' in element.type:
      mideNodeConnectivity = element.connectivity[4:]
    elif 'C3D15' in element.type:
      mideNodeConnectivity = element.connectivity[6:]
    elif 'C3D20' in element.type[:5]:
      mideNodeConnectivity = element.connectivity[8:]
    for nodeNum in nodeLabels:
      if nodeNum in mideNodeConnectivity:
        nodeNumList.append(nodeNum)
        nodeLabels.remove(nodeNum)
        nodeNumList.append(nodeLabels[-1])
        break
  return nodeNumList


def createNodeNumLoopFromSet(instanceName, nSet, elSet):
  """return a list of sequenced node numbers forming a closed loop"""
  mag = [[numpy.linalg.norm(node.coordinates), node.label] for node in nSet.nodes]
  startNodeNum = min(mag)[1]
  # find adjacent elements to startNode
  elList = findElementWithNodeNum(startNodeNum, elSet.elements)
  # initialise the sequence using the first element in the sequence
  nodeSequenceList = findNodeSequenceInElement(startNodeNum, nSet.nodes, elList[0])
  oldElement = elList[0]
  # loop through the remaining elements until the loop is closed
  while len(nodeSequenceList) < len(nSet.nodes):
    # determine which elements are connected to last node in list
    newElList = findElementWithNodeNum(nodeSequenceList[-1], elSet.elements)
    if len(newElList)== 2:
      newElList.remove(oldElement)
```

```
    else:
      print "Error: node list does not form a closed loop"
    newNodeSequenceList = findNodeSequenceInElement(nodeSequenceList[-1], nSet.nodes, newElList[0])
    oldElement = newElList[0]
    for nodeNum in newNodeSequenceList[1:]:
      nodeSequenceList.append(nodeNum)
  return nodeSequenceList


def createCoordinateListFromNodeNumList(stepName,nodeNumList):
  """return a sequence of nodal coordinates from a list of node numbers"""
#  stepName = odb.steps.keys()[-1]
  step = odb.steps[stepName]
  frame = step.frames[-1]
  coordinateFieldOutput = frame.fieldOutputs['COORD'].getSubset(region=instance.nodeSets[setName])
  displacementFieldOutput = frame.fieldOutputs['U'].getSubset(region=instance.nodeSets[setName])
  coordinateList = []
  if step.nlgeom:
    for nodeNum in nodeNumList:
      for value in coordinateFieldOutput.values:
        if value.nodeLabel == nodeNum:
          coordinateList.append(value.data)
          break
  else:
    for nodeNum in nodeNumList:
      for i, value in enumerate(coordinateFieldOutput.values):
        if value.nodeLabel == nodeNum:
          coordinateList.append(value.data+displacementFieldOutput.values[i].data)
          break
```

```
  return tuple(coordinateList)


def meanCoordinates(list):
  """returns the mean coordinates from a list of coordinates"""
  sum = list[0]
  for i in range(1,len(list)-1):
    sum = sum + list[i]
  return sum/(len(list)-1)


def polygonProjectedArea(list):
  """compute the area projected along the x-axis of a 3D irregular polygon"""
  area = 0.0
  centre = meanCoordinates(list)
  for i in range(1,len(list)):
    mean = (list[i-1] + list[i])/2.
    pnt1= copy.deepcopy(list[i-1])
    pnt2= copy.deepcopy(list[i])
    pnt1[0] = mean[0]
    pnt2[0] = mean[0]
    centre[0] = mean[0]
    vector1 = pnt1 - centre
    vector2 = pnt2 - centre
    area += numpy.linalg.norm(numpy.cross(vector1,vector2))/2.0
  return area




# start the process
# obtain current viewport and odb based on what is on the current display
```

```
VP          = session.viewports[session.currentViewportName]
odb         = VP.displayedObject
instanceName = odb.rootAssembly.instances.keys()[0]

instance = odb.rootAssembly.instances[instanceName]
nSet     = instance.nodeSets[setName]
elSet    = instance.elementSets[setName]

# obtain the sequence of node numbers and deformed coordinates
nodeSequenceList = createNodeNumLoopFromSet(instanceName, nSet, elSet)
for stepName in odb.steps.keys():
  coordinateList   = createCoordinateListFromNodeNumList(stepName, nodeSequenceList)
  area = polygonProjectedArea(coordinateList)
  print 'Step = %s:  Area of deformed opening is %s\n' %(stepName, area)
```

B 1mm hole in HDPE

1. Summary results for area, gradient (m) and leakage exponent (N1)

HDPE	Area of deformed holes with A_0 =0.7832mm^2					
Pressure (MPa)	0.2		0.4		0.6	
Time (s)	Uniaxial	Biaxial	Uniaxial	Biaxial	Uniaxial	Biaxial
0 (Elastic)	0.7864	0.7879	0.7896	0.7926	0.7928	0.7974
10	0.7864	0.7879	0.7896	0.7927	0.7928	0.7974
100	0.7864	0.7879	0.7897	0.7927	0.7929	0.7976
1000	0.7867	0.7884	0.7903	0.7936	0.7938	0.7989
5000	0.7877	0.7898	0.7923	0.7966	0.7968	0.8033
10000	0.7885	0.7910	0.7938	0.7989	0.7991	0.8068
50000	0.7896	0.7926	0.7961	0.8022	0.8024	0.8117
100000	0.7897	0.7927	0.7961	0.8022	0.8025	0.8118

Table B-1: Deformed area (mm^2) for 1mm round hole in HDPE

HDPE	Uniaxial		Biaxial	
Time (s)	N1	m	N1	m
0 (Elastic)	0.5072	1.570E-10	0.5107	2.330E-10
10	0.5072	1.570E-10	0.5107	2.330E-10
100	0.5073	1.594E-10	0.5109	2.379E-10
1000	0.5080	1.741E-10	0.5118	2.575E-10
5000	0.5102	2.232E-10	0.5151	3.311E-10
10000	0.5119	2.600E-10	0.5176	3.875E-10
50000	0.5143	3.139E-10	0.5212	4.684E-10
100000	0.5143	3.139E-10	0.5212	4.684E-10

Table B-2: Gradients (m) and leak exponents (N1) from the power law graphs for 1mm hole in HDPE

2. Variation of leak area with time

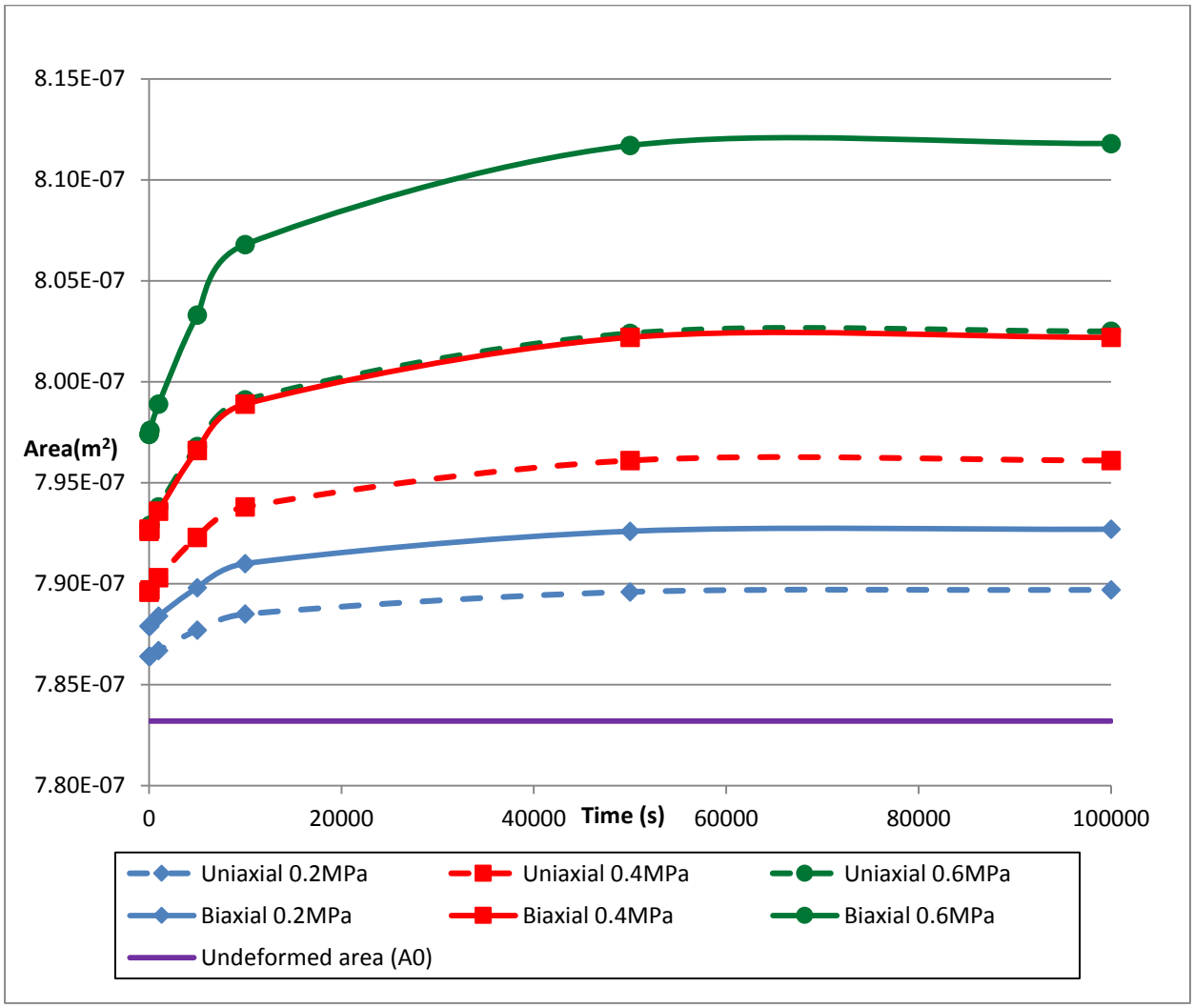

Figure B-1: Area against time for the 1mm hole in HDPE

3. Variation of leak area with pressure

a) Uniaxial

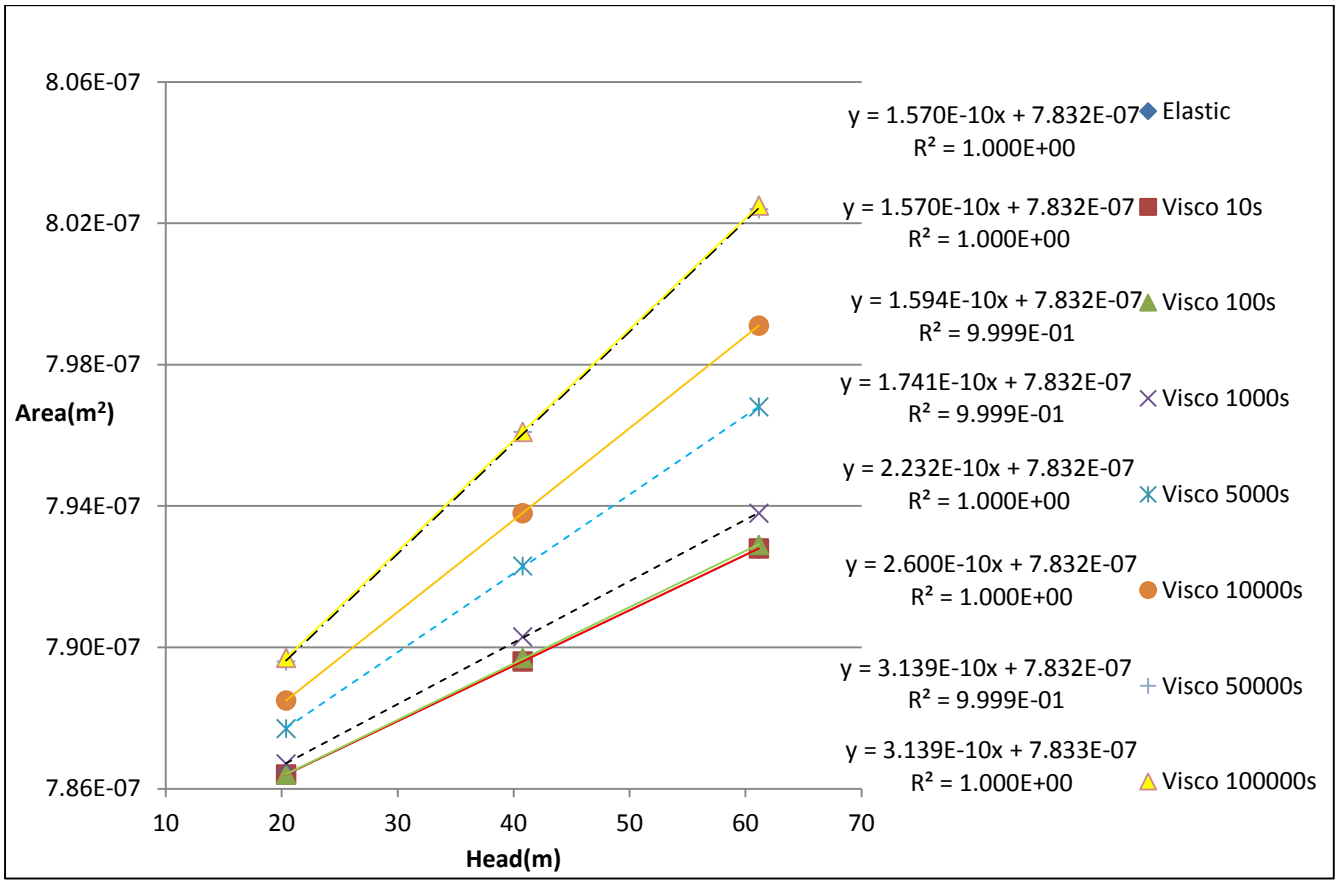

Figure B-2: Area against pressure head for 1mm hole in HDPE, uniaxial state

b) Biaxial

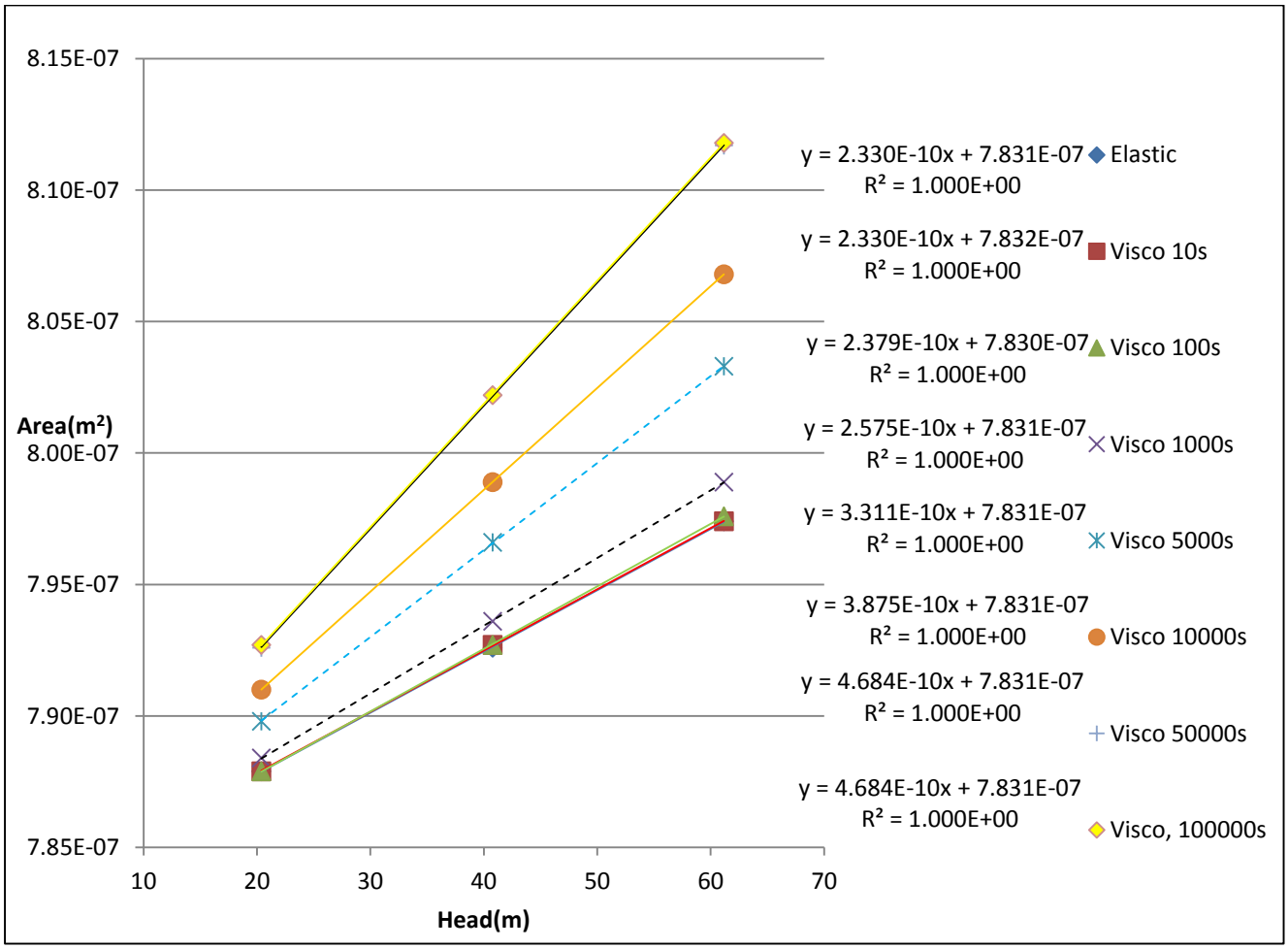

Figure B-3: Area against pressure head for 1mm hole in HDPE, biaxial state

4. Variation of leak discharge with time

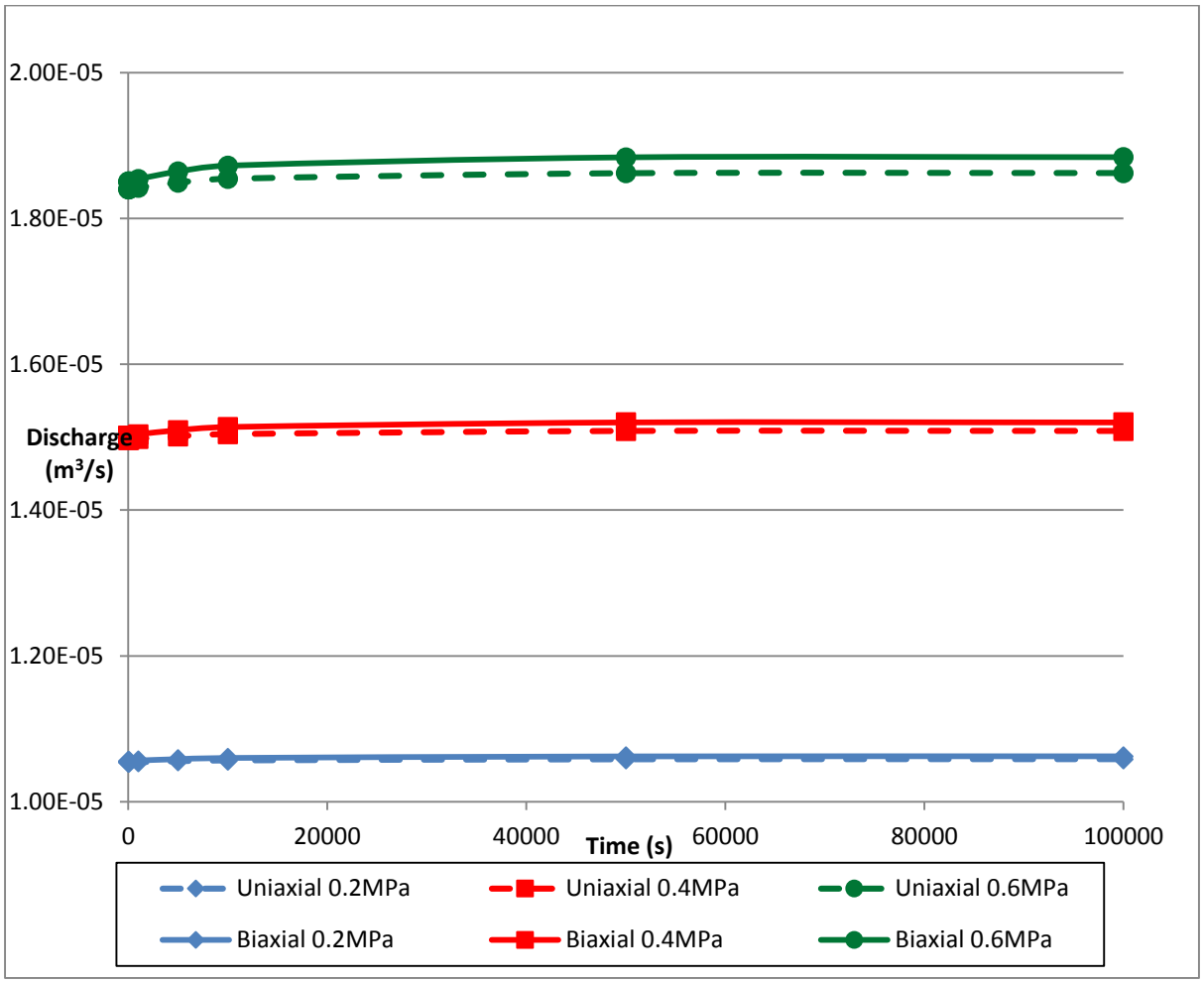

Figure B-4: Discharge against time for 1mm hole in HDPE

5. Variation of leak discharge with pressure

a) Uniaxial

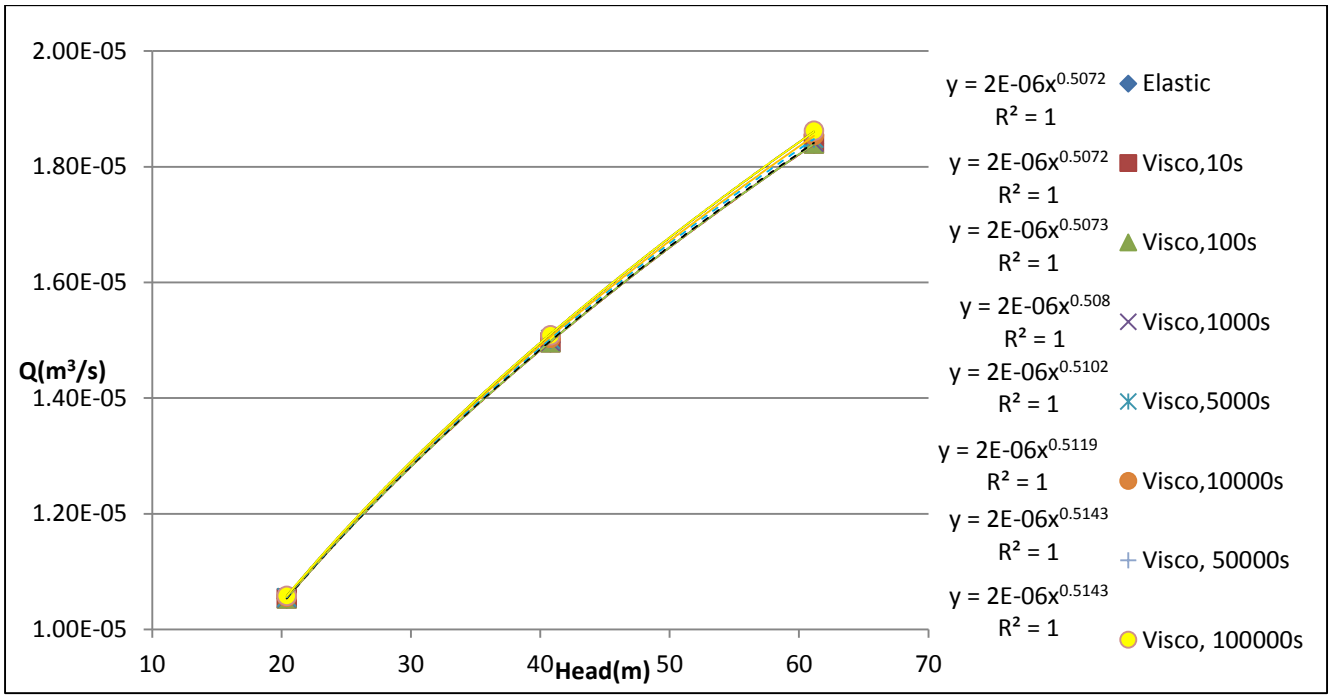

Figure B-5: Discharge against pressure head for 1mm hole in HDPE, uniaxial state

b) Biaxial

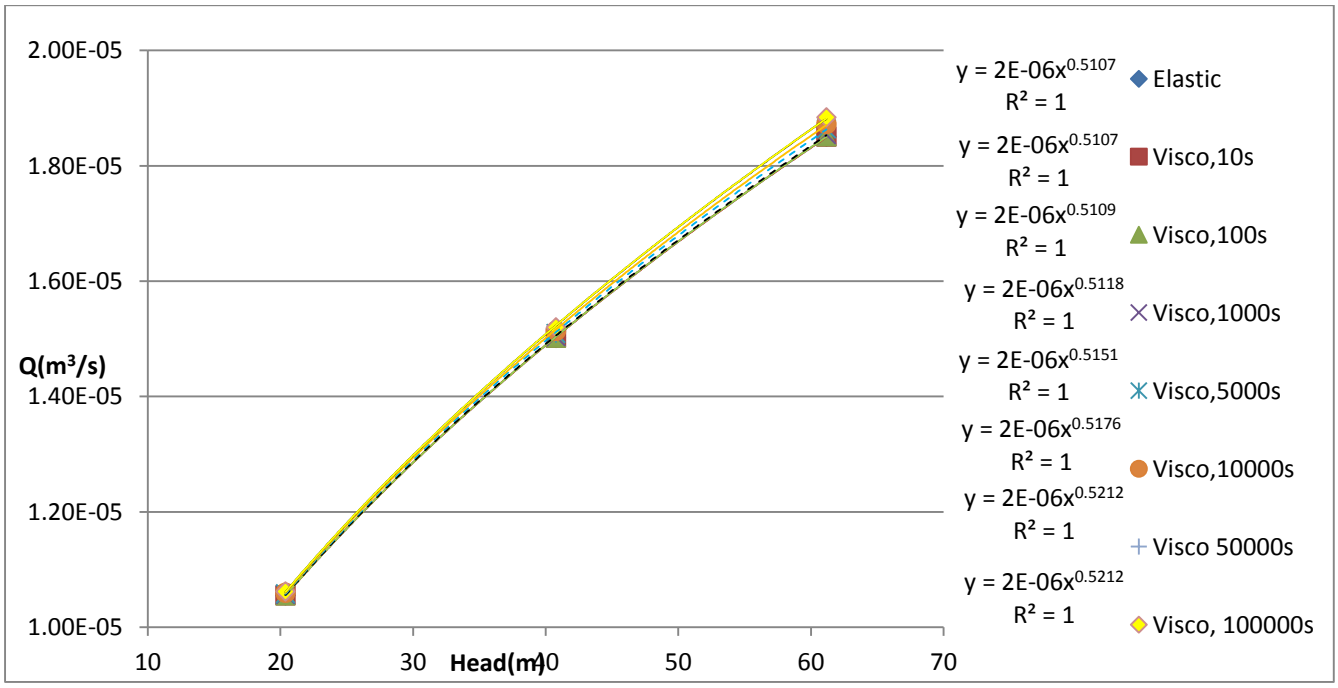

Figure B-6: Discharge against pressure head for 1mm hole in HDPE, biaxial state

6. Gradient (m) and leakage exponent (N1)

a) Gradient (m) against time

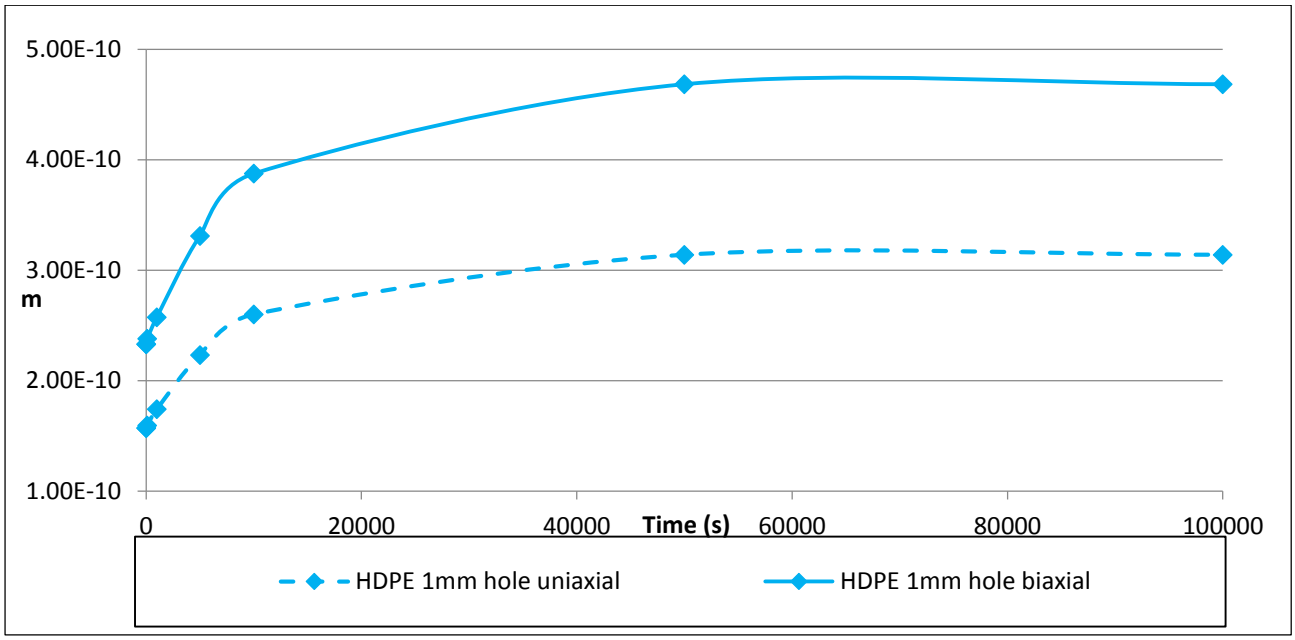

Figure B-7: Gradient (m) against time for 1mm hole in HDPE

b) Leakage exponent (N1) against time

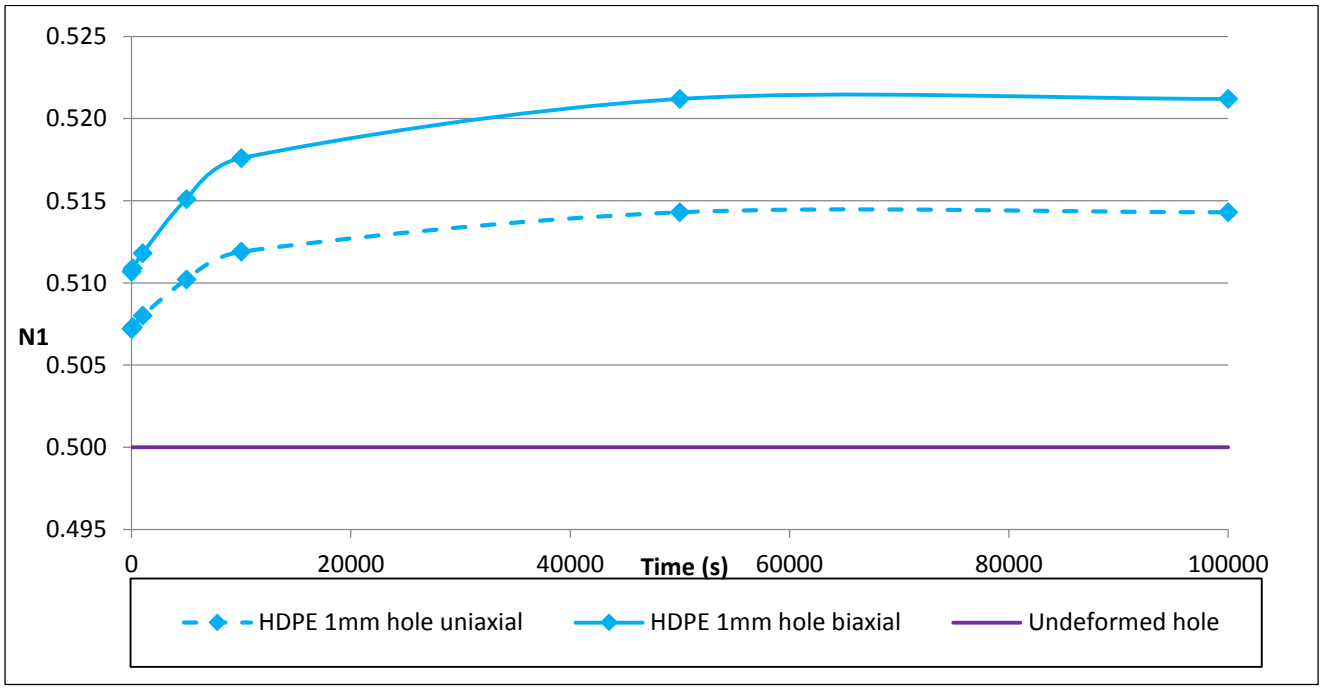

Figure B-8: Leakage exponent (N1) against time for a 1m hole in HDPE

7. Percentage change in area with pressure

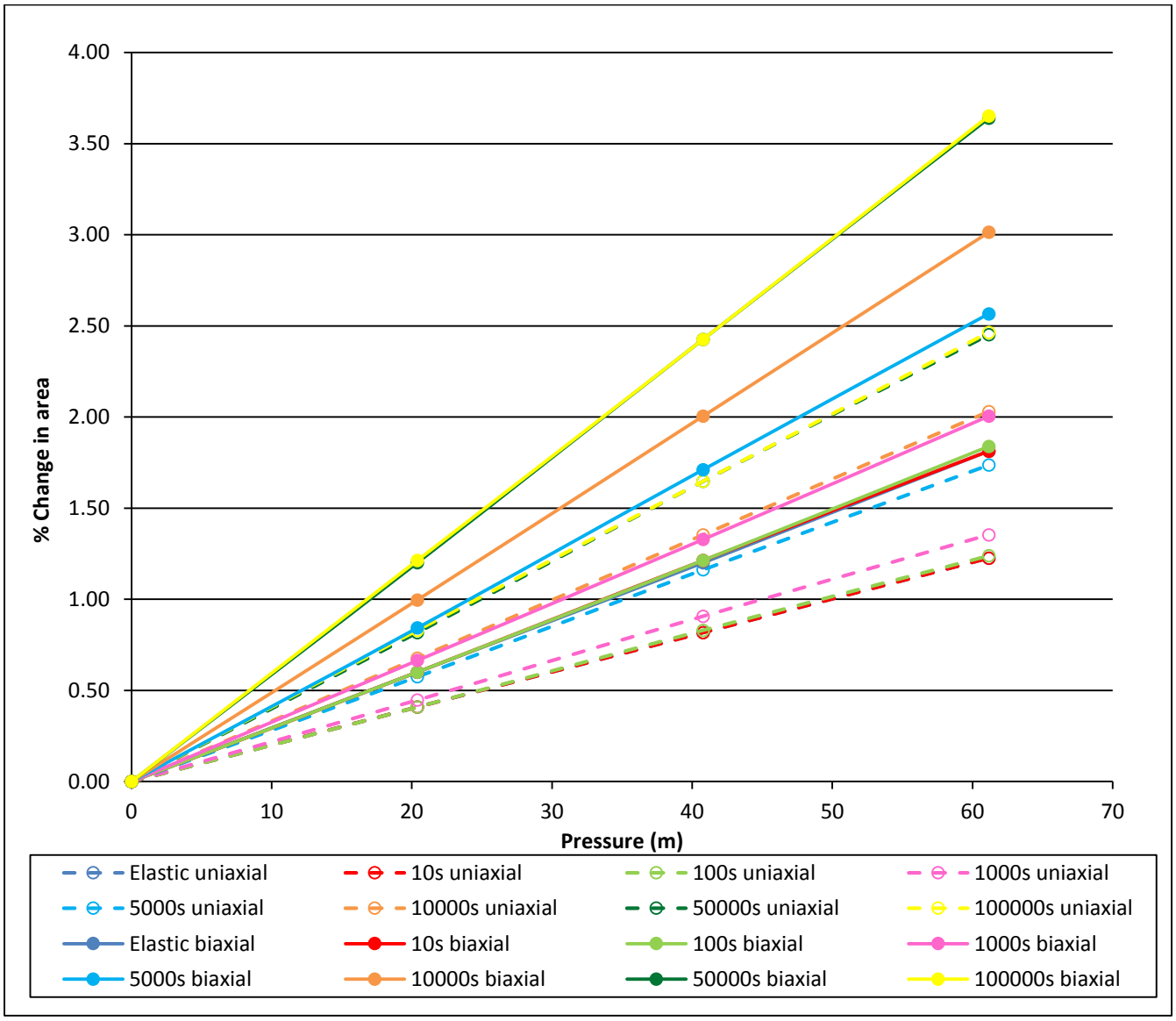

Figure B-9: Percentage change in area against pressure for 1mm hole in HDPE

8. Ratio of total change in area to elastic change in area

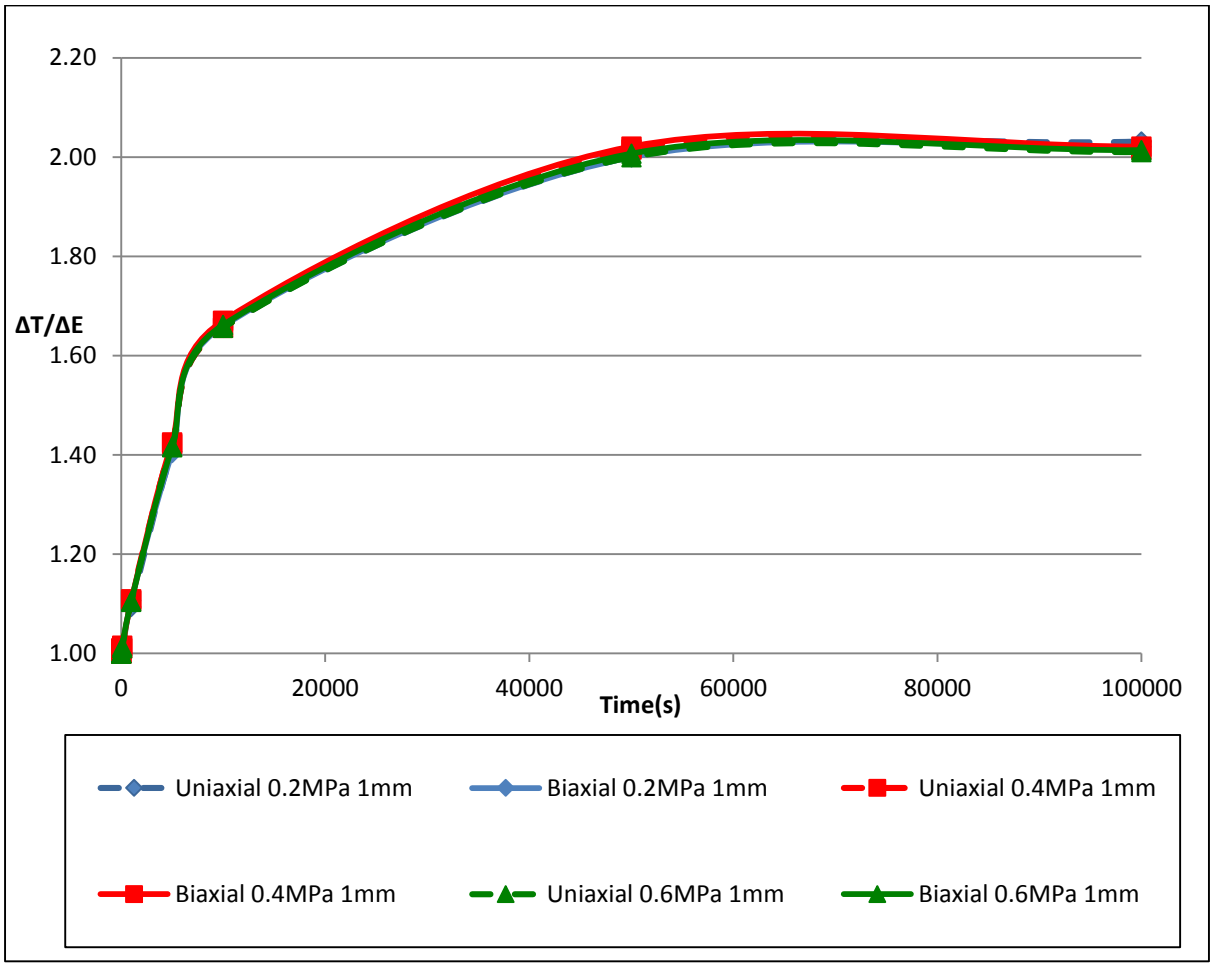

Figure B-10: ΔT/ΔE against time for 1mm hole in HDPE

9. Cyclic results

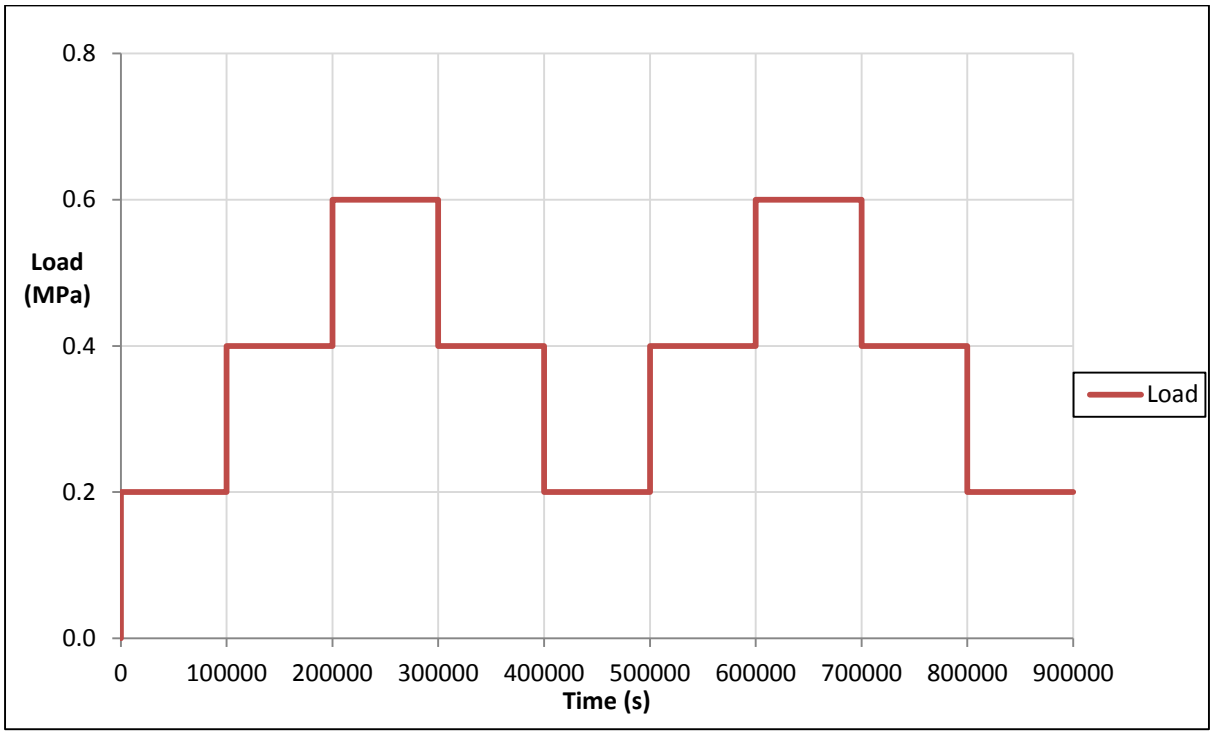

Figure B-11: Cyclic loading for a 1mm hole in HDPE pipe

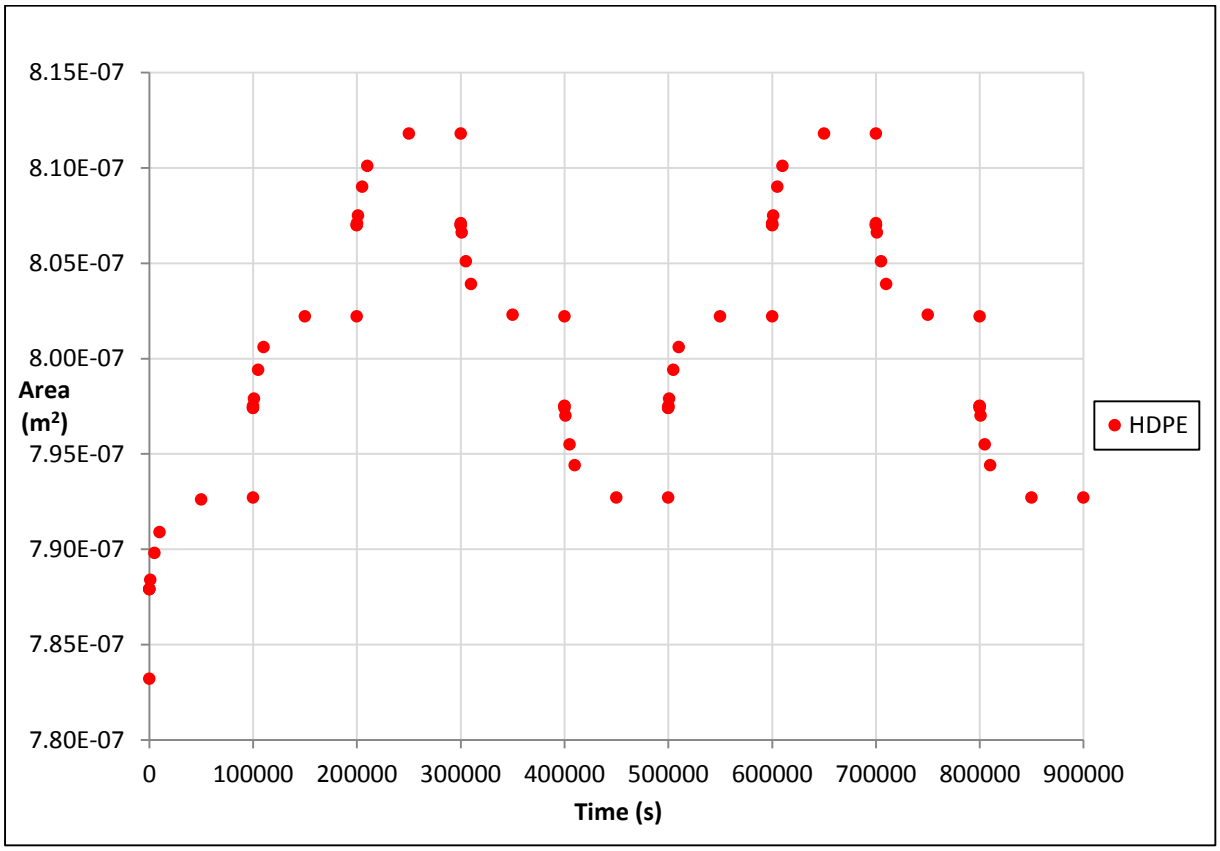

Figure B-12: Deformed area against time for 1mm hole in HDPE during cyclic loading, biaxial

10. Leakage number, calculated leak exponents, m/A_0 and m/m_E

a) Uniaxial

Time (s)	N1 from power law	m	L_N	N1	m/A_0	m/m_E
			Pressure = 0.4MPa	**Pressure = 0.4MPa**		
0	0.5072	1.570E-10	0.008174	0.5081	0.0002	1.00000
10	0.5072	1.570E-10	0.008174	0.5081	0.0002	1.00000
100	0.5073	1.594E-10	0.008299	0.5082	0.0002	1.01529
1000	0.508	1.741E-10	0.009064	0.5090	0.0002	1.10892
5000	0.5102	2.232E-10	0.011620	0.5115	0.0003	1.42166
10000	0.5119	2.600E-10	0.013536	0.5134	0.0003	1.65605
50000	0.5143	3.139E-10	0.016342	0.5161	0.0004	1.99936
100000	0.5143	3.139E-10	0.016342	0.5161	0.0004	1.99936

Table B-3: Leakage numbers, calculated leak exponents, m/A_0 and m/m_E for the 1mm hole in HDPE, uniaxial

b) Biaxial

Time (s)	N1 from power law	m	L_N	N1	m/A_0	m/m_E
			Pressure = 0.4MPa	**Pressure = 0.4MPa**		
0	0.5107	2.330E-10	0.0121	0.5120	0.0003	1.00000
10	0.5107	2.330E-10	0.0121	0.5120	0.0003	1.00000
100	0.5109	2.379E-10	0.0124	0.5122	0.0003	1.02103
1000	0.5118	2.575E-10	0.0134	0.5132	0.0003	1.10515
5000	0.5151	3.311E-10	0.0172	0.5169	0.0004	1.42103
10000	0.5176	3.875E-10	0.0202	0.5198	0.0005	1.66309
50000	0.5212	4.684E-10	0.0244	0.5238	0.0006	2.01030
100000	0.5212	4.684E-10	0.0244	0.5238	0.0006	2.01030

Table B-4: Leakage numbers, calculated leak exponents, m/A_0 and m/m_E for the 1mm hole in HDPE, biaxial

C 1mm hole in PVC

1. Summary results for area, gradient (m) and leakage exponent (N1)

PVC	Area of deformed holes with A_0 = 0.7832mm^2					
Pressure (MPa)	0.2		0.4		0.6	
Time (s)	Uniaxial	Biaxial	Uniaxial	Biaxial	Uniaxial	Biaxial
0 (Elastic)	0.7845	0.7852	0.7859	0.7872	0.7873	0.7892
10	0.7845	0.7852	0.7859	0.7872	0.7873	0.7892
100	0.7845	0.7852	0.7859	0.7872	0.7873	0.7892
1000	0.7846	0.7853	0.7860	0.7874	0.7875	0.7895
5000	0.7847	0.7855	0.7863	0.7878	0.7879	0.7901
10000	0.7848	0.7856	0.7864	0.7880	0.7881	0.7904
50000	0.7848	0.7856	0.7865	0.7881	0.7882	0.7905
100000	0.7848	0.7856	0.7865	0.7881	0.7882	0.7905

Table C-1: Deformed areas (mm^2) for the 1mm hole in PVC

PVC	Uniaxial		Biaxial	
Time (s)	N1	m	N1	m
0 (Elastic)	0.5032	6.867E-11	0.5045	9.810E-11
10	0.5032	6.867E-11	0.5045	9.810E-11
100	0.5032	6.867E-11	0.5045	9.810E-11
1000	0.5033	7.112E-11	0.5047	1.030E-10
5000	0.5036	7.848E-11	0.5052	1.128E-10
10000	0.5037	8.093E-11	0.5054	1.177E-10
50000	0.5038	8.339E-11	0.5055	1.202E-10
100000	0.5038	8.339E-11	0.5055	1.202E-10

Table C-2: Gradients (m) and leak exponents (N1) from the power law graphs for the 1mm hole in PVC

2. Variation of leak area with time

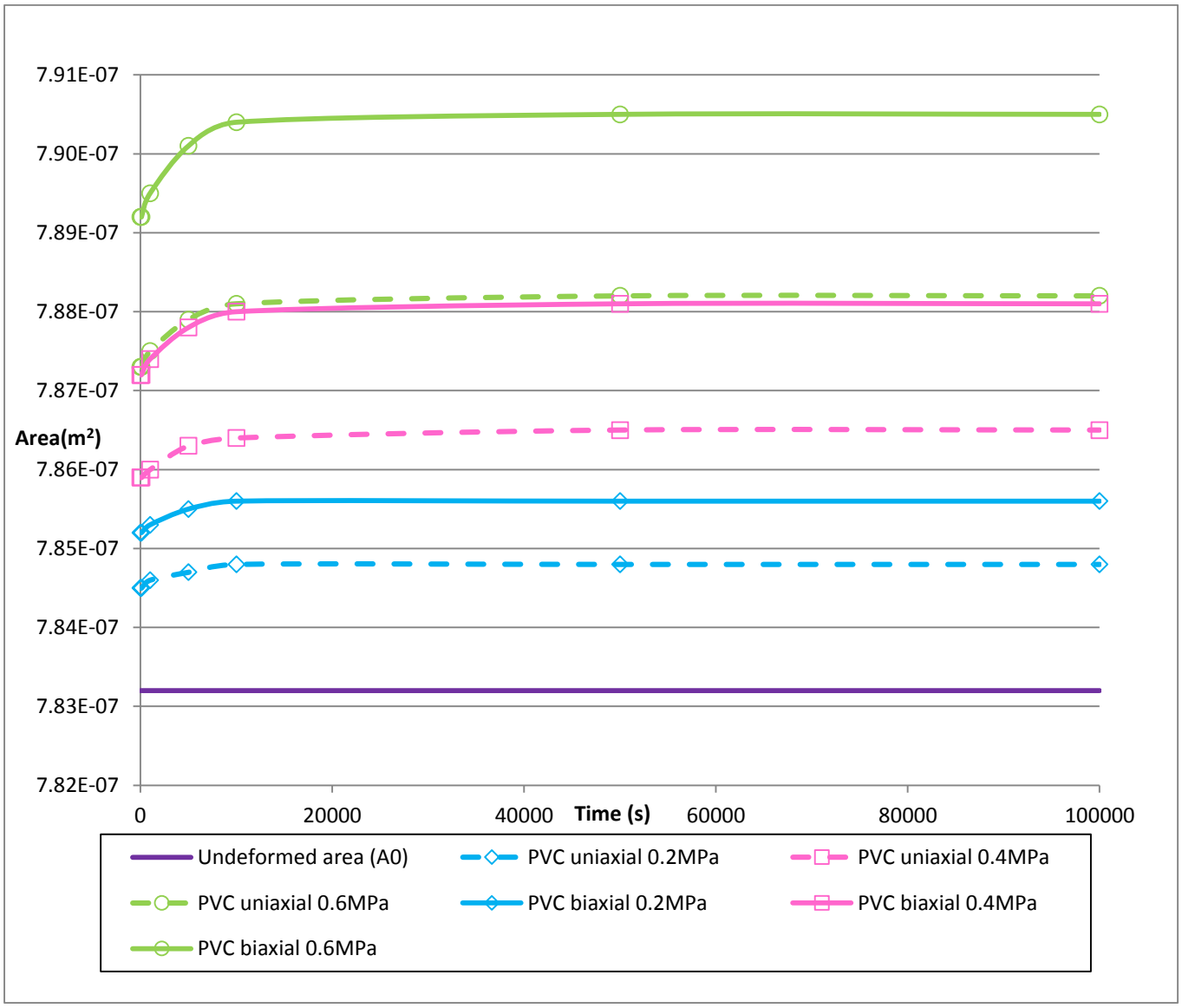

Figure C-1: Area against time for the 1mm hole in PVC

3. Variation of leak area with pressure

a) Uniaxial

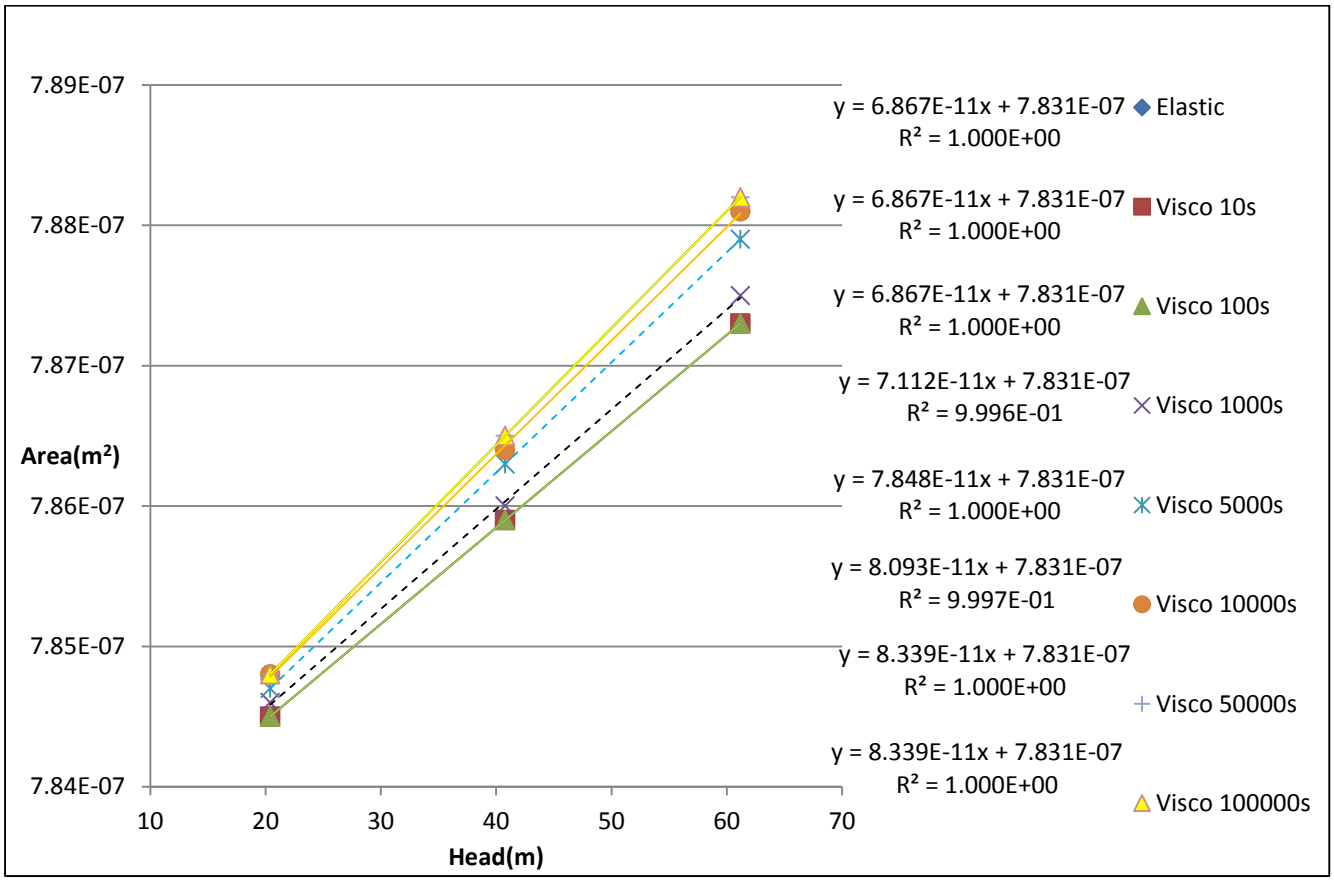

Figure C-2: Area against pressure head for 1mm hole in PVC pipe, uniaxial state

b) Biaxial

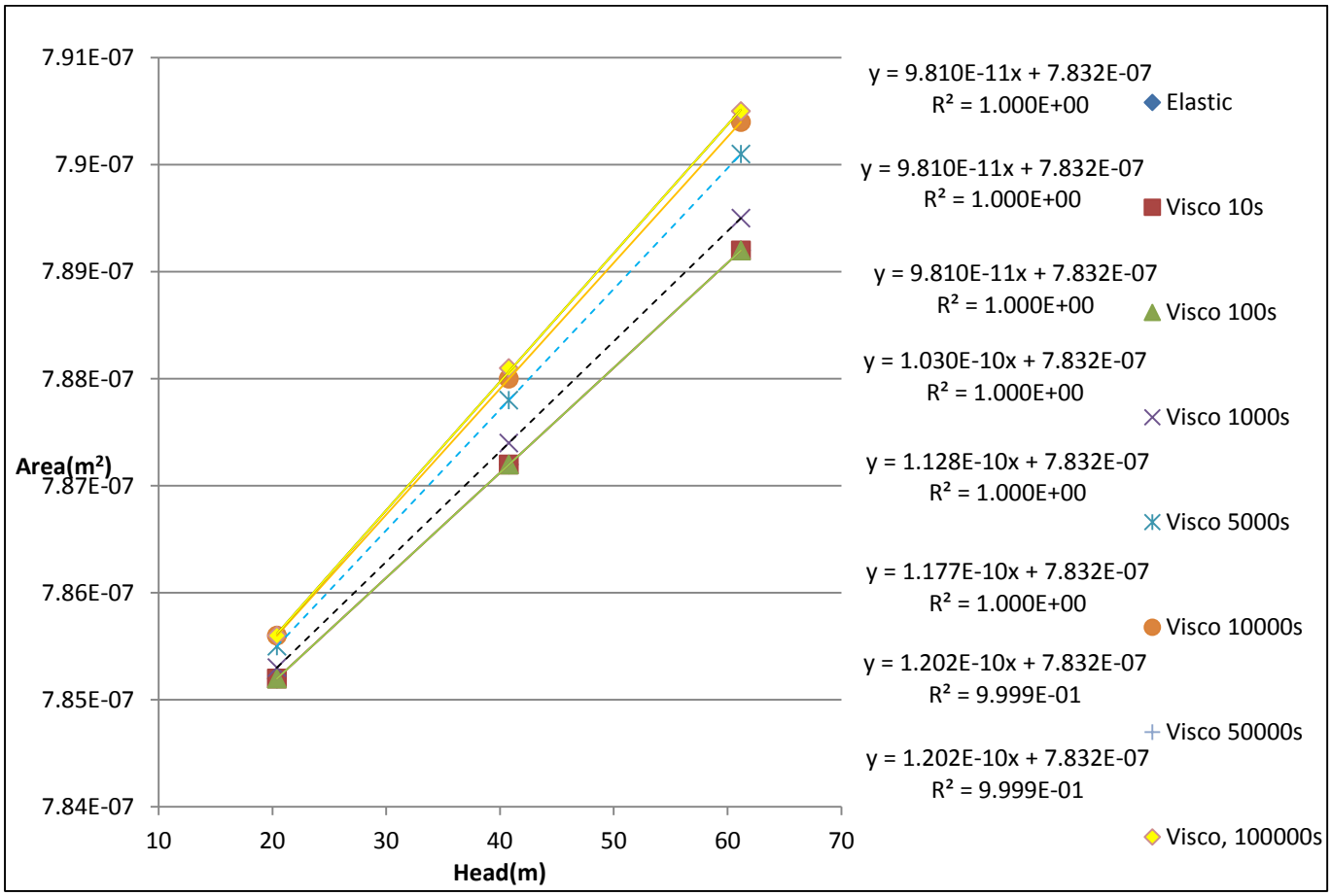

Figure C-3: Area against pressure head for 1mm hole in PVC pipe, biaxial state

4. Variation of leak discharge with time

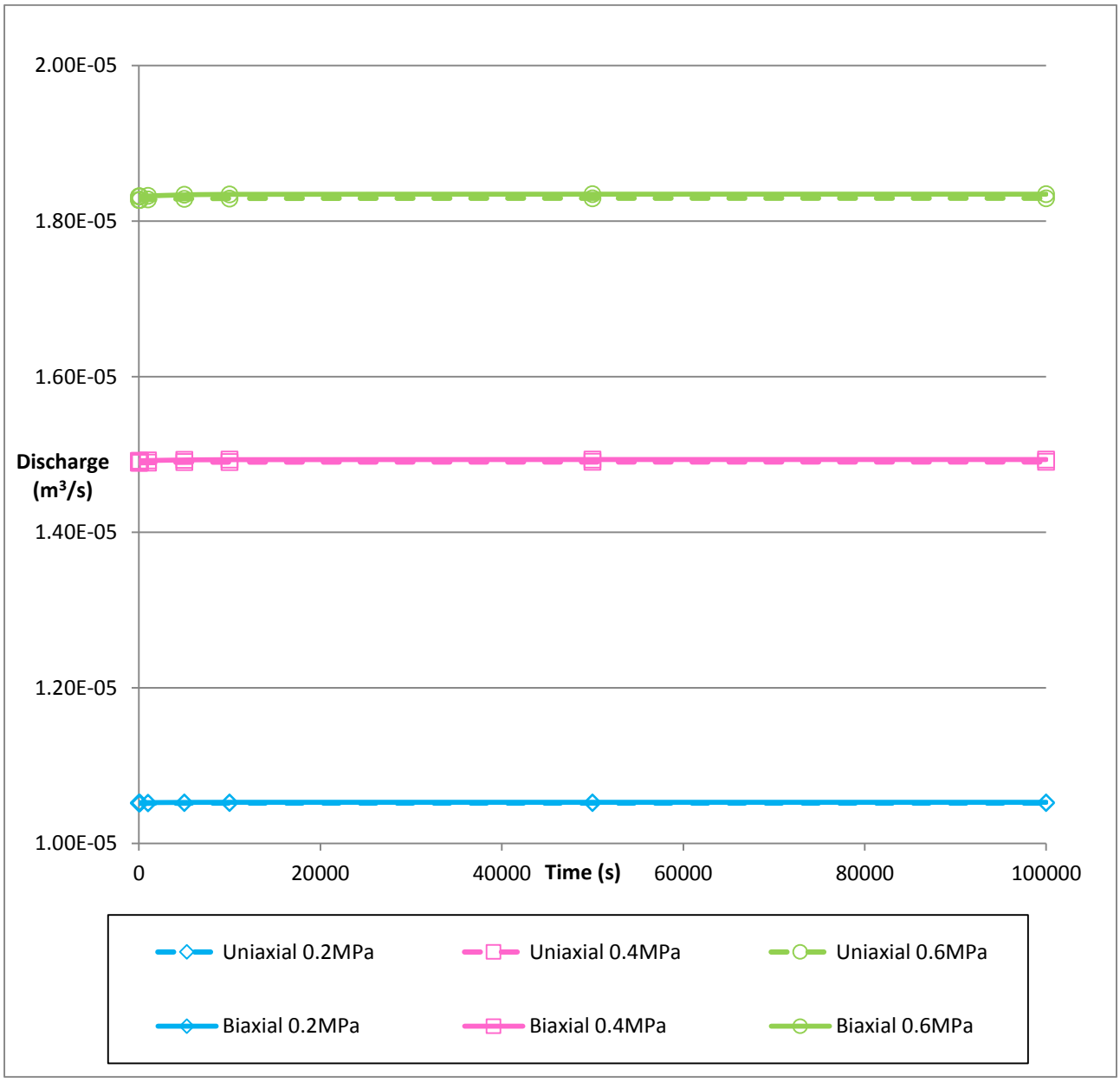

Figure C-4: Discharge against time for the 1mm hole in PVC

5. Variation of leak discharge with pressure

a) Uniaxial

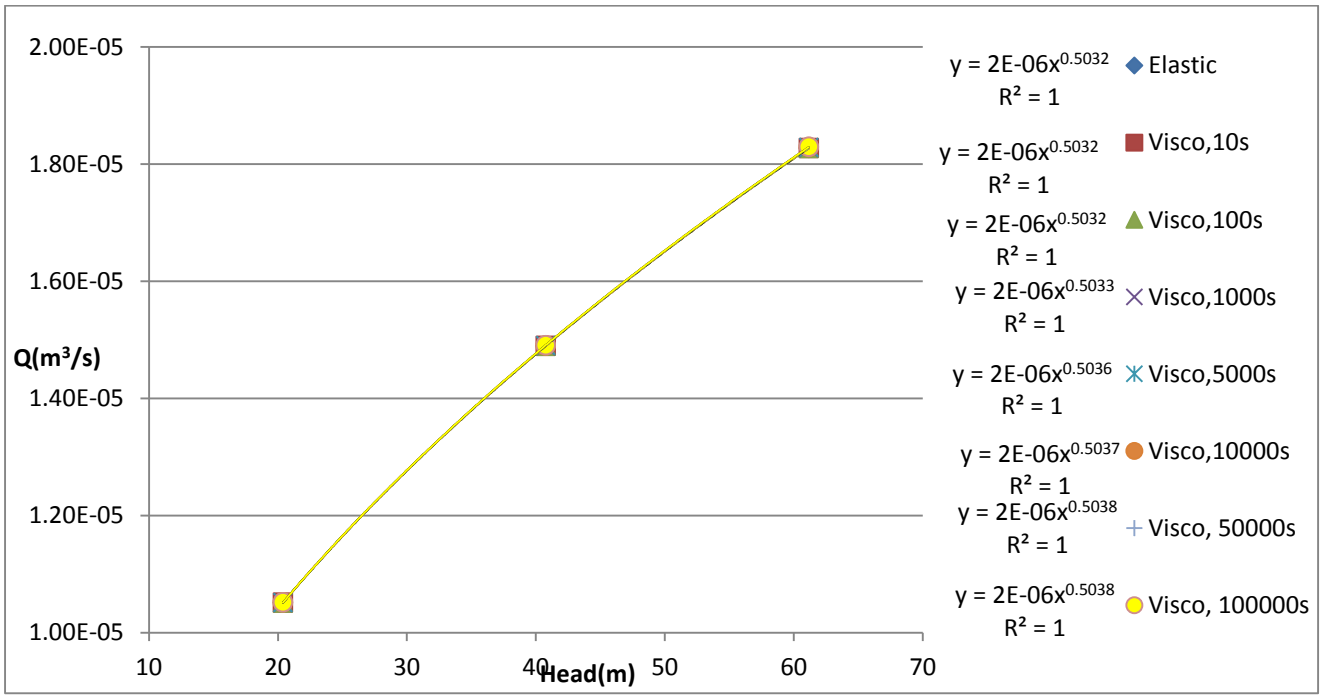

Figure C-5: Discharge against pressure head for 1mm hole in PVC, uniaxial state

b) Biaxial

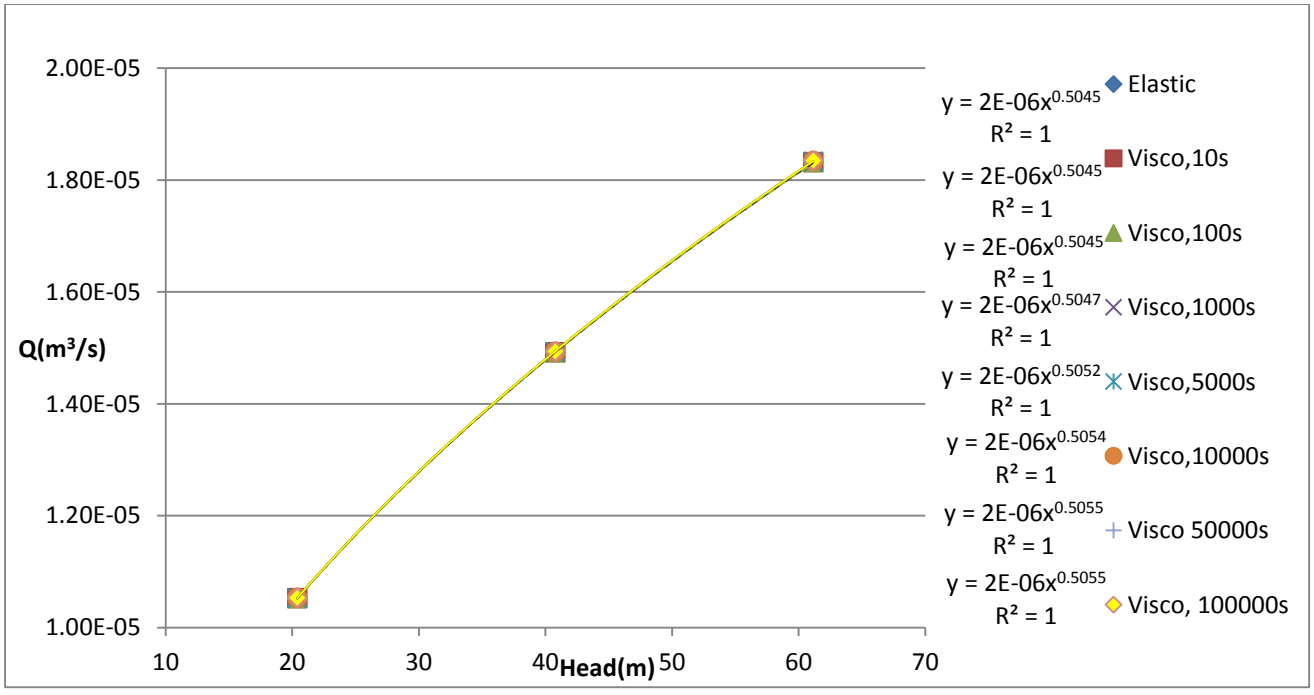

Figure C-6: Discharge against pressure head for 1mm hole in PVC, biaxial state

6. Gradient (m) and leakage exponent (N1)

a) Gradient (m) against time

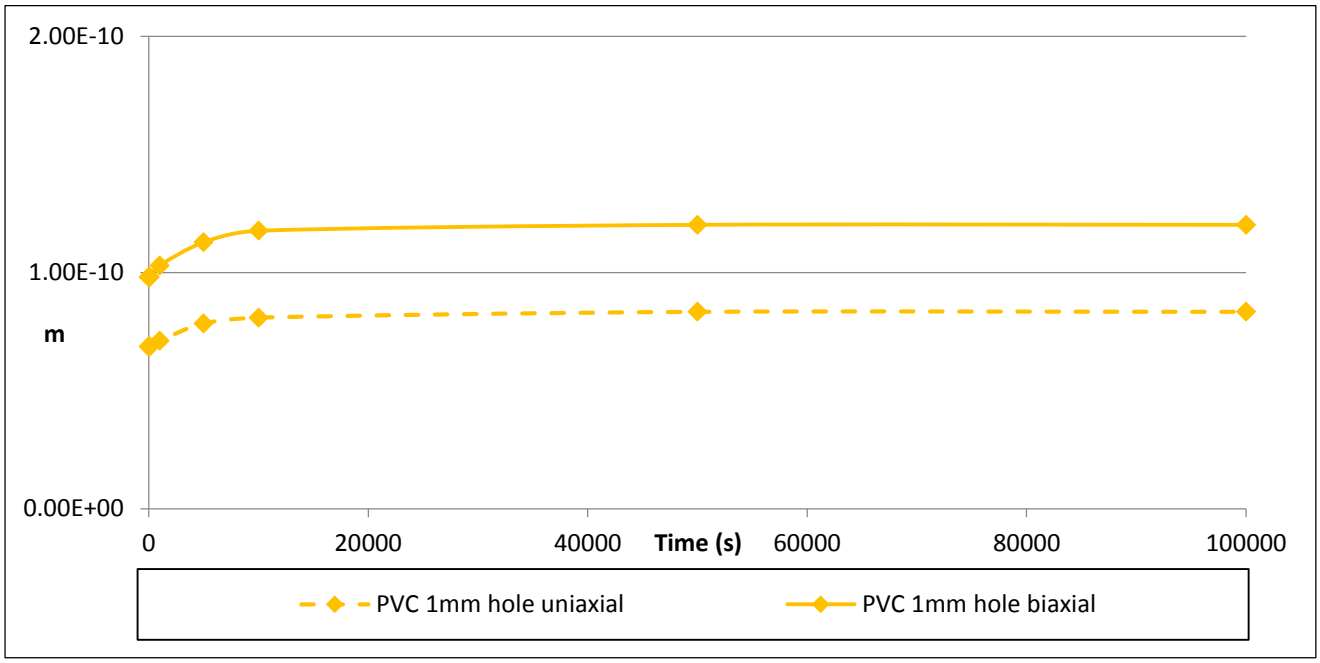

Figure C-7: Gradient (m) against time for 1mm hole in PVC

b) Leakage exponent (N1) against time

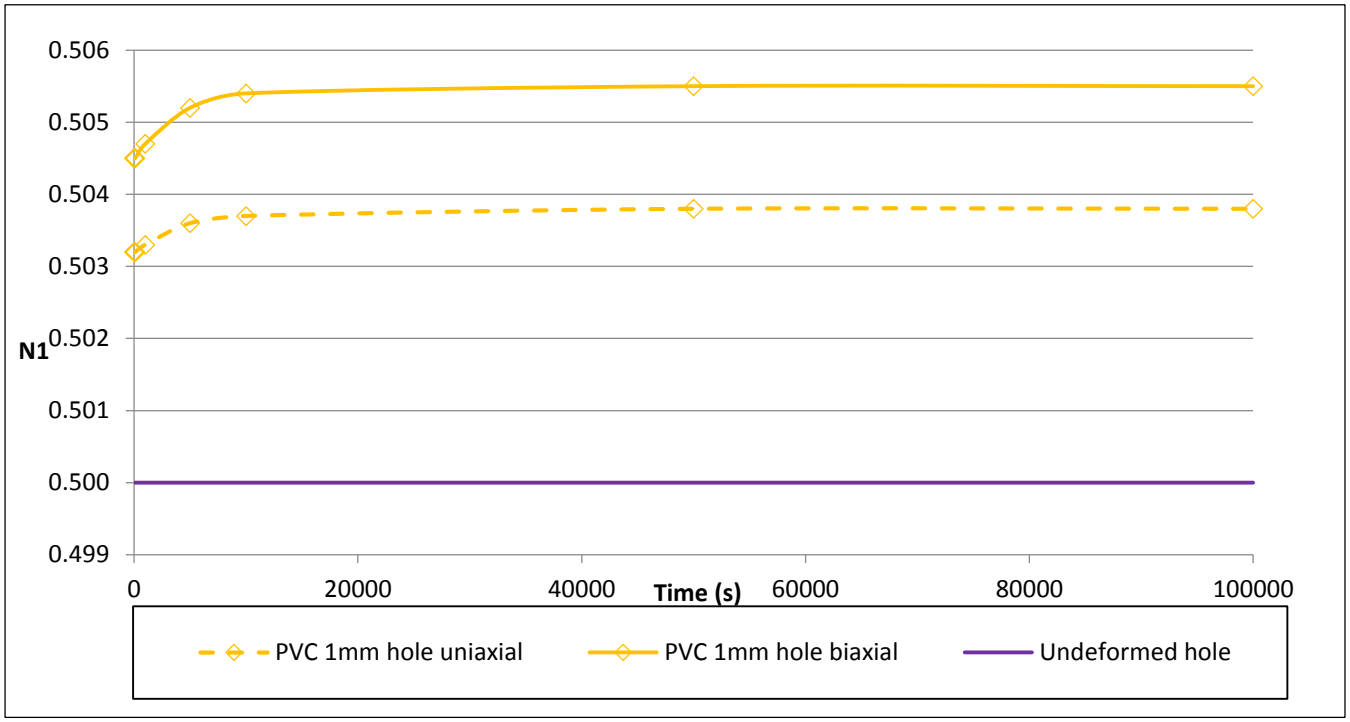

Figure C-8: Leakage exponent (N1) against time for 1mm hole in PVC

7. Percentage change in area with pressure

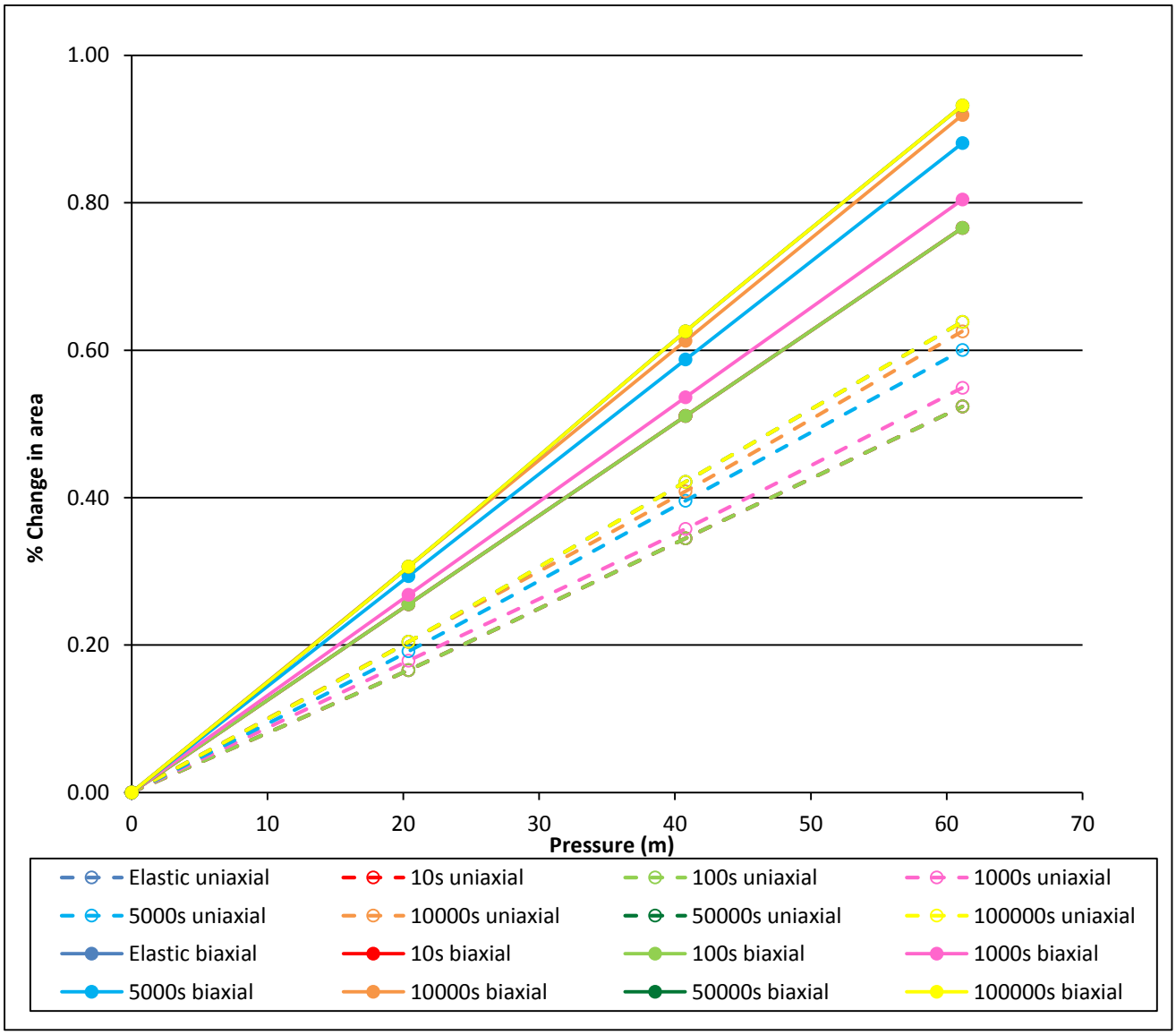

Figure C-9: Percentage change in area against pressure for the 1mm hole in PVC pipe

8. Ratio of total change in area to elastic change in area

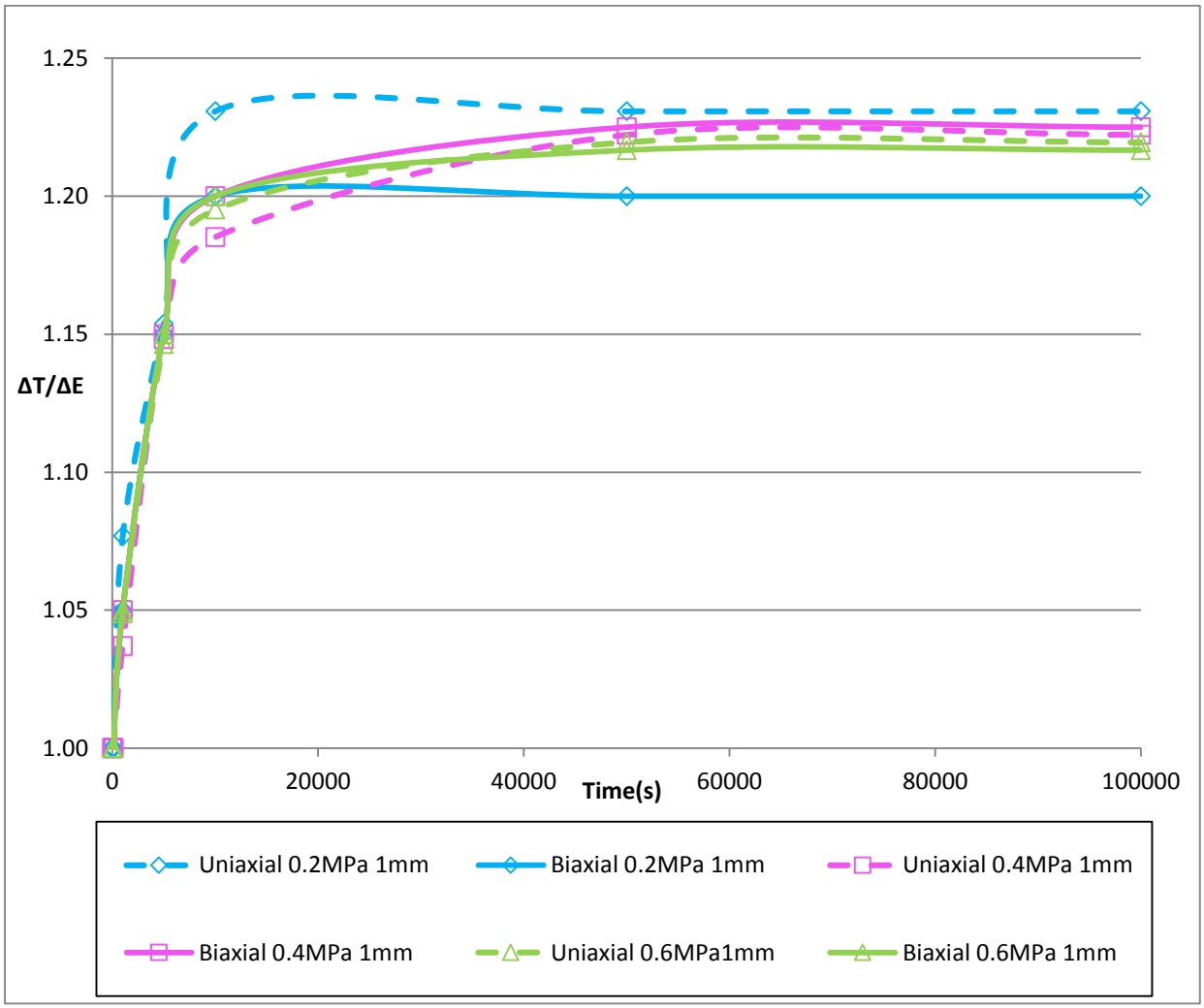

Figure C-10: ΔT/ΔE against time for 1mm hole in PVC

9. Cyclic results

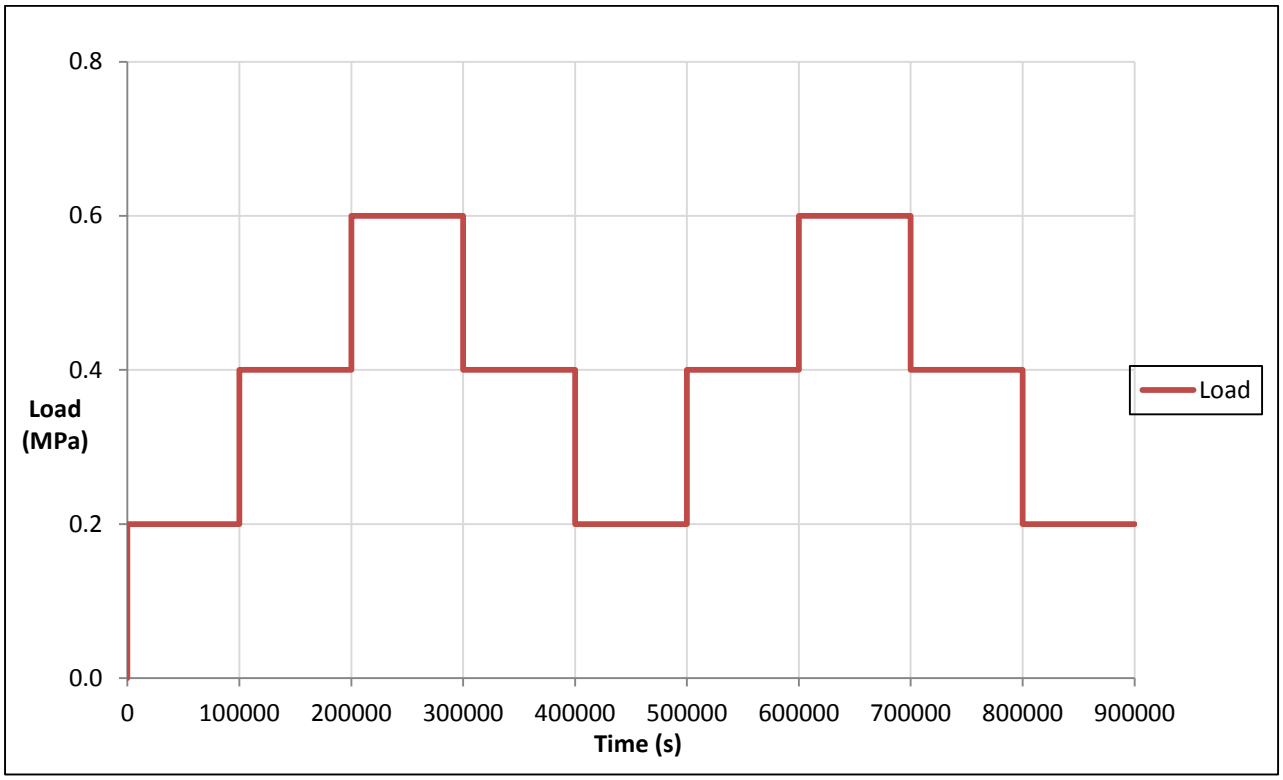

Figure C-11: Cyclic loading for a 1mm hole in PVC pipe

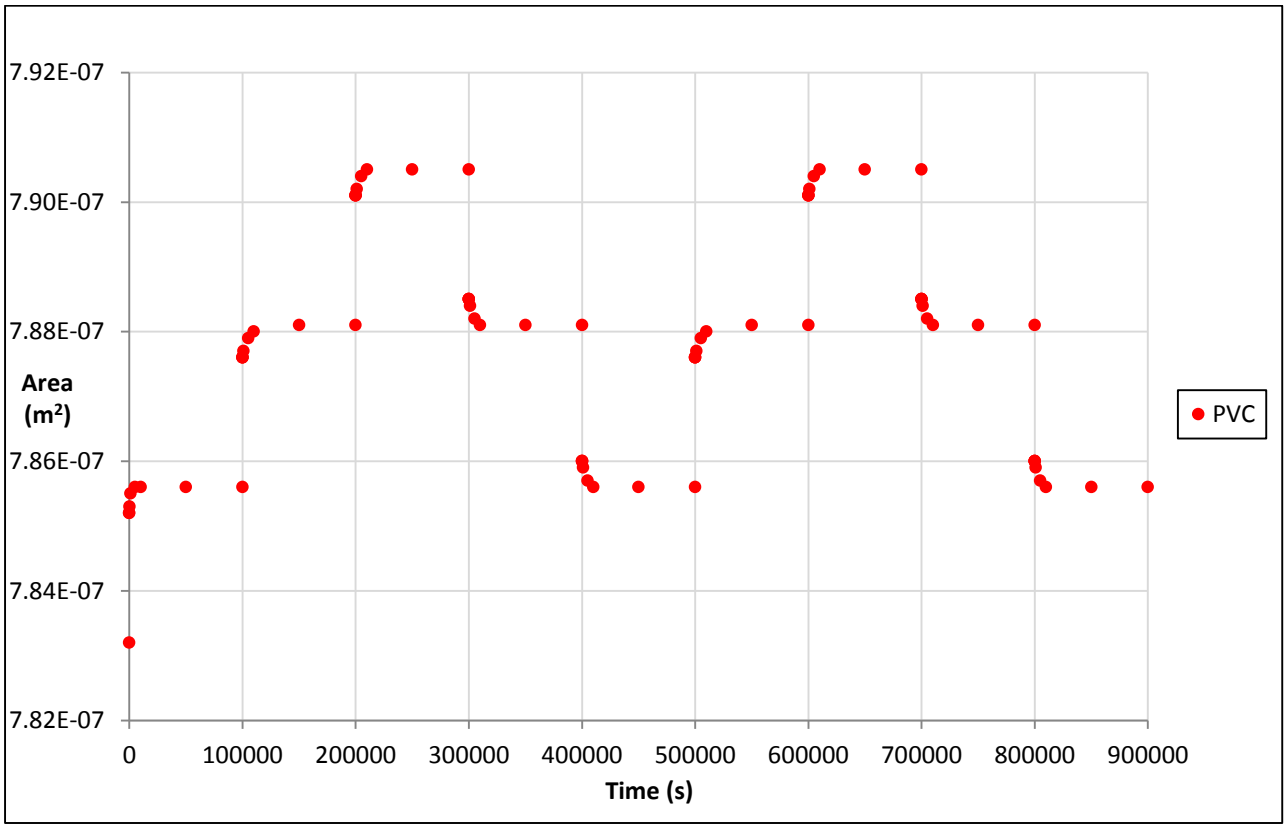

Figure C-12: Deformed area against time for 1mm hole in PVC during cyclic loading, biaxial

10. Leakage number, calculated leak exponents, m/A_0 and m/m_E

a) Uniaxial

Time (s)	N1 from power law	m	L_N	N1	m/A_0	m/m_E
			Pressure = 0.4MPa	**Pressure = 0.4MPa**		
0	0.5032	6.867E-11	0.0036	0.5036	0.00009	1.0000
10	0.5032	6.867E-11	0.0036	0.5036	0.00009	1.0000
100	0.5032	6.867E-11	0.0036	0.5036	0.00009	1.0000
1000	0.5033	7.112E-11	0.0037	0.5037	0.00009	1.0357
5000	0.5036	7.848E-11	0.0041	0.5041	0.00010	1.1429
10000	0.5037	8.093E-11	0.0042	0.5042	0.00010	1.1785
50000	0.5038	8.339E-11	0.0043	0.5043	0.00011	1.2144
100000	0.5038	8.339E-11	0.0043	0.5043	0.00011	1.2144

Table C-3: Leakage numbers, calculated leak exponents, m/A_0 and m/m_E for the 1mm hole in PVC, uniaxial

b) Biaxial

Time (s)	N1 from power law	m	L_N	N1	m/A_0	m/m_E
			Pressure = 0.4MPa	**Pressure = 0.4MPa**		
0	0.5045	9.81E-11	0.0051	0.5051	0.00013	1.0000
10	0.5045	9.81E-11	0.0051	0.5051	0.00013	1.0000
100	0.5045	9.81E-11	0.0051	0.5051	0.00013	1.0000
1000	0.5047	1.03E-10	0.0054	0.5053	0.00013	1.0499
5000	0.5052	1.13E-10	0.0059	0.5058	0.00014	1.1498
10000	0.5054	1.18E-10	0.0061	0.5061	0.00015	1.1998
50000	0.5055	1.20E-10	0.0063	0.5062	0.00015	1.2253
100000	0.5055	1.20E-10	0.0063	0.5062	0.00015	1.2253

Table C-4: Leakage numbers, calculated leak exponents, m/A_0 and m/m_E for the 1mm hole in PVC, biaxial

D 12mm hole in HDPE

1. Summary results for area, gradient (m) and leakage exponent (N1)

HDPE	Area of deformed holes with A_0 = 112.98mm^2					
Pressure (MPa)	0.2		0.4		0.6	
Time (s)	Uniaxial	Biaxial	Uniaxial	Biaxial	Uniaxial	Biaxial
0 (Elastic)	113.7139	113.9704	114.4410	114.9615	115.1623	115.9541
10	113.7148	113.9716	114.4427	114.9639	115.1649	115.9577
100	113.7227	113.9823	114.4585	114.9855	115.1884	115.9902
1000	113.7984	114.0849	114.6087	115.1911	115.4118	116.2990
5000	114.0628	114.4439	115.1323	115.9107	116.1894	117.3809
10000	114.2734	114.7308	115.5484	116.4862	116.8060	118.2467
50000	114.5901	115.1637	116.1726	117.3554	117.7283	119.5551
100000	114.5960	115.1718	116.1840	117.3714	117.7451	119.5792

Table D-1: Deformed areas (mm^2) for the 12mm hole in HDPE

HDPE	Uniaxial		Biaxial	
Time (s)	N1	m	N1	m
0 (Elastic)	0.5113	3.552E-08	0.5154	4.865E-08
10	0.5113	3.556E-08	0.5154	4.871E-08
100	0.5114	3.595E-08	0.5155	4.924E-08
1000	0.5125	3.957E-08	0.5171	5.430E-08
5000	0.5165	5.215E-08	0.5226	7.203E-08
10000	0.5195	6.211E-08	0.5269	8.623E-08
50000	0.5241	7.696E-08	0.5333	1.077E-07
100000	0.5242	7.723E-08	0.5334	1.081E-07

Table D-2: Gradients (m) and Leak exponents (N1) from the power law graphs for the 12mm hole in HDPE

2. Variation of leak area with time

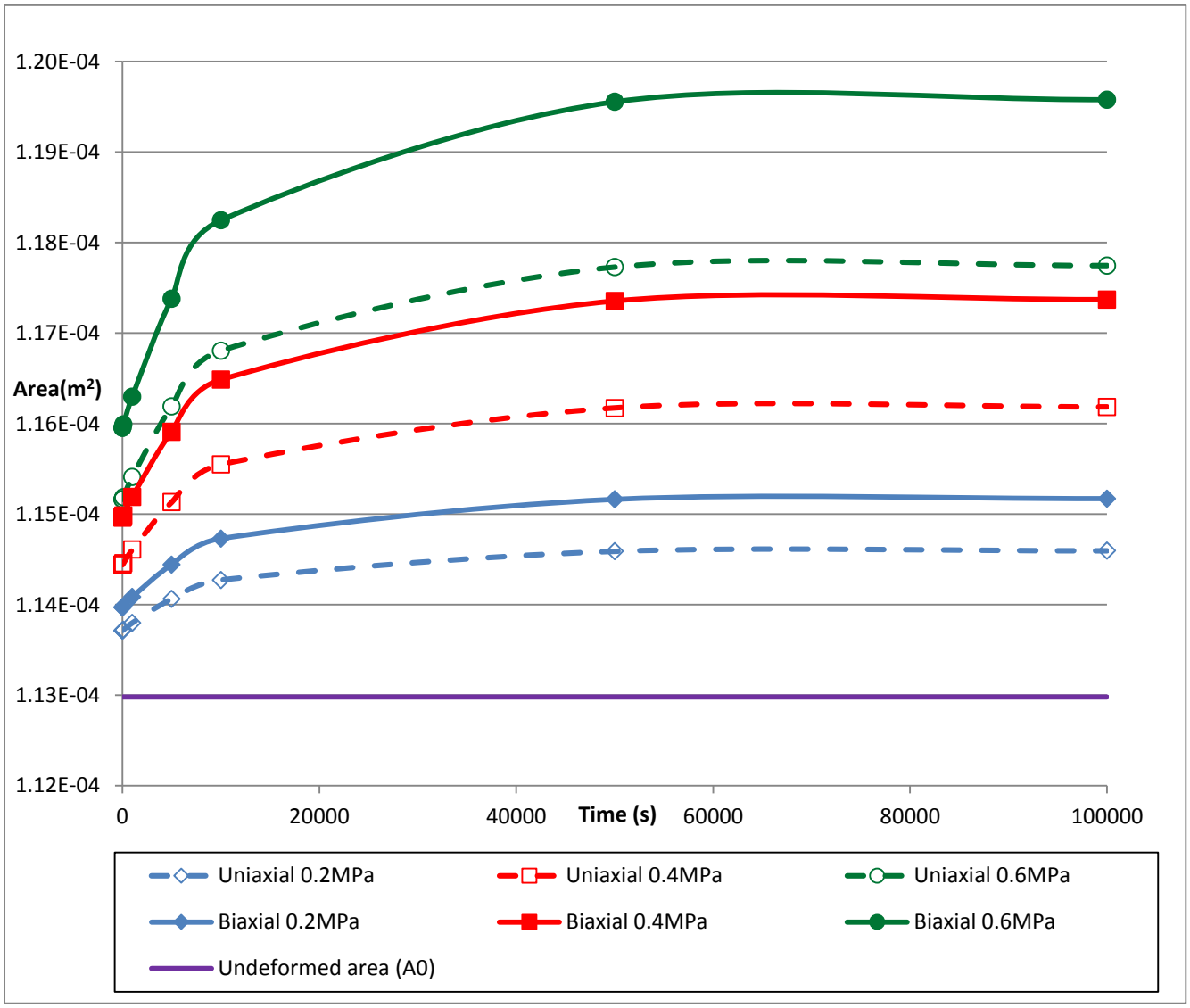

Figure D-1: Area against time for a 12mm hole in HDPE pipe

3. Variation of leak area with pressure

a) Uniaxial

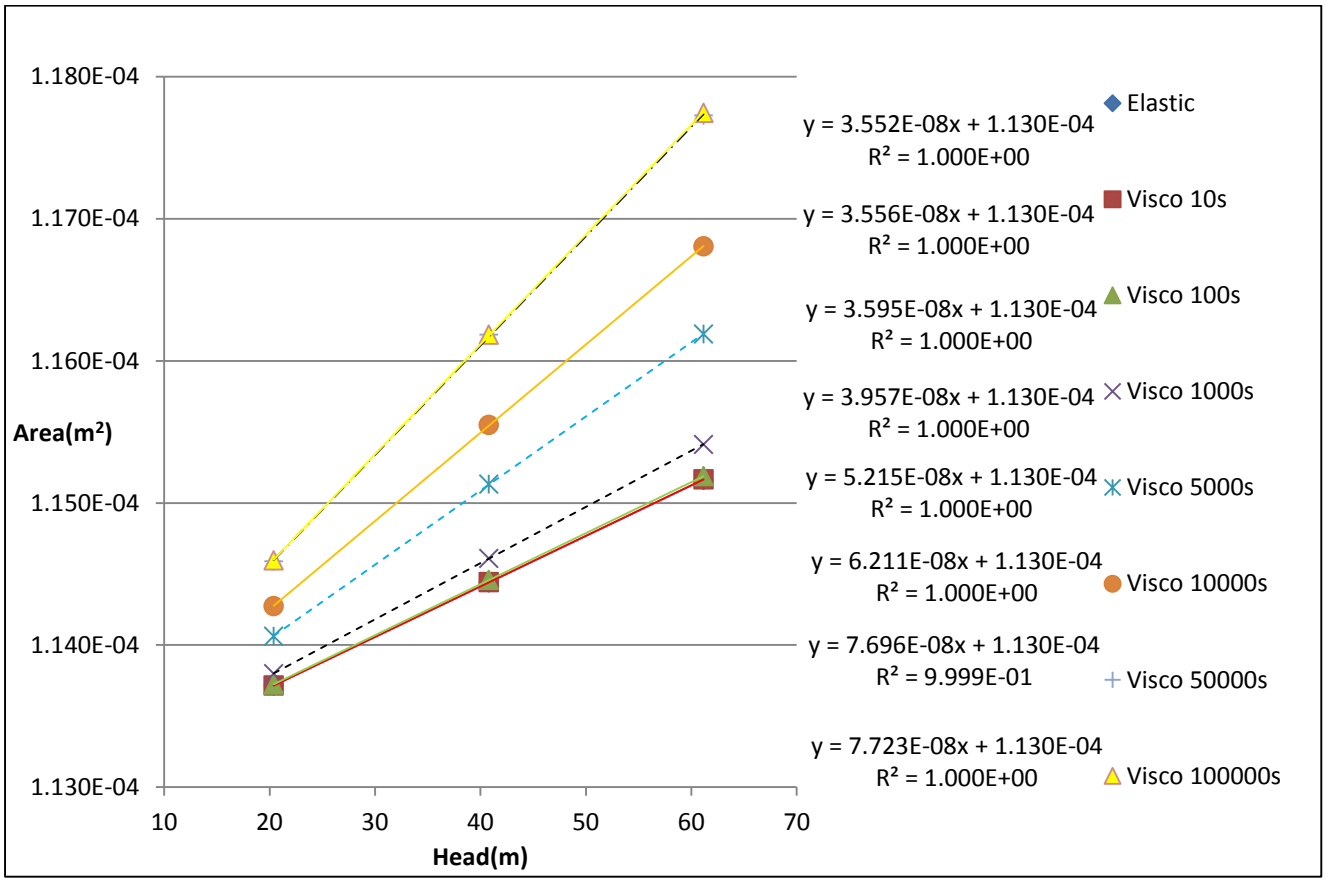

Figure D-2: Area against pressure for 12mm hole in HDPE pipe, uniaxial state

b) Biaxial

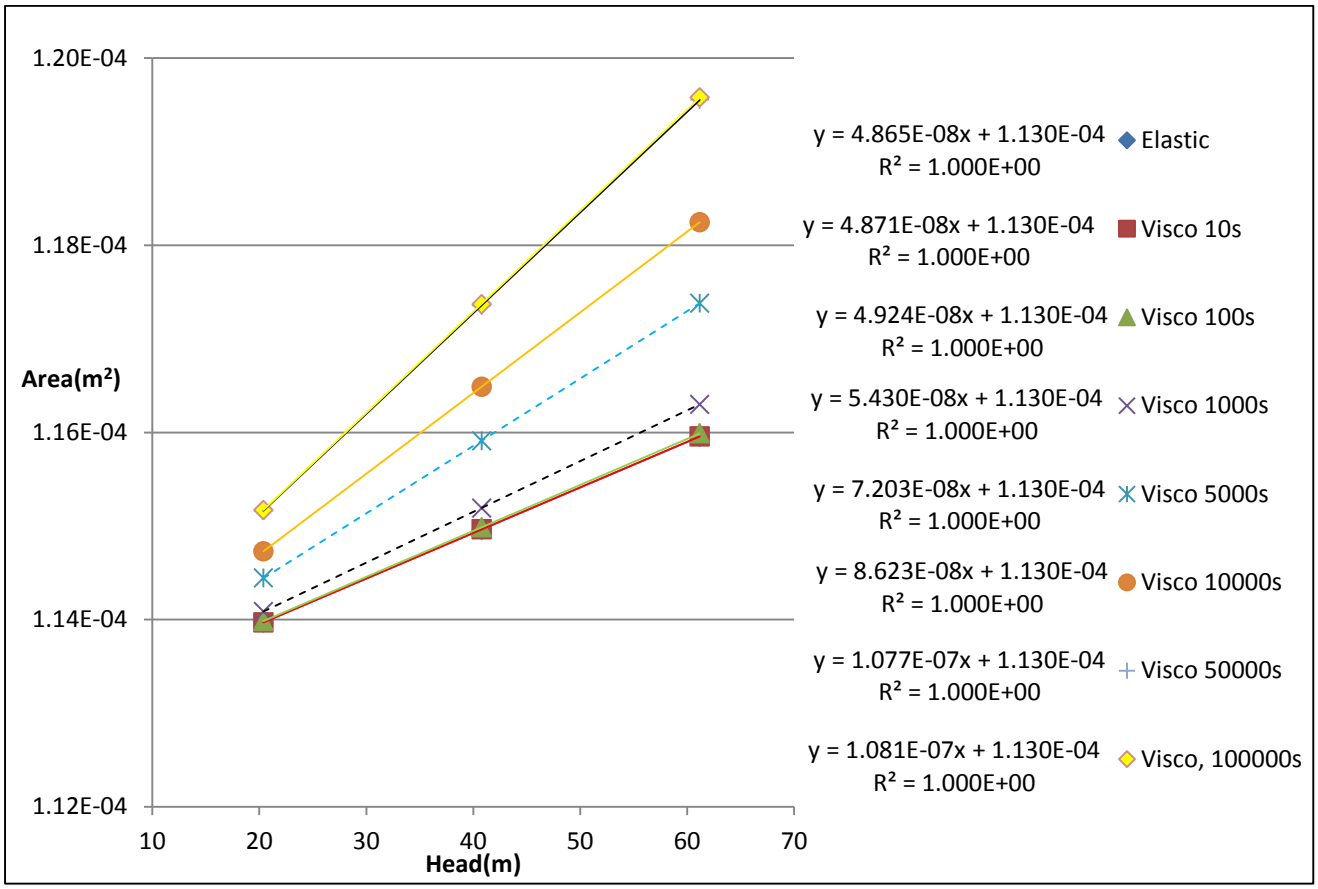

Figure D-3: Area against pressure for 12mm hole in HDPE pipe biaxial state

4. Variation of leak discharge with time

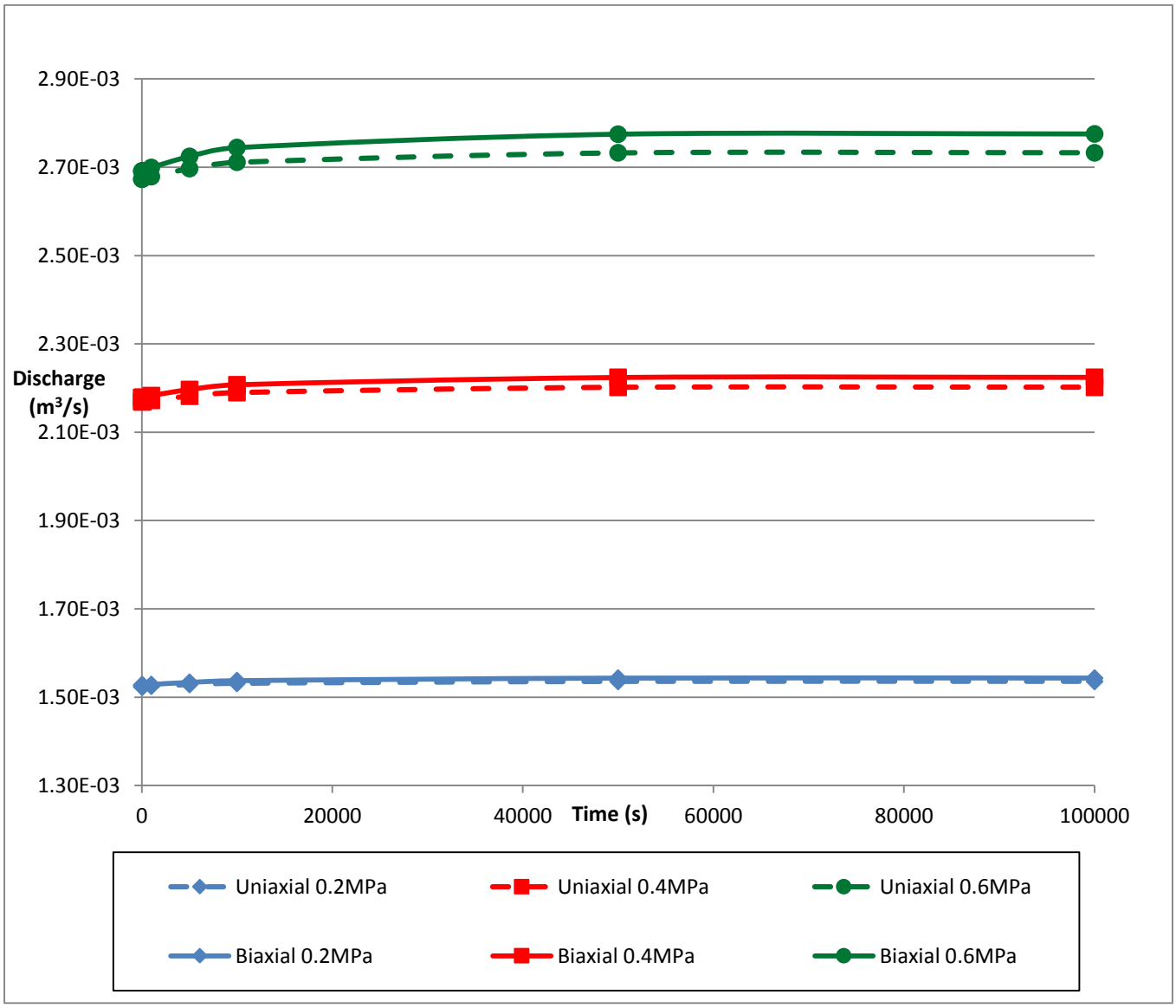

Figure D-4: Discharge against time for a 12mm hole in HDPE pipe

5. Variation of leak discharge with pressure

a) Uniaxial

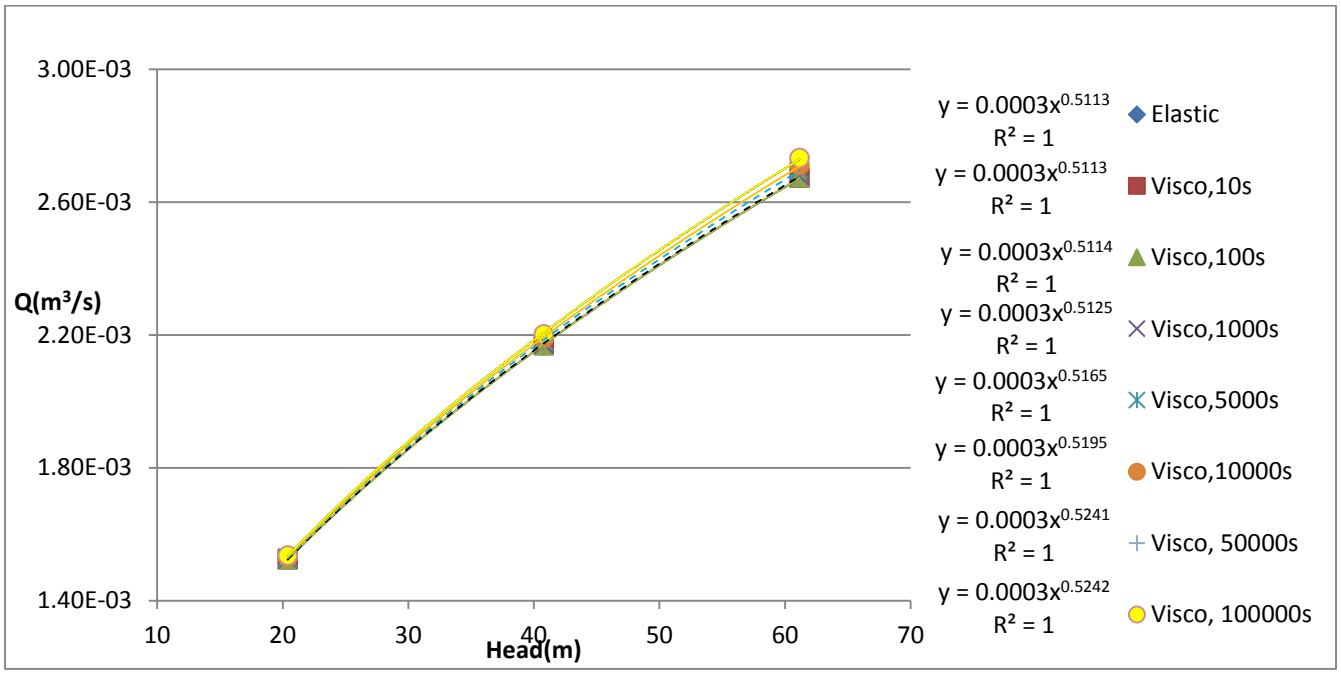

Figure D-5: Discharge against pressure head for 12mm hole in HDPE, uniaxial state

b) Biaxial

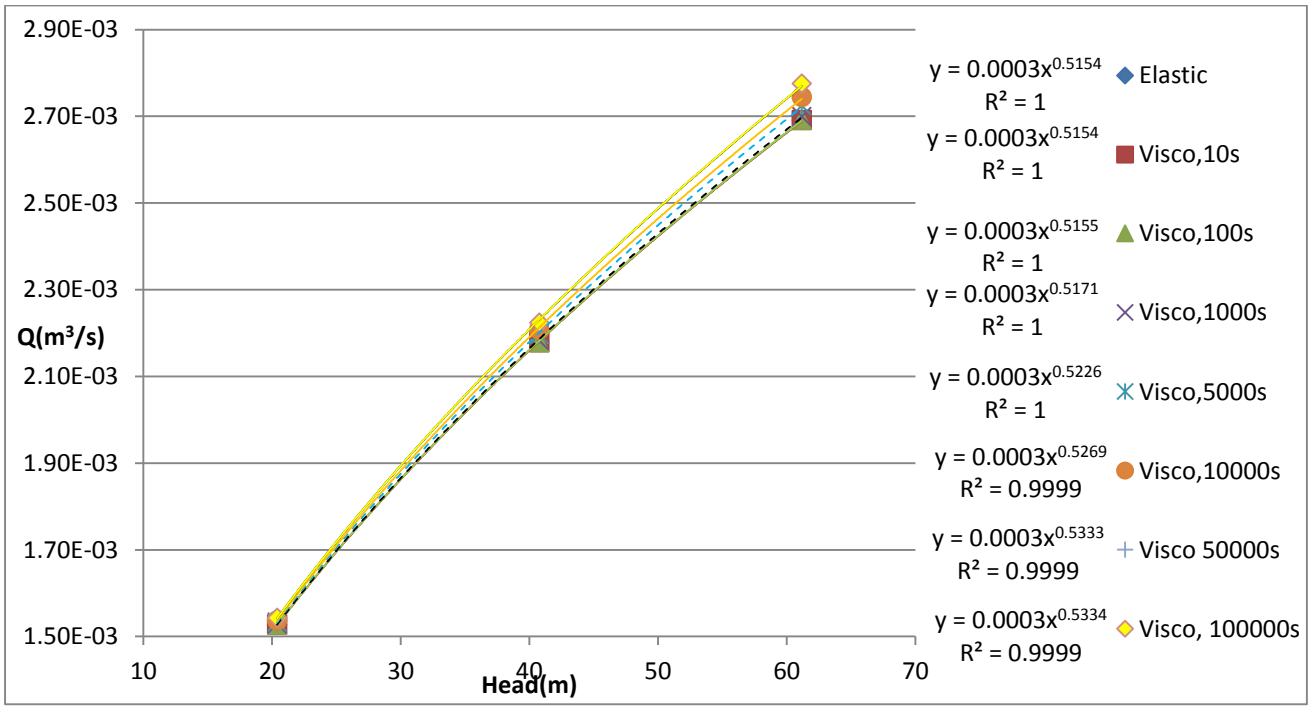

Figure D-6: Discharge against pressure head for 12mm hole in HDPE, biaxial state

6. Gradient (m) and leakage exponent (N1)

a) Gradient (m) against time

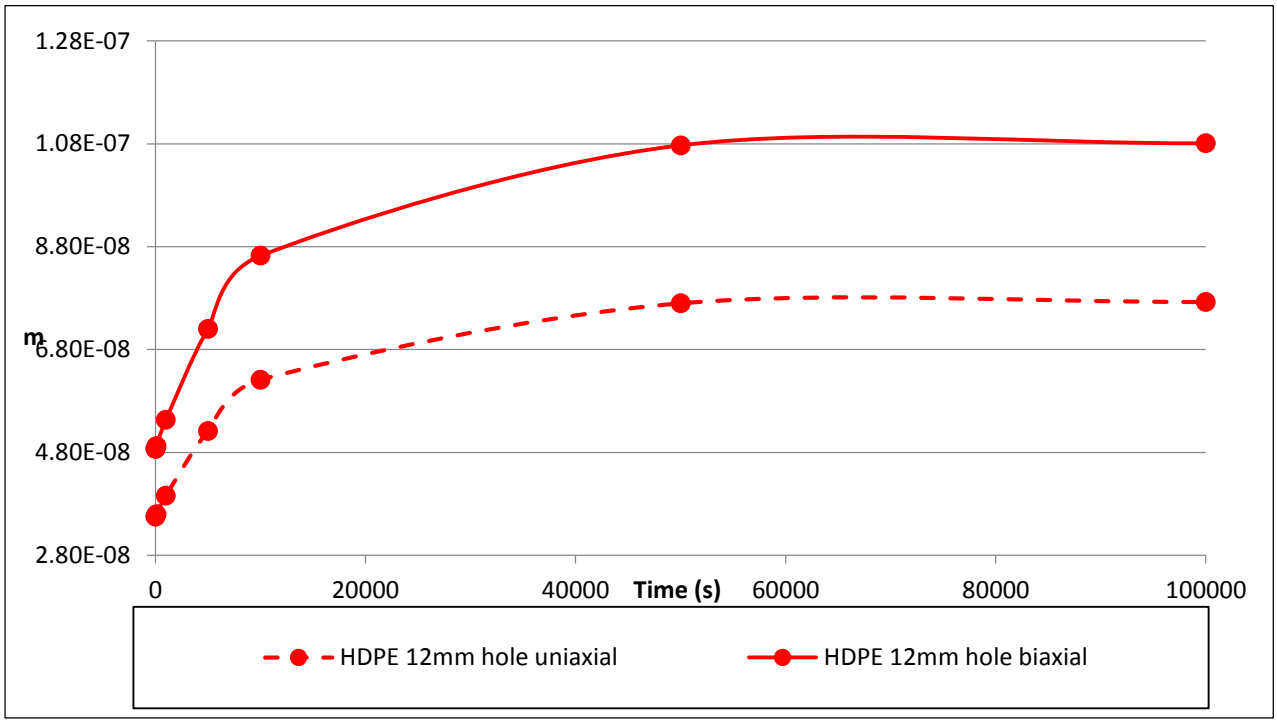

Figure D-7: Gradient (m) against time for 12mm hole in HDPE

b) Leakage exponent (N1) against time

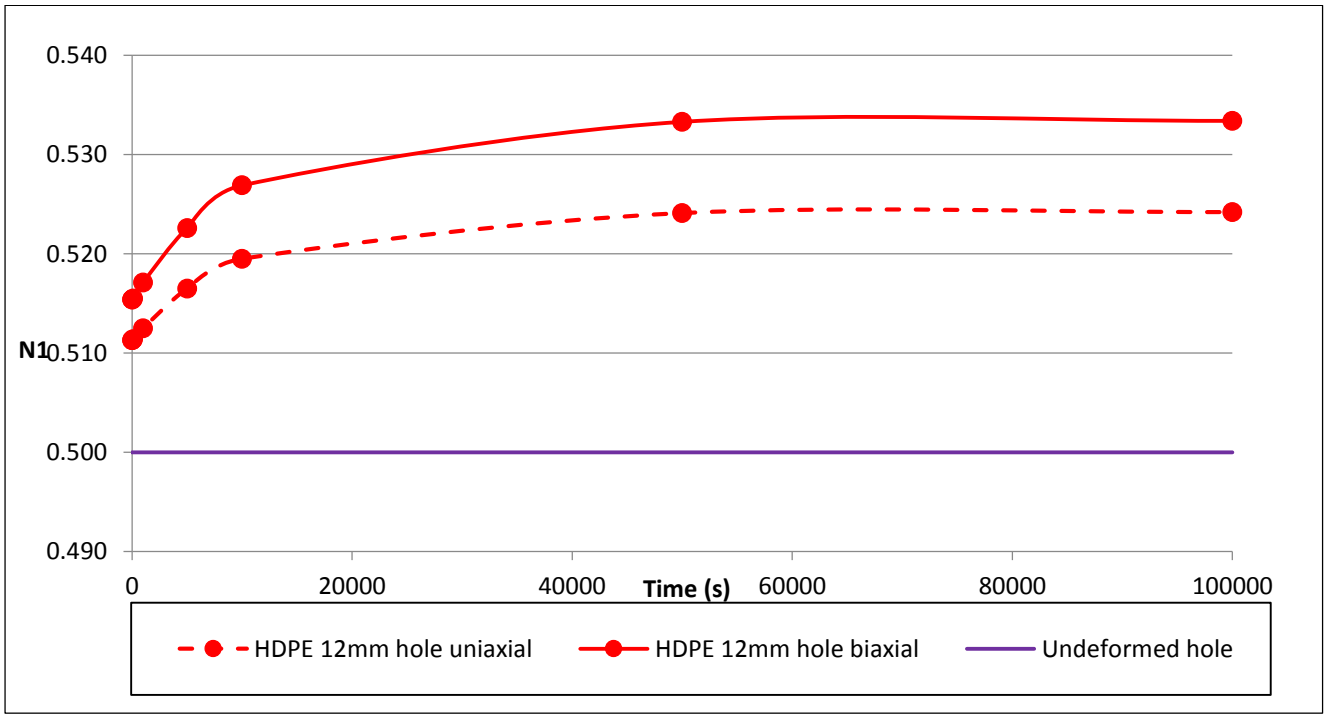

Figure D-8: Leakage exponent (N1) against time for 12mm hole in HDPE

7. Percentage change in area with pressure

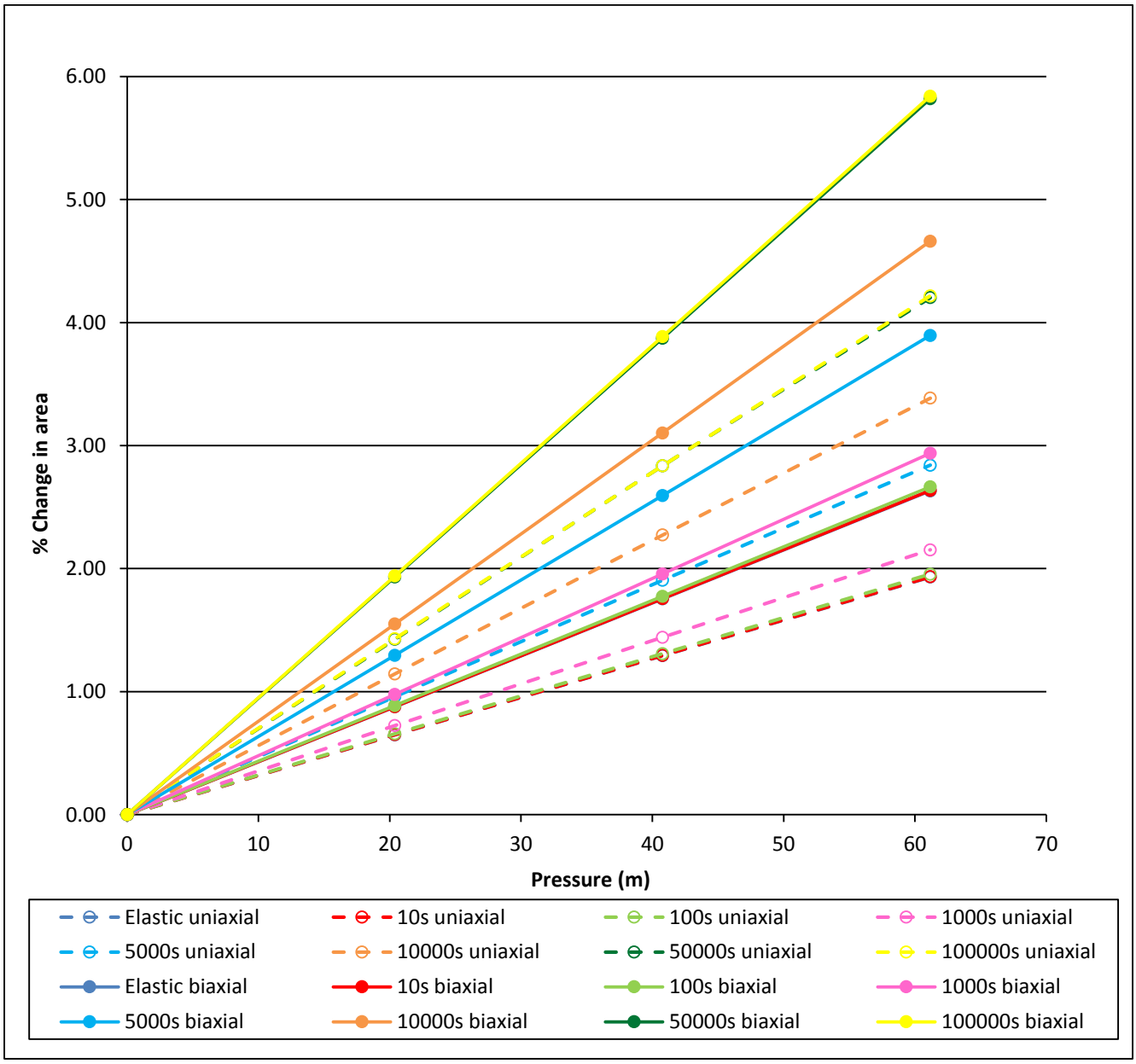

Figure D-9: Percentage change in area for the 12mm hole in HDPE pipe

8. Ratio of total change in area to elastic change in area

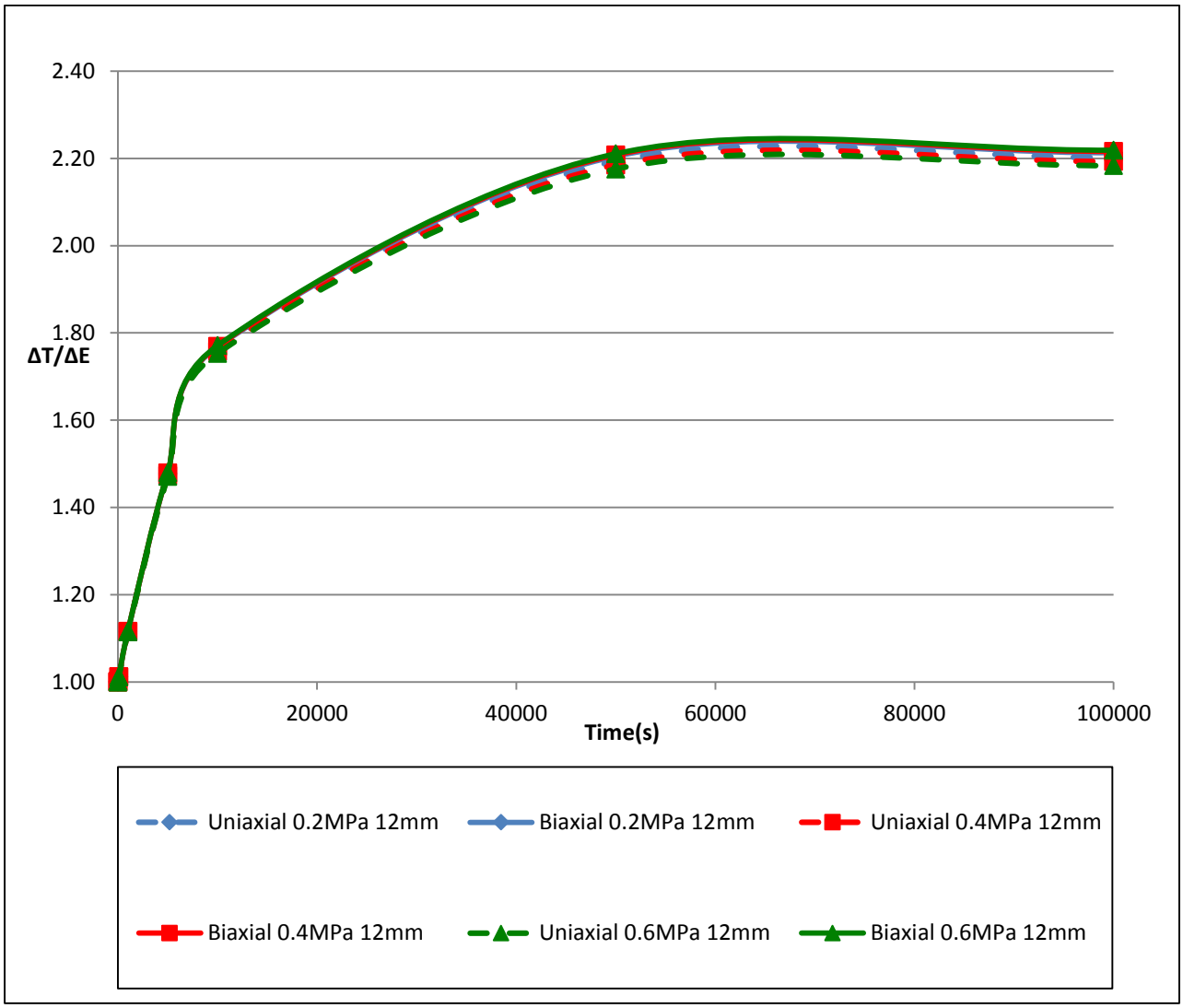

Figure D-10: ΔT/ΔE against time for 12mm hole in HDPE

9. Leakage number, calculated leak exponents, m/A_0 and m/m_E

a) Uniaxial

Time (s)	N1 from power law	m	L_N	N1	m/A_0	m/m_E
			Pressure = 0.4MPa	**Pressure = 0.4MPa**		
0	0.5113	3.55E-08	0.0130	0.5128	0.00032	1.0000
10	0.5113	3.56E-08	0.0130	0.5129	0.00032	1.0011
100	0.5114	3.60E-08	0.0132	0.5130	0.00032	1.0121
1000	0.5125	3.96E-08	0.0145	0.5143	0.00036	1.1140
5000	0.5165	5.22E-08	0.0191	0.5187	0.00047	1.4682
10000	0.5195	6.21E-08	0.0228	0.5222	0.00056	1.7486
50000	0.5241	7.70E-08	0.0282	0.5274	0.00069	2.1667
100000	0.5242	7.72E-08	0.0283	0.5275	0.00069	2.1743

Table D-3: Leakage numbers, calculated leak exponents, m/A_0 and m/m_E for the 12mm hole in HDPE, uniaxial

b) Biaxial

Time (s)	N1 from power law	m	L_N	N1	m/A_0	m/m_E
			Pressure = 0.4MPa	**Pressure = 0.4MPa**		
0	0.5154	4.87E-08	0.0178	0.5175	0.00044	1.0000
10	0.5154	4.87E-08	0.0178	0.5175	0.00044	1.0012
100	0.5155	4.92E-08	0.0180	0.5177	0.00044	1.0121
1000	0.5171	5.43E-08	0.0199	0.5195	0.00049	1.1161
5000	0.5226	7.20E-08	0.0264	0.5257	0.00065	1.4806
10000	0.5269	8.62E-08	0.0316	0.5306	0.00077	1.7725
50000	0.5333	1.08E-07	0.0395	0.5380	0.00097	2.2138
100000	0.5334	1.08E-07	0.0396	0.5381	0.00097	2.2220

Table D-4: Leakage numbers, calculated leak exponents, m/A_0 and m/m_E for the 12mm hole in HDPE, biaxial

E 12mm hole in PVC

1. Summary results for area, gradient (m) and leakage exponent (N1)

PVC	Area of deformed holes with A_0 = 112.98mm^2					
Pressure (MPa)	0.2		0.4		0.6	
Time (s)	Uniaxial	Biaxial	Uniaxial	Biaxial	Uniaxial	Biaxial
0 (Elastic)	113.3134	113.4205	113.6446	113.8602	113.9746	114.3002
10	113.3135	113.4207	113.6449	113.8607	113.9750	114.3009
100	113.3152	113.4230	113.6483	113.8652	113.9801	114.3077
1000	113.3304	113.4430	113.6785	113.9054	114.0253	114.3680
5000	113.3697	113.4950	113.7567	114.0094	114.1421	114.5241
10000	113.3871	113.5181	113.7915	114.0557	114.1941	114.5935
50000	113.3949	113.5285	113.8071	114.0765	114.2173	114.6247
100000	113.3949	113.5286	113.8071	114.0765	114.2173	114.6247

Table E-1: Deformed areas (mm^2) for the 12mm in PVC

PVC	Uniaxial		Biaxial	
Time (s)	N1	m	N1	m
0 (Elastic)	0.5052	1.622E-08	0.5069	2.157E-08
10	0.5052	1.622E-08	0.5069	2.159E-08
100	0.5052	1.631E-08	0.5069	2.170E-08
1000	0.5054	1.704E-08	0.5072	2.269E-08
5000	0.5060	1.894E-08	0.5080	2.524E-08
10000	0.5063	1.979E-08	0.5084	2.637E-08
50000	0.5064	2.017E-08	0.5086	2.668E-08
100000	0.5064	2.017E-08	0.5086	2.668E-08

Table E-2: Gradients (m) and Leak exponents (N1) from the power law graphs for the 12mm hole in PVC

2. Variation of leak area with time

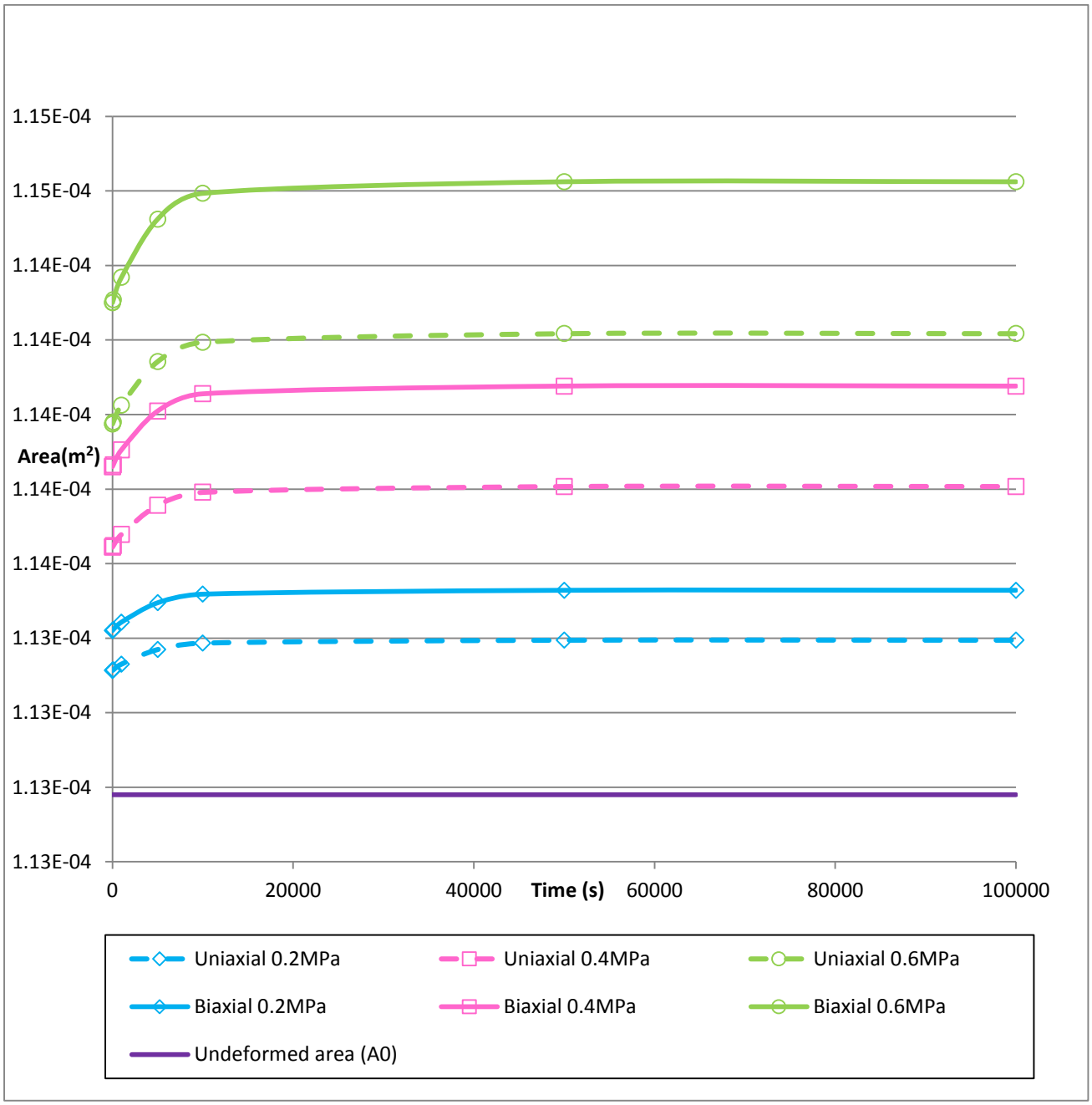

Figure E-1: Area against time for a 12mm hole in PVC pipe

3. Variation of leak area with pressure

a) Uniaxial

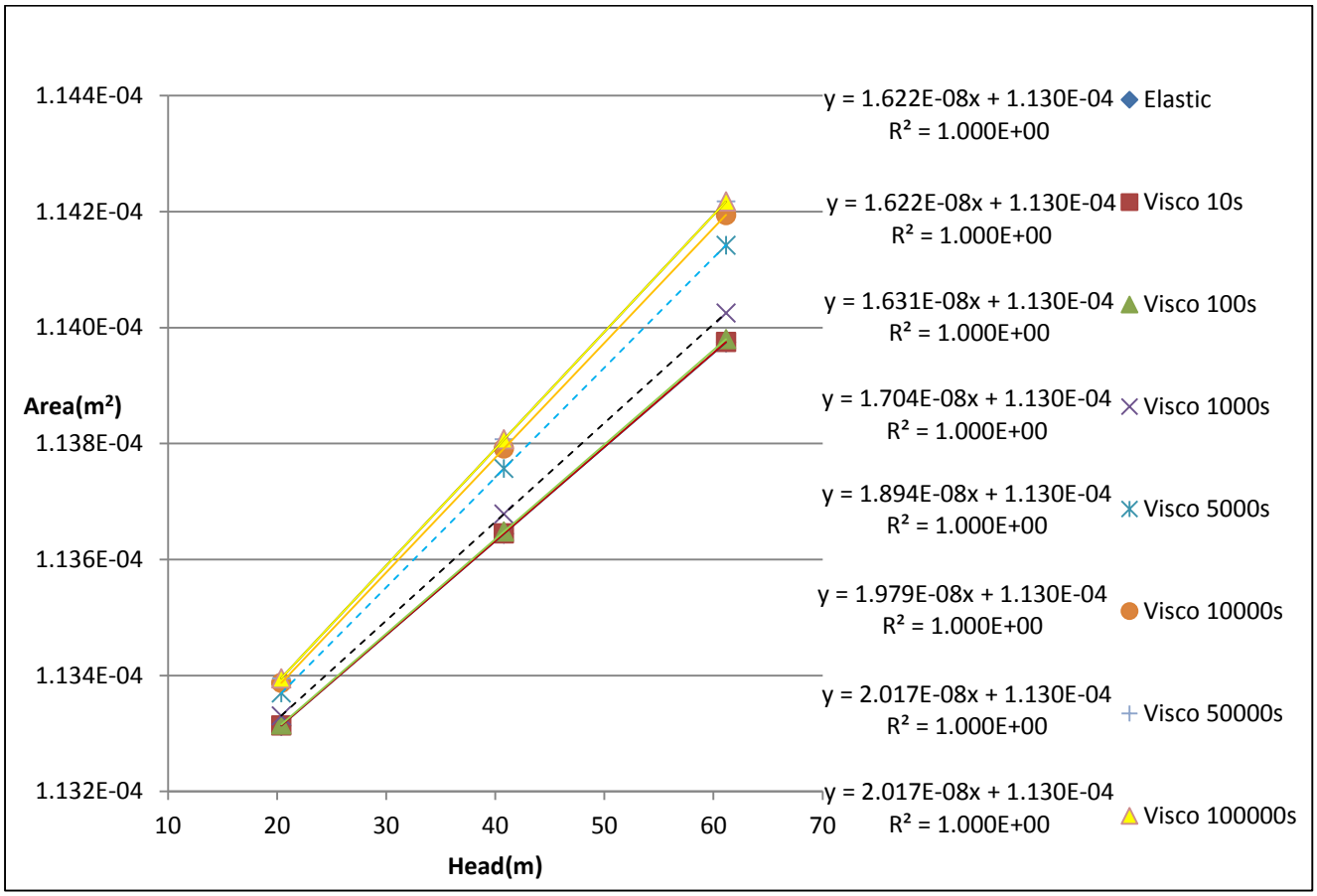

Figure E-2: Area against pressure for 12mm hole in PVC pipe, uniaxial state

b) Biaxial

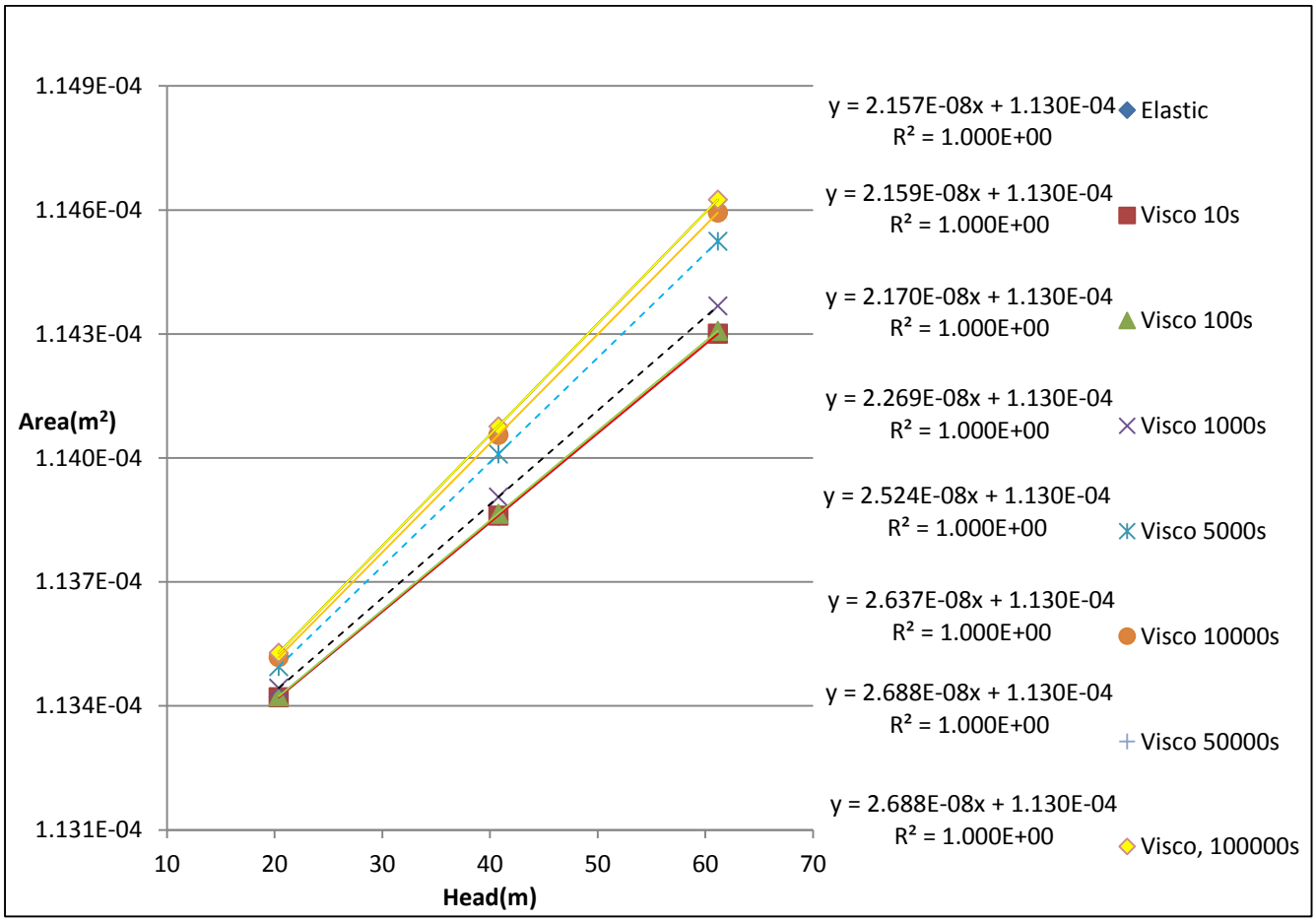

Figure E-3: Area against pressure for 12mm hole in PVC pipe, biaxial state

4. Variation of leak discharge with time

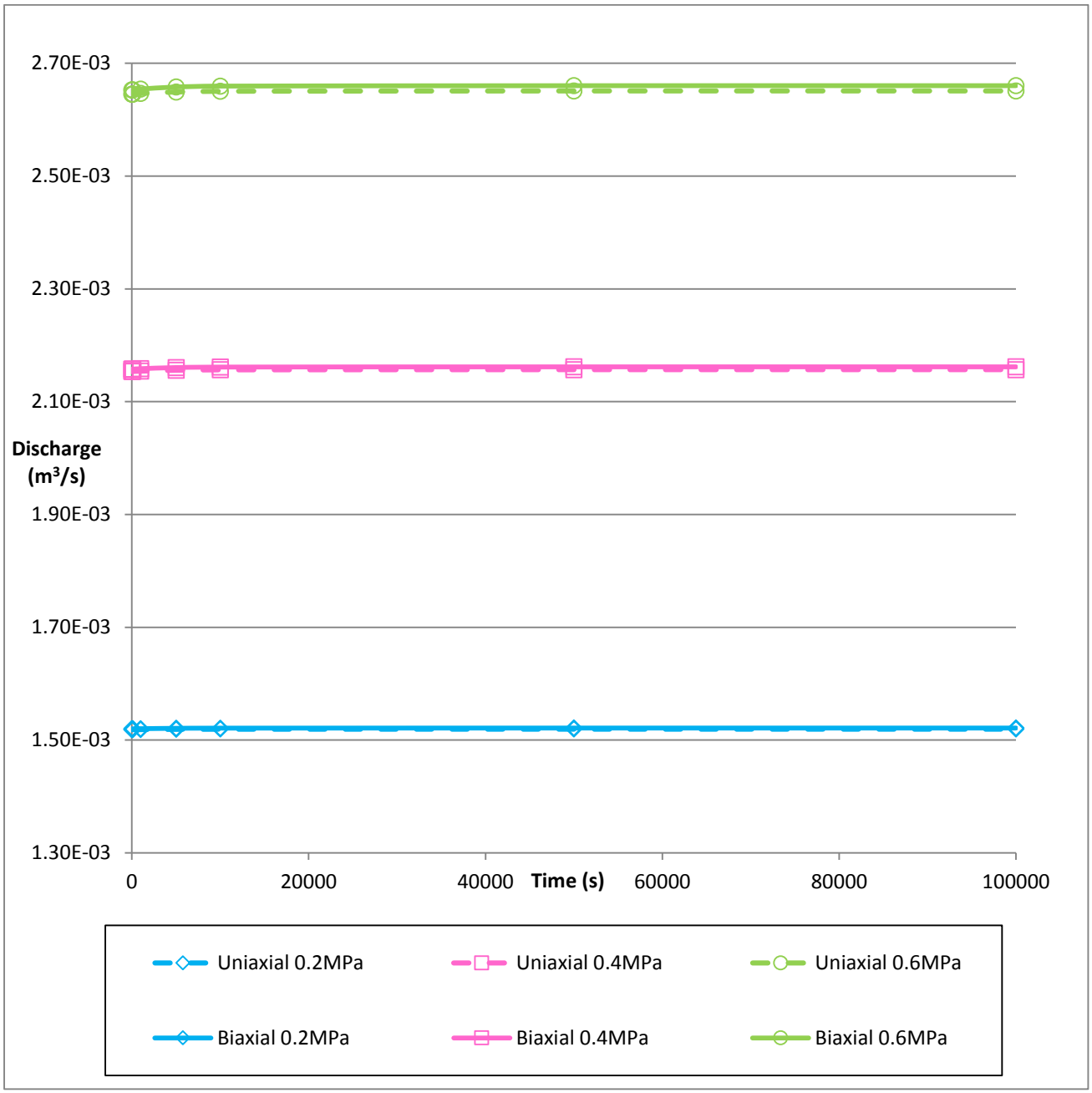

Figure E-4: Discharge against time for 12mm hole in PVC

5. Variation of leak discharge with pressure

a) Uniaxial

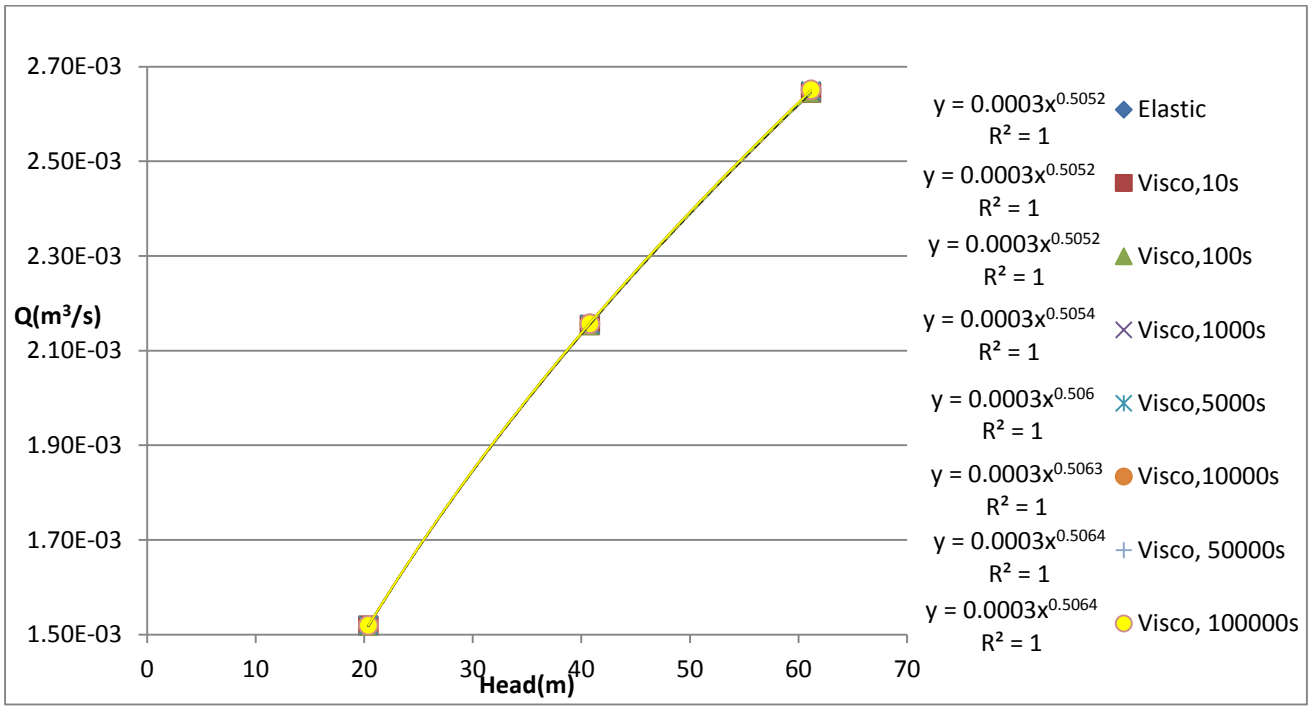

Figure E-5: Discharge against pressure head for 12mm hole in PVC, uniaxial state

b) Biaxial

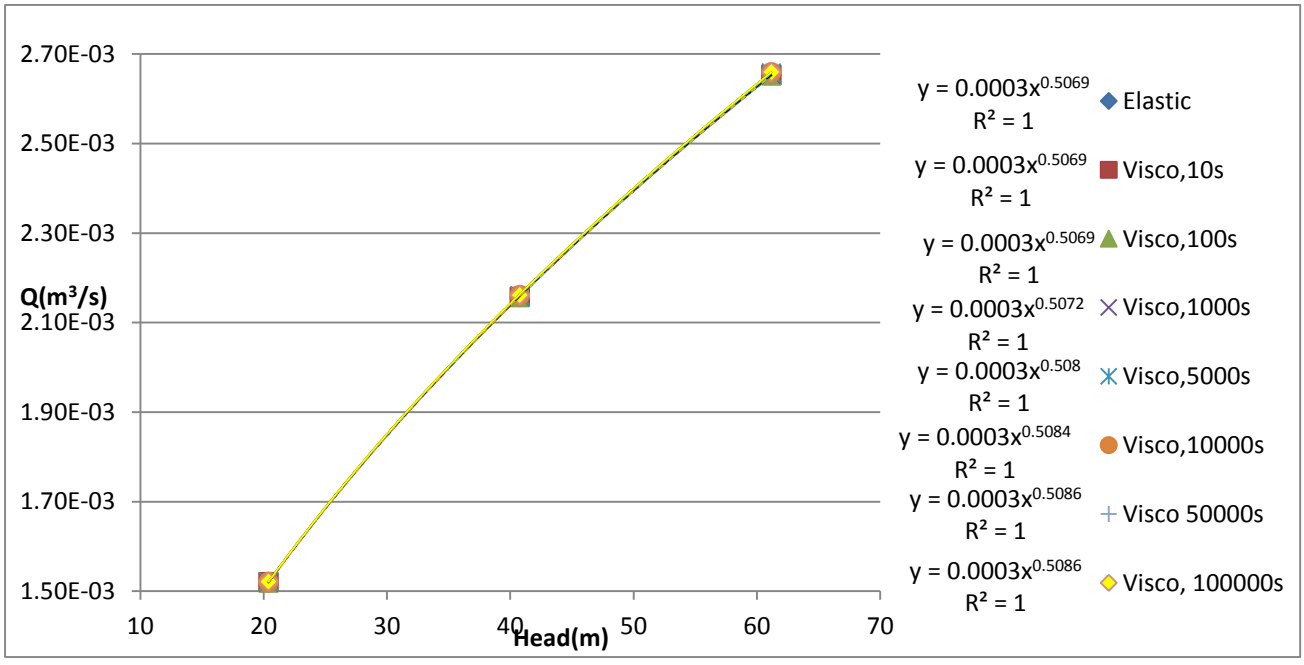

Figure E-6: Discharge against pressure head for 12mm hole in PVC, biaxial state

6. Gradient (m) and leakage exponent (N1)

a) Gradient (m) against time

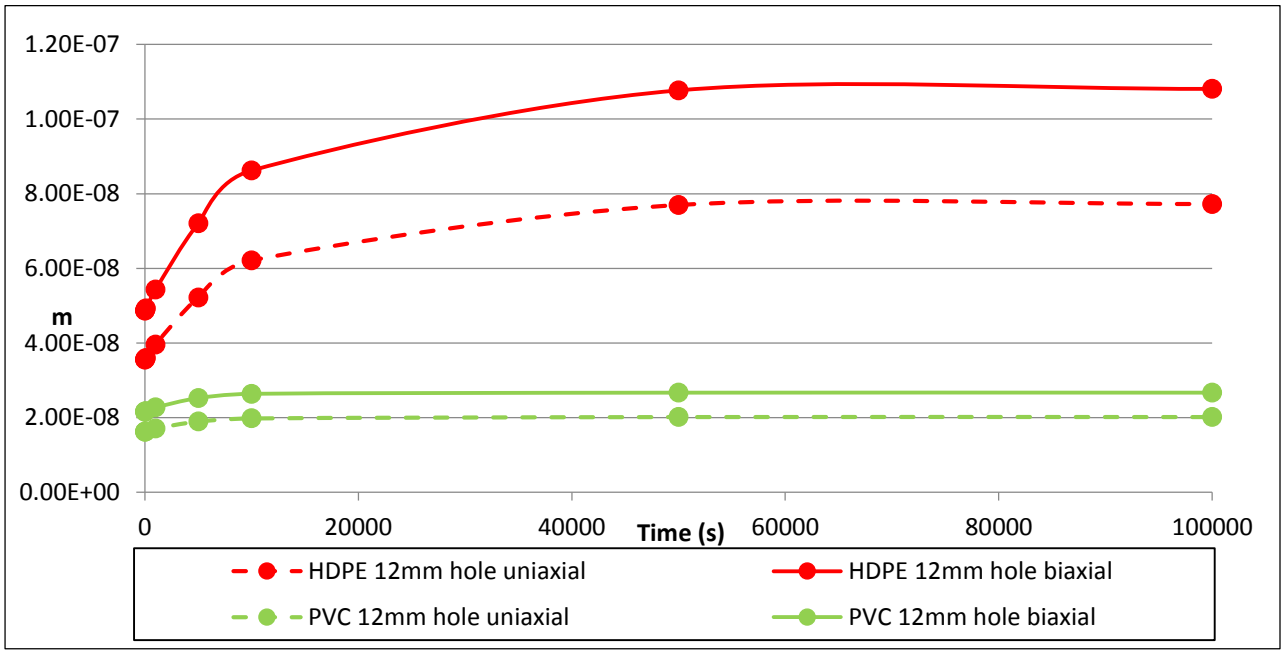

Figure E-7: Gradient (m) against time for 12mm hole in PVC

b) Leakage exponent (N1) against time

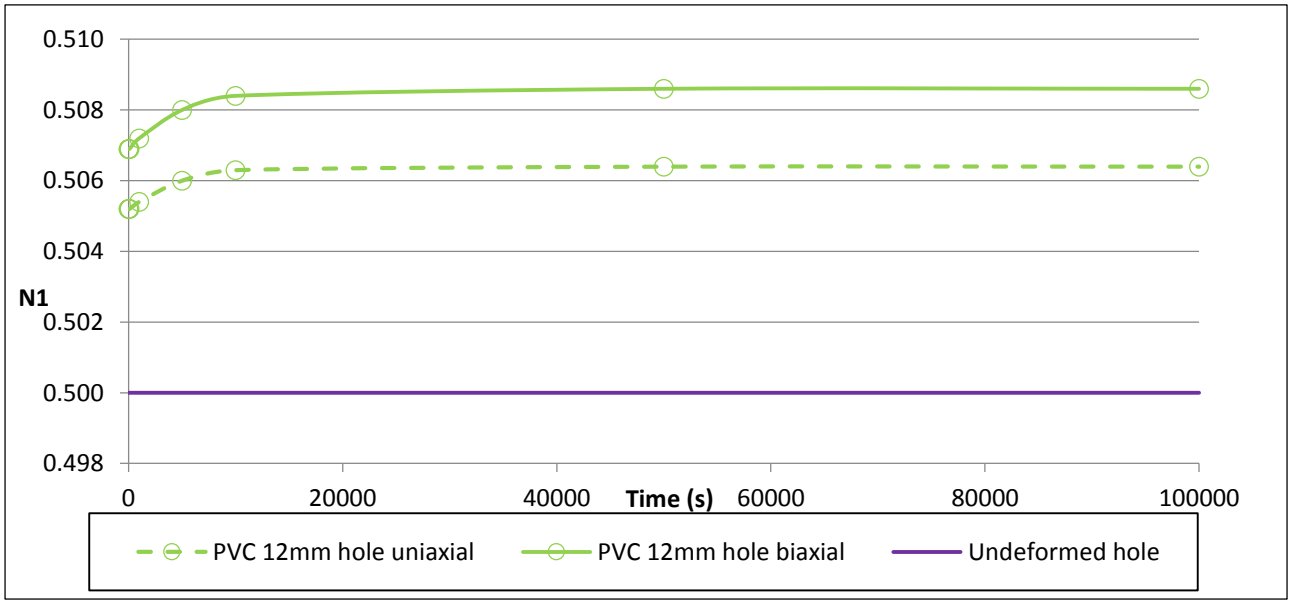

Figure E-8: Leakage exponent (N1) against time for 12mm hole in PVC

7. Percentage change in area with pressure

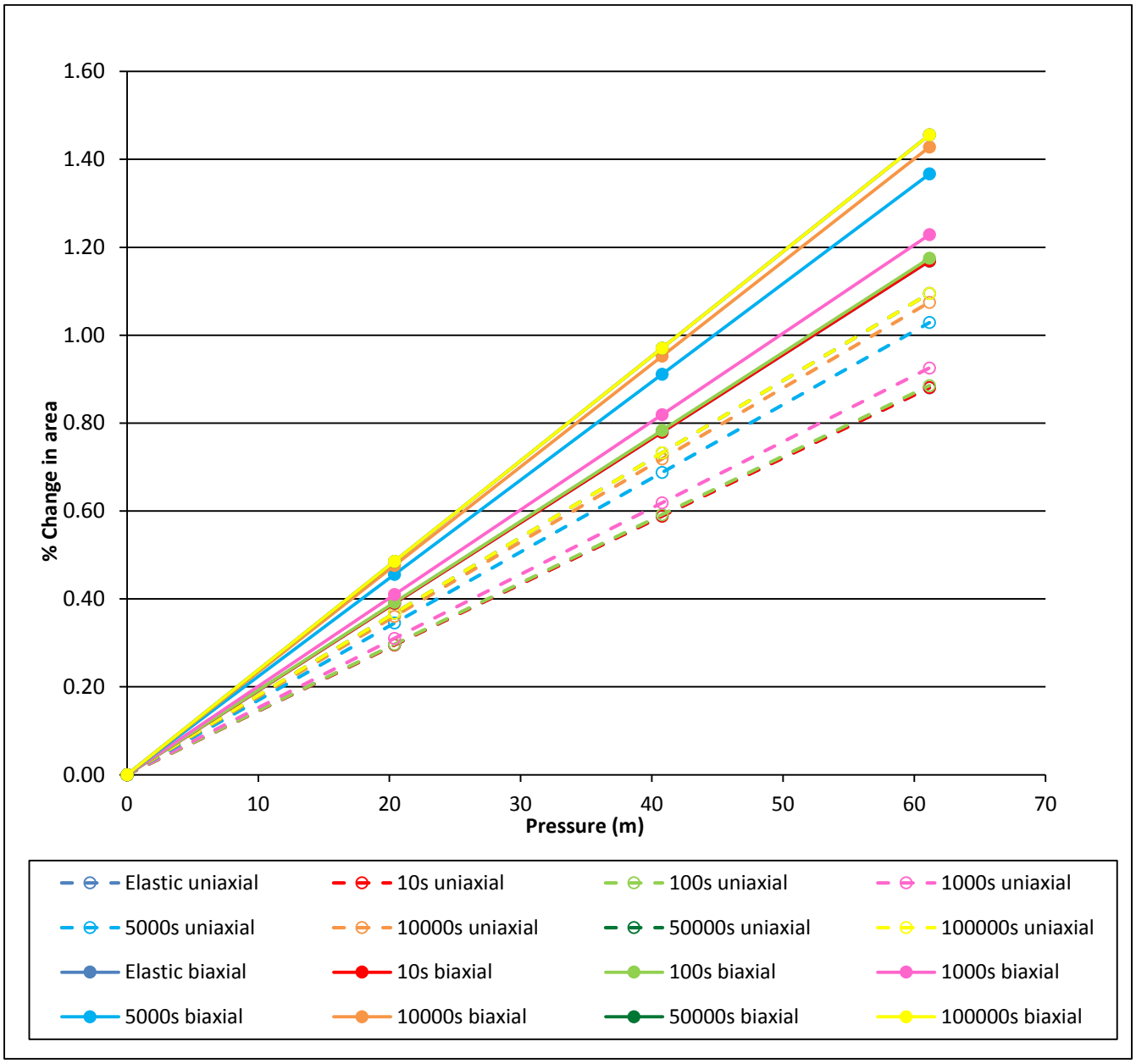

Figure E-9: Percentage change in area against time for the 12mm hole in PVC pipe

8. Ratio of total change in area to elastic change in area

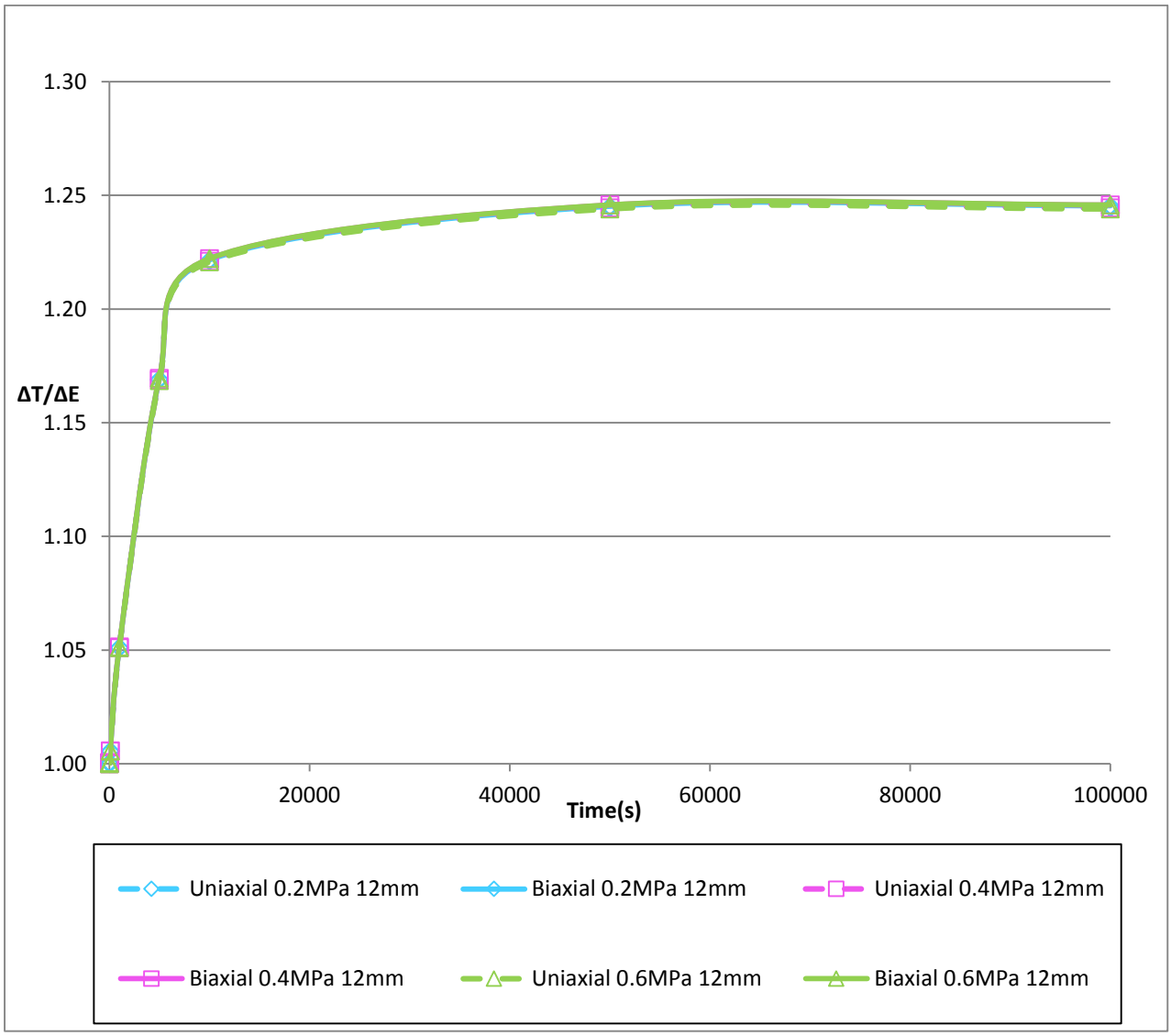

Figure E-10: ΔT/ΔE against time for 12mm hole in PVC

9. Leakage number, calculated leak exponents, m/A_0 and m/m_E

a) Uniaxial

Time (s)	N1 from power law	m	L_N	N1	m/A_0	m/m_E
			Pressure = 0.4MPa	**Pressure = 0.4MPa**		
0	0.5052	1.62E-08	0.0059	0.5059	0.00015	1.0000
10	0.5052	1.62E-08	0.0059	0.5059	0.00015	1.0000
100	0.5052	1.63E-08	0.0060	0.5059	0.00015	1.0055
1000	0.5054	1.70E-08	0.0062	0.5062	0.00015	1.0506
5000	0.506	1.89E-08	0.0069	0.5069	0.00017	1.1677
10000	0.5063	1.98E-08	0.0073	0.5072	0.00018	1.2201
50000	0.5064	2.02E-08	0.0074	0.5073	0.00018	1.2435
100000	0.5064	2.02E-08	0.0074	0.5073	0.00018	1.2435

Table E-3: Leakage numbers, calculated leak exponents, m/A_0 and m/m_E for the 12mm hole in PVC, uniaxial

b) Biaxial

Time (s)	N1 from power law	m	L_N	N1	m/A_0	m/m_E
			Pressure = 0.4MPa	**Pressure = 0.4MPa**		
0	0.5069	2.16E-08	0.0079	0.5078	0.00019	1.0000
10	0.5069	2.16E-08	0.0079	0.5078	0.00019	1.0009
100	0.5069	2.17E-08	0.0079	0.5079	0.00019	1.0060
1000	0.5072	2.27E-08	0.0083	0.5082	0.00020	1.0519
5000	0.508	2.52E-08	0.0092	0.5092	0.00023	1.1701
10000	0.5084	2.64E-08	0.0097	0.5096	0.00024	1.2225
50000	0.5086	2.67E-08	0.0098	0.5097	0.00024	1.2369
100000	0.5086	2.67E-08	0.0098	0.5097	0.00024	1.2369

Table E-4: Leakage numbers, calculated leak exponents, m/A_0 and m/m_E for the 12mm hole in PVC, biaxial

F 1mm by 10mm longitudinal crack in HDPE

1. Summary results for area, gradient (m) and leakage exponent (N1)

HDPE	Area of deformed cracks with A_0 = 9.77mm^2					
Pressure (MPa)	0.2		0.4		0.6	
Time (s)	Uniaxial	Biaxial	Uniaxial	Biaxial	Uniaxial	Biaxial
0 (Elastic)	10.1587	10.1640	10.5425	10.5543	10.9243	10.9438
10	10.1592	10.1645	10.5434	10.5553	10.9256	10.9452
100	10.1633	10.1686	10.5515	10.5635	10.9377	10.9575
1000	10.2019	10.2080	10.6285	10.6420	11.0525	11.0750
5000	10.3370	10.3453	10.8967	10.9160	11.4519	11.4848
10000	10.4444	10.4548	11.1097	11.1341	11.7687	11.8108
50000	10.6054	10.6190	11.4284	11.4612	12.2416	12.2993
100000	10.6084	10.6220	11.4341	11.4671	12.2501	12.3082

Table F-1: Deformed areas (mm^2) for the 1mm by 10mm longitudinal crack in HDPE

HDPE	Uniaxial		Biaxial	
Time (s)	N1	m	N1	m
0 (Elastic)	0.5648	1.878E-08	0.5659	1.912E-08
10	0.5648	1.880E-08	0.566	1.915E-08
100	0.5655	1.899E-08	0.5666	1.935E-08
1000	0.5714	2.086E-08	0.5727	2.126E-08
5000	0.5914	2.734E-08	0.5932	2.795E-08
10000	0.6066	3.248E-08	0.6088	3.326E-08
50000	0.6281	4.013E-08	0.6312	4.121E-08
100000	0.6285	4.026E-08	0.6316	4.135E-08

Table F-2: Gradients (m) and leakage exponents (N1) from the power law graphs for 1mm by 10mm longitudinal crack in HDPE

2. Variation of leak area with time

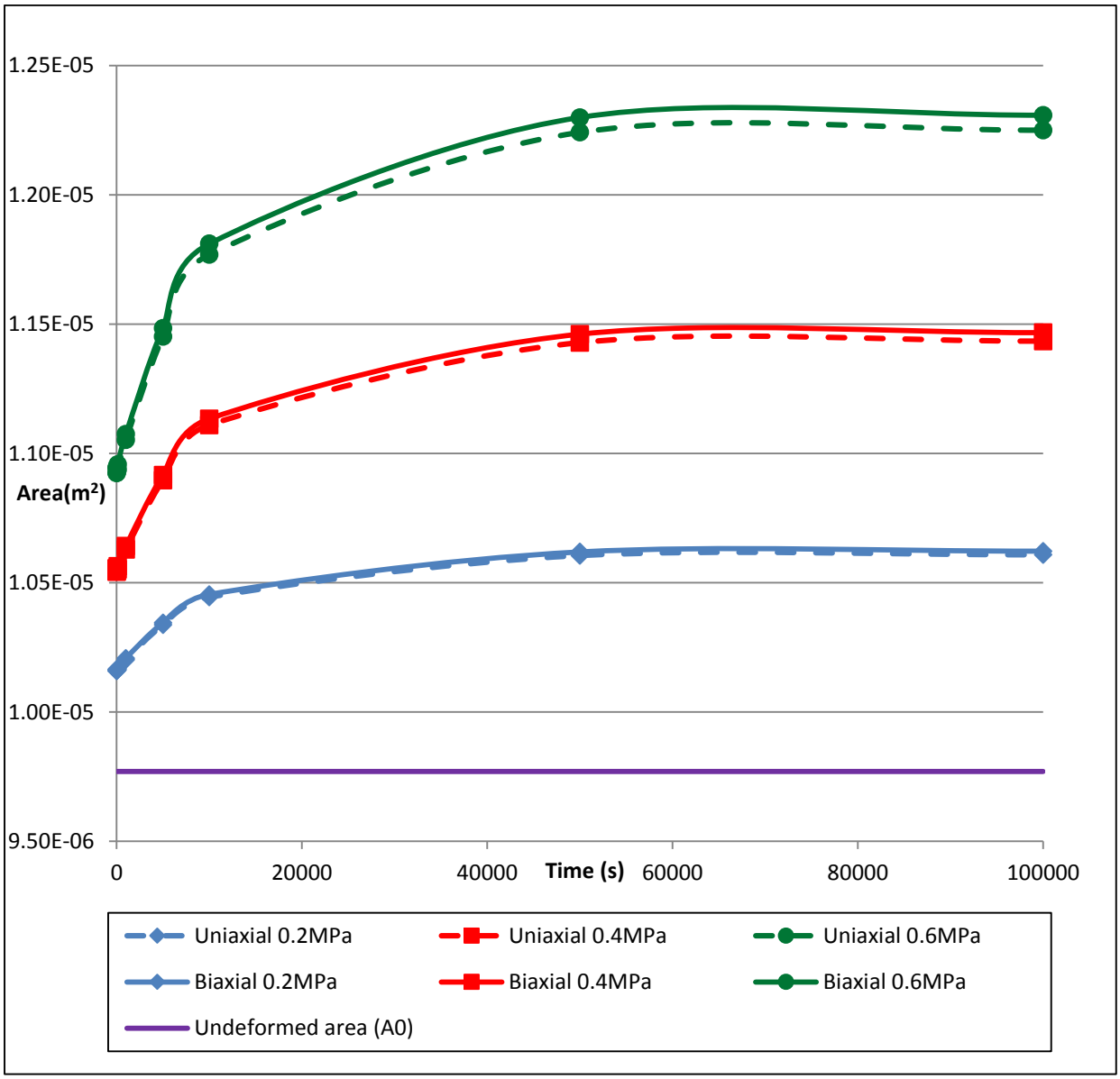

Figure F-1: Area against time for 1mm by 10mm longitudinal crack in HDPE

3. Variation of leak area with pressure

a) Uniaxial

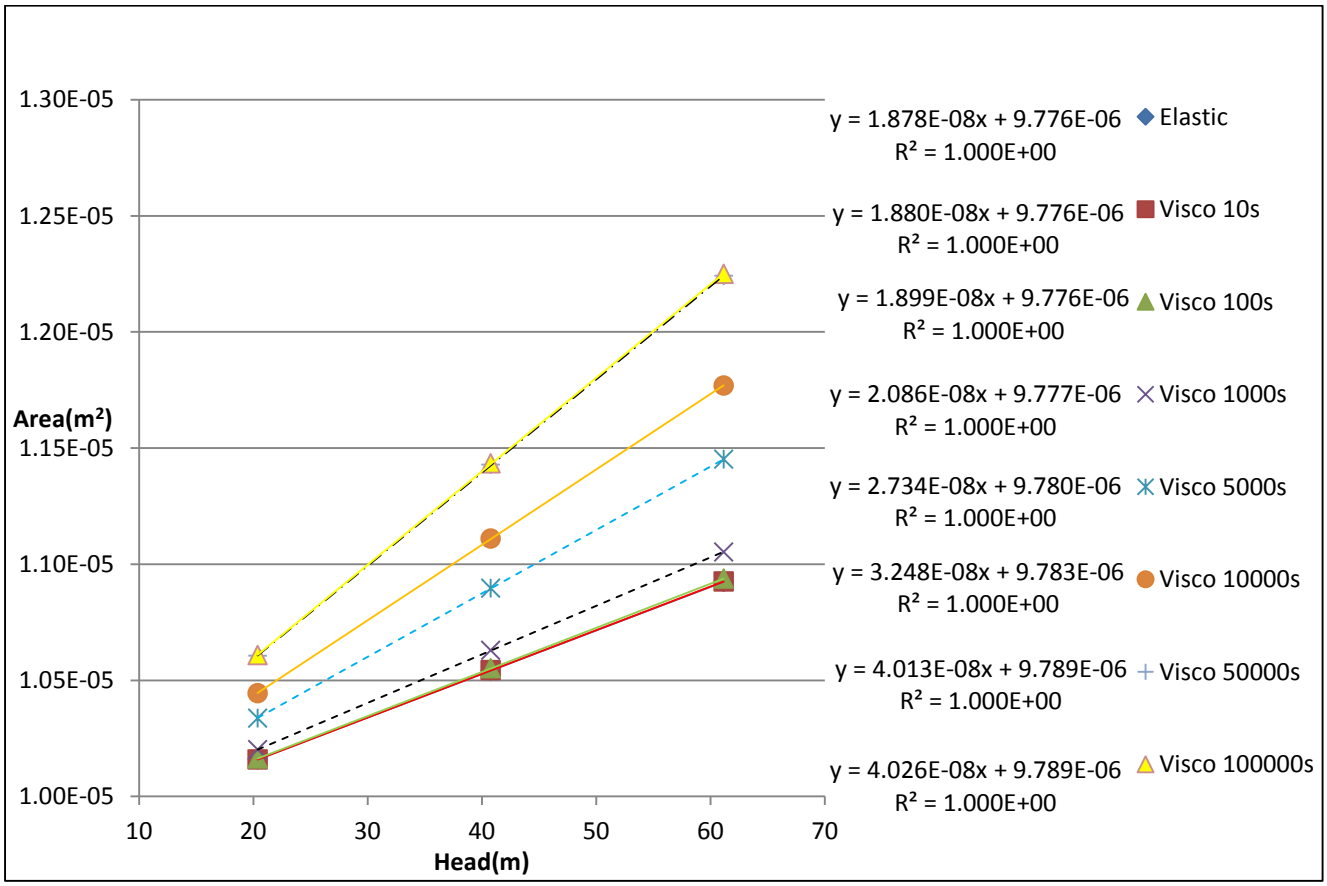

Figure F-2: Area against pressure head for 1mm by 10mm longitudinal crack in HDPE, uniaxial state

b) Biaxial

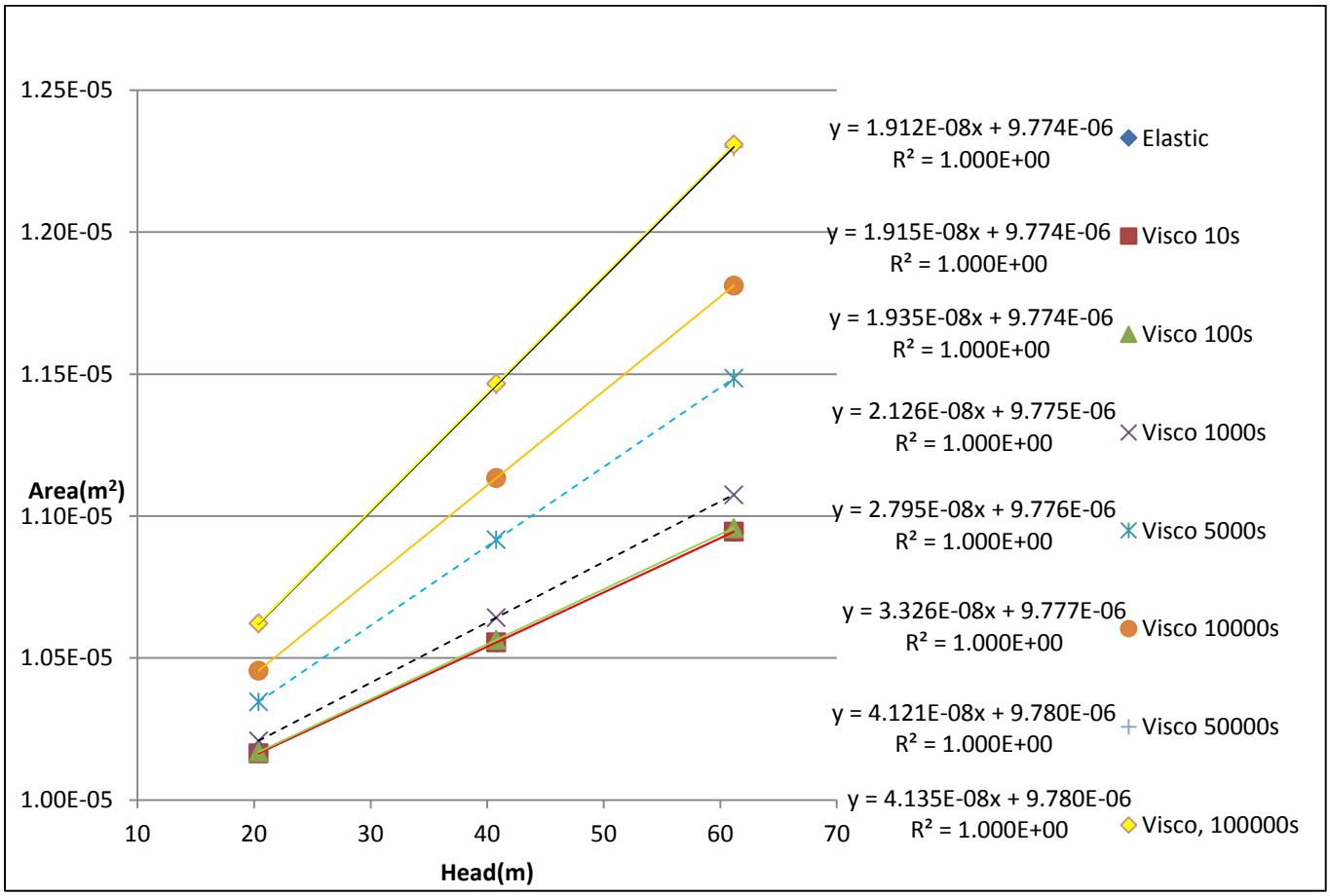

Figure F-3: Area against pressure head for 1mm by 10mm longitudinal crack in HDPE, biaxial state

4. Variation of leak discharge with time

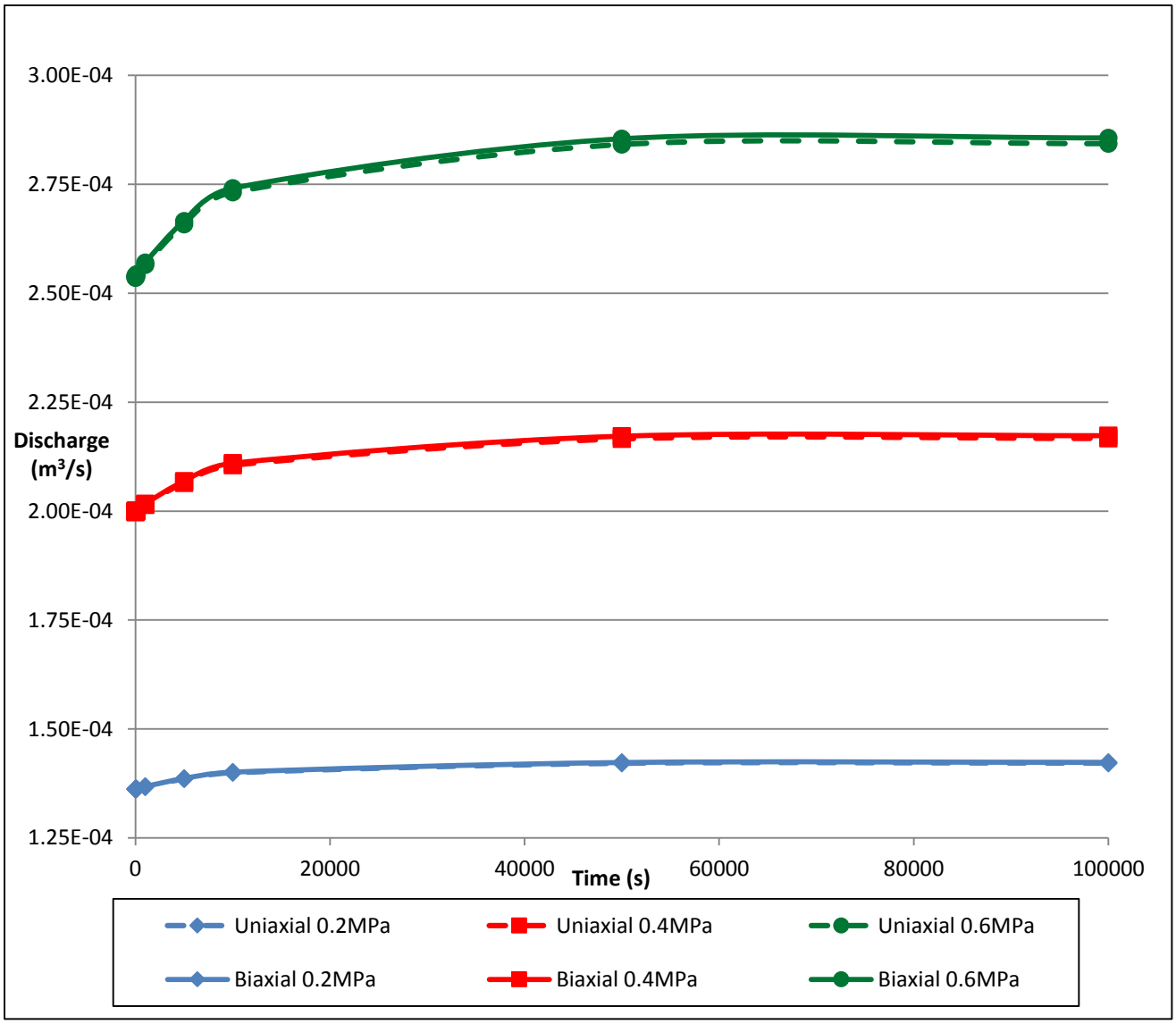

Figure F-4: Discharge against time for 1mm by 10mm longitudinal crack in HDPE

5. Variation of leak discharge with pressure

a) Uniaxial

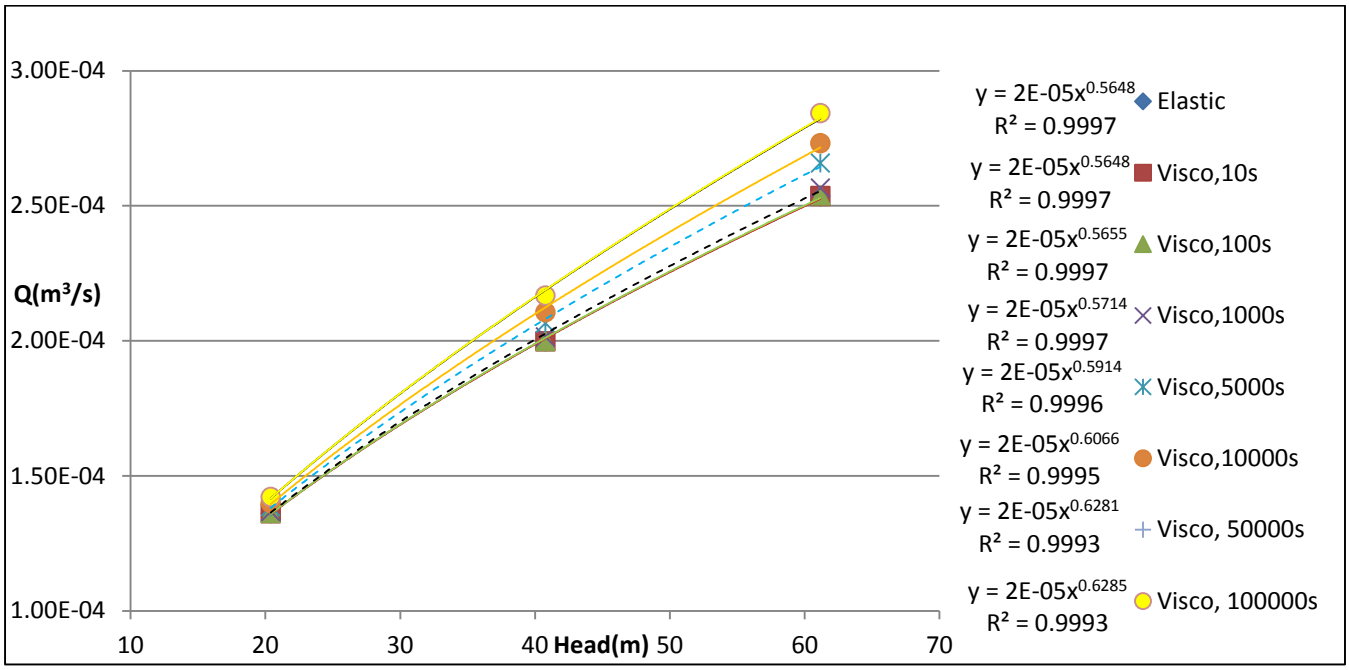

Figure F-5: Discharge against pressure head for 1mm by 10mm longitudinal crack in HDPE, uniaxial

b) Biaxial

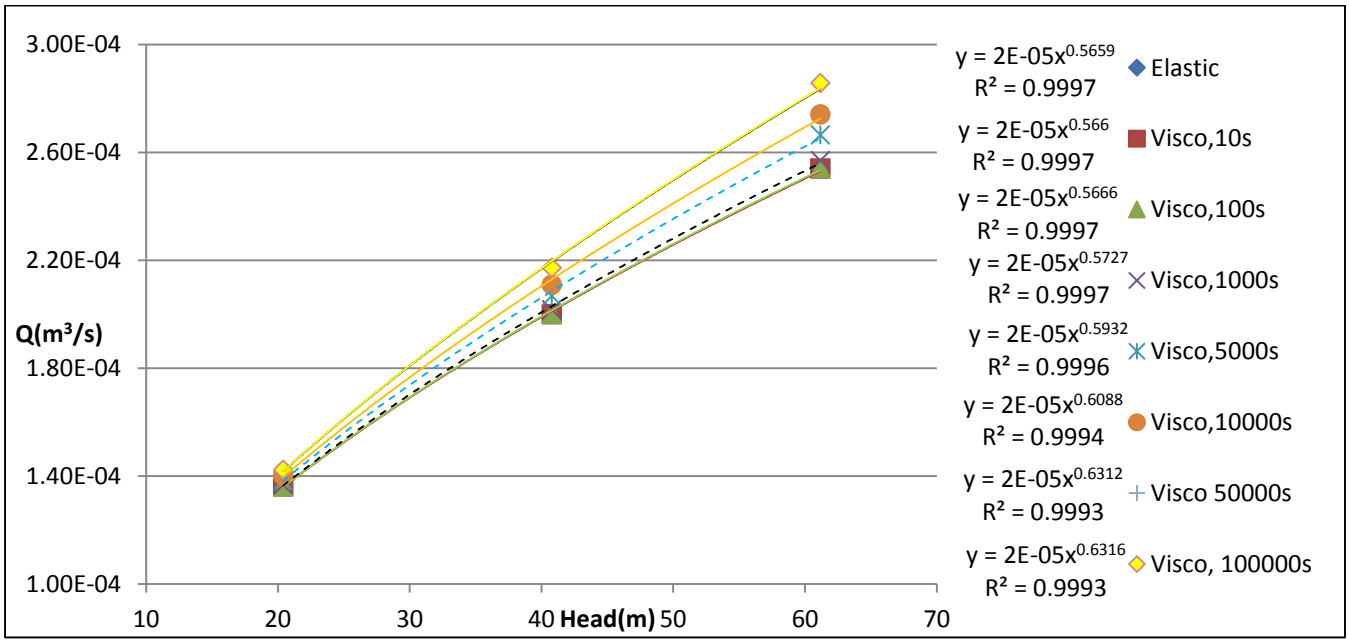

Figure F-6: Discharge against pressure head for 1mm by 10mm longitudinal crack in HDPE, biaxial

6. Gradient (m) and leakage exponent (N1)

a) Gradient (m) against time

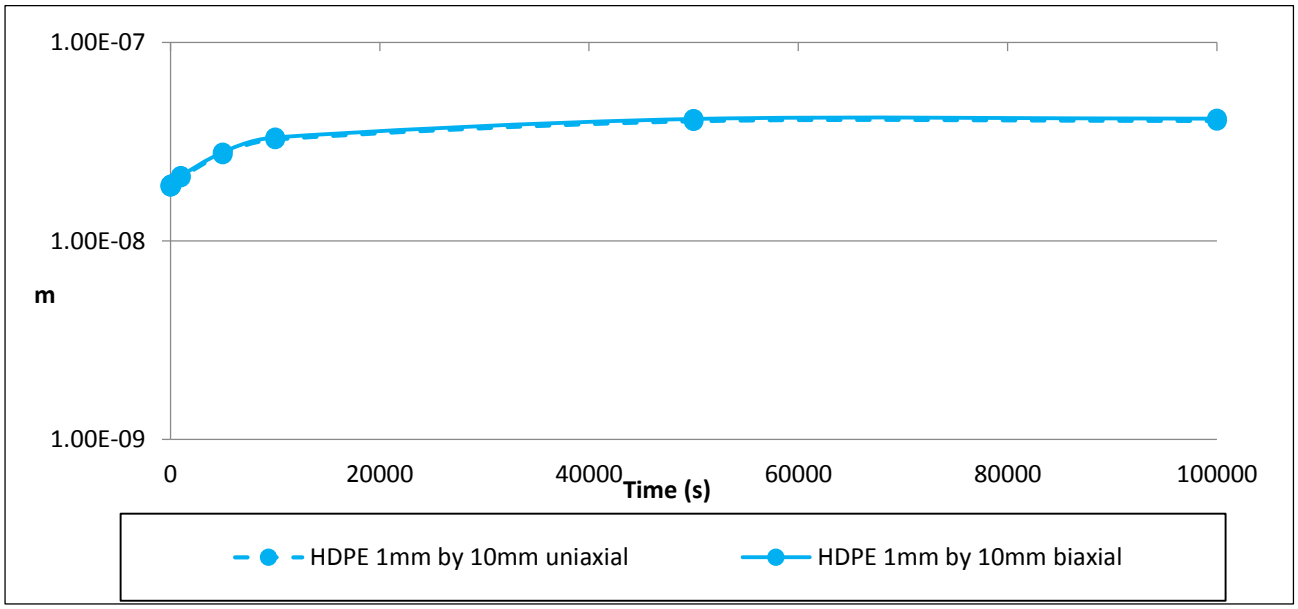

Figure F-7: Gradient (m) against time for 1mm by 10mm longitudinal crack in HDPE

b) Leakage exponent (N1) against time

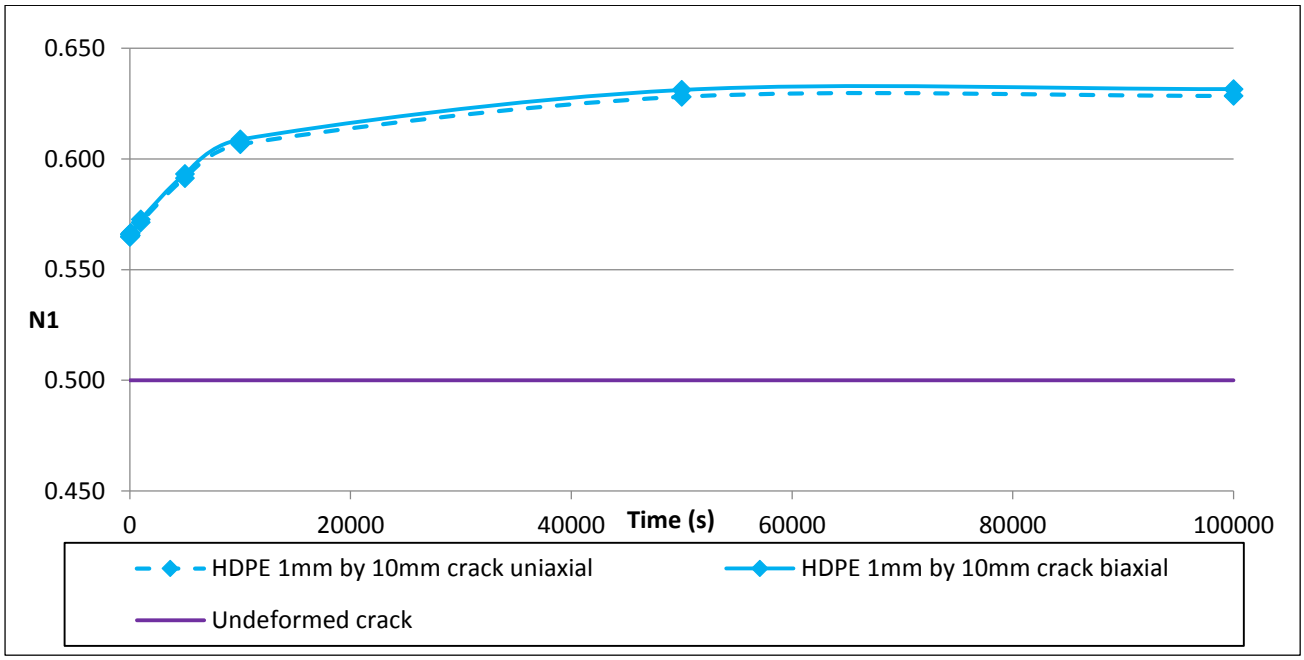

Figure F-8: Leakage exponent (N1) against time for 1mm by 10mm longitudinal crack in HDPE

7. Percentage change in area with pressure

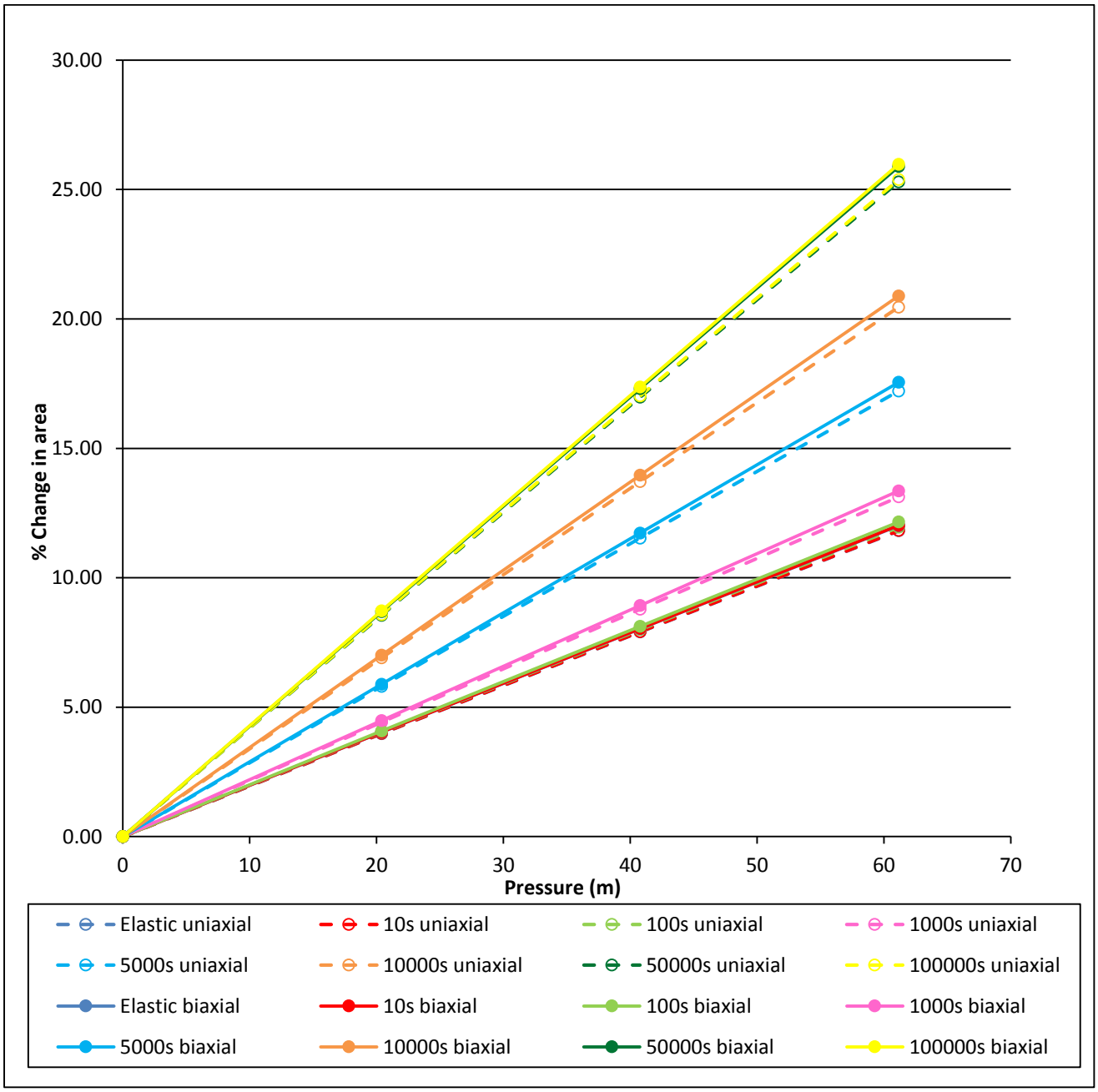

Figure F-9: Percentage change in area against pressure head for 1mm by 10mm longitudinal crack in HDPE

8. Ratio of total change in area to elastic change in area

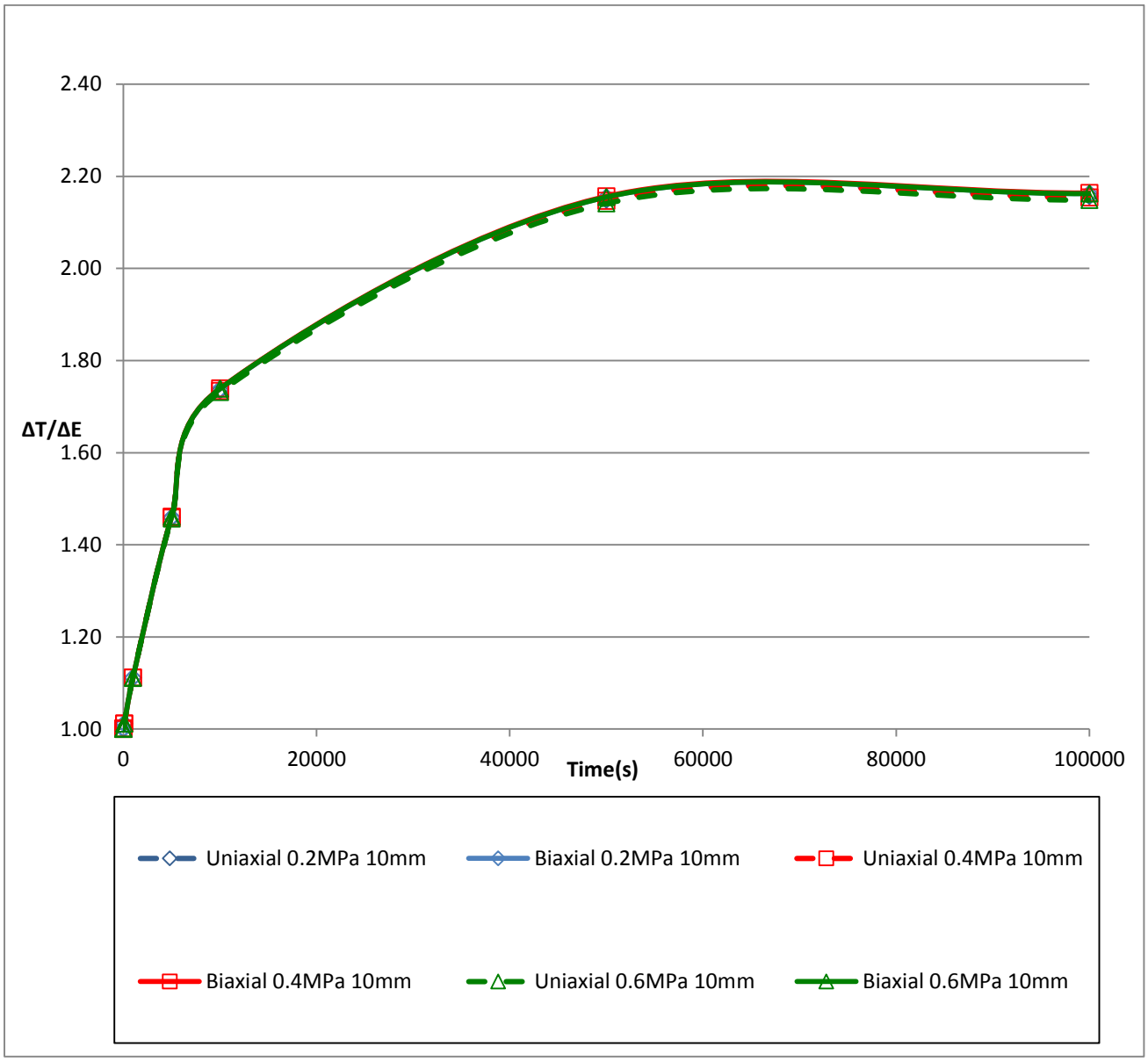

Figure F-10: ΔT/ΔE against time for 1mm by 10mm longitudinal crack in HDPE

9. Cyclic results

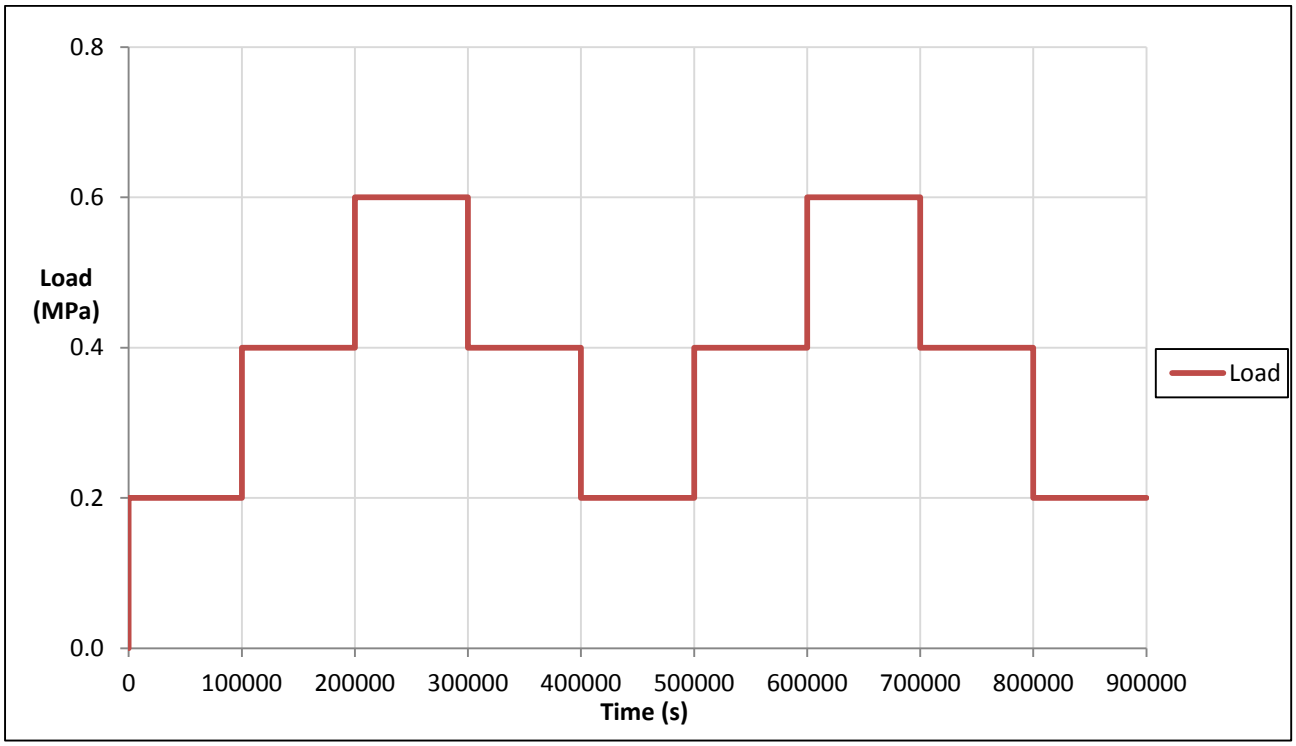

Figure F-11: Cyclic loading for 1mm by 10mm longitudinal crack in HDPE

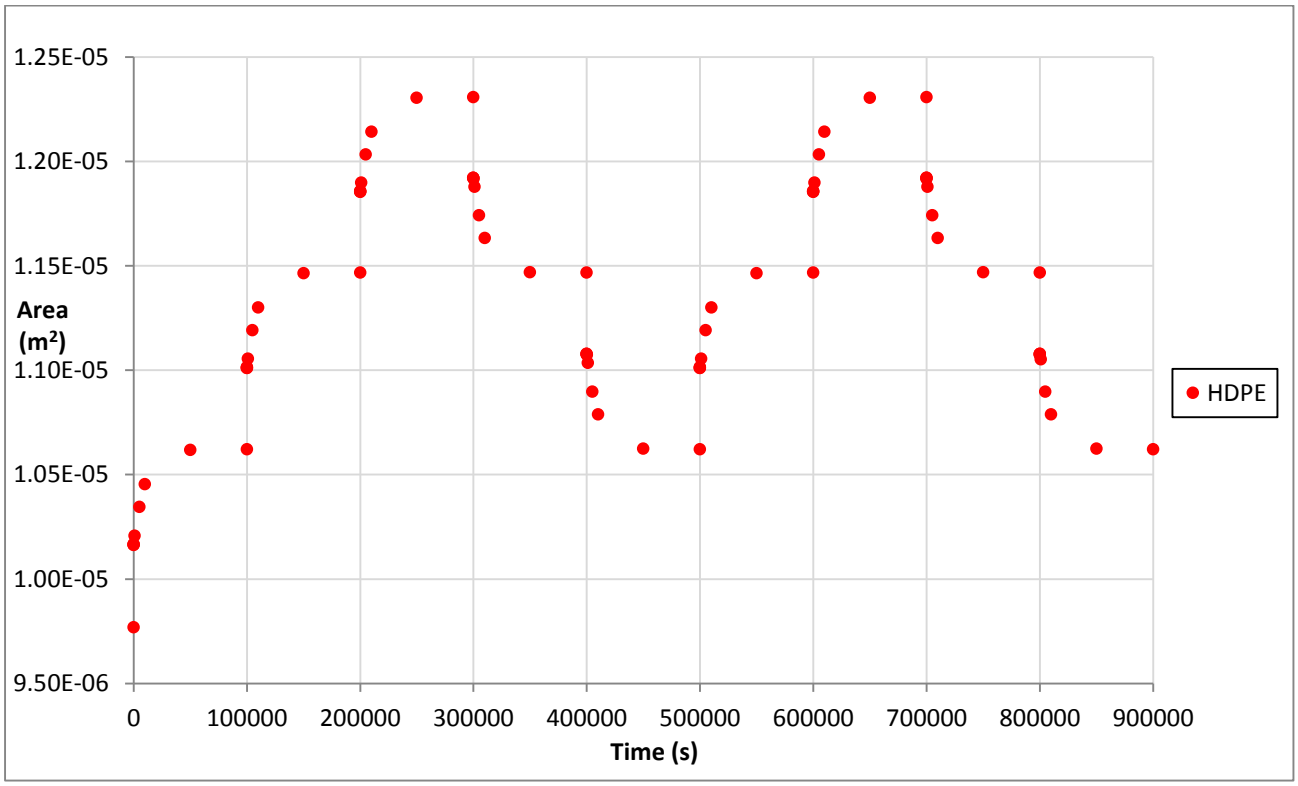

Figure F-12: Deformed area against time for 1mm by 10mm longitudinal crack in HDPE during cyclic loading, biaxial state

10. Leakage number, calculated leak exponents, m/A_0 and m/m_E

a) Uniaxial

Time (s)	N1 from power law	m	L_N	N1	m/A_0	m/m_E
			Pressure = 0.4MPa	Pressure = 0.4MPa		
0	0.5648	1.88E-08	0.0784	0.5727	0.00192	1.0000
10	0.5648	1.88E-08	0.0785	0.5728	0.00192	1.0011
100	0.5655	1.90E-08	0.0793	0.5734	0.00194	1.0112
1000	0.5714	2.09E-08	0.0871	0.5801	0.00214	1.1108
5000	0.5914	2.73E-08	0.1141	0.6024	0.00280	1.4558
10000	0.6066	3.25E-08	0.1356	0.6194	0.00332	1.7295
50000	0.6281	4.01E-08	0.1675	0.6435	0.00411	2.1368
100000	0.6285	4.03E-08	0.1680	0.6439	0.00412	2.1438

Table F-3: Leakage numbers, calculated leak exponents, m/A_0 and m/m_E for the 1mm by 10mm crack in HDPE, uniaxial

b) Biaxial

Time (s)	N1 from power law	m	L_N	N1	m/A_0	m/m_E
			Pressure = 0.4MPa	Pressure = 0.4MPa		
0	0.5659	1.91E-08	0.0798	0.5739	0.00196	1.0000
10	0.566	1.92E-08	0.0799	0.5740	0.00196	1.0016
100	0.5666	1.94E-08	0.0808	0.5747	0.00198	1.0120
1000	0.5727	2.13E-08	0.0887	0.5815	0.00218	1.1119
5000	0.5932	2.80E-08	0.1166	0.6045	0.00286	1.4618
10000	0.6088	3.33E-08	0.1388	0.6219	0.00340	1.7395
50000	0.6312	4.12E-08	0.1720	0.6467	0.00422	2.1553
100000	0.6316	4.14E-08	0.1726	0.6472	0.00423	2.1627

Table F-4: Leakage numbers, calculated leak exponents, m/A_0 and m/m_E for the 1mm by 10mm crack in HDPE, biaxial

11. Change in deformation

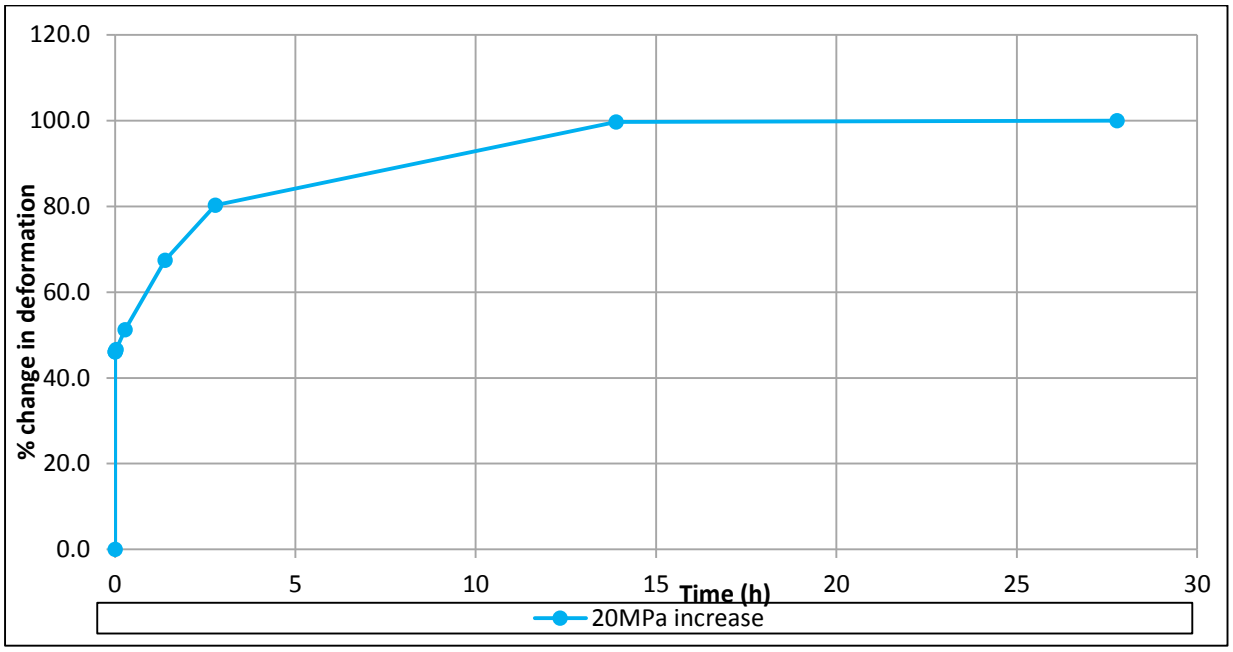

Figure F-13: Percentage change in deformation against time for a 20MPa increase in pressure, 1mm by 10mm crack in HDPE, biaxial

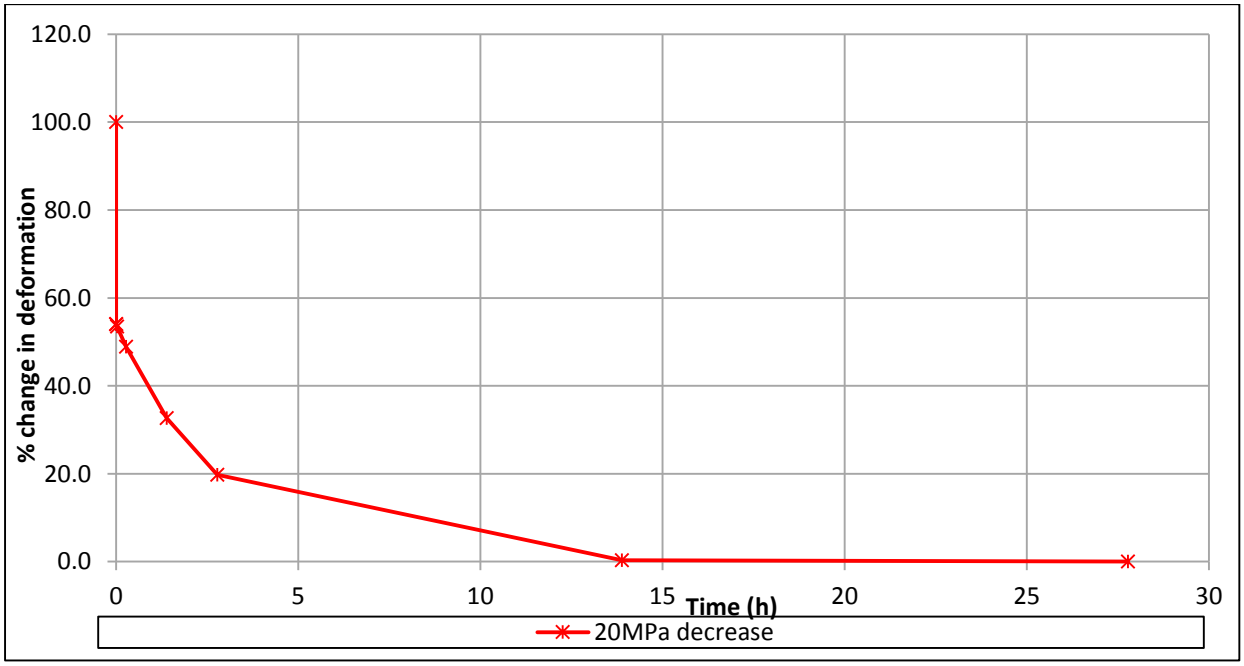

Figure F-14: Percentage change in deformation against time for a 20MPa decrease in pressure, 1mm by 10mm crack in HDPE, biaxial

G 1mm by 10mm longitudinal crack in PVC

12. Summary results for area, gradient (m) and leakage exponent (N1)

PVC	Area of deformed cracks with A_0 = 9.77mm^2					
Pressure (MPa)	0.2		0.4		0.6	
Time (s)	Uniaxial	Biaxial	Uniaxial	Biaxial	Uniaxial	Biaxial
0 (Elastic)	9.9401	9.9422	10.1070	10.1113	10.2734	10.2802
10	9.9402	9.9423	10.1072	10.1115	10.2737	10.2805
100	9.9410	9.9431	10.1088	10.1131	10.2762	10.2830
1000	9.9484	9.9506	10.1236	10.1281	10.2982	10.3054
5000	9.9676	9.9700	10.1618	10.1669	10.3554	10.3636
10000	9.9761	9.9787	10.1788	10.1842	10.3808	10.3894
50000	9.9799	9.9825	10.1864	10.1919	10.3922	10.4010
100000	9.9799	9.9825	10.1864	10.1919	10.3922	10.4010

Table G-1: Deformed areas for 1mm by 10mm longitudinal crack in PVC

PVC	Uniaxial		Biaxial	
Time (s)	N1	m	N1	m
0 (Elastic)	0.5294	8.174E-09	0.5298	8.289E-09
10	0.5294	8.179E-09	0.5298	8.294E-09
100	0.5295	8.221E-09	0.5299	8.336E-09
1000	0.5308	8.579E-09	0.5312	8.701E-09
5000	0.5340	9.511E-09	0.5345	9.653E-09
10000	0.5354	9.925E-09	0.5359	1.007E-08
50000	0.5361	1.011E-08	0.5366	1.026E-08
100000	0.5361	1.011E-08	0.5366	1.026E-08

Table G-2: Gradients (m) and leakage exponents (N1) from the power law graphs for 1mm by 10mm longitudinal crack in PVC

13. Variation of leak area with time

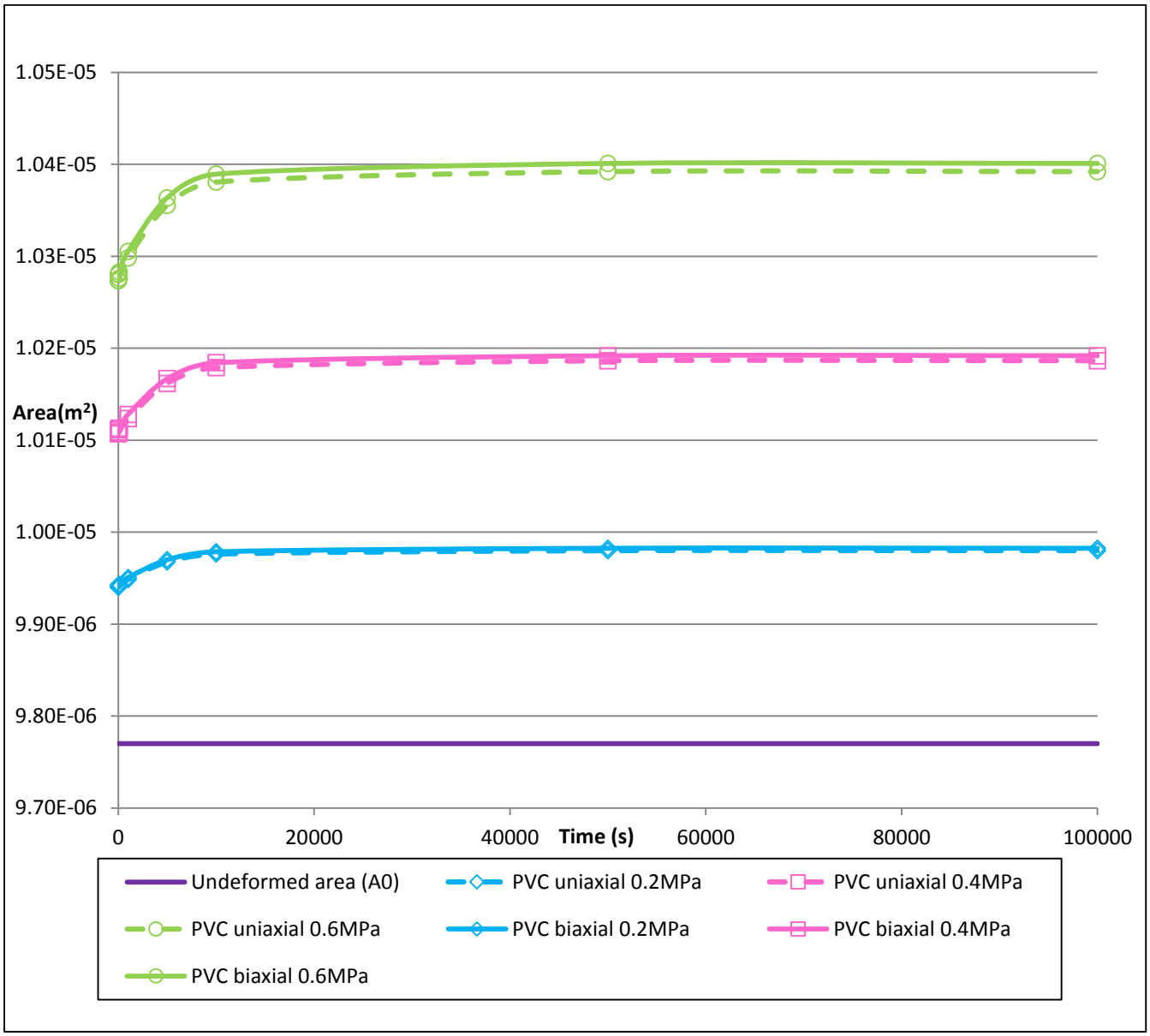

Figure G-1: Area against time for 1mm by 10mm longitudinal crack in PVC

14. Variation of leak area with pressure

a) Uniaxial

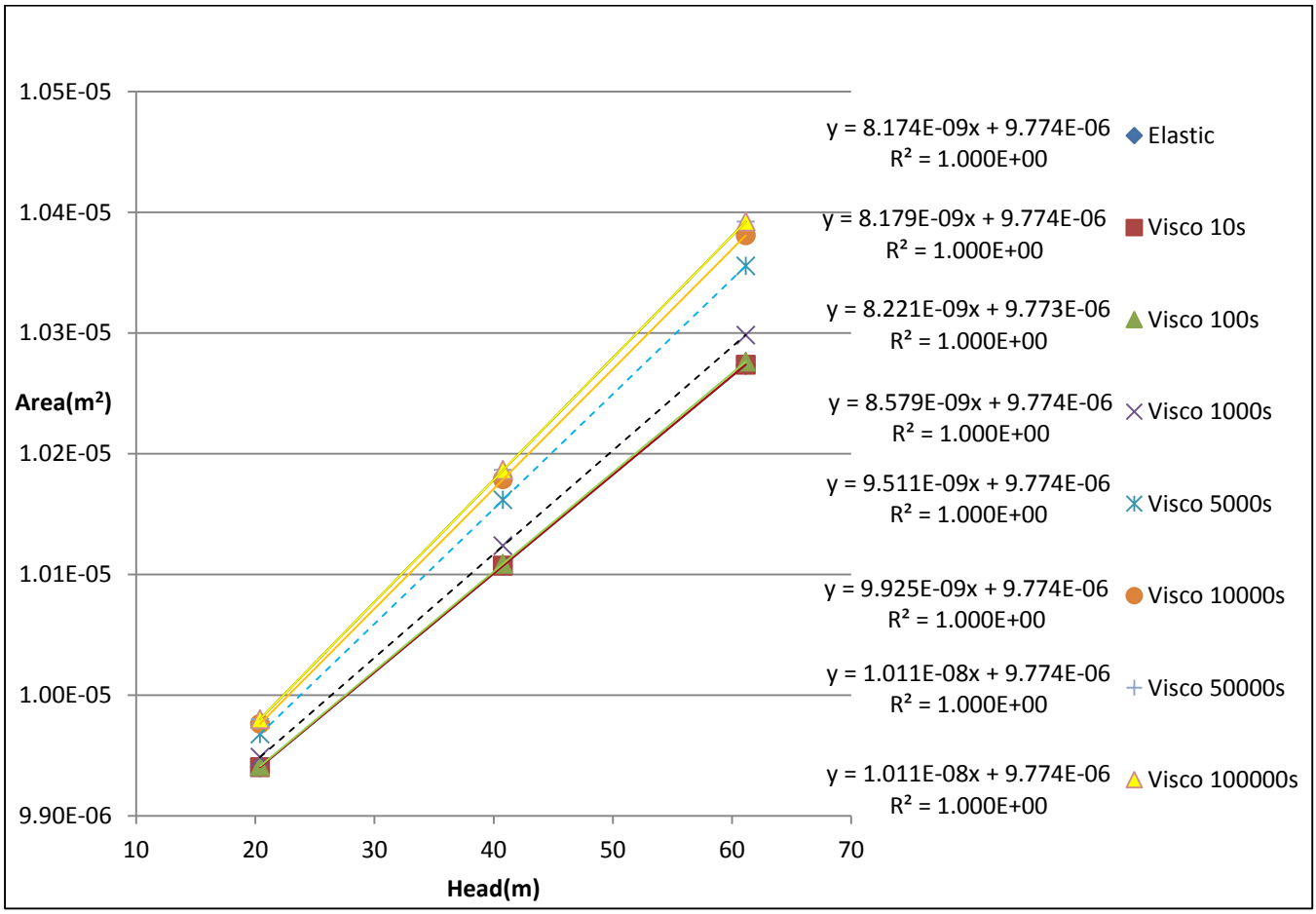

Figure G-2: Area against pressure head for 1mm by 10mm longitudinal crack in PVC, uniaxial

b) Biaxial

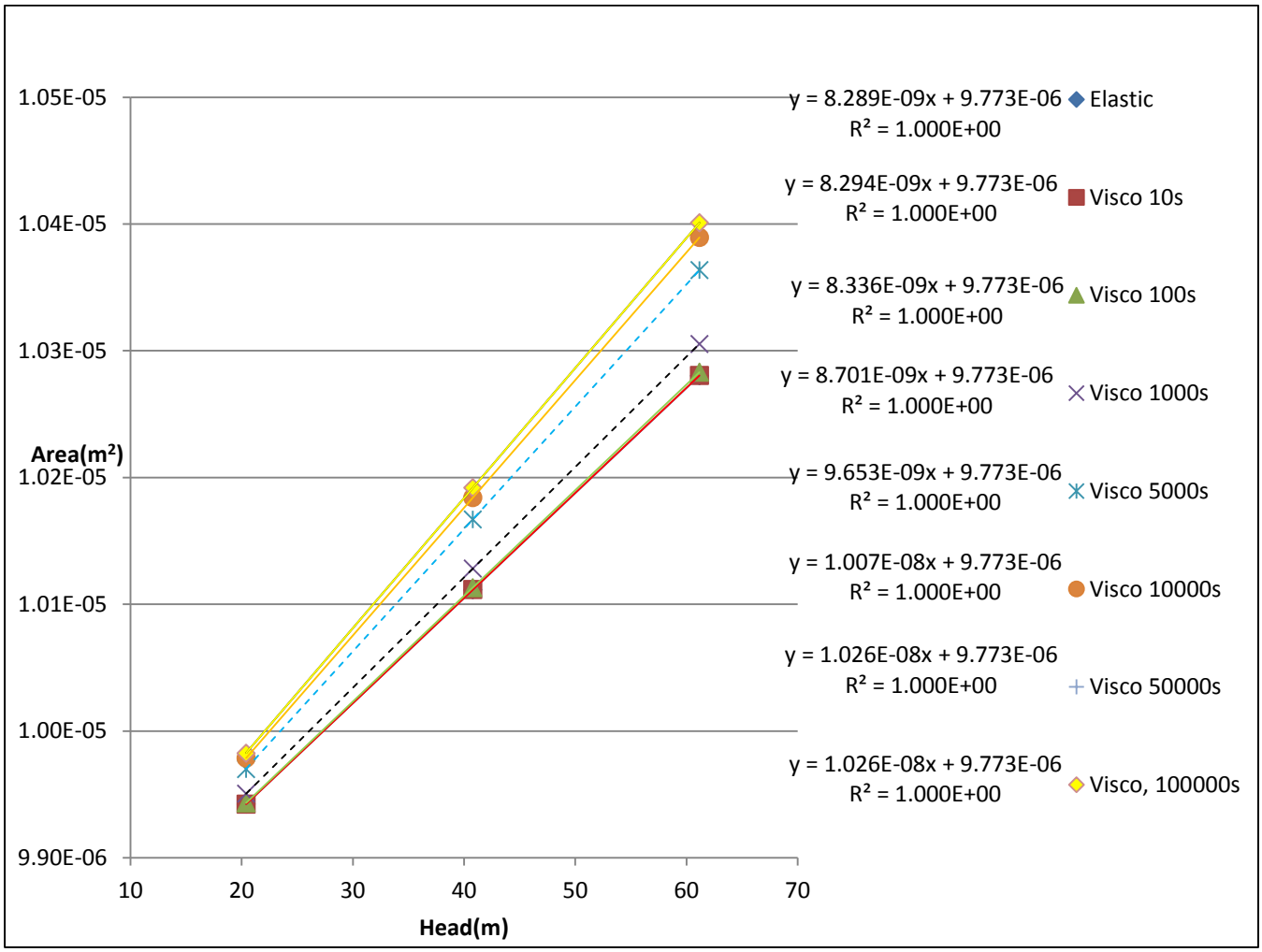

Figure G-3: Area against head for 1mm by 10mm longitudinal crack in PVC, biaxial

15. Variation of leak discharge with time

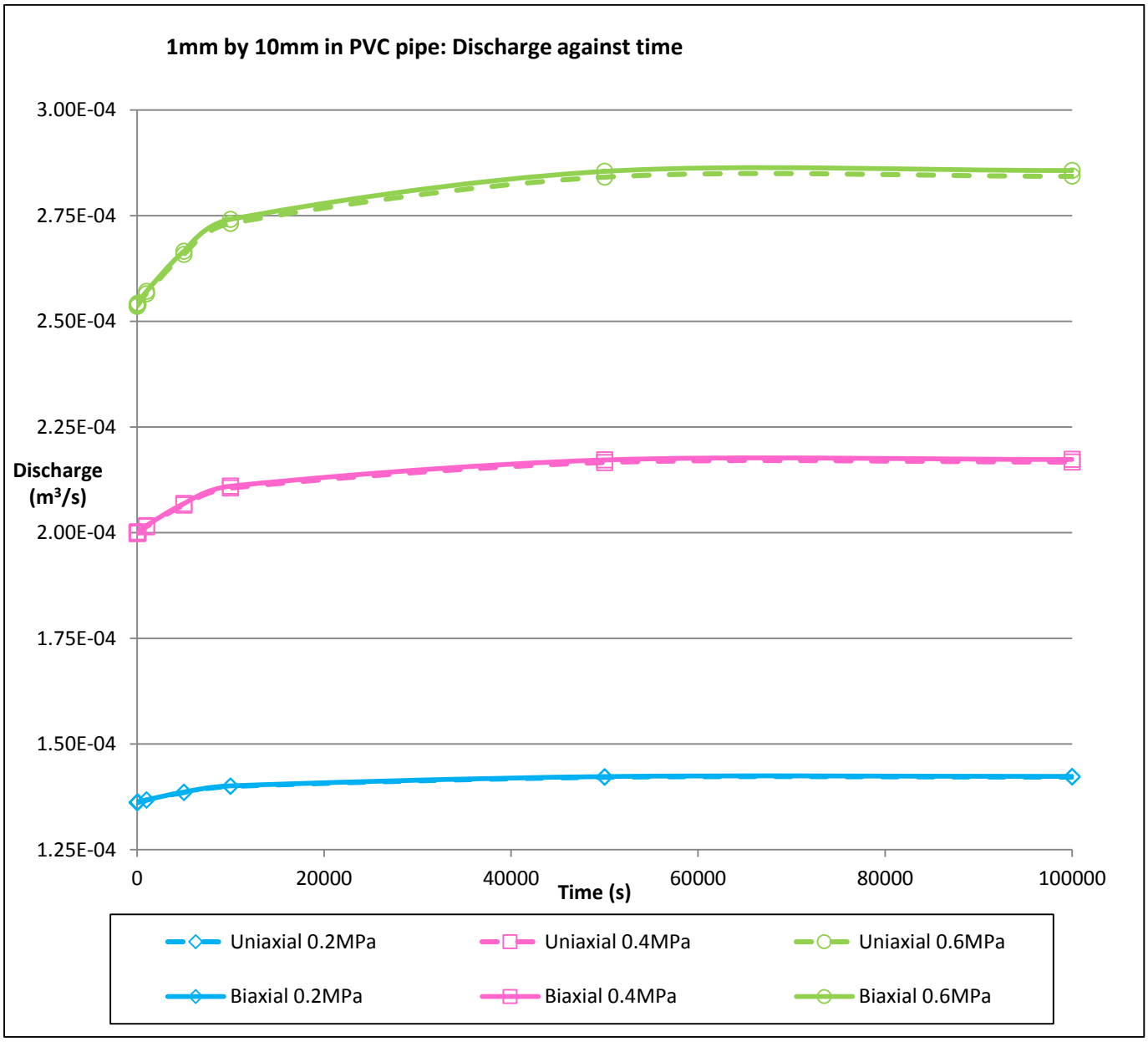

Figure G-4: Discharge against time for 1mm by 10mm longitudinal crack in PVC

16. Variation of leak discharge with pressure

a) Uniaxial

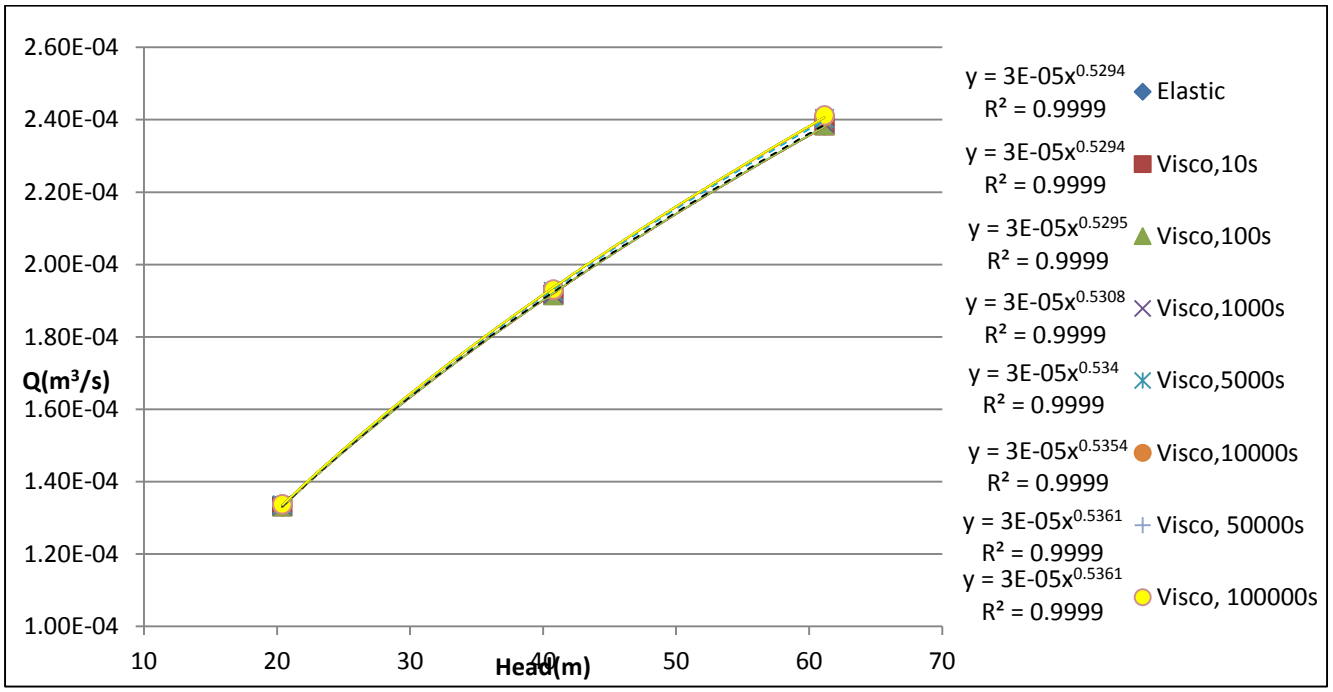

Figure G-5: Discharge against pressure head for 1mm by 10mm longitudinal crack in PVC, uniaxial

b) Biaxial

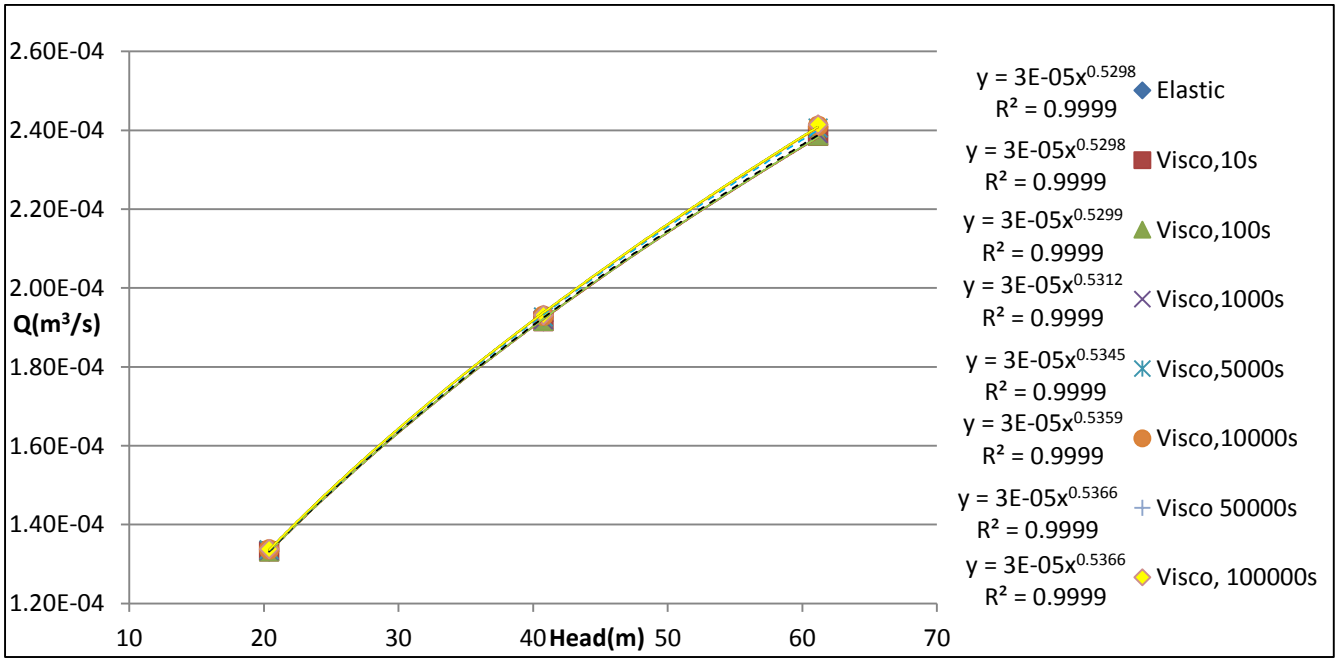

Figure G-6: Discharge against pressure head for 1mm by 10mm longitudinal crack in PVC, biaxial

17. Gradient (m) and leakage exponent (N1)

a) Gradient (m) against time

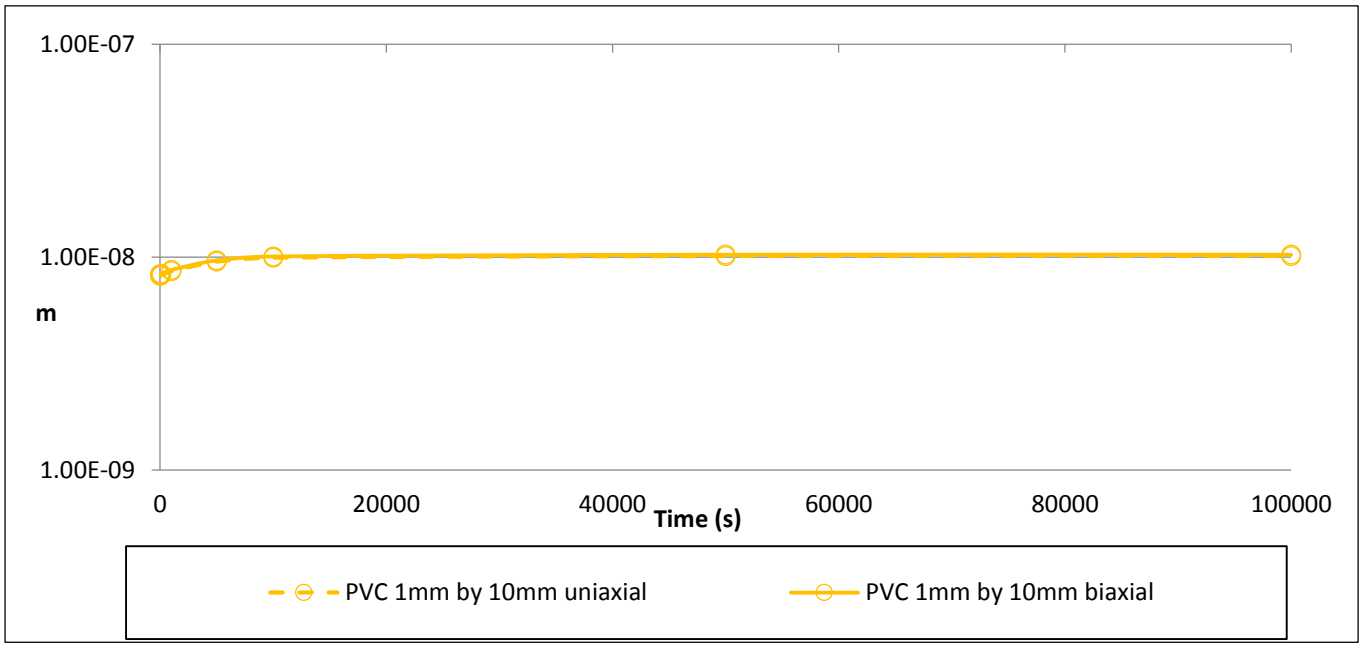

Figure G-7: Gradient (m) against time for 1mm by 10mm longitudinal crack in PVC

b) Leakage exponent (N1) against time

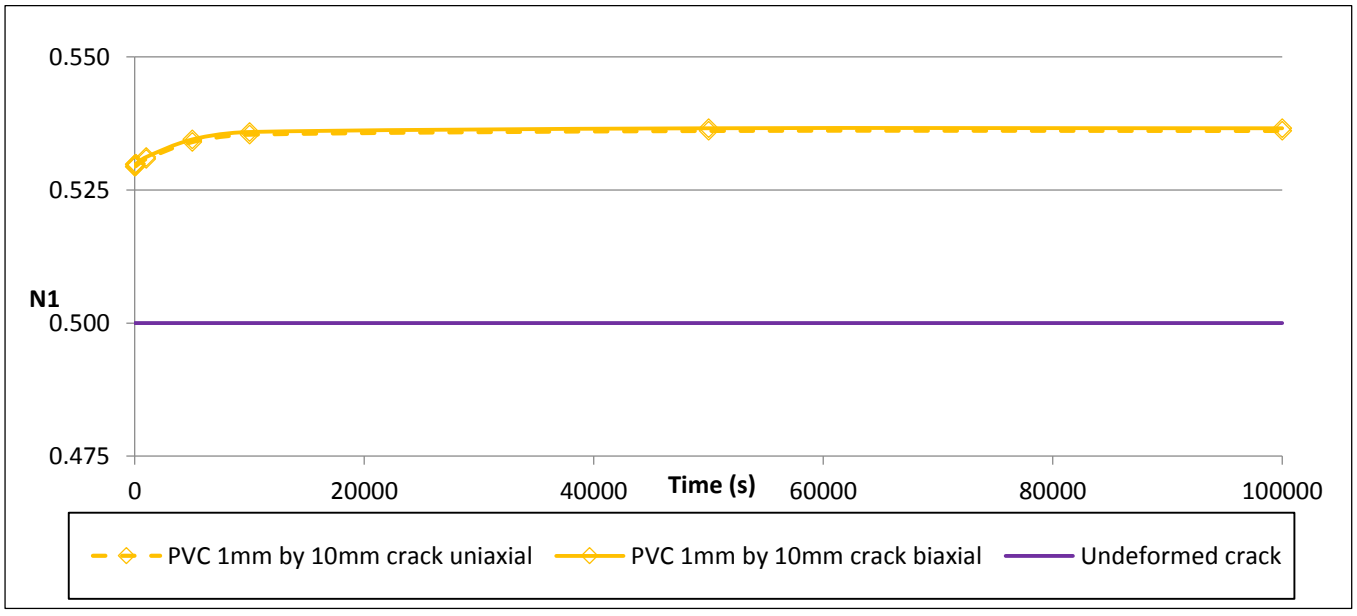

Figure G-8: Leakage exponent (N1) against time for 1mm by 10mm longitudinal crack in PVC

18. Percentage change in area with pressure

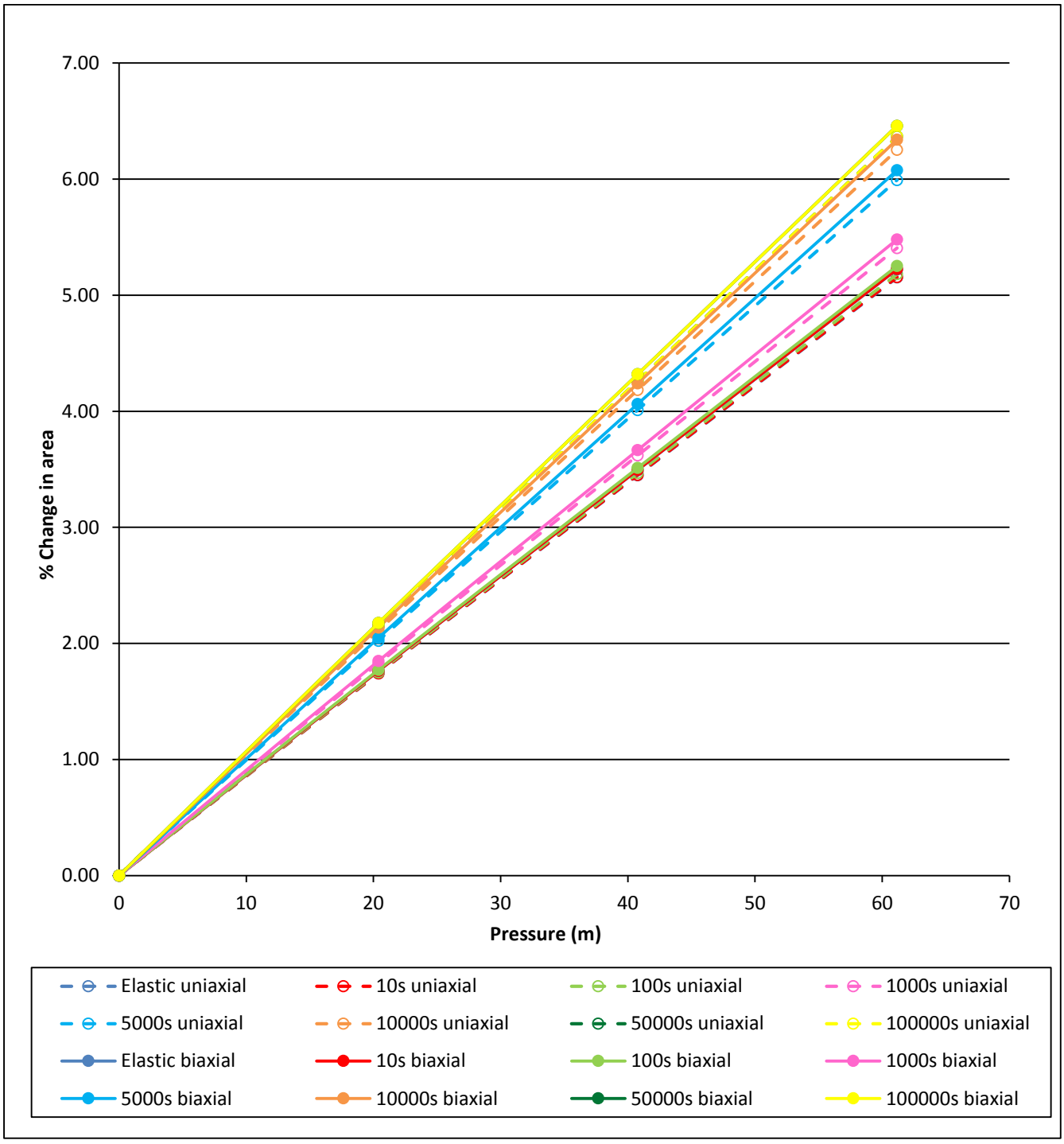

Figure G-9: Percentage change in area against pressure for 1mm by 10mm longitudinal crack in PVC

19. Ratio of total change in area to elastic change in area

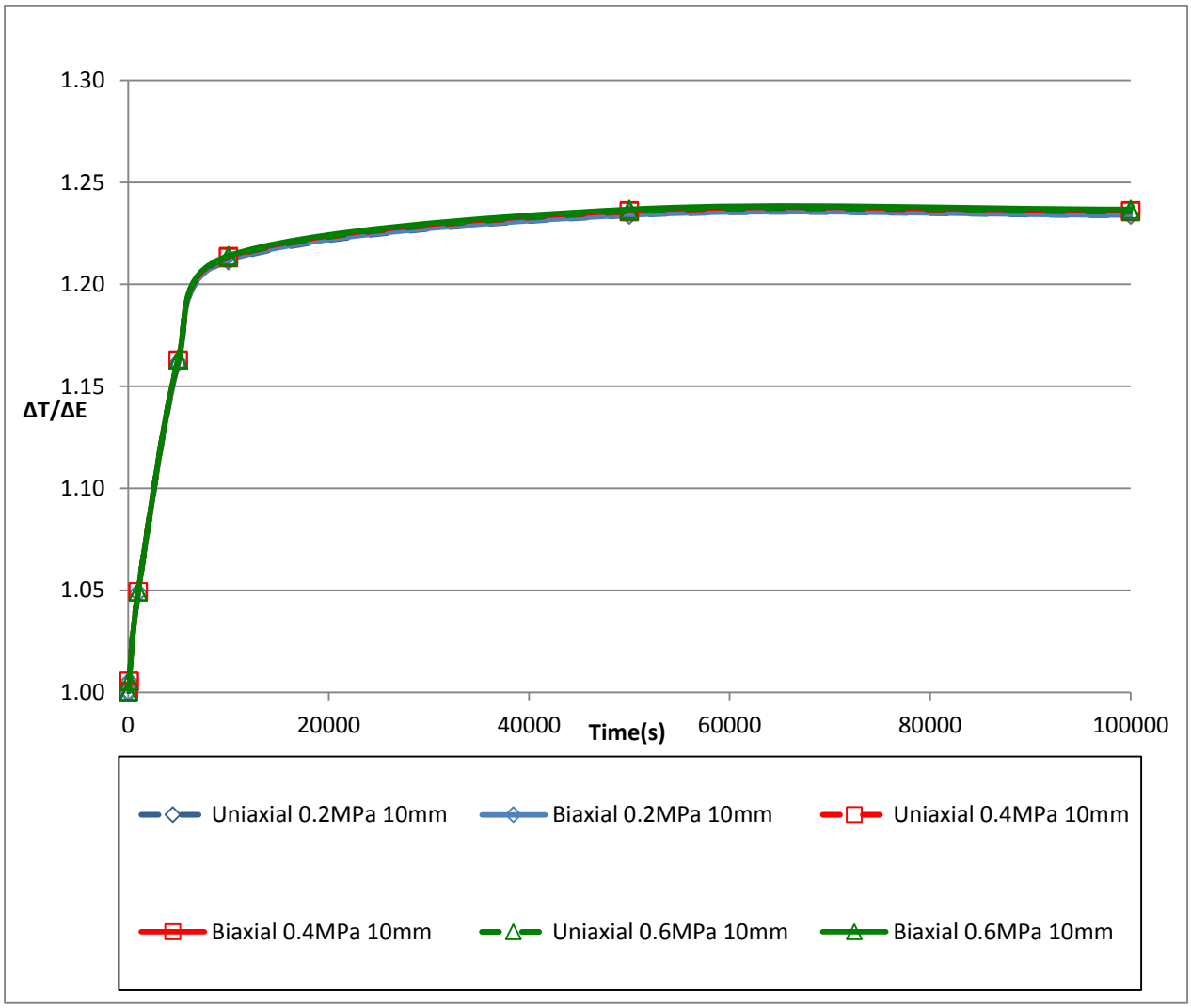

Figure G-10: ΔT/ΔE against time for 1mm by 10mm longitudinal crack in PVC

20. Cyclic results

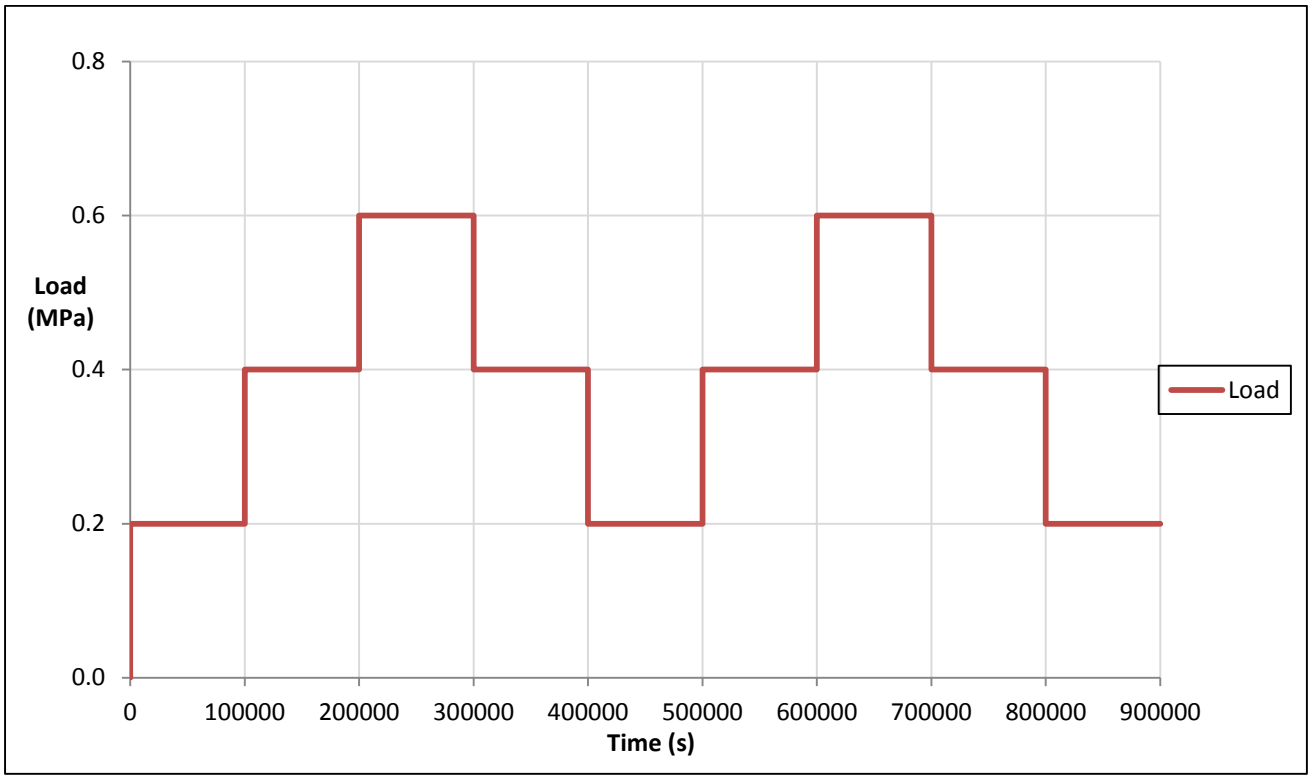

Figure G-11: Cyclic loading for a 1mm by 10mm longitudinal crack in PVC

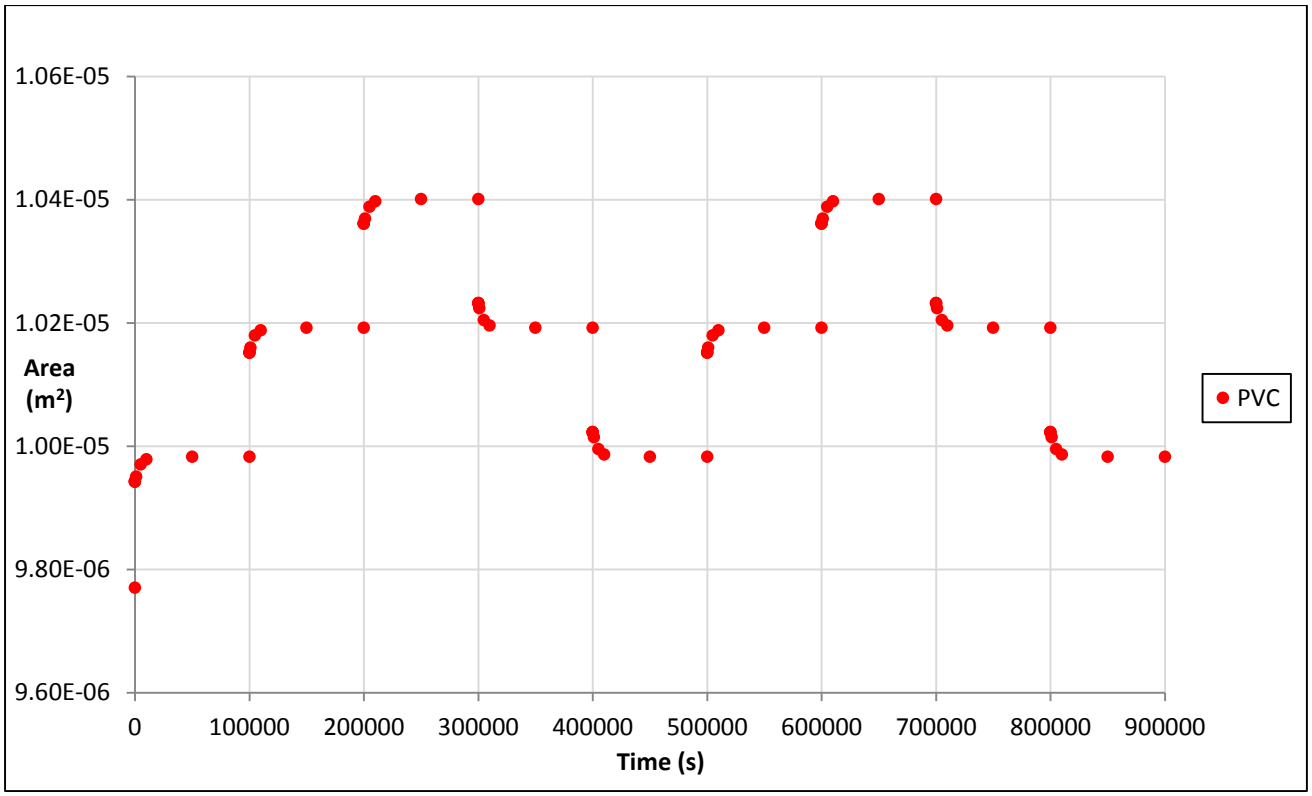

Figure G-12: Deformed area against time for a 1mm by 10mm longitudinal crack in PVC during cyclic loading

21. Leakage number, calculated leak exponents, m/A_0 and m/m_E

a) Uniaxial

Time (s)	N1 from power law	m	L_N	N1	m/A_0	m/m_E
			Pressure = 0.4MPa	**Pressure = 0.4MPa**		
0	0.5294	8.17E-09	0.0341	0.5330	0.00084	1.0000
10	0.5294	8.18E-09	0.0341	0.5330	0.00084	1.0006
100	0.5295	8.22E-09	0.0343	0.5332	0.00084	1.0057
1000	0.5308	8.58E-09	0.0358	0.5346	0.00088	1.0495
5000	0.534	9.51E-09	0.0397	0.5382	0.00097	1.1636
10000	0.5354	9.93E-09	0.0414	0.5398	0.00102	1.2142
50000	0.5361	1.01E-08	0.0422	0.5405	0.00103	1.2368
100000	0.5361	1.01E-08	0.0422	0.5405	0.00103	1.2368

Table G-3: Leakage numbers, calculated leak exponents, m/A_0 and m/m_E for the 1mm by 10mm crack in PVC, uniaxial

b) Biaxial

Time (s)	N1 from power law	m	L_N	N1	m/A_0	m/m_E
			Pressure = 0.4MPa	**Pressure = 0.4MPa**		
0	0.5298	8.29E-09	0.0346	0.5334	0.00085	1.0000
10	0.5298	8.29E-09	0.0346	0.5335	0.00085	1.0006
100	0.5299	8.34E-09	0.0348	0.5336	0.00085	1.0057
1000	0.5312	8.70E-09	0.0363	0.5350	0.00089	1.0497
5000	0.5345	9.65E-09	0.0403	0.5387	0.00099	1.1646
10000	0.5359	1.01E-08	0.0420	0.5403	0.00103	1.2149
50000	0.5366	1.03E-08	0.0428	0.5411	0.00105	1.2378
100000	0.5366	1.03E-08	0.0428	0.5411	0.00105	1.2378

Table G-4: Leakage numbers, calculated leak exponents, m/A_0 and m/m_E for the 1mm by 10mm crack in PVC, biaxial

22. Change in deformation

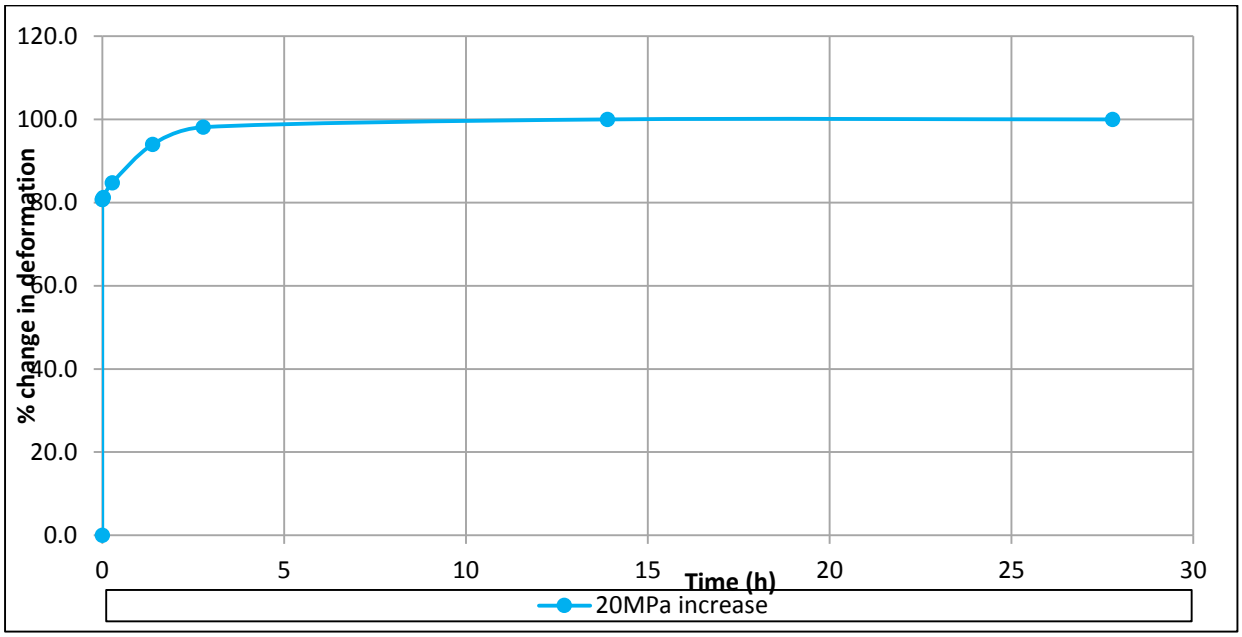

Figure G-13: Percentage change in deformation against time for a 20MPa increase in pressure, 1mm by 10mm crack in PVC, biaxial

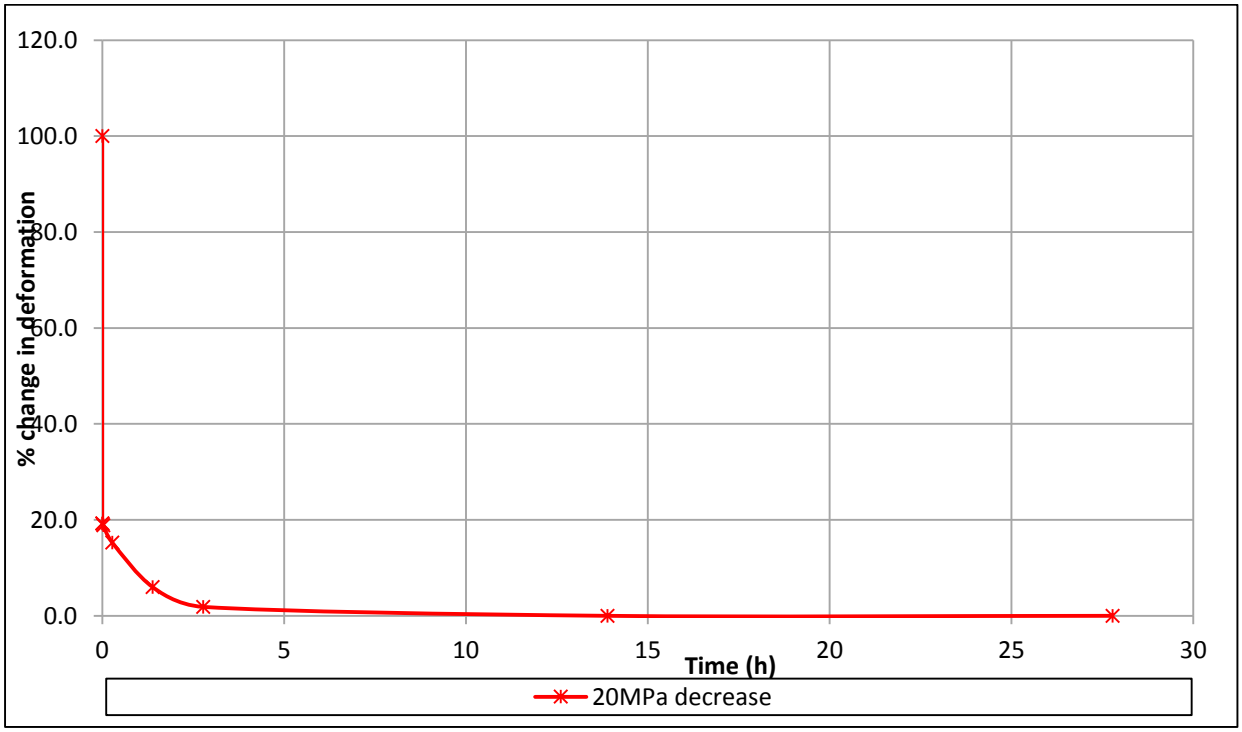

Figure G-14: Percentage change in deformation against time for a 20MPa decrease in pressure, 1mm by 10mm crack in PVC, biaxial

H 1mm by 40mm longitudinal crack in HDPE

1. Summary results for area, gradient (m) and leakage exponent (N1)

HDPE	Area of deformed cracks with A_0 = 39.785mm^2					
Pressure (MPa)	0.2		0.4		0.6	
Time (s)	Uniaxial	Biaxial	Uniaxial	Biaxial	Uniaxial	Biaxial
0 (Elastic)	50.9974	50.9941	62.0549	62.0779	72.9575	73.0365
10	51.0104	51.0070	62.0804	62.1035	72.9951	73.0744
100	51.1260	51.1228	62.3085	62.3324	73.3323	73.4139
1000	52.2259	52.2241	64.4752	64.5084	76.5330	76.6380
5000	56.0556	56.0612	71.9950	72.0701	87.6032	87.8116
10000	59.0949	59.1090	77.9349	78.0540	96.3050	96.6198
50000	63.6398	63.6713	86.7707	86.9738	109.1772	109.6923
100000	63.7226	63.7545	86.9309	87.1359	109.4098	109.9290

Table H-1: Deformed areas (mm^2) for 1mm by 40mm longitudinal crack in HDPE

HDPE	Uniaxial		Biaxial	
Time (s)	N1	m	N1	m
0 (Elastic)	0.8213	5.386E-07	0.8223	5.406E-07
10	0.8216	5.392E-07	0.8226	5.412E-07
100	0.8237	5.446E-07	0.8247	5.467E-07
1000	0.8431	5.961E-07	0.8443	5.988E-07
5000	0.9015	7.737E-07	0.9035	7.787E-07
10000	0.9397	9.126E-07	0.9423	9.200E-07
50000	0.9865	1.117E-06	0.9903	1.129E-06
100000	0.9873	1.120E-06	0.9910	1.132E-06

Table H-2: Gradients (m) and leakage exponents (N1) from the power law graphs for 1mm by 40mm longitudinal crack in HDPE

2. Variation of leak area with time

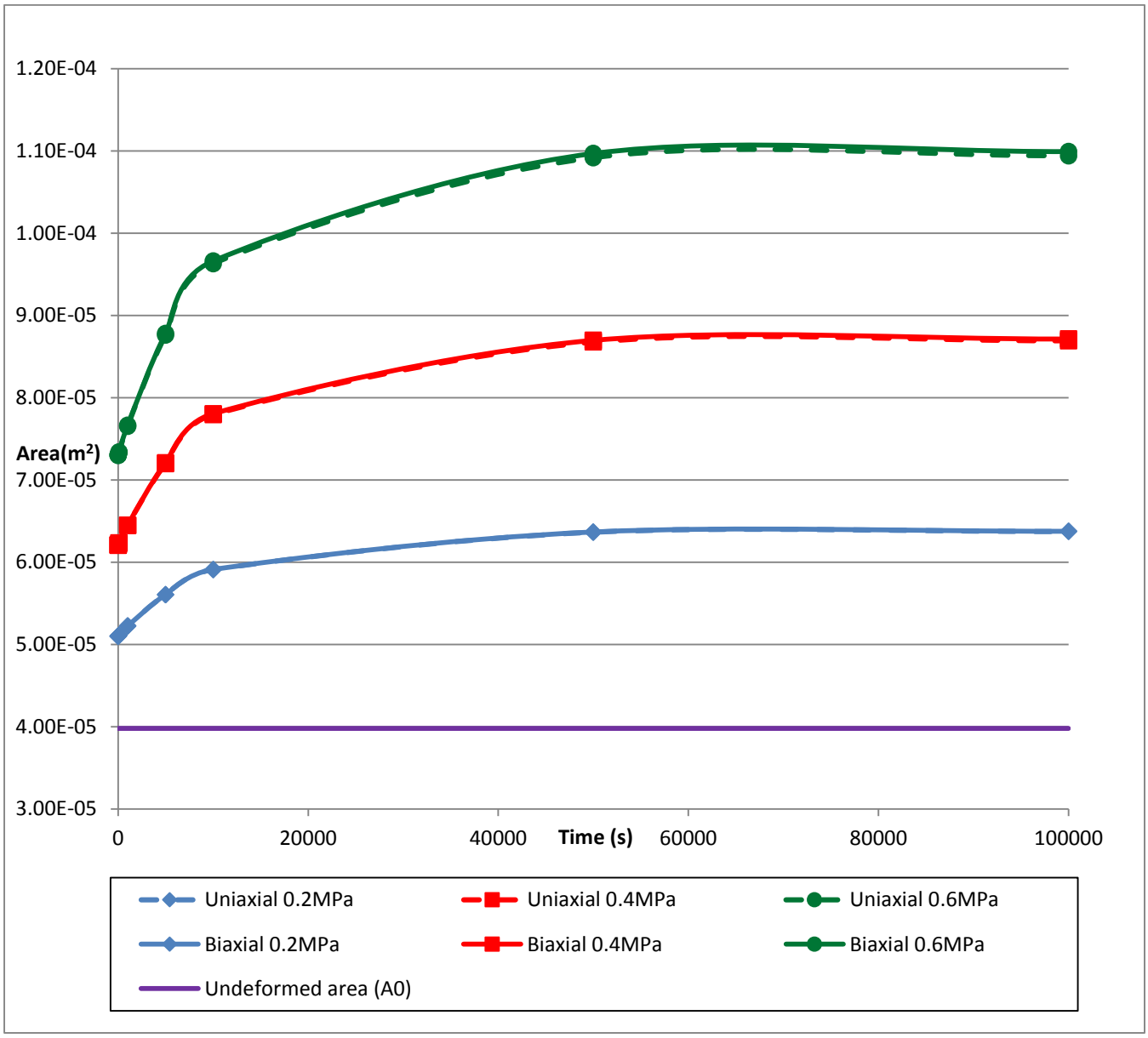

Figure H-1: Area against time for 1mm by 40mm longitudinal crack in HDPE

3. Variation of leak area with pressure

a) Uniaxial

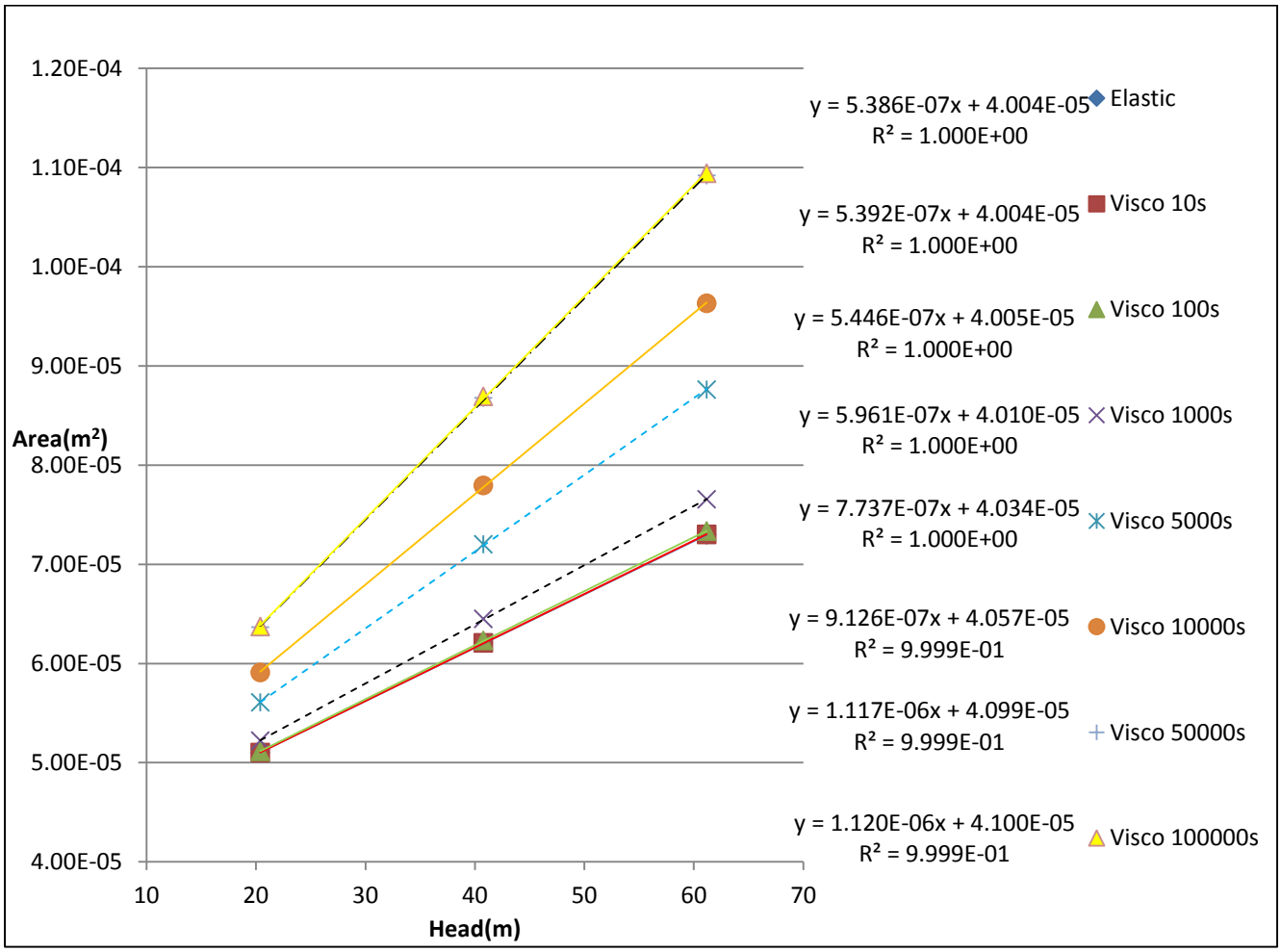

Figure H-2: Area against pressure head for 1mm by 40mm longitudinal crack in HDPE, uniaxial

b) Biaxial

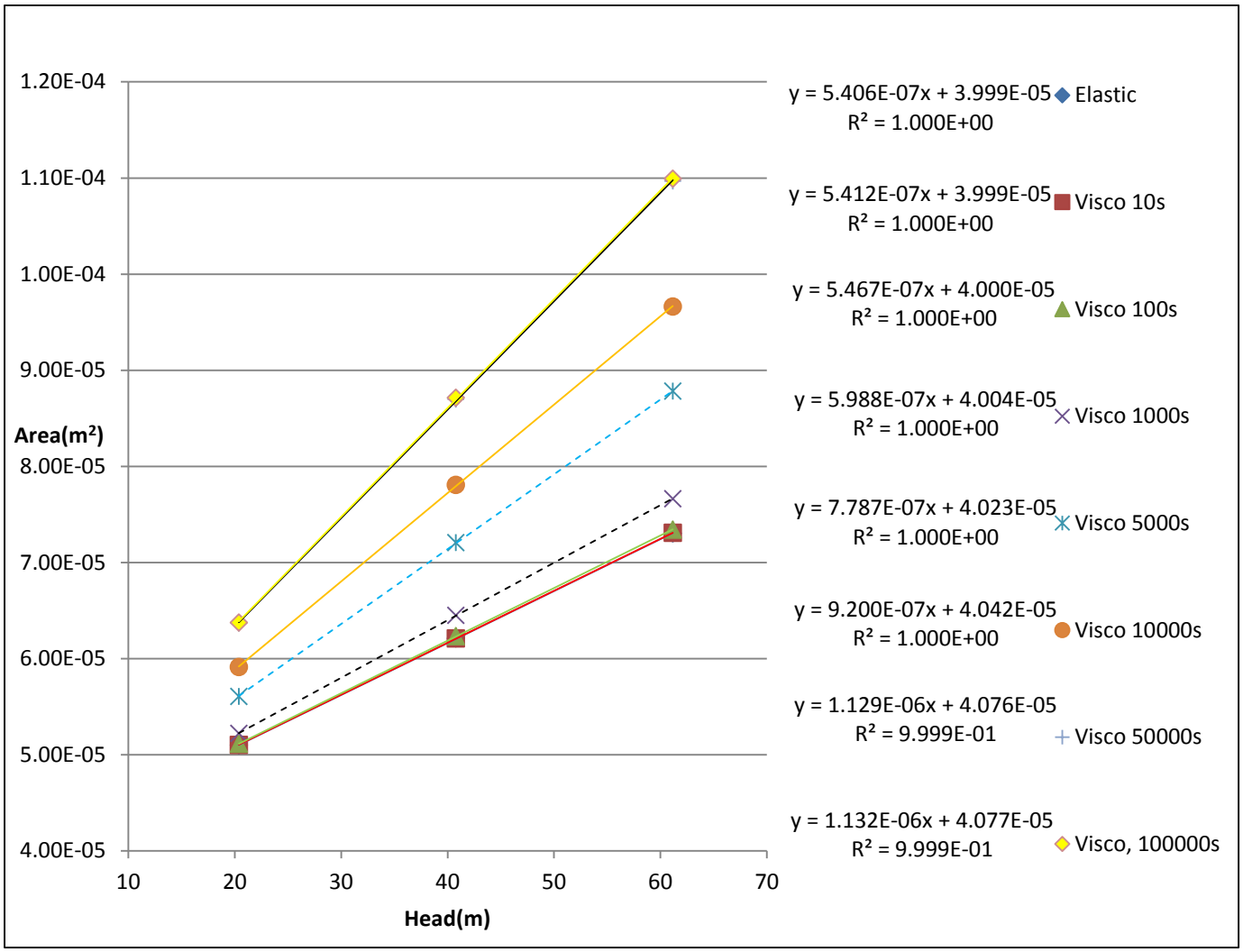

Figure H-3: Area against pressure head for 1mm by 40mm longitudinal crack in HDPE, biaxial

4. Variation of leak discharge with time

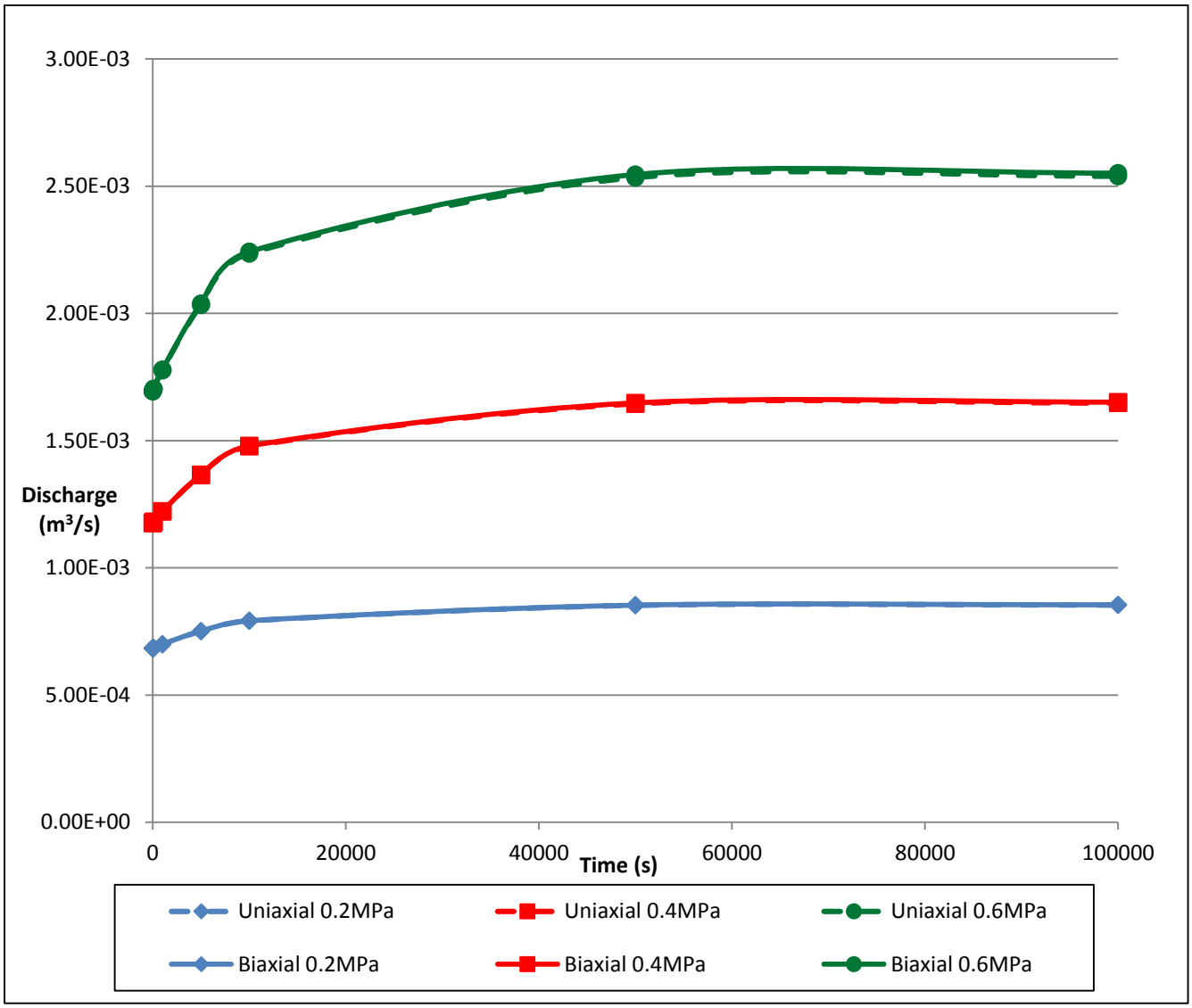

Figure H-4: Discharge against time for 1mm by 40mm longitudinal crack in HDPE

5. Variation of leak discharge with pressure

a) Uniaxial

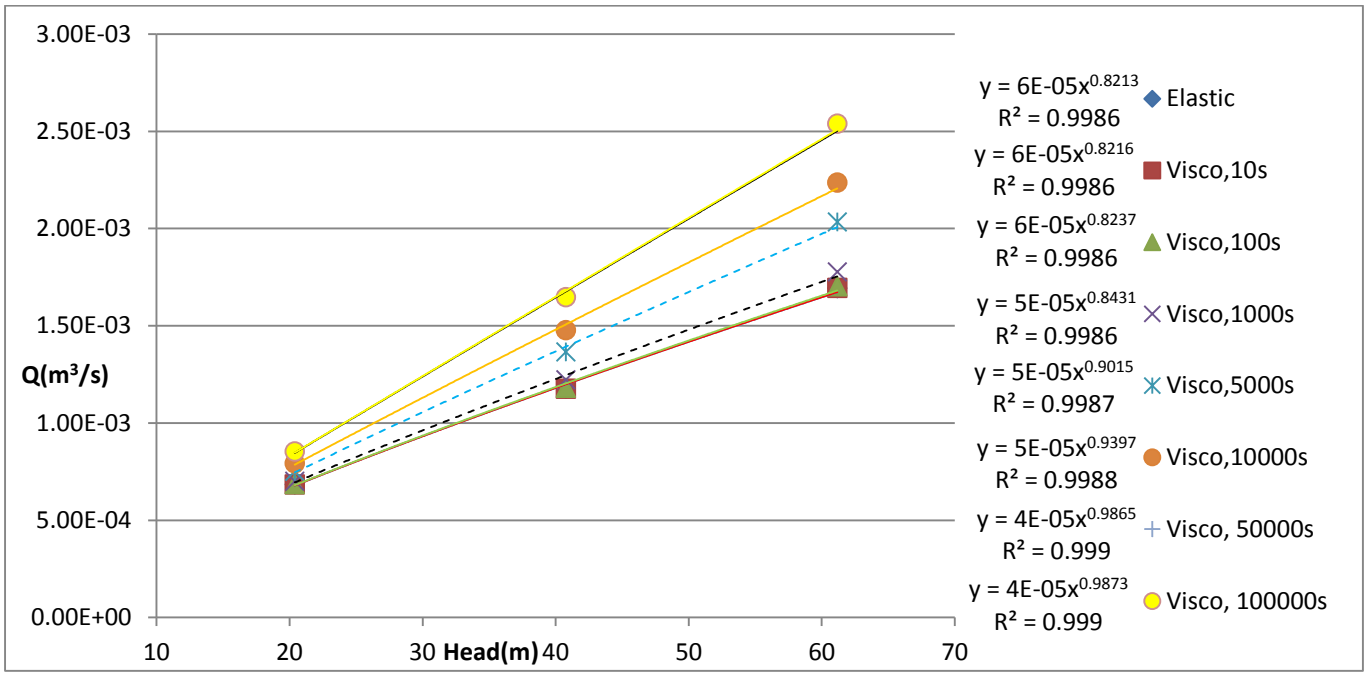

Figure H-5: Discharge against pressure head for 1mm by 40mm longitudinal crack in HDPE, uniaxial

b) Biaxial

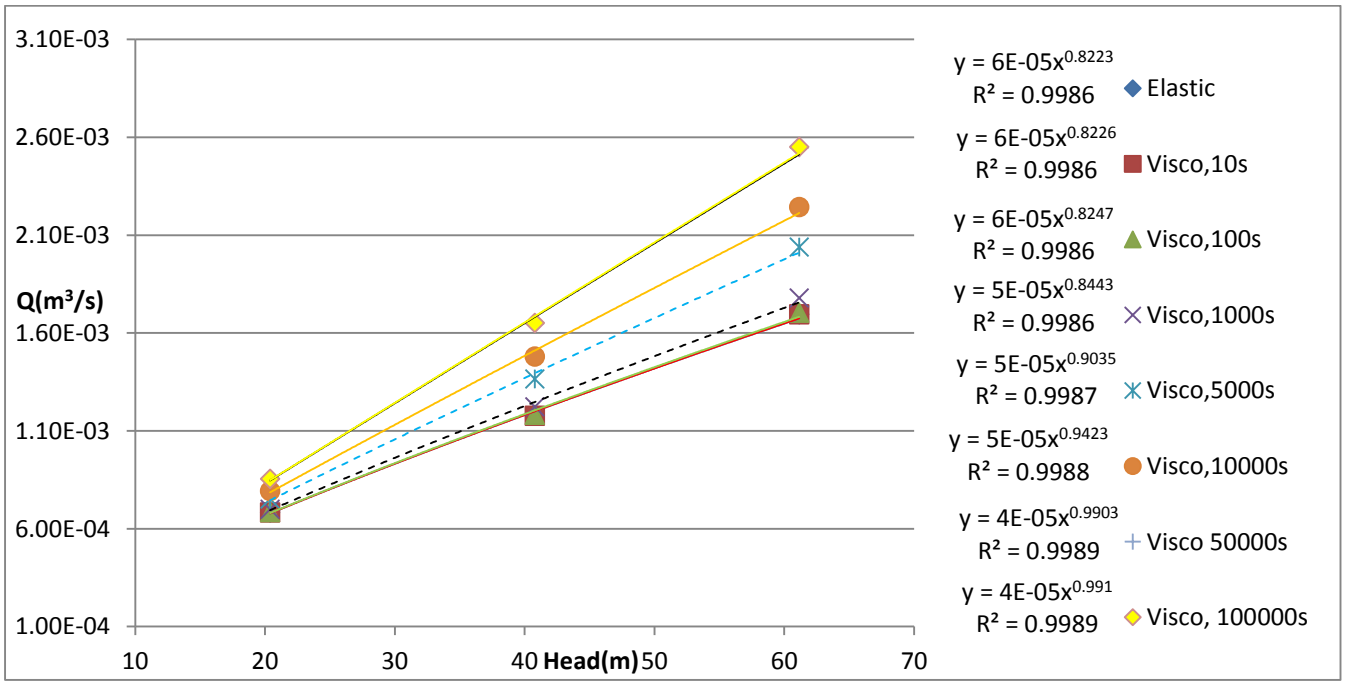

Figure H-6: Discharge against pressure head for 1mm by 40mm longitudinal crack in HDPE, biaxial

6. Gradient (m) and leakage exponent (N1)

a) Gradient (m) against time

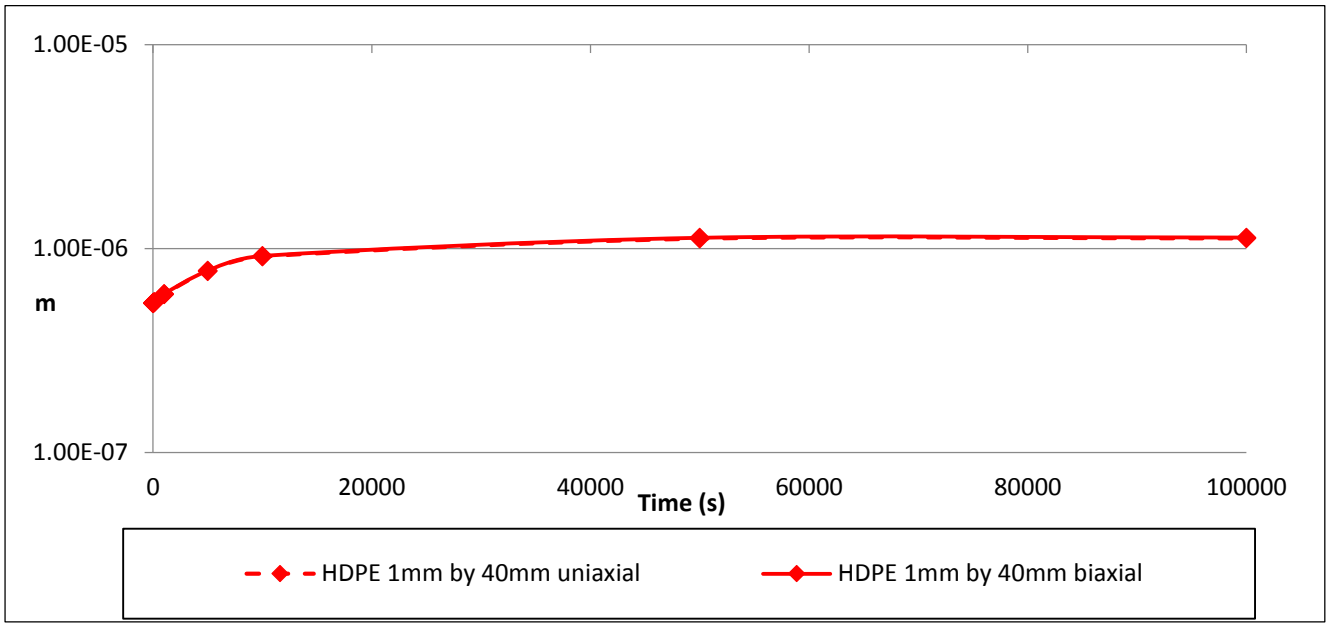

Figure H-7: Gradient (m) against time for 1mm by 40mm longitudinal crack in HDPE

b) Leakage exponent (N1) against time

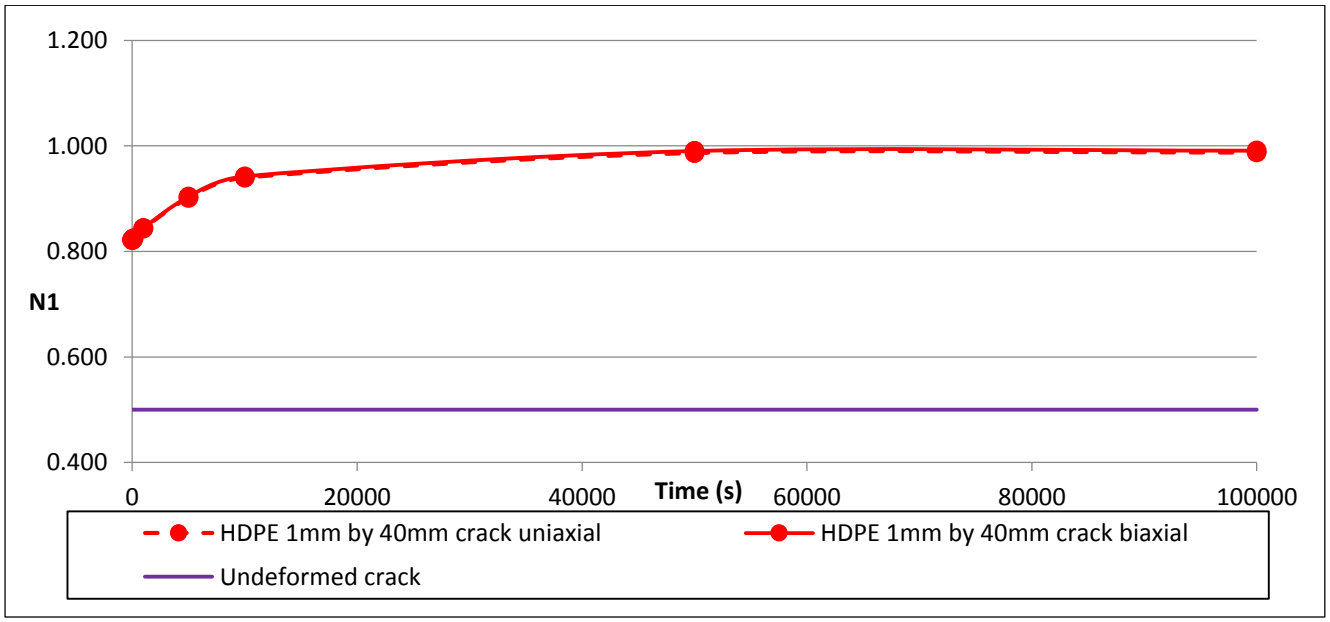

Figure H-8: Leakage exponent (N1) against time for 1mm by 40mm longitudinal crack in HDPE

7. Percentage change in area with pressure

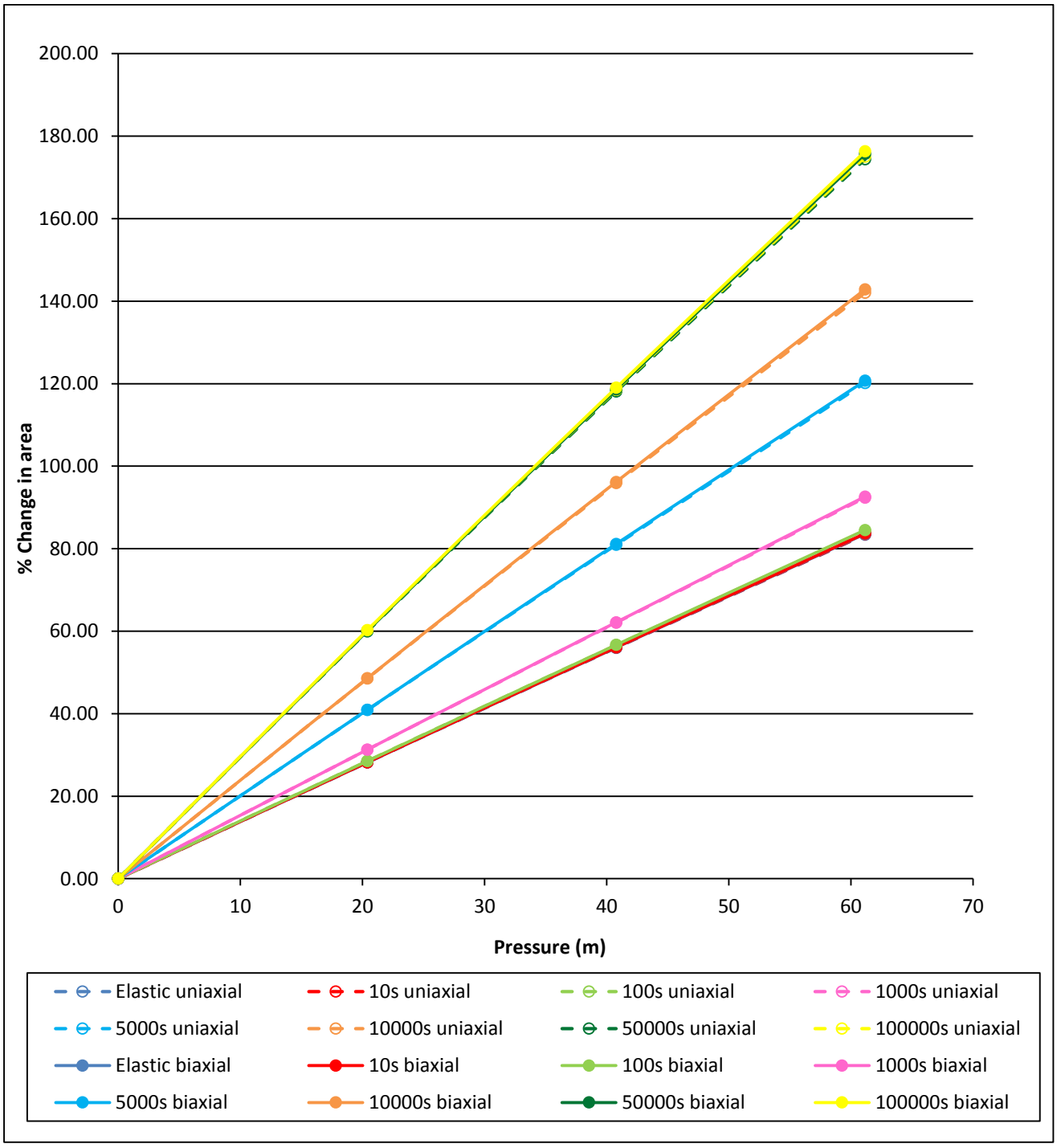

Figure H-9: Percentage change in area against pressure for 1mm by 40mm longitudinal crack in HDPE

8. Ratio of total change in area to elastic change in area

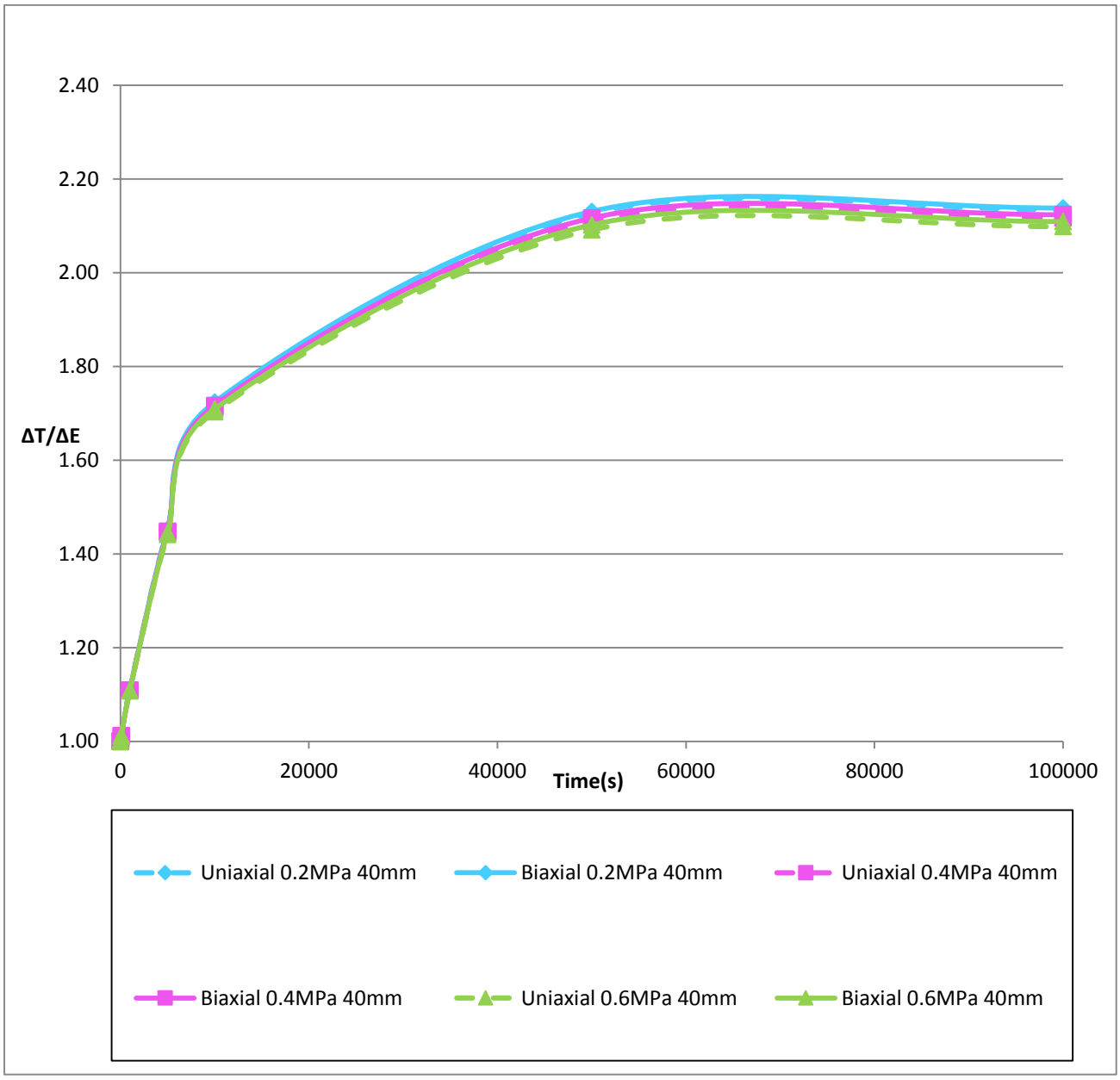

Figure H-10: ΔT/ΔE against time for 1mm by 40mm longitudinal crack in HDPE

9. Leakage number , calculated leak exponents, m/A_0 and m/m_E

a) Uniaxial

Time (s)	N1 from power law	m	L_N	N1	m/A_0	m/m_E
			Pressure = 0.4MPa	Pressure = 0.4MPa		
0	0.8213	5.39E-07	0.5520	0.8557	0.01354	1.0000
10	0.8216	5.39E-07	0.5526	0.8559	0.01355	1.0011
100	0.8237	5.45E-07	0.5581	0.8582	0.01369	1.0111
1000	0.8431	5.96E-07	0.6109	0.8792	0.01498	1.1068
5000	0.9015	7.74E-07	0.7929	0.9423	0.01945	1.4365
10000	0.9397	9.13E-07	0.9353	0.9833	0.02294	1.6944
50000	0.9865	1.12E-06	1.1448	1.0338	0.02808	2.0739
100000	0.9873	1.12E-06	1.1479	1.0344	0.02815	2.0795

Table H-3: Leakage numbers, calculated leak exponents, m/A_0 and m/m_E for the 1mm by 40mm crack in HDPE, uniaxial

b) Biaxial

Time (s)	N1 from power law	m	L_N	N1	m/A_0	m/m_E
			Pressure = 0.4MPa	Pressure = 0.4MPa		
0	0.8223	5.41E-07	0.5540	0.8565	0.01359	1.0000
10	0.8226	5.41E-07	0.5547	0.8568	0.01360	1.0011
100	0.8247	5.47E-07	0.5603	0.8591	0.01374	1.0113
1000	0.8443	5.99E-07	0.6137	0.8803	0.01505	1.1077
5000	0.9035	7.79E-07	0.7981	0.9438	0.01957	1.4404
10000	0.9423	9.20E-07	0.9429	0.9853	0.02312	1.7018
50000	0.9903	1.13E-06	1.1571	1.0364	0.02838	2.0884
100000	0.991	1.13E-06	1.1602	1.0371	0.02845	2.0940

Table H-4: Leakage numbers, calculated leak exponents, m/A_0 and m/m_E for the 1mm by 40mm crack in HDPE, biaxial

I 1mm by 40mm longitudinal crack in PVC

1. Summary results for area, gradient (m) and leakage exponent (N1)

PVC	Area of deformed cracks with A_0 = 39.785mm^2					
Pressure (MPa)	0.2		0.4		0.6	
Time (s)	Uniaxial	Biaxial	Uniaxial	Biaxial	Uniaxial	Biaxial
0 (Elastic)	45.7370	45.7292	51.6466	51.6382	57.5139	57.5121
10	45.7402	45.7325	51.6531	51.6448	57.5236	57.5217
100	45.7694	45.7616	51.7109	51.7026	57.6097	57.6080
1000	46.0291	46.0212	52.2265	52.2186	58.3773	58.3772
5000	46.7016	46.6933	53.5607	53.5539	60.3625	60.3668
10000	47.0001	46.9917	54.1527	54.1465	61.2427	61.2492
50000	47.1341	47.1257	54.4183	54.4124	61.6376	61.6452
100000	47.1342	47.1257	54.4183	54.4124	61.6376	61.6452

Table I-1: Deformed areas (mm^2) for 1mm by 40mm longitudinal crack in PVC

PVC	Uniaxial		Biaxial	
Time (s)	N1	m	N1	m
0 (Elastic)	0.7050	2.888E-07	0.7051	2.890E-07
10	0.7051	2.890E-07	0.7052	2.891E-07
100	0.7058	2.904E-07	0.7059	2.905E-07
1000	0.7127	3.028E-07	0.7128	3.030E-07
5000	0.7297	3.350E-07	0.7299	3.353E-07
10000	0.7370	3.493E-07	0.7372	3.497E-07
50000	0.7402	3.557E-07	0.7405	3.561E-07
100000	0.7402	3.557E-07	0.7405	3.561E-07

Table I-2: Gradients (m) and leakage exponents (N1) from the power law graphs for 1mm by 40mm longitudinal crack in PVC

2. Variation of leak area with time

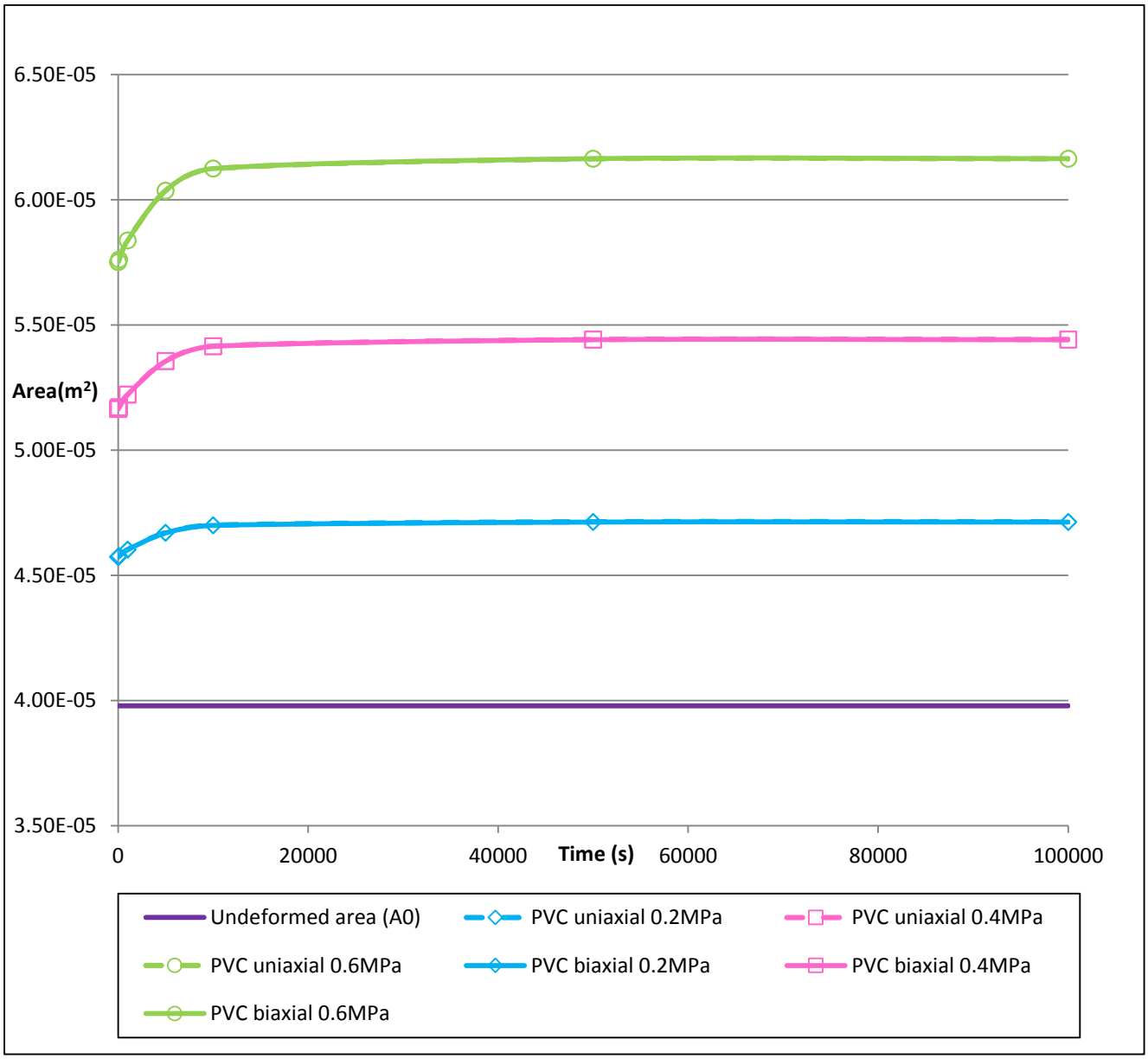

Figure I-1: Area against time for 1mm by 40mm longitudinal crack in PVC

3. Variation of leak area with pressure

a) Uniaxial

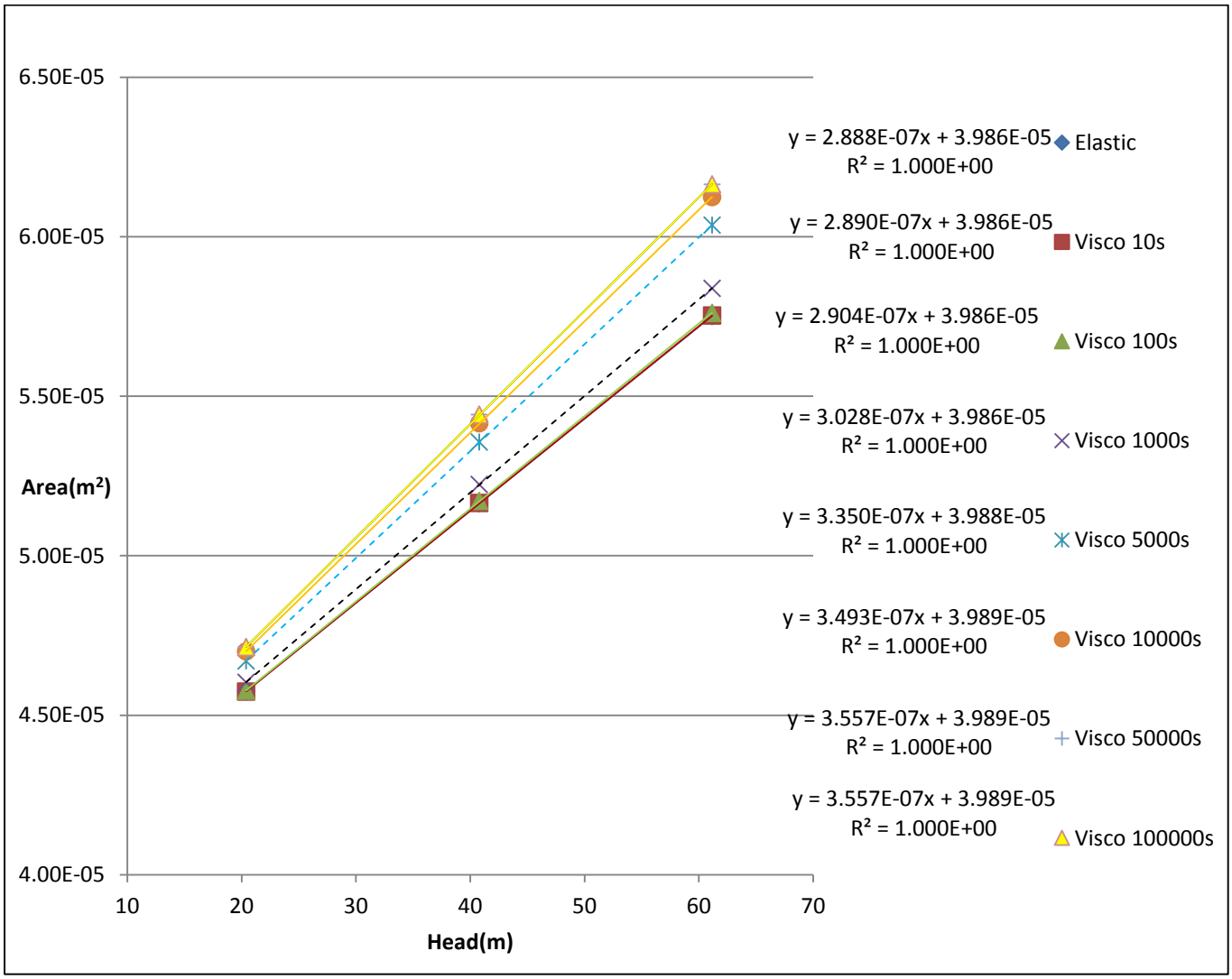

Figure I-2: Area against pressure head for 1mm by 40mm longitudinal crack in PVC, uniaxial

b) Biaxial

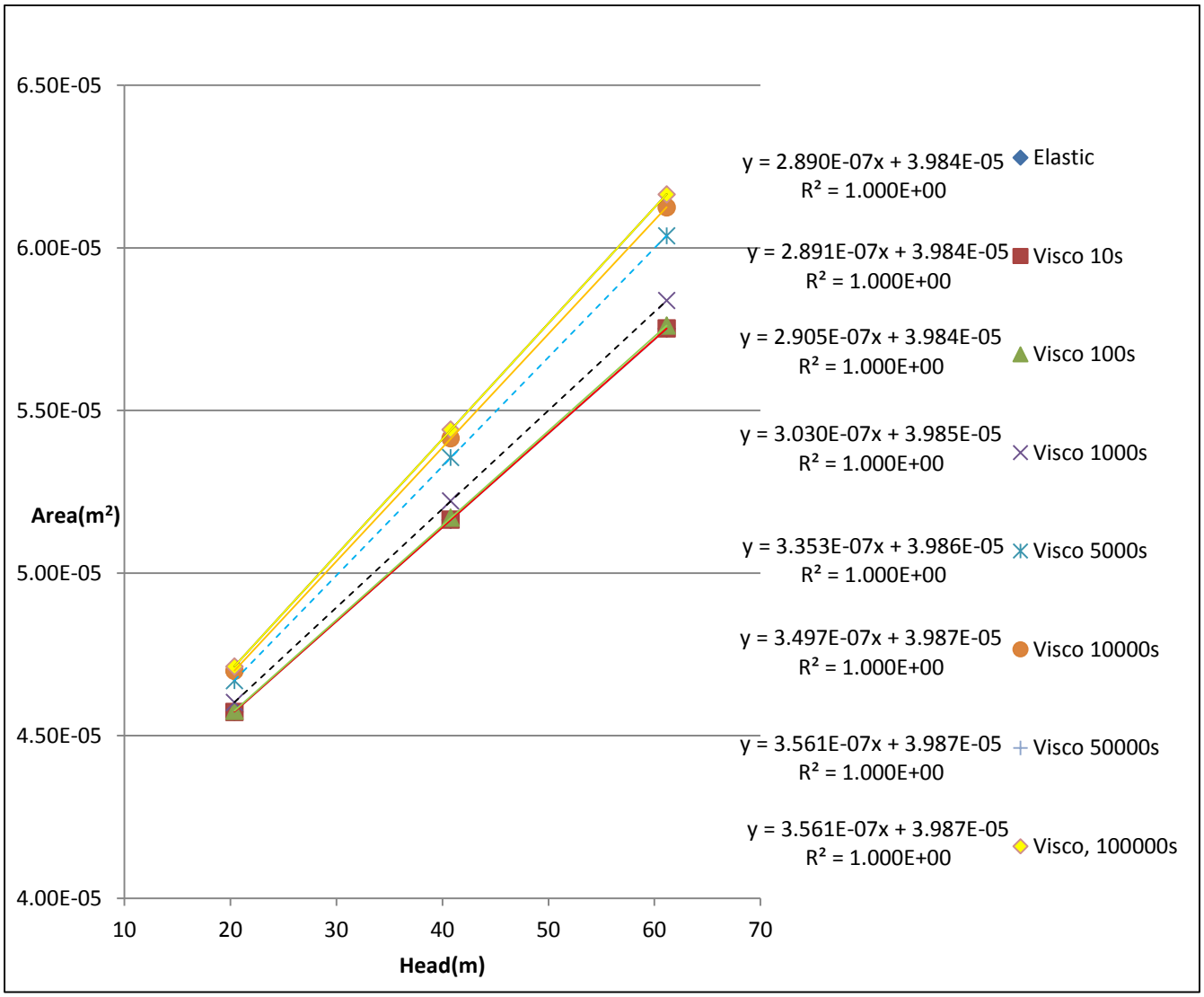

Figure I-3: Area against pressure head for 1mm by 40mm longitudinal crack in PVC, biaxial

4. Variation of leak discharge with time

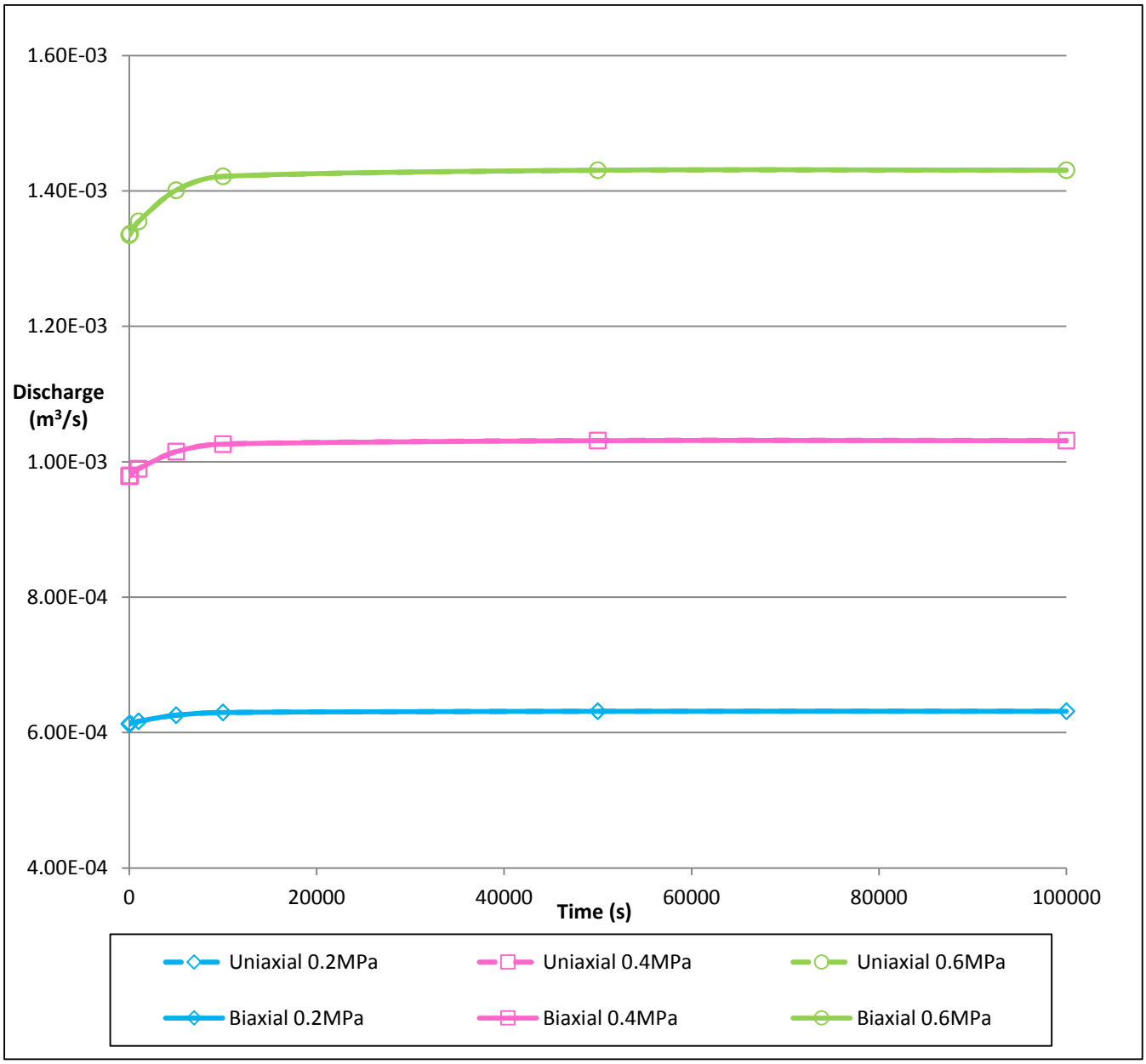

Figure I-4: Discharge against time for 1mm by 40mm longitudinal crack in PVC

5. Variation of leak discharge with pressure

a) Uniaxial

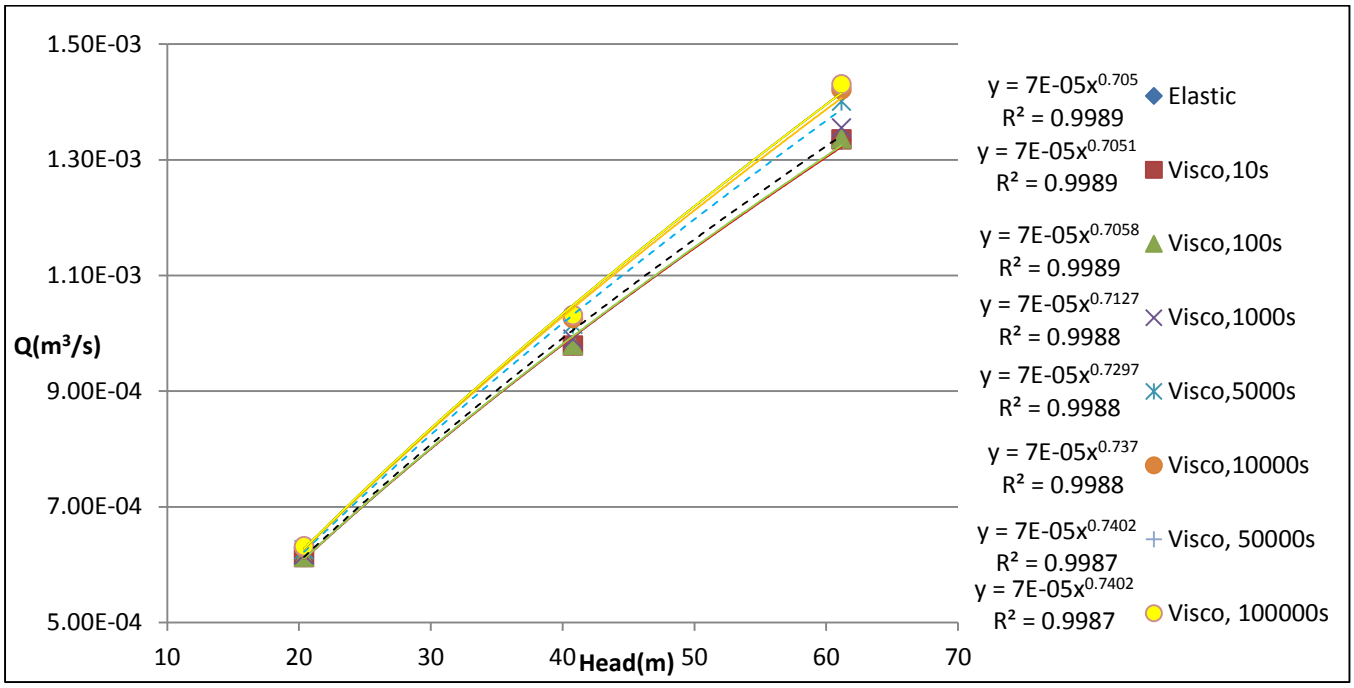

Figure I-5: Discharge against pressure head for 1mm by 40mm longitudinal crack in PVC, uniaxial

b) Biaxial

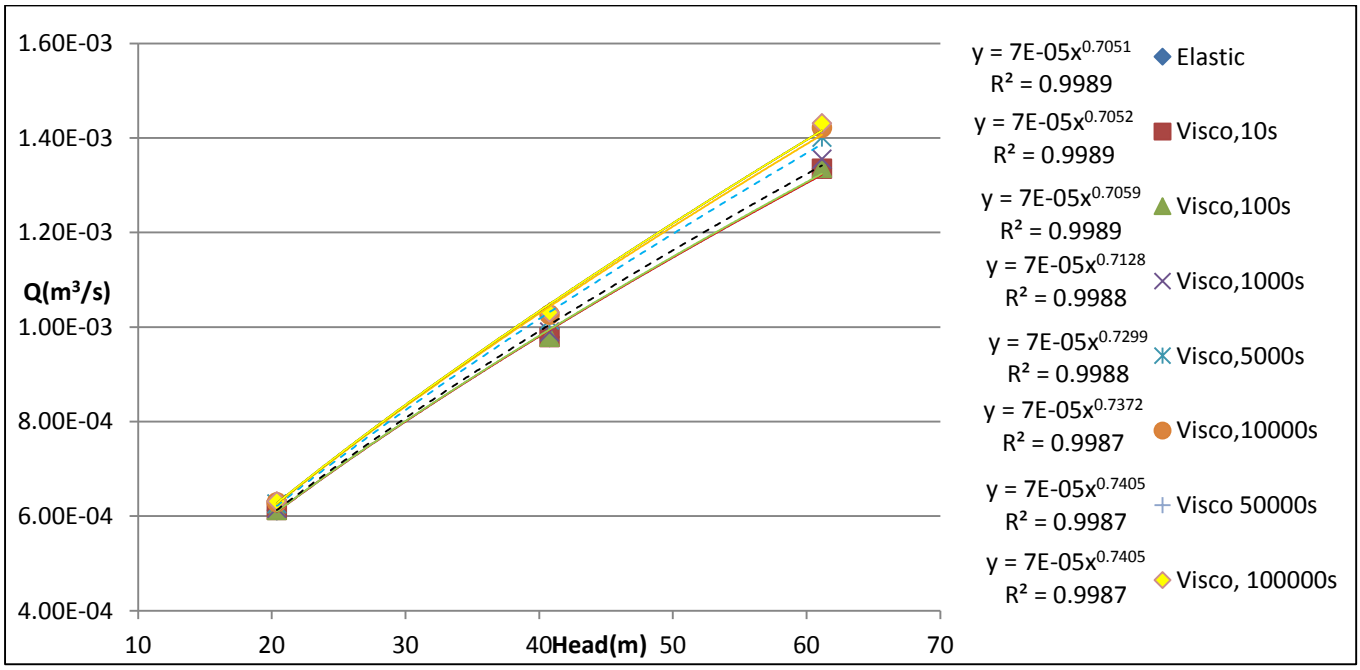

Figure I-6: Discharge against pressure head for 1mm by 40mm longitudinal crack in PVC, biaxial

6. Gradient (m) and leakage exponent (N1)

a) Gradient (m) against time

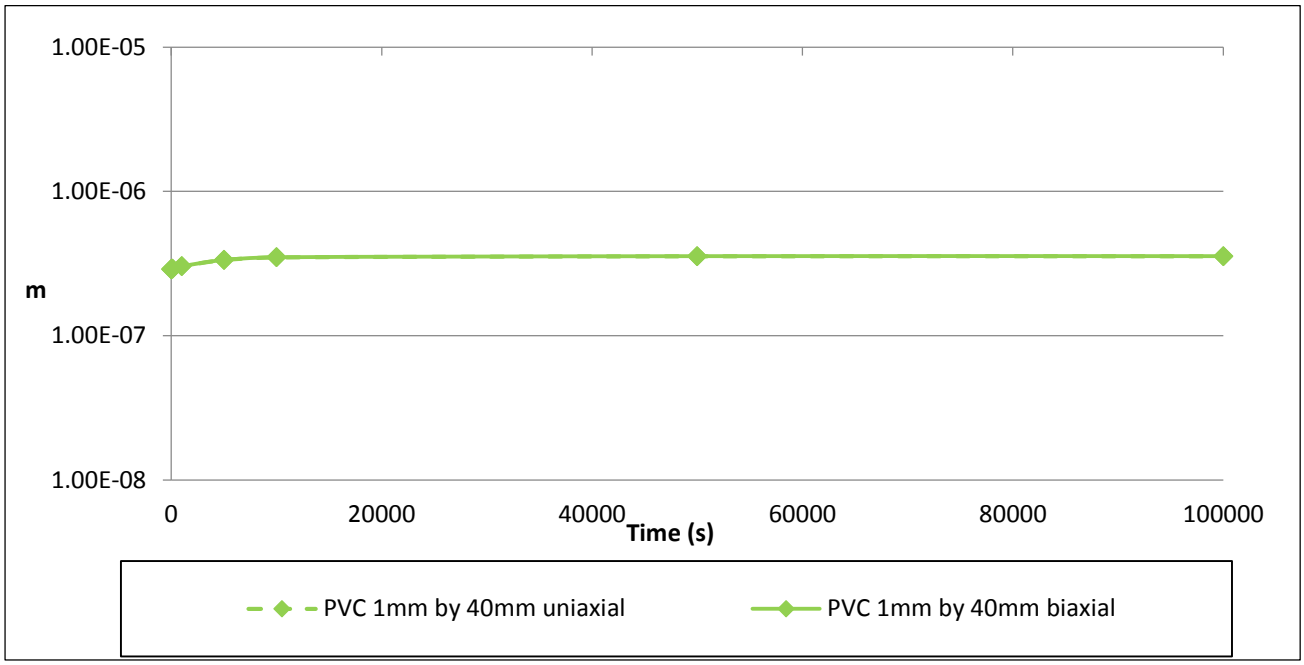

Figure I-7: Gradient (m) against time for 1mm by 40mm longitudinal crack in PVC

b) Leakage exponent (N1) against time

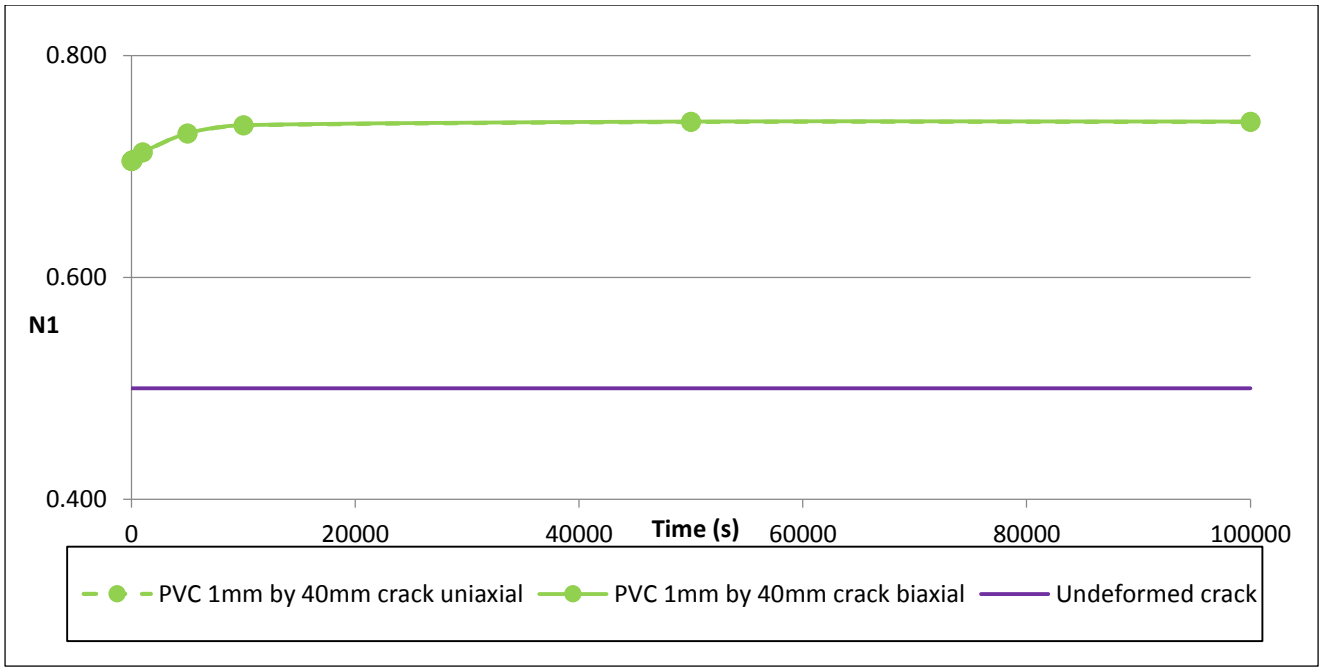

Figure I-8: Leakage exponent (N1) against time for 1mm by 40mm longitudinal crack in PVC

7. Percentage change in area with pressure

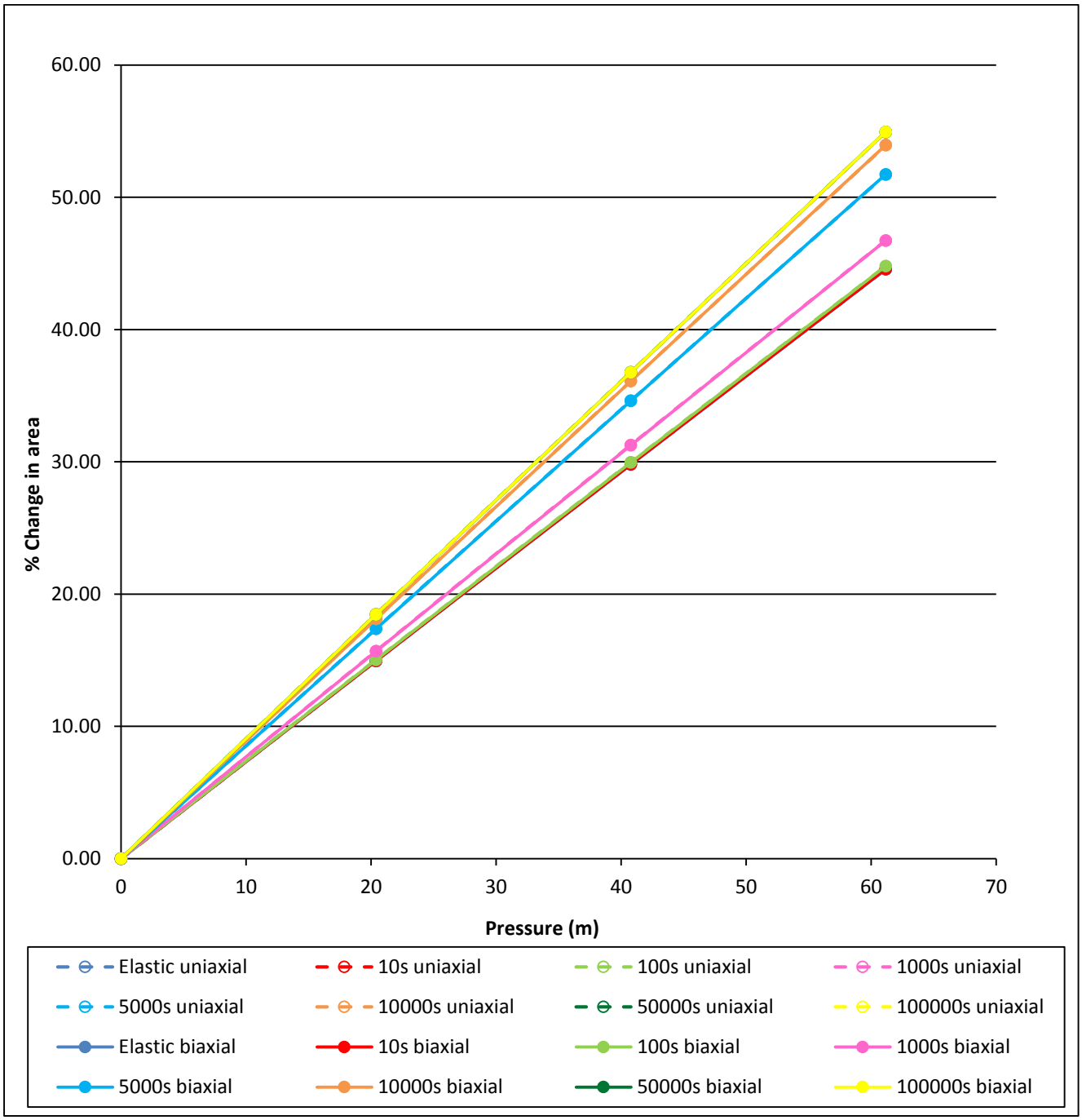

Figure I-9: Percentage change in area against pressure for 1mm by 40mm longitudinal crack in PVC

8. Ratio of total change in area to elastic change in area

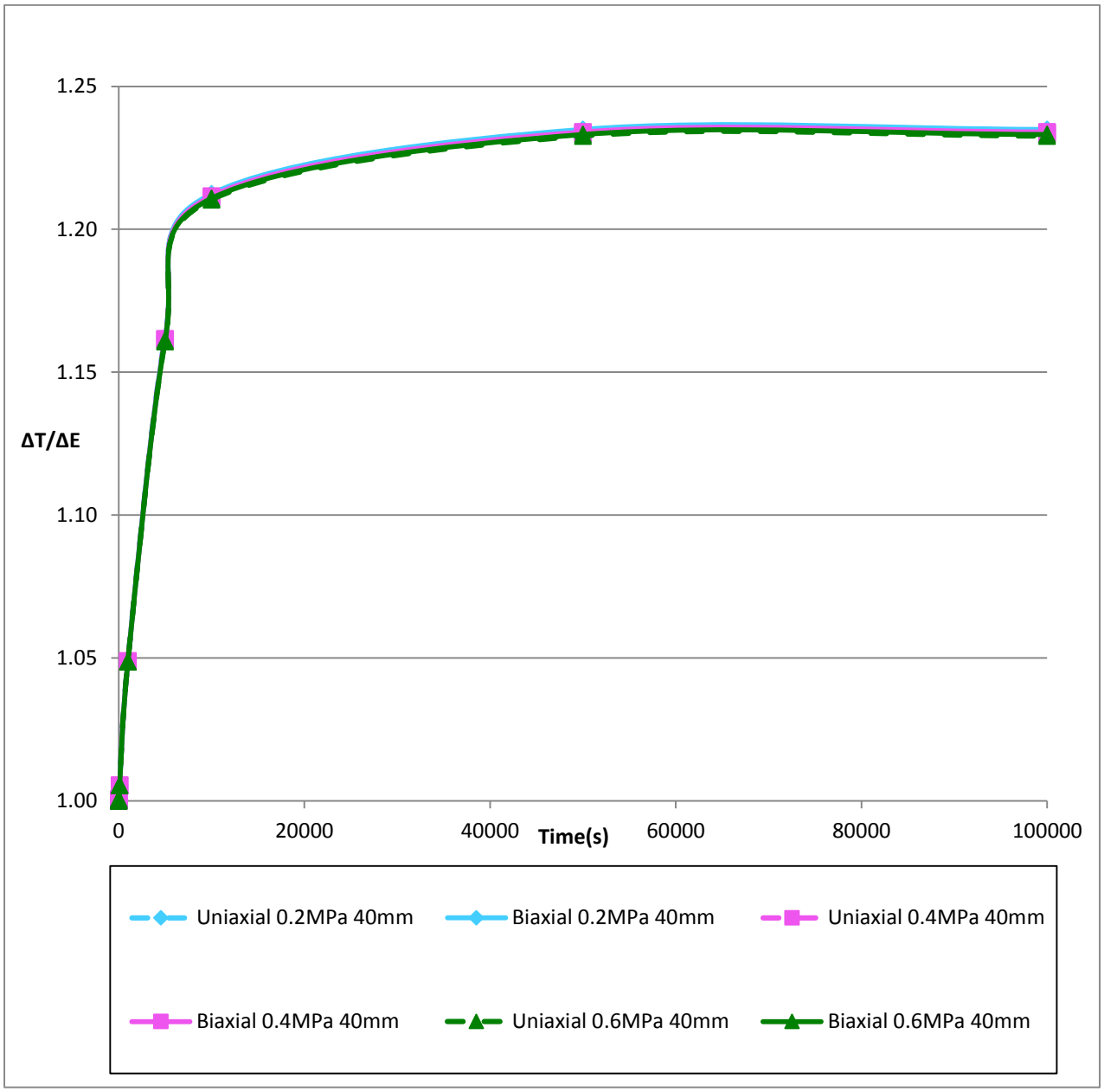

Figure I-10: ΔT/ΔE against time for 1mm by 40mm longitudinal crack in PVC

9. Leakage number, calculated leak exponents, m/A_0 and m/m_E

a) Uniaxial

Time (s)	N1 from power law	m	L_N	N1	m/A_0	m/m_E
			Pressure = 0.4MPa	**Pressure = 0.4MPa**		
0	0.705	2.89E-07	0.2960	0.7284	0.00726	1.0000
10	0.7051	2.89E-07	0.2962	0.7285	0.00726	1.0007
100	0.7058	2.90E-07	0.2976	0.7294	0.00730	1.0055
1000	0.7127	3.03E-07	0.3103	0.7368	0.00761	1.0485
5000	0.7297	3.35E-07	0.3433	0.7556	0.00842	1.1600
10000	0.737	3.49E-07	0.3580	0.7636	0.00878	1.2095
50000	0.7402	3.56E-07	0.3645	0.7672	0.00894	1.2316
100000	0.7402	3.56E-07	0.3645	0.7672	0.00894	1.2316

Table I-3: Leakage numbers, calculated leak exponents, m/A_0 and m/m_E for the 1mm by 40mm crack in PVC, uniaxial

b) Biaxial

Time (s)	N1 from power law	m	L_N	N1	m/A_0	m/m_E
			Pressure = 0.4MPa	**Pressure = 0.4MPa**		
0	0.7051	2.89E-07	0.2962	0.7285	0.00726	1.0000
10	0.7052	2.89E-07	0.2963	0.7286	0.00727	1.0003
100	0.7059	2.91E-07	0.2977	0.7294	0.00730	1.0052
1000	0.7128	3.03E-07	0.3105	0.7370	0.00762	1.0484
5000	0.7299	3.35E-07	0.3436	0.7558	0.00843	1.1602
10000	0.7372	3.50E-07	0.3584	0.7638	0.00879	1.2100
50000	0.7405	3.56E-07	0.3650	0.7674	0.00895	1.2322
100000	0.7405	3.56E-07	0.3650	0.7674	0.00895	1.2322

Table I-4: Leakage numbers, calculated leak exponents, m/A_0 and m/m_E for the 1mm by 40mm crack in PVC, biaxial

J 1mm by 80mm longitudinal crack in HDPE

1. Summary results for area, gradient (m) and leakage exponent (N1)

HDPE	Area of deformed cracks with A_0 = 79.765mm^2					
Pressure (MPa)	0.2		0.4		0.6	
Time (s)	Uniaxial	Biaxial	Uniaxial	Biaxial	Uniaxial	Biaxial
0 (Elastic)	191.3013	191.3092	299.7896	300.0906	405.2300	406.1093
10	191.4318	191.4398	300.0432	300.3452	405.5996	406.4815
100	192.5999	192.6096	302.3139	302.6255	408.9074	409.8129
1000	203.6987	203.7260	323.8539	324.2627	440.2312	441.3753
5000	242.2430	242.3554	398.1506	398.9928	547.4883	549.6773
10000	272.7212	272.9278	456.3287	457.6217	630.5876	633.8461
50000	318.1328	318.5251	542.0461	544.1935	751.5046	756.7690
100000	318.9575	319.3537	543.5916	545.7567	753.6672	758.9726

Table J-1 Deformed areas (mm^2) for 1mm by 80mm longitudinal crack in HDPE

HDPE	Uniaxial		Biaxial	
Time (s)	N1	m	N1	m
0 (Elastic)	1.1794	5.247E-06	1.1813	5.268E-06
10	1.1797	5.252E-06	1.1815	5.274E-06
100	1.1815	5.305E-06	1.1834	5.327E-06
1000	1.1980	5.801E-06	1.2001	5.828E-06
5000	1.2395	7.486E-06	1.2426	7.537E-06
10000	1.2608	8.777E-06	1.2650	8.854E-06
50000	1.2810	1.063E-05	1.2861	1.075E-05
100000	1.2812	1.066E-05	1.2864	1.078E-05

Table J-2: Gradients (m) and leakage exponents (N1) from the power law graphs for 1mm by 80mm longitudinal crack in HDPE

2. Variation of leak area with time

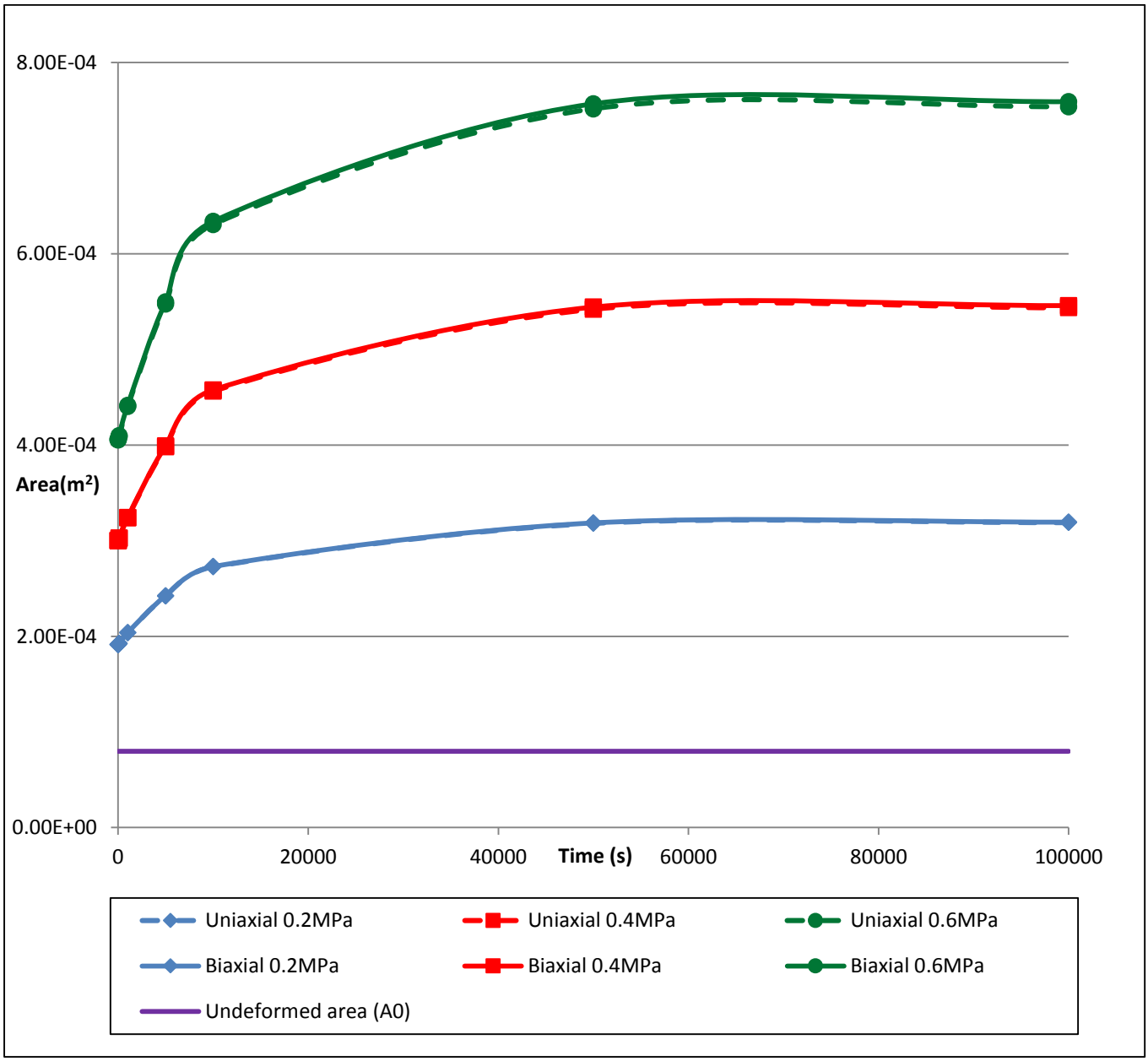

Figure J-1: Area against time for 1mm by 80mm longitudinal crack in HDPE

J

3. Variation of leak area with pressure

a) Uniaxial

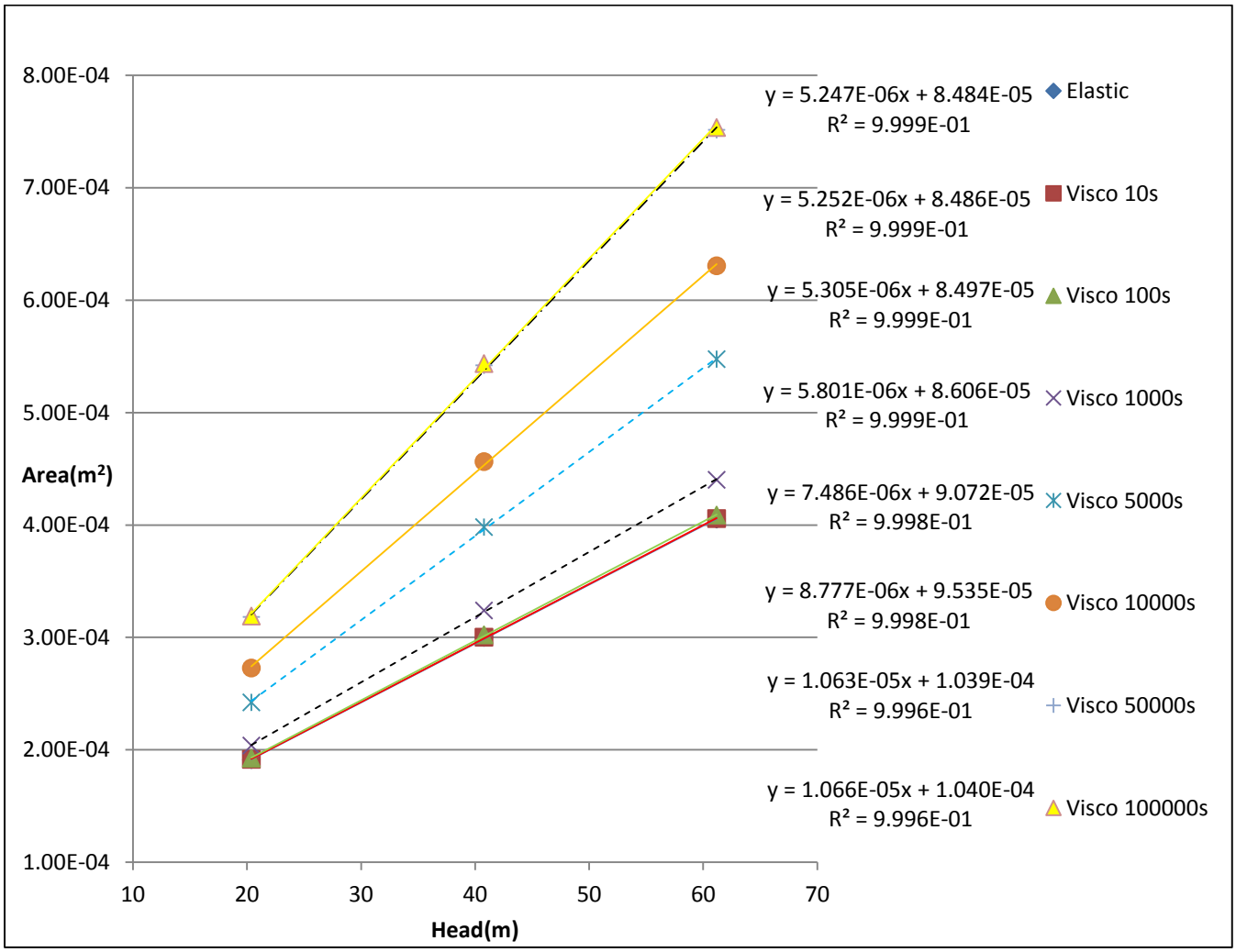

Figure J-2: Area against pressure for 1mm by 80mm longitudinal crack in HDPE, uniaxial

b) Biaxial

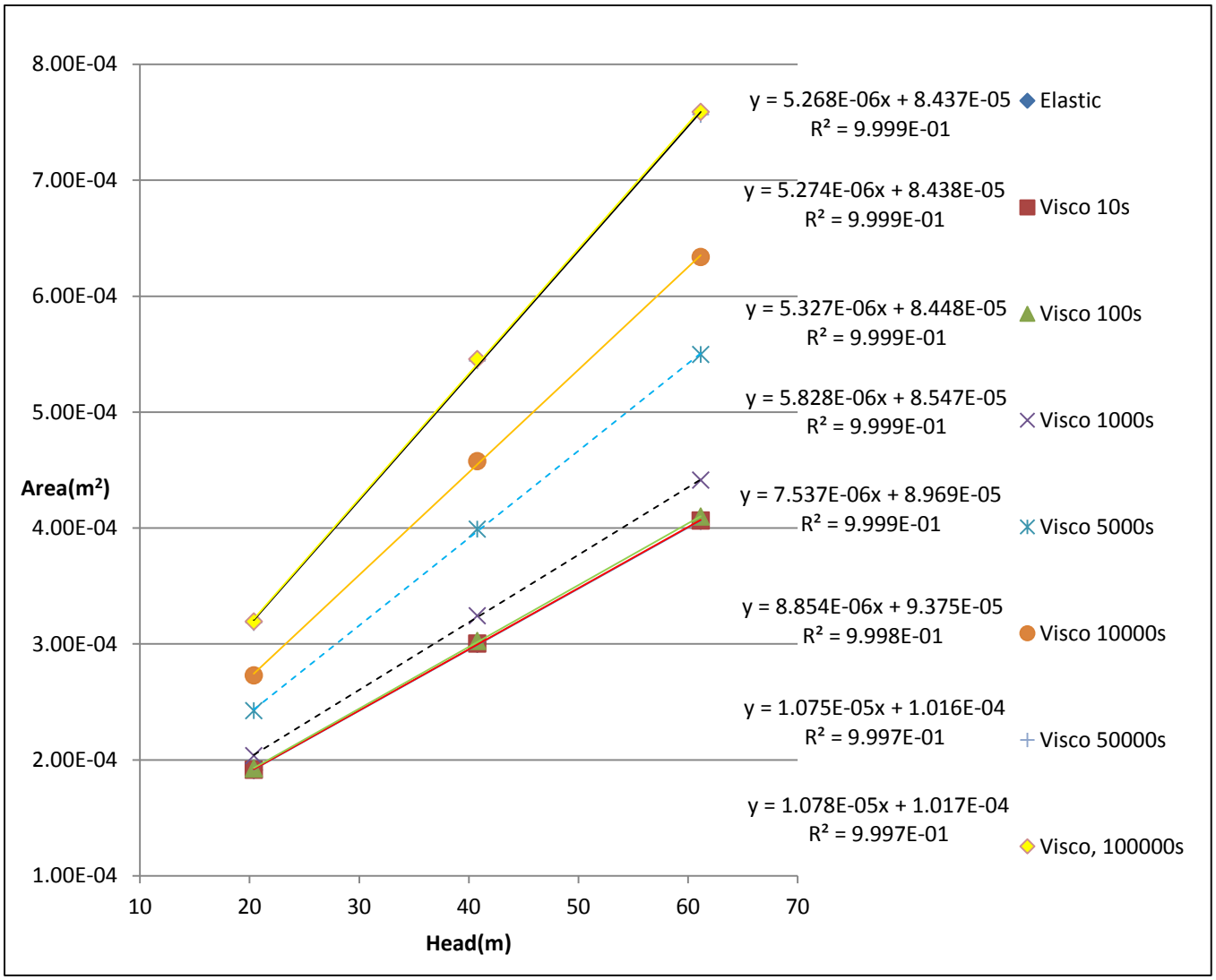

Figure J-3: Area against pressure for 1mm by 80mm longitudinal crack in HDPE, biaxial

4. Variation of leak discharge with time

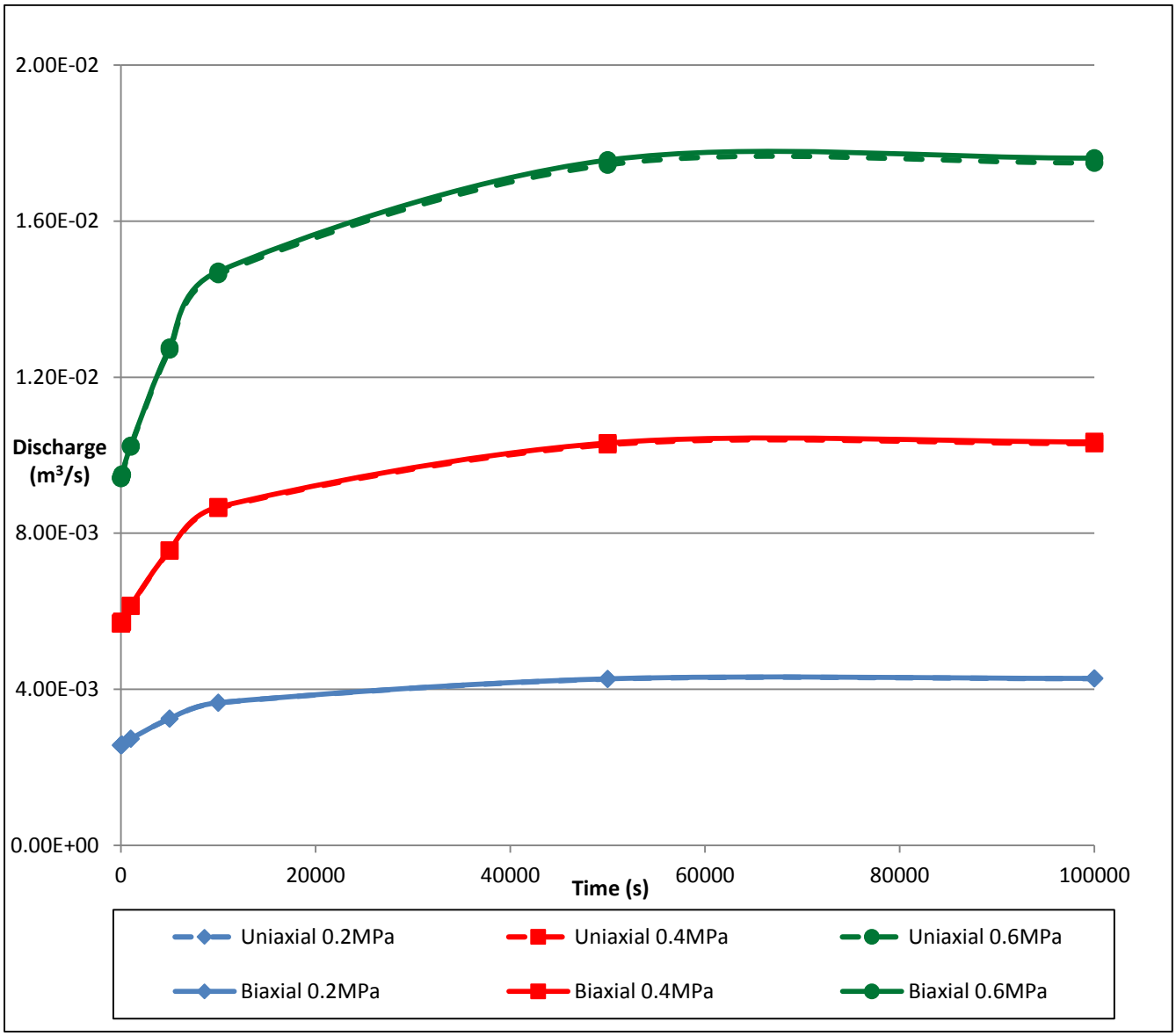

Figure J-4: Discharge against time for 1mm by 80mm longitudinal crack in HDPE

5. Variation of leak discharge with pressure

a) Uniaxial

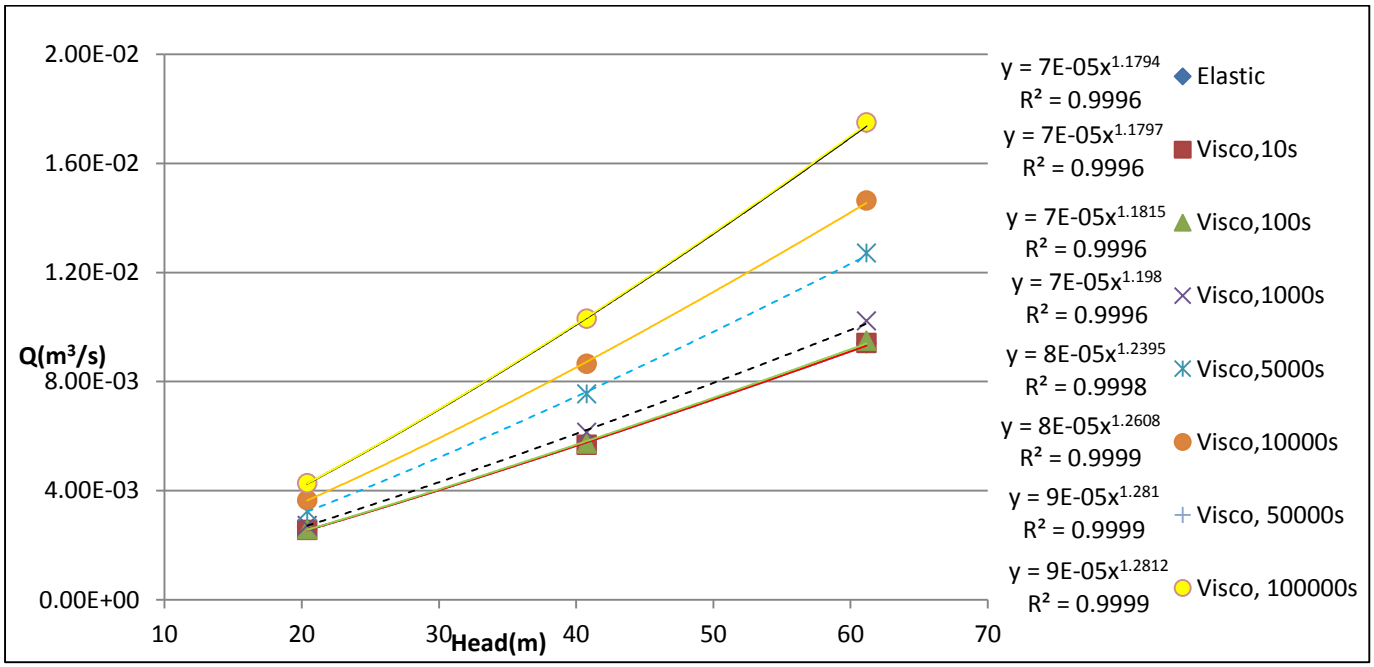

Figure J-5: Discharge against pressure head for 1mm by 80mm longitudinal crack in HDPE, uniaxial

b) Biaxial

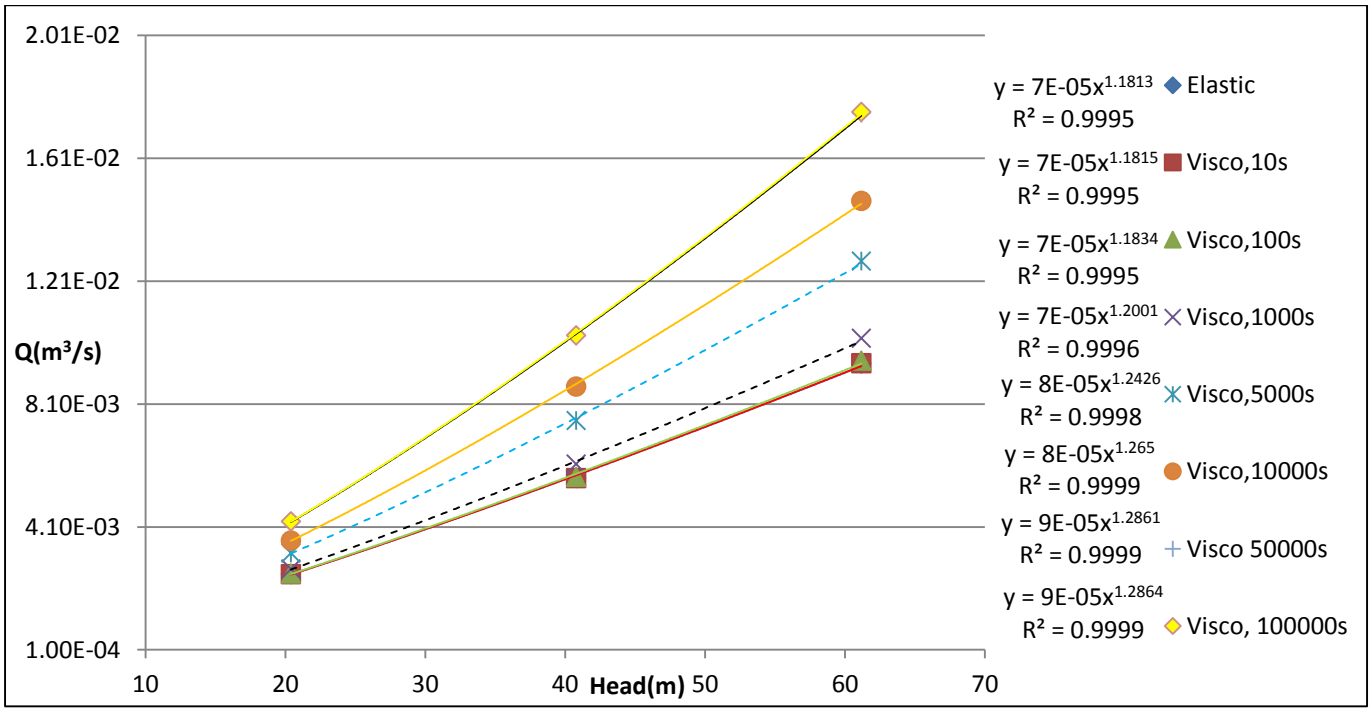

Figure J-6: Discharge against head for 1mm by 80mm longitudinal crack in HDPE, biaxial

6. Gradient (m) and leakage exponent (N1)

a) Gradient (m) against time

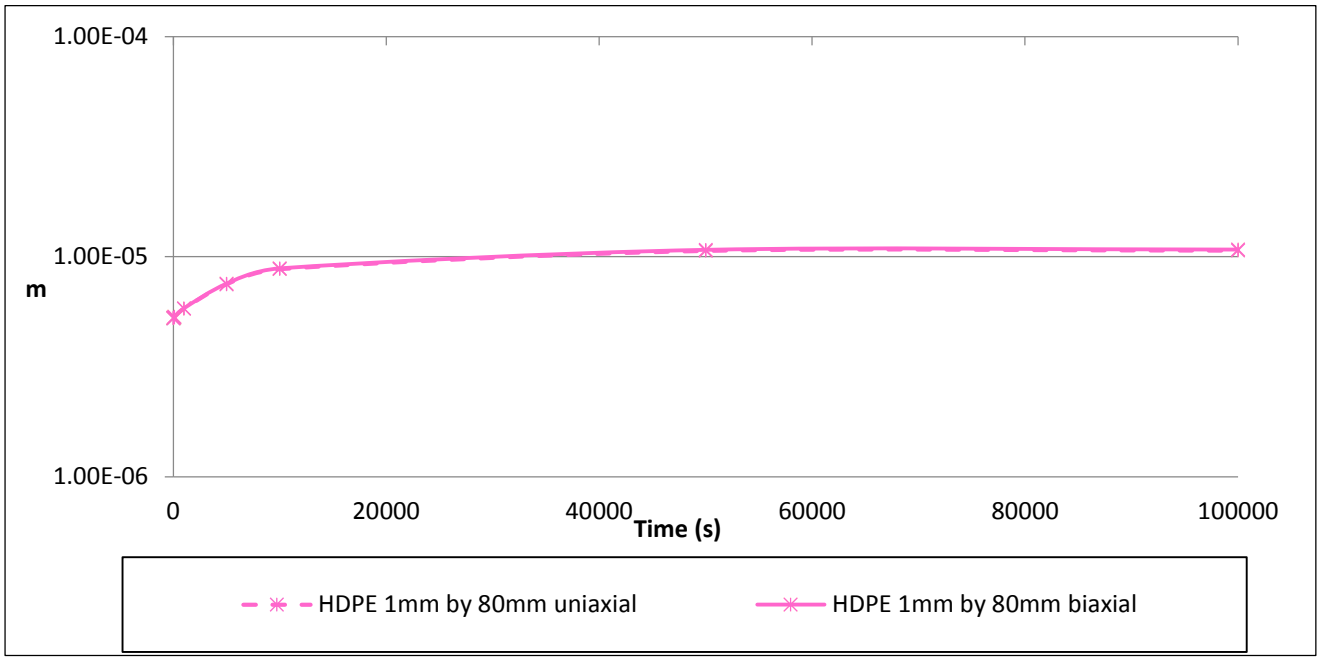

Figure J-7: Gradient (m) against time for 1mm by 80mm longitudinal crack in HDPE

b) Leakage exponent (N1) against time

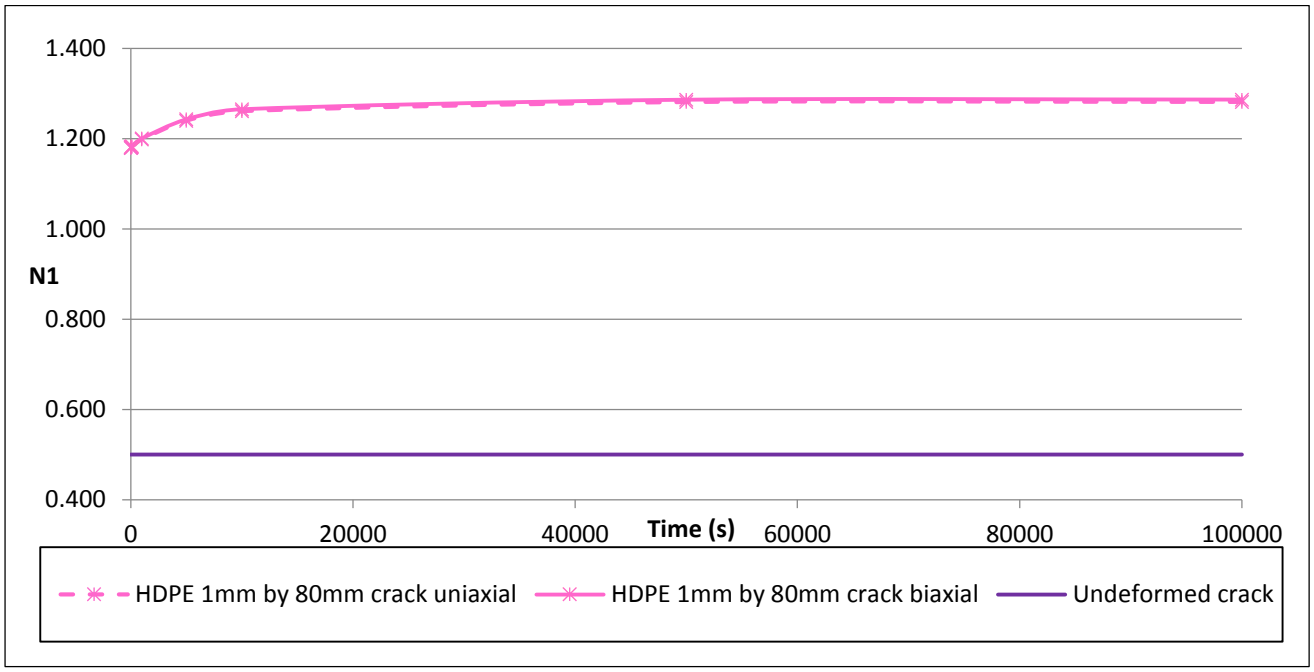

Figure J-8: Leakage exponent (N1) against time for 1mm by 80mm longitudinal crack in HDPE

7. Percentage change in area with pressure

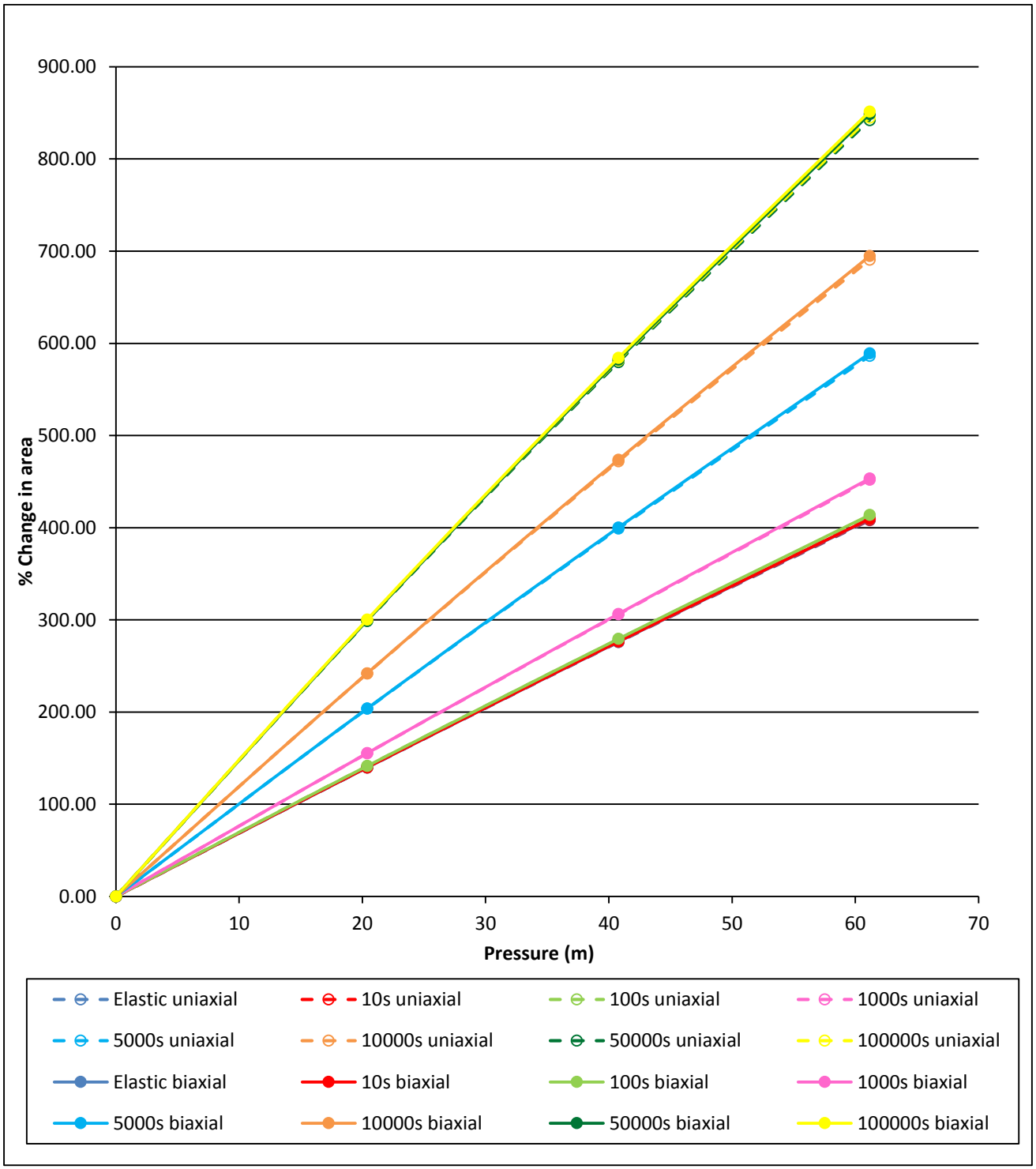

Figure J-9: Percentage change in area against pressure for 1mm by 80mm longitudinal crack in HDPE

8. Ratio of total change in area to elastic change in area

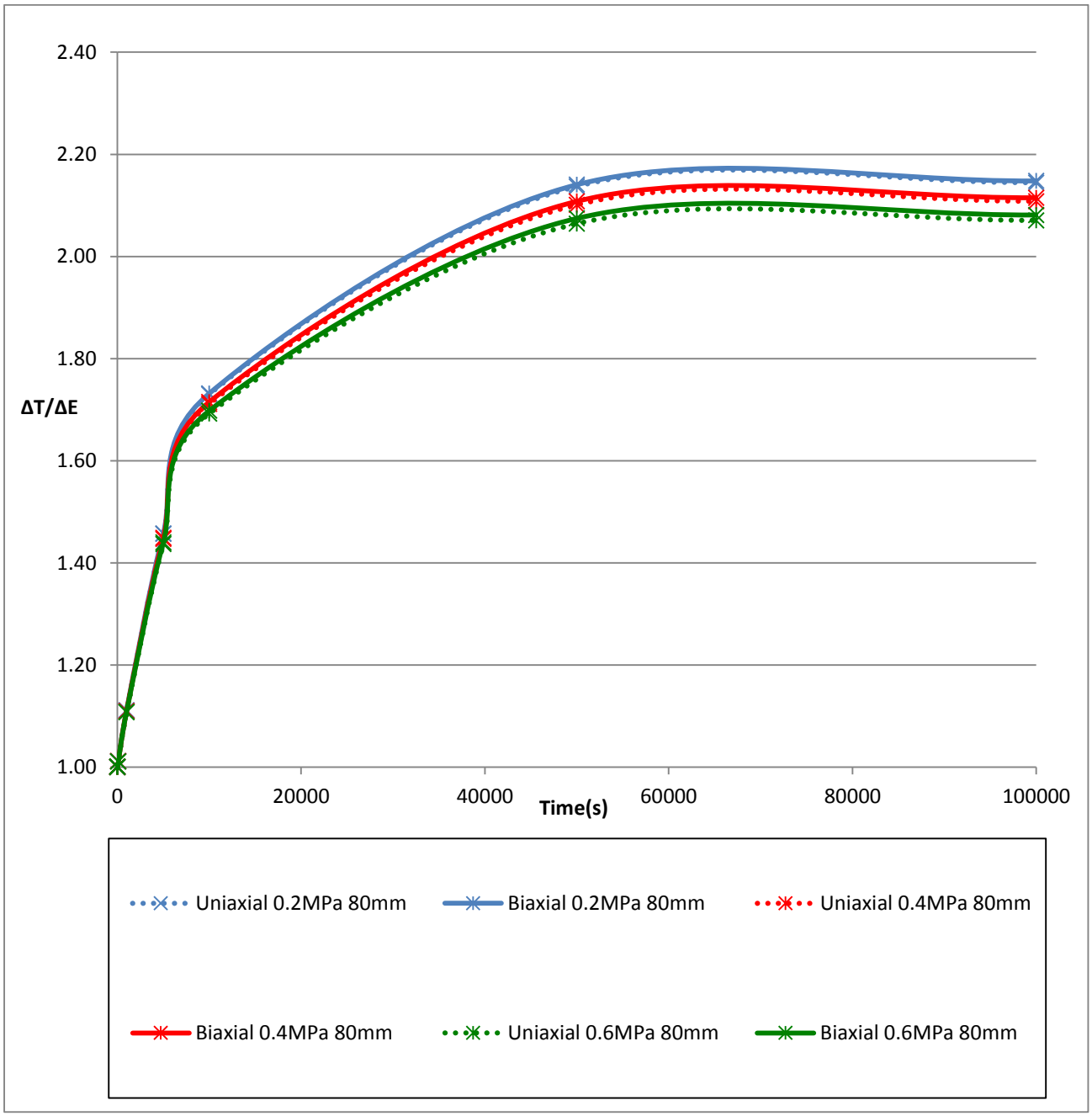

Figure J-10: ΔT/ΔE against time for 1mm by 80mm longitudinal crack in HDPE

9. Leakage number, calculated leak exponents, m/A_0 and m/m_E

a) Uniaxial

Time (s)	N1 from power law	m	L_N	N1	m/A_0	m/m_E
			Pressure = 0.4MPa	Pressure = 0.4MPa		
0	1.1794	5.25E-06	2.6822	1.2284	0.06578	1.0000
10	1.1797	5.25E-06	2.6847	1.2286	0.06584	1.0010
100	1.1815	5.31E-06	2.7118	1.2306	0.06651	1.0111
1000	1.198	5.80E-06	2.9654	1.2478	0.07273	1.1056
5000	1.2395	7.49E-06	3.8267	1.2928	0.09385	1.4267
10000	1.2608	8.78E-06	4.4867	1.3177	0.11004	1.6728
50000	1.281	1.06E-05	5.4339	1.3446	0.13327	2.0259
100000	1.2812	1.07E-05	5.4492	1.3449	0.13364	2.0316

Table J-3: Leakage numbers, calculated leak exponents, m/A_0 and m/m_E for the 1mm by 80mm crack in HDPE, uniaxial

b) Biaxial

Time (s)	N1 from power law	m	L_N	N1	m/A_0	m/m_E
			Pressure = 0.4MPa	Pressure = 0.4MPa		
0	1.1813	5.27E-06	2.6929	1.2292	0.06604	1.0000
10	1.1815	5.27E-06	2.6960	1.2294	0.06612	1.0011
100	1.1834	5.33E-06	2.7231	1.2314	0.06678	1.0112
1000	1.2001	5.83E-06	2.9792	1.2487	0.07306	1.1063
5000	1.2426	7.54E-06	3.8528	1.2939	0.09449	1.4307
10000	1.265	8.85E-06	4.5260	1.3190	0.11100	1.6807
50000	1.2861	1.08E-05	5.4952	1.3460	0.13477	2.0406
100000	1.2864	1.08E-05	5.5106	1.3464	0.13515	2.0463

Table J-4: Leakage numbers, calculated leak exponents, m/A_0 and m/m_E for the 1mm by 80mm crack in HDPE, biaxial

K 1mm by 80mm longitudinal crack in PVC

1. Summary results for area, gradient (m) and leakage exponent (N1)

PVC	Area of deformed cracks with A_0 = 79.765mm^2					
Pressure (MPa)	0.2		0.4		0.6	
Time (s)	Uniaxial	Biaxial	Uniaxial	Biaxial	Uniaxial	Biaxial
0 (Elastic)	139.5652	139.5275	198.5584	198.5482	256.7450	256.8275
10	139.5987	139.5610	198.6244	198.6143	256.8427	256.9254
100	139.8966	139.8589	199.2121	199.2026	257.7120	257.7966
1000	142.5532	142.5155	204.4511	204.4475	265.4588	265.5613
5000	149.4291	149.3918	217.9949	218.0091	285.4725	285.6176
10000	152.4813	152.4445	223.9998	224.0231	294.3207	294.5010
50000	153.8516	153.8151	226.6942	226.7218	298.2932	298.4855
100000	153.8517	153.8152	226.6945	226.7220	298.2935	298.4859

Table K-1: Deformed areas (mm^2) against time for a 1mm by 80mm longitudinal crack in PVC

PVC	Uniaxial		Biaxial	
Time (s)	N1	m	N1	m
0 (Elastic)	1.0499	2.874E-06	1.0504	2.877E-06
10	1.0500	2.875E-06	1.0505	2.878E-06
100	1.0511	2.889E-06	1.0517	2.892E-06
1000	1.0610	3.014E-06	1.0616	3.018E-06
5000	1.0844	3.336E-06	1.0851	3.341E-06
10000	1.0939	3.479E-06	1.0946	3.484E-06
50000	1.0980	3.542E-06	1.0988	3.548E-06
100000	1.0980	3.542E-06	1.0988	3.548E-06

Table K-2: Gradients (m) and leakage exponents (N1) from the power law graphs for 1mm by 80mm longitudinal crack in PVC

2. Variation of leak area with time

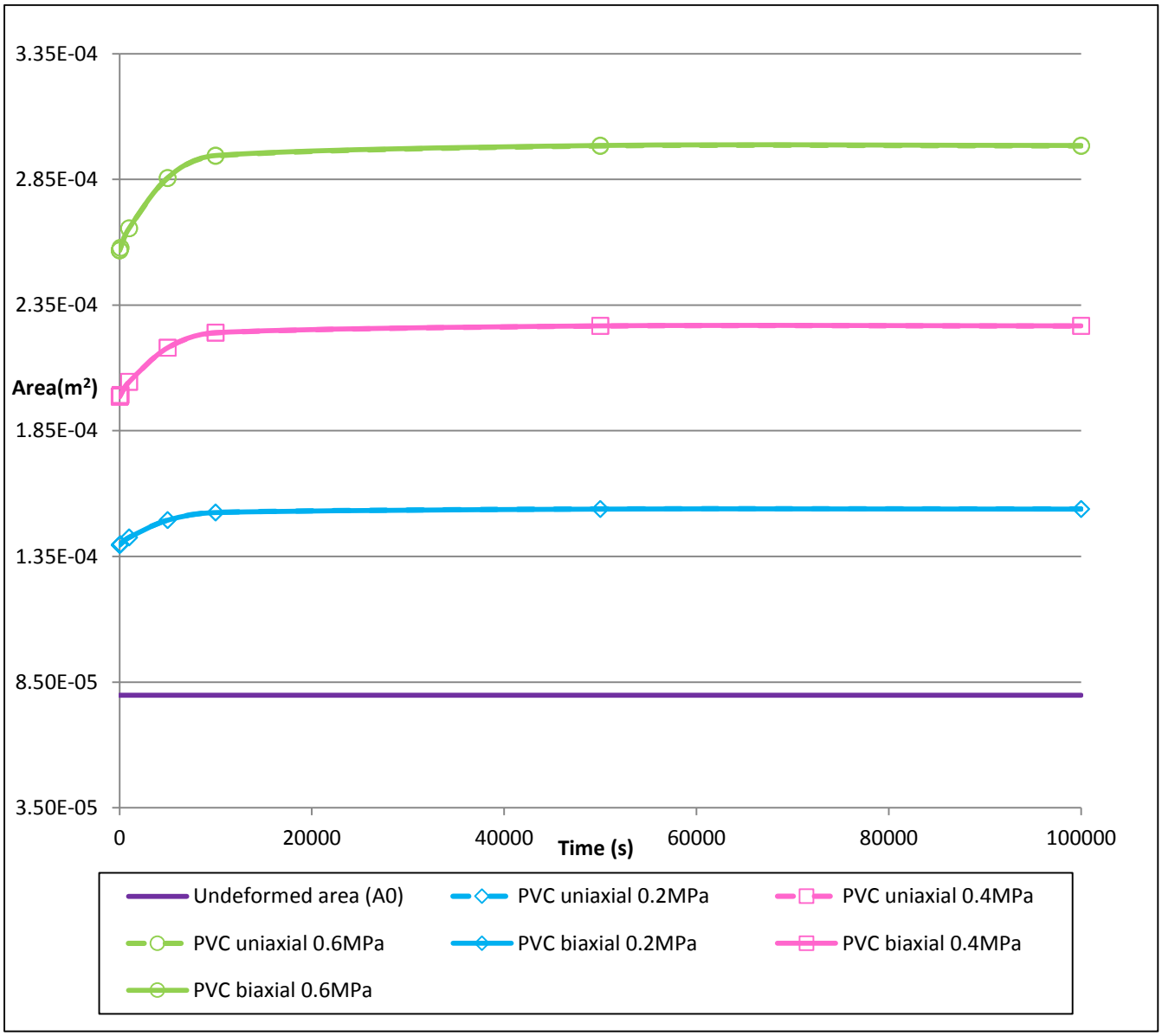

Figure K-1: Area against time for 1mm by 80mm longitudinal crack in PVC

3. Variation of leak area with pressure

a) Uniaxial

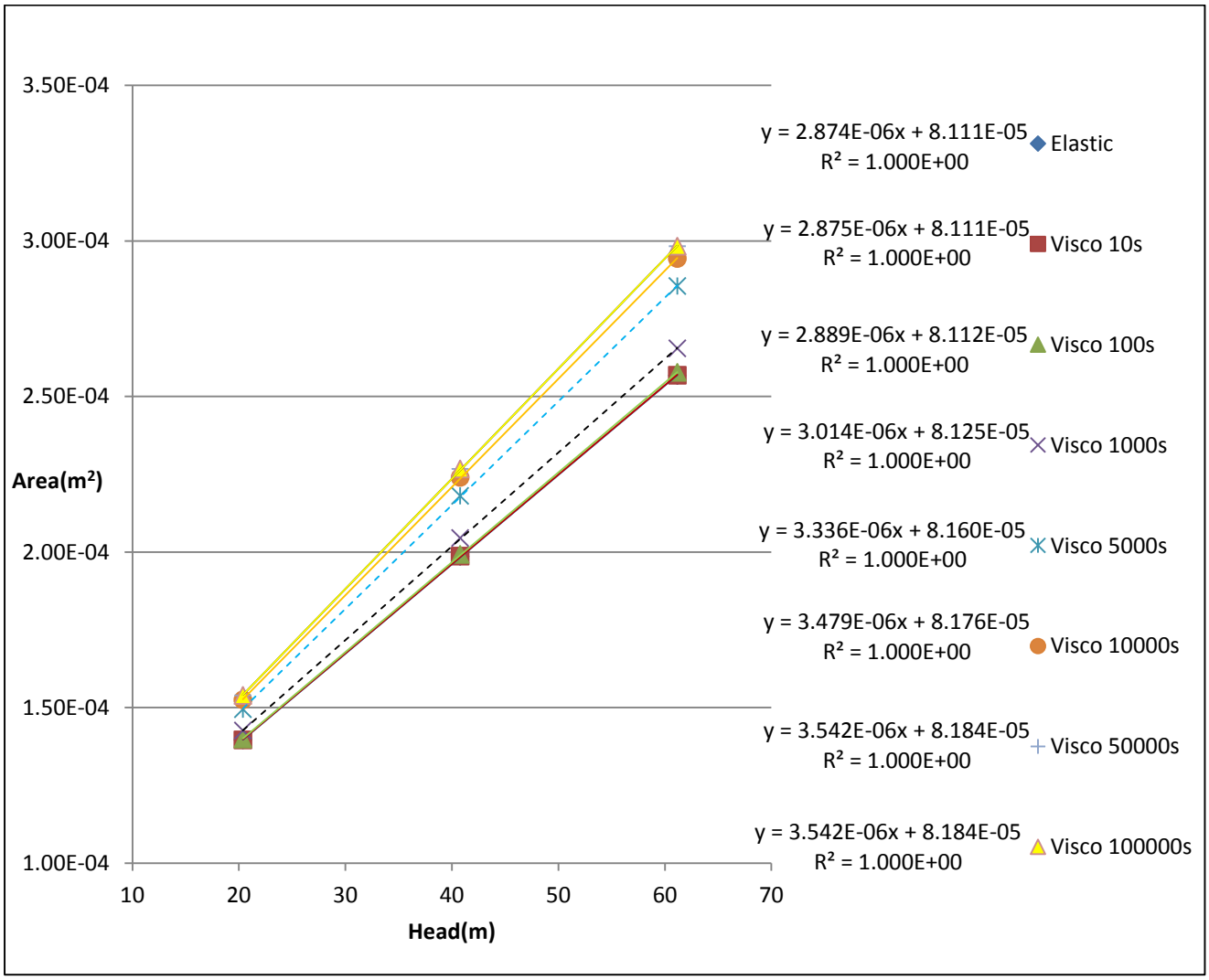

Figure K-2: Area against pressure head for 1mm by 80mm longitudinal crack in PVC, uniaxial

b) Biaxial

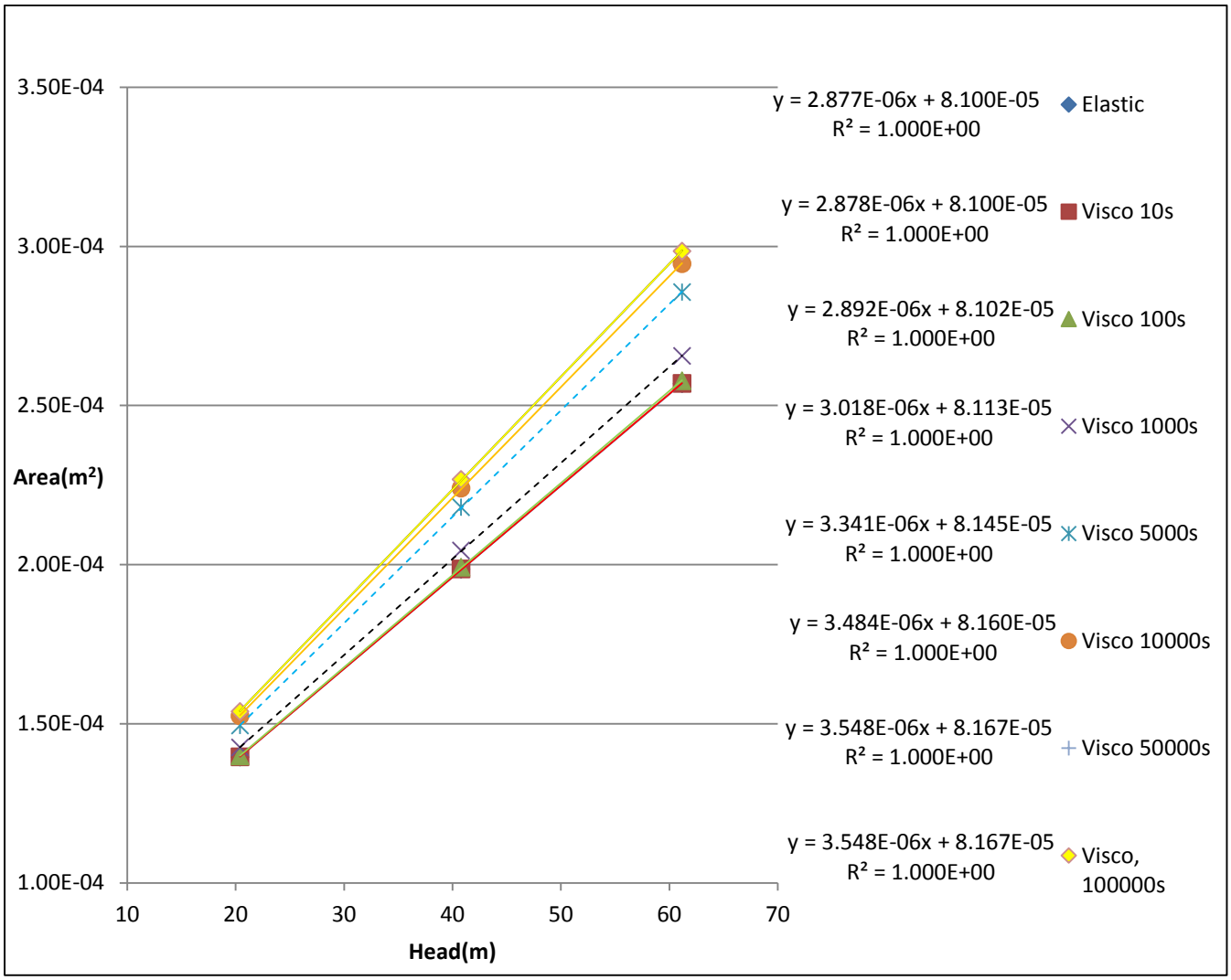

Figure K-3: Area against pressure head for 1mm by 80mm longitudinal crack in PVC, biaxial

4. Variation of leak discharge with time

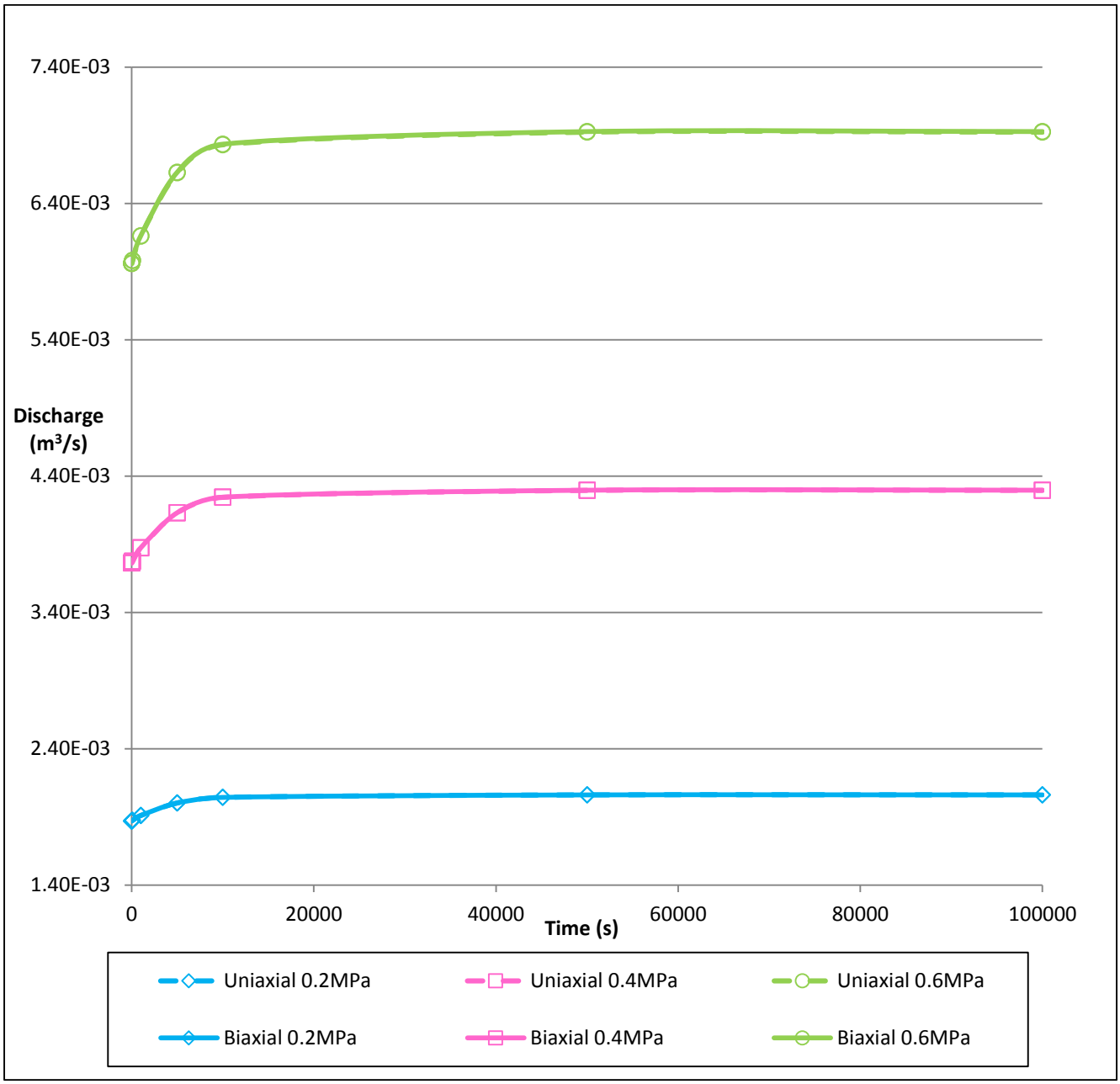

Figure K-4: Discharge against time for 1mm by 80mm longitudinal crack in PVC

5. Variation of leak discharge with pressure

a) Uniaxial

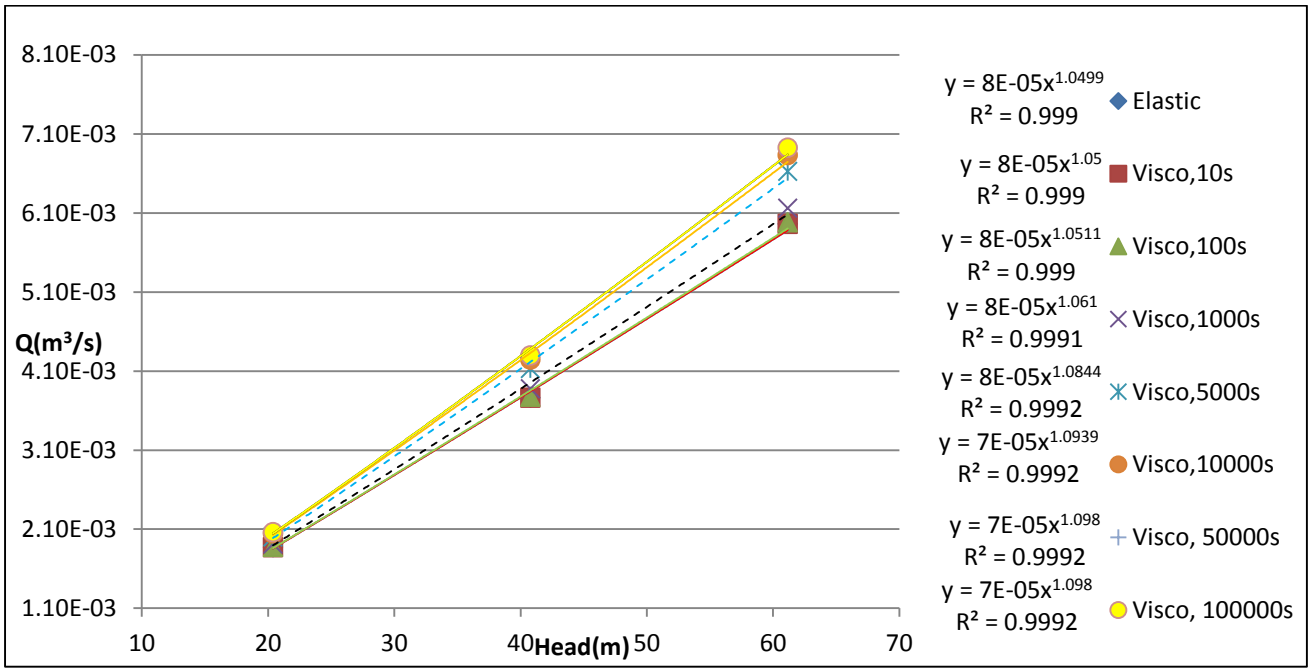

Figure K-5: Discharge against pressure head for 1mm by 80mm longitudinal crack in PVC, uniaxial

b) Biaxial

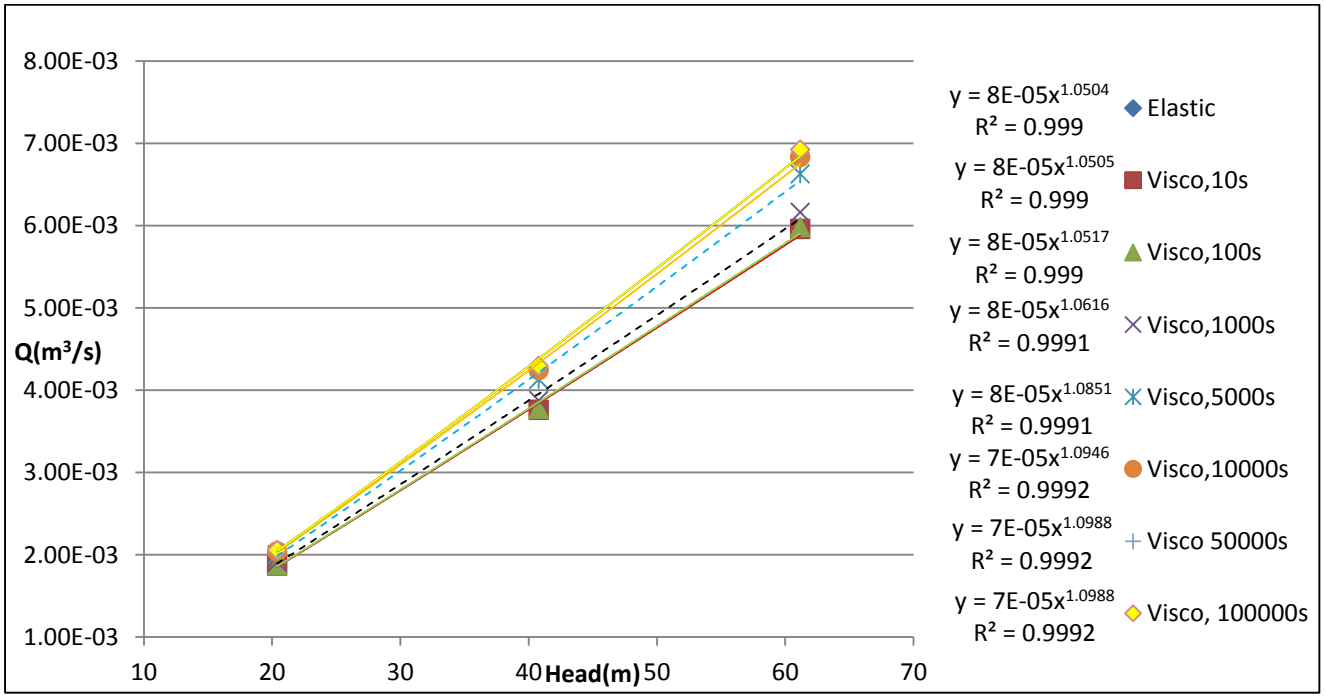

Figure K-6: Discharge against pressure head for 1mm by 80mm longitudinal crack in PVC, biaxial

6. Gradient (m) and leakage exponent (N1)

a) Gradient (m) against time

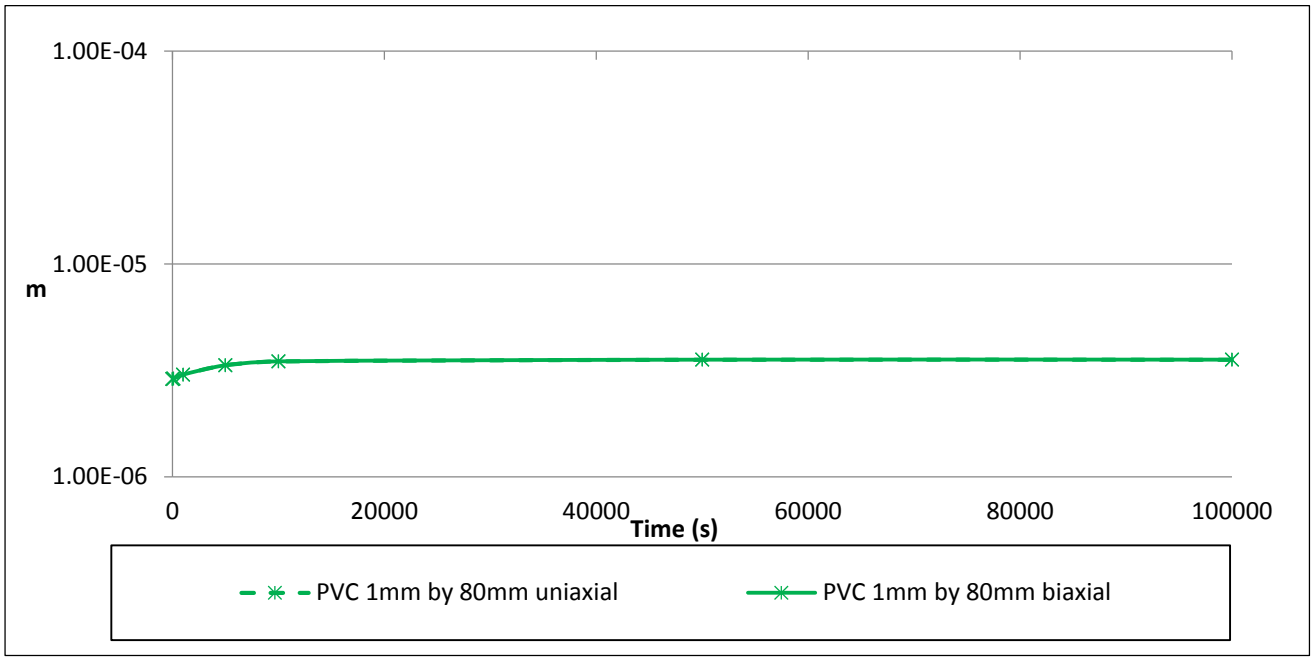

Figure K-7: Gradient (m) against time for 1mm by 80mm longitudinal crack in PVC

b) Leakage exponent (N1) against time

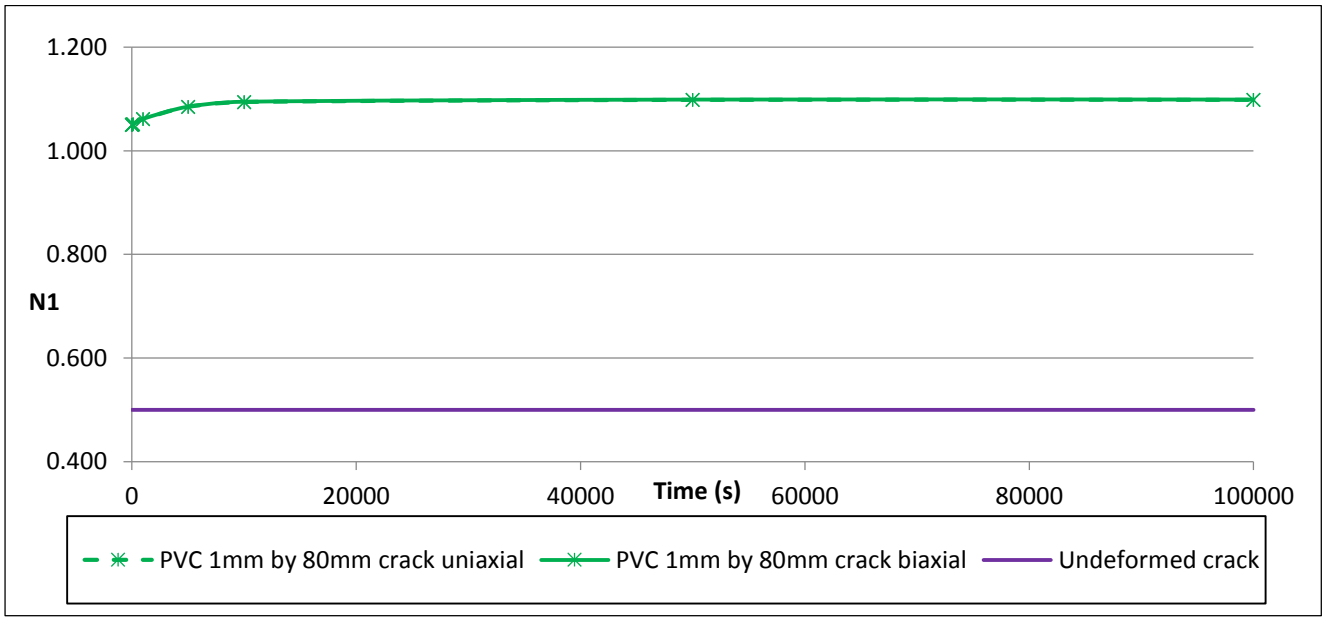

Figure K-8: Leakage exponent (N1) against time for 1mm by 80mm longitudinal crack in PVC

7. Percentage change in area with pressure

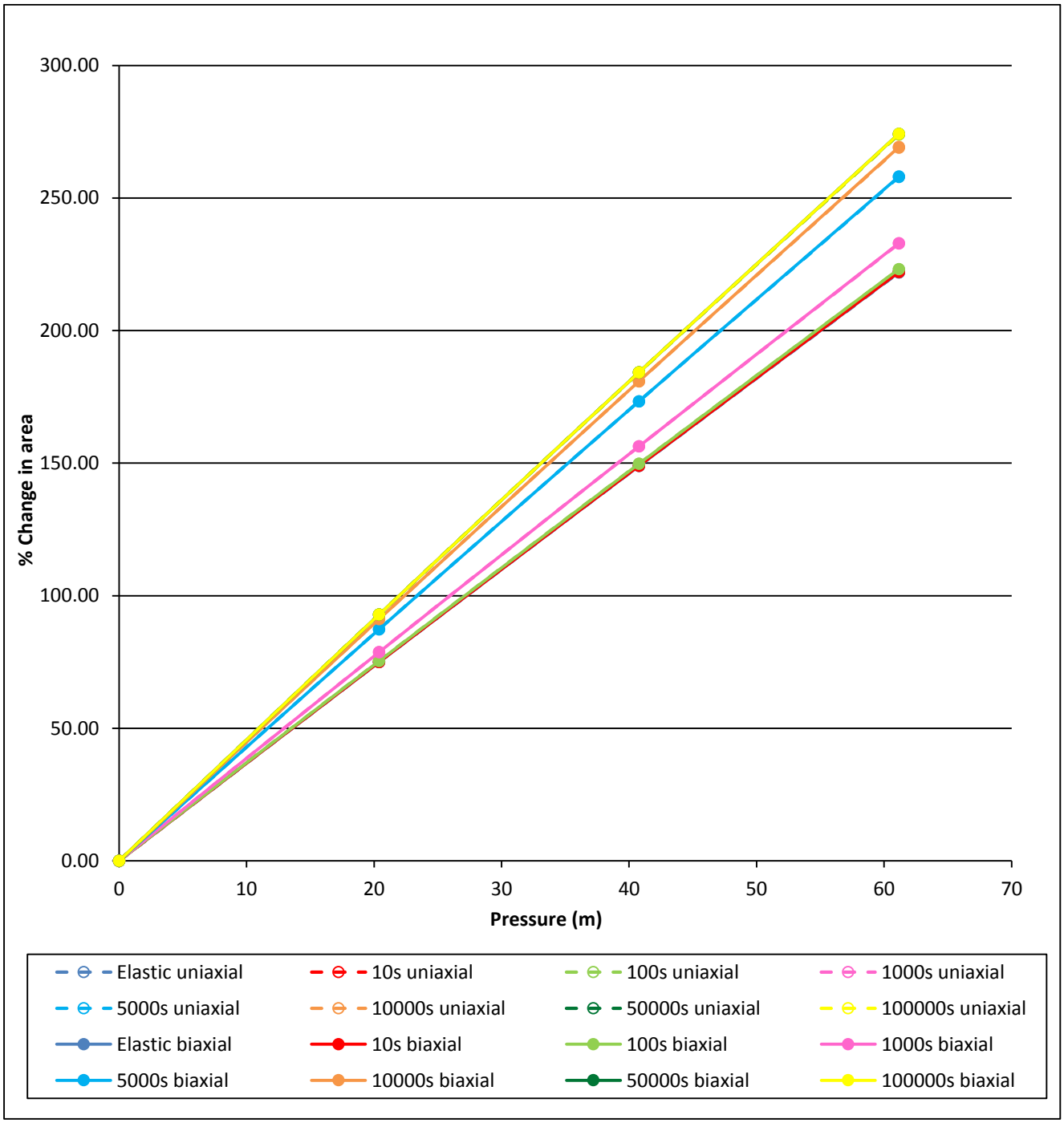

Figure K-9: Percentage change in area against pressure for 1mm by 80mm longitudinal crack in PVC

8. Ratio of total change in area to elastic change in area

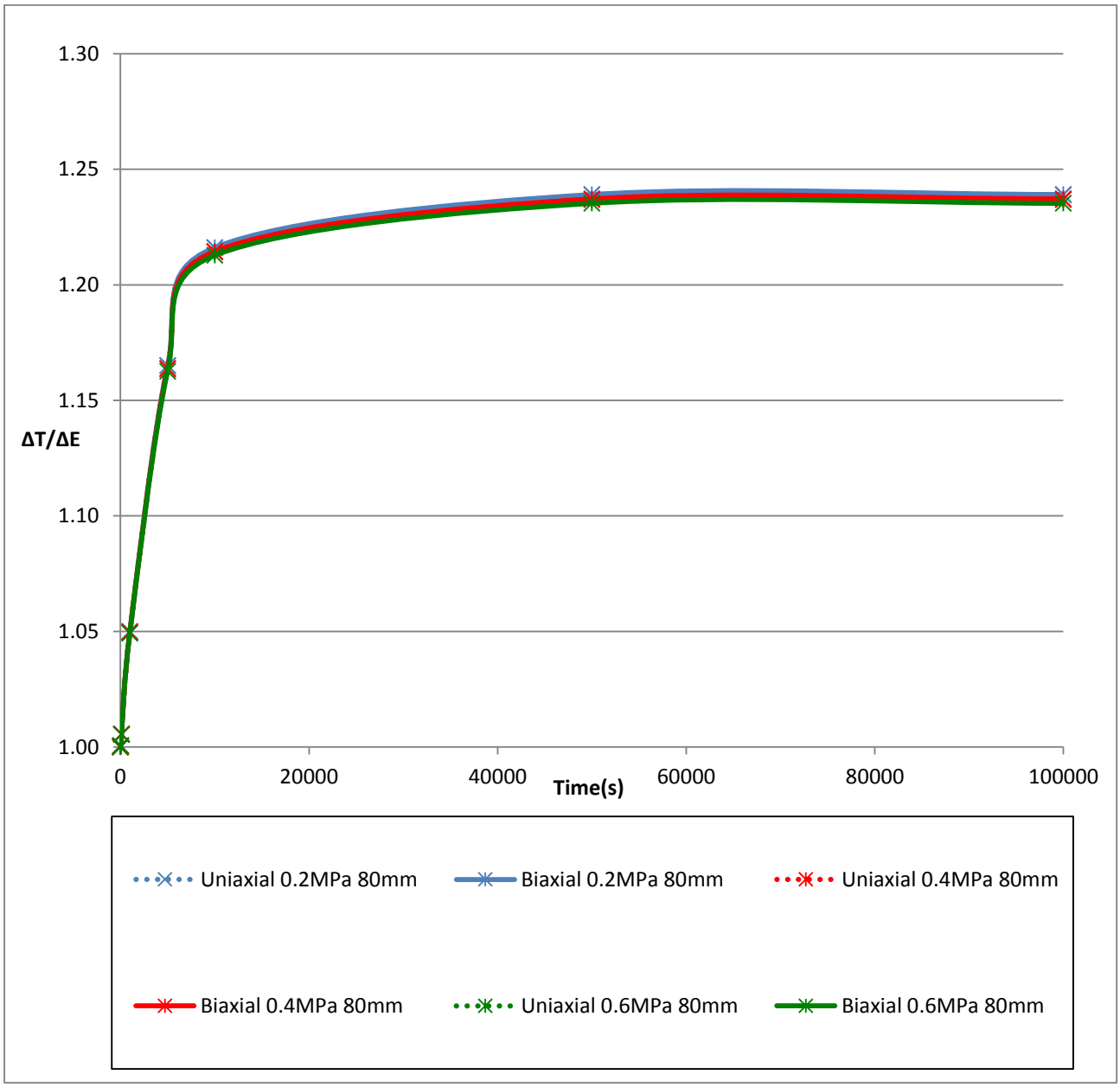

Figure K-10: ΔT/ΔE against time for 1mm by 80mm longitudinal crack in PVC

9. Leakage number, calculated leak exponents, m/A_0 and m/m_E

a) Uniaxial

Time (s)	N1 from power law	m	L_N	N1	m/A_0	m/m_E
0	1.0499	2.87E-06	1.4691	1.0950	0.03603	1.0000
10	1.05	2.88E-06	1.4697	1.0951	0.03604	1.0003
100	1.0511	2.89E-06	1.4768	1.0963	0.03622	1.0052
1000	1.061	3.01E-06	1.5407	1.1064	0.03779	1.0487
5000	1.0844	3.34E-06	1.7053	1.1304	0.04182	1.1608
10000	1.0939	3.48E-06	1.7784	1.1401	0.04362	1.2105
50000	1.098	3.54E-06	1.8106	1.1442	0.04441	1.2324
100000	1.098	3.54E-06	1.8106	1.1442	0.04441	1.2324

Table K-3: Leakage numbers calculated leak exponents, m/A_0 and m/m_E for the 1mm by 80mm crack in PVC, uniaxial

b) Biaxial

Time (s)	N1 from power law	m	L_N	N1	m/A_0	m/m_E
0	1.0504	2.877E-06	1.4707	1.0953	0.03607	1.0000
10	1.0505	2.878E-06	1.4712	1.0953	0.03608	1.0003
100	1.0517	2.892E-06	1.4783	1.0965	0.03626	1.0052
1000	1.0616	3.018E-06	1.5428	1.1067	0.03784	1.0490
5000	1.0851	3.341E-06	1.7079	1.1307	0.04189	1.1613
10000	1.0946	3.484E-06	1.7810	1.1404	0.04368	1.2110
50000	1.0988	3.548E-06	1.8137	1.1446	0.04448	1.2332
100000	1.0988	3.548E-06	1.8137	1.1446	0.04448	1.2332

Table K-4: Leakage numbers, calculated leak exponents, m/A_0 and m/m_E for the 1mm by 80mm crack in PVC, biaxial

L Sample Abaqus Input file: Input file for a 12mm hole in HDPE, biaxial load state

NOTE: Only details of the first three nodes and elements are included here.

*Heading

Deformation

** Job name: HDPE12mmroundhole Model name: HDPE 12mm round hole

** Generated by: Abaqus/CAE 6.13-1

*Preprint, echo=NO, model=NO, history=NO, contact=NO

**

** PARTS

**

*Part, name="Pipe segement solid 12mm hole"

*Node

1, 54.5967941, -12., 0.

2, 54.5967941, -12., 238.

3, 0., -55.9000015, 238.

(etc.)

*Element, type=C3D20

1, 480, 6461, 40564, 6415, 1, 75, 2827, 276, 58759, 58758, 58757, 58756, 58760, 58761, 58762,

58763, 58765, 58764, 58766, 58767

2, 6461, 6462, 40565, 40564, 75, 76, 2828, 2827, 58770, 58769, 58768, 58758, 58771, 58772, 58773,

58761, 58764, 58774, 58775, 58766

3, 6462, 6463, 40566, 40565, 76, 77, 2829, 2828, 58778, 58777, 58776, 58769, 58779, 58780, 58781,

58772, 58774, 58782, 58783, 58775

(etc)

*Elset, elset=__PickedSurf27_S4, internal, instance="Pipe segement solid 12mm hole-1", generate

13458, 13556, 2

*Surface, type=ELEMENT, name=_PickedSurf27, internal

__PickedSurf27_S1, S1

__PickedSurf27_S5, S5

__PickedSurf27_S2, S2

__PickedSurf27_S4, S4

*End Assembly

**

** MATERIALS

**

*Material, name=HDPE

*Elastic, moduli=INSTANTANEOUS

1126.76, 0.4

*Viscoelastic, time=PRONY

0.564, 0., 4348.76

**

** BOUNDARY CONDITIONS

**

** Name: line xy Type: Displacement/Rotation

*Boundary

_PickedSet18, 1, 1

_PickedSet18, 2, 2

_PickedSet18, 4, 4

_PickedSet18, 5, 5

** Name: point xyz Type: Displacement/Rotation

*Boundary

_PickedSet17, 1, 1

_PickedSet17, 2, 2

_PickedSet17, 3, 3

_PickedSet17, 4, 4

_PickedSet17, 5, 5

_PickedSet17, 6, 6

** --

**

** STEP: Apply pressure

**

*Step, name="Apply pressure", nlgeom=NO, inc=1000

apply pressure

*Static

1., 1., 1e-05, 1.

**

** LOADS

**

** Name: Biaxial add on   Type: Pressure

*Dsload

_PickedSurf26, P, -1.333

** Name: Internal pressure   Type: Pressure

*Dsload

_PickedSurf27, P, 0.2

**

** OUTPUT REQUESTS

**

*Restart, write, frequency=0

**

** FIELD OUTPUT: F-Output-1

**

*Output, field, frequency=100

*Node Output

CF, COORD, RF, U

*Element Output, directions=YES

NFORC, S

**

** HISTORY OUTPUT: H-Output-1

**

*Output, history, frequency=100

*Node Output, nset="Pipe segement solid 12mm hole-1".HolePerimeterOD

COOR1, COOR2, COOR3, U1, U2, U3

*End Step

** --

**

** STEP: Creep1

**

*Step, name=Creep1, nlgeom=NO, inc=1000

Creep

*Visco, cetol=1e-05

1., 10., 0.1, 10.

**

** OUTPUT REQUESTS

**

*Restart, write, frequency=0

**

** FIELD OUTPUT: F-Output-1

**

*Output, field, frequency=100

*Node Output

CF, COORD, RF, U

*Element Output, directions=YES

```
NFORC, S
**
** HISTORY OUTPUT: H-Output-1
**
*Output, history, frequency=100
*Node Output, nset="Pipe segement solid 12mm hole-1".HolePerimeterOD
COOR1, COOR2, COOR3, U1, U2, U3
*End Step
** ----------------------------------------------------------------
**
** STEP: Creep2
**
*Step, name=Creep2, nlgeom=NO, inc=1000
creep
*Visco, cetol=1e-05
1., 90., 0.1, 90.
**
** OUTPUT REQUESTS
**
*Restart, write, frequency=0
**
** FIELD OUTPUT: F-Output-1
**
*Output, field, frequency=100
*Node Output
CF, COORD, RF, U
*Element Output, directions=YES
NFORC, S
**
```

```
** HISTORY OUTPUT: H-Output-1
**
*Output, history, frequency=100
*Node Output, nset="Pipe segement solid 12mm hole-1".HolePerimeterOD
COOR1, COOR2, COOR3, U1, U2, U3
*End Step
** ----------------------------------------------------------------
**
** STEP: Creep3
**
*Step, name=Creep3, nlgeom=NO, inc=1000
creep
*Visco, cetol=1e-05
1., 900., 0.1, 900.
**
** OUTPUT REQUESTS
**
*Restart, write, frequency=0
**
** FIELD OUTPUT: F-Output-1
**
*Output, field, frequency=100
*Node Output
CF, COORD, RF, U
*Element Output, directions=YES
NFORC, S
**
** HISTORY OUTPUT: H-Output-1
**
```

*Output, history, frequency=100

*Node Output, nset="Pipe segement solid 12mm hole-1".HolePerimeterOD

COOR1, COOR2, COOR3, U1, U2, U3

*End Step

** --

**

** STEP: Creep4

**

*Step, name=Creep4, nlgeom=NO, inc=1000

creep

*Visco, cetol=1e-05

1., 4000., 0.1, 4000.

**

** OUTPUT REQUESTS

**

*Restart, write, frequency=0

**

** FIELD OUTPUT: F-Output-1

**

*Output, field, frequency=100

*Node Output

CF, COORD, RF, U

*Element Output, directions=YES

NFORC, S

**

** HISTORY OUTPUT: H-Output-1

**

*Output, history, frequency=100

*Node Output, nset="Pipe segement solid 12mm hole-1".HolePerimeterOD

COOR1, COOR2, COOR3, U1, U2, U3

*End Step

** --

**

** STEP: Creep5

**

*Step, name=Creep5, nlgeom=NO, inc=1000

creep

*Visco, cetol=1e-05

10., 5000., 0.1, 5000.

**

** OUTPUT REQUESTS

**

*Restart, write, frequency=0

**

** FIELD OUTPUT: F-Output-1

**

*Output, field, frequency=100

*Node Output

CF, COORD, RF, U

*Element Output, directions=YES

NFORC, S

**

** HISTORY OUTPUT: H-Output-1

**

*Output, history, frequency=100

*Node Output, nset="Pipe segement solid 12mm hole-1".HolePerimeterOD

COOR1, COOR2, COOR3, U1, U2, U3

*End Step

```
** ----------------------------------------------------------------
**
** STEP: Creep6
**
*Step, name=Creep6, nlgeom=NO, inc=1000
creep
*Visco, cetol=1e-05
10., 40000., 0.1, 10000.
**
** OUTPUT REQUESTS
**
*Restart, write, frequency=0
**
** FIELD OUTPUT: F-Output-1
**
*Output, field, frequency=100
*Node Output
CF, COORD, RF, U
*Element Output, directions=YES
NFORC, S
**
** HISTORY OUTPUT: H-Output-1
**
*Output, history, frequency=100
*Node Output, nset="Pipe segement solid 12mm hole-1".HolePerimeterOD
COOR1, COOR2, COOR3, U1, U2, U3
*End Step
** ----------------------------------------------------------------
**
```

```
** STEP: Creep7
**
*Step, name=Creep7, nlgeom=NO, inc=1000
creep
*Visco, cetol=1e-05
10., 50000., 0.5, 50000.
**
** OUTPUT REQUESTS
**
*Restart, write, frequency=0
**
** FIELD OUTPUT: F-Output-1
**
*Output, field, frequency=100
*Node Output
CF, COORD, RF, U
*Element Output, directions=YES
NFORC, S
**
** HISTORY OUTPUT: H-Output-1
**
*Output, history, frequency=100
*Node Output, nset="Pipe segement solid 12mm hole-1".HolePerimeterOD
COOR1, COOR2, COOR3, U1, U2, U3
*End Step
```